

**Distribution Agreement:**

In presenting this thesis or dissertation as a partial fulfillment of the requirements for an advanced degree from Emory University, I hereby grant to Emory University and its agents the non-exclusive license to archive, make accessible, and display my thesis or dissertation in whole or in part in all forms of media, now or hereafter known, including display on the world wide web. I understand that I may select some access restrictions as part of the online submissions of this thesis or dissertation. I retain all ownership rights to the copyright of the thesis or dissertation. I also retain the right to use in future works (such as articles or books) all or part of this thesis or dissertation.

Signature

\_\_\_\_\_  
Nina Mace Weldy

\_\_\_\_\_  
Date

Development of Transition Metal Catalyzed  
Metallonitrene and Metallocarbene Group Transfer Reactions

By

Nina Mace Weldy  
Doctor of Philosophy

Chemistry

---

Simon B. Blakey, Ph.D.  
Advisor

---

Christopher C. Scarborough, Ph.D.  
Committee Member

---

Huw M. L. Davies, Ph.D.  
Committee Member

Accepted:

---

Lisa A. Tedesco, Ph.D.  
Dean of the James T. Laney School of Graduate Studies

---

Date

Development of Transition Metal Catalyzed  
Metallonitrene and Metallocarbene Group Transfer Reactions

By

Nina Mace Weldy

B.S., Davidson College, 2010

Advisor: Simon B. Blakey, Ph.D.

An abstract of  
a dissertation submitted to the Faculty of the  
James T. Laney School of Graduate Studies of Emory University  
in partial fulfillment of the requirements for the degree of  
Doctor of Philosophy  
in Chemistry

2015

## Abstract

### Development of Transition Metal Catalyzed

### Metallonitrene and Metallocarbene Group Transfer Reactions

By Nina Mace Weldy

Group transfer reactions provide a powerful approach for formation of complex molecules for pharmaceutical and natural product synthesis. Our study of group 9 transition metal complexes has provided a range of group transfer reactions for formation of C–C, C–N, and C–O bonds from simple starting materials. In Chapter 1, we discuss the intermolecular metallonitrene/alkyne cascade. Previous studies in our laboratory established the direct unveiling of an intermediate with an  $\alpha$ -iminometallocarbene reactivity profile by an intramolecular metallonitrene-initiated oxidative cascade process. We extended the utility of this cascade process to intermolecular trapping of the reactive intermediate by a variety of allyl ethers to provide  $\alpha$ -oxyimine products in which new C=N, C–O and C–C bonds have all been generated. A variety of substrates were explored, enantioenriched products were able to be generated by efficient transfer of stereochemical information from simple enantioenriched allyl ethers, and the usefulness of the process was demonstrated by an efficient synthesis of the core ring system of the Securinega alkaloids.

Our study of racemic and enantioselective C–H amination strategies is described in Chapter 2. A quinoline-oxazoline amide ligand framework was designed for C–H amination with aryl azides. Ir(I) complexes of this ligand were synthesized. Iridium(III) bis(oxazoliny)phenyl and bis(imidazoliny)phenyl complexes were capable of benzylic C–H amination in moderate enantioselectivity. In collaboration with the MacBeth laboratory, a dinuclear Co(II) complex with a redox-active ligand system was found to efficiently catalyze C–H amination to form indolines from aryl azides. The catalyst system was capable of forming 5-, 6-, and 7-membered rings and tolerated medicinally relevant heterocycles, such as pyridine and indole. The ease of synthesis and tunability of the redox-active ligand system make this method advantageous for selective C–H amination.

Finally, Chapter 3 details our enantioselective C–H functionalization with acceptor-only metallocarbenes catalyzed by an iridium(III) bis(imidazoliny)phenyl catalyst family to give phthalan- and 2,5-dihydrofuran derivatives in excellent yield and enantioselectivity. The reaction was found tolerant of a variety of substitution patterns of the diazoacetate, while the steric and electronic properties of the substrate greatly influenced the reaction yield and selectivity. These results showcased the potential for reaction design based on an interaction of experimental and computational results in developing a foundation for further expansion into highly selective reactions with novel classes of acceptor-only metallocarbenes.

Development of Transition Metal Catalyzed  
Metallonitrene and Metallocarbene Group Transfer Reactions

By

Nina Mace Weldy  
B.S., Davidson College, 2010

Advisor: Simon B. Blakey, Ph.D.

A dissertation submitted to the Faculty of the  
James T. Laney School of Graduate Studies of Emory University  
in partial fulfillment of the requirements for the degree of  
Doctor of Philosophy  
in Chemistry

2015

*In Memory of Drs. Karl and Marguerite Murphy*

## Acknowledgements

First, thank you to Dr. Simon Blakey, for being a wonderful advisor. You've taught me so much about scientific inquiry, research, teaching, writing, and using precise language. Thank you for accepting me into your lab and for the supportive atmosphere you've fostered throughout my time at Emory. Coming to Emory and joining your lab is the best decision I could have made for my Ph.D.

Thank you to Dr. Huw Davies for your insightful feedback on my work, as well as everything you've done for the Center for Selective C–H Functionalization. Being a part of the Center has enriched my graduate experience so much, by being able to meet and collaborate with incredible chemists. I feel very fortunate to have been a part of the Center and look forward to continuing to witness the amazing impact it is having in our field.

Thank you to Dr. Christopher Scarborough for your comments and encouragement throughout my time here. Thank you for all your help in my career development and for being so supportive.

I benefited greatly from amazing collaborators and coauthors throughout my time at Emory. Thank you to Dr. Cora MacBeth, I am so glad that I got to be a part of the beginning of scientific collaboration between our two groups. Thank you also for all of your enthusiasm and for teaching me so much about inorganic chemistry, as well as for your help in my job search. Dr. Omar Villanueva, I could not have had a better person to collaborate with. You are a great chemist, and a kind and encouraging person. Thank

you to Dr. Aaron Thornton and Dr. Clayton Owens, whose excellent science established projects that I had the joy of building upon.

Thank you to Dr. Dan Morton for training me during my rotation in the Davies laboratory. You taught me so much about how to operate in lab, and thank you for being so patient and kind to me when I had no idea how to do anything.

Thank you to all the current and former members of the Blakey lab. Thank you to Dr. Danny Mancheno for your good advice and enthusiastic participation in “group time.” Thank you to Dr. Aidi Kong for reassuring me and for your excellent example in lab. Thank you to Dr. Jennifer Bon and Eric Andreansky for being awesome people to share a lab with.

Dr. Katie Chepiga, I am so incredibly blessed you were in my class and that we got to be good friends. I look forward to seeing the amazing things you will accomplish in chemistry.

Thank you to Jessica Petree for praying for me and always being a bright light.

Thank you to Glenn and Marilee Mace for always loving me, being proud of me, and encouraging me to get “straight A’s.” Although, I have a confession: I did not get straight A’s in graduate school.

This work is in memory of Karl and Marguerite Murphy. They met while working on their English Ph.D.’s at Harvard, when Karl mistakenly used Marguerite’s coat hanger when she sat in the carrel next to him in the library. I love and miss you, Nannie and Grandpop, and thank you for making my pursuing a Ph.D. a lifelong aspiration for me.



Thank you to my parents, Keith and Elizabeth Mace, for more than I can articulate on an acknowledgements page. You have supported me endlessly throughout my education, and more importantly, you're the people who first taught me what love is.

Thank you to my brother, Dashiell Mace, for being so encouraging and always being proud of what I'm doing. You are an incredible person, and I'm proud of you too. And lastly, thank you to Zachary Weldy. Meeting and marrying you is the best thing to happen to me in graduate school. You are helping me become my glory self every day, and I praise God for putting you in my life. Thank you for always being excited about becoming "Mr. and Dr."

Studying chemistry consistently amazes me with the power and artistry of our Creator God. Throughout graduate school, in the struggles and the triumphs of research, I've been reminded of words attributed to Johannes Kepler, that scientific discovery is "thinking God's thoughts after Him." There can be no better motivation for scientific inquiry than to marvel at the God who created it all and understands it better than we ever could.

"[T]o the only God, our Savior, through Jesus Christ our Lord, be glory, majesty, dominion, and authority, before all time and now and forever. Amen." (Jude 1:25)

## Table of Contents

### Chapter 1. Intermolecular Cascade Reactions Through Alkyne Oxidative Amination with Metallonitrenes

1.1 Introduction to Metallonitrene Cascade Reactions .....	2
1.1.1 Background of Cascade Reactions.....	2
1.1.2 Generation of Metallonitrenes .....	3
1.1.3 Metallonitrene Cascade Reactions .....	6
1.1.3.1 Metallonitrene/Alkene Cascade Reactions .....	6
1.1.3.1.1 Azide-Initiated Metallonitrene/Alkene Cascade Reactions .....	6
1.1.3.1.2 Intermolecular Alkene Oxyamination.....	14
1.1.3.2 Metallonitrene/Allene Cascade Reactions .....	15
1.1.3.2.1 Aminocyclopropane-Forming Metallonitrene/Allene Cascade Reactions .....	15
1.1.3.2.2 2-Amidoallylcation [3+2] Annulation .....	19
1.1.3.2.3 Cascades with 1,4-Diazaspiro[2.2]pentane (DASP) Scaffolds.....	22
1.1.3.3 Metallonitrene/Alkyne Cascade Reactions .....	27
1.1.3.3.1 Intramolecular Metallonitrene/Alkyne Cascade Reactions .....	27
1.1.3.3.2 Intermolecular Metallonitrene/Alkyne Cascade Reactions .....	36
1.2 Intermolecular Metallonitrene/Alkyne Cascade Optimization .....	42
1.3 Intermolecular Metallonitrene/Alkyne Cascade Substrate Scope.....	44
1.4 Viroallosecurinine Core Synthesis.....	59
1.4.1. Previous Syntheses of <i>Securinega</i> Alkaloids.....	59

1.4.2 Retrosynthetic Analysis of Viroallosecurinine and Preliminary Results.....	63
1.4.3 Streamlined Route to Viroallosecurinine Core .....	68
1.5 Conclusions.....	71
1.6. Experimental Procedures and Compound Characterization .....	73
References.....	96

## **Chapter 2. Group 9 Transition Metal Catalyzed C–H Amination with Aryl Azides**

2.1 Introduction to Metallonitrene C–H Amination .....	104
2.1.1 Qualities of an Ideal C–H Amination .....	104
2.1.2 Azides as Metallonitrene Precursors.....	105
2.1.2.1 Metallonitrene C–H Amination Utilizing Azides with Electron-Withdrawing Groups.....	106
2.1.2.2 Metallonitrene C–H Amination Utilizing Aryl and Vinyl Azides.....	111
2.1.2.3 Metallonitrene C–H Amination Utilizing Alkyl Azides.....	113
2.1.3 Challenges in C–H Amination Utilizing Azide Metallonitrene Precursors.....	114
2.1.3.1 Use of First Row Transition Metals in Metallonitrene C–H Amination Utilizing Aryl Azides.....	115
2.1.3.2 Enantioselectivity in Metallonitrene C–H Amination Utilizing Aryl Azides .....	116
2.2 Modular Ligand Design for Enantioselective Catalysis .....	119
2.2.1 Oxazoline-Based Modular Ligands .....	119
2.2.2 Linear Regression Mathematical Modeling for Catalyst Optimization.....	120

2.2.3 Planned Synthetic Routes to Quinoline/Oxazoline Amide Ligands .....	123
2.3 Enantioselective C–H Amination with Iridium(I) and Iridium(III) Catalysts .....	126
2.3.1 Quinoline/Oxazoline Amide Ligand Synthesis .....	126
2.3.2 Quinoline/Oxazoline Amide Ligand Metalation and Resultant Complex Characterization .....	135
2.3.3 Iridium(I) quinoline-oxazoline amide Catalyzed C–H Amination with Aryl Azides .....	145
2.3.4 Iridium(III) Phebox and Phebim Catalyzed Enantioselective C–H Amination with Aryl Azides .....	148
2.4 Cobalt(II) Catalyzed C–H Amination with Aryl Azides .....	160
2.4.1 Catalysis with a Cobalt(II) Dimer with Redox-Active Ligand Scaffold $\text{NH}(o\text{-PhNHC(O)}^i\text{Pr})_2$ .....	160
2.4.2 Aryl Azide Substrate Syntheses .....	161
2.4.3 Cobalt(II) Catalyzed C–H Amination Results .....	174
2.5 Conclusions .....	180
2.6 Experimental Procedures and Compound Characterization .....	182
References .....	237

### **Chapter 3. Enantioselective Acceptor-Only Metallocarbene C–H Functionalization**

#### 3.1 Introduction to Enantioselective C–H Functionalization

Utilizing Metallocarbenes .....	244
---------------------------------	-----

3.1.1 Intermolecular Enantioselective C–H Insertion with Acceptor-Only Diazoacetate Metallocarbene Precursors .....	245
3.1.1.1 Intermolecular Enantioselective C–H Insertion with Alkyl Diazoacetates .....	246
3.1.1.2 Racemic C–H Insertion and Enantioselective Cyclopropanation with Ethyl Diazoacetate .....	251
3.1.2 Iridium(III) Phebox and Phebim Catalysts for C–H Functionalization .....	253
3.1.2.1 Development and Previous Uses of the Phebox and Phebim Ligand Scaffolds .....	253
3.1.2.2 Enantioselective Iridium(III) Phebox Catalyzed Donor/Acceptor Metallocarbene C–H Functionalization .....	258
3.1.2.3 Enantioselective Iridium(III) Phebox Catalyzed Ethyl Diazoacetate C–H Functionalization .....	260
3.2 Enantioselective Iridium(III) Phebim Catalyzed Acceptor-Only Diazoacetate C–H Functionalization .....	263
3.2.1 Iridium(III) Phebim Catalyst Synthesis .....	264
3.2.2 Iridium(III) Phebim Catalyst Optimization with Ethyl Diazoacetate .....	266
3.2.3 Acceptor-Only Diazoacetate Scope .....	267
3.2.4 Phthalan-Derived Substrate Synthesis .....	271
3.2.5 Ethyl Diazoacetate C–H Insertion Substrate Scope .....	276
3.2.6 Kinetic Resolution .....	279
3.2.7 Determination of Absolute Stereochemistry of C–H Insertion Products .....	281

3.2.8 Kinetic Isotope Effect of Ethyl Diazoacetate C–H Insertion into Tetrahydrofuran .....	282
3.3 Conclusions.....	285
3.4 Experimental Procedures and Compound Characterization .....	287
References.....	326

## List of Schemes

### Chapter 1:

Scheme 1.1	Johnson's classic synthesis of progesterone through a cationic polyolefin cyclization cascade reaction .....	3
Scheme 1.2	Preliminary Rh(II)-catalyzed aryl azide cascade reaction to form 2,3-diphenyl indole <b>9</b> .....	8
Scheme 1.3	Selective formation of 2,3-diphenylindole <b>11</b> from $\beta,\beta$ -diphenylstyryl azide <b>10</b> .....	8
Scheme 1.4	Mechanism for rhodium-catalyzed synthesis of 2,3-disubstituted indole <b>11</b> from $\beta,\beta$ -disubstituted styryl azide <b>10</b> . ....	9
Scheme 1.5	Nitro-group migration reaction to form 3-nitroindole <b>16</b> from $\beta$ -nitro styryl azide <b>17</b> .....	10
Scheme 1.6	Migrating group selectivity in the styryl azide cascade.....	10
Scheme 1.7	Selective aminomethylene migration from styryl azide <b>18</b> to form 2,3-disubstituted indole <b>19</b> .....	11
Scheme 1.8	New electrocyclization/migration cascade reaction with $\alpha,\beta,\beta$ -trisubstituted styryl azides <b>20</b> to form 1,2,3-trisubstituted indoles <b>21</b> .....	12
Scheme 1.9	Postulated mechanism for the formation of 1,2,3-trisubstituted indole <b>29</b> from styryl azide <b>24</b> .....	13
Scheme 1.10	General FeBr <sub>2</sub> -catalyzed cascade reaction of <i>ortho</i> -alkyl-substituted aryl azides <b>30</b> to form 2,3-disubstituted indoles <b>31</b> .....	13

Scheme 1.11	Scope of the FeBr <sub>2</sub> catalyzed cascade reaction of <i>ortho</i> -alkyl-substituted aryl azides .....	14
Scheme 1.12	Postulated oxyamination mechanism with metallonitrene <b>32</b> and alkene <b>33</b> to form 1,2-amino ester <b>35</b> .....	15
Scheme 1.13	Metallonitrene/allene cascade concept .....	16
Scheme 1.14	Transfer of stereochemistry from a chiral allene through the metallonitrene/allene cascade .....	17
Scheme 1.15	Metallonitrene/allene cascade with bulkier allene substitution .....	18
Scheme 1.16	Metallonitrene/allene cascade mechanism.....	19
Scheme 1.17	Mechanism for [3+2] and [3+3] 2-amidoallylcation annulation .....	22
Scheme 1.18	Allenic <i>N</i> -tosyloxy-carbamate aziridination to form a methylene aziridine.....	23
Scheme 1.19	Aziridination of an allenic carbamate to form a methylene aziridine.....	23
Scheme 1.20	Synthesis of a 1,4-diazaspiro[2.2]pentane (DASP) scaffold <b>59</b> from an allenic carbamate <b>58</b> and subsequent C1 or formal C3 ring-opening .....	24
Scheme 1.21	Formal C3 ring opening of 1,4-diazaspiro[2.2]pentane (DASP) scaffold <b>60</b> .....	25
Scheme 1.22	C2 ring opening of 1,4-diazaspiro[2.2]pentane (DASP) scaffolds .....	26
Scheme 1.23	Cascade formation of 1,3-diaminated ketone <b>66</b> from carbamate <b>65</b> .....	26
Scheme 1.24	One-pot aziridination and ring-opening of allenic sulfamate <b>67</b> with transfer of chirality to oxathiazepane <b>68</b> .....	27
Scheme 1.25	Intramolecular metallonitrene/alkyne cascade mechanism .....	28



Scheme 1.26	Metallonitrene/alkyne cascade control experiment with sulfamate ester <b>75</b> .....	29
Scheme 1.27	Intramolecular metallonitrene/alkyne substrate scope.....	30
Scheme 1.28	Metallonitrene/alkyne cascade Friedel-Crafts termination mechanism.....	31
Scheme 1.29	Electronic substitution effects on Friedel-Crafts termination of the metallonitrene/alkyne cascade .....	32
Scheme 1.30	Mechanism of cyclopropanation termination of the metallonitrene/alkyne cascade with sulfamate ester <b>83</b> .....	33
Scheme 1.31	Effect of olefin substitution on cyclopropanation termination of the metallonitrene/alkyne cascade .....	34
Scheme 1.32	Metallonitrene/alkyne cascade termination by aryl cyclopropanation .....	34
Scheme 1.33	Importance of the benzylic ether in favoring aryl cyclopropanation over electrophilic aromatic substitution in the metallonitrene/alkyne cascade .....	35
Scheme 1.34	Enantioselective catalysis of the intramolecular metallonitrene/alkyne cascade reaction of sulfamate ester <b>96</b> .....	36
Scheme 1.35	1,2,3-Triazole <b>97</b> as an $\alpha$ -iminometallobutene precursor for C–H functionalization .....	37
Scheme 1.36	Intermolecular metallonitrene/alkyne cascade mechanism, with possible unproductive pathways .....	38
Scheme 1.37	Use of $\text{Rh}_2(\text{tfacam})_4$ for intermolecular metallonitrene aziridination .....	38
Scheme 1.38	Derivatization of oxathiazepane <b>102</b> to form disubstituted cyclohexene <b>104</b> .....	41

Scheme 1.39	Activation of intermolecular metallonitrene/alkyne cascade product <b>101</b> for ring-opening .....	41
Scheme 1.40	Synthesis of Rh <sub>2</sub> (tfacam) <sub>4</sub> .....	42
Scheme 1.41	Synthesis of methyl crotyl ether ( <b>111</b> ) by methylation of crotyl alcohol ( <b>112</b> ).....	45
Scheme 1.42	Intermolecular cascade reaction with methyl crotyl ether ( <b>111</b> ) .....	45
Scheme 1.43	Silyl cupration of propargyl methyl ether ( <b>117</b> ) to yield <i>E</i> -vinyl silane <b>115</b> .....	47
Scheme 1.44	Intermolecular cascade reaction with chiral ether <b>120</b> to yield imine <b>122</b> .....	50
Scheme 1.45	Synthesis of benzyl ether <b>123</b> .....	51
Scheme 1.46	Intermolecular cascade reaction with benzyl ether <b>123</b> .....	52
Scheme 1.47	Synthesis of enantiomerically enriched benzyl ether ( <i>R</i> )- <b>123</b> .....	52
Scheme 1.48	Intermolecular cascade reaction with enantiomerically enriched benzyl allyl ether ( <i>R</i> )- <b>123</b> .....	53
Scheme 1.49	Derivatization of oxathiazepine <b>124</b> with 4-nitrobenzyl chloride for crystallization.....	54
Scheme 1.50	Benzyl allyl ether ( <b>128</b> ) metallonitrene/alkyne cascade termination to yield imine <b>101</b> .....	56
Scheme 1.51	Cyclohexyl allyl ether ( <b>130</b> ) metallonitrene/alkyne cascade termination .....	56
Scheme 1.52	Metallonitrene/alkyne cascade with <i>in situ</i> Grignard addition to imine <b>101</b> .....	58

Scheme 1.53	Oxathiazepane ring-opening/ring-closing reaction to form pyrrolidine <b>131</b> .....	58
Scheme 1.54	Honda and coworkers' synthesis of viroallosecurinine: key step for generation of 1,2-amino oxygenated stereocenters.....	61
Scheme 1.55	Key steps of Kerr and coworkers' synthesis of allosecurinine .....	62
Scheme 1.56	Key steps of Busqué, de March, and coworkers' synthesis of viroallosecurinine and allosecurinine .....	63
Scheme 1.57	Retrosynthesis of viroallosecurinine using the intermolecular metallonitrene/alkyne cascade .....	64
Scheme 1.58	Synthesis of racemic chiral vinyl silane <b>151</b> .....	66
Scheme 1.59	Intermolecular metallonitrene/alkyne cascade with chiral vinyl silane <b>151</b> to form oxathiazepine <b>156</b> .....	67
Scheme 1.60	Retrosynthetic analysis of viroallosecurinine core <b>157</b> .....	67
Scheme 1.61	Intermolecular cascade reaction with sulfamate ester <b>144</b> and enantiomerically enriched benzyl ether <b>123</b> .....	69
Scheme 1.62	Viroallosecurinine core ring system synthesis.....	70

## Chapter 2:

Scheme 2.1	General scheme for the ideal intramolecular (top) and intermolecular (bottom) C–H amination.....	104
Scheme 2.2	Copper powder catalyzed C–H amination and aziridination of cyclohexene ( <b>2</b> ) with benzenesulfonyl azide ( <b>1</b> ) .....	107

Scheme 2.3	Cobalt(II) tetraphenyl porphyrin (Co(TPP)) catalyzed C–H amination with sulfonyl azide <b>7</b> .....	107
Scheme 2.4	C–H amination with sulfamoyl azides ( <b>9</b> ) using [Co(3,5-DitBu-IbuPhyrin)] <b>8</b> .....	108
Scheme 2.5	Intramolecular allylic C–H amination with sulfamoyl azide <b>10</b> to form sulfamide <b>11</b> using [Co(3,5-DitBu-IbuPhyrin)] .....	109
Scheme 2.6	Directed intermolecular arene C–H amidation with sulfonyl azide <b>14</b> and aryl azide <b>15</b> .....	109
Scheme 2.7	Intermolecular sp <sup>3</sup> C–H amidation with sulfonyl azide <b>14</b> .....	110
Scheme 2.8	Intermolecular C–H amidation of arene <b>17</b> with acyl azide <b>16</b> using [IrCp*Cl <sub>2</sub> ] <sub>2</sub> .....	110
Scheme 2.9	Rh <sub>2</sub> (O <sub>2</sub> CC <sub>3</sub> F <sub>7</sub> ) <sub>4</sub> catalyzed intramolecular aryl C–H amination with vinyl azide <b>18</b> .....	111
Scheme 2.10	Rh <sub>2</sub> (O <sub>2</sub> CC <sub>3</sub> F <sub>7</sub> ) <sub>4</sub> catalyzed intramolecular vinyl C–H amination with aryl azide <b>19</b> .....	112
Scheme 2.11	[(cod)Ir(OMe)] <sub>2</sub> catalyzed intramolecular benzylic C–H amination with aryl azide <b>20</b> to form indoline <b>21</b> and indole <b>22</b> .....	112
Scheme 2.12	Rh <sub>2</sub> (esp) <sub>2</sub> catalyzed intramolecular amination of unactivated, aliphatic C–H bonds with aryl azides ( <b>23</b> ) to give indolines ( <b>24</b> ) .....	113
Scheme 2.13	Iron-dipyrrinato catalyzed intramolecular amination of aliphatic sp <sup>3</sup> C–H bonds with alkyl azides ( <b>25</b> ) to form pyrrolidines ( <b>26</b> ) .....	114
Scheme 2.14	[RhCp*Cl <sub>2</sub> ] <sub>2</sub> catalyzed intermolecular amination of aryl sp <sup>2</sup> C–H bonds of arene <b>27</b> with alkyl azide <b>28</b> .....	114

Scheme 2.15	Iron-porphyrin catalyzed intramolecular benzylic C–H amination with aryl azide <b>29</b> .....	116
Scheme 2.16	Intermolecular benzylic C–H insertion with 1-adamantylazide ( <b>30</b> ).....	116
Scheme 2.17.	Iridium-salen <b>33</b> catalyzed intramolecular enantioselective benzylic intramolecular C–H amination with aryl sulfonyl azide <b>31</b> to form sultam <b>32</b> .....	117
Scheme 2.18.	Ruthenium-salen <b>34</b> catalyzed intermolecular enantioselective benzylic and allylic intermolecular C–H amination with 2-(trimethylsilyl)ethanesulfonyl azide ( <b>35</b> ) .....	118
Scheme 2.19	P411 catalyzed enantioselective intramolecular C–H amination with sulfonyl azide <b>36</b> .....	118
Scheme 2.20	Synthetic route to quinoline-oxazoline amide ligand <b>39</b> for electronic turning of the quinoline fragment .....	125
Scheme 2.21	Synthetic route to quinoline-oxazoline amide ligand <b>39</b> for steric turning of the oxazoline fragment. ....	126
Scheme 2.22	Synthesis of Cbz-protected oxazoline <b>51</b> .....	127
Scheme 2.23	Oxazoline <b>54</b> synthesis and deprotection.....	128
Scheme 2.24	Proline-oxazoline amide ligand <b>55</b> synthesis under Mitsunobu conditions.....	129
Scheme 2.25	Benzyl-substituted quinoline-oxazoline amide ligand <b>61</b> synthesis .....	129
Scheme 2.26	Synthesis of isobutyl-substituted quinoline amide <b>63</b> .....	130
Scheme 2.27	Synthesis of diastereomeric quinoline-oxazoline amide ligands <b>64</b> and <b>65</b> .....	131

Scheme 2.28	Synthesis of isopropyl-substituted quinoline-oxazoline amide ligand <b>68</b> .....	131
Scheme 2.29	Alternate oxazoline-forming reaction for synthesis of bis(oxazoline) <b>71</b> .....	132
Scheme 2.30	Cyclization of amide <b>69</b> with catalytic DMAP to yield quinoline-oxazoline amide <b>68</b> .....	132
Scheme 2.31	Synthesis of benzyl-substituted quinoline-oxazoline amide ligand <b>72</b> ....	133
Scheme 2.32	Synthesis of <i>tert</i> -butyl-substituted quinoline-oxazoline amide ligand <b>76</b> .....	134
Scheme 2.33	Synthesis of methoxy-substituted quinoline-oxazoline amide ligand <b>80</b> .....	134
Scheme 2.34	Planned synthesis of <i>gem</i> -dimethyl-substituted quinoline-oxazoline amide ligand <b>84</b> .....	135
Scheme 2.35	Attempted metalation of quinoline-oxazoline amide ligand <b>72</b> with IrCl <sub>3</sub> •3H <sub>2</sub> O and NaHCO <sub>3</sub> at room temperature to 45 ° C .....	136
Scheme 2.36	Cobalt(II) metalation of HN( <i>o</i> -PhNHC(O) <sup><i>t</i></sup> Pr) <sub>2</sub> ligand ( <b>86</b> ) to form cobalt(II) complex <b>85</b> .....	137
Scheme 2.37	Formation of ligand-potassium salt <b>87</b> from quinoline-oxazoline amide <b>72</b> .....	137
Scheme 2.38	Metalation of quinoline-oxazoline ligand <b>72</b> with IrCl <sub>3</sub> to form iridium(III) complex <b>88</b> (tentatively characterized by mass spectrometry) .....	139

Scheme 2.39	Metalation of quinoline-oxazoline ligand <b>72</b> with IrBr <sub>3</sub> •4H <sub>2</sub> O to form iridium(III) complex <b>89</b> (tentatively characterized by mass spectrometry) .....	139
Scheme 2.40	Metalation of quinoline-oxazoline ligand <b>72</b> with CoCl <sub>2</sub> to form cobalt(II) complexes <b>90</b> , <b>91</b> , and <b>92</b> (tentatively characterized by mass spectrometry) .....	140
Scheme 2.41	Metalation of quinoline-oxazoline ligand <b>72</b> with RhCl <sub>3</sub> and crystallization from acetonitrile and diethyl ether to yield rhodium(III) complex <b>93</b> .....	141
Scheme 2.42	Tejel and coworkers' metalation of amide ligand <b>94</b> with [(cod)Ir(OMe)] <sub>2</sub> to form iridium(I) complex <b>95</b> .....	143
Scheme 2.43	Metallation of quinoline-oxazoline amide ligand <b>72</b> to form iridium(I) complex <b>96</b> and proposed oxidation to iridium(III) complex <b>97</b> .....	143
Scheme 2.44	Metallation of quinoline-oxazoline amide ligand <b>76</b> to form iridium(I) complex <b>98</b> .....	144
Scheme 2.45	Metallation of quinoline-oxazoline amide ligand <b>80</b> to form iridium(I) complex <b>99</b> .....	145
Scheme 2.46	Driver and coworkers' iridium(I) catalyzed benzylic C–H amination with aryl azide <b>20</b> to form indoline <b>21</b> , indole <b>22</b> and aniline <b>100</b> .....	146
Scheme 2.47	Synthesis of aryl azide <b>20</b> .....	146
Scheme 2.48	Iridium(III) phebox <b>104</b> catalyzed enantioselective amination with aryl azide <b>20</b> to form indoline <b>21</b> and indole <b>22</b> .....	149
Scheme 2.49	Synthesis of <sup>i</sup> Bu- and Me-substituted iridium(III) phebox complexes <b>105</b> and <b>106</b> .....	156

Scheme 2.50	Examination of aryl azide <b>113</b> for unactivated primary sp <sup>3</sup> C–H insertion with iridium(III) phebox <b>114</b> .....	158
Scheme 2.51	Synthesis of methoxy- and trifluoromethyl-substituted aryl azides <b>121</b> , <b>122</b> , and <b>123</b> .....	162
Scheme 2.52	Synthesis of trifluoromethyl-substituted aryl azide <b>124</b> .....	162
Scheme 2.53	Optimized synthesis of azide <b>127</b> by Sonogashira coupling .....	163
Scheme 2.54	Synthesis of azide <b>130</b> by Sonogashira reaction.....	164
Scheme 2.55	Synthesis of pyridinyl azide <b>133</b> .....	164
Scheme 2.56	Failed Sonogashira coupling with 2-ethynyl-pyridine ( <b>136</b> ) and 2-bromoaniline ( <b>128</b> ) in the synthesis of 2-pyridinyl azide <b>135</b> .....	165
Scheme 2.57	Sonogashira coupling with 2-ethynyl-pyridine ( <b>136</b> ) and 2-bromobenzaldehyde ( <b>138</b> ).....	165
Scheme 2.58	Failed Sonogashira coupling with 2-ethynyl-pyridine ( <b>136</b> ).....	166
Scheme 2.59	Synthesis of 3-thiophenyl azide <b>139</b> .....	167
Scheme 2.60	Synthesis of indolyl azide <b>140</b> .....	168
Scheme 2.61	Synthesis of azide <b>145</b> .....	169
Scheme 2.62	Synthesis of alkyne <b>150</b> and use toward azide <b>149</b> .....	170
Scheme 2.63	Synthesis of <i>ortho</i> -homoallylic aryl azide <b>153</b> .....	171
Scheme 2.64	Synthesis of alkyl azide <b>157</b> for intramolecular benzylic C–H amination .....	171
Scheme 2.65	Synthesis of <i>ortho</i> -alkyl azides <b>158</b> and <b>159</b> .....	172
Scheme 2.66	Synthesis of mesityl azide ( <b>162</b> ).....	172
Scheme 2.67	Failed synthesis of deuterated azide <b>164</b> .....	173



Scheme 2.68 Synthesis of deuterated aryl azide **165** via reduction of styryl azide **166**.....174

Scheme 2.69 Kinetic isotope effect experiment with aryl azide **165** .....177

### Chapter 3:

Scheme 3.1 Calculated energy barriers for Rh<sub>2</sub>(OAc)<sub>4</sub> catalyzed C–H insertion of methyl diazoacetate (**7**) and methyl phenyldiazoacetate (**8**) into cyclopentane (**6**).....246

Scheme 3.2 Competitive β-hydride elimination of alkyl diazoacetates (**9**) to give alkenes (**10**).....247

Scheme 3.3 Rh<sub>2</sub>(*S*-NTTL)<sub>4</sub> (**11**) catalyzed enantioselective C–H insertion of α-alkyl-α-diazoester **13** with indole **12**.....248

Scheme 3.4 Proposed mechanism of Rh<sub>2</sub>(*S*-NTTL)<sub>4</sub> (**11**) catalyzed enantioselective C–H insertion of alkyl metallocarbene **14** with indole **12** .....249

Scheme 3.5 Rh<sub>2</sub>(*S*-PTTEA)<sub>4</sub> (**20**) catalyzed enantioselective C–H insertion of α-diazopropionate **18** with 2,3-unsubstituted indole **19** .....249

Scheme 3.6 Iridium-salen **21** and **22** catalyzed enantioselective C–H insertion of alkyl diazoacetates **23** and **24** into tetrahydrofuran (**4**) and 1,4-cyclohexadiene (**25**).....251

Scheme 3.7 Tp<sup>Ms</sup>Cu **26** Catalyzed racemic C–H functionalization with ethyl diazoacetate (**27**) into tetrahydrofuran (**4**) and tetrahydropyran (**28**) .....252

Scheme 3.8	Ruthenium pybox <b>29</b> catalyzed enantioselective cyclopropanation of styrene ( <b>30</b> ) with ethyl diazoacetate ( <b>27</b> ).....	253
Scheme 3.9	Iridium(III) phebox <b>31</b> and rhodium(III) phebox <b>35</b> catalyzed conjugate reduction and asymmetric reductive aldol reaction .....	254
Scheme 3.10	Iridium(III) phebox <b>36</b> catalyzed borylation of arenes .....	255
Scheme 3.11	Platinum(II) phebim <b>39</b> catalyzed asymmetric Friedel-Crafts alkylation of indole <b>40</b> with nitroalkene <b>41</b> .....	256
Scheme 3.12	Palladium(II) phebim <b>42</b> catalyzed enantioselective aza-Morita-Baylis-Hillman reaction of imine <b>43</b> with nitrile <b>44</b> .....	257
Scheme 3.13	Rhodium(III) phebim <b>45</b> and <b>46</b> catalyzed allylation of aldehyde <b>47</b> and carbonyl-ene reaction.....	258
Scheme 3.14	Iridium(III) phebox <b>52</b> catalyzed enantioselective C–H functionalization of 1,4-cyclohexadiene ( <b>25</b> ) with methyl phenyldiazoacetate ( <b>8</b> ).....	259
Scheme 3.15	Iridium(III) phebox <b>56</b> catalyzed enantioselective insertion of ethyl diazoacetate ( <b>27</b> ) into tetrahydrofuran ( <b>4</b> ) to give insertion product <b>57</b> .....	261
Scheme 3.16	Iridium(III) phebox <b>56</b> catalyzed enantioselective insertion of ethyl diazoacetate ( <b>27</b> ) into phthalan ( <b>58</b> ) .....	262
Scheme 3.17	Synthesis of iridium(III) phebim complexes <b>59-62</b> .....	265
Scheme 3.18	CH <sub>2</sub> - <sup>t</sup> Bu-substituted iridium(III) phebim <b>68</b> catalyzed C–H insertion with ethyl diazoacetate ( <b>27</b> ) .....	267
Scheme 3.19	Synthesis of methyl diazoacetate ( <b>7</b> ) .....	268

Scheme 3.20	Iridium(III) phebim <b>61</b> and <b>62</b> catalyzed C–H insertion with phthalan ( <b>58</b> ) and methyl diazoacetate ( <b>7</b> ).....	268
Scheme 3.21	Iridium(III) phebim <b>61</b> and <b>62</b> catalyzed C–H insertion with phthalan ( <b>58</b> ) and 2,2,2-trichloroethyl diazoacetate ( <b>69</b> ) at 0.5 mol % catalyst loading .....	269
Scheme 3.22	Iridium(III) phebim <b>61</b> and <b>62</b> catalyzed C–H insertion with phthalan ( <b>58</b> ) and 2,2,2-trichloroethyl diazoacetate ( <b>69</b> ) at 2 mol % catalyst loading .....	269
Scheme 3.23	Synthesis of 3-nitro-substituted phthalan <b>71</b> .....	271
Scheme 3.24	Unsuccessful syntheses of phthalan derivatives .....	272
Scheme 3.25	Arene C–H borylation of phthalan ( <b>58</b> ) to afford phthalan derivatives <b>76</b> and <b>77</b> .....	273
Scheme 3.26	Improved arene C–H borylation of phthalan ( <b>58</b> ) to afford phthalan derivative <b>76</b> .....	273
Scheme 3.27	Arene C–H borylation of phthalan ( <b>58</b> ) with 4,4'-di-tert-butyl-2,2'-dipyridyl ligand ( <b>78</b> ) to afford phthalan derivative <b>76</b> .....	274
Scheme 3.28	Synthesis of 3-methoxy phthalan ( <b>80</b> ) .....	274
Scheme 3.29	Bromination of pinacol boronate <b>76</b> to yield 3-bromo-phthalan ( <b>81</b> ).....	274
Scheme 3.30	Suzuki-Miyaura cross-coupling of pinacol boronate <b>76</b> and phenyl iodide to yield 3-phenyl-phthalan ( <b>82</b> ) .....	275
Scheme 3.31	Synthesis of 2-methyl-phthalan ( <b>83</b> ) by TBAF-promoted cyclization of alcohol <b>85</b> .....	276

Scheme 3.32	Derivatization of insertion product <b>100</b> to form 3,5 dinitrobenzoate <b>101</b> .....	281
Scheme 3.33	Kinetic isotope effect for ethyl diazoacetate ( <b>27</b> ) insertion into tetrahydrofuran ( <b>4</b> ).....	283

## List of Figures

### Chapter 1:

Figure 1.1	Nitrene and metallonitrene representations .....	4
Figure 1.2	Metallonitrene precursor classes.....	5
Figure 1.3	Complex products formed from metallonitrene cascades.....	6
Figure 1.4	Mechanistic hypotheses for the aryl C–H amination of aryl azides ( <b>4</b> ) to form carbazoles ( <b>5</b> ) .....	7
Figure 1.5	MO diagram for the [3+2] annulation of a homoallenyl sulfamate ester <b>48</b> and benzaldehyde ( <b>49</b> ) to form trisubstituted tetrahydrofuran <b>50</b> .....	20
Figure 1.6	Metallonitrene/alkyne cascade concept development.....	27
Figure 1.7	Continuum of metallonitrene/alkyne cascade intermediates .....	29
Figure 1.8	Literature precedent for [2,3]-Wittig rearrangement of terminal alkynes (top) compared with stereochemical models for poor diastereoselectivity observed in metallonitrene/alkyne cascade reaction (bottom).....	46
Figure 1.9	Literature precedent for [2,3]-Wittig rearrangement of enantiomerically enriched allyl ether <b>127</b> (top) with stereochemical models for metallonitrene/alkyne cascade reaction .....	55
Figure 1.10	Comparison of reduced metallonitrene/alkyne cascade product with viroallosecurinine.....	59
Figure 1.11	Representative members of the <i>Securinega</i> alkaloids .....	60
Figure 1.12	Three-dimensional representation of amine <b>147</b> for selective oxidation .....	65
Figure 1.13	NOE correlations of ring-closed product <b>159</b> .....	70

## Chapter 2:

Figure 2.1	Representative oxazoline ligand classes. ....	120
Figure 2.2	Enantioselective ketone propargylation with proline-oxazoline ligand <b>37</b> for mathematical modeling .....	121
Figure 2.3	Enantioselective ketone propargylation with quinoline-proline ligand <b>38</b> for mathematical modeling .....	122
Figure 2.4	Comparison of proposed quinoline-oxazoline amide ligand structure <b>39</b> with inspiration ligands.....	123
Figure 2.5	Proposed iridium(I) and iridium(III) quinoline-oxazoline amide complexes <b>40</b> and <b>41</b> .....	124
Figure 2.6	Possible coordination modes for rhodium(III) quinoline-oxazoline amide complex <b>93</b> .....	141
Figure 2.7	Crystal structure of rhodium(III) quinoline-oxazoline amide complex <b>93</b> .....	142
Figure 2.8	Comparison of iridium(III) phebox and iridium(III) phebim complexes .....	149
Figure 2.9	Iridium(III) indanyl phebox <b>112</b> structure, synthesized by Dr. Andrew Schafer .....	157
Figure 2.10	Dinuclear cobalt(II) complexes with redox active NH( <i>o</i> -PhNHC(O) <sup><i>i</i></sup> Pr) <sub>2</sub> ligand scaffold .....	161
Figure 2.11	<sup>1</sup> H NMR spectra for <b>A</b> ) deuterated azide <b>165</b> , <b>B</b> ) indoline product <b>21</b> , <b>C</b> ) aniline precursor <b>169</b> and azide <b>165</b> , and <b>D</b> ) reaction mixture of indoline products <b>180-D</b> and <b>180-H</b> .....	178

### Chapter 3:

Figure 3.1	Metallo-carbene C–H functionalization mechanism.....	245
Figure 3.2	Phebim <b>37</b> and phebox <b>38</b> ligand frameworks.....	255
Figure 3.3	Calculated pro- <i>R</i> and pro- <i>S</i> transition states of ethyl diazoacetate ( <b>27</b> ) insertion into tetrahydrofuran (top) and phthalan (bottom) with Ir(III)-phebox <b>56</b> .....	262
Figure 3.4	Crystal structure of 4-methoxy-phenyl diazoacetate insertion product <b>102</b> .....	282
Figure 3.5	<sup>1</sup> H NMR spectra for determination of kinetic isotope effect: A) <sup>1</sup> H NMR spectrum of <b>104-H</b> ; B) <sup>1</sup> H NMR spectrum of kinetic isotope effect experiment.....	284

## List of Tables

### Chapter 1:

Table 1.1	Substrate scope for metallonitrene/allene cascade for synthesis of aminocyclopropanes .....	16
Table 1.2	Substrate scope of [3+3] annulation of 2-amidoallylcations and substituted nitrones <b>51</b> .....	21
Table 1.3	Allenic carbamate one-pot synthesis of <i>N,N</i> -spiroaminals .....	25
Table 1.4	Initial substrate scope of the intermolecular metallonitrene/alkyne cascade reaction to yield imines <b>100</b> .....	39
Table 1.5	Reported inverse temperature dependence of diastereoselectivity of Grignard addition to imine <b>101</b> .....	40
Table 1.6	Intermolecular cascade reaction GC optimization of the metallonitrene/alkyne cascade with sulfamate ester <b>109</b> and methyl allyl ether to give imine <b>110</b> .....	43
Table 1.7	Synthesis of vinyl silanes <b>116</b> and <b>115</b> .....	48
Table 1.8	Intermolecular metallonitrene/alkyne cascade optimization with vinyl silanes <b>115</b> and <b>116</b> and sulfamate <b>109</b> .....	49
Table 1.9	Synthesis of chiral allyl ether <b>120</b> .....	50
Table 1.10	Temperature dependence of diastereoselectivity of Grignard addition to imine <b>101</b> .....	57
Table 1.11	Optimization of intermolecular metallonitrene/alkyne cascade with sulfamate ester <b>144</b> .....	69



## Chapter 2:

Table 2.1	Summary of ideality in C–H amination methodology .....	105
Table 2.2	Cbz Deprotection attempts of oxazoline <b>51</b> .....	127
Table 2.3	Metalation conditions for quinoline-oxazoline ligand <b>72</b> to form iridium(III) complex <b>88</b> (tentatively characterized by mass spectrometry) .....	138
Table 2.4	Iridium(I) quinoline-oxazoline amide catalyst optimization for benzylic C–H amination with aryl azide <b>20</b> .....	147
Table 2.5	Optimization of iridium(III) phehim R <sup>2</sup> substitution for enantioselective C–H amination with aryl azide <b>20</b> .....	150
Table 2.6	Optimization of iridium(III) phehim R <sup>1</sup> substitution for enantioselective C–H amination with aryl azide <b>20</b> .....	151
Table 2.7	Optimization of iridium(III) phehim ancillary ligand for enantioselective C–H amination with aryl azide <b>20</b> .....	151
Table 2.8	Optimization of iridium(III) phehim reaction temperature for enantioselective C–H amination with aryl azide <b>20</b> .....	152
Table 2.9	Optimization of iridium(III) phebox and phehim R <sup>1</sup> -substitution for enantioselective C–H amination with aryl azide <b>20</b> .....	153
Table 2.10	Optimization of iridium(III) phebox backbone substitution for enantioselective C–H amination with aryl azide <b>20</b> .....	153
Table 2.11	Solvent optimization for iridium(III) phebox catalyzed enantioselective C–H amination with aryl azide <b>20</b> .....	154

Table 2.12	Control reactions for iridium(III) phebox catalyzed enantioselective C–H amination with aryl azide <b>20</b> .....	155
Table 2.13	Study of iridium(III) phebox R <sup>1</sup> substitution for enantioselective C–H amination with aryl azide <b>20</b> .....	156
Table 2.14	Preliminary optimization of iridium(III) phebox <b>104</b> catalyzed enantioselective benzylic C–H amination with sulfamate ester <b>115</b> .....	158
Table 2.15	Optimization of iridium(III) phebox and phebim catalyzed enantioselective C–H amination with sulfamate ester <b>116</b> .....	159
Table 2.16	Optimization of intramolecular benzylic C–H amination with <i>ortho</i> -homobenzyl aryl azide <b>20</b> .....	175
Table 2.17	Substrate scope of cobalt(II) catalyzed C–H amination with aryl azides .....	176
Table S2.1.	Optimization of iridium(III) phebox and phebim catalyzed enantioselective C–H amination with aryl azide <b>20</b> .....	214
Table S2.2	Crystal data and structure refinement for <b>93</b> .....	235
 <b>Chapter 3:</b>		
Table 3.1	Iridium(III) phebox <b>52</b> catalyzed enantioselective C–H functionalization of cyclohexadiene derivatives ( <b>54</b> ) with methyl phenyldiazoacetates ( <b>55</b> ).....	260
Table 3.2	Catalyst optimization of enantioselective ethyl diazoacetate ( <b>27</b> ) insertion into phthalan ( <b>58</b> ).....	264

Table 3.3	Additional catalyst optimization of enantioselective ethyl diazoacetate (27) insertion into phthalan (58).....	266
Table 3.4	Diazoacetate scope for C–H insertion into phthalan with iridium(III) phebim complexes 61 and 62.....	270
Table 3.5	Phthalan derivative substrate scope of iridium(III) phebim 62 catalyzed enantioselective C–H functionalization with ethyl diazoacetate (27).....	277
Table 3.6	Phthalan 2,5-dihydrofuran derivative substrate scope of iridium(III) phebim 62 catalyzed enantioselective C–H functionalization with ethyl diazoacetate (27) by Dr. Clay Owens and Dr. Andrew Schafer.....	278
Table 3.7	Optimization of iridium(III) phebim- and phebox-catalyzed acceptor-only C–H functionalization of tetrahydrofuran (4) with ethyl diazoacetate (27).....	279
Table 3.8	Optimization of iridium(III) phebim-catalyzed kinetic resolution of 2-methyl-phthalan (83) with ethyl diazoacetate (27).....	280
Table S3.1	Structural refinement data for (R)-4-methoxyphenyl 2-(1,3-dihydroisobenzofuran-1-yl)acetate (102).....	323

## Abbreviations

Ac	acetyl
AcOH	acetic acid
Boc	<i>tert</i> -butoxycarbonyl
Bn	benzyl
br	broad
<i>n</i> -BuLi	<i>n</i> -butyllithium
Cbz	benzyloxycarbonyl
cod	cyclooctadiene
d	doublet
DABCO	1,4-diazabicyclo[2.2.2]octane
DCE	1,2-dichloroethane
DCM	dichloromethane
DDQ	2,3-dichloro-5,6-dicyano-1,4-benzoquinone
DIAD	diisopropyl azodicarboxylate
DIBAL	diisobutylaluminum hydride
DMAP	<i>N, N</i> -dimethylaminopyridine
DME	1, 2-dimethoxyethane
DMF	<i>N, N</i> -dimethylformamide
DMPU	<i>N, N'</i> -dimethyl- <i>N, N'</i> -propylene urea
DMSO	dimethylsulfoxide
ee	enantiomeric excess

equiv	equivalent
ESI	electrospray ionization
EtOAc	ethyl acetate
HMPA	hexamethylphosphoric triamide
HRMS	high resolution mass spectroscopy
KHMDS	potassium <i>bis</i> (trimethylsilyl)amide
LAH	lithium aluminum hydride
LDA	lithium diisopropylamide
LiHMDS	lithium <i>bis</i> (trimethylsilyl)amide
LG	leaving group
m	multiplet
MG	migrating group
mmol	millimole
MOM	methoxymethyl ether
NMR	nuclear magnetic resonance
Ns	4-nitrobenzenesulfonyl
OMe	methoxy
OPiv	pivaloate
Ph	phenyl
phebim	bis(imidazoliny)phenyl
phebox	bis(oxazoliny)phenyl
ppm	parts per million
pybox	bis(oxazoliny)pyridine

q	quartet
quint	quintet
Rh <sub>2</sub> (esp) <sub>2</sub>	bis[rhodium( $\alpha,\alpha,\alpha',\alpha'$ -tetramethyl-1,3-benzenedipropionic acid)]
Rh <sub>2</sub> ( <i>S</i> -NTTL) <sub>4</sub>	dirhodium(II) tetrakis[ <i>N</i> -1,8-naphthaloyl-( <i>S</i> )- <i>tert</i> -leucinate]
Rh <sub>2</sub> (OAc) <sub>4</sub>	dirhodium(II) tetraacetate
Rh <sub>2</sub> ( <i>S</i> -PTTL) <sub>4</sub>	dirhodium(II) tetrakis[ <i>N</i> -phthaloyl-( <i>S</i> )- <i>tert</i> -leucinate]
Rh <sub>2</sub> (TPA) <sub>4</sub>	tetrakis(triphenylacetato)dirhodium(II)
RT	room temperature
s	singlet
t	triplet
TBAF	tetrabutylammonium fluoride hydrate
TBDMS	<i>tert</i> -butyldimethylsilyl
TBDPS	<i>tert</i> -butyldiphenylsilyl
Tf	trifluoromethanesulfonyl
TFA	trifluoroacetic acid
TFAA	trifluoroacetic anhydride
tfacam	trifluoroacetamide
TFT	trifluorotoluene
THF	tetrahydrofuran
TMS	trimethylsilyl
Ts	<i>para</i> -toluenesulfonyl
w	weak

**Chapter 1. Intermolecular Cascade Reactions Through Alkyne  
Oxidative Amination with Metallonitrenes**

## 1.1 Introduction to Metallonitrene Cascade Reactions

### 1.1.1 Background of Cascade Reactions

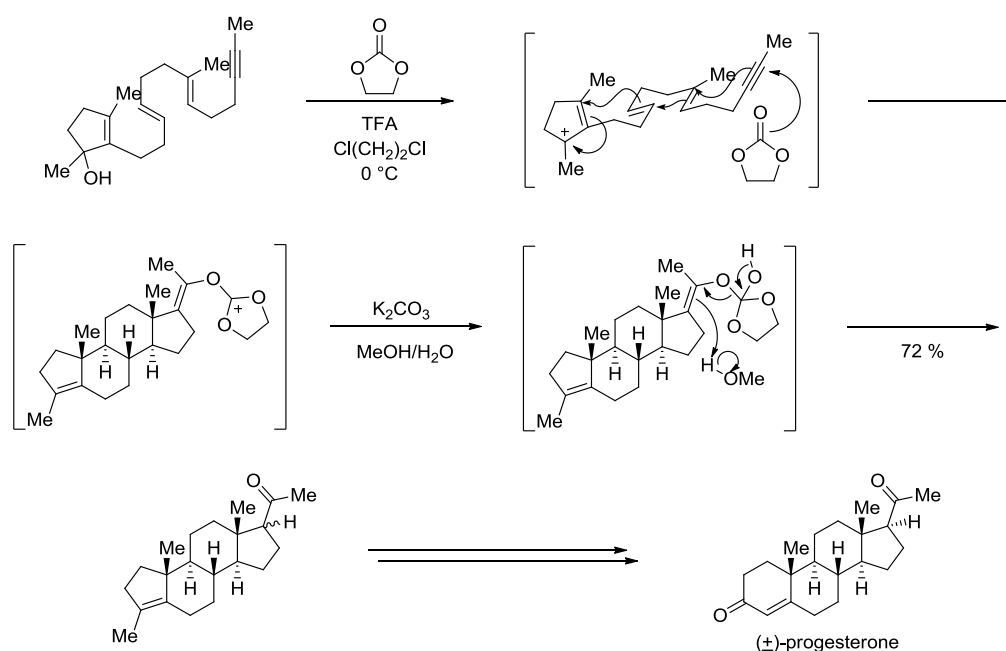
In recent years, cascade reactions have grown in recognition for the elegant routes to complex molecules they can provide.<sup>1</sup> Nicolaou defines cascade reactions as “sequences of chemical transformations in which the starting substrate is designed so as to (or happens to) undergo a reaction whose product becomes the substrate for the next step, whose product again becomes the substrate for the next step, and so on, until a product stable to the reaction conditions is reached.”<sup>2</sup> Cascade reactions are notoriously difficult to classify, and the strictest definition of a cascade reaction does not allow reaction conditions to be altered at any point in the process. However, under a more liberal definition, many reactions that fall under the heading of cascade reactions include addition of additional reagents at various points in the reaction, so long as the reaction sequence occurs in “one pot.”<sup>3</sup>

Cascade reactions, also known as “domino reactions,” have been used to great effect in numerous examples of total synthesis.<sup>4</sup> Cascade reactions provide a number of practical benefits, often falling under the umbrella of green chemistry. These methodologies can improve atom economy, save time and labor spent on purification and performing multiple separate reactions in succession, and generate less waste. They also bring benefits to the art of total synthesis, by enhancing the aesthetic appeal of a synthesis through a single complex transformation, instead of a series of manipulations. Cascades may also permit transformations that would not be possible through a series of reactions,



by employing intermediates that would not be isolable. While many impressive examples have been disclosed within the past ten to twenty years,<sup>5-7</sup> one notable historical example involves a cationic polyolefin cyclization cascade in Johnson's classic synthesis of progesterone (Scheme 1.1).<sup>8,9</sup>

**Scheme 1.1.** Johnson's classic synthesis of progesterone through a cationic polyolefin cyclization cascade reaction.<sup>8,9</sup>



### 1.1.2 Generation of Metallonitrenes

As highly reactive species, metallonitrenes are attractive intermediates for use in cascade reactions. A nitrene is defined as a neutral nitrogen species with six valence electrons.<sup>10</sup> These species are highly electrophilic, analogous to carbenes, and may exist in a singlet (**1**) or triplet (**2**) state, each featuring distinct reactivity modes (Figure 1.1). A

destabilized nitrene often favors the triplet state. However, when a transition metal catalyst stabilizes the nitrene species, it most often acts as an electrophile, providing metallonitrene **3** in the singlet state.

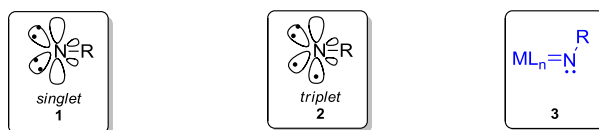


**Figure 1.1.** Nitrene and metallonitrene representations.

Metallonitrenes may be generated from a number of different precursors. These precursors fall into two general categories: those that require addition of an external oxidant to achieve the metallonitrene oxidation state (Box A, Figure 1.2) and those that are initially in the appropriate oxidation state for formation of the nitrene (Box B, Figure 1.2). Carbamates, sulfamates, sulfamides, sulfonamides, and ureas/guanidines are examples of nitrene precursors that require addition of a hypervalent iodine oxidant to form an iminoiodinane, which may then interact with the catalyst to form a metallonitrene.<sup>11,12</sup> *N*-Tosyloxycarbamates and azides are used as pre-oxidized metallonitrene precursors, without the requirement of addition of an oxidant, most commonly a hypervalent iodine oxidant. In the case of *N*-tosyloxycarbamates, addition of a base (e.g.,  $K_2CO_3$ ) induces formation of metallonitrene in the necessary oxidation state.<sup>13</sup> With azides, release of  $N_2$  gas upon interaction with the catalyst provides the metallonitrene (see Chapter 2).

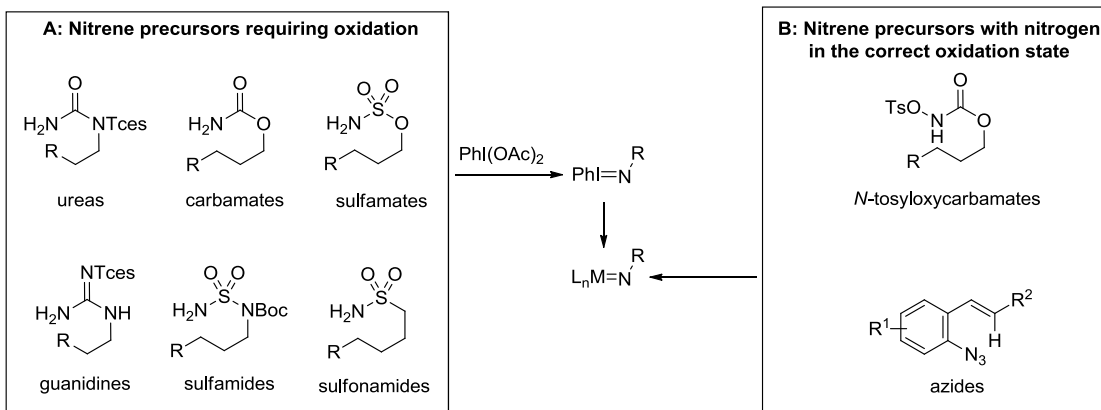


**Figure 1.2.** Metallonitrene precursor classes.

Most transformations with metallonitrenes fall into the classifications of C-H amination and aziridination. Most early examples of metallonitrene C-H amination focused on insertion into benzylic C-H bonds, but more recently the substrate scope has been expanded to aryl, vinyl, and even unactivated tertiary, secondary, and primary  $sp^3$  C-H bonds.<sup>14</sup> Though many different ligand structures and metal centers catalyze C-H amination, dirhodium tetracarboxylates have been particularly effective for amination.<sup>15,16</sup> Aziridination through nitrene transfer to olefins has also been extensively studied.<sup>17</sup> Copper catalysts have been very effective in this area, beginning with copper powder by Kwart and Khan<sup>18,19</sup> and extending to copper complexes with bis(oxazoline) ligands by Evans<sup>20</sup> and Jacobsen.<sup>21</sup> However, metallonitrene chemistry is not bound by these two classes, and metallonitrenes can also be used to initiate complex cascade reactions.

### 1.1.3 Metallonitrene Cascade Reactions

Many different metallonitrene cascade reactions have been discovered to generate complex functionality in a single transformation. Often, cascades begin with a C–H amination or aziridination step, which is then intercepted with some kind of trapping agent and/or rearrangement. This initiates a sequence of new bond formations in one pot. For convenience, we have categorized the cascade reactions by the type of  $\pi$  system interacting with the metallonitrene: alkenes, allenes, and alkynes. Many of these reactions form products with an array of contiguous stereocenters in high selectivity, providing facile routes to complex molecules, such as those shown in Figure 1.3.

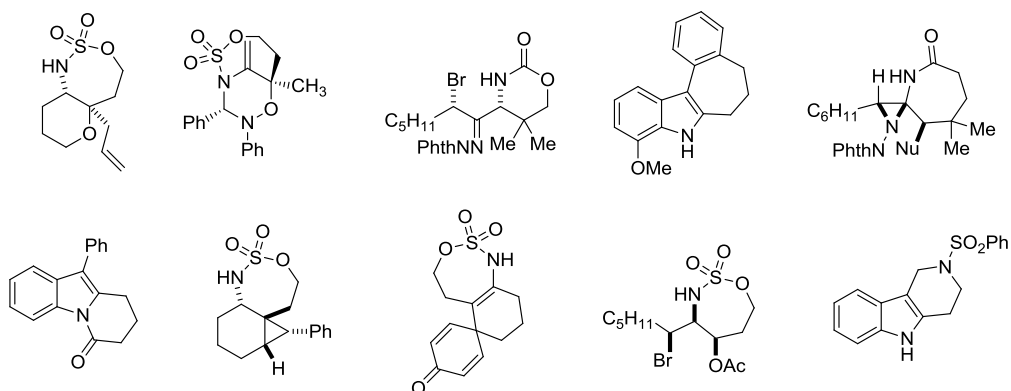


**Figure 1.3.** Complex products formed from metallonitrene cascades.

#### 1.1.3.1 Metallonitrene/Alkene Cascade Reactions

##### 1.1.3.1.1 Azide-Initiated Metallonitrene/Alkene Cascade Reactions

Early examples of metallonitrene/alkene cascades evolved from Driver and coworkers' studies of aryl and vinyl C–H amination using vinyl and aryl azides (**4**) to

form indoles, pyrroles, and carbazoles (Figure 1.4, **5**).<sup>22-24</sup> From a mechanistic study of C–H insertion with biaryl azides to form carbazoles, Driver and coworkers observed evidence of distinct metallonitrene intermediate **6** formed prior to breaking the C–H bond.<sup>25</sup> As the reaction is not believed to be concerted, it was theorized that without the presence of a functionalizable C–H bond, the metallonitrene intermediate could be intercepted for cascade reactions.

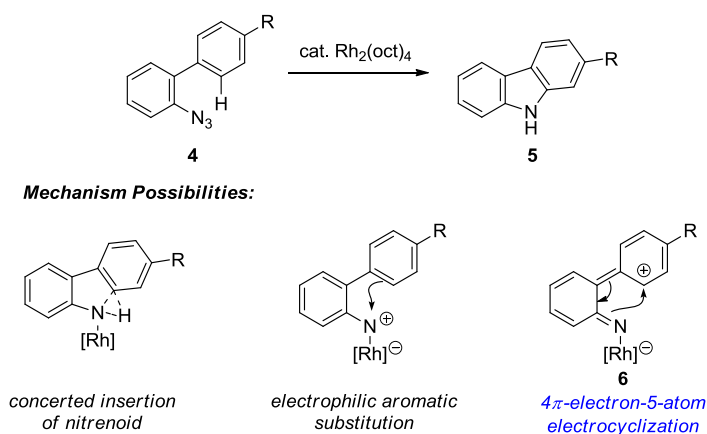
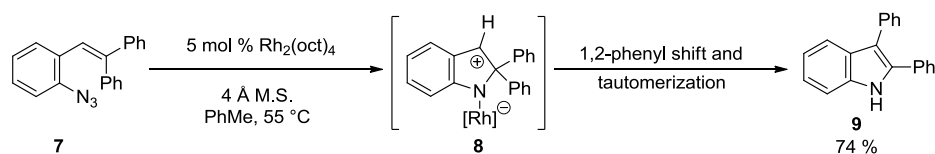


**Figure 1.4.** Mechanistic hypotheses for the aryl C–H amination of aryl azides (**4**) to form carbazoles (**5**).<sup>25</sup>

In a preliminary reaction during C–H amination studies, it was found that with gem-diphenyl-substituted aryl azide **7**, generation of a metallonitrene initiated a migratory process.<sup>24</sup> The alkene attacks the electrophilic metallonitrene, generating a new C–N bond in benzylic cation **8**. This intermediate triggers a 2,3-phenyl shift to form the 2,3-diphenyl indole **9** (Scheme 1.2).

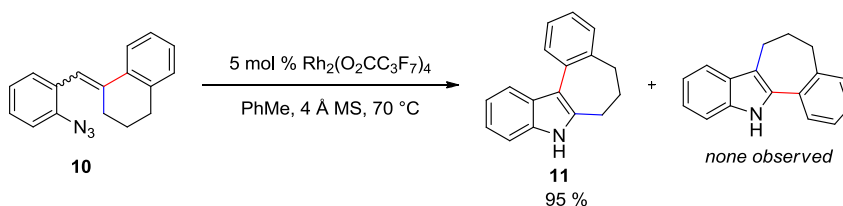
**Scheme 1.2.** Preliminary Rh(II)-catalyzed aryl azide cascade reaction to form 2,3-diphenyl indole **9**.<sup>24</sup>



In further studies, the cascade was found to extend beyond the migration of phenyl rings to the selective migration of various  $\beta$  substituents, beginning with aryl groups (Scheme 1.3).<sup>26</sup> It is important to note that in the presence of a  $\beta$ -hydrogen, the hydride is more likely to migrate than the aryl ring, resulting in formal C–H insertion.

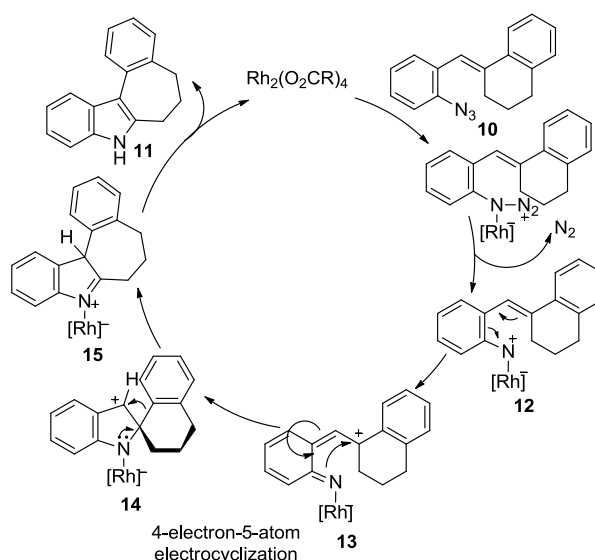
Both  $\text{Rh}_2(\text{O}_2\text{CC}_3\text{F}_7)_4$  and  $\text{Rh}_2(\text{esp})_2$  are competent catalysts for the cascade. In a control reaction, a mixture of the *E* and *Z* isomer of the  $\beta,\beta$ -diphenylstyryl azide **10** show the same selectivity for 2,3-disubstituted indole product **11**, demonstrating that the selectivity is independent of starting olefin geometry. Though alkyl groups are also competent of undergoing migration, when both an alkyl and aryl group are substituents on the olefin, only aryl group migration is observed in a ratio greater than 95:5. An electron-donating group on the migrating aryl ring increases reaction efficiency slightly, but has no bearing on selectivity.

**Scheme 1.3.** Selective formation of 2,3-diphenylindole **11** from  $\beta,\beta$ -diphenylstyryl azide **10**.<sup>26</sup>



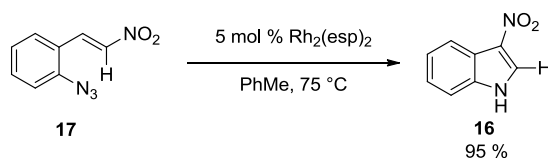
Mechanistically, the cascade is thought to begin with coordination of the rhodium carboxylate complex to the azide **10**, followed by extrusion of  $N_2$  to form the metallonitrene **12** (Scheme 1.4). Electron migration gives the more stable resonance form **13**, which is then able to participate in the 4-electron-5-atom electrocyclization to give intermediate **14**. Aryl migration then forms the iminium **15**, and tautomerization yields the product indole **11**.

**Scheme 1.4.** Mechanism for rhodium-catalyzed synthesis of 2,3-disubstituted indole **11** from  $\beta,\beta$ -disubstituted styryl azide **10**.<sup>26</sup>



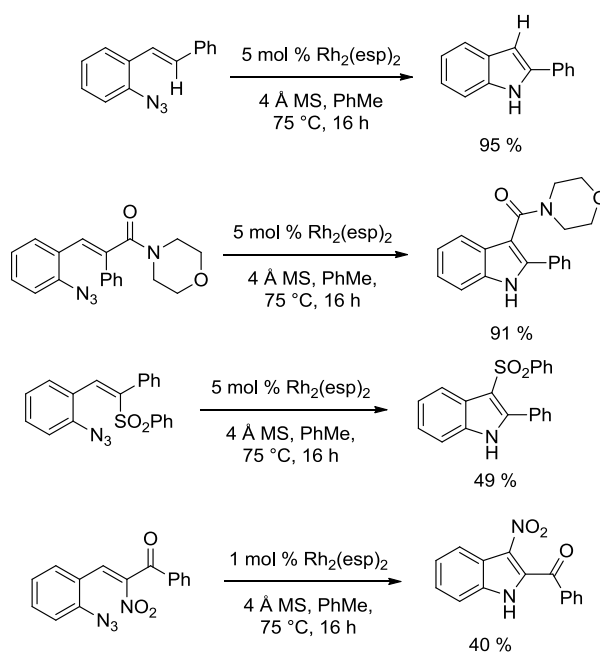
The migration also extends to  $\beta$ -nitro groups for forming 3-nitroindoles, such as **16** (Scheme 1.5).<sup>27</sup> In contrast to aryl group migration, a nitro group will migrate preferentially even in the presence of a  $\beta$ -hydride, as in azide **17**. The mechanism is likely similar to the mechanism in Scheme 1.4, though the nitro group migration may occur via a [1,5]-nitro shift or via homolysis of the C–N bond and radical recombination.

**Scheme 1.5.** Nitro-group migration reaction to form 3-nitroindole **16** from  $\beta$ -nitro styryl azide **17**.<sup>27</sup>



Due to the differences in proposed mechanisms among classes of migrating groups, it is not possible to postulate a general rule for migratory aptitude that extends to all migrating groups. Rather, migration preferences must be determined experimentally. To this point, the migration was shown to distinguish between a number of quite different  $\beta$ -substituents (Scheme 1.6).

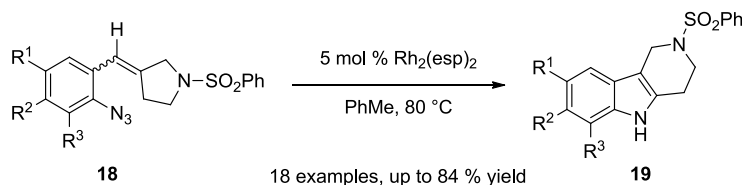
**Scheme 1.6.** Migrating group selectivity in the styryl azide cascade.<sup>27</sup>





In order to investigate the ability of the migration to distinguish between more similar migratory groups, styryl azide **18** was employed (Scheme 1.7).<sup>28</sup> In this reaction, the migration is found to distinguish between two  $\beta$ -methylene units, where one is substituted with an amine. After initial electrocyclicization of the rhodium nitrene, an aminomethylene 1,2-shift occurs selectively to form 2,3-disubstituted indole **19** exclusively. The migration is postulated to proceed either in a similar fashion to a retro-Mannich reaction, or by a diradical pair.

**Scheme 1.7.** Selective aminomethylene migration from styryl azide **18** to form 2,3-disubstituted indole **19**.<sup>28</sup>

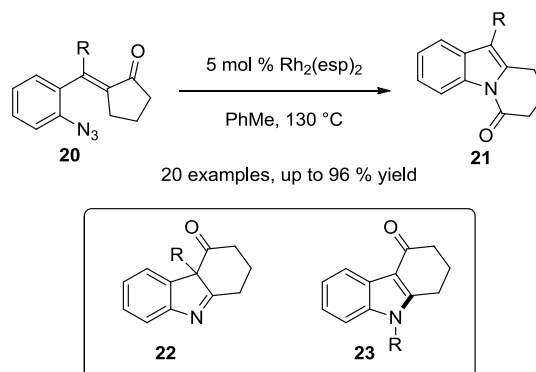


Based on these reports, a preference for migration in the cascade has been established empirically as: ester  $\ll$  alkyl  $\ll$  aryl  $\ll$  aminomethylene  $\ll$  amide  $\ll$  H  $\ll$  sulfone  $\ll$  ketone  $\ll$  nitro.

After demonstrating in previous examples of the cascade that the benzylic hydrogen would migrate to the nitrogen atom (Scheme 1.4), studies turned to the effect of replacing this  $\alpha$ -hydrogen with an alkyl or aryl group (Scheme 1.8). In the case of  $\alpha,\beta,\beta$ -trisubstituted styryl azides **20**, a new cascade process is observed with exclusive migration of the  $\beta$ -carbonyl to form 1,2,3-trisubstituted indoles **21**.<sup>29</sup> This is contrary to

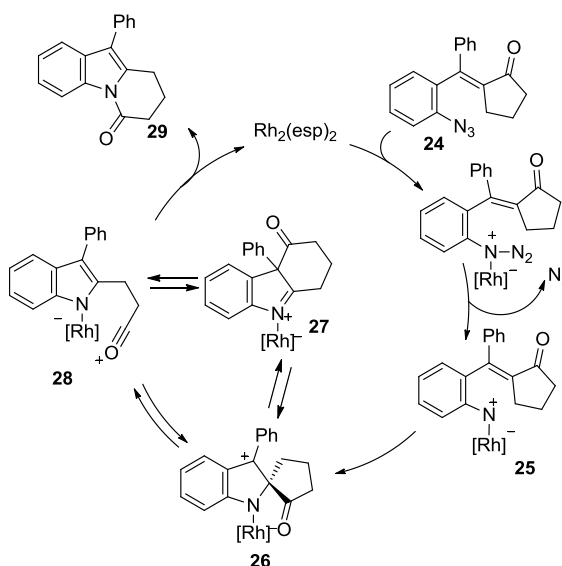
the production of indolenine **22** or indole **23**, which was expected from previously observed migrations.

**Scheme 1.8.** New electrocyclization/migration cascade reaction with  $\alpha,\beta,\beta$ -trisubstituted styryl azides **20** to form 1,2,3-trisubstituted indoles **21**.<sup>29</sup>



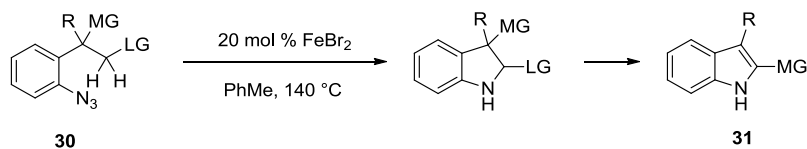
The postulated mechanism is similar to that observed with other migrating groups (Scheme 1.9). As in Scheme 1.4, azide **24** coordinates to the rhodium(II) catalyst and extrudes  $N_2$  to form metallonitrene **25**. A  $4\pi$ -electron-5-atom electrocyclization yields spirocycle **26**, which may then undergo a 1,2-carbonyl shift to form **27** or may form acylium ion **28** directly, with the rhodium(II) catalyst acting as a Lewis acid. This dual reactivity of the catalyst in forming the metallonitrene and behaving as a Lewis acid is a more recent development with a number of possible uses in metallonitrene cascades (see Section 1.1.3.1.2). Acylium ion **28** may then be attacked by the indole to form the product **29**.

**Scheme 1.9.** Postulated mechanism for the formation of 1,2,3-trisubstituted indole **29** from styryl azide **24**.<sup>29</sup>



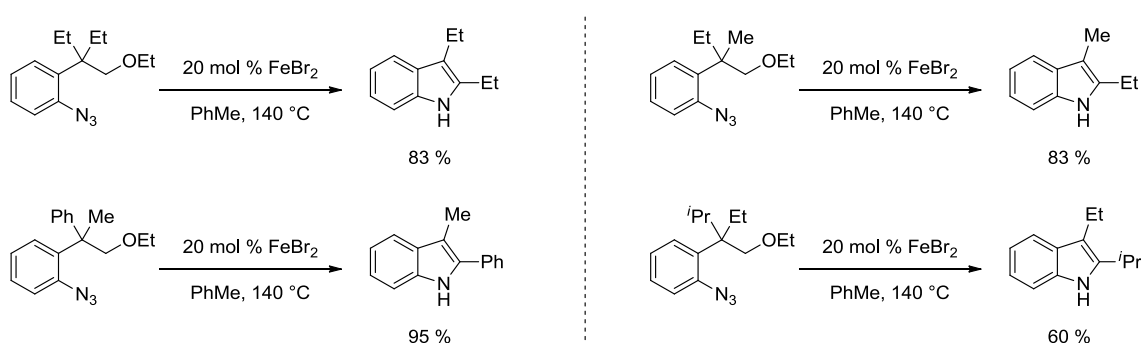
The cascade reactivity is not limited to styryl azides. If an aryl azide (**30**) is substituted with an *ortho*-alkyl group with both an appropriate leaving group and migrating group, FeBr<sub>2</sub> catalyzes a C–H amination step, which prompts a [1,2]-shift to form 2,3-disubstituted indoles (Scheme 1.10, **31**).<sup>30</sup> Notably, rhodium, cobalt, ruthenium, and copper catalysts were not found competent for the tandem reaction, and the FeBr<sub>2</sub> is hypothesized to act as both an N-atom transfer catalyst and Lewis acid.

**Scheme 1.10.** General FeBr<sub>2</sub>-catalyzed cascade reaction of *ortho*-alkyl-substituted aryl azides **30** to form 2,3-disubstituted indoles **31**.<sup>30</sup>



While ethoxy was employed exclusively as the leaving group, a variety of migratory groups were tolerated, as with styryl azides (Scheme 1.11). The migration was found dependent upon the nature of the migratory group, showing a preference of methyl < 1° < 2° < phenyl.

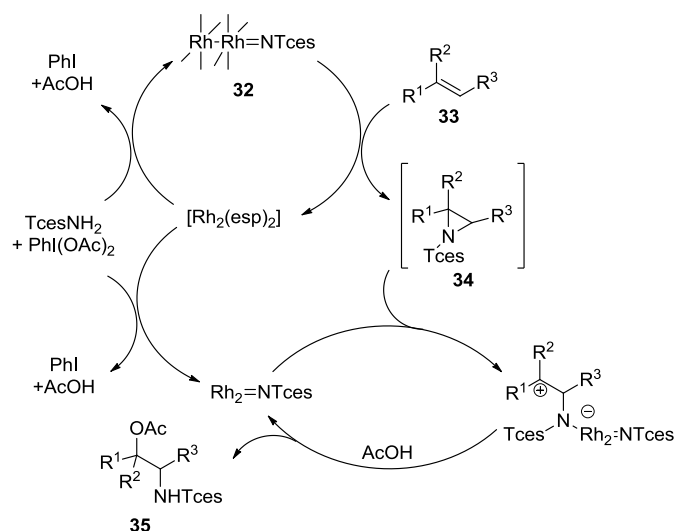
**Scheme 1.11.** Scope of the FeBr<sub>2</sub> catalyzed cascade reaction of *ortho*-alkyl-substituted aryl azides.<sup>30</sup>



### 1.1.3.1.2 Intermolecular Alkene Oxyamination

Cascade reactions of other non-azide nitrene precursors and alkenes have seen relatively little exploration. Dauban and coworkers observed a useful oxyamination tandem reaction when an alkene is exposed to trichloroethylsulfamate with a Rh(II) catalyst in the presence of a hypervalent iodine oxidant and acetic acid (Scheme 1.12).<sup>31</sup> The metallonitrene **32** aziridinate the alkene **33**. It also acts as a Lewis acid for nucleophilic ring opening of the aziridine intermediate **34** with acetate to form 1,2-amino ester **35**. This represents a unique role for the Rh-bound metallonitrene, as well as providing a direct route to protected 1,2-amino alcohols.

**Scheme 1.12.** Postulated oxyamination mechanism with metallonitrene **32** and alkene **33** to form 1,2-amino ester **35**.<sup>31</sup>

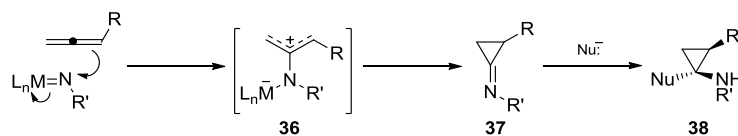


### 1.1.3.2 Metallonitrene/Allene Cascade Reactions

#### 1.1.3.2.1 Aminocyclopropane-Forming Metallonitrene/Allene Cascade Reactions

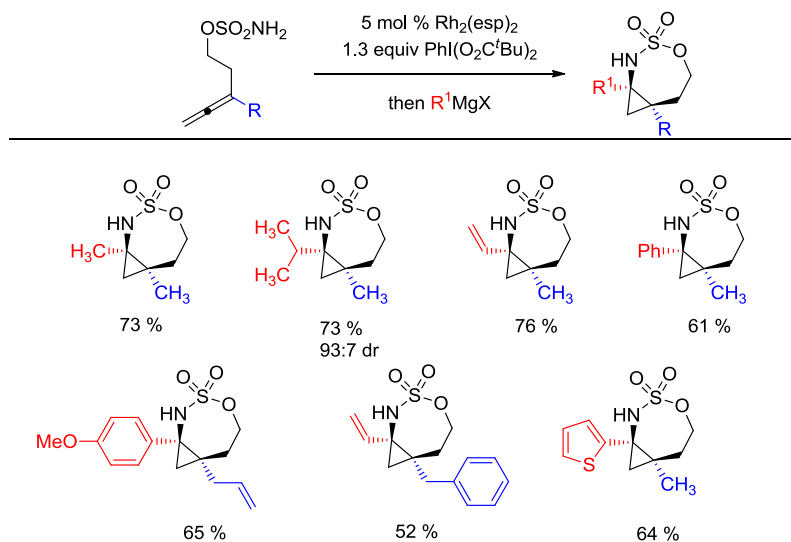
Metallonitrene/allene cascades have received the most study of any of the cascade classifications to be reviewed. These cascades were first studied by Blakey and coworkers, with the concept of generating a 2-amidoallyl cation **36** from the interaction of an allene with a metallonitrene, which would then behave as a 1,3-dipole equivalent for further reactivity (Scheme 1.13).<sup>32</sup> In fact, it was found that the highly reactive intermediate 2-amidoallyl cation shut down to a cyclopropyl imine **37**, which could then be attacked by a nucleophile to yield a highly substituted aminocyclopropane **38**.

**Scheme 1.13.** Metallonitrene/allene cascade concept.<sup>32</sup>



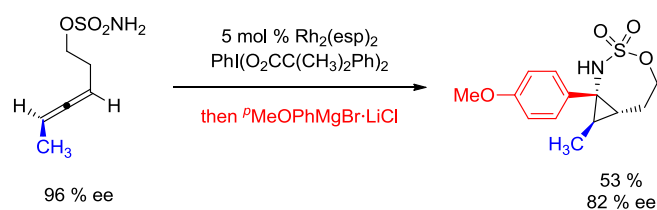
In this cascade, a sulfamate in the presence of  $\text{Rh}_2(\text{esp})_2$  serves to generate a metallonitrene, which attacks a tethered allene. The cascade is then typically terminated with a Grignard reagent (Table 1.1). This nucleophilic attack occurs preferentially from the convex face of the cyclopropane/oxathiazepane system. The cascade can be extended to a variety of allene substituents, with the reaction proceeding smoothly until the steric bulk is increased to *tert*-butyl.

**Table 1.1.** Substrate scope for metallonitrene/allene cascade for synthesis of aminocyclopropanes.<sup>32</sup>



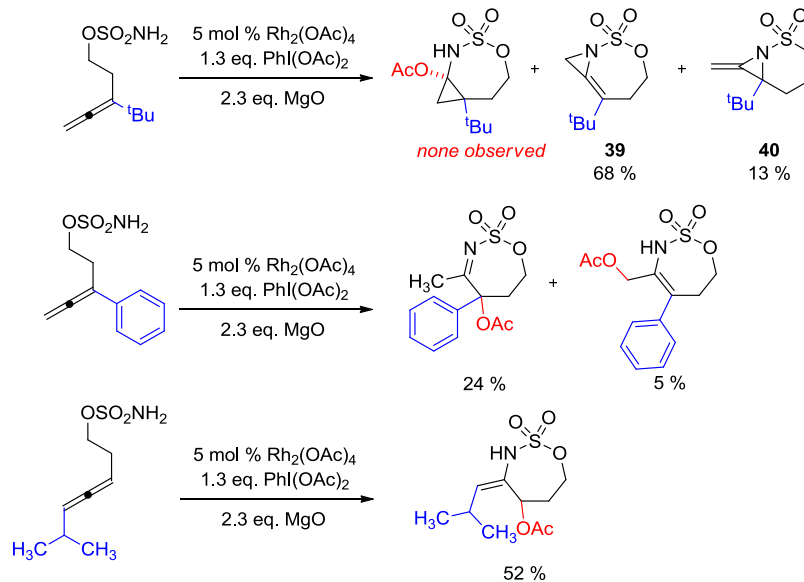
Notably, transfer of stereochemistry from an enantiomerically enriched allene to the cyclopropane product is possible (Scheme 1.14). This result indicates that the mechanism is not as simple as the truly flat amido allyl cation intermediate **36** initially proposed.

**Scheme 1.14.** Transfer of stereochemistry from a chiral allene through the metallonitrene/allene cascade.<sup>32</sup>



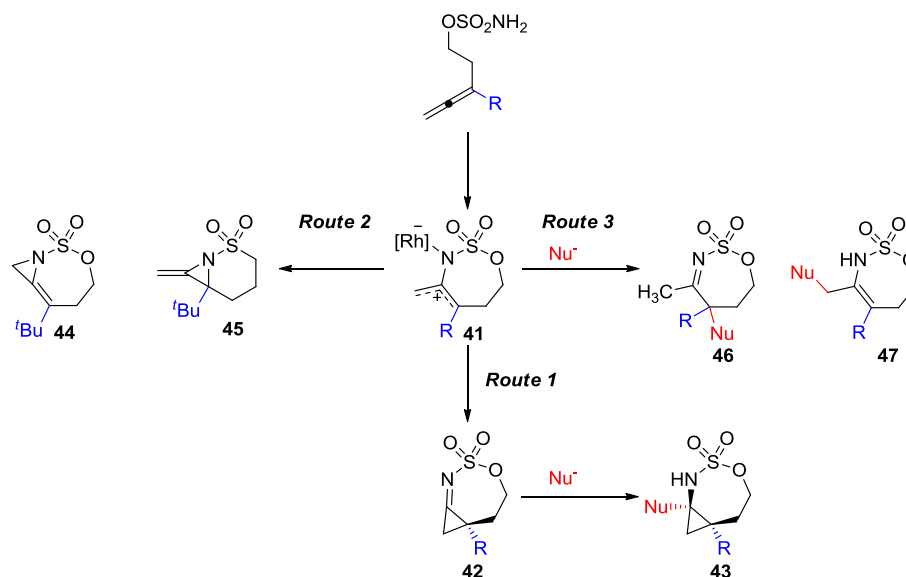
Robertson and coworkers extended this work to bulkier allene substituents that were previously unsuccessful, though reaction efficiency was greatly reduced (Scheme 1.15).<sup>33</sup> Depending upon the substitution pattern, products were isolated as imines or enamines. With the bulkiest substitution of the allene, they saw formation of unprecedented bicyclic methylene aziridines **39** and **40**. These side products highlight the mechanistic complexity of the reaction.

**Scheme 1.15.** Metallonitrene/allene cascade with bulkier allene substitution.<sup>33</sup>



The behavior of these variously substituted allenes provides insight into the mechanism of the reaction. All variations of the cascade appear to proceed through a common 2-amidoallylcation intermediate (Scheme 1.16, **41**). In the first route, intermediate **41** collapses into the cyclopropylimine **42**, which is attacked by a nucleophile to form cyclopropylimine **43**. In route 2, intermediate **41** forms either aziridine **44** or **45** depending upon which position of the allyl cation is attacked. Finally, by route 3, the nucleophile attacks the 2-amidoallylcation directly to form imine **46** or enamine **47** without the formation of an aziridine or cyclopropane.



**Scheme 1.16.** Metallonitrene/allene cascade mechanism.

### 1.1.3.2.2 2-Amidoallylcation [3+2] Annulation

The versatility of the 2-amidoallylcation intermediate was expanded upon by Blakey and coworkers, hinging upon the recognition that the 1,3-dipole could also be useful in what is described in their first report as a “[3+2] cycloaddition” (Figure 1.5).<sup>32</sup> Using homoallenyl sulfamate ester **48**, with benzaldehyde (**49**) as the dipolarophile, followed by a reductive workup, gave the trisubstituted tetrahydrofuran **50**. However, as shown below, the orbitals of the 2-amidoallylcation and benzaldehyde (**49**) do not overlap according to Woodward-Hoffman rules to allow for a concerted cycloaddition, and in a follow-up communication, this reaction is more properly described as an annulation.<sup>34</sup>

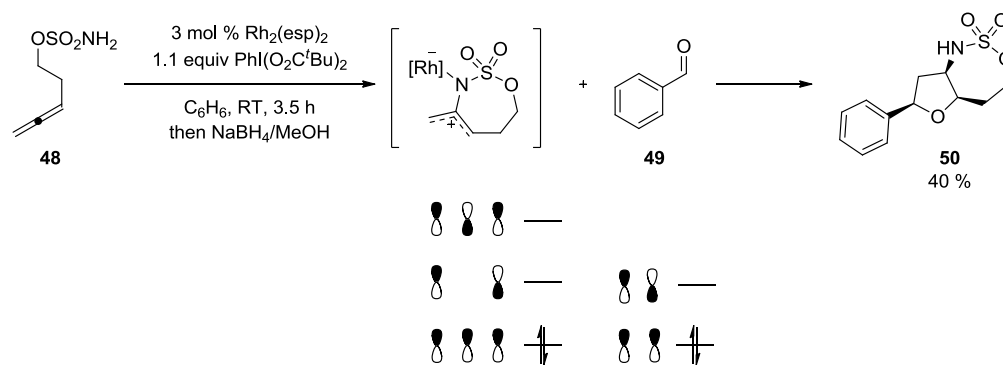
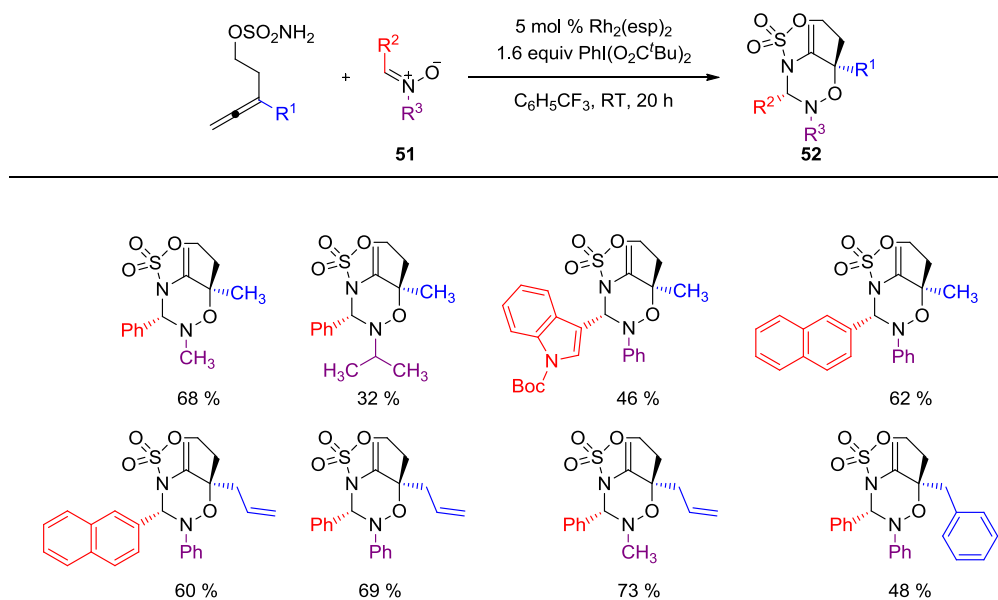


**Figure 1.5.** MO diagram for the [3+2] annulation of a homoallenyl sulfamate ester **48** and benzaldehyde (**49**) to form trisubstituted tetrahydrofuran **50**.<sup>32</sup>

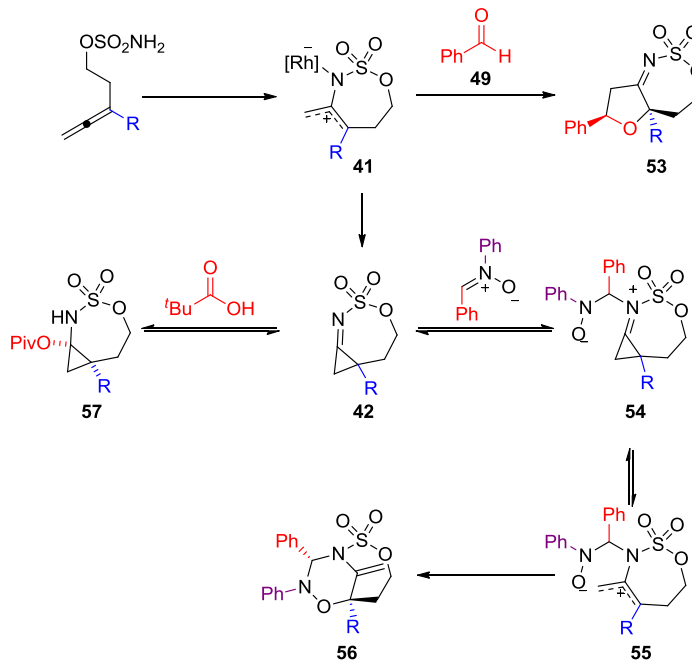
In a further extension of this annulation, nitrones **51** were found to be competent reaction partners in a [3+3] annulation with complementary regioselectivity to the [3+2] to give the bicyclic aminal **52** (Table 1.2). The reaction is highly regioselective and stereoselective, giving **52** as a single isomer. A range of 1,1-disubstituted allenes with moderately sized substituents were effective in the annulation. Aryl and heteroaryl substituents were tolerated on the nitron **51** at the  $\text{R}^2$ -position, though alkyl substitution was not effective in the cascade. At the  $\text{R}^3$ -position of the nitron **51**, aryl and small alkyl groups gave good yields, but larger alkyl groups such as isopropyl decreased the yield, with *tert*-butyl substitution suppressing the reaction completely.

**Table 1.2.** Substrate scope of [3+3] annulation of 2-amidoallylcations and substituted nitrones **51**.<sup>34</sup>



As shown previously, the cascade begins with oxidation to form the 2-amidoallylcation intermediate **41** (Scheme 1.17). A small, excellent nucleophile like benzaldehyde gives the formal [3+2] product **53**. If a comparable nucleophile is not present, 2-amidoallylcation **41** shuts down to the cyclopropylimine **42**. In the presence of a nitron, nucleophilic attack leads to cyclopropyliminium **54** which opens to the allyl cation **55**. This species is then trapped by the nitron oxygen to yield the annulation product **56**. In the absence of a suitable annulation partner, imine **42** will be attacked by any nucleophile available, including pivaloate oxidant byproduct to yield cyclopropane **57**.

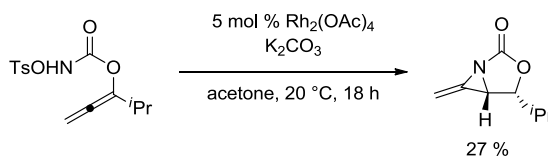
**Scheme 1.17.** Mechanism for [3+2] and [3+3] 2-amidoallylcation annulation.<sup>32,34</sup>



### 1.1.3.2.3 Cascades with 1,4-Diazaspiro[2.2]pentane (DASP) Scaffolds

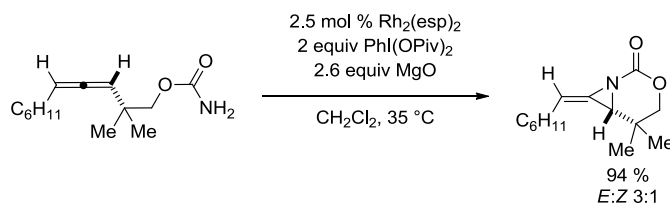
Robertson and coworkers observed that when allenic *N*-tosyloxy-carbamates are used in place of sulfamates for the intramolecular metallonitrene/allene cascade, methylene aziridines, previously isolated as a side product (Scheme 1.15), can be generated selectively in poor yield (Scheme 1.18).<sup>35</sup> This is likely due to the chain length difference in carbamates, which are better equipped to form 5- or 6-membered rings than the sulfamates previously studied. Later studies indicate competing C–H amination may have contributed to the poor yields observed initially.

**Scheme 1.18.** Allenic *N*-tosyloxy-carbamate aziridination to form a methylene aziridine.<sup>35</sup>



Schomaker and coworkers built upon this work with sulfamates and *N*-tosyloxy-carbamates, finding allenic carbamates to be the most useful nitrene precursors for generating methylene aziridines in excellent yields (Scheme 1.19).<sup>36,37</sup> In itself, this reaction is a more straightforward aziridination, but this work provides a foundation for later studies that better fit our definition of a cascade reaction. The selectivity for methylene aziridines was achieved in part by shortening the tether length to form six-membered rings, as well as blocking potential C–H amination sites with methyl groups.

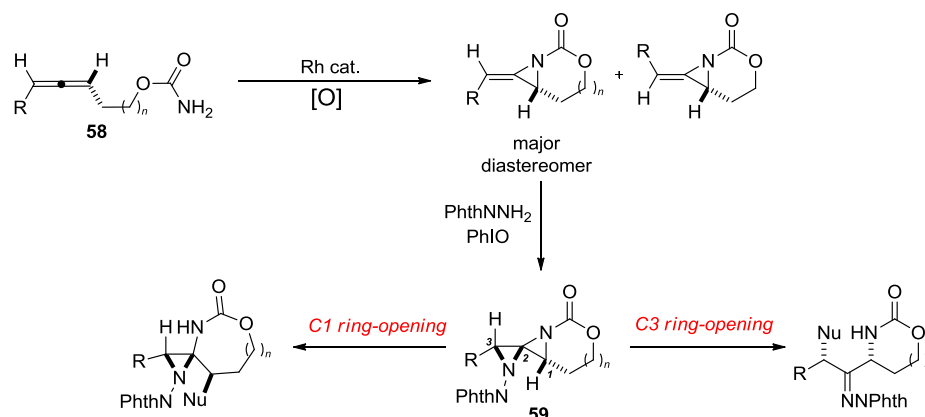
**Scheme 1.19.** Aziridination of an allenic carbamate to form a methylene aziridine.<sup>36</sup>



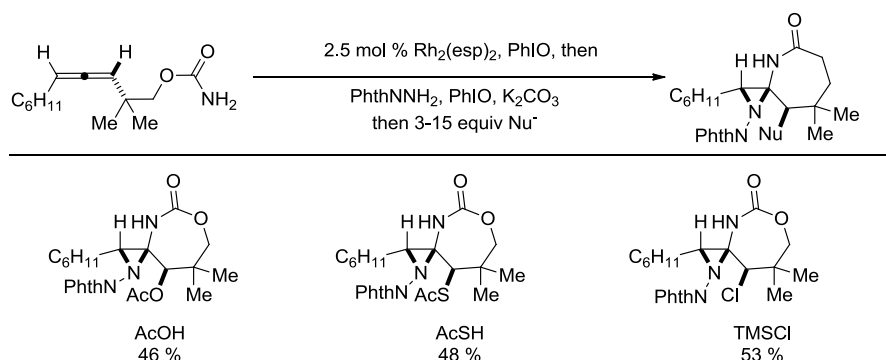
This reactivity was applied in an intramolecular/intermolecular allene bis-aziridination by following the rhodium-catalyzed intramolecular aziridination of an allenic carbamate **58** with subsequent addition of *N*-aminophthalimide in a metal-free aziridination (Scheme 1.20).<sup>38</sup> These 1,4-diazaspiro[2.2]pentane (DASP) scaffolds **59**

may then be opened at the C1 position or formally at the C3 position, providing a useful route for the synthesis of biologically active molecules containing adjacent C-N/C-O/C-O stereocenters.<sup>39</sup>

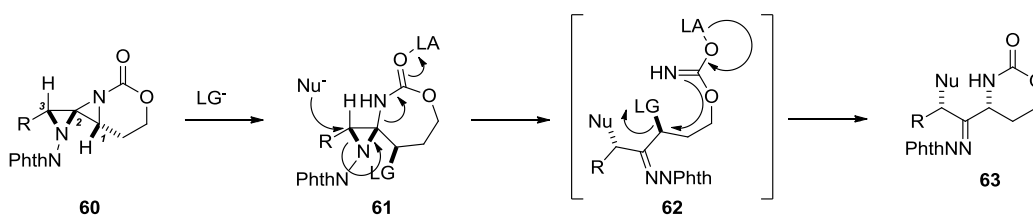
**Scheme 1.20.** Synthesis of a 1,4-diazaspiro[2.2]pentane (DASP) scaffold **59** from an allenic carbamate **58** and subsequent C1 or formal C3 ring-opening.<sup>38</sup>



In a “one-pot” reaction, the allenic carbamate can form the DASP scaffold *in situ*, with subsequent nucleophilic aziridine-opening at C1 to form *N,N*-spiroaminals (Table 1.3). Showcasing one of the useful features of cascade reactions, the one-pot transformation provided a 13 % boost in yield over the same transformation done stepwise.

**Table 1.3.** Allenic carbamate one-pot synthesis of *N,N*-spiroaminals.<sup>38</sup>

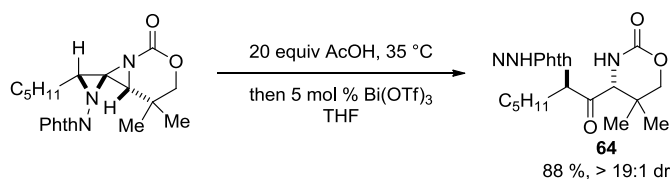
It is with some difficulty that ring opening at C3 was achieved. More electron-withdrawing groups on the aziridine second formed would direct the nucleophile to C3, but unfortunately, the second aziridination was limited to *N*-aminophthalamide. Instead, a formal C3 opening was achieved by opening at C1 of the DASP scaffold **60** to form bicyclic intermediate **61**, followed by opening at C3 to give intermediate **62**, and re-closing to form the product imine **63** (Scheme 1.21).

**Scheme 1.21.** Formal C3 ring opening of 1,4-diazaspiro[2.2]pentane (DASP) scaffold **60**.<sup>38</sup>

A third transformation from these DASP scaffolds was subsequently disclosed, using C2 ring-opening to make 1,3-diaminated compounds, such as ketone **64** (Scheme

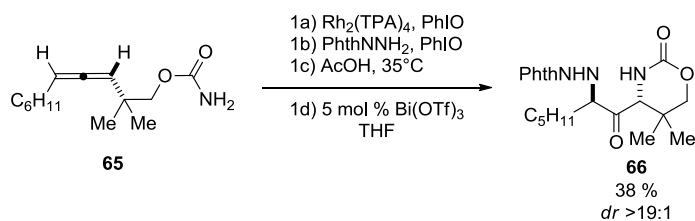
1.22).<sup>39</sup> In this process, acetate opening at C1 takes place first. The Lewis acid then activates the remaining aziridine ring for C2 ring-opening and rearrangement.

**Scheme 1.22.** C2 ring opening of 1,4-diazaspiro[2.2]pentane (DASP) scaffolds.<sup>39</sup>



In applying this reaction as a metallonitrene/allene cascade, the complete transformation from carbamate **65** to 1,3-diaminated ketone **66** can be achieved in one pot in an overall yield of 38 % and very good diastereoselectivity (Scheme 1.23).

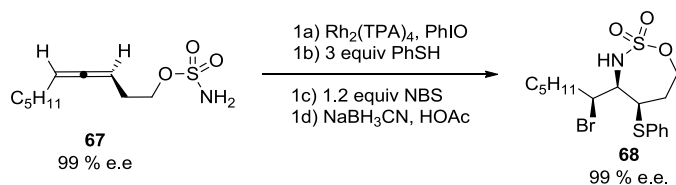
**Scheme 1.23.** Cascade formation of 1,3-diaminated ketone **66** from carbamate **65**.<sup>39</sup>



From their observations in allenic carbamate reactivity, Schomaker and coworkers revisited allenic sulfamates for forming methylene aziridines.<sup>40</sup> Upon exposure of allenic sulfamate **67** to  $\text{Rh}_2(\text{TPA})_4$  with oxidant, followed by nucleophile addition and reduction, product **68** was formed in one pot (Scheme 1.24). Complete transfer of axial chirality in allene **67** to point chirality in oxathiazepane **68** was observed. The cascade was effective with a variety of weak nucleophiles.



**Scheme 1.24.** One-pot aziridination and ring-opening of allenic sulfamate **67** with transfer of chirality to oxathiazepane **68**.<sup>40</sup>



### 1.1.3.3 Metallonitrene/Alkyne Cascade Reactions

#### 1.1.3.3.1 Intramolecular Metallonitrene/Alkyne Cascade Reactions

In 2007, one of the earliest metallonitrene cascade reactions to be discovered was the metallonitrene/alkyne cascade. The metallonitrene/alkyne cascade concept was inspired by ene/yne metathesis, with a metallonitrene in place of the carbene (Figure 1.6).<sup>41</sup> The metallonitrene is envisioned to undergo a [2+2] reaction to generate a new C–N double bond and  $\alpha$ -iminometallobutene capable of initiating a cascade.

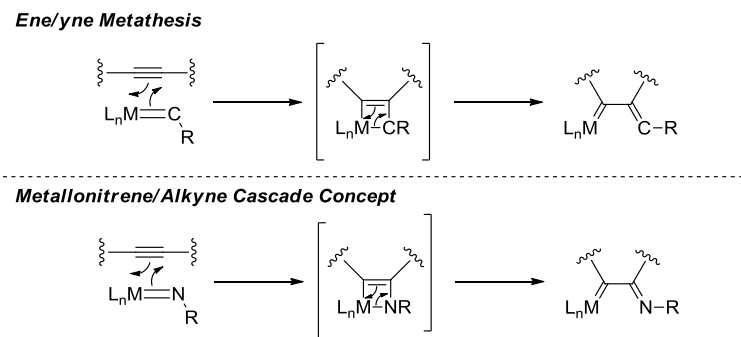
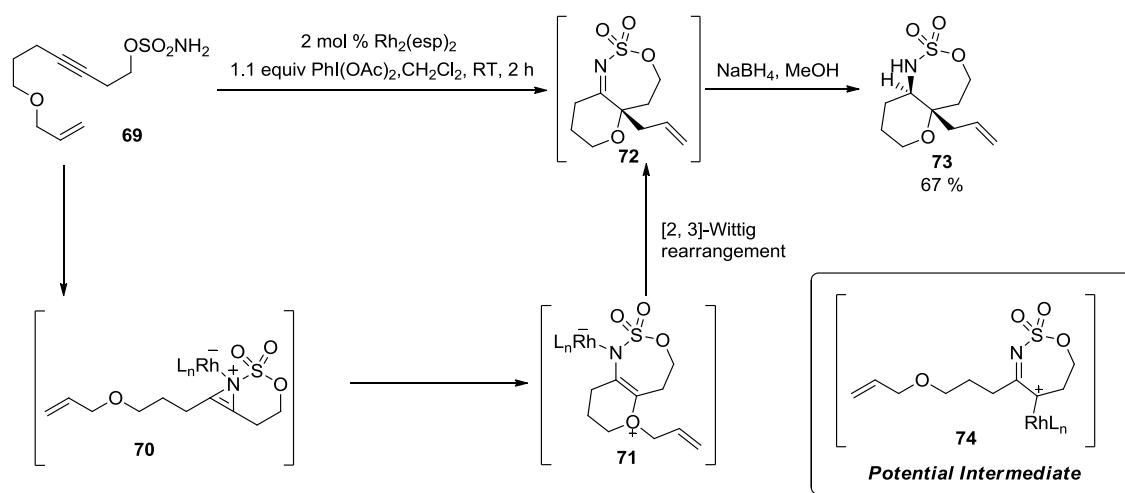


**Figure 1.6.** Metallonitrene/alkyne cascade concept development.<sup>41</sup>

When a metallonitrene is generated from a sulfamate ester, hypervalent iodine oxidant, and  $\text{Rh}_2(\text{esp})_2$  catalyst, a cascade process is indeed initiated (Scheme 1.25). The electrophilic rhodium nitrene species generated from sulfamate **69** is trapped by a tethered alkyne to form azirinium intermediate **70**. The cascade is terminated by a tethered allyl ether to form intermediate **71**, followed by migration of the allyl group through a [2,3]-Wittig rearrangement to form imine **72**. The imine is then reduced with  $\text{NaBH}_4$  *in situ* to form the bicyclic product **73**.

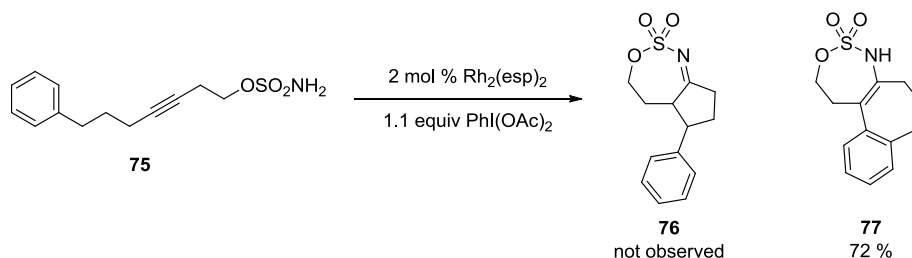
**Scheme 1.25.** Intramolecular metallonitrene/alkyne cascade mechanism.<sup>41</sup>



Initially, it was hypothesized that the intermediate prior to allyl ether trapping would involve generation of a new metallocarbene, as in  $\alpha$ -iminometallobenoid intermediate **74** (Scheme 1.25). For this purpose, substrate **75** was designed for trapping of a transient  $\alpha$ -iminometallobenoid intermediate (Scheme 1.26).<sup>42</sup> If such an intermediate were involved, with C–H amination catalyst  $\text{Rh}_2(\text{esp})_2$ , one would expect

benzylic C–H insertion to form imine **76** (or perhaps aryl cyclopropanation). What is observed instead is electrophilic aromatic substitution product **77**.

**Scheme 1.26.** Metallonitrene/alkyne cascade control experiment with sulfamate ester **75**.<sup>42</sup>



In considering the nature of the intermediate generated from the metallonitrene, it is conceivable to envision the metallonitrene interacting with the alkyne to form a  $\pi$ -complex, with several potential intermediates lying close together on the energy surface, including azirinium **70** (Figure 1.7). With most substrates, a seven membered ring is favored in the cascade, implying an intermediate endocyclic enaminium **78**. But, by varying the structure of the sulfamate ester, formation of the six-membered ring may also be favored, which implies an intermediate exocyclic enaminium **79**. Therefore, the cascade intermediate is best described as a continuum of intermediates **70**, **78**, **79**.

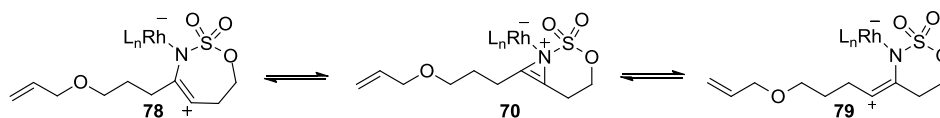
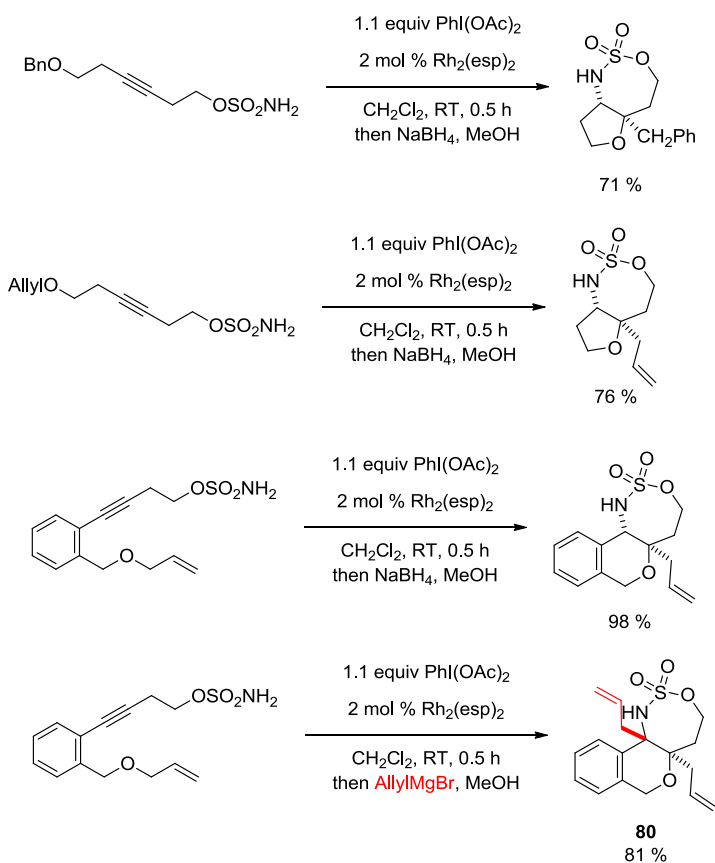


**Figure 1.7.** Continuum of metallonitrene/alkyne cascade intermediates.

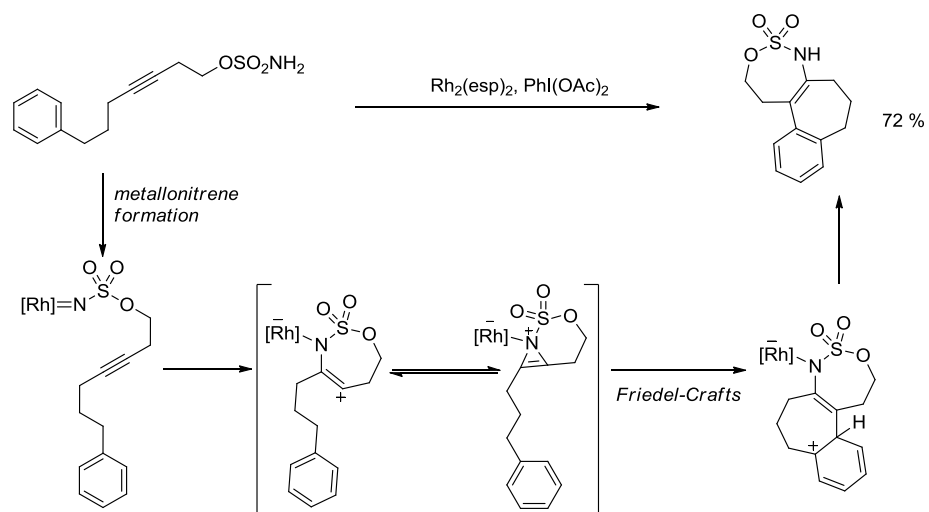
The cascade could also be terminated by a tethered benzyl ether and was tolerant of a phenyl ring incorporated into the tether (Scheme 1.27). In addition to quenching with NaBH<sub>4</sub>, the imine could be attacked with a Grignard reagent to afford **80** in good yield of 81 %.

**Scheme 1.27.** Intramolecular metallonitrene/alkyne substrate scope.<sup>41</sup>



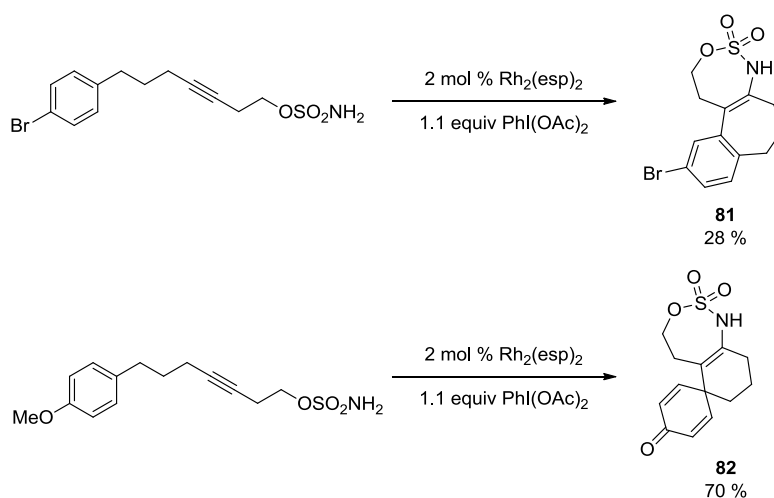
With the cascade established and a mechanistic hypothesis in place, Blakey and coworkers further extended the cascade termination beyond allyl and benzyl ethers.<sup>42</sup> They found that aromatic rings were efficient for cascade termination via electrophilic aromatic substitution (Scheme 1.28).

**Scheme 1.28.** Metallonitrene/alkyne cascade Friedel-Crafts termination mechanism.<sup>42</sup>



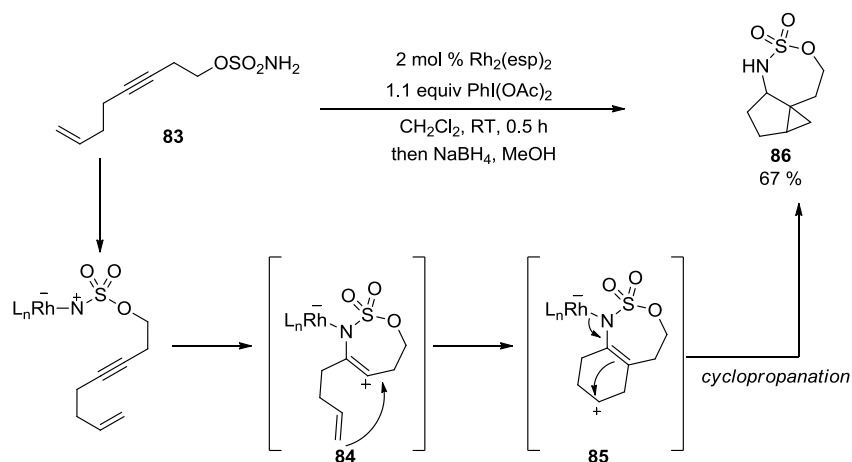
Consistent with electrophilic aromatic substitution, the reaction efficiency decreases when an electron withdrawing group is substituted on the aromatic ring (28 % **81**, Scheme 1.29). In contrast, a methoxy group on the aromatic ring acts as a *para* director. Subsequently, the methyl group is lost rather than eliminating a proton to restore aromaticity and give **82** in good yield, which is also consistent with electrophilic aromatic substitution.

**Scheme 1.29.** Electronic substitution effects on Friedel-Crafts termination of the metallonitrene/alkyne cascade.<sup>42</sup>



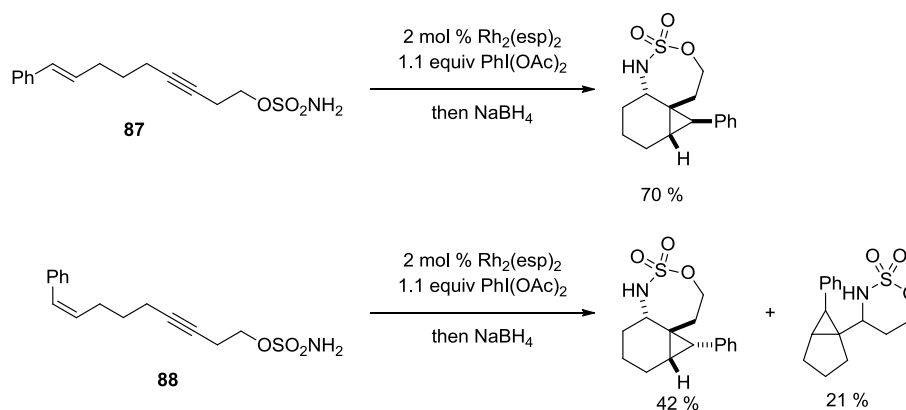
The unique nature of the cascade intermediate is again illustrated in cascade termination by cyclopropanation in the presence of a tethered olefin, as in sulfamate ester **83** (Scheme 1.30). In this case, intermediate **84** behaves as an enaminium intermediate. The olefin attacks the enaminium to yield bicyclic intermediate **85**. The enamine then terminates the cascade by cyclopropanation to form product **86**. Consistent with the proposed mechanism, substrates with substitution on the alkene stabilize the cation in the intermediate, leading to better yields than the unsubstituted alkene. This is consistent with stepwise, two-electron chemistry, rather than a radical process.

**Scheme 1.30.** Mechanism of cyclopropanation termination of the metallonitrene/alkyne cascade with sulfamate ester **83**.<sup>42</sup>



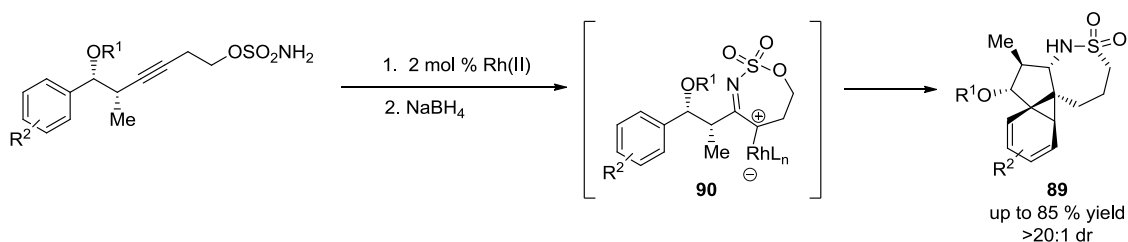
Generally, if it were a stepwise, two-electron mechanism, then one would expect both the *E* and *Z* alkene to give the same product due to free rotation around the double bond in the enaminium intermediate. However, when substrates with tethered *E* alkene **87** or *Z* alkene **88** are employed in the cascade, scrambling of olefin stereochemistry is not observed (Scheme 1.31). This result suggests the mechanism is more complex than a simple stepwise process, and is concerted, though probably asynchronous.

**Scheme 1.31.** Effect of olefin substitution on cyclopropanation termination of the metallonitrene/alkyne cascade.<sup>42</sup>



In a recent extension of this work, Panek and coworkers demonstrated cascade termination with cyclopropanation of an arene (Scheme 1.32).<sup>43</sup> The method is capable of selectively forming norcaradienes (**89**) in good yield and excellent diastereoselectivity. Unlike previous work from Blakey and coworkers, the intermediate is neither trapped by the ether or in Friedel-Crafts termination by the arene, but instead cyclopropanates the arene in a Buchner reaction. Though intermediate **90** is given in their report, there is no mechanistic evidence given for formation of a metalcarbene intermediate. As mentioned previously (Scheme 1.26), control experiments have indicated generation of this  $\alpha$ -iminometallobenzyloxy intermediate **90** is unlikely.

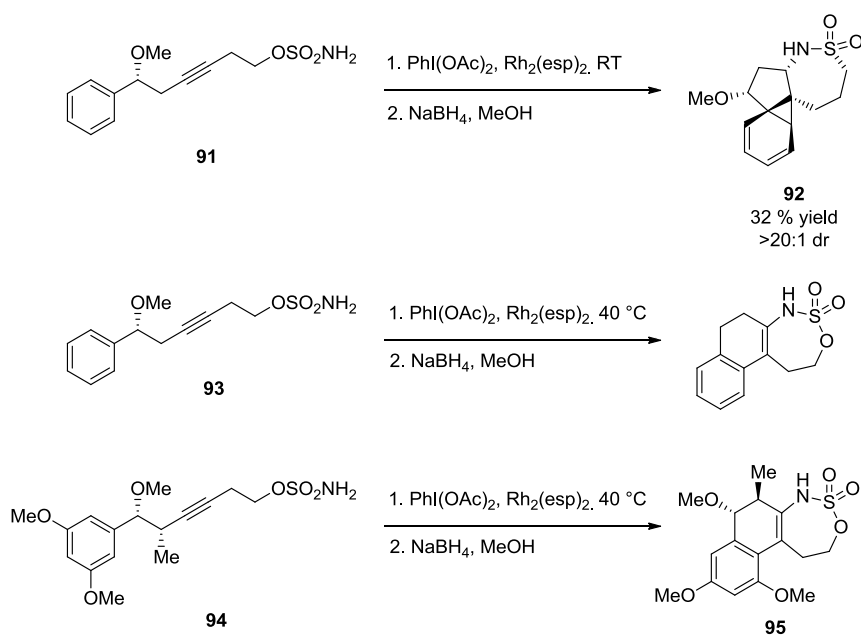
**Scheme 1.32.** Metallonitrene/alkyne cascade termination by aryl cyclopropanation.<sup>43</sup>





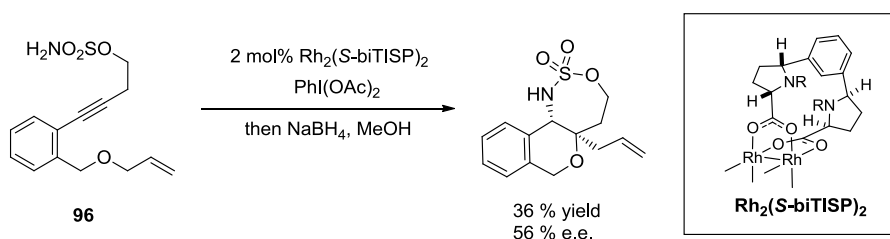
The methyl group adjacent to the alkyne was found necessary for thermal stability at 40 °C, but substrate **91** was effective in the cascade at room temperature in a reduced yield of 32 % (Scheme 1.33). The benzylic ether is believed to play an important role through electron-donation in favoring aryl cyclopropanation product **92** over Friedel Crafts termination. The Friedel Crafts termination observed by Blakey and coworkers is confirmed in this work with substrates not substituted with the benzylic ether (**93**). In addition, the strongly electron donating groups in 2,3-dimethoxy substituted sulfamate ester **94** favored electrophilic aromatic substitution to form **95**, even in the presence of the benzylic ether. The norcaradienes products formed in the cascade are also shown capable of further transformation to take advantage of the four contiguous stereocenters.

**Scheme 1.33.** Importance of the benzylic ether in favoring aryl cyclopropanation over electrophilic aromatic substitution in the metallonitrene/alkyne cascade.<sup>43</sup>



Based on the success of the metallonitrene/alkyne cascade reaction, expansion to an enantioselective methodology would further add to the utility of the transformation. Examination of a variety of chiral dirhodium catalysts and sulfamate ester substrates with the intramolecular metallonitrene/alkyne cascade reaction found enantioselectivity varied greatly, dependent upon the substitution of the sulfamate ester.<sup>44</sup> The greatest enantiomeric excess was achieved with  $\text{Rh}_2(\text{S-biTISP})_2$  and sulfamate ester **96** (Scheme 1.34). Although the observed enantioselectivity was promising, the level of enantioselectivity achieved was not synthetically useful. This result led to the pursuit of other strategies for enantioselectivity, such as substrate-based transfer of stereochemical information (Section 1.3).

**Scheme 1.34.** Enantioselective catalysis of the intramolecular metallonitrene/alkyne cascade reaction of sulfamate ester **96**.<sup>44</sup>

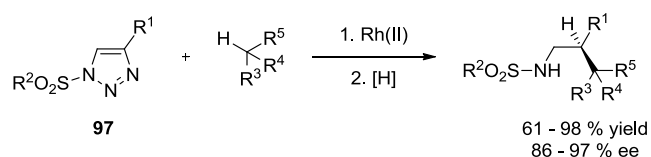


### 1.1.3.3.2 Intermolecular Metallonitrene/Alkyne Cascade Reactions

As has been discussed, the intermediate generated in the intramolecular metallonitrene/alkyne cascade, though not a true  $\alpha$ -iminometallobenzyne, behaves in a similar manner.  $\alpha$ -Iminometallobenzyne intermediates are difficult to synthesize directly, as the necessary diazo precursors rapidly isomerize to the 1,2,3-triazoles.<sup>45</sup> Fokin and

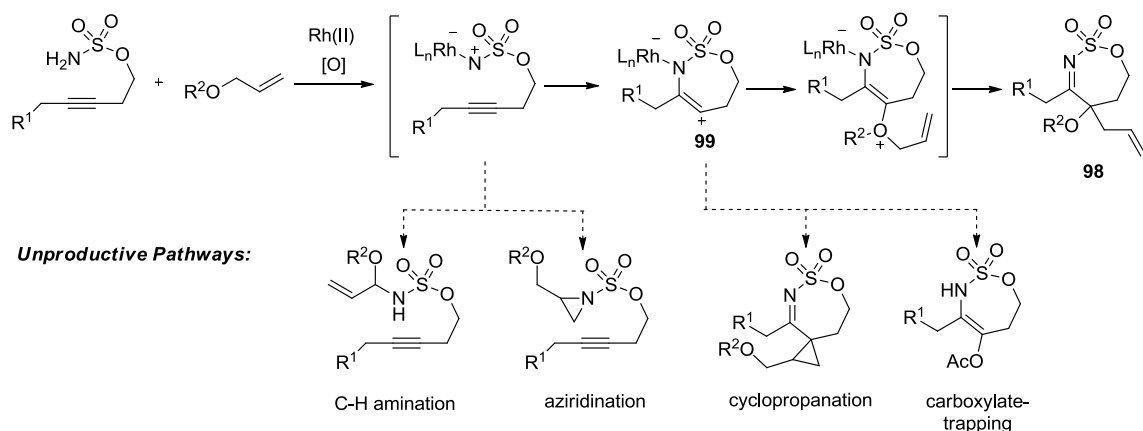
coworkers have shown these 1,2,3-triazoles **97** are capable of unveiling  $\alpha$ -iminometallobenzenes in the presence of an appropriate transition metal catalyst and can be subsequently used for C–H functionalization or other reactions typical of carbenes (Scheme 1.35).<sup>46-53</sup>

**Scheme 1.35.** 1,2,3-Triazole **97** as an  $\alpha$ -iminometallobenzene precursor for C–H functionalization.<sup>46</sup>



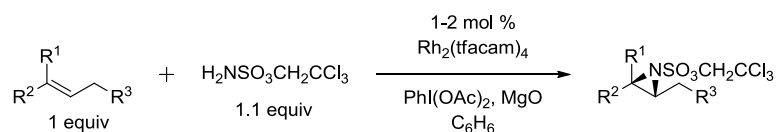
The metallonitrene/alkyne cascade presents an alternative method for unveiling an  $\alpha$ -iminometallobenzene-like intermediate directly from an alkyne and metallonitrene. However, the necessity of tethering the allyl ether for trapping to the homo propargylic sulfamate ester limited the method's utility. In order to be synthetically useful, Blakey and coworkers next sought to establish the cascade with intermolecular termination (Scheme 1.36).<sup>54</sup> Beginning from an allyl ether and homopropargylic sulfamate ester, the desired allyl ether termination and [2,3]-Wittig rearrangement leads to oxathiazepine **98**. However, possible undesired reaction pathways were of concern. By eliminating the tethered allyl ether for intramolecular trapping, cascade intermediates could be trapped by a number of different nucleophiles. For instance, one might expect allylic C–H amination or aziridination by the metallonitrene to compete with cascade termination. From the enaminium intermediate **99**, cyclopropanation of the allyl ether or nucleophilic attack of the acetate oxidant byproduct is also a potential competing pathway.

**Scheme 1.36.** Intermolecular metallonitrene/alkyne cascade mechanism, with possible unproductive pathways.<sup>54</sup>



Initially, it was observed that under standard intramolecular cascade conditions with  $\text{Rh}_2(\text{esp})_2$ , synthetically useful quantities of the desired cascade product were not isolated due to competing C–H amination. A report from Du Bois and coworkers described  $\text{Rh}_2(\text{tfacam})_4$  as promoting intermolecular interaction of metallonitrenes with  $\pi$ -systems in preference to C–H amination (Scheme 1.37).<sup>55</sup> Therefore, it was hypothesized that employing  $\text{Rh}_2(\text{tfacam})_4$  in place of C–H amination catalyst  $\text{Rh}_2(\text{esp})_2$  might yield reaction conditions selective for the desired cascade product.

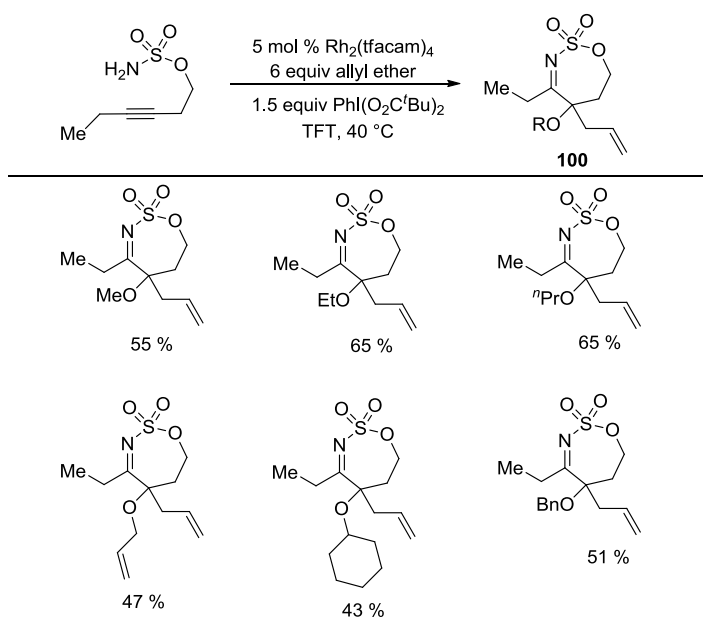
**Scheme 1.37.** Use of  $\text{Rh}_2(\text{tfacam})_4$  for intermolecular metallonitrene aziridination.<sup>55</sup>



$\text{Rh}_2(\text{tfacam})_4$  at 5 mol % catalyst loading gave the desired cascade termination to yield oxathiazepine products **100** (Table 1.4).<sup>56</sup> Due to the initial goals for the

application of the intermolecular metallonitrene/alkyne cascade, Dr. Aaron Thornton optimized reaction conditions using bis-allyl ether and a more complex sulfamate ester. Thornton and Blakey found the cascade could be terminated with a variety of commercially available allyl ethers in moderate yield. The intermolecular cascade provided the unexpected benefit of yielding an isolable imine **100**, eliminating the necessity of *in situ* reduction.

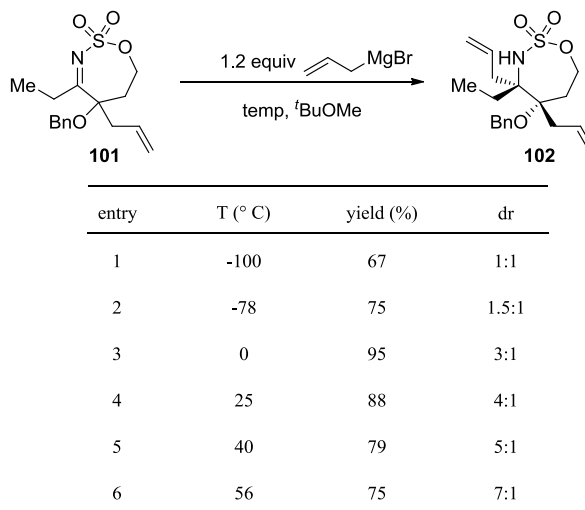
**Table 1.4.** Initial substrate scope of the intermolecular metallonitrene/alkyne cascade reaction to yield imines **100**.<sup>56</sup>



Since the products were able to be isolated as the imine, the cascade products could be subjected to a variety of subsequent transformations, such as the addition of a Grignard reagent to isolated cascade product **101** to give amine **102** (Table 1.5). A surprising inverse temperature dependence on diastereoselectivity was initially

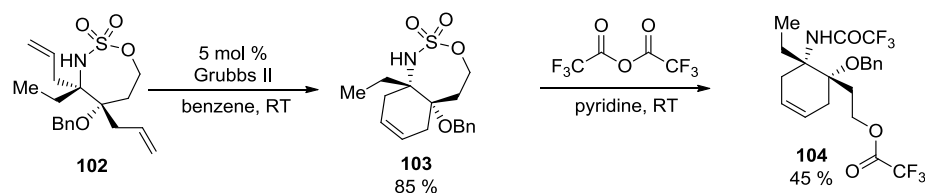
observed;<sup>56</sup> however, subsequent investigation revealed this observation to be erroneous (see Section 1.4).

**Table 1.5.** Reported inverse temperature dependence of diastereoselectivity of Grignard addition to imine **101**.<sup>56</sup>



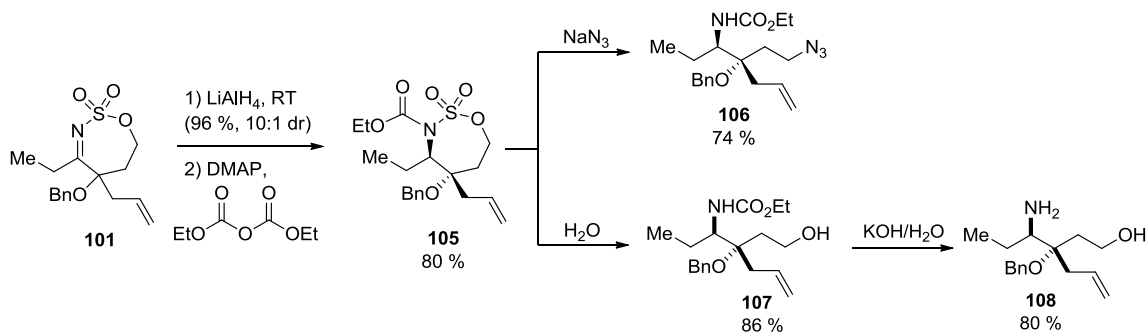
Following Grignard addition to form oxathiazepane **102**, ring-closing metathesis with Grubbs II catalyst formed bicyclic cyclohexene **103** in 85 % yield (Scheme 1.38). Traditional acylation agents were not found effective for activating oxathiazepane **103**. However, reaction of oxathiazepane **103** with trifluoroacetic anhydride gave the corresponding trifluoroacetamide. As this protecting group is extremely electron-withdrawing, the trifluoroacetate anion byproduct was then capable of attacking the activated oxathiazepane to generate the highly substituted cyclohexene **104** in 45 % yield.

**Scheme 1.38.** Derivatization of oxathiazepane **102** to form disubstituted cyclohexene **104**.<sup>56</sup>



The intermolecular cascade reaction products were found useful in a number of further transformations (Scheme 1.39). Starting from imine **101**, lithium aluminum hydride reduction at room temperature proceeded with 96 % yield and a diastereomeric ratio of 10:1. To subsequently open the sulfamate ester with an external nucleophile, activation by *N*-acylation was necessary.<sup>57</sup> Activated sulfamate ester **105** can be opened with sodium azide to yield **106** in 74 % yield or with water to yield **107** in 86 %. The ethyl carbamate protecting group may then be cleaved under strongly basic conditions, yielding the free amine **108** in 80 % yield.

**Scheme 1.39.** Activation of intermolecular metallonitrene/alkyne cascade product **101** for ring-opening.<sup>56</sup>

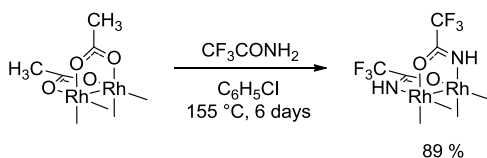


## 1.2 Intermolecular Metallonitrene/Alkyne Cascade Optimization

After the initial discovery of the intermolecular metallonitrene/alkyne cascade reaction, a preliminary optimization by Dr. Aaron Thornton indicated that  $\text{Rh}_2(\text{tfacam})_4$  was the best catalyst for the transformation.<sup>56</sup> However, the optimization was incomplete and did not present a systematic and detailed study from which clear conclusions could be reached. Therefore, this research was initiated by conducting a systematic optimization with a simple substrate.

Several dirhodium catalysts were screened, including  $\text{Rh}_2(\text{tfacam})_4$ .  $\text{Rh}_2(\text{tfacam})_4$  was prepared in excellent yield (89 %) according to the literature by refluxing  $\text{Rh}_2(\text{OAc})_4$  with trifluoroacetamide in chlorobenzene over six days (Scheme 1.40).<sup>58</sup>

**Scheme 1.40.** Synthesis of  $\text{Rh}_2(\text{tfacam})_4$ .



The optimization was conducted with methyl allyl ether and homopropargylic sulfamate ester **109**.  $\text{Rh}_2(\text{esp})_2$  (the intramolecular cascade catalyst),  $\text{Rh}_2(\text{TPA})_4$ ,  $\text{Rh}_2(\text{OAc})_4$ , and  $\text{Rh}_2(\text{tfacam})_4$  were examined in benzene with  $\text{PhI}(\text{OAc})_2$  as oxidant (Table 1.6, entries 1-4) and with  $\text{PhI}(\text{O}_2\text{C}^t\text{Bu})_2$  as oxidant (entries 5-8). Due in part to the poor solubility of  $\text{PhI}(\text{OAc})_2$ ,  $\text{PhI}(\text{O}_2\text{C}^t\text{Bu})_2$  was found to be the more efficient oxidant and was employed for the remainder of the optimization.  $\text{Rh}_2(\text{OAc})_4$  and  $\text{Rh}_2(\text{tfacam})_4$  generated the only significant quantities of imine **110** through the cascade





metallonitrene/alkyne cascade were not stable flash chromatography. This observation led us to hypothesize that product decomposition was taking place during purification, an idea confirmed by subjecting the product to two-dimensional thin layer chromatography.

Therefore, new conditions for flash chromatography purification that would render the imine **110** less susceptible to decomposition were investigated. Replacing silica gel with alumina offered no improvement, nor did 1 % triethylamine additive to the solvent system. An additive of 1 % acetic acid improved the isolated yield significantly, giving an isolated yield of 75 % imine **110** (Table 1.6, entry 16). We theorize that acetic acid serves to neutralize any trace quantities of base in the eluent, suppressing a base-mediated hydrolysis of imine **110**.

### 1.3. Intermolecular Metallonitrene/Alkyne Cascade Substrate Scope

The intermolecular metallonitrene/alkyne cascade reaction was previously found generalizable to a variety of simple allyl ethers (Table 1.4). However, allyl ethers with olefinic substitution had not yet been examined. The anticipated introduction of a second stereocenter through the cascade would make the methodology more useful for the synthesis of complex molecules. In an effort to observe the effect of terminal allyl substitution, we began our studies with methyl crotyl ether.

Methyl *E*-crotyl ether (**111**) was obtained by methylation of crotyl alcohol (**112**). Using literature conditions for methylation with methyl iodide in DMSO,<sup>59</sup> methyl ether **111** was isolated in low yield (Scheme 1.41). As the crude <sup>1</sup>H NMR spectrum showed

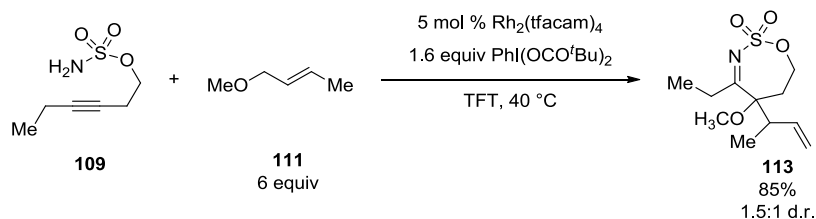
clean conversion, the low yield was likely due to difficulty in purifying volatile methyl ether **111**.

**Scheme 1.41.** Synthesis of methyl crotyl ether (**111**) by methylation of crotyl alcohol (**112**).



The intermolecular metallonitrene/alkyne cascade reaction with standard sulfamate ester **109** proceeded in 85 % yield with a 1.5:1 ratio of diastereomers of oxathiazepine **113** (Scheme 1.42). The relative stereochemistry of the separable isomers was not determined experimentally, as the structure is not rigid enough for NOE to be informative.

**Scheme 1.42.** Intermolecular cascade reaction with methyl crotyl ether (**111**).



The poor diastereoselectivity of the reaction can be explained by examination of transition state models. In contrast to the selectivity we observed, good diastereoselectivity has been previously observed for terminal alkynes in [2,3]-Wittig rearrangements (such as alkyne **114**, Figure 1.8).<sup>60-63</sup> In the transition state model given,

1,3-diaxial interactions between the alkyne and H<sub>a</sub> caused favoring of transition state TS<sub>1</sub>, which gave almost complete selectivity for the *anti* diastereomer.<sup>61</sup> In contrast, allyl ethers with olefinic substitution exhibited very poor diastereoselectivity in the [2,3]-Wittig rearrangement in our system. This difference in selectivity may be attributed to the disubstituted alkyne of **109**, which led to comparable steric clashes in both transition states, causing TS<sub>1</sub> to be closer in energy to TS<sub>2</sub>.

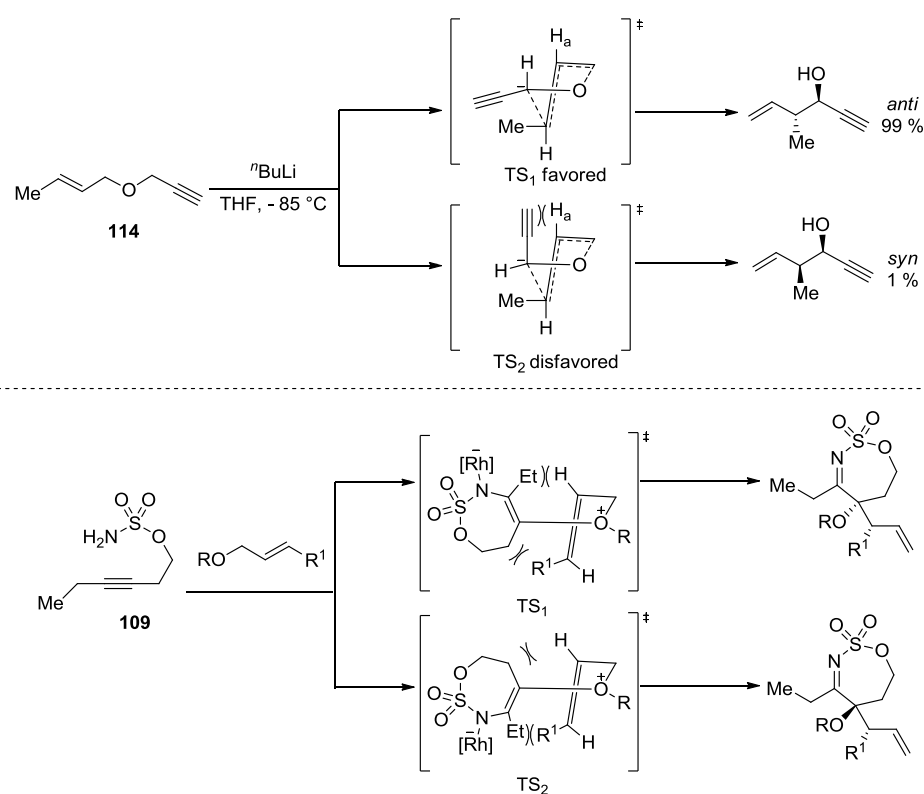
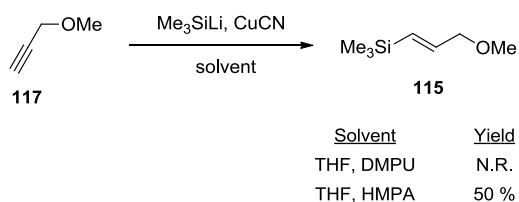


**Figure 1.8.** Literature precedent for [2,3]-Wittig rearrangement of terminal alkynes (top)<sup>61</sup> compared with stereochemical models for poor diastereoselectivity observed in metallonitrene/alkyne cascade reaction (bottom).

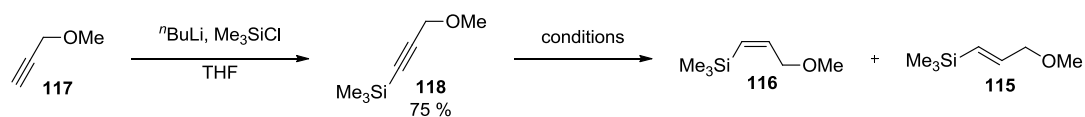
After demonstrating that the metallonitrene cascade reaction proceeded extremely well with terminal methyl substitution, both *E*- and *Z*-vinyl silanes **115** and **116** were synthesized to gauge the compatibility of a trimethylsilyl group, whose incorporation in the product would provide a functional handle for subsequent transformations (Scheme 1.43 and Table 1.7). By examining both *E*- and *Z*-vinyl silanes, the effect of the olefinic substitution pattern on yield and diastereomeric ratio could be examined.

A literature precedent for silyl cupration of propargyl methyl ether with HMPA additive (**117**) afforded *E*-vinyl silane **115** in 50 % yield (Scheme 1.43).<sup>64</sup> Initially, DMPU was used as an additive in THF to decrease toxicity. However, trimethylsilyl lithium could not be formed under these conditions, and use of HMPA was required.

**Scheme 1.43.** Silyl cupration of propargyl methyl ether (**117**) to yield *E*-vinyl silane **115**.



To synthesize *Z*-vinyl silane **116**, we began with a simple silylation of propargyl ether **117** to yield propargyl silane **113** in 75 % yield (Table 1.7).<sup>65</sup> Initially, hydroboration-protodeborylation was attempted for selective *cis* reduction.<sup>66</sup> *Z*-Vinyl silane **116** was observed by <sup>1</sup>H NMR spectroscopy but was not isolable from the residual borane byproducts by flash chromatography. Hydrogenation with Lindlar's catalyst yielded an inseparable mixture of **115** and **116**. Selective reduction to vinyl silane **118** was achieved with DIBAL-H in 90 % yield.<sup>67</sup>

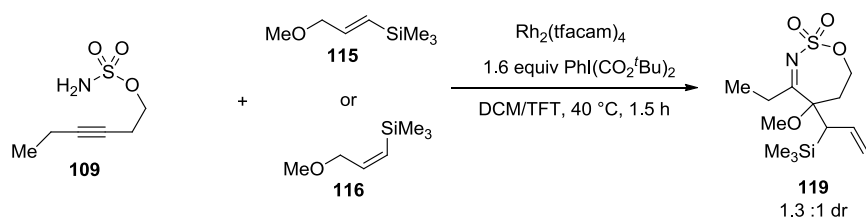
**Table 1.7.** Synthesis of vinyl silanes **116** and **115**.

reagents	solvent	yield (%)	products
$\text{HB}(\text{Hex})_2$ , AcOH	THF	nd	<b>116</b>
$\text{H}_2$ , Lindlar's cat.	MeOH	nd	<b>115</b> + <b>116</b>
1. DIBAL, 2. $\text{H}_2\text{SO}_4$	$\text{Et}_2\text{O}$	90 %	<b>116</b>

Both  $E$ - and  $Z$ -vinylsilanes **115** and **116** were competent reaction partners for the cascade. Under standard conditions, both **115** and **116** gave equivalent yields of 39 % (Table 1.8, entries 1 and 2,) with diastereoselectivities of 1.3:1 and 1:1.3. The vinyl silane geometry translated into selectivity for the major diastereomer, with vinyl silanes **115** and **116** giving opposite major diastereomers of imine **119**. The diastereomers were again inseparable by column chromatography and relative stereochemistry was not determined.

By increasing the excess of vinyl silane **116** from 6 equivalents to 12, the yield was boosted to 43 % (entry 3). The reaction was run in 80% trifluorotoluene/20 % dichloromethane (due to results discussed in Table 1.11) with no improvement (Table 1.8, entry 4). Increasing catalyst loading from 5 to 10 mol % with 6 equivalents of vinyl silane **116** gave a yield of 40 %, and increasing both equivalents of vinyl silane **116** and catalyst loading gave comparable yields (entries 5 and 6).

**Table 1.8.** Intermolecular metallonitrene/alkyne cascade optimization with vinyl silanes **115** and **116** and sulfamate **109**.



entry	allyl ether	DCM (%)	equiv allyl ether	cat. loading (mol %)	yield (%) <sup>a</sup>	dr
1	<b>116</b>	0 %	6	5 mol %	39 %	1.3:1
2	<b>115</b>	0 %	6	5 mol %	39 %	1:1.3
3	<b>116</b>	0 %	12	5 mol %	43 %	1.3:1
4	<b>116</b>	20 %	12	5 mol %	43 %	1.3:1
5	<b>116</b>	0 %	6	10 mol %	40 %	1.3:1
6	<b>116</b>	0 %	12	10 mol %	37 %, 41 %	1.3:1


<sup>a</sup>Isolated yield of **119** after silica gel chromatography.

After establishing the viability of terminating the metallonitrene/alkyne cascade with a vinyl silane, we turned our attention to the introduction of an allylic stereocenter, which had not been previously examined in either the intermolecular or intramolecular cascade.

3-Methoxybut-1-ene was selected as the target allyl ether for introducing an allylic stereocenter. Methyl-substitution for the allylic stereocenter was selected to provide the least potential steric hindrance for the cascade, with the methyl ether for consistency. To synthesize 3-methoxybut-1-ene (**120**), we first applied conditions reported in the literature for deprotonation of alcohol **121** with potassium hydroxide and methylation with methyl iodide (Table 1.9, entry 1).<sup>68</sup> Though it was observed by crude <sup>1</sup>H NMR spectroscopy, methyl ether **126** was not able to be isolated. Using *n*-butyllithium as the base and increasing the equivalents of methyl iodide did not yield any isolable product (entry 2).<sup>69</sup> Finally, under the conditions previously established for

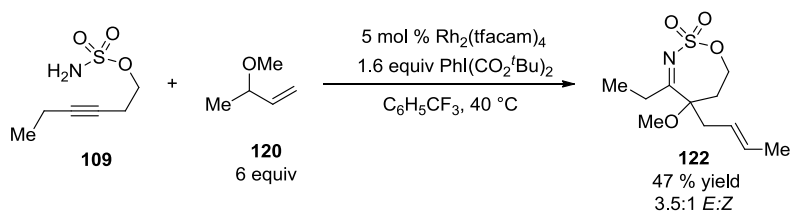
methylation of alcohol **112**, methyl ether **120** was successfully synthesized, albeit in low yield over two trials (entry 3). The low yields likely arose from the significant volatility of methyl ether **120**.

**Table 1.9.** Synthesis of chiral allyl ether **120**.

		
entry	conditions	yield (%)
1	1) 4 equiv KOH, 2) 2 equiv MeI	trace
2	1) 1 equiv <sup>t</sup> BuLi, 2) 8 equiv MeI	trace
3	1) 1.7 equiv NaH, 2) 1 equiv MeI	12,17

Carrying out the intermolecular cascade reaction with chiral allyl ether **120** was successful, proceeding in 47 % yield of imine **122** in a 3.5:1 *E:Z* ratio, as determined by the <sup>1</sup>H NMR spectrum (Scheme 1.44).

**Scheme 1.44.** Intermolecular cascade reaction with chiral ether **120** to yield imine **122**.



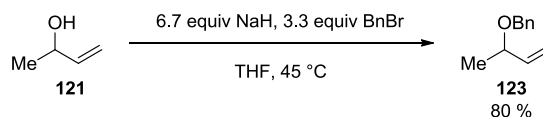
After establishing the reaction's tolerance for the introduction of an allylic stereocenter in allyl ether **120**, we next sought to synthesize enantiomerically enriched cascade products through transfer of stereochemical information from an enantiomerically pure allyl ether. While the cascade reaction proceeded in moderate



yield with ether **120**, the purification difficulties in its synthesis were a concern in producing enantiomerically enriched allyl ether **120** without sacrificing precious enantiomerically enriched starting material. Also, incorporation of a benzyl-protected alcohol into the oxathiazepine product would make it more versatile for further transformations. For these reasons, benzyl allyl ether **123** was employed in studies on the usage of an enantiomerically enriched allyl ether (Scheme 1.45).

Previous use of benzyl allyl ether in the intermolecular cascade reaction indicated that the allyl group would migrate preferentially to the benzyl group (Table 1.4). Benzyl protection of racemic but-3-en-2-ol with excess sodium hydride and benzyl bromide proceeded in 80 % yield to give benzyl ether **123** (Scheme 1.45).<sup>70</sup>

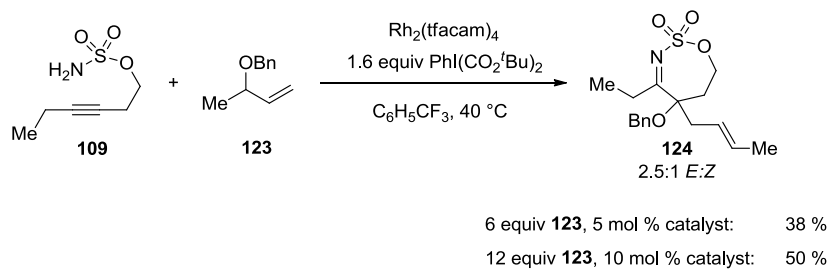
**Scheme 1.45.** Synthesis of benzyl ether **123**.



The cascade reaction with benzyl ether **123** under standard conditions of 6 equivalents **123** and 5 mol % catalyst loading gave racemic imine **124** in 38 % yield and 2.5:1 *E:Z* ratio, with a slightly reduced yield compared to termination with methyl ether **120** (Scheme 1.46). The difference in yield between methyl ether **120** and benzyl ether **123** is reflective of the difference in efficiency previously observed between the unsubstituted benzyl ether and methyl ether as well (75 % and 52 %, respectively; Table 1.6 and Scheme 1.48). This disparity may be attributed to competing 1,2 benzyl migration (though products of this migration were not isolated). However, increasing the

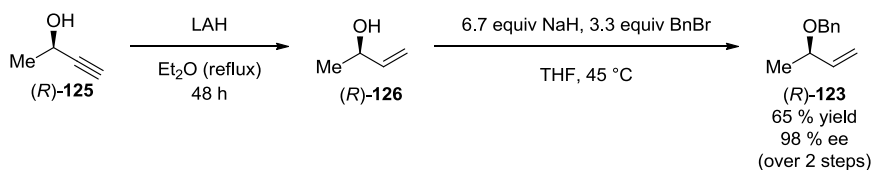
catalyst loading from 5 mol % to 10 mol % and equivalents of benzyl ether **123** from 6 equivalents to 12 equivalents resulted in a significant increase in yield to 50 % oxathiazepine **124**.

**Scheme 1.46.** Intermolecular cascade reaction with benzyl ether **123**.



Synthesis of the enantiomerically enriched allyl ether **123** began from commercially available propargyl alcohol (*R*)-**125**. Reduction with LAH<sup>71</sup> to afford allyl alcohol (*R*)-**126** and subsequent benzyl protection provided benzyl allyl ether (*R*)-**123** in 65 % yield over two steps (Scheme 1.47).

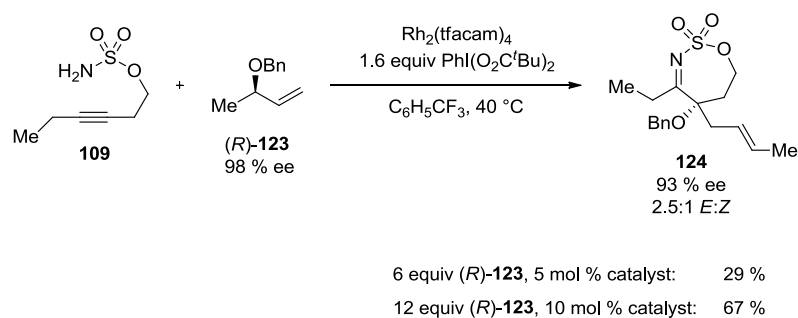
**Scheme 1.47.** Synthesis of enantiomerically enriched benzyl ether (*R*)-**123**.



Cascade termination with enantiomerically enriched benzyl ether (*R*)-**123** yielded 29 % imine **124** under standard conditions with an *E:Z* ratio of 2.5:1 (Scheme 1.48). To our delight, stereochemical information was transferred through the [2,3]-Wittig rearrangement, resulting in 93 % ee. This represents only a slight loss of enantiomeric

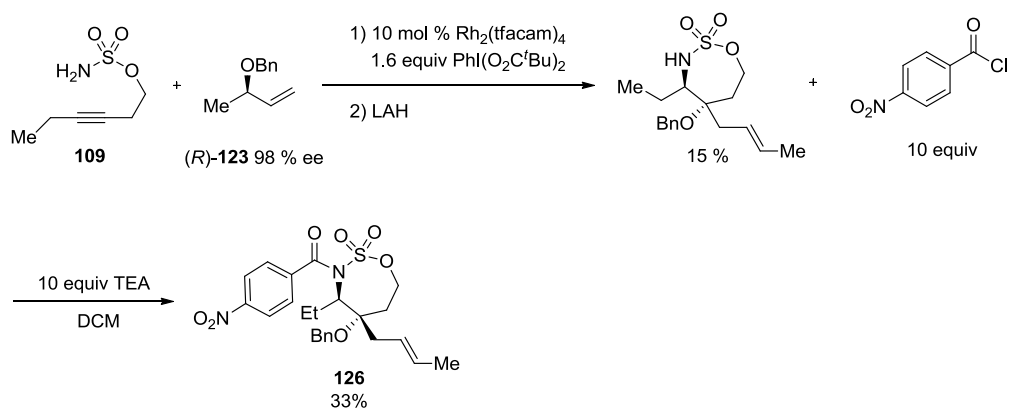
purity from the 98 % ee of allyl ether (*R*)-**123**. Again, when catalyst loading was increased to 10 mol % and excess allyl ether to 12 equivalents, the yield increased to 67 % and enantioselectivity was constant.

**Scheme 1.48.** Intermolecular cascade reaction with enantiomerically enriched benzyl allyl ether (*R*)-**123**.



Imine **124** was a crystalline solid, but, unfortunately, we were not able to obtain X-ray quality crystals. Formation of a derivative was attempted to determine the absolute stereochemistry of oxathiazepine **124** by *in situ* reduction with lithium aluminum hydride and acylation with 4-nitrobenzoyl chloride. Although 33 % of the amide **126** was produced, the amide **126** did not yield crystals suitable for X-ray crystallography (Scheme 1.49).

**Scheme 1.49.** Derivatization of oxathiazepine **124** with 4-nitrobenzyl chloride for crystallization.



In the absence of an X-ray crystal structure, literature precedent for the [2,3]-Wittig rearrangement of enantiomerically enriched allyl ethers was used for transition state analysis to assign the absolute stereochemistry of imine **124** (Figure 1.9).<sup>72,73</sup> Based on the demonstrated preference for keeping the methyl group equatorial shown in the Wittig reaction of alkyne **127**,<sup>73</sup> we qualitatively predict transition state TS<sub>1</sub> to be lower in energy, resulting in (*S*)-**124**.

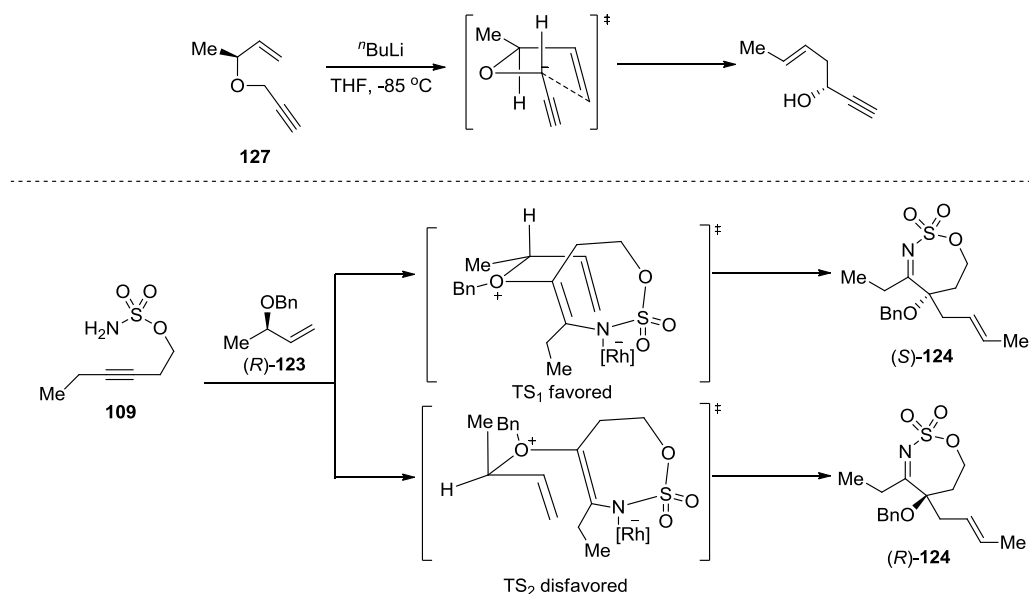
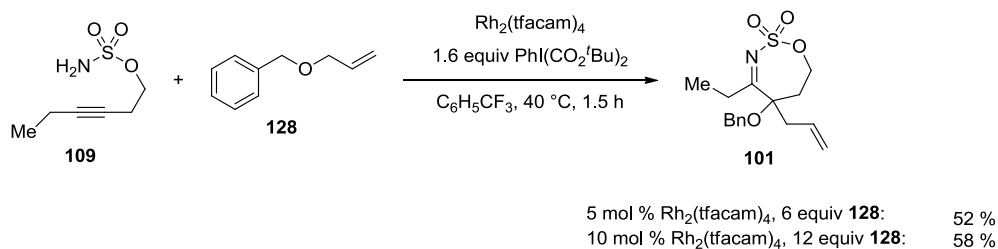


**Figure 1.9.** Literature precedent for [2,3]-Wittig rearrangement of enantiomerically enriched allyl ether **127** (top)<sup>73</sup> with stereochemical models for metallonitrene/alkyne cascade reaction.

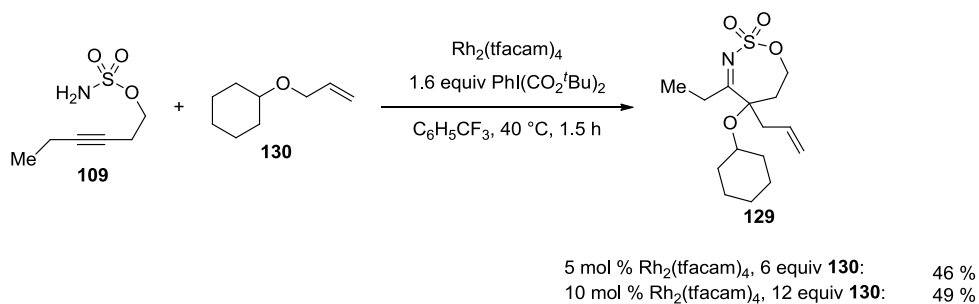
Based on our results that increasing the catalyst loading to 10 mol %  $\text{Rh}_2(\text{tfacam})_4$  and the excess of allyl ether to 12 equivalents improved the cascade yield for imines **119** and **124**, we wished to examine previous substrates (Table 1.4) utilizing these conditions. Additionally, our new chromatography conditions (1 % acetic acid) may provide us with yields that would be an improvement to what was previously reported.<sup>56</sup> Yield of imine **101** with benzyl allyl ether (**128**) under improved purification conditions was comparable at 52 % (Scheme 1.50; from 51 % yield, Scheme 1.39). Increasing the equivalents of allyl ether **128** from 6 to 12 and catalyst loading to 10 mol % increased the yield to 58 %.

**Scheme 1.50.** Benzyl allyl ether (**128**) metallonitrene/alkyne cascade termination to yield imine **101**.



Likewise, the improved flash chromatography conditions did not provide significant improvement in yield of imine **129** with cyclohexyl allyl ether (**130**, Scheme 1.51; from 43 % yield, Table 1.4). Increasing the catalyst loading and excess of allyl ether **130** improved the yield somewhat to 49 % imine **129**.

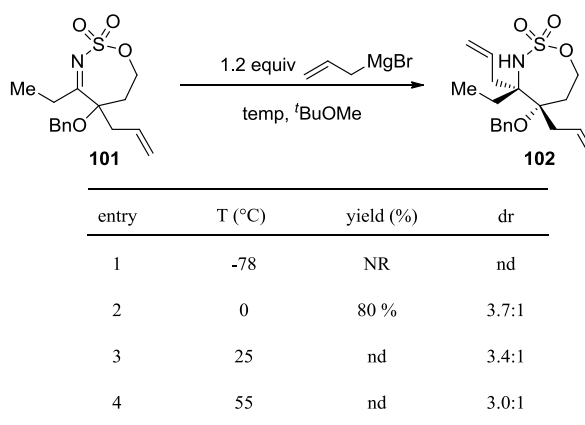
**Scheme 1.51.** Cyclohexyl allyl ether (**130**) metallonitrene/alkyne cascade termination.



As discussed previously, one of the more surprising initial results in the intermolecular metallonitrene/alkyne cascade, was the report of an unusual inverse temperature dependence with regard to the stereoselectivity of Grignard addition to imine **101** (Table 1.5).<sup>56</sup> However, upon repetition of these experiments, a more conventional temperature dependence was observed, with the reaction showing a slight decrease in

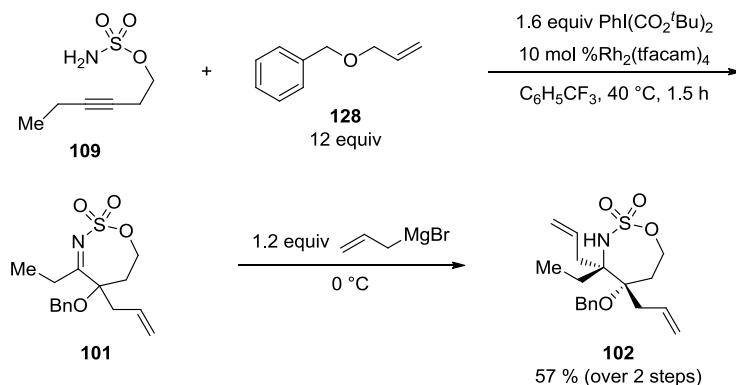
selectivity with increasing temperature (Table 1.10). Upon review of the crude  $^1\text{H}$  NMR spectra for the data presented in Table 1.5, peaks had been previously misidentified and incorrect peaks were integrated in calculating the diastereoselectivity. These data were therefore determined to be invalid. The optimal yield and selectivity were found at 0 °C with a yield of 80 % of **102** and diastereoselectivity of 3.7:1 (entry 4).

**Table 1.10.** Temperature dependence of diastereoselectivity of Grignard addition to imine **101**.



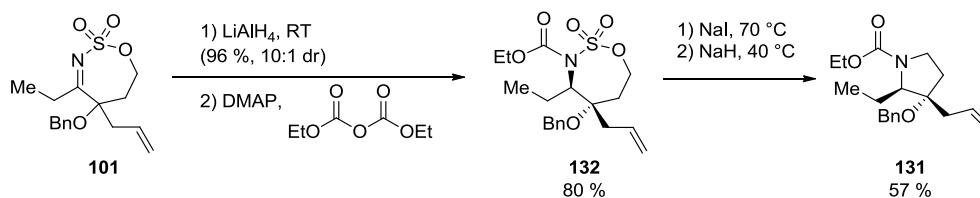
We also found the Grignard addition could be accomplished *in situ* following the cascade reaction, without intermediate purification. This *in situ* addition resulted in an increased overall yield of 57 % yield, likely due to the increased stability of amine **102**, compared to imine **101** (Scheme 1.52).

**Scheme 1.52.** Metallonitrene/alkyne cascade with *in situ* Grignard addition to imine **101**.



Previous work established an activation and ring-opening procedure for the oxathiazepane ring to produce an array of cyclic and acyclic building blocks out of the rich functionality of the cascade products (Scheme 1.41). Unfortunately, characterization data could not be found for the pyrrolidine **131**, which had been formed on a very small scale (2.3 mg). After reduction and *N*-acylation of imine **101** to form amide **132**, nucleophilic ring-opening and sulfur trioxide extrusion with sodium iodide was followed by ring-closing displacement of iodide. Pyrrolidine **131** was formed in 57 % on a larger scale (13 mg; Scheme 1.53).

**Scheme 1.53.** Oxathiazepane ring-opening/ring-closing reaction to form pyrrolidine **131**.





## 1.4 Viroallosecurinine Core Synthesis

We next sought to apply our intermolecular metallonitrene/alkyne cascade methodology to the synthesis of complex molecules. The cascade rapidly generates 1,2-aminoxygenated centers with excellent stereoselectivity following selective reduction. These stereocenters are analogous to those at the center of the azabicyclo[3.2.1] ring system of viroallosecurinine, a member of the *Securinega* alkaloids (Figure 1.10). Using substrate-controlled stereoselectivity, we investigated an enantioselective synthesis of viroallosecurinine.

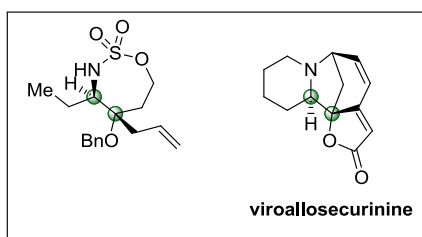


**Figure 1.10.** Comparison of reduced metallonitrene/alkyne cascade product with viroallosecurinine.

### 1.4.1. Previous Syntheses of *Securinega* Alkaloids

The *Securinega* alkaloids are a class of molecules for which we propose the intermolecular metallonitrene/alkyne cascade reaction could provide a streamlined synthetic sequence (Figure 1.11). This class of more than 50 members has been known for more than 50 years and has been shown biologically active.<sup>74</sup> The plants from which these alkaloids are derived have been employed in a variety of traditional Chinese

medicines.<sup>75</sup> For example, securinine, the most studied member of the class, has been shown to have central nervous system activity, as well as antimalarial and antibacterial activity.<sup>76-79</sup>

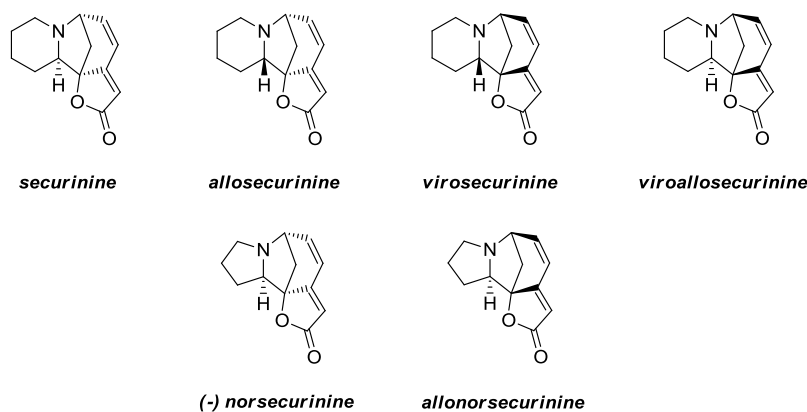


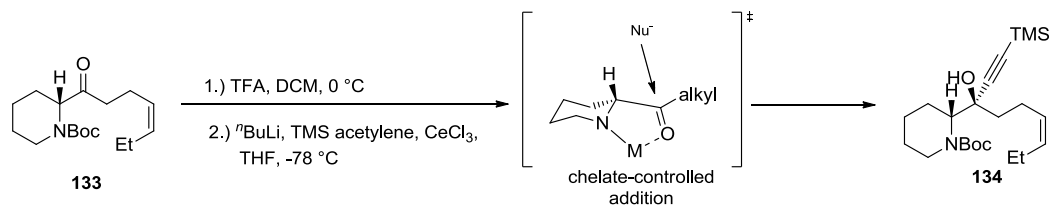
**Figure 1.11.** Representative members of the *Securinega* alkaloids.<sup>74</sup>

The intermolecular metallonitrene/alkyne cascade reaction has great potential as an elegant entry into this class of molecules through the generation of the 1,2-amino oxygenated stereocenters central to the class. Due to the predicted enantioselectivity and observed diastereoselectivity in reduction of the cascade products, as well as the potential for forming the adjoining six-membered ring, viroallosecurinine is the most attractive target molecule of this class. Though viroallosecurinine and its enantiomer allosecurinine have been synthesized previously, elegantly setting the 1,2-amino oxygenated stereocenters remains an outstanding goal.<sup>80,81</sup>

Viroallosecurinine was first synthesized by Honda and coworkers in 2004, starting from optically active ketone intermediate **133** (Scheme 1.54).<sup>82</sup> Similar to their previous synthesis of (-)-securinine,<sup>83</sup> intermediate **133** was derived from (+)-pipercolinic acid. Upon chelation-controlled addition of TMS-acetylene to intermediate **133**, a single

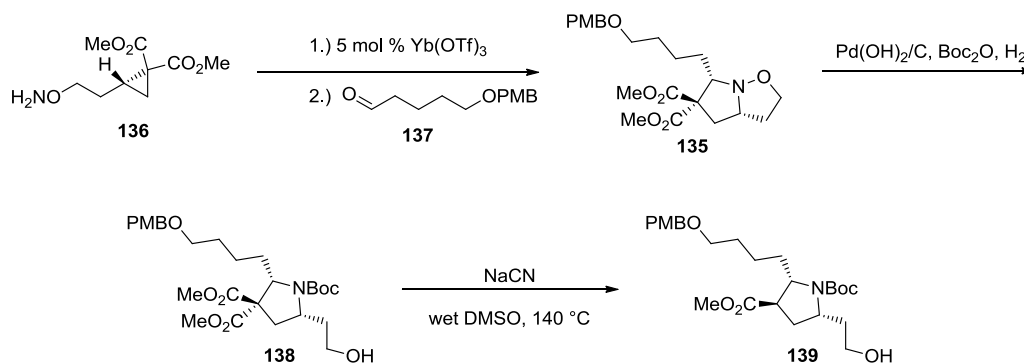
enantiomer of alcohol **134** was generated. Following the setting of these stereocenters, seven additional steps produced viroallosecurinine, for a total of 14 steps.

**Scheme 1.54.** Honda and coworkers' synthesis of viroallosecurinine: key step for generation of 1,2-amino oxygenated stereocenters.<sup>82</sup>



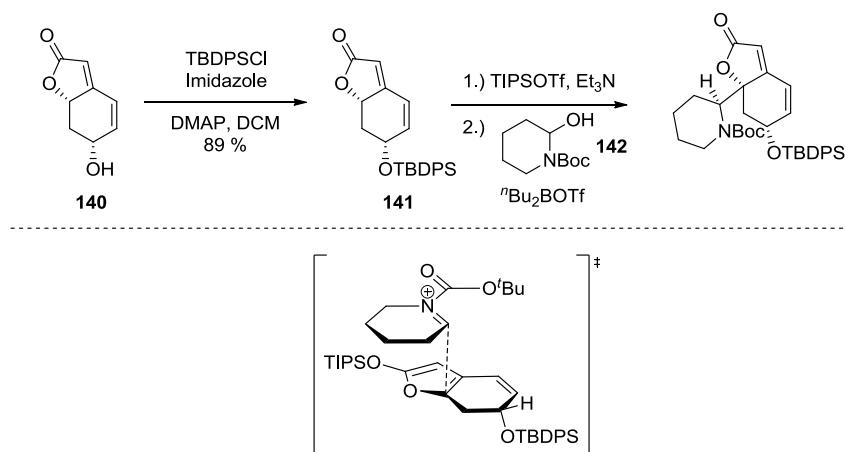
The first synthesis of allosecurinine was reported in 2008 by Kerr and coworkers.<sup>84</sup> The key step they identified allowed access to 2,5-*cis* pyrroloisoxazolidine **135** from enantiomerically pure cyclopropane **136** (Scheme 1.55). Optically active cyclopropane **136** was obtained via asymmetric dihydroxylation and subsequent manipulation of the diol. The amine stereocenter was set from cyclization of cyclopropane **136** and treatment with protected aldehyde **137**, to yield **135**. The oxygenated stereocenter was generated in Krapcho decarboxylation of geminal diester **138**, to yield the thermodynamic product, monoester **139**. The complete synthesis yielded allosecurinine in an overall yield of 5 % in 22 steps from commercially available material.

**Scheme 1.55.** Key steps of Kerr and coworkers' synthesis of allosecurinine.<sup>84</sup>



In 2008, Busqué, de March and coworkers applied methods from previous syntheses of natural products (+)- and (-)-menisdaurilide to synthesize allosecurinine and viroallosecurinine from common intermediates.<sup>85</sup> Intermediate **140** (with the oxygenated stereocenter in place), from a previously reported synthesis of menisdaurilide, was protected and then treated with TIPSOTf and triethylamine to generate silyloxyfuran **141** (Scheme 1.56).<sup>86</sup> The key step of this synthesis involved a Mannich reaction of **141** and the piperidinium ion generated from **142**. The Mannich reaction yielded two diastereomers (out of four possible) that were separable by column chromatography. The observed selectivity was credited to an *endo* Diels-Alder-like transition state, with the acyliminium ion approaching from the opposite face of the furan to the OTBDPS group of **141** (the identities of the minor diastereomers were not established). While separation of the diastereomers was possible, it leaves room for improvement in selectivity in future syntheses. The overall synthesis was completed in 14 steps with an overall 4.4 % yield for allosecurinine and 3.8 % for viroallosecurinine.

**Scheme 1.56.** Key steps of Busqué, de March, and coworkers' synthesis of viroallosecurinine and allosecurinine.<sup>85,86</sup>

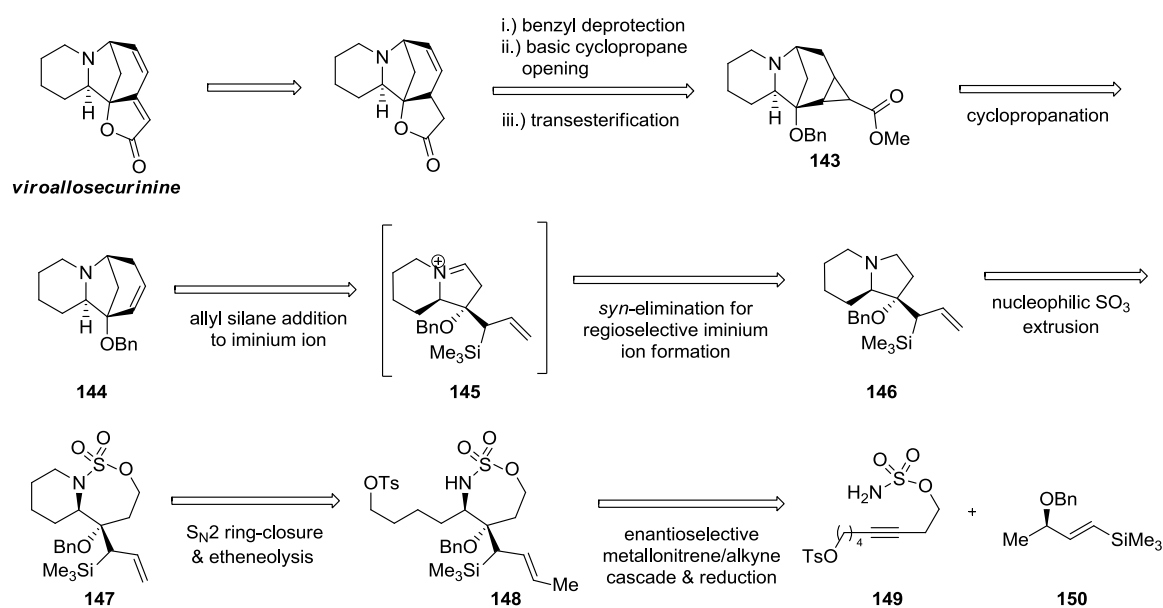


Therefore, while both allosecurinine and viroallosecurinine have been synthesized previously, a route involving our intermolecular metallonitrene/alkyne cascade reaction as the key step has the potential to both streamline the synthesis and provide access in sequential steps to the key 1,2-amino oxygenated stereocenters of these molecules.

#### 1.4.2 Retrosynthetic Analysis of Viroallosecurinine and Preliminary Results

Utilizing our metallonitrene/alkyne cascade reaction, we designed a streamlined and versatile route to viroallosecurinine, which may easily be adapted to allosecurinine as well. The key transformation will be the generation of oxathiazepane **143** via the intermolecular metallonitrene/alkyne cascade and subsequent reduction (Scheme 1.57).

**Scheme 1.57.** Retrosynthesis of viroallosecurinine using the intermolecular metallonitrene/alkyne cascade.



From cyclopropane **143**, benzyl deprotection, followed by a base-induced cyclopropane opening/transesterification/oxidation sequence is planned to furnish viroallosecurinine (Scheme 1.57). Cyclopropane **143** will be afforded from cyclopropanation of alkene **144**. Ring-closure of iminium **145** to tricyclic core **144** is made possible by the installation of the allylic trimethylsilyl group during the intramolecular cascade reaction, to increase the nucleophilicity of the terminal alkene.<sup>87</sup> Iminium ion **145** will be generated by a selenation/oxidation sequence of **146**, followed by selective *syn* oxidation to eliminate the hydrogen aligned with the nitrogen lone pair (Figure 1.12). Bicyclic amine **146** will be supplied by nucleophilic extrusion of SO<sub>3</sub> with NaI from bicyclic intermediate **147**. S<sub>N</sub>2 ring-closure of the primary tosylate of oxathiazepane **148**, followed by ruthenium-catalyzed etheneolysis of the olefinic methyl will yield intermediate **147**. Amine **148** is produced from diastereoselective reduction

with lithium aluminum hydride from the oxygenated face of the cascade product produced by sulfamate ester **149** and enantiomerically enriched allyl ether **150**. Transfer of stereochemistry from allyl ether **150** sets the oxygenated stereocenter in the cascade product.

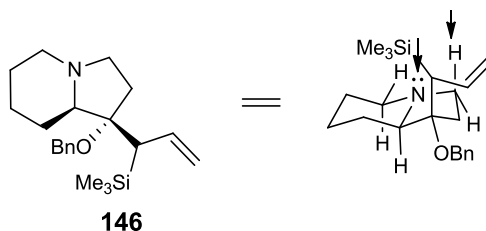


**Figure 1.12.** Three-dimensional representation of amine **147** for selective oxidation.

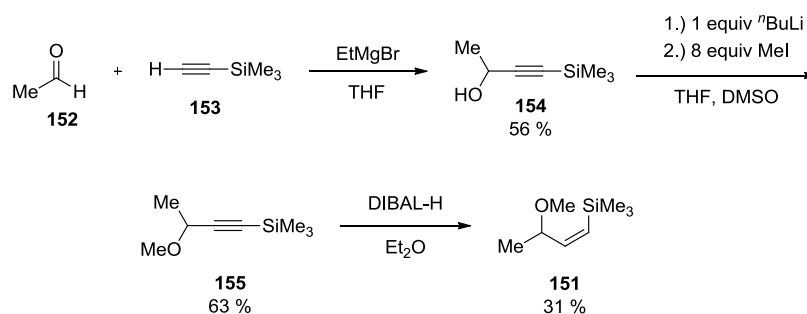
To address enantioselectivity, we will employ a chiral allyl ether to induce stereochemistry at the quaternary stereocenter during the [2,3]-Wittig rearrangement that concludes the cascade. This stereocenter will then determine the chirality at the amine stereocenter via the diastereoselectivity of the subsequent lithium aluminum hydride reduction. One minor drawback of this method is the residual olefinic methyl in oxathiazepane **143**. However, removal should be possible, as ruthenium-catalyzed ethenolysis has been shown effective with similar substrates.<sup>88</sup>

In considering this synthesis, we identified both the introduction of chirality in the product by stereochemical transfer in the [2,3]-Wittig rearrangement and the utilization of vinyl silanes to generate allyl silane products as important extensions of the intermolecular cascade that required investigation.

In order to provide proof of principle for the first key transformation, racemic vinyl silane **151** was synthesized, incorporating both the necessary allylic stereocenter

and vinyl silane functionality (Scheme 1.58). A methyl ether was again employed to allow for direct comparison with previously used vinyl silanes. Beginning with acetaldehyde (**152**), trimethylsilyl acetylene (**153**) was deprotonated with EtMgBr, which then underwent addition to **152** in 56 % yield of propargyl alcohol **154**.<sup>89</sup> Methylation of propargyl alcohol **154** was accomplished with *n*-butyl lithium and methyl iodide in large excess to give propargyl ether **155**.<sup>69</sup> Finally, DIBAL-H reduction of the ether **155** yielded exclusively *Z*-vinyl silane **151** in 31 % yield.

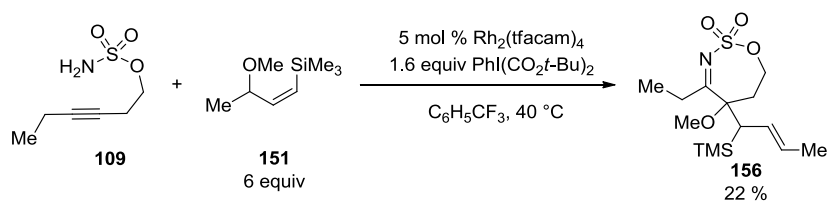
**Scheme 1.58.** Synthesis of racemic chiral vinyl silane **151**.



Unfortunately, when racemic vinyl silane **151** was used to terminate the metallonitrene/alkyne cascade under standard conditions with sulfamate ester **109**, the yield decreased sharply from that observed for both vinyl silanes **115** and **116** (Scheme 1.59; compare to 43 %, Table 1.8). Imine **156** was formed in 22 % yield, possibly due to accumulation of steric effects from the combination of both olefinic and allylic substituents. Overlapping peaks of the <sup>1</sup>H NMR spectrum made determination of the ratio of the four inseparable diastereomeric products unfeasible.

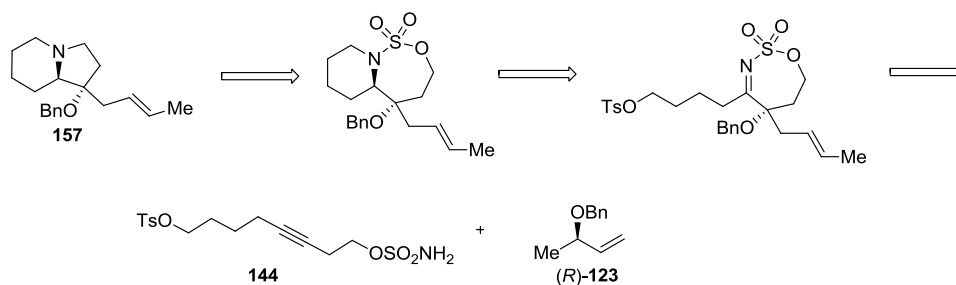


**Scheme 1.59.** Intermolecular metallonitrene/alkyne cascade with chiral vinyl silane **151** to form oxathiazepine **156**.



Due to this poor result, we decided to instead apply the intermolecular metallonitrene/alkyne cascade to a streamlined synthesis of the viroallosecurinine bicyclic core **157**, rather than a longer synthesis of the complete natural product (Scheme 1.60). Similar to the previous retrosynthesis, the key step of this synthesis is the intermolecular metallonitrene/alkyne cascade reaction with sulfamate ester **144** and previously synthesized benzyl allyl ether (*R*)-**123** for substrate-based transfer of stereochemical information.

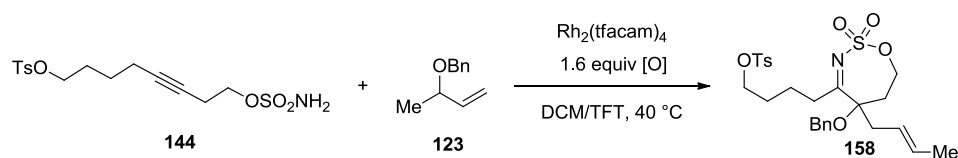
**Scheme 1.60.** Retrosynthetic analysis of viroallosecurinine core **157**.



### 1.4.3 Streamlined Route to Viroallosecurinine Core

Under standard cascade conditions, the reaction of racemic benzyl allyl ether **123** and sulfamate ester **144** initially proceeded with only 15 % yield of imine **155** (Table 1.11, entry 1). However, we recognized sulfamate ester **144** exhibited low solubility in trifluorotoluene. Addition of a 15 % dichloromethane as a co-solvent resulted in improved solubility of sulfamate ester **144** and improved the yield by 20 % (entry 2). Use of 20 % dichloromethane gave a slight increase in yield to 37 % with complete solubility of sulfamate ester **144** (entry 3). Further additions of dichloromethane (50 % and 100 % dichloromethane) did not improve the yield further (entries 4 and 5). Increasing the excess of allyl ether **123** to 12 equivalents and increased catalyst loading to 10 mol % resulted in slight increases in yield (42 % and 44 %, respectively; entries 6 and 8). However, the combined effect of increasing allyl ether excess and catalyst loading resulted in an improved yield of imine **158** (59 %, entry 9).

**Table 1.11.** Optimization of intermolecular metallonitrene/alkyne cascade with sulfamate ester **144**.

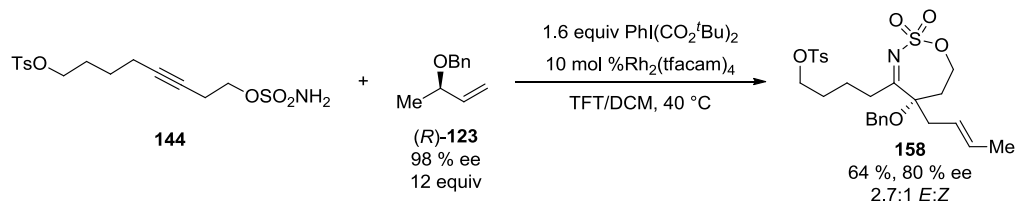


entry	DCM (%)	equiv <b>123</b>	oxidant	cat. loading (%)	yield (%) <sup>a</sup>
1	0	6	$\text{PhI}(\text{CO}_2^t\text{Bu})_2$	5 mol %	15 %
2	15	6	$\text{PhI}(\text{CO}_2^t\text{Bu})_2$	5 mol %	35 %
3	20	6	$\text{PhI}(\text{CO}_2^t\text{Bu})_2$	5 mol %	37 %
4	50	6	$\text{PhI}(\text{CO}_2^t\text{Bu})_2$	5 mol %	34 %
5	100	6	$\text{PhI}(\text{CO}_2^t\text{Bu})_2$	5 mol %	37 %
6	20	12	$\text{PhI}(\text{CO}_2^t\text{Bu})_2$	5 mol %	42 %
7	20	6	$\text{PhI}(\text{tpa})_2$	5 mol %	27 %
8	20	6	$\text{PhI}(\text{CO}_2^t\text{Bu})_2$	10 mol %	44 %
9	20	12	$\text{PhI}(\text{CO}_2^t\text{Bu})_2$	10 mol %	59 %

<sup>a</sup>Isolated yield of **158** after silica gel chromatography.

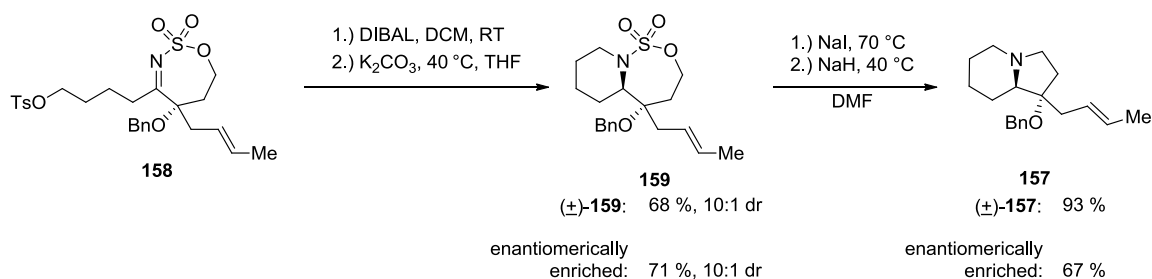
With enantiomerically enriched benzyl allyl ether (*R*)-**123**, enantiomerically enriched imine **158** was furnished in 64 % yield under optimized conditions (Scheme 1.61). The olefin geometry of **158** was determined to be 2.7:1 *E:Z* by <sup>1</sup>H NMR spectroscopy.

**Scheme 1.61.** Intermolecular cascade reaction with sulfamate ester **144** and enantiomerically enriched benzyl ether **123**.



Following cyclization, oxathiazepine **158** was reduced in 10:1 dr with DIBAL-H and treated with  $K_2CO_3$  in THF, leading to an intramolecular  $S_N2$  displacement of the primary tosylate to afford bicyclic amine **159** in 68 % yield from racemic oxathiazepine **158** and 71 % yield from enantiomerically enriched oxathiazepine **158** (Scheme 1.62). For the reduction, hydride delivery was determined by NOE experiments to occur from the same face as the  $\alpha$ -oxygenated center.

**Scheme 1.62.** Viroallosecurinine core ring system synthesis.



Following assignment of all protons through COSY, NOE experiments conducted on bicyclic amine **159** revealed the correlations identified in Figure 1.13.

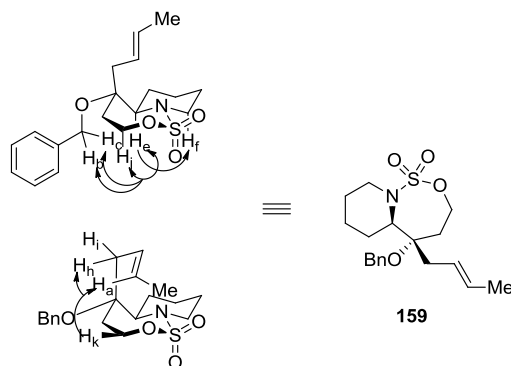


**Figure 1.13.** NOE correlations of ring-closed product **159**.

From bicycle **159**, sequential nucleophilic extrusion of sulfur trioxide with sodium iodide and ring-closing displacement of iodide formed the pyrrolidine ring of octahydroindolizine **157** in 93 % yield with racemic bicyclic amine **159** and 67 % with enantiomerically enriched **159** (Scheme 1.62).<sup>90</sup> **157** represents the enantioenriched core of viroallosecurinine with the challenging vicinal amino alcohol stereocenters appropriately set.

## 1.5 Conclusions

In conclusion, we have expanded the methodology for the intermolecular metallonitrene/alkyne cascade, as well as completed a synthesis of the bicyclic viroallosecurinine core **157**. The cascade reaction was systematically optimized, and the reaction conditions and purification were revised, increasing the yield for most substrates. The substrate scope has been expanded to more highly substituted allyl ethers than those previously studied, including both olefinic and allylic substitution. Substrate-controlled transfer of stereochemical information has been established, providing cascade products in excellent enantiomeric excess. These developments are important not only for future applications of the intermolecular metallonitrene/alkyne cascade reaction, but also as an important expansion in the field of metallonitrene chemistry, capable of streamlining the synthesis of complex nitrogen-containing molecules.

In terms of future work, catalyst-controlled enantioselectivity has not yet been investigated, though it is possible intramolecularly with  $\text{Rh}_2(\text{biTISP})_2$  (Scheme 1.35). Extending the cascade reaction to chiral catalysis would not only broaden its applicability

in general, but also allow the required cascade for the total synthesis without the necessity of the allylic stereocenter. As we have shown, vinyl silanes without allylic substitution were tolerated in decent yields; however, incorporation of the allylic methyl group necessary for transfer of stereochemical information resulted in a dramatic decrease in yield. The development of an appropriate chiral catalyst would enable the use of vinyl silanes in an efficient synthesis of viroallosecurinine with our cascade reaction as the key step would again be more feasible.

Further mechanistic studies would also be of interest. Computational modeling of the rhodium nitrenoid species that initiates the cascade could provide insight into the nature of the nitrene. Preliminary calculations indicated formation of a triplet nitrene, rather than a singlet as had been previously theorized. Radical-trapping experiments could investigate this hypothesis.

Additional methods of trapping the metallonitrene/alkyne intermediate could be pursued intermolecularly. The intermolecular cascade should be investigated in any context  $\alpha$ -iminocarbenes are used.

## 1.6. Experimental Procedures and Compound Characterization

### General Information.

$^1\text{H}$  and  $^{13}\text{C}$  NMR spectra were recorded on a Varian Inova 600 spectrometer (600 MHz  $^1\text{H}$ , 150 MHz  $^{13}\text{C}$ ) and a Varian Inova 400 spectrometer (400 MHz  $^1\text{H}$ , 100 MHz  $^{13}\text{C}$ ) at room temperature in  $\text{CDCl}_3$  (neutralized and dried with anhydrous  $\text{K}_2\text{CO}_3$ ) with internal  $\text{CHCl}_3$  as the reference (7.27 ppm for  $^1\text{H}$  and 77.23 ppm for  $^{13}\text{C}$ ). Chemical shifts ( $\delta$  values) were reported in parts per million (ppm) and coupling constants ( $J$  values) in Hz. Multiplicity is indicated using the following abbreviations: s = singlet, d = doublet, t = triplet, q = quartet, qn = quintet, sext = sextet, m = multiplet, br = broad signal. ). Infrared (IR) spectra were recorded using Thermo Electron Corporation Nicolet 380 FT-IR spectrometer. High-resolution mass spectra were obtained using a Thermo Electron Corporation Finigan LTQFTMS (at the Mass Spectrometry Facility, Emory University). Gas chromatography (GC) was carried out on an Agilent 6850 Network GC System equipped with a CHIRASIL-DEX CB column. High performance liquid chromatography (HPLC) was carried out on an Agilent 1100 Series equipped with a Chirasil Chiralpak AS-H column and a variable wavelength detector. We acknowledge the use of shared instrumentation provided by grants from the NIH and the NSF. Analytical thin layer chromatography (TLC) was performed on precoated glass backed EMD 0.25 mm silica gel 60 plates. Visualization was accomplished with UV light or ethanolic anisaldehyde, followed by heating. Flash column chromatography was carried out using Silicycle® silica gel 60 (40-63  $\mu\text{m}$ ).

All reactions were conducted with anhydrous solvents in oven-dried and nitrogen- or argon-charged glassware. Anhydrous solvents were purified by passage through activated alumina using a *Glass Contours* solvent purification system unless otherwise noted. Benzene, DMSO, DMA, DMF, and TFT were dried over activated 4 Å molecular sieves. Solvents for workup, extraction and column chromatography were used as received from commercial suppliers. All reagents were purchased from Sigma-Aldrich and used as received unless otherwise noted.  $\text{PhI}(\text{O}_2\text{C}^t\text{Bu})_2$  and  $\text{PhI}(\text{OAc})_2$  were dried under vacuum (0.02 mmHg) for 12 hours prior to use. Pyridine, 2,6-lutidine, and HMPA were purified by distillation from calcium hydride.  $\text{Rh}_2(\text{OAc})_4$  was purchased from Strem. Other rhodium catalysts were purchased from Sigma-Aldrich and used as received.

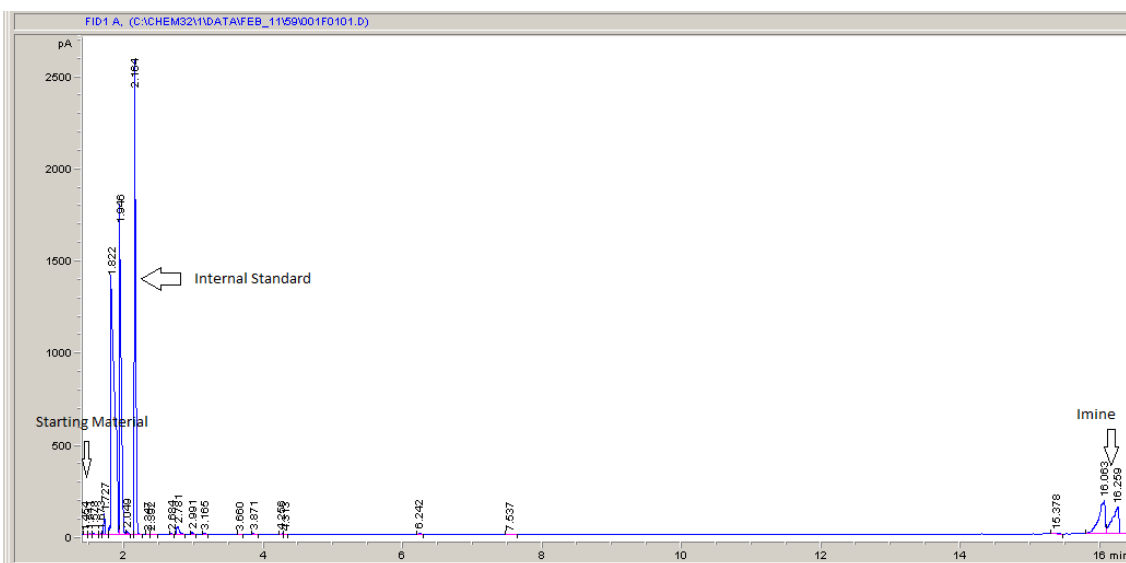


**$\text{Rh}_2(\text{tfacam})_4$ .** Prepared according to the literature,<sup>90</sup> using  $\text{Rh}_2(\text{OAc})_4$  (141 mg, 0.325 mmol) and  $\text{CF}_3\text{CONH}_2$  (4.6 g, 0.41 mol). 189 mg  $\text{Rh}_2(\text{tfacam})_4$  was isolated in 89 % yield (cf. 82 % reported).  $^{19}\text{F}$  NMR, IR, and HRMS were identical to those reported. **IR** (thin film,  $\text{cm}^{-1}$ ) 3650, 2174, 2096, 1667, 1268, 1200, 1164, 851, 730;  **$^{19}\text{F}$  NMR** (282 MHz,  $\text{CD}_3\text{CN}$ ,  $\text{C}_6\text{H}_5\text{CF}_3$  standard at -63.7 ppm) -75.5; **HRMS** (+ESI) calculated for  $\text{C}_8\text{H}_4\text{F}_{12}\text{N}_4\text{O}_4\text{Rh}_2$  653.8151, found 655.89253 [M+2].



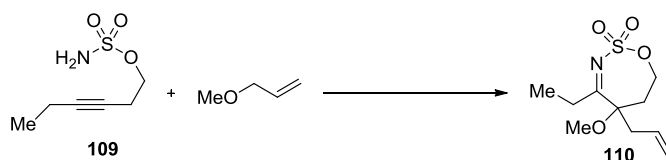
### GC Optimization of Intermolecular Cascade (Table 1.6)

Rh<sup>II</sup> catalyst (5 mol %) in solvent (0.025 M) was stirred in a round bottom flask at 40 °C. A solution of hex-3-yn-1-sulfamate (**109**, 1 equiv), oxidant (1.6 equiv), and methyl allyl ether (6 equiv) in solvent (0.025 M) was added via syringe pump over 1.5 h. After complete addition, the reaction was stirred for 5 min. The reaction mixture was then concentrated onto a pad of SiO<sub>2</sub> and immediately flushed with 20 mL EtOAc, followed by addition of 1 eq. internal standard 3,5-dimethylanisole. A 1 mL aliquot was analyzed by gas chromatography (CHIRASIL DEX, 120 → 200 °C, 5 °C/min), and percent yield was calculated using the conversion factor of 1.15 peak ratio of oxathiazepine **110** (*t*<sub>r</sub>: 16.0 min and 16.2 min) to 3,5-dimethylanisole (*t*<sub>r</sub>: 2.16 min). Percent conversion was calculated using the conversion factor of 1.07 peak ratio of sulfamate ester **109** (*t*<sub>r</sub>: 1.42 min) to 3,5-dimethylanisole to give percent sulfamate ester **109** consumed.



**General procedure (A) for intermolecular cascade termination.**  $\text{Rh}_2(\text{tfacam})_4$  (5 mol %) in  $\text{CF}_3\text{C}_6\text{H}_5$  (0.025 M) was stirred in a round bottom flask at 40 °C. A solution of sulfamate ester (1 equiv),  $\text{PhI}(\text{O}_2\text{C}^t\text{Bu})_2$  (1.6 equiv), and allyl ether (6 equiv) in  $\text{CF}_3\text{C}_6\text{H}_5$  (0.025 M) was added via syringe pump over 1.5 h. After complete addition, the reaction was stirred until thin layer chromatography indicated complete consumption of starting sulfamate ester (0.5-2 h). Once judged to be complete, the reaction mixture was concentrated onto a pad of  $\text{SiO}_2$  and immediately purified by flash column chromatography on silica gel as indicated, with an additive of 1 % HOAc.

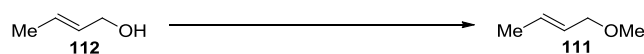
**General procedure (B) for intermolecular cascade termination.**  $\text{Rh}_2(\text{tfacam})_4$  (10 mol %) in  $\text{CF}_3\text{C}_6\text{H}_5$  (0.025 M) was stirred in a round bottom flask at 40 °C. A solution of sulfamate ester (1 equiv),  $\text{PhI}(\text{O}_2\text{C}^t\text{Bu})_2$  (1.6 equiv), and allyl ether (12 equiv) in  $\text{CF}_3\text{C}_6\text{H}_5$  (0.025 M) was added via syringe pump over 1.5 h. After complete addition, the reaction was stirred until thin layer chromatography indicated complete consumption of starting sulfamate ester (0.5-2 h). Once judged to be complete, the reaction mixture was concentrated onto a pad of  $\text{SiO}_2$  and immediately purified by flash column chromatography on silica gel as indicated, with an additive of 1 % HOAc.



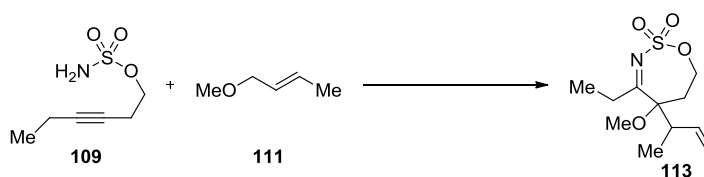
**5-allyl-4-ethyl-5-methoxy-6,7-dihydro-5H-1,2,3-oxathiazepine 2,2-dioxide (110).**

Prepared by general procedure A using hex-3-yn-1-sulfamate<sup>54</sup> (**109**, 50 mg, 0.28 mmol),  $\text{PhI}(\text{O}_2\text{C}^t\text{Bu})_2$  (0.18 g, 0.451 mmol), and  $\text{Rh}_2(\text{tfacam})_4$  (9.2 mg, 0.014 mmol). Flash

chromatography (5:1 hexanes/EtOAc with 1 % HOAc) afforded oxathiazepine **110** as a colorless oil (51 mg, 75 %);  $R_f$  0.45 (3:1 hexanes: EtOAc); **IR** (thin film,  $\text{cm}^{-1}$ ) 2980, 2197, 2027, 1627, 1365, 1180;  $^1\text{H NMR}$  ( $\text{CDCl}_3$ , 400 MHz)  $\delta$  5.96-5.85 (m, 1H), 5.23-5.18 (m, 2H), 4.41 (ddd,  $J = 11.4, 6.9, 1.2$  Hz, 1H), 4.27 (m, 1H), 3.25 (s, 3H), 2.98-2.87 (m, 1H), 2.78 (dq,  $J = 30.5, 11.9$  Hz, 1H), 2.62-2.50 (m, 3H), 1.97 (dd,  $J = 15.3, 12.5$  Hz, 1H), 1.12 (t,  $J = 7.2$  Hz, 3H);  $^{13}\text{C NMR}$  ( $\text{CDCl}_3$ , 75 MHz)  $\delta$  84.6, 77.0, 73.9, 69.4, 19.8, 14.2, 12.5; **HRMS** (+ESI) calculated for  $\text{C}_{10}\text{H}_{18}\text{NO}_4\text{S}$  248.0962, found 248.09508  $[\text{M}+\text{H}]^+$ .

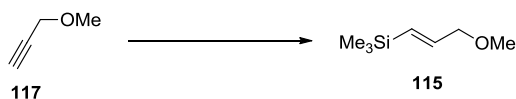


**(E)-1-methoxybut-2-ene (111)**. Prepared according to the literature,<sup>59</sup> using (*E*)-but-2-en-1-ol (**112**, 1.85 mL, 21.7 mmol), NaH (1.5 g of a 60 % dispersion, 38 mmol), and MeI (1.74 mL, 28.0 mmol). 0.289 g **111** was isolated in 15 % yield (cf. 93 % reported).  $^1\text{H NMR}$  was identical to that reported.<sup>59</sup>  $^1\text{H NMR}$  ( $\text{CDCl}_3$ , 400 MHz)  $\delta$  5.72 (dq,  $J = 15.9, 6.4$  Hz, 1H), 5.56 (dt,  $J = 15.9, 6.2$  Hz, 1H), 3.83 (dt,  $J = 6.2, 1$  Hz, 2H), 3.30 (s, 3H), 1.76 (dd,  $J = 6.4, 1.2$  Hz, 3H).



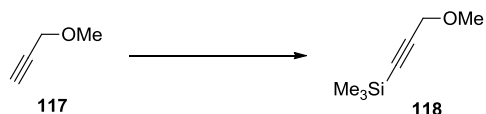
**5-(but-3-en-2-yl)-4-ethyl-5-methoxy-6,7-dihydro-5H-1,2,3-oxathiazepine 2,2-dioxide (113)**. Prepared according to general procedure A using hex-3-yn-1-yl sulfamate<sup>54</sup> (**109**, 30 mg, 0.17 mmol),  $\text{PhI}(\text{O}_2\text{C}^t\text{Bu})_2$  (0.11 g, 0.28 mmol), (*E*)-1-methoxybut-2-ene (**111**,

85 mg, 0.99 mmol), and  $\text{Rh}_2(\text{tfacam})_4$  ( 5.9 mg, 0.009 mmol). Flash chromatography (5:1 hexane/EtOAc with 1 % HOAc) afforded two separable diastereomers of **113**: (23 mg, 51 %) and (15 mg, 34 %):  $R_f$  0.29 (3:1 hexanes/EtOAc); **IR** (thin film,  $\text{cm}^{-1}$ ) 2975, 2939, 1625, 1460, 1368, 1179;  **$^1\text{H NMR}$**  ( $\text{CDCl}_3$ , 400 MHz)  $\delta$  5.89 (ddd,  $J = 17.3, 10.3, 9.2$  Hz, 1H), 5.18-5.09 (m, 2H), 4.40-4.34 (m, 2H), 3.27 (s, 3H), 2.96-2.81 (m, 2H), 2.76 (ddd,  $J = 14.9, 11.5, 7.6$  Hz, 1H), 2.5 (dq,  $J = 18.4, 7$  Hz, 1H), 1.96 (ddd,  $J = 12, 3.7, 2.2$  Hz, 1H), 1.14 (t,  $J = 7.0$  Hz, 3H), 1.07 (d,  $J = 6.7$  Hz, 3H);  **$^{13}\text{C NMR}$**  ( $\text{CDCl}_3$ , 100 MHz)  $\delta$  193.8, 138.7, 117.3, 86.2, 64.5, 53.2, 44.1, 31.8, 31.4, 16.3, 10.2; **HRMS** (-ESI) calculated for  $\text{C}_{11}\text{H}_{18}\text{O}_4\text{NS}$  260.0962, found 260.09615  $[\text{M}-\text{H}]^-$ ; and  $R_f$  0.25 (3:1 hexanes/EtOAc); **IR** (thin film,  $\text{cm}^{-1}$ ) 2975, 1625, 1368, 1179, 1100;  **$^1\text{H NMR}$**  ( $\text{CDCl}_3$ , 400 MHz)  $\delta$  5.87 (ddd,  $J = 17.2, 10.1, 8.7$  Hz, 1H), 5.08-4.99 (m, 2H), 4.43 (ddd,  $J = 11.4, 6.3, 1.8$  Hz, 1H), 4.27 (td,  $J = 12.1, 4.1$  Hz, 1H), 3.26 (s, 3H), 2.81 (dtd,  $J = 14.7, 12.0, 6.7$  Hz, 3H), 2.44-2.33 (m, 1H), 2.03 (ddd,  $J = 15.2, 4.2, 1.7$  Hz, 1H), 1.09-1.01 (m, 6H);  **$^{13}\text{C NMR}$**  ( $\text{CDCl}_3$ , 100 MHz)  $\delta$  194.2, 138.0, 116.9, 87.6, 64.6, 53.2, 43.2, 31.5, 30.8, 15, 9.6; **HRMS** (-ESI) calculated for  $\text{C}_{11}\text{H}_{18}\text{O}_4\text{NS}$  260.0962, found 260.09615  $[\text{M}-\text{H}]^-$ .

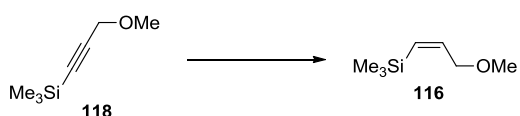


**(E)-(3-methoxyprop-1-en-1-yl)trimethylsilane (115)**. Prepared according to the literature,<sup>64</sup> using hexamethyldisilane (7.2 mL, 35.2 mmol), MeLi (24 mL, 28 mmol), CuCN (1.26 g, 14.1 mmol) and 3-methoxyprop-1-yne (**117**, 1.1 mL, 13.0 mmol). 0.174 g **115** was isolated in 50 % yield (cf. 41 % reported).  $^1\text{H NMR}$  was identical to that

reported.<sup>64</sup>  $^1\text{H NMR}$  (400 MHz;  $\text{CDCl}_3$ )  $\delta$  6.07 (dt,  $J = 18.8, 4.9$  Hz, 1H), 5.91 (dt,  $J = 18.8, 1.4$  Hz, 1H), 3.93 (dd,  $J = 4.9, 1.5$  Hz, 2H), 3.34 (s, 3H), 0.06 (s, 9H).

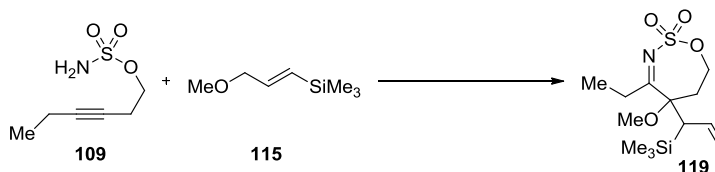


**(3-methoxyprop-1-yn-1-yl)trimethylsilane (118).** Prepared according to a procedure modified from the literature.<sup>65</sup> To a mixture of  $n\text{BuLi}$  (5.6 mL, 10.5 mmol), and THF (8 mL) was added 3-methoxyprop-1-yne (117, 1.0 mL, 11.8 mmol) at  $-50$  °C with stirring. The mixture was allowed to warm up to room temperature for 45 min and trimethylsilyl chloride (1.3 mL, 10.2 mmol) was then added at  $-20$  °C. The mixture was stirred for 60 min while warming up to room temperature and added to a mixture of ether (10 mL) and saturated  $\text{NH}_4\text{Cl}$  (10 mL). The organic layer was separated, washed with phosphate buffer (pH 7) and water, and dried over  $\text{Na}_2\text{SO}_4$ . Concentration *in vacuo* and distillation afforded 0.883 g 118 in 53 % yield as a colorless oil.  $^1\text{H NMR}$  was identical to that reported.<sup>91</sup>  $^1\text{H NMR}$  ( $\text{CDCl}_3$ , 400 MHz)  $\delta$  4.08 (s, 2H), 3.37 (s, 3H), 0.17 (s, 9H).

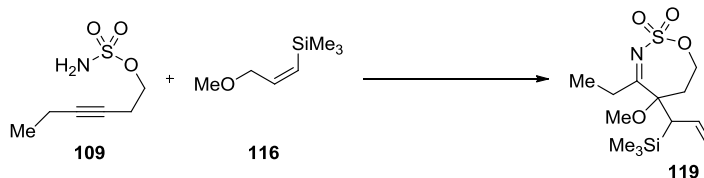


**(Z)-(3-methoxyprop-1-en-1-yl)trimethylsilane (116).** Prepared according to the literature,<sup>67</sup> using (3-methoxyprop-1-yn-1-yl)trimethylsilane (118, 1.34 g, 9.42 mmol) and DIBAL-H (16 mL, 11 mmol). 1.22 g 116 was isolated in 90 % yield (cf. 91 % reported).  $^1\text{H NMR}$  was identical to that reported.  $^1\text{H NMR}$  ( $\text{CDCl}_3$ , 400 MHz)  $\delta$  6.37 (dt,  $J = 14.5,$

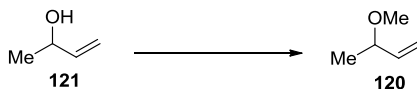
6.3 Hz, 1H), 5.73 (dt,  $J = 14.5, 1.4$  Hz, 1H), 3.97 (dd,  $J = 6.3, 1.6$  Hz, 2H), 3.32 (s, 3H), 0.11 (s, 9H).



**4-ethyl-5-methoxy-5-(1-(trimethylsilyl)allyl)-6,7-dihydro-5H-1,2,3-oxathiazepine 2,2-dioxide (119).** Prepared according to general procedure A using hex-3-yn-1-yl sulfamate<sup>54</sup> (**109**, 31 mg, 0.18 mmol),  $\text{PhI}(\text{O}_2\text{C}^t\text{Bu})_2$  (0.12 g, 0.282 mmol), (*E*)- (3-methoxyprop-1-en-1-yl)trimethylsilane (0.15 g, 1.02 mmol), and  $\text{Rh}_2(\text{tfacam})_4$  (5.5 mg, 0.008 mmol). Flash chromatography (5:1 hexane/EtOAc with 1 % HOAc) afforded the title compound as a colorless oil (22 mg, 39 %) with a diastereomeric ratio of 1.3:1 inseparable diastereomers;  $R_f$  0.23 (3:1 hexanes/EtOAc); **IR** (thin film,  $\text{cm}^{-1}$ ) 2953, 2255, 2039, 1715, 1624, 1368, 1181;  **$^1\text{H NMR}$**  ( $\text{CDCl}_3$ , 400 MHz)  $\delta$  6.07 (ddd,  $J = 17.4, 7.6, 5.5$  Hz, 1H), 5.89-5.80 (m, 1H), 5.02-4.89 (m, 1H), 4.39 (ddd,  $J = 12.0, 6.1, 1.2$  Hz, 1H), 4.22 (ddd,  $J = 12.2, 4.6, 1.2$  Hz, 1H), 3.26 (s, 3H), 2.83-2.72 (m, 2H), 2.65-2.50 (m, 2H), 1.94 (ddd,  $J = 14.9, 4.6, 1.2$  Hz, 1H), 1.1 (t,  $J = 7.0$  Hz, 3H), 0.04 (s, 9H);  **$^{13}\text{C NMR}$**  ( $\text{CDCl}_3$ , 100 MHz)  $\delta$  192.9, 138.9, 133.8, 118.0, 89.1, 64.7, 52.9, 42.1, 32.5, 9.6; -0.3 (3C); **HRMS** (-ESI) calculated for  $\text{C}_{13}\text{H}_{24}\text{O}_4\text{NSSi}$  318.12008, found 318.12056 [M-H]<sup>-</sup>.

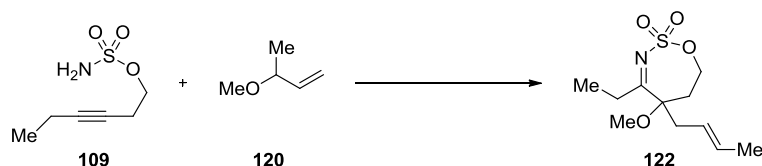


**4-ethyl-5-methoxy-5-(1-(trimethylsilyl)allyl)-6,7-dihydro-5H-1,2,3-oxathiazepine 2,2-dioxide (119).** Prepared according to general procedure B using hex-3-yn-1-yl sulfamate<sup>54</sup> (**109**, 31 mg, 0.18 mmol),  $\text{PhI}(\text{O}_2\text{C}^t\text{Bu})_2$  (0.11 g, 0.28 mmol), (Z)-(3-methoxyprop-1-en-1-yl)trimethylsilane (**116**, 0.30 g, 2.0 mmol), and  $\text{Rh}_2(\text{tfacam})_4$  (5.5 mg, 0.008 mmol). Flash chromatography (5:1 hexane/EtOAc with 1 % HOAc) afforded the title compound as a colorless oil (24 mg, 43 %) with a diastereomeric ratio of 1:1.3 inseparable diastereomers;  $R_f$  0.23 (3:1 hexanes/EtOAc); **IR** (thin film,  $\text{cm}^{-1}$ ) 2949, 2251, 2035, 1698, 1375, 1190; **<sup>1</sup>H NMR** ( $\text{CDCl}_3$ , 400 MHz)  $\delta$  6.07 (ddd,  $J = 18.4, 7.6, 5.3$  Hz, 1H), 5.89-5.78 (m, 1H), 5.12-5.03 (m, 1H), 4.39 (ddd,  $J = 11.7, 7.0, 1.2$  Hz, 1H), 4.25 (ddd,  $J = 12.3, 4.5, 1.2$  Hz, 1H), 3.26 (s, 3H), 2.95-2.76 (m, 2H), 2.66-2.48 (m, 2H), 2.05 (ddd,  $J = 14.9, 3.9, 0.8$  Hz, 1H), 1.21 (t,  $J = 7.0$  Hz, 3H), 0.06 (s, 9H); **<sup>13</sup>C NMR** ( $\text{CDCl}_3$ , 100 MHz)  $\delta$  193.9, 138.5, 137.3, 118.4, 89.1, 65.0, 53.1, 44.6, 32.5, 10.2, -0.3 (3C); **HRMS** (-ESI) calculated for  $\text{C}_{13}\text{H}_{24}\text{O}_4\text{NSSi}$  318.12008, found 318.12056  $[\text{M}-\text{H}]^-$ .

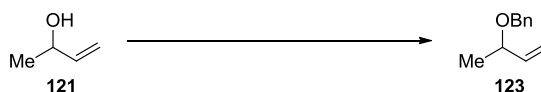


**3-methoxybut-1-ene (120).** Prepared according to conditions modified from the literature,<sup>59</sup> using but-3-en-2-ol (**121**, 0.5 mL, 5.77 mmol), NaH (400 mg of a 60 % dispersion, 10 mmol), and MeI (360  $\mu\text{L}$ , 5.8 mmol). 84 mg **120** was isolated in 17 % yield. **<sup>1</sup>H NMR** was identical to that reported.<sup>92</sup> **<sup>1</sup>H NMR** ( $\text{CDCl}_3$ , 400 MHz)  $\delta$  5.7 (ddd,

$J = 17.3, 10.1, 7.4$  Hz, 1H), 5.19-5.11 (m, 2H), 3.72-3.66 (m, 1H), 3.26 (s, 3H), 1.22 (d,  $J = 6.3$  Hz, 3H).



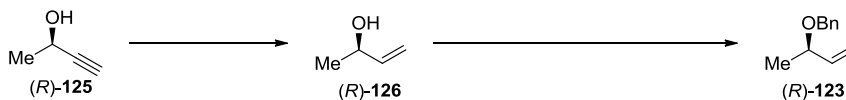
**5-(but-2-en-1-yl)-4-ethyl-5-methoxy-6,7-dihydro-5H-1,2,3-oxathiazepine 2,2-dioxide (122).** Prepared according to general procedure A using hex-3-yn-1-yl sulfamate<sup>54</sup> (**109**, 31 mg, 0.17 mmol),  $\text{PhI}(\text{O}_2\text{C}^t\text{Bu})_2$  (0.11 g, 0.27 mmol), 3-methoxybut-1-ene (**120**, 88 mg, 1.0 mmol), and  $\text{Rh}_2(\text{tfacam})_4$  (5.4 mg, 0.008 mmol). Flash chromatography (5:1 hexane/EtOAc with 1 % HOAc) afforded the title compound as a colorless oil (21.3 mg, 47 %) with an *E:Z* ratio of 3.5:1 inseparable isomers;  $R_f$  0.44 (3:1 hexanes/EtOAc); **IR** (thin film,  $\text{cm}^{-1}$ ) 2974, 2939, 2139, 1627, 1366, 1182; **<sup>1</sup>H NMR** ( $\text{CDCl}_3$ , 400 MHz)  $\delta$  5.61-5.56 (m, 1H), 5.52 (ddd,  $J = 7.9, 5.6, 1.4$  Hz, 1H), 4.4 (ddd,  $J = 11.3, 6.8, 1.4$  Hz, 1H), 4.26 (td,  $J = 12, 4.5$  Hz, 1H), 3.24 (s, 3H), 2.88 (dq,  $J = 14.9, 7.04, 0.78$  Hz, 1H), 2.76 (dq,  $J = 19, 7.1$  Hz, 1H), 2.64-2.39 (m, 3H), 1.97 (ddd,  $J = 14.9, 4.7, 1.2$  Hz, 1H), 1.68 (dd,  $J = 6.3, 0.8$  Hz, 3H), 1.11 (t,  $J = 7.2$  Hz, 3H); **<sup>13</sup>C NMR** ( $\text{CDCl}_3$ , 100 MHz)  $\delta$  193.6, 130.9, 123.5, 85.1, 64.7, 52.9, 38.5, 31.4, 30.2, 18.3, 10.2; **HRMS** (-ESI) calculated for  $\text{C}_{11}\text{H}_{18}\text{NO}_4\text{S}$  260.09620, found 260.09653  $[\text{M}-\text{H}]^-$ .



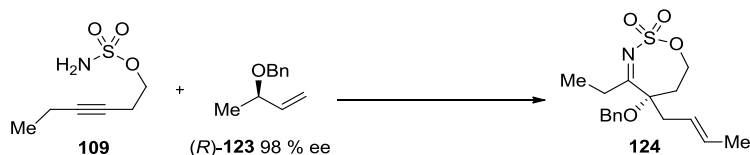
**((but-3-en-2-yloxy)methyl)benzene (123).** Prepared according to the literature,<sup>70</sup> using 3-buten-2-ol (**121**, 3.0 mL, 34.6 mmol), benzyl bromide (14.0 mL, 114 mmol), and NaH



(9 g of a 60 % dispersion, 225 mmol). 2.8 g **123** was isolated in 80 % yield (cf. 67 % reported);  $^1\text{H NMR}$  was identical to that reported.<sup>70</sup>  $^1\text{H NMR}$  ( $\text{CDCl}_3$ , 400 MHz)  $\delta$  7.34-7.25 (m, 5H), 5.78 (ddd,  $J = 17.4, 10.4, 7.4$  Hz, 1H), 5.23-5.14 (m, 2H), 4.56 (d,  $J = 12.1$  Hz, 1H), 4.38 (d,  $J = 11.7$  Hz, 1H), 3.95-3.87 (m, 1H), 1.28 (d,  $J = 6.7$  Hz, 3H).

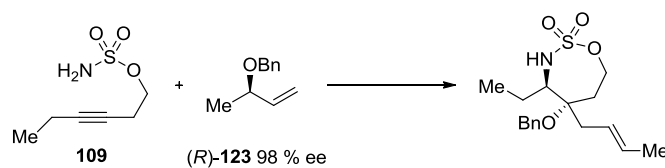


**(R)-((but-3-en-2-yloxy)methyl)benzene ((R)-123)**. A solution of (*R*)-3-butyn-2-ol (**125**) in  $\text{Et}_2\text{O}$  (2 mL) was added dropwise to a solution of LAH (4.6 mL, 1 M in  $\text{Et}_2\text{O}$ ) at 0 °C. The reaction was warmed to reflux and heated overnight. The reaction was quenched with Rochelle's salt (aq.) and extracted with  $\text{Et}_2\text{O}$ , dried, and concentrated *in vacuo*. The crude residue was dissolved in THF (8 mL) and added to a solution of NaH (1.5 g, 38.2 mmol) and benzyl bromide (2.24 mL, 18.8 mmol) in THF (23 mL) over 20 minutes. The reaction was quenched after 1 hour and purified by flash chromatography (99:1 hexanes/ $\text{EtOAc}$ ) to give **123** (601 mg, 65 % yield over 2 steps);  $^1\text{H NMR}$  was identical to that reported above.<sup>70</sup>



**5-(benzyloxy)-5-(but-2-en-1-yl)-4-ethyl-6,7-dihydro-5H-1,2,3-oxathiazepine 2,2-dioxide (124)**. Prepared according to general procedure B using hex-3-yn-1-yl sulfamate<sup>54</sup> (**109**, 0.12 g, 0.67 mmol),  $\text{PhI}(\text{O}_2\text{C}^t\text{Bu})_2$  (0.43 g, 1.07 mmol), (*R*)-((but-3-en-2-yloxy)methyl)benzene (**123**, 0.65 g, 4.01 mmol), and  $\text{Rh}_2(\text{tfacam})_4$  (23 mg, 0.04

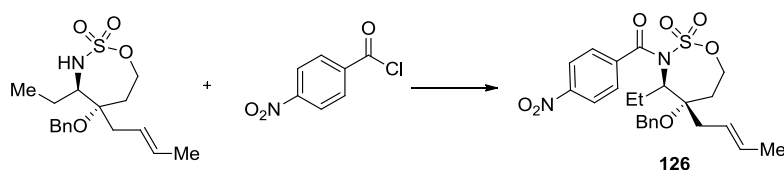
mmol). Flash chromatography (5:1 hexane/EtOAc with 1 % HOAc) afforded **124** as a white amorphous solid (84 mg, 29 %) with an *E:Z* ratio of 2.5:1 inseparable isomers and an ee of 93 %;  $R_f$  0.40 (3:1 hexanes/EtOAc); **IR** (thin film,  $\text{cm}^{-1}$ ) 2973, 2937, 1626, 1363, 1178, 1090, 733;  **$^1\text{H NMR}$**  ( $\text{CDCl}_3$ , 400 MHz)  $\delta$  7.40-7.28 (m, 5H), 5.69-5.56 (m, 2H), 4.6 (d,  $J = 11.7$  Hz, 1H), 4.42 (ddd,  $J = 11.7, 7.0, 0.78$  Hz, 1H), 4.33-4.25 (m, 2H), 3.00 (td,  $J = 13.7, 6.7$  Hz, 1H), 2.82 (dd,  $J = 19.2, 7$  Hz, 1H), 2.71-2.48 (m, 3H), 2.1 (dd,  $J = 14.9, 3.9$  Hz, 1H), 1.69 (d,  $J = 4.7$  Hz, 3H), 1.09 (t,  $J = 7.0$  Hz, 3H);  **$^{13}\text{C NMR}$**  ( $\text{CDCl}_3$ , 100 MHz)  $\delta$  193.4, 137.5, 131.1, 128.8, 128.1, 126.8, 123.6, 85.4, 66.8, 64.9, 38.8, 32.3, 30.5, 18.4, 10.3; **HRMS** (-ESI) calculated for  $\text{C}_{17}\text{H}_{22}\text{O}_4\text{NS}$  336.1275, found 336.12778 [M-H] $^-$ ; **GC** (CHIRASIL DEX, 90  $\rightarrow$  200  $^\circ\text{C}$ , 2  $^\circ\text{C}/\text{min}$ )  $t_r(\text{maj}) = 27.76$  min,  $t_r(\text{min}) = 27.92$  min;  $[\alpha]_D^{20} + 13.4$  ( $c$  2.70,  $\text{CHCl}_3$ ); **GC** (CHIRASIL DEX, 90  $\rightarrow$  200  $^\circ\text{C}$ , 2  $^\circ\text{C}/\text{min}$ )  $t_r(\text{maj}) = 27.76$  min,  $t_r(\text{min}) = 27.92$  min.



**(4*R*,5*S*)-5-(benzyloxy)-5-((*E*)-but-2-en-1-yl)-4-ethyl-1,2,3-oxathiazepane 2,2-dioxide.**

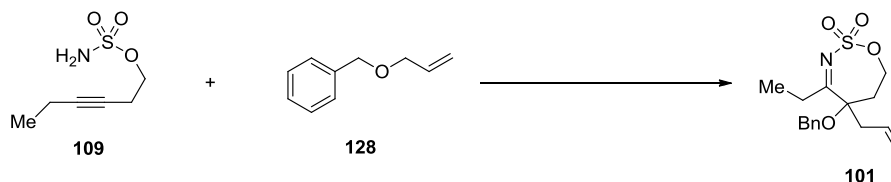
Prepared according to general procedure A using hex-3-yn-1-yl sulfamate<sup>54</sup> (**109**, 190 mg, 1.07 mmol),  $\text{PhI}(\text{O}_2\text{C}^t\text{Bu})_2$  (0.68 g, 1.67 mmol), (*R*)-((but-3-en-2-yloxy)methyl)benzene (**123**, 1.37 g, 8.5 mmol), and  $\text{Rh}_2(\text{tfacam})_4$  (40 mg, 0.06 mmol). The crude residue prior to chromatography was dissolved in THF (1.5 mL) and LAH (1.0 mL, 2.5 M in  $\text{Et}_2\text{O}$ ) was added dropwise at 0  $^\circ\text{C}$ , then warmed to room temperature. After chromatography indicated complete consumption of starting material, the reaction was stirred with Rochelle's salt (aq) and  $\text{Et}_2\text{O}$  and extracted with  $\text{Et}_2\text{O}$ , dried, and

concentrated. Flash chromatography (5:1 hexanes/EtOAc) afforded the title compound as a colorless oil (53 mg, 15 %);  $R_f$  0.28 (5:1 hexanes/EtOAc);  $^1\text{H NMR}$  ( $\text{CDCl}_3$ , 400 MHz)  $\delta$  7.34-7.24 (m, 5H), 5.53 (dd,  $J = 15.3, 6.7$  Hz, 1H), 5.37 (dd,  $J = 15.3, 7.8$  Hz, 1H), 5.21 (br d,  $J = 2.7$  Hz, 1H), 4.47-4.40 (m, 2H), 4.3 (d,  $J = 10.6$ , 1H), 4.11-4.09 (m, 2H), 3.14 (br d,  $J = 12.1$  Hz, 1H), 2.47 (dd,  $J = 15.5, 6.1$  Hz, 1H), 2.23 (dd,  $J = 15.5, 8.0$  Hz, 1H), 1.90-1.82 (m, 1H), 1.65 (d,  $J = 6.3$  Hz, 3H), 1.61-1.56 (m, 1H), 1.08 (t,  $J = 7.0$  Hz, 3H).



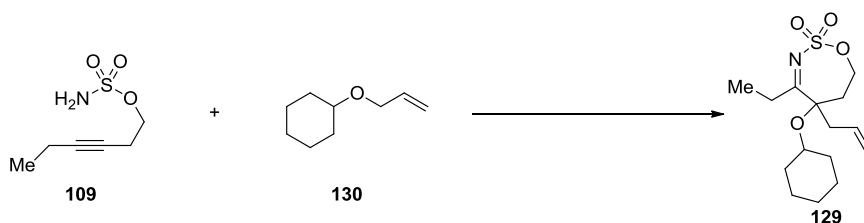
**((4*R*,5*S*)-5-(benzyloxy)-5-((*E*)-but-2-en-1-yl)-4-ethyl-2,2-dioxido-1,2,3-oxathiazepan-3-yl)(4-nitrophenyl)methanone (126).** (4*R*,5*S*)-5-(benzyloxy)-5-((*E*)-but-2-en-1-yl)-4-ethyl-1,2,3-oxathiazepane 2,2-dioxide (53 mg, 0.16 mmol, 1 equiv) was dissolved in DCM (1 mL). Triethylamine (255  $\mu\text{L}$ , 1.8 mmol, 12 equiv) was added to the reaction vessel. 4-Nitrobenzoyl chloride (348 mg, 1.9 mmol, 12 equiv) in DCM (1.5 mL) was added dropwise. The reaction was allowed to stir overnight, then quenched with NaOH (3N aq soln) and extracted with DCM, dried, and concentrated. Flash chromatography (3:1 hexanes:EtOAc  $\rightarrow$  EtOAc) afforded the title compound **126** as a white amorphous solid (25 mg, 33 %);  $R_f$  0.8 (3:1 hexanes/EtOAc);  $^1\text{H NMR}$  ( $\text{CDCl}_3$ , 400 MHz)  $\delta$  8.27 (d,  $J = 8.6$  Hz, 2H), 7.83 (d,  $J = 8.6$  Hz, 2H), 7.35-7.29 (m, 5H), 6.4 (d,  $J = 10.2$  Hz, 1H), 5.70-5.63 (m, 1H), 5.57 (dd,  $J = 8.4, 7.2$  Hz, 1H), 4.52 (d,  $J = 7.0$  Hz, 2H), 4.32 (td,  $J = 10.6, 2.0$  Hz, 1H), 3.73 (td,  $J = 10.8, 5.5$  Hz, 1H), 3.61 (tt,  $J = 10.9, 5.6$  Hz, 1H), 2.48 (d,  $J = 7.0$  Hz, 2H), 2.41-2.31 (m, 1H), 2.27-2.20 (m, 1H), 1.95 (ddd,  $J = 14.1, 7.4,$

2.3 Hz, 1H), 1.71 (d,  $J = 6.3$  Hz, 3H), 0.95 (t,  $J = 7.2$  Hz, 3H); **HRMS** (+ESI) calculated for  $C_{24}H_{29}N_2O_7S$  489.1695, found 489.1801  $[M+H]^+$ .

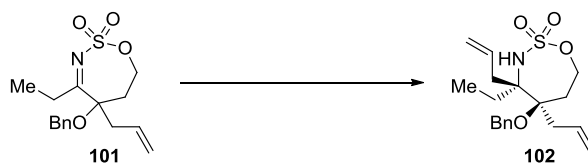


**5-allyl-5-(benzyloxy)-4-ethyl-6,7-dihydro-5H-1,2,3-oxathiazepine 2,2-dioxide (101).**

Prepared by general procedure B using hex-3-yn-1-sulfamate<sup>54</sup> (**109**, 30 mg, 0.17 mmol),  $PhI(O_2C^tBu)_2$  (0.11 g, 0.28 mmol), benzyl allyl ether (**128**, 0.31 mL, 2.0 mmol) and  $Rh_2(tfacam)_4$  (11 mg, 0.017 mmol). Flash chromatography (5:1  $\rightarrow$  3:1 hexanes/EtOAc with 1% HOAc) afforded the title compound as a white amorphous solid (32 mg, 58 %);  $R_f$  0.40 (3:1 hexanes/EtOAc); **IR** (thin film,  $cm^{-1}$ ) 2977, 2937, 1627, 1365, 1181;  **$^1H$  NMR** ( $CDCl_3$ , 600 MHz)  $\delta$  7.40-7.33 (m, 5H), 6.07-6.00 (m, 1H), 5.29-5.26 (m, 2H), 4.62 (d,  $J = 11.4$  Hz, 1H), 4.46 (ddd,  $J = 11.4, 6.7, 1.0$  Hz, 1H), 4.36-4.31 (m, 2H), 3.05 (dt,  $J = 14.8, 6.7$  Hz, 1H), 2.86 (dq,  $J = 19.1, 7.1$  Hz, 1H), 2.72 (ddd,  $J = 14.3, 5.2, 1.0$  Hz, 1H), 2.68-2.60 (m, 2H), 2.13 (dd,  $J = 14.3, 3.8$  Hz, 1H), 1.13 (t,  $J = 7.2$  Hz, 3H);  **$^{13}C$  NMR** ( $CDCl_3$ , 150 MHz)  $\delta$  192.9, 137.3, 131.3, 128.8, 128.1, 126.8, 120.4, 84.9, 66.9, 64.7, 39.9, 32.3, 30.3, 10.3; **HRMS** (+APCI) calculated for  $C_{16}H_{22}NO_4S$  324.1270, found 324.1259  $[M+H]^+$ .



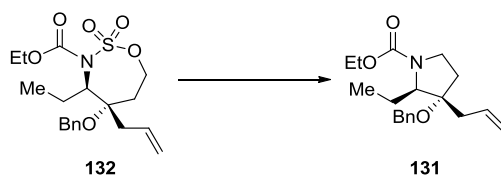
**5-allyl-5-(cyclohexyloxy)-4-ethyl-6,7-dihydro-5H-1,2,3-oxathiazepine 2,2-dioxide (129).** Prepared by general procedure A using hex-3-yn-1-sulfamate<sup>54</sup> (**109**, 30 mg, 0.16 mmol),  $\text{PhI}(\text{O}_2\text{C}^t\text{Bu})_2$  (0.11 g, 0.27 mmol), cyclohexyl allyl ether (**130**, 0.14 g, 1.0 mmol) and  $\text{Rh}_2(\text{tfacam})_4$  (5.5 mg, 0.008 mmol). Flash chromatography (5:1→4:1 hexanes/EtOAc with 1% HOAc) afforded the title compound as a colorless oil (26 mg, 46 %);  $R_f$  0.50 (3:1 hexanes/EtOAc); **IR** (thin film,  $\text{cm}^{-1}$ ) 2934, 2857, 1625, 1366, 1178; **<sup>1</sup>H NMR** ( $\text{CDCl}_3$ , 600 MHz)  $\delta$  5.97-5.90 (m, 1H), 5.22-5.19 (m, 2H), 4.41 (ddd,  $J = 11.9$ , 6.7, 1.4 Hz, 1H), 4.26 (dt,  $J = 11.9$ , 4.3 Hz, 1H), 3.47 (tt,  $J = 9.1$ , 3.3 Hz, 1H), 2.87 (dt,  $J = 13.3$ , 6.7 Hz, 1H), 2.79-2.71 (m, 2H), 2.63 (dd,  $J = 14.3$ , 5.7 Hz, 1H), 2.45 (dd,  $J = 14.3$ , 8.1 Hz, 1H), 2.13 (ddd,  $J = 14.8$ , 4.3, 1.4 Hz, 1H), 1.84-1.74 (m, 4H), 1.55-1.53 (m, 1H), 1.47-1.19 (m, 5H), 1.11 (t,  $J = 7.2$  Hz, 3H); **<sup>13</sup>C NMR** ( $\text{CDCl}_3$ , 150 MHz)  $\delta$  194.3, 131.7, 119.9, 84.7, 73.4, 65.0, 39.7, 35.0, 33.2, 30.8, 27.2, 25.6, 24.5; **HRMS** (+APCI) calculated for  $\text{C}_{15}\text{H}_{26}\text{NO}_4\text{S}$  316.1583, found 316.1573  $[\text{M}+\text{H}]^+$ .



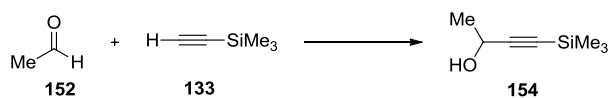
**4,5-diallyl-5-(benzyloxy)-4-ethyl-1,2,3-oxathiazepane 2,2-dioxide (102).** To a solution of 5-allyl-5-(benzyloxy)-4-ethyl-6,7-dihydro-5H-1,2,3-oxathiazepine 2,2-dioxide (**101**, 25 mg, 0.08 mmol) in MTBE (0.6 mL) at 0 °C was added allylmagnesium bromide

(0.11 mL, 0.09 mmol, 0.84 M solution in Et<sub>2</sub>O). Once thin layer chromatography indicated complete consumption of starting material (4.5 h), reaction was quenched with 1 N HCl and extracted with EtOAc and brine. The combined organic extracts were dried over MgSO<sub>4</sub> and concentrated *in vacuo*. Preparatory TLC (3:1 hexane/EtOAc with 1 % Et<sub>3</sub>N) afforded two separable diastereomers of **102**, (18 mg, 63 %) and (5 mg, 17 %): **R<sub>f</sub>** 0.31 (3:1 hexanes/EtOAc); **IR** (thin film, cm<sup>-1</sup>) 3341, 2922, 2382, 2115, 1343, 1275, 1253, 1181; **<sup>1</sup>H NMR** (CDCl<sub>3</sub>, 400 MHz) δ 7.39-7.28 (m, 5H), 5.95-5.85 (m, 2H), 5.32 (s, 1H), 5.18-5.14 (m, 2H), 5.06-4.99 (m, 2H), 4.59 (d, *J* = 10.6 Hz, 1H), 4.45 (td, *J* = 12.2, 1.0 Hz, 1H), 4.35 (d, *J* = 11.0 Hz, 1H), 4.13 (dt, *J* = 13.0, 3.5 Hz, 1H), 2.69-2.56 (m, 3H), 2.49-2.47 (m, 2H), 2.30-2.20 (m, 2H), 2.14 (d, *J* = 3.5 Hz, 1H), 1.84 (ddd, *J* = 14.9, 7.4, 1.2 Hz, 1H), 1.09 (t, *J* = 7.4 Hz, 3H); **<sup>13</sup>C NMR** (CDCl<sub>3</sub>, 100 MHz) δ 137.6, 134.7, 133.7, 129.0, 127.5, 127.5, 119.3, 117.6, 83.3, 66.8, 64.8, 64.4, 40.1, 38.7, 32.1, 24.3, 9.5; **HRMS** (+ESI) calculated for C<sub>19</sub>H<sub>28</sub>NO<sub>4</sub>S 366.17336, found 366.17369 [M+H]<sup>+</sup>;

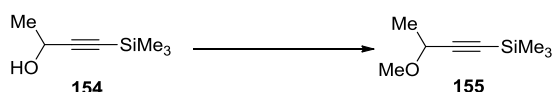
**R<sub>f</sub>** 0.29 (3:1 hexanes/EtOAc); **IR** (thin film, cm<sup>-1</sup>) 3336, 2924, 2359, 2205, 1413, 1350, 1182; **<sup>1</sup>H NMR** (CDCl<sub>3</sub>, 400 MHz) δ 7.39-7.27 (m, 5H), 5.92-5.81 (m, 2H), 5.37 (s, 1H), 5.23-5.18 (m, 2H), 5.14-5.06 (m, 2H), 4.58 (d, *J* = 10.6 Hz, 1H), 4.50-4.43 (m, 1H), 4.35 (d, *J* = 10.6 Hz, 1H), 4.20-4.13 (m, 1H), 3.27 (q, *J* = 7.3 Hz, 1H), 3.02 (ddt, *J* = 15.7, 4.3, 2.2 Hz, 1H), 2.78 (dd, *J* = 15.7, 10.2 Hz, 2H), 2.66 (dd, *J* = 10.6, 7.4 Hz, 2H), 2.30-2.16 (m, 2H), 1.94 (d, *J* = 6.7 Hz, 1H), 0.97 (t, *J* = 7.4 Hz, 3H); **<sup>13</sup>C NMR** (CDCl<sub>3</sub>, 100 MHz) δ 137.7, 133.9, 129.1, 129.0, 127.5, 123.0, 118.8, 96.6, 83.0, 66.9, 65.0, 64.5, 40.2, 39.4, 32.9, 25.5, 8.4; **HRMS** (+ESI) calculated for C<sub>19</sub>H<sub>28</sub>NO<sub>4</sub>S 366.17336, found 366.17368 [M+H]<sup>+</sup>.



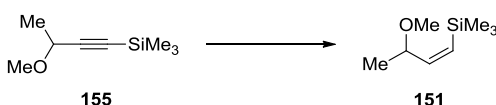
**Ethyl 3-allyl-3-(benzyloxy)-2-ethylpyrrolidine-1-carboxylate (131).** A mixture of ethyl 5-allyl-5-(benzyloxy)-4-ethyl-1,2,3-oxathiazepane-3-carboxylate 2,2-dioxide<sup>54</sup> (**132**, 28 mg, 0.07 mmol) and NaI (27 mg, 0.18 mmol) in DMF (1 mL) was heated to 70 °C for 14 h. The reaction was cooled to ambient temperature and NaH (4 mg, 0.1 mmol, 60 % dispersion in mineral oil) was added in a single portion. The resulting mixture was warmed to 40 °C and stirred 14 h. This solution was cooled to ambient temperature and quenched by the addition of saturated aqueous NH<sub>4</sub>Cl. This mixture was extracted with EtOAc, the organic extracts were combined, dried over MgSO<sub>4</sub> and concentrated *in vacuo*. Preparatory TLC (3:1 hexanes/EtOAc with 1 % Et<sub>3</sub>N) afforded **131** as a colorless residue (13 mg, 57 %); **R<sub>f</sub>** 0.60 (5:1 hexanes/EtOAc); **IR** (thin film, cm<sup>-1</sup>) 2976, 1693, 1415, 1105, 907; **<sup>1</sup>H NMR** (CDCl<sub>3</sub>, 400 MHz) δ 7.32-7.21 (m, 5H), 5.95-5.85 (m, 1H), 5.18-5.11 (m, 2H), 4.46-4.38 (m, 2H), 4.16-4.06 (m, 2H), 4.02-3.96 (m, 1H), 3.62 (dd, *J* = 10.6, 8.2 Hz, 1H), 3.55-3.44 (m, 1H), 3.35 (dt, *J* = 18.8, 9.4 Hz, 1H), 2.59 (ddd, *J* = 32.1, 15.3, 6.3 Hz, 1H), 2.41-2.29 (m, 1H), 2.17-2.07 (m, 1H), 1.84-1.73 (m, 1H), 1.69-1.56 (m, 1H), 1.16 (t, *J* = 7.2 Hz, 3H), 0.93 (t, *J* = 7.4 Hz, 3H); **<sup>13</sup>C NMR** (CDCl<sub>3</sub>, 150 MHz) δ 156.6, 138.9, 133.6, 128.5, 127.6, 127.3, 118.1, 86.7, 85.9, 64.1, 61.0, 44.2, 35.8, 32.8, 25.2, 14.9, 11.0; **HRMS** (+ESI) calculated for C<sub>19</sub>H<sub>28</sub>NO<sub>3</sub> 318.20637, found 318.20654 [M+H]<sup>+</sup>.



**4-(trimethylsilyl)but-3-yn-2-ol (154)**. Prepared according to the literature,<sup>89</sup> using trimethylsilyl acetylene (**133**, 6 mL, 43 mmol), ethylmagnesium bromide (18 mL, 54 mmol), and acetaldehyde (**152**, 3.6 mL, 64.2 mmol). 3.4 g **154** was isolated in 56 % yield (cf. 87 % reported). <sup>1</sup>H NMR was identical to that reported. <sup>1</sup>H NMR (CDCl<sub>3</sub>, 400 MHz) δ 4.50 (qd, *J* = 6.7, 5.5 Hz, 1H), 1.76 (d, *J* = 5.5 Hz, 1H), 1.43 (d, *J* = 6.7 Hz, 3H), 0.15 (s, 9H).



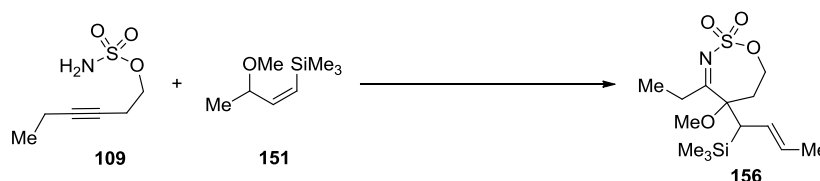
**(3-methoxybut-1-yn-1-yl)trimethylsilane (155)**. Prepared according to the literature,<sup>69</sup> using 4-(trimethylsilyl)but-3-yn-2-ol (**154**, 0.30 g, 2.12 mmol), <sup>n</sup>BuLi (1.1 mL, 2.1 mmol), and methyl iodide (1.1 mL, 16.9 mmol). 208 mg **155** was isolated in 63 % yield (cf. 90 % reported). <sup>1</sup>H NMR was identical to that reported. <sup>1</sup>H NMR (CDCl<sub>3</sub>, 400 MHz) δ 4.04 (q, *J* = 6.4 Hz, 1H), 3.38 (s, 3H), 1.40 (d, *J* = 6.7 Hz, 3H), 0.16 (s, 9H).



**(Z)-(3-methoxybut-1-en-1-yl)trimethylsilane (151)**. Prepared according to a procedure modified from the literature.<sup>67</sup> To a stirring solution of (3-methoxybut-1-yn-1-yl)trimethylsilane (**155**, 0.854 g, 5.46 mmol) in ether (3 mL) was slowly added DIBAL-H (6.3 mL, 6.3 mmol). After stirring for an additional 3 h at ambient temperature, the reaction mixture was added to a separatory funnel containing cold 10 % H<sub>2</sub>SO<sub>4</sub> (20 mL)

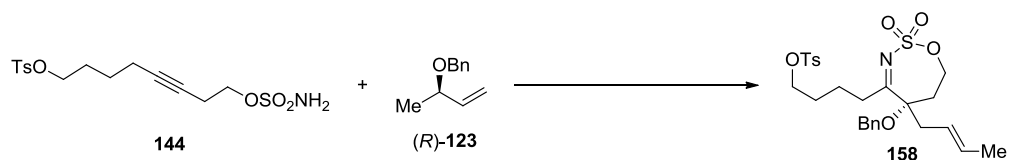


and ice. The mixture was shaken and the layers separated quickly. After extraction of the aqueous layer with fresh ether, the organic layers were combined and washed with saturated sodium chloride solution and dried with anhydrous  $\text{Mg}_2\text{SO}_4$ . Purification on silica gel (pentane/ $\text{Et}_2\text{O}$ , 99:1) gave **151** as a colorless oil (271 mg, 31 % yield);  $R_f$  0.5 (99:1 hexanes/ $\text{EtOAc}$ ); **IR** (thin film,  $\text{cm}^{-1}$ ) 3866, 3668, 2604, 2224, 2135, 1984, 1605;  **$^1\text{H}$  NMR** ( $\text{CDCl}_3$ , 400 MHz)  $\delta$  6.10 (dd,  $J = 14.5, 9$  Hz, 1H), 5.68 (d,  $J = 14.5$  Hz, 1H), 3.90 (dd,  $J = 9.0, 6.3$  Hz, 1H), 3.25 (s, 3H), 0.9 (d,  $J = 6.7$  Hz, 3H), 0.12 (s, 9H);  **$^{13}\text{C}$  NMR** ( $\text{CDCl}_3$ , 75 MHz)  $\delta$  150.4, 131.7, 77.2, 56.2, 21.6, 0.6 ; **HRMS** (-ESI) calculated for  $\text{C}_8\text{H}_{17}\text{OSi}$  157.10432, found 157.10135  $[\text{M}-\text{H}]^-$ .



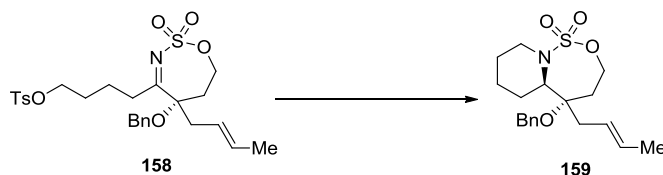
**(5-methoxy-4-methyl-5-(1-(trimethylsilyl)but-2-en-1-yl)-6,7-dihydro-5H-1,2,3-oxathiazepine 2,2-dioxide (156)**. Prepared according to general procedure A using hex-3-yn-1-yl sulfamate<sup>54</sup> (**109**, 31 mg, 0.17 mmol),  $\text{PhI}(\text{OC}^t\text{Bu})_2$  (0.11 g, 0.27 mmol), (Z)-3-methoxybut-1-en-1-yltrimethylsilane (**151**, 0.16 mg, 1.02 mmol), and  $\text{Rh}_2(\text{tfacam})_4$  (5.8 mg, 0.009 mmol). Flash chromatography (5:1 hexane/ $\text{EtOAc}$  with 1 % HOAc additive) afforded **156** as a colorless oil (12 mg, 22 %) as a mixture of inseparable diastereomers;  $R_f$  0.55 (3:1 hexanes/ $\text{EtOAc}$ ); **IR** (thin film,  $\text{cm}^{-1}$ ) 3273, 2956, 2096, 1736, 1625, 1370, 1182;  **$^1\text{H}$  NMR** ( $\text{CDCl}_3$ , 600 MHz)  $\delta$  5.9 (dd,  $J = 12.0, 2.7$  Hz, 1H), 5.40-5.28 (m, 1H), 4.45-4.25 (m, 2H), 3.26 (s, 3H), 2.87-2.68 (m, 2H), 2.59-2.45 (m, 1H), 2.35-2.24 (m, 1H), 2.09 (ddt,  $J = 16.0, 9.4, 1.6$  Hz, 1H), 1.65 (ddd,  $J = 13.1, 5.9, 1.2$

Hz, 3H), 0.07 (s, 9H);  $^{13}\text{C}$  NMR ( $\text{CDCl}_3$ , 150 MHz)  $\delta$  170.7, 145.7, 128.9, 66.3, 52.4, 40.3, 33.8, 18.4, 9.7, 0.1 (3C) ; HRMS (-ESI) calculated for  $\text{C}_{13}\text{H}_{24}\text{NO}_4\text{SSi}$  318.11953, found 318.12051  $[\text{M}-\text{H}]^-$ .



**4-(5-(benzyloxy)-5-(but-2-en-1-yl)-2,2-dioxido-6,7-dihydro-5H-1,2,3-oxathiazepin-4-yl)butyl 4-methylbenzenesulfonate (158)**. Prepared according to general procedure B, with the following modification.  $\text{Rh}_2(\text{tfacam})_4$  (18 mg, 0.03 mmol) in  $\text{CF}_3\text{C}_6\text{H}_5$  (0.025 M) was stirred in a round bottom flask at 40 °C. A solution of 8-(tosyloxy)oct-3-yn-1-yl sulfamate (**144**, 0.93 g, 0.25 mmol),  $\text{PhI}(\text{O}_2\text{C}^t\text{Bu})_2$  (0.16 g, 0.41 mmol), and (R)-((but-3-en-2-yloxy)methyl)benzene<sup>54</sup> (**123**, 0.48 g, 3.0 mmol) in  $\text{CF}_3\text{C}_6\text{H}_5/\text{CH}_2\text{Cl}_2$  (0.025 M, 5:1) was added via syringe pump over 1.5 h. After complete addition the reaction was stirred until TLC indicated complete consumption of starting sulfamate ester (30 min). Once judged to be complete, the reaction mixture was concentrated onto a pad of  $\text{SiO}_2$  and immediately purified by flash column chromatography on silica gel (5:1 hexane/EtOAc with 1 % HOAc) to afford **158** as a white amorphous solid (58 mg, 64 %, 80% ee) with an *E:Z* ratio of 2.7:1 inseparable isomers;  $R_f$  0.26 (3:1 hexanes/EtOAc); IR (thin film,  $\text{cm}^{-1}$ ) 2922, 1626, 1357, 1173, 910, 730;  $^1\text{H}$  NMR ( $\text{CDCl}_3$ , 400 MHz)  $\delta$  7.75 (d,  $J = 8.2$  Hz, 2H), 7.39-7.27 (m, 7H), 5.68-5.53 (m, 2H), 4.57 (d,  $J = 11.7$  Hz, 1H), 4.4 (ddd,  $J = 11.0, 7.0, 1.2$  Hz, 1H), 4.31-4.24 (m, 2H), 3.99-3.94 (m, 2H), 2.94 (ddd,  $J = 14.4, 12.8, 6.5$  Hz, 1H), 2.79-2.71 (m, 1H), 2.63-2.54 (m, 2H), 2.52-2.46 (m, 1H), 2.42 (s, 3H), 2.09 (ddd,  $J = 15.7, 5.1, 1.2$  Hz, 1H), 1.68 (d,  $J = 5.9$  Hz, 3H), 1.64-1.55 (m,

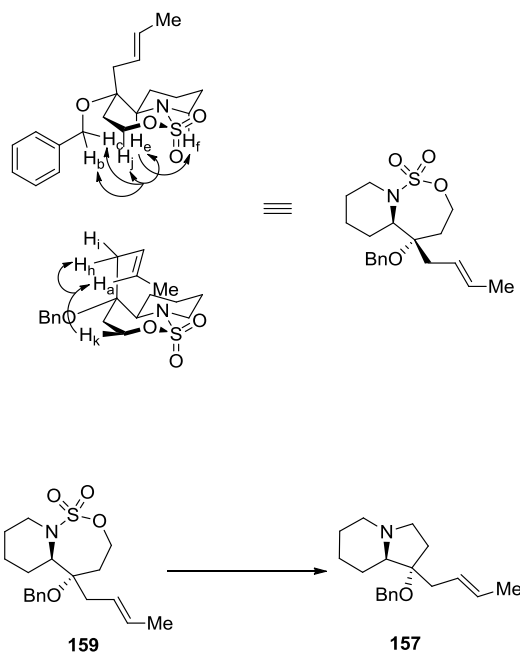
4H);  $^{13}\text{C}$  NMR ( $\text{CDCl}_3$ , 100 MHz)  $\delta$  191.4, 145.1, 137.3, 133.1, 131.3, 130.1, 128.9, 128.2, 128.1, 126.8, 123.4, 85.2, 70.3, 66.9, 64.9, 38.6, 36.1, 32.3, 28.3, 21.9, 21.7, 18.4; **m.p.** 91-92 °C; **HRMS** (-ESI) calculated for  $\text{C}_{26}\text{H}_{32}\text{O}_7\text{N}_1\text{S}_2$  534.16257, found 534.16316  $[\text{M}-\text{H}]^-$ ;  $[\alpha]_D^{20}$  + 26.4 (*c* 1.48,  $\text{CHCl}_3$ ); **HPLC** (AS-H, 2  $\rightarrow$  15 % IPA/HEX, 1 mL/min),  $\lambda$  210 nm,  $t_r(\text{maj})$  = 8.36 min,  $t_r(\text{min})$  = 7.58 min.



**5-(benzyloxy)-5-(but-2-en-1-yl)octahydropyrido[1,2-c][1,2,3]oxathiazepine 1,1-dioxide (159).** DIBAL-H (0.11 mL, 0.11 mmol) was added dropwise to a stirring solution of 4-(5-(benzyloxy)-5-(but-2-en-1-yl)-2,2-dioxido-6,7-dihydro-5H-1,2,3-oxathiazepin-4-yl)butyl 4-methylbenzenesulfonate (**158**, 30 mg, 0.056 mmol) in  $\text{CH}_2\text{Cl}_2$  (0.5 mL) at ambient temperature. Once thin layer chromatography indicated complete consumption of starting material (30 min), the reaction mixture was added to a vigorously stirring solution of saturated aqueous Rochelle's salt (10 mL) and  $\text{Et}_2\text{O}$  (20 mL).  $\text{Et}_2\text{O}$  (50 mL) was added, and the resulting biphasic mixture was stirred vigorously for approximately 3 h. The organic layer was separated, washed with brine, dried over  $\text{MgSO}_4$  and concentrated *in vacuo*. The crude mixture was dissolved in THF (0.5 mL), and  $\text{K}_2\text{CO}_3$  (20 mg, 0.14 mmol) was added at ambient temperature. The reaction was warmed to 40 °C and stirred for 14 h, until TLC indicated complete consumption of starting material. The reaction was quenched with a saturated solution of  $\text{NH}_4\text{Cl}$  and extracted with  $\text{EtOAc}$  (3 x 20 mL). The combined organic extracts were washed with brine, dried over  $\text{MgSO}_4$  and concentrated *in vacuo*. Purification by flash chromatography (7:1

hexanes/EtOAc) afforded **17** as a colorless oil (13.8 mg, 71 %);  $R_f$  0.46 (3:1 hexanes/EtOAc); **IR** (thin film,  $\text{cm}^{-1}$ ) 2926, 2856, 2000, 1343, 1177, 979;  **$^1\text{H}$  NMR** (400 MHz;  $\text{CDCl}_3$ )  $\delta$  7.37-7.19 (m, 5H), 5.54-5.50 (m, 2H), 4.55 (d,  $J = 11.7$  Hz, 1H), 4.45 (d,  $J = 11.3$  Hz, 1H), 4.32 (dd,  $J = 7.8, 2.7$  Hz, 2H), 4.09 (dd,  $J = 8.4, 6.1$  Hz, 1H), 3.75 (ddd,  $J = 14.4, 6.4, 2.3$  Hz, 1H), 3.17 (ddd,  $J = 14.5, 10.6, 4.7$  Hz, 1H), 2.66 (d,  $J = 13.3$  Hz, 1H), 2.44-2.37 (m, 1H), 2.36-2.28 (m, 1H), 2.07-2.00 (m, 1H), 1.92-1.71 (m, 4H), 1.67 (d,  $J = 2.7$  Hz, 3H), 1.65-1.57 (m, 2H);  **$^{13}\text{C}$  NMR** (100 MHz,  $\text{CDCl}_3$ )  $\delta$  138.7, 129.5, 128.6, 127.7, 127.1, 125.9, 80.6, 77.4, 67.6, 63.9, 59.3, 42.4, 36.6, 35.5, 29.9, 22.8, 21.8, 19.2, 18.4; **HRMS** (-ESI) calculated for  $\text{C}_{19}\text{H}_{26}\text{O}_4\text{NS}$  364.1588, found 364.15933.

**Key NOE correlations for 159:**



**1-(benzyloxy)-1-((E)-but-2-en-1-yl)octahydroindolizine (157).** A mixture of 5-(benzyloxy)-5-(but-2-en-1-yl)octahydropyrido[1,2-c][1,2,3]oxathiazepine 1,1-dioxide (**159**, 120 mg, 0.328 mmol) and NaI (170 mg, 1.13 mmol) in DMF (0.5 mL) was heated

to 70 °C for 14 h. The reaction was cooled to ambient temperature and NaH (50 mg, 1.25 mmol, 60 % dispersion in mineral oil) was added in a single portion. The resulting mixture was warmed to 40 °C and stirred for 14 h. The solution was again cooled to ambient temperature and quenched by addition of saturated NH<sub>4</sub>Cl. This mixture was extracted with EtOAc. The organic extracts were combined, washed with brine, dried over MgSO<sub>4</sub>, and concentrated *in vacuo*. Preparative TLC (9:1 hexanes:Et<sub>3</sub>N) afforded **157** as a colorless oil (63 mg, 67 %); **R<sub>f</sub>** 0.21 (3:1 hexanes/EtOAc); **IR** (thin film, cm<sup>-1</sup>) 2930, 2786, 2156, 1973, 571; **<sup>1</sup>H NMR** (CDCl<sub>3</sub>, 400 MHz) δ 7.37-7.29 (m, 5H), 5.57-5.53 (m, 2H); 4.47 (d, *J* = 11.3 Hz, 1H), 4.40 (d, *J* = 11.4 Hz, 1H), 3.07 (dd, *J* = 10.4, 0.8 Hz, 1H), 2.93 (t, *J* = 8.4 Hz, 1H), 2.68 (d, *J* = 13.3 Hz, 1H), 2.27 (ddd, *J* = 10.8, 8.8, 7.8 Hz, 1H), 2.12-2.01 (m, 3H), 1.86-1.78 (m, 4H), 1.67 (dd, *J* = 3.5, 1.1 Hz, 3H), 1.56-1.44 (m, 2H), 1.38-1.27 (m, 2H); **<sup>13</sup>C NMR** (CDCl<sub>3</sub>, 100 MHz) δ 139.5, 128.5, 127.5, 126.4, 85.6, 77.4, 72.8, 64.9, 54.5, 53.8, 37.3, 35.5, 29.9, 28.0, 25.4, 24.6, 18.4; **HRMS** (+ESI) calculated for C<sub>19</sub>H<sub>28</sub>NO 286.21654, found 286.21709 [M+H]<sup>+</sup>; **[α]<sub>D</sub><sup>20</sup>** +5.2 (*c* 1.02, CHCl<sub>3</sub>).

## References

- (1) *Catalytic Cascade Reactions*; Xu, P.-F., Wang, W., Eds.; John Wiley & Sons, Inc: Hoboken, NJ, 2013.
- (2) Nicolaou, K. C.; Chen, J. S. *Chem. Soc. Rev.* **2009**, *38*, 2993.
- (3) Nicolaou, K. C.; Edmonds, D. J.; Bulger, P. G. *Angew. Chem., Int. E.* **2006**, *45*, 7134.
- (4) *Domino Reactions: Concepts for Efficient Organic Synthesis*; Tietze, L. F., Eds.; Wiley-VCH: Weinheim, Germany, 2014.
- (5) Smith, J. M.; Moreno, J.; Boal, B. W.; Garg, N. K. *Angew. Chem., Int. Ed.* **2015**, *54*, 400.
- (6) Chu, S.; Wallace, S.; Smith, M. D. *Angew. Chem., Int. Ed.* **2014**, *53*, 13826.
- (7) Barrett, T. N.; Barrett, A. G. M. *J. Am. Chem. Soc.* **2014**, *136*, 17013.
- (8) Johnson, W. S.; Gravestock, M. B.; McCarry, B. E. *J. Am. Chem. Soc.* **1971**, *93*, 4332.
- (9) Gravestock, M. B.; Johnson, W. S.; McCarry, B. E.; Parry, R. J.; Ratcliffe, B. E. *J. Am. Chem. Soc.* **1978**, *100*, 4274.
- (10) Platz, M. S. Nitrenes. In *Reactive Intermediate Chemistry*; Moss, R. A., Platz, M. S., Jones, M., Eds.; John Wiley & Sons, Inc.: Hoboken, NJ, 2005; pp 501-559.
- (11) Espino, C. G.; Du Bois, J. Rhodium(II)-Catalyzed Oxidative Amination. In *Modern Rhodium-Catalyzed Organic Reactions*; Evans, P. A., Ed.; Wiley-VCH: Weinheim, 2005; pp 379-416.

- (12) Dauban, P.; Dodd, R. H. Catalytic C–H Amination with Nitrenes. In *Amino Group Chemistry*; Ricci, A., Ed.; Wiley-VCH: Weinheim, 2008; pp 55-92.
- (13) Lebel, H.; Huard, K.; Lectard, S. *J Am Chem. Soc.* **2005**, *127*, 14198.
- (14) Du Bois, J. *Org. Process Res. Dev.* **2011**, *15*, 758.
- (15) Breslow, R. G., S. H. *J. Chem. Soc., Chem. Commun.* **1982**, 1400.
- (16) Espino, C. G.; Du Bois, J. *Angew. Chem., Int. Ed.* **2001**, *40*, 598.
- (17) Müller, P.; Fruit, C. *Chem. Rev.* **2003**, *103*, 2905.
- (18) Kwart, H.; Kahn, A. A. *J. Am. Chem. Soc.* **1967**, *89*, 1950.
- (19) Kwart, H.; Khan, A. A. *J. Am. Chem. Soc.* **1967**, *89*, 1951.
- (20) Evans, D. A.; Faul, M. M.; Bilodeau, M. T.; Anderson, B. A.; Barnes, D. M. *J. Am. Chem. Soc.* **1993**, *115*, 5328.
- (21) Li, Z.; Conser, K. R.; Jacobsen, E. N. *J. Am. Chem. Soc.* **1993**, *115*, 5326.
- (22) Stokes, B. J.; Dong, H.; Leslie, B. E.; Pumphrey, A. L.; Driver, T. G. *J. Am. Chem. Soc.* **2007**, *129*, 7500.
- (23) Dong, H.; Shen, M.; Redford, J. E.; Stokes, B. J.; Pumphrey, A. L.; Driver, T. G. *Org. Lett.* **2007**, *9*, 5191.
- (24) Shen, M.; Leslie, B. E.; Driver, T. G. *Angew. Chem., Int. Ed.* **2008**, *47*, 5056.
- (25) Stokes, B. J.; Richert, K. J.; Driver, T. G. *J. Org. Chem.* **2009**, *74*, 6442.
- (26) Sun, K.; Liu, S.; Bec, P. M.; Driver, T. G. *Angew. Chem., Int. Ed.* **2011**, *50*, 1702.
- (27) Stokes, B. J.; Liu, S.; Driver, T. G. *J. Am. Chem. Soc.* **2011**, *133*, 4702.
- (28) Kong, C.; Jana, N.; Driver, T. G. *Org. Lett.* **2013**, *15*, 824.
- (29) Jones, C.; Nguyen, Q.; Driver, T. G. *Angew. Chem., Int. Ed.* **2014**, *53*, 785.

- (30) Nguyen, Q.; Nguyen, T.; Driver, T. G. *J. Am. Chem. Soc.* **2013**, *135*, 620.
- (31) Dequirez, G.; Ciesielski, J.; Retailleau, P.; Dauban, P. *Chem. – Eur. J.* **2014**, *20*, 8929.
- (32) Stoll, A. H.; Blakey, S. B. *J. Am. Chem. Soc.* **2010**, *132*, 2108.
- (33) Feast, G. C.; Page, L. W.; Robertson, J. *Chem. Commun.* **2010**, *46*, 2835.
- (34) Stoll, A. H.; Blakey, S. B. *Chem. Sci.* **2011**, *2*, 112.
- (35) Robertson, J.; Feast, G. C.; White, L. V.; Steadman, V. A.; Claridge, T. D. W. *Org. Biomol. Chem.* **2010**, *8*, 3060.
- (36) Boralsky, L. A.; Marston, D.; Grigg, R. D.; Hershberger, J. C.; Schomaker, J. M. *Org. Lett.* **2011**, *13*, 1924.
- (37) Grigg, R. D.; Schomaker, J. M.; Timokhin, V. *Tetrahedron* **2011**, *67*, 4318.
- (38) Rigoli, J. W.; Boralsky, L. A.; Hershberger, J. C.; Marston, D.; Meis, A. R.; Guzei, I. A.; Schomaker, J. M. *J. Org. Chem.* **2012**, *77*, 2446.
- (39) Weatherly, C. D.; Rigoli, J. W.; Schomaker, J. M. *Org. Lett.* **2012**, *14*, 1704.
- (40) Adams, C. S.; Boralsky, L. A.; Guzei, I. A.; Schomaker, J. M. *J. Am. Chem. Soc.* **2012**, *134*, 10807.
- (41) Thornton, A. R.; Blakey, S. B. *J. Am. Chem. Soc.* **2008**, *130*, 5020.
- (42) Thornton, A. R.; Martin, V. I.; Blakey, S. B. *J. Am. Chem. Soc.* **2009**, *131*, 2434.
- (43) Brawn, R. A.; Zhu, K.; Panek, J. S. *Org. Lett.* **2014**, *16*, 74.
- (44) Martin, V. Explorations of Metallocarbene and Metallonitrene Reactive Intermediate Chemistry for the Development of Synthetically Useful New Reactions. Ph.D. Dissertation, Emory University, Atlanta, GA, 2010.



- (45) Harmon, R. E.; Stanley, F.; Gupta, S. K.; Johnson, J. *J. Org. Chem.* **1970**, *35*, 3444.
- (46) Horneff, T.; Chuprakov, S.; Chernyak, N.; Gevorgyan, V.; Fokin, V. V. *J. Am. Chem. Soc.* **2008**, *130*, 14972.
- (47) Chuprakov, S.; Kwok, S. W.; Zhang, L.; Lercher, L.; Fokin, V. V. *J. Am. Chem. Soc.* **2009**, *131*, 18034.
- (48) Chuprakov, S.; Malik, J. A.; Zibinsky, M.; Fokin, V. V. *J. Am. Chem. Soc.* **2011**, *133*, 10352.
- (49) Grimster, N.; Zhang, L.; Fokin, V. V. *J. Am. Chem. Soc.* **2010**, *132*, 2510.
- (50) Selander, N.; Worrell, B. T.; Chuprakov, S.; Velaparthi, S.; Fokin, V. V. *J. Am. Chem. Soc.* **2012**, *134*, 14670.
- (51) Selander, N.; Fokin, V. V. *J. Am. Chem. Soc.* **2012**, *134*, 2477.
- (52) Chuprakov, S.; Kwok, S. W.; Fokin, V. V. *J. Am. Chem. Soc.* **2013**, *135*, 4652.
- (53) Chuprakov, S.; Worrell, B. T.; Selander, N.; Sit, R. K.; Fokin, V. V. *J. Am. Chem. Soc.* **2014**, *136*, 195.
- (54) Mace, N.; Thornton, A. R.; Blakey, S. B. *Angew. Chem., Int. Ed.* **2013**, *52*, 5836.
- (55) Guthikonda, K.; Du Bois, J. *J. Am. Chem. Soc.* **2002**, *124*, 13672.
- (56) Thornton, A. R. Metallonitrene/Alkyne Cascade Reactions: Development of a Versatile Process for Organic Synthesis. Ph.D. Dissertation, Emory University, Atlanta, GA, 2010.
- (57) Meléndez, R. E.; Lubell, W. D. *Tetrahedron* **2003**, *59*, 2581.
- (58) Guthikonda, K.; Du Bois, J. *J. Am. Chem. Soc.* **2002**, *124*, 13672.
- (59) Brown, H. C.; Lynch, G. J. *J. Org. Chem.* **1981**, *46*, 531.

- (60) Nakai, T.; Mikami, K.; Taya, S.; Fujita, Y. *J. Am. Chem. Soc.* **1981**, *103*, 6492.
- (61) Mikami, K.; Kimura, Y.; Kishi, N.; Nakai, T. *J. Org. Chem.* **1983**, *48*, 279.
- (62) Nakai, T.; Mikami, K. *Chem. Rev.* **1986**, *86*, 885.
- (63) Mikami, K.; Nakai, T. *Synthesis* **1991**, *1991*, 594.
- (64) Alvisi, D.; Blart, E.; Bonini, B. F.; Mazzanti, G.; Ricci, A.; Zani, P. *J. Org. Chem.* **1996**, *61*, 7139.
- (65) Valenti, E.; Pericas, M. A.; Serratos, F. *J. Org. Chem.* **1990**, *55*, 395.
- (66) Soderquist, J. A.; Santiago, B. *Tetrahedron Lett.* **1990**, *31*, 5113.
- (67) Miller, R. B.; McGarvey, G. *J. Org. Chem.* **1978**, *43*, 4424.
- (68) Johnstone, R. A. W.; Rose, M. E. *Tetrahedron* **1979**, *35*, 2169.
- (69) Turlington, M.; Yue, Y.; Yu, X.-Q.; Pu, L. *J. Org. Chem.* **2010**, *75*, 6941.
- (70) Bischofberger, N.; Waldmann, H.; Saito, T.; Simon, E. S.; Lees, W.; Bednarski, M. D.; Whitesides, G. M. *J. Org. Chem.* **1988**, *53*, 3457.
- (71) Hoveyda, A. H.; Lombardi, P. J.; O'Brien, R. V.; Zhugralin, A. R. *J. Am. Chem. Soc.* **2009**, *131*, 8378.
- (72) Tsai, D. J. S.; Midland, M. M. *J. Org. Chem.* **1984**, *49*, 1842.
- (73) Sayo, N.; Azuma, K.-i.; Mikami, K.; Nakai, T. *Tetrahedron Lett.* **1984**, *25*, 565.
- (74) Chirkin, E.; Atkalian, W.; Porée, F.-H. The *Securinega* Alkaloids In *The Alkaloids: Chemistry and Biology*; Hans-Joachim, K., Ed.; Academic Press: Waltham, 2015; Vol. 74, pp 1-120.
- (75) Weinreb, S. M. *Nat. Prod. Rep.* **2009**, *26*, 758.
- (76) Weenen, H.; Nkunya, M. H. H.; Bray, D. H.; Mwasumbi, L. B.; Kinabo, L. S.; Kilimali, V. A. E. B.; Wijnberg, J. B. P. A. *Planta Med* **1990**, *56*, 371.

- (77) Mensah, J. L.; Lagarde, I.; Ceschin, C.; Michelb, G.; Gleye, J.; Fouraste, I. *J. Ethnopharmacology* **1990**, *28*, 129.
- (78) Tatematsu, H.; Mori, M.; Yang, T.-H.; Chang, J.-J.; Lee, T. T.-Y.; Lee, K.-H. *J. Pharm. Sci.* **1991**, *80*, 325.
- (79) Dong NZ, G. Z., Chou WH, Kwok CY *Acta Pharmacol. Sin.* **1999**, *20*, 267.
- (80) Sampath, M.; Lee, P.-Y. B.; Loh, T.-P. *Chem. Sci.* **2011**, *2*, 1988.
- (81) Chen, J.-H.; Levine, S. R.; Buegler, J. F.; McMahon, T. C.; Medeiros, M. R.; Wood, J. L. *Org. Lett.* **2012**, *14*, 4531.
- (82) Honda, T.; Namiki, H.; Watanabe, M.; Mizutani, H. *Tetrahedron Lett.* **2004**, *45*, 5211.
- (83) Honda, T.; Namiki, H.; Kaneda, K.; Mizutani, H. *Org. Lett.* **2004**, *6*, 87.
- (84) Leduc, A. B.; Kerr, M. A. *Angew. Chem., Int. Ed.* **2008**, *47*, 7945.
- (85) Bardají, G. G.; Cantó, M.; Alibés, R.; Bayón, P.; Busqué, F.; de March, P.; Figueredo, M.; Font, J. *J. Org. Chem.* **2008**, *73*, 7657.
- (86) Busqué, F.; Cantó, M.; de March, P.; Figueredo, M.; Font, J.; Rodríguez, S. *Tetrahedron: Asymmetry* **2003**, *14*, 2021.
- (87) Son, Y. W.; Kwon, T. H.; Lee, J. K.; Pae, A. N.; Lee, J. Y.; Cho, Y. S.; Min, S.-J. *Org. Lett.* **2011**, *13*, 6500.
- (88) Thomas, R. M.; Keitz, B. K.; Champagne, T. M.; Grubbs, R. H. *J. Am. Chem. Soc.* **2011**, *133*, 7490.
- (89) Fleming, I.; Takaki, K.; Thomas, A. P. *J. Chem. Soc., Perkin Trans. 1* **1987**, 2269.
- (90) Guthikonda, K.; When, P. M.; Caliendo, B. J.; Du Bois, J. *Tetrahedron* **2006**, *62*, 11331.

- (91) Hopf, H.; Naujoks, E. *Tetrahedron Lett.* **1988**, 29, 609.
- (92) Tzeng, D.; Weber, W. P. *J. Org. Chem.* **1981**, 46, 693.

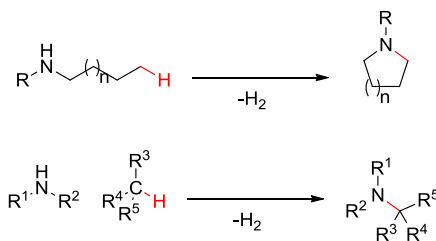
**Chapter 2. Group 9 Transition Metal Catalyzed C–H  
Amination with Aryl Azides**

## 2.1 Introduction to Metallonitrene C–H Amination

### 2.1.1 Qualities of an Ideal C–H Amination

Nitrogen-containing functional groups are extremely prevalent and important in biologically active molecules, making efficient methods for forming C–N bonds essential.<sup>1</sup> Introduction of nitrogen-containing functionality is a particular challenge. Amination methods in nature almost exclusively rely on the reaction of a nucleophilic nitrogen species with an activated carbon center. In contrast, enzymatic oxygenation of C–H bonds can occur without such activation.<sup>2-5</sup> The challenge for the synthetic chemist lies in addressing these natural limitations in C–H amination with methods to form C–N bonds from unactivated C–H bonds, with the least amount of byproducts possible (Scheme 2.1).<sup>6,7</sup> Though the simplest possible amination would yield H<sub>2</sub> the byproduct, thermodynamically the reaction given in Scheme 2.1 (bottom) would be unfavorable by approximately 13 kcal/mol.<sup>8</sup> For this reason, a more thermodynamically feasible ideal C–H amination might include molecular oxygen as an oxidant, with evolution of water.

**Scheme 2.1.** General scheme for an ideal intramolecular (top) and intermolecular (bottom) C–H amination.



In considering C–H amination methods, there are several factors that contribute to ideality (Table 2.1). While many of these reactions are transition-metal mediated, in an ideal method, metals would be used in catalytic quantities, and preferably be earth-abundant. Required ligands would be simple to synthesize, and reaction conditions would be mild, with limited additives. An ideal method would generate minimal, easily removable byproducts. It would be versatile for use with a range of substrates and show excellent chemoselectivity for a particular class of C–H bond ( $sp^3$ ,  $sp^2$ , etc.), as well as stereoselectivity. Finally, such a method would give the desired product with no need to post-functionalize.

**Table 2.1.** Summary of ideality in C–H amination methodology.

<b>Qualities of an Ideal C-H Amination</b>	
• <i>Catalytic Transition Metal</i>	• <i>Versatile Substrates</i>
• <i>Simple Ligand Synthesis</i>	• <i>Chemoselective</i>
• <i>Minimal Byproducts</i>	• <i>Diastereoselective</i>
• <i>Limited Additives</i>	• <i>Enantioselective</i>
• <i>Mild Conditions</i>	• <i>Atom Economical</i>

### 2.1.2 Azides as Metallonitrene Precursors

One of the most effective methods for introducing C–N bonds, which has seen a great amount of progress in recent years, is metallonitrene-initiated C–H functionalization.<sup>9</sup> As described in Chapter 1, a variety of metallonitrene precursors are competent for amination (Figure 1.2). Though azides do not meet all of the criteria for ideality (Table 2.1), they do have a number of attractive features. For instance, they do

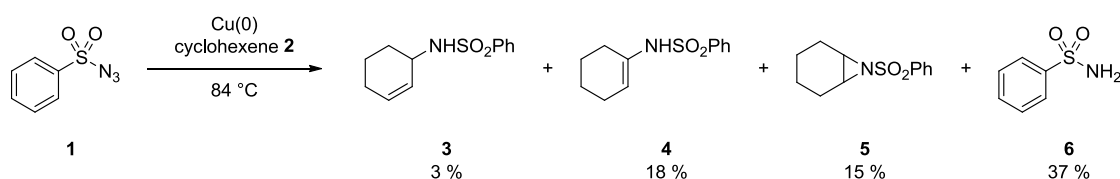
not require addition of an oxidant and release nitrogen gas as the only byproduct.<sup>10-12</sup> However, one of the limitations of azides as metallonitrene precursors C–H amination is that they often require electron withdrawing groups to increase the nitrogen electrophilicity for functionalization of inherently unreactive C–H bonds.<sup>13</sup> These electron withdrawing groups also assist in preventing unproductive rearrangement pathways.<sup>14</sup> For this reason, initial studies of amination with azides examined electron deficient azides, such as sulfonyl and phosphoryl azides. Since that time, rational design of new catalyst systems and amination mechanisms have enabled the use of aryl, acyl, and even alkyl azides without unproductive rearrangements. In reviewing the previous work with azides, it will be organized by three categories: azides with electron withdrawing groups, aryl and vinyl azides, and alkyl azides. Aryl and alkyl azides have seen significant preliminary advances in catalytic C–H amination in recent years. However, limitations still lie in extensions to intermolecular transformations, and effective enantioselective catalysis with these substrates has yet to be developed.

#### **2.1.2.1 Metallonitrene C–H Amination Utilizing Azides with Electron-Withdrawing Groups**

The first C–H amination and aziridination with azides was reported by Kwart and Khan nearly fifty years ago using benzenesulfonyl azide (**1**) and copper powder with cyclohexene (**2**, Scheme 2.2).<sup>15</sup> C–H amination products **3** and **4** and aziridination product **5** were observed in 21 % and 15 %, respectively, along with benzenesulfonamide (**6**) byproduct.

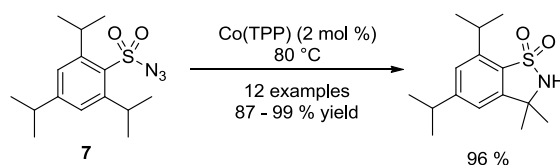


**Scheme 2.2.** Copper powder catalyzed C–H amination and aziridination of cyclohexene (**2**) with benzenesulfonyl azide (**1**).<sup>15</sup>



Metalloporphyrins were among the first catalysts used for C–H amination with electron deficient azides.<sup>16</sup> In early examples, Cenini and coworkers reported cobalt(II) porphyrin catalyzed benzylic amination with 4-nitrophenyl azide.<sup>17,18</sup> Also utilizing metalloporphyrin complexes, Zhang and coworkers have made significant advances in C–H amination with azides. Cobalt(II) tetraphenyl porphyrin intramolecularly aminated tertiary, secondary, and primary benzylic C–H bonds with sulfonyl azides (e.g., **7**) under mild conditions (Scheme 2.3).<sup>19</sup> This discovery was followed by a similar C–H amination with aryl phosphoryl azides in the presence of an amide-functionalized metalloporphyrin.<sup>20</sup>

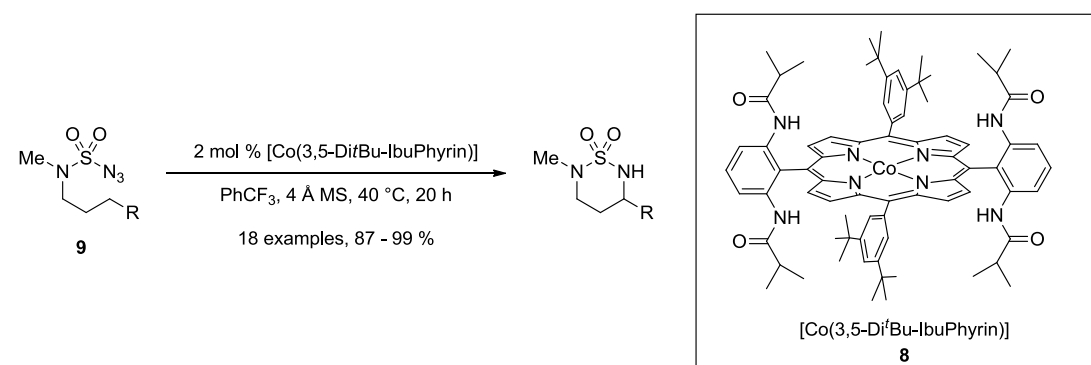
**Scheme 2.3.** Cobalt(II) tetraphenyl porphyrin (Co(TPP)) catalyzed C–H amination with sulfonyl azide **7**.<sup>19</sup>



This amide-functionalized porphyrin **8** proved integral for expanding beyond benzylic C–H amination. Zhang and coworkers hypothesize porphyrin **8** provided added

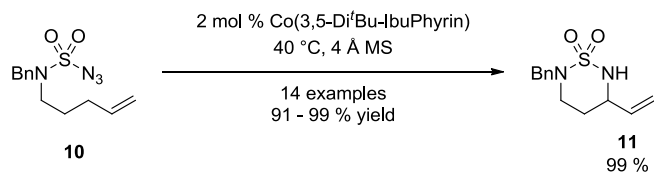
stabilization of the postulated nitrene intermediate through hydrogen-bonding (Scheme 2.4).<sup>21</sup> Using sulfamoyl azides (**9**), Zhang and coauthors were able to aminate unactivated primary, secondary, and tertiary C–H bonds. With this system, the first example of amination of primary C–H bonds was achieved.

**Scheme 2.4.** C–H amination with sulfamoyl azides (**9**) using [Co(3,5-Di*t*Bu-IbuPhyrin)] **8**.<sup>21</sup>



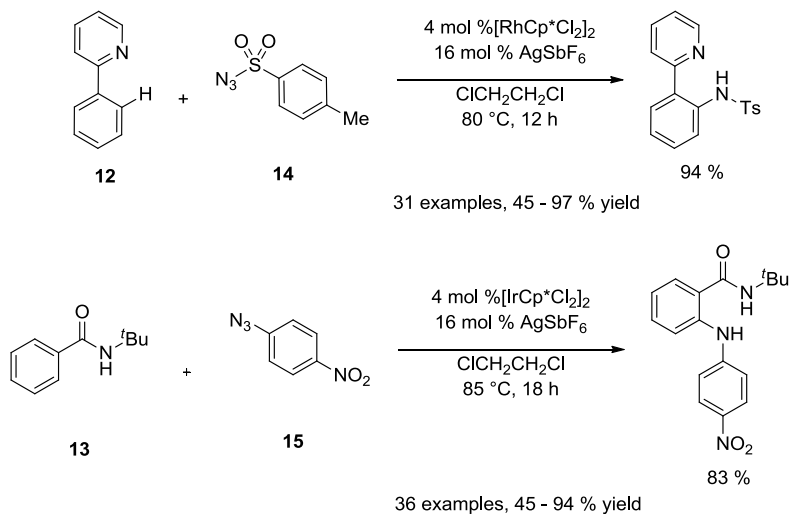
With the use of a first-row metal and porphyrin ligand framework, a radical mechanism is operative in the amination. Zhang and coworkers were able to use this mechanistic insight for chemoselective intramolecular allylic amination, without aziridination, using sulfamoyl azide **10** to give sulfamide **11** (Scheme 2.5).<sup>22</sup> Similarly, sulfamoyl azides were able to aminate sp<sup>3</sup> C–H bonds activated by electron withdrawing esters, amides, and ketones.<sup>23</sup> Subsequently, cobalt(II) tetraphenyl porphyrin was also found capable of accessing a limited number of benzylic bonds in an intermolecular context using electron-poor 2,2,2-trichloroethoxycarbonyl azide and an excess of substrate.<sup>24</sup>

**Scheme 2.5.** Intramolecular allylic C–H amination with sulfamoyl azide **10** to form sulfamide **11** using  $[\text{Co}(\text{3,5-DitBu-IbuPhyrin})]$ .<sup>22</sup>



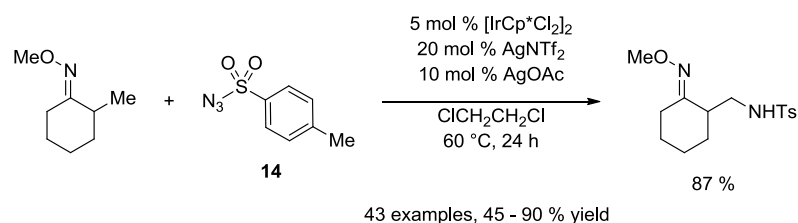
In broadening the scope and usefulness of intermolecular amination, Chang and coworkers found arenes containing chelating directing groups (**12** or **13**) could be amidated by 4-toluenesulfonyl azide (**14**) or 4-nitrophenyl azide (**15**) with  $[\text{RhCp}^*\text{Cl}_2]_2$  or  $[\text{IrCp}^*\text{Cl}_2]_2$  (Scheme 2.6).<sup>25-27</sup> Treatment of the dimer with a silver salt generates the cationic rhodium or iridium catalyst *in situ*. From this active species, amidation is proposed to occur through a five-membered metallocyclic intermediate, in a C–H insertion mechanism.

**Scheme 2.6.** Directed intermolecular arene C–H amidation with sulfonyl azide **14** and aryl azide **15**.<sup>25,26</sup>



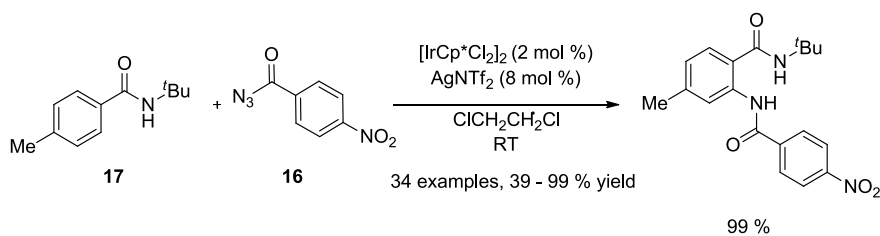
Chang and coworkers also discovered that the use of a directing group enabled the amidation of the  $sp^3$  C–H bonds of unactivated methyl groups with 4-toluenesulfonyl azide (**14**, Scheme 2.7).<sup>28</sup> Other azides with electron-withdrawing functionality were also tolerated, and the methodology was applied in the late stage amidation of  $sp^3$  C–H bonds.

**Scheme 2.7.** Intermolecular  $sp^3$  C–H amidation with sulfonyl azide **14**.<sup>28</sup>



Notably, electron-poor acyl azides (**16**) are also capable of C–H amidation with arenes (**17**) using  $[\text{IrCp}^*\text{Cl}_2]_2$  (Scheme 2.8).<sup>29</sup> This result is particularly notable, as acyl azides would be expected to react via Curtius rearrangement to give the isocyanates. The amidation was also extended to olefinic C–H bonds to produce *Z*-enamides. Amination with aryl sulfonyl azides also proceeded intermolecularly under the same conditions.<sup>30</sup>

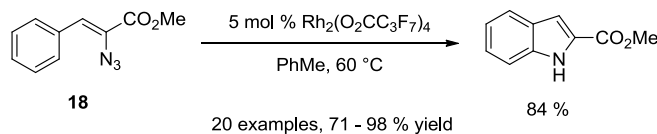
**Scheme 2.8.** Intermolecular C–H amidation of arene **17** with acyl azide **16** using  $[\text{IrCp}^*\text{Cl}_2]_2$ .<sup>29</sup>



### 2.1.2.2 Metallonitrene C–H Amination Utilizing Aryl and Vinyl Azides

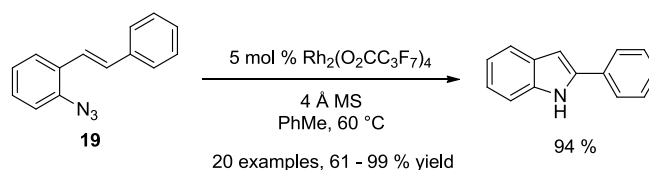
Despite their lack of electron-withdrawing functionality, vinyl and aryl azides are capable of revealing a metallonitrene suitable for C–H amination. In initial studies,  $\text{Rh}_2(\text{O}_2\text{CC}_3\text{F}_7)_4$  was found uniquely active for intramolecular aryl C–H amination with vinyl azides, such as **18** (Scheme 2.9).<sup>31</sup> The reaction forms indoles and other *N*-heteroaromatics in excellent yield.

**Scheme 2.9.**  $\text{Rh}_2(\text{O}_2\text{CC}_3\text{F}_7)_4$  catalyzed intramolecular aryl C–H amination with vinyl azide **18**.<sup>31</sup>



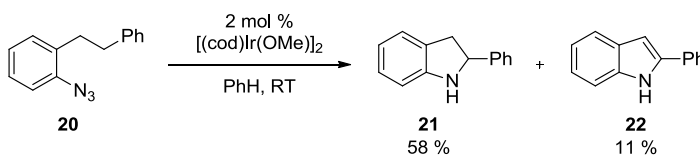
Similarly, aryl azides (**19**) are capable of insertion into vinyl C–H bonds with both iron<sup>32</sup> and rhodium<sup>33</sup> catalysts (Scheme 2.10). Amination with aryl azides is most effective into benzylic  $\text{sp}^2$  C–H bonds, and it is tolerant of both electron-withdrawing and electron-donating substitution on both aromatic rings. Biaryl azides also undergo rhodium catalyzed insertion to form carbazoles,<sup>34,35</sup> and vinyl azides undergo zinc catalyzed insertion into  $\text{sp}^2$  C–H bonds to form pyrroles.<sup>36</sup>

**Scheme 2.10.**  $\text{Rh}_2(\text{O}_2\text{CC}_3\text{F}_7)_4$  catalyzed intramolecular vinyl C–H amination with aryl azide **19**.<sup>33</sup>



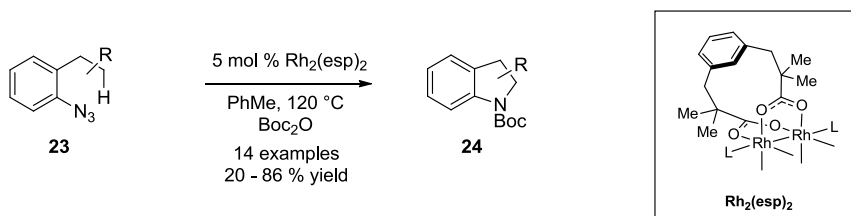
Beyond  $\text{sp}^2$  C–H bonds, Driver and coworkers found *ortho*-homobenzyl-substituted aryl azides (e.g., **20**) are capable of intramolecular benzylic  $\text{sp}^3$  C–H bond amination to form indolines (e.g., **21**) as well as indoles (e.g., **22**) by oxidation (Scheme 2.11).<sup>37</sup> After an expansive screen of catalysts, an iridium(I) dimer,  $[(\text{cod})\text{Ir}(\text{OMe})]_2$ , catalyzed the insertion at  $25 \text{ } ^\circ\text{C}$ . This reaction system was limited to the amination of secondary benzylic C–H bonds, and was functional even in the absence of electron withdrawing substitution of the aryl azide. However, increasing electron density further by substitution of a methoxy group on the aryl ring *para* to the azide suppressed the reaction completely. The system was also plagued by competing indole and aniline formation.

**Scheme 2.11.**  $[(\text{cod})\text{Ir}(\text{OMe})]_2$  catalyzed intramolecular benzylic C–H amination with aryl azide **20** to form indoline **21** and indole **22**.<sup>37</sup>



In order to extend the methodology to unactivated C–H bonds, C–H amination catalyst  $\text{Rh}_2(\text{esp})_2$  was found to catalyze intramolecular insertion into primary, secondary, and tertiary aliphatic C–H bonds from aryl azides (**23**) to form indolines (**24**, Scheme 2.12).<sup>38</sup> Interestingly,  $[(\text{cod})\text{Ir}(\text{OMe})]_2$  did not catalyze the reaction, and an electron donating substituent *para* to the azide did not suppress the reaction. These differences highlight the nuances of C–H amination and the need for additional catalyst systems to both understand the mechanism and expand the applicability.

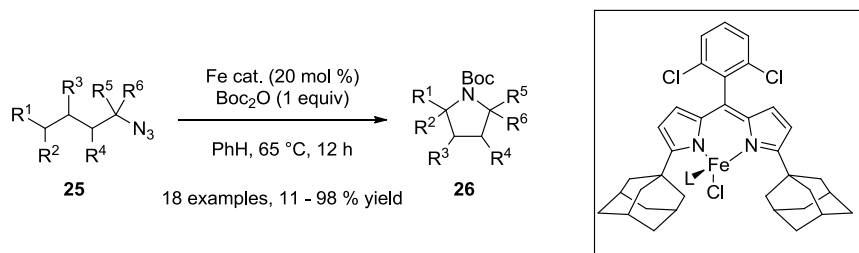
**Scheme 2.12.**  $\text{Rh}_2(\text{esp})_2$  catalyzed intramolecular amination of unactivated, aliphatic C–H bonds with aryl azides (**23**) to give indolines (**24**).<sup>38</sup>



### 2.1.2.3 Metallonitrene C–H Amination Utilizing Alkyl Azides

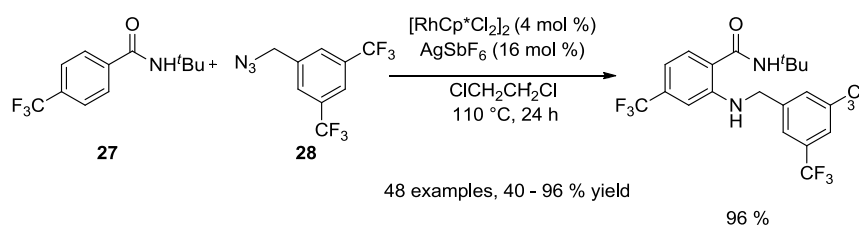
Alkyl azides (**25**) are particularly challenging for use as nitrene precursors in C–H amination, due to their propensity for rearrangement to form linear amines and imines via  $\beta$ -hydride elimination or intermolecular C–H activation (Scheme 2.13).<sup>39</sup> Using an iron-dipyrrinato catalyst inspired by the heme iron in cytochrome P450, Betley and coworkers found a range of aliphatic C–H bonds could be intramolecularly aminated, including allylic, benzylic, tertiary, and secondary bonds. Boc-Protection of pyrrolidine products (**26**) was necessary to prevent product-inhibition of the catalyst.

**Scheme 2.13.** Iron-dipyrrinato catalyzed intramolecular amination of aliphatic  $sp^3$  C–H bonds with alkyl azides (**25**) to form pyrrolidines (**26**).<sup>39</sup>



Using their  $[RhCp^*Cl_2]_2$  catalyst system, Chang and coworkers were also able to aminate aryl C–H bonds of arenes with appropriate directing groups (e.g., **27**) with alkyl azides (Scheme 2.14).<sup>40</sup> A variety of alkyl azides and chelating groups were well-tolerated, though most examples employed 3,5-di(trifluoromethyl)benzyl azide (**28**).

**Scheme 2.14.**  $[RhCp^*Cl_2]_2$  catalyzed intermolecular amination of aryl  $sp^2$  C–H bonds of arene **27** with alkyl azide **28**.<sup>40</sup>



### 2.1.3 Challenges in C–H Amination Utilizing Azide Metallonitrene Precursors

While an array of impressive work has contributed to the broadening applicability of azide-derived nitrenes for C–H amination, several challenges remain. One of these is the use of earth abundant transition metals for catalysis. Though first row metals have

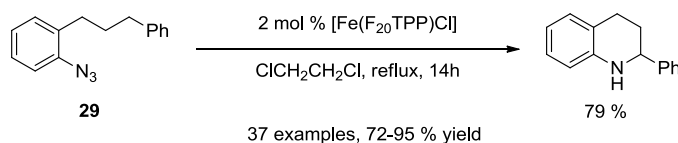


found more use in amination than in some other areas of catalysis, many transformations are still only possible with precious metals. Enantioselectivity also remains an outstanding challenge. Enantioselective aminations with azides are significantly more limited than other nitrene precursors, such as sulfamate esters, and have not been extensively studied.

### **2.1.3.1 Use of First Row Transition Metals in Metallonitrene C–H Amination Utilizing Aryl Azides**

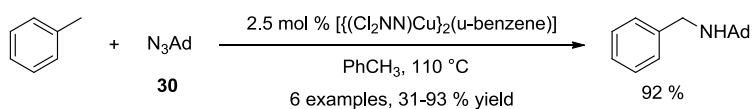
In addressing the challenge of coinage metals for C–H amination, Zhang and co-workers have made extensive contributions by expanding cobalt(II)-porphyrin metalloradical systems to mediate a variety of catalytic C–H aminations (Schemes 2.2-4). Che and coworkers have also used an iron-porphyrin complex for benzylic amination with vinyl and aryl azides (**29**), similar to the transformations catalyzed with [(cod)Ir(OMe)]<sub>2</sub> by Driver and coworkers (Scheme 2.15; Scheme 2.11).<sup>41</sup> Betley and coworkers have also demonstrated the capacity for incorporating a redox-active ligand framework in iron(II) complexes to catalyze reactions that are otherwise untenable (Scheme 2.13). Betley and coworkers also extended this ligand system to a cobalt(I) complex capable of intraligand amination, though not yet in a catalytic manner.<sup>42</sup>

**Scheme 2.15.** Iron-porphyrin catalyzed intramolecular benzylic C–H amination with aryl azide **29**.<sup>41</sup>



Warren and coworkers have employed a  $\beta$ -diketimide dicopper complex for C–H amination reactions with 1-adamantylazide (**30**), primarily into benzylic C–H bonds (Scheme 2.16).<sup>43</sup> Use of an adamantyl or *tert*-butyl substituent for introducing steric bulk in the azide was necessary to aid in the dissociation of the copper fragments to form a monomeric active species.<sup>44</sup>

**Scheme 2.16.** Intermolecular benzylic C–H insertion with 1-adamantylazide (**30**).<sup>43</sup>



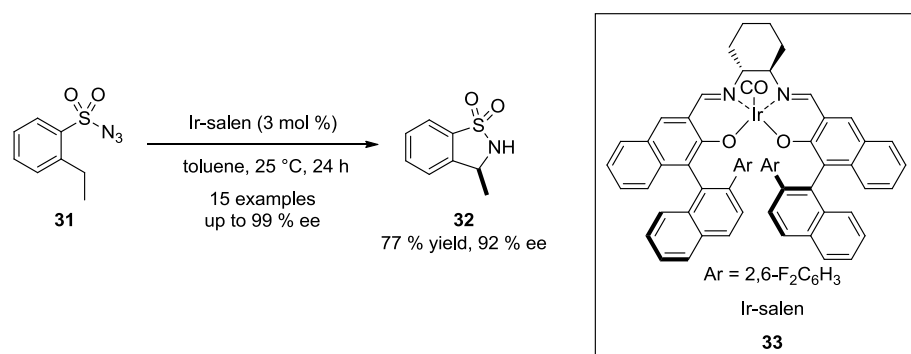
As shown in these examples, the incorporation of redox-active ligands<sup>45-47</sup> has proven critical for promoting multi-electron processes with first-row transition metals, which might not be innately useful in C–H amination.

### 2.1.3.2 Enantioselectivity in Metallonitrene C–H Amination Utilizing Aryl Azides

Enantioselective C–H amination with azides is far less developed than racemic variants. Based on the discovery that their chiral iridium(III)-salen complexes catalyze

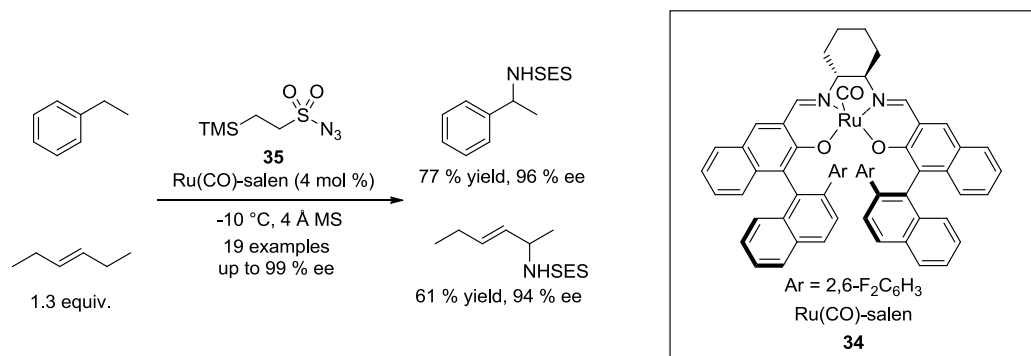
enantioselective C–H functionalization with carbenes, Katsuki and coworkers found these complexes could also catalyze intramolecular and intermolecular C–H amination with azides in excellent enantioselectivity. Sulfonyl azide **31** undergoes benzylic C–H amination in 77 % yield of sultam **32** in 92 % ee with iridium(III)-salen **33** (Scheme 2.17).<sup>48</sup> A variety of electronic variation around the aryl ring is also tolerated.

**Scheme 2.17.** Iridium-salen **33** catalyzed intramolecular enantioselective benzylic intramolecular C–H amination with aryl sulfonyl azide **31** to form sultam **32**.<sup>48</sup>



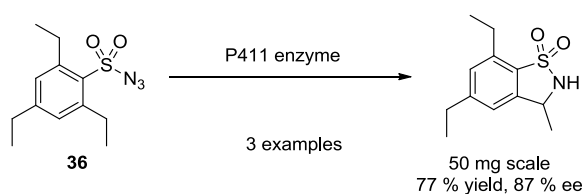
Likewise, ruthenium-salen complex **34** catalyzed intermolecular C–H amination with 2-(trimethylsilyl)ethanesulfonyl azide (**35**) in excellent enantioselectivity (Scheme 2.18).<sup>49</sup> The insertion was generalizable to ethyl, methyl, and cyclic methylene groups in allylic or benzylic positions.

**Scheme 2.18.** Ruthenium-salen **34** catalyzed intermolecular enantioselective benzylic and allylic intermolecular C–H amination with 2-(trimethylsilyl)ethanesulfonyl azide (**35**).<sup>49</sup>



Intramolecular benzylic amination with aryl sulfonyl azides (**36**) may also be catalyzed in moderate to good enantioselectivity with cytochrome P450 variant P411 in the first enzyme catalyzed C–H amination by Lewis, Arnold, and coworkers (Scheme 2.19).<sup>50</sup> This amination method was found effective *in vivo* in *E. Coli* cells as well. Subsequently, complementary variants were developed for differing regioselectivity modes, with one P411 enzyme selective for benzylic C–H bonds and the other for homo-benzylic C–H bonds.<sup>43</sup> Both proceeded with excellent enantioselectivity.

**Scheme 2.19.** P411 catalyzed enantioselective intramolecular C–H amination with sulfonyl azide **36**.<sup>50</sup>



## 2.2 Modular Ligand Design for Enantioselective Catalysis

Through this survey of the azide amination literature, many of the catalyst systems are quite specialized, requiring optimization with particular metals and ligand frameworks for each class of azide or target C–H bond. We still do not have broadly applicable mechanistic rules that would enable *de novo* prediction of useful ligand systems; experimental optimization is necessary. As William Knowles wrote of asymmetric hydrogenation (as quoted by Sigman and coauthors): “Since achieving 95 % [enantiomeric excess] only involves energy differences of about 2 kcal [per mol], which is no more than a barrier encountered in a simple rotation of ethane, it is unlikely that before the fact one can predict what kind of ligand structures will be effective.”<sup>51,52</sup> More easily tunable ligands would be extremely useful in addressing this concern, allowing facile catalyst evolution in keeping with experimental results. Such ligands would have easily adjustable chiral pockets and be amenable to complexation with both coinage and precious metals. Additionally, these modular ligands will be amenable to mathematical modeling strategies to enable the prediction of optimal ligand substitution. Though azides are the target substrate of our study, the catalysts we discuss may be useful for C–H functionalization and other reactions with both nitrenes and carbenes.

### 2.2.1 Oxazoline-Based Modular Ligands

In considering modular, enantioselective ligand systems, oxazoline-based systems have been recognized as privileged structures.<sup>53</sup> One of the particular advantages of

oxazolines, compared to other privileged catalysts such as salen or BINOL derivatives, is their ease of synthesis. In addition to bis(oxazoline) ligands,<sup>54</sup> a single oxazoline moiety can be incorporated alongside other functionality in unsymmetrical oxazoline ligand variants (Figure 2.1)<sup>55,56</sup>

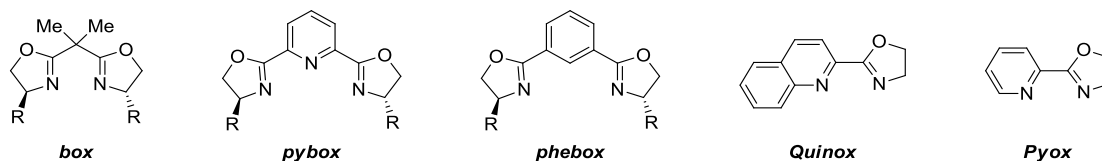


**Figure 2.1.** Representative oxazoline ligand classes.<sup>54-56</sup>

## 2.2.2 Linear Regression Mathematical Modeling for Catalyst Optimization

Ligand design has long involved mostly reaction screening and chemical intuition, especially before the desired reaction mechanism is well-understood. Although there may not be enough information about the mechanism of nitrene C–H amination to make design from first principles possible, the Sigman group has recently made significant strides in methods for three-dimensional correlation of steric and electronic free energy relationships for systematic catalyst optimization. Instead of relying on guesswork and empirical catalyst synthesis and testing, their method takes into account the synergistic interactions of both effects for prediction of optimal catalyst structures. Sigman and coworkers have applied their method to optimize ligand structures to great effect with oxazoline-based ligands.

For example, in the case of chromium catalyzed enantioselective ketone propargylation, a limited library of proline-oxazoline ligand **37** was synthesized for

modeling (Figure 2.2).<sup>57</sup> In this case, the Charton values of groups “X” and “Y” were graphed against enantioselectivity on a three dimensional surface. A predicted maximum across the surface then gave the catalyst system with the maximum enantioselectivity possible using their proline-oxazoline ligand system **37**. Through the use of mathematical modeling, empirical enantioselectivity measurements and synthesis of catalysts were drastically reduced. This methods saves time and resources spent in synthesizing and applying a variety of catalysts. All that is needed is a sufficient data table of ligand variants and corresponding enantioselectivities (in this case, a total of nine catalysts).

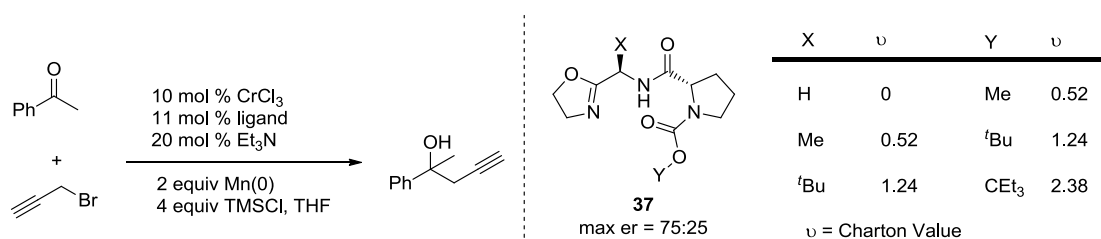


**Figure 2.2.** Enantioselective ketone propargylation with proline-oxazoline ligand **37** for mathematical modeling.<sup>57</sup>

Unfortunately, according to the model, the oxazoline-proline ligand structure **37** was only capable of a maximum er of 75:25. This enabled Sigman and coworkers to modify their ligand structure before extensive experimental work was performed. The ligand was modified to a quinoline-proline ligand scaffold **38** (Figure 2.3). Modeling of both the steric impact of the proline fragment (“S”) and electronic variation around the quinoline ring (“E”) led to a maximum predicted er of 92:8. Experimentally with the optimal catalyst **38** (E = OMe, S = *t*-Bu), an er of 96:4 was observed in the test

propargylation. This method provides an attractive method for optimizing reactions where mechanistic understanding is limited, and applications extend even beyond predictions of enantioselectivity. One condition of this methodology is that it does not require a catalyst with several turning points for easy variability.

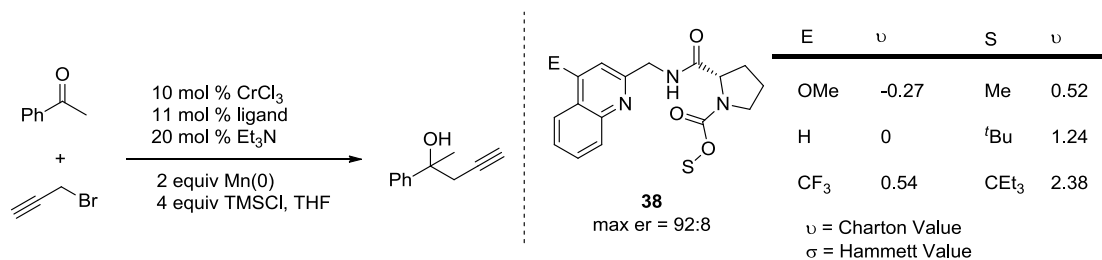


**Figure 2.3.** Enantioselective ketone propargylation with quinoline-proline ligand **38** for mathematical modeling.<sup>57</sup>

This mathematical modeling technique has been further expanded to include complementary empirical modeling of both the substrate substitution as well as catalyst tuning.<sup>58</sup> This data-driven approach has also been applied in the enantioselective allylation of benzaldehyde under Nozaki-Hiyama-Kishi conditions.<sup>59-61</sup> It is not limited to oxazoline-based catalysis, but has been used for chiral anion catalysis,<sup>62</sup> as well as for interpreting site selectivity of a reaction.<sup>63</sup> Though for our purposes, we are primarily interested in steric and electronic catalyst tuning, a variety of physical parameters of the catalyst may be used in the analysis, such as acidity and polarizability.<sup>64</sup>



### 2.2.3 Planned Synthetic Routes to Quinoline/Oxazoline Amide Ligands

In collaboration with the Sigman group, we designed a modular ligand system to take advantage of this three-dimensional modeling method. We plan to synthesize a novel, flexible, tridentate mono-anionic ligand **39**. The ligand will include a quinoline ring for electronic tuning, an amide linker, and an oxazoline ring for steric tuning and introduction of chirality. Though Quinox ligands have been used in catalysis,<sup>65-68</sup> an amide linker has not previously been introduced (Figure 2.4).

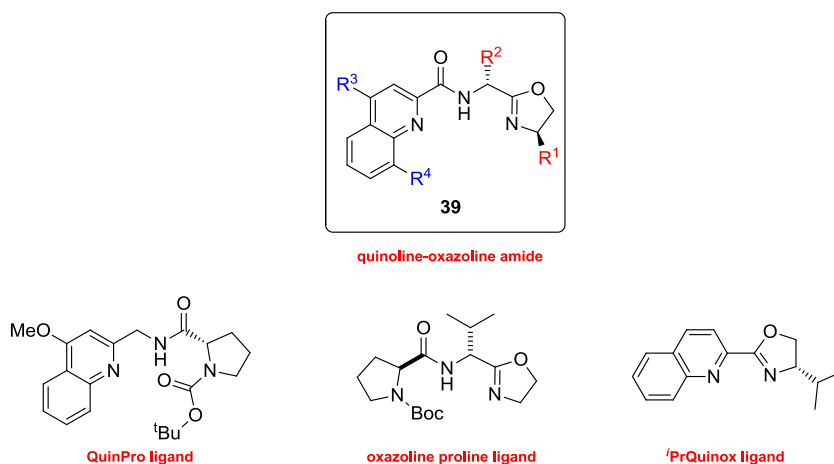


**Figure 2.4.** Comparison of proposed quinoline-oxazoline amide ligand structure **39** with inspiration ligands.<sup>65-68</sup>

Many of the above ligands form active catalyst species when mixed *in situ* with an appropriate metal salt. However, we will seek to isolate and characterize the metal-ligand complex prior to introduction to reaction conditions. Based on the results from Driver and coworkers with aryl azide amination (Scheme 2.11), we will seek to synthesize the iridium(I) and iridium(III) complexes **40** and **41**, respectively, as well as

the other Group 9 complexes with cobalt and rhodium (Figure 2.5). The chiral pocket may be tuned at  $R^1$  and  $R^2$ , and electron-donating and electron-withdrawing groups may be introduced at  $R^3$  and  $R^4$ . The iridium(III) complex **41** is shown with meridional ligand coordination geometry, though facial coordination is also a possibility, which may cause difficulties for chiral catalysis.

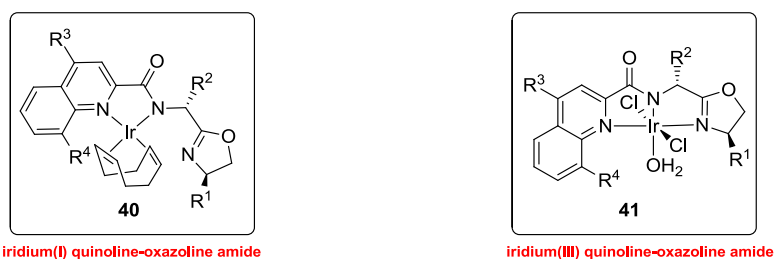
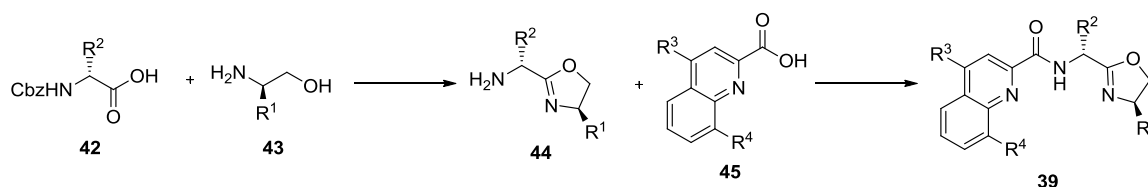


**Figure 2.5.** Proposed iridium(I) and iridium(III) quinoline-oxazoline amide complexes **40** and **41**.

Because of the ligand design, we anticipate a modular synthesis, with facile introduction of both the quinoline and oxazoline fragments. We propose two routes for ligand synthesis. In the first method, the synthesis begins with coupling of the Cbz protected amino acid **42** with an amino alcohol **43**, to form the Cbz-protected oxazoline, with chirality introduced via the commercially available amino acid and amino alcohol building blocks (Scheme 2.20). The protecting group is removed by hydrogenolysis to give the oxazoline **44**.<sup>59,69</sup>

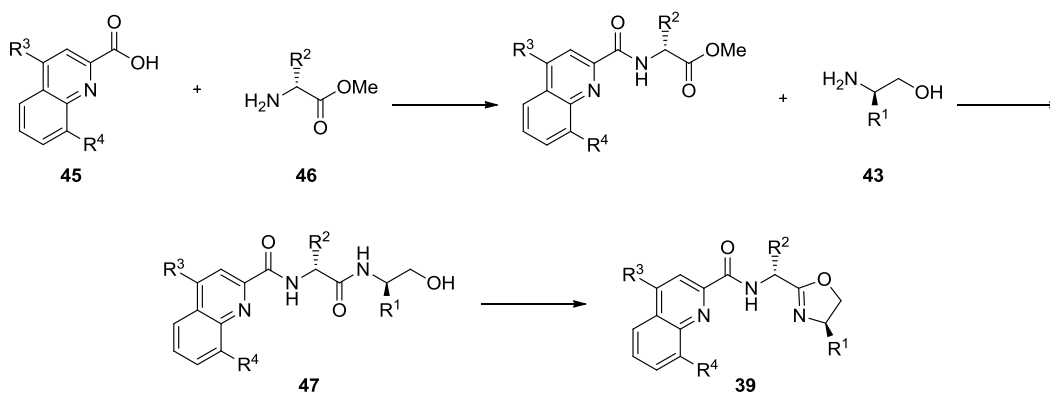
**Scheme 2.20.** Synthetic route to quinoline-oxazoline amide ligand **39** for electronic turning of the quinoline fragment.



The final step is amide bond formation with the appropriate quinaldic acid **45** to form the quinoline-oxazoline amide **39**. One benefit of this route is that it introduces the quinoline portion in the final step, so it will be particularly useful for varying electronic substituents around the ring. However, it does include the Cbz-protection and deprotection, which is not necessary via the second route.

The second method begins with coupling of a quinaldic acid **45** and an amino ester **46** (Scheme 2.21). This is followed by acyl transfer with an enantioenriched amino alcohol **43** to give amide **47**. A similar route has been pursued in the synthesis of proline-oxazoline amide ligands.<sup>70</sup> Final cyclization of the oxazoline gives the quinoline-oxazoline amide **39**. One of the benefits of this route is that the oxazoline is formed in the final step, so there are no concerns about ring-opening throughout the rest of the sequence. It will also be more useful for varying the steric substitution of the oxazoline, since this fragment is introduced at a later step. An additional benefit of this route is that it does not require Cbz protection and deprotection. It also does not involve exposure of a potentially fragile oxazoline moiety to the entire synthetic sequence.

**Scheme 2.21.** Synthetic route to quinoline-oxazoline amide ligand **39** for steric turning of the oxazoline fragment.

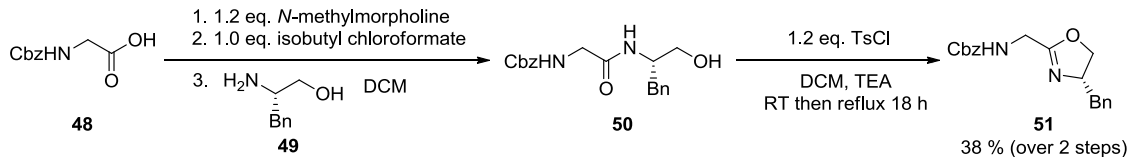


## 2.3 Enantioselective C–H Amination with Iridium(I) and Iridium(III) Catalysts

### 2.3.1 Quinoline/Oxazoline Amide Ligand Synthesis

Ligand synthesis began with the first route presented, in part due to the robust precedent for oxazolanyl amine synthesis (Scheme 2.20). In keeping with literature precedent,<sup>59</sup> commercially available Cbz-protected amino acid **48** is coupled with commercially available (*S*)-phenylalaninol (**49**) to introduce the chiral center in amide **50** (Scheme 2.22). Cyclization was accomplished by tosylation of the alcohol moiety of **50** followed by ring-closing at reflux to yield 38 % of Cbz-protected oxazoline **51**. Initially, no substitution was introduced adjacent to the oxazoline for simplicity.

**Scheme 2.22.** Synthesis of Cbz-protected oxazoline **51**.



Unfortunately, though oxazoline synthesis proceeded smoothly, Cbz deprotection posed some difficulty. Initial efforts with Pd/C in a variety of solvents (Table 2.2, entries 1-3) resulted in recovery of starting material **51**. Sigman and coworkers also report that they were unable to remove a Cbz group from a similar oxazoline, though they attributed it to the presence of a sulfur-containing impurity from a previous step.<sup>71</sup> Use of Pearlman's catalyst also resulted in no conversion (entry 4). Finally, with a fresh bottle of Pd/C, slight conversion to oxazoline **52** was observed.

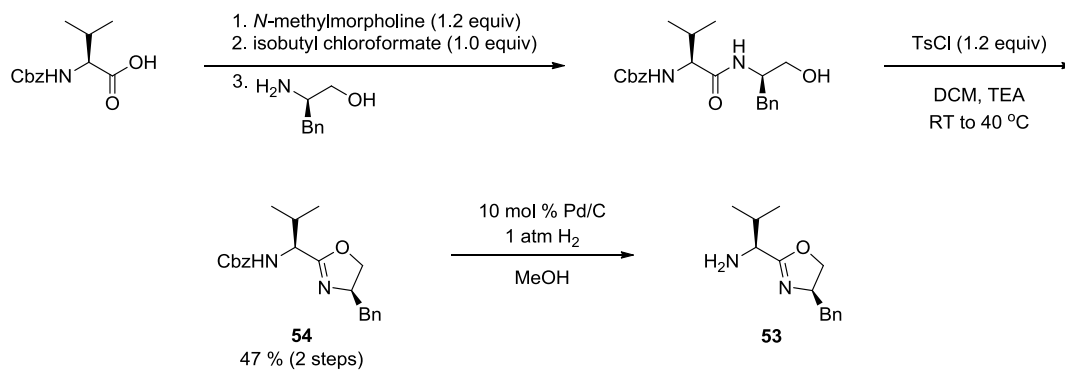
**Table 2.2.** Cbz Deprotection attempts of oxazoline **51**.

entry	catalyst	catalyst loading (mol %)	solvent	outcome
1	Pd/C	5	MeOH	<b>51</b>
2	Pd/C	5	EtOH	<b>51</b>
3	Pd/C	5	THF	<b>51</b>
4	Pd(OH) <sub>2</sub> /C	20	MeOH	<b>51</b>
5	Pd/C	5	EtOH	<b>51 + 52</b>

Based on these difficulties, isopropyl substitution was introduced to the ligand backbone in order to reproduce the literature synthesis of **53** (Scheme 2.23).<sup>59</sup> In Sigman and coworkers' report on the synthesis of amine functionalized oxazolines, they describe

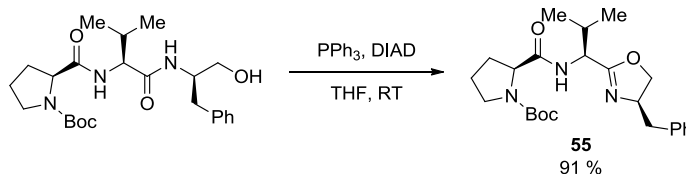
the deprotection of substrate **54** as “sluggish,” and it did not proceed to completion.<sup>71</sup> We observed some conversion to **53**, but overall it was found that the deprotection was inefficient and batch-dependent upon the palladium catalyst.

**Scheme 2.23.** Oxazoline **54** synthesis and deprotection.



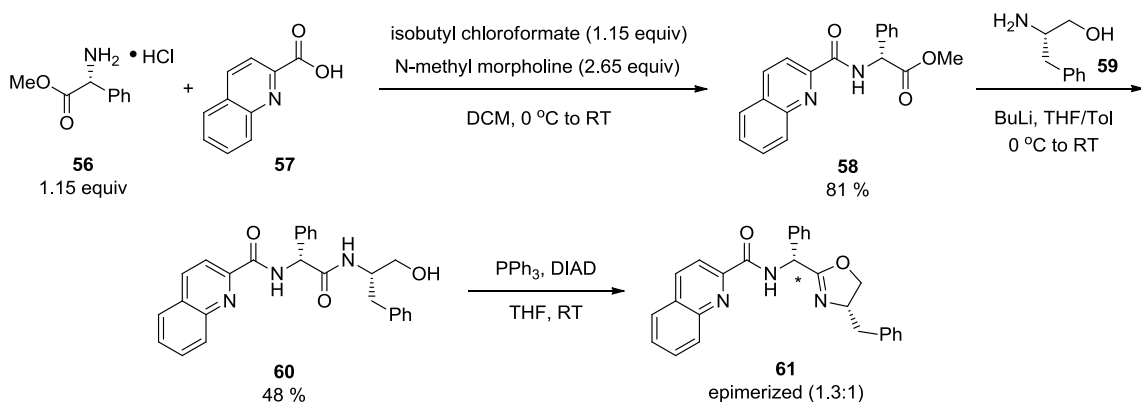
Though this first route would be complementary for tuning the electronics around the quinoline ring, the second synthetic strategy to quinoline-oxazoline amides (**39**) was pursued to avoid the problematic deprotection (Scheme 2.21). The synthesis begins with coupling of a chiral amino ester and quinaldic acid, based on the literature synthesis of proline-oxazoline amide ligands.<sup>57</sup> Then, acyl transfer with an enantioenriched amino alcohol leads to the pre-cyclized ligand with two stereocenters in place. The oxazoline is then formed under Mitsunobu conditions, following a precedent for proline-oxazoline amide **55** formation (Scheme 2.24).<sup>71</sup>

**Scheme 2.24.** Proline-oxazoline amide ligand **55** synthesis under Mitsunobu conditions.<sup>71</sup>



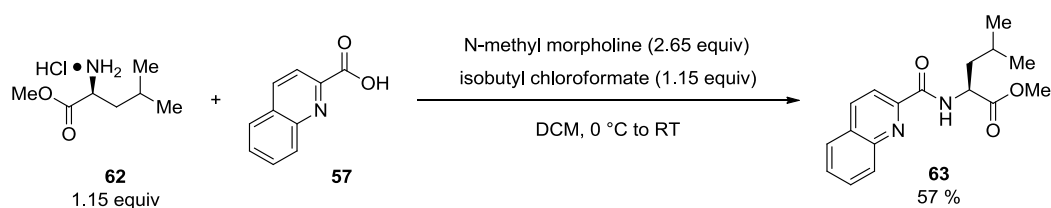
Coupling (*R*)-phenylglycine methyl ester (**56**) with quinaldic acid (**57**) proceeded to afford 81% of amide **58**, with a simple recrystallization for purification (Scheme 2.25). Reaction with (*S*)-phenylalaninol (**59**) gave 48 % yield of the cyclization precursor **60**. Unfortunately, the final cyclization resulted in epimerization of the marked stereocenter in **61**. To provide evidence that **61** was a mixture of epimers, rather than rotamers, high temperature <sup>1</sup>H NMR showed no coalescence of peaks. Some separation of the epimers was also possible by flash chromatography, without interconversion. Unfortunately, the hydrazide byproduct from the Mitsunobu reaction also proved extremely difficult to separate from quinoline-oxazoline amide **61**.

**Scheme 2.25.** Benzyl-substituted quinoline-oxazoline amide ligand **61** synthesis.



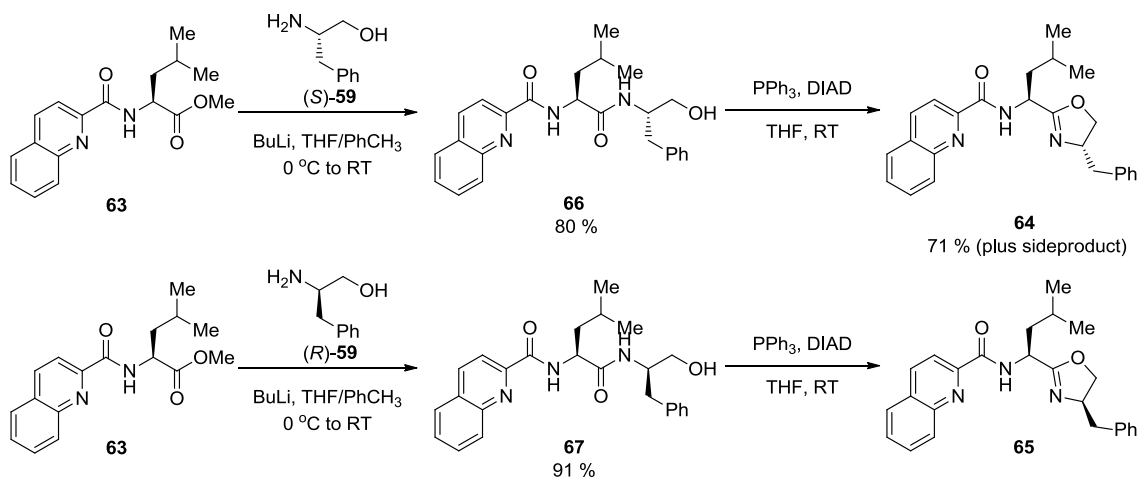
We hypothesized that this difficulty with epimerization of ligand **61** might be caused by the acidity imparted by the phenyl-substitution of the backbone. For this reason, we next employed the isobutyl amino ester **62** to synthesize amide **63** in 57 % yield (Scheme 2.26).

**Scheme 2.26.** Synthesis of isobutyl-substituted quinoline amide **63**.

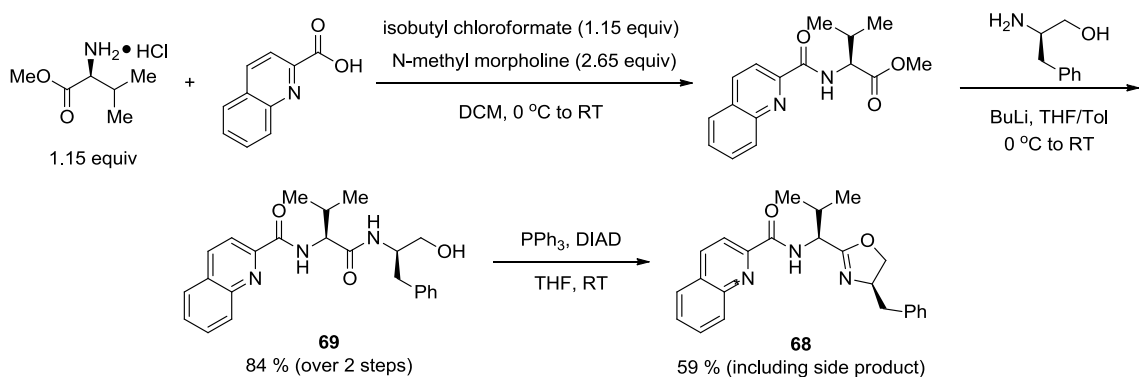


In order to determine which step in the ligand synthesis might induce epimerization, we synthesized ligand diastereomers **64** and **65** based on phenylalaninol enantiomers (*R*)-**59** and (*S*)-**59** and amide **63** (Scheme 2.27). By synthesizing diastereomers **64** and **65**, comparison of the  $^1\text{H}$  NMR spectra would allow us to determine if any epimerization had taken place. By  $^1\text{H}$  NMR, both amides **66** and **67** were each distinct diastereomers, with no minor diastereomers observable. Nor were minor diastereomers observed in **64** and **65**. Fortunately, epimerization was not occurring with this substrate; however, a co-eluting side product from the cyclization reaction could not be separated from quinoline-oxazoline amides **64** and **65**.



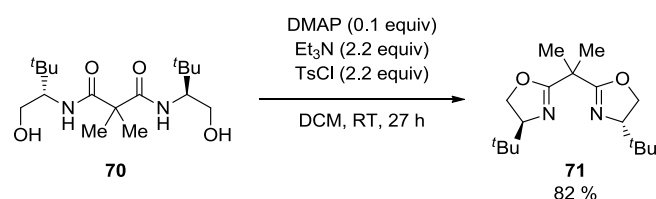
**Scheme 2.27.** Synthesis of diastereomeric quinoline-oxazoline amide ligands **64** and **65**.

Unfortunately, even synthesis of isopropyl-substituted ligand **68** still resulted in a side product (in addition to the hydrazide) that could not be separated (Scheme 2.28). However, as in previous syntheses, the formation of amide **69** proceeded smoothly in 84 %. This led us to seek out different cyclization conditions for oxazoline formation to avoid the problematic side product.

**Scheme 2.28.** Synthesis of isopropyl-substituted quinoline-oxazoline amide ligand **68**.

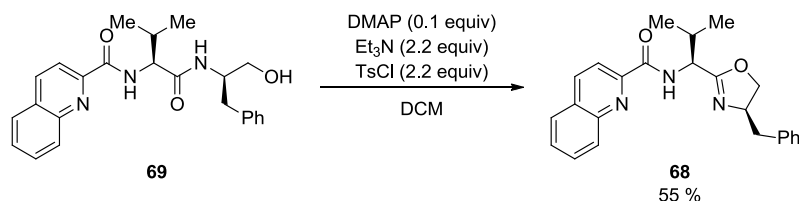
A variety of ring-closure methods for oxazolines have been evaluated throughout the literature. Evans and coauthors disclosed a method using catalytic 4-(dimethylamino)pyridine, *p*-toluenesulfonyl chloride, and triethylamine for cyclization of amide **70** to yield bis(oxazoline) **71** in 82 % (Scheme 2.29).<sup>72</sup> We expect that by applying this method to eliminate the use of Mitsunobu conditions, we can simplify ligand purification.

**Scheme 2.29.** Alternate oxazoline-forming reaction for synthesis of bis(oxazoline) **71**.<sup>72</sup>



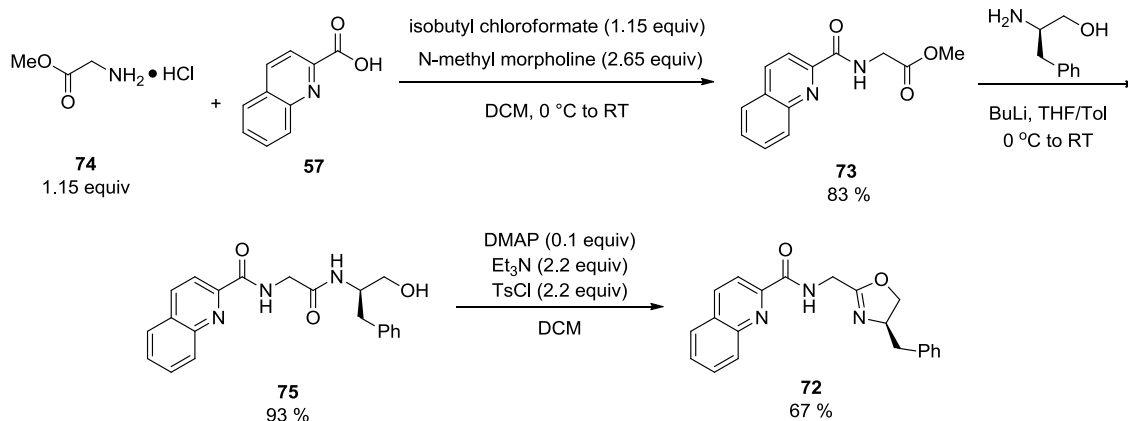
In our hands, these cyclization conditions proved much more successful for the synthesis of quinoline-oxazoline amide **68** in 55 % yield, with no problematic side products (Scheme 2.30).

**Scheme 2.30.** Cyclization of amide **69** with catalytic DMAP to yield quinoline-oxazoline amide **68**.



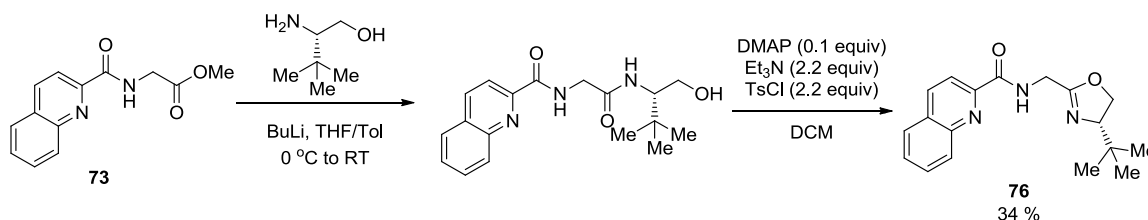
Subsequently, glycine-based ligand **72** was designed to provide a simple ligand for ease of metallation (Scheme 2.31). By keeping the backbone substitution constant, initial catalyst studies will be designed to vary substitution only at the 4-position of the oxazoline and 4-position of the quinoline. Amide **73** was synthesized in 83 % from quinaldic acid **57** and amino methyl ester **74**. Cyclization precursor **75** was afforded in 93 % from **73**, or in 80 % yield from **74** and **57** without intermediate purification. Subsequent cyclization proceeded cleanly to yield quinoline-oxazoline amide **72** in 67 % yield.

**Scheme 2.31.** Synthesis of benzyl-substituted quinoline-oxazoline amide ligand **72**.



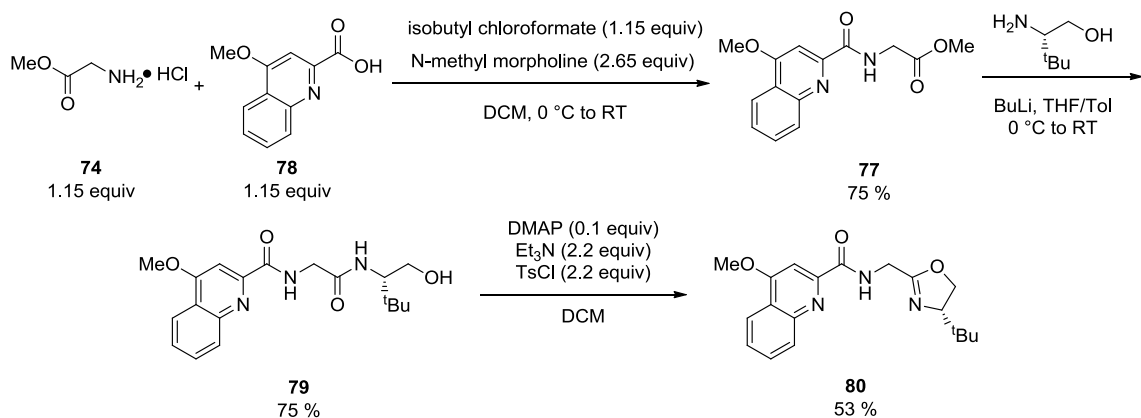
For studies of the resultant transition-metal complexes, we incorporated a *tert*-butyl substituent at the 4-position of the oxazoline to aid in crystallization. From amide **73**, quinoline-oxazoline amide ligand **76** was afforded in 34 % yield over two steps (Scheme 2.32).

**Scheme 2.32.** Synthesis of *tert*-butyl-substituted quinoline-oxazoline amide ligand **76**.



To introduce variation in the electronics of the quinoline, a methoxy group was substituted at the 4-position. The methoxy amide **77** was synthesized in 75 % yield from the commercially available 4-methoxy quinaldic acid **78** and amino methyl ester **74** (Scheme 2.33). Formation of cyclization precursor **79** was also accomplished in good yield (75 %), and subsequent cyclization gave quinoline-oxazoline amide ligand **80** in 53 % yield. Ligand **80** was found to be a crystalline, white solid, which we anticipated would be beneficial for crystallization of the resultant transition metal complexes.

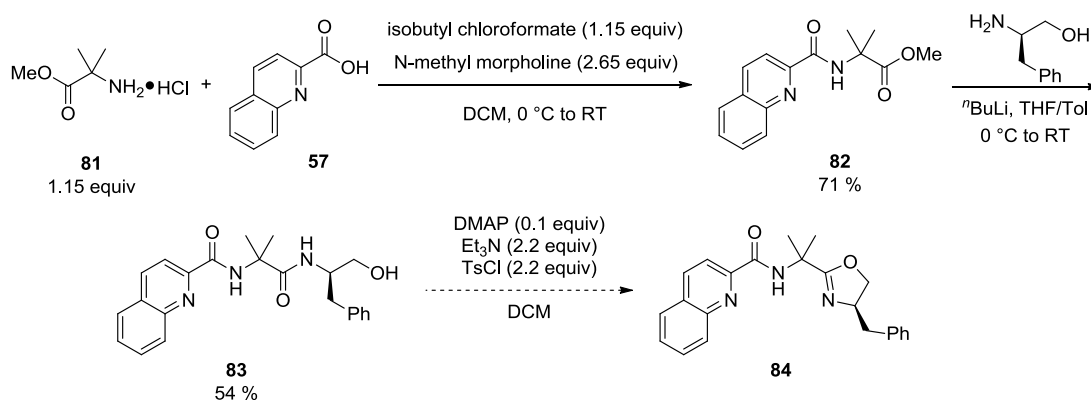
**Scheme 2.33.** Synthesis of methoxy-substituted quinoline-oxazoline amide ligand **80**.



Lastly, backbone substitution was investigated. Introduction of *gem*-dimethyl substitution was intended to aid in rigidifying the ligand backbone were any difficulties

in coordination of the metal experienced. From reaction of *gem*-dimethyl amino ester **81** and unsubstituted quinaldic acid **57**, amide **82** was produced in 71 % yield (Scheme 2.34). Benzyl-substituted cyclization precursor **83** was afforded in 54 % yield. However, the final step in ligand synthesis of quinoline-oxazoline ligand **84** has not been completed.

**Scheme 2.34.** Planned synthesis of *gem*-dimethyl-substituted quinoline-oxazoline amide ligand **84**.

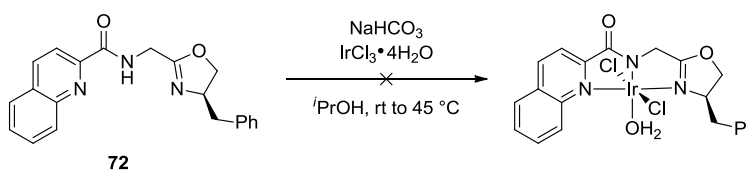


### 2.3.2 Quinoline/Oxazoline Amide Ligand Metalation and Resultant Complex Characterization

With quinoline-oxazoline amide ligands in hand, our studies next turned to metalation with iridium(III) and iridium(I) salts. Due to our group's studies of iridium(III) bis(oxazoliny)phenyl (phebox) complexes,<sup>73</sup> the simple 4-benzyl-substituted oxazoline ligand **72** was first exposed to IrCl<sub>3</sub>·3H<sub>2</sub>O with sodium bicarbonate in refluxing isopropanol for metalation (see Section 2.3.4). However, no metalation was observed, and only decomposed ligand was recovered.

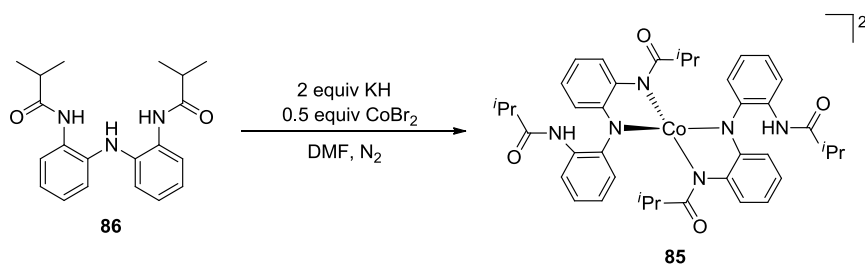
Upon gentler heating, no reaction was observed (Scheme 2.35). Though both the quinoline-oxazoline amide ligand and phebox ligand are tridentate, monoanionic ligands, the C–H insertion into the  $sp^2$  aryl C–H bond required to form iridium(III) phebox complexes represents a considerable difference from the amide deprotonation required to form our iridium(III) quinoline-oxazoline amide complexes. Therefore, it is reasonable that different metalation conditions are required.

**Scheme 2.35.** Attempted metalation of quinoline-oxazoline amide ligand **72** with  $\text{IrCl}_3 \cdot 3\text{H}_2\text{O}$  and  $\text{NaHCO}_3$  at room temperature to  $45^\circ\text{C}$ .



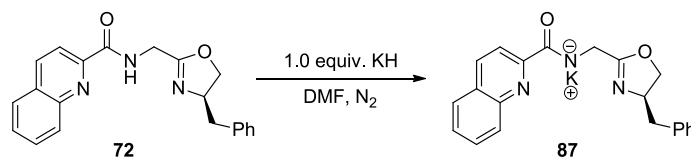
In collaboration with the MacBeth group, metallation conditions similar to those used for their cobalt(II) amidate complex **85** were investigated (Scheme 2.36).<sup>74</sup> Deprotonation of amide ligands with hydride bases has been well-established in the literature for generation of salts of these ligands *in situ*, which can then be metalated easily with transition metal ions.<sup>75-79</sup> In this instance, two equivalents of potassium hydride are added to deprotonate the two amide arms of the ligand **86**, forming a potassium-ligand salt. Then, stirring with a simple cobalt(II) salt results in formation of complex **85**.

**Scheme 2.36.** Cobalt(II) metalation of  $\text{HN}(o\text{-PhNHC(O)}^i\text{Pr})_2$  ligand (**86**) to form cobalt(II) complex **85**.<sup>74</sup>



With this in mind, the potassium-ligand salt **87** was first isolated to confirm deprotonation (Scheme 2.37). Addition of one equivalent of potassium hydride to a solution of ligand **72** in the glovebox resulted in observable bubbling and a light orange solution. The clean potassium-ligand salt **87** was observed by  $^1\text{H}$  NMR.

**Scheme 2.37.** Formation of ligand-potassium salt **87** from quinoline-oxazoline amide **72**.



Following isolation of the ligand salt **87**, a variety of metalation conditions were examined with ligand **72** and iridium(III) salts in the glovebox (Table 2.3). The most promising results were observed with extended heating in dimethylformamide, which was required as solvent for solubility of the potassium hydride. Throughout metalation attempts, insolubility of the iridium(III) salt was a challenge, as black, insoluble salt was consistently observed in the reaction flask. Reactions were monitored by mass spectrometry.

Under mild heating, deprotonation with potassium hydride and metalation with  $\text{IrCl}_3$  in dimethylformamide over three days was unsuccessful (Table 2.3, entry 1). The  $\text{IrCl}_3 \cdot 3\text{H}_2\text{O}$  salt was more soluble under reaction conditions, but without heating did not produce complex **88** (entry 2). The hydrate was not investigated further, as reprotonation of the ligand could be problematic. Silver carbonate was also attempted for deprotonation, with the aim of aiding in chloride abstraction, but no reaction was observed (entry 3). Strong heating to  $125^\circ\text{C}$  over 12 days resulted in minor observation and tentative characterization of **88** by mass spectrometry, but complex **88** could not be isolated.

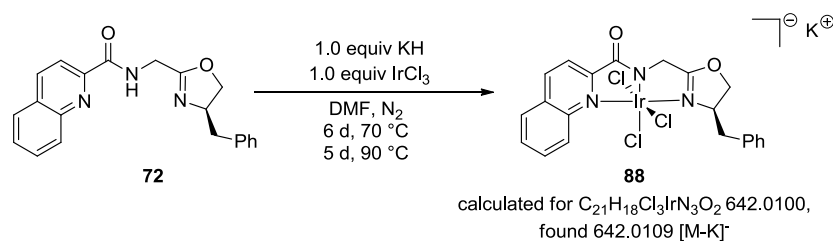
**Table 2.3.** Metalation conditions for quinoline-oxazoline ligand **72** to form iridium(III) complex **88** (tentatively characterized by mass spectrometry).

entry	Ir(III) salt	base	solvent	time	T ( $^\circ\text{C}$ )	outcome
1	$\text{IrCl}_3$	KH	DMF	RT to $45^\circ\text{C}$	24 h to 48 h	NR
2	$\text{IrCl}_3 \cdot 3\text{H}_2\text{O}$	KH	DMF	RT	48 h	NR
3	$\text{IrCl}_3$	$\text{Ag}_2\text{CO}_3$	MeOH	RT to reflux	24 h to 72 h	NR
4	$\text{IrCl}_3$	KH	DMF	$125^\circ\text{C}$	12 days	minor <b>88</b>

Exposure of ligand **72** to potassium hydride and anhydrous  $\text{IrCl}_3$  in dimethylformamide with heating at  $70^\circ\text{C}$  for six days, followed by heating at  $90^\circ\text{C}$  for 5 days, resulted in observation and tentative characterization of **88** by mass spectrometry (Scheme 2.38). Unfortunately, multiple crystallizations, as well as flash chromatography, failed to yield pure complex **88**.

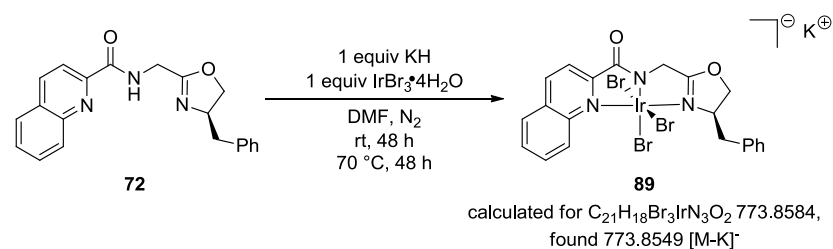


**Scheme 2.38.** Metalation of quinoline-oxazoline ligand **72** with  $\text{IrCl}_3$  to form iridium(III) complex **88** (tentatively characterized by mass spectrometry).



Use of the  $\text{IrBr}_3 \cdot 4\text{H}_2\text{O}$  salt was also attempted for metalation (Scheme 2.39). The hydrate was observed to be more soluble in dimethylformamide than the  $\text{IrCl}_3$  salt, and complex **89** was observed and tentatively characterized by mass spectrometry, although isolation was again unsuccessful.

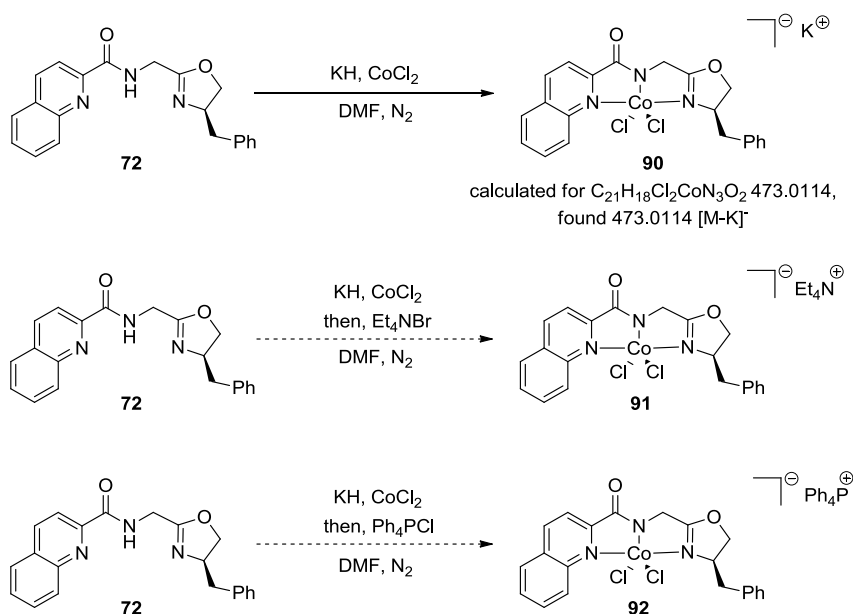
**Scheme 2.39.** Metalation of quinoline-oxazoline ligand **72** with  $\text{IrBr}_3 \cdot 4\text{H}_2\text{O}$  to form iridium(III) complex **89** (tentatively characterized by mass spectrometry).



Ligand **72** was exposed to metalation conditions with  $\text{CoCl}_2$ , both for understanding of quinoline-oxazoline amide coordination and also for potential catalysis (Scheme 2.40). Under standard conditions of ligand deprotonation with potassium hydride and exposure to  $\text{CoCl}_2$  in dimethylformamide in the glove box at room temperature, complex **90** was observed by mass spectrometry. Crystallization was

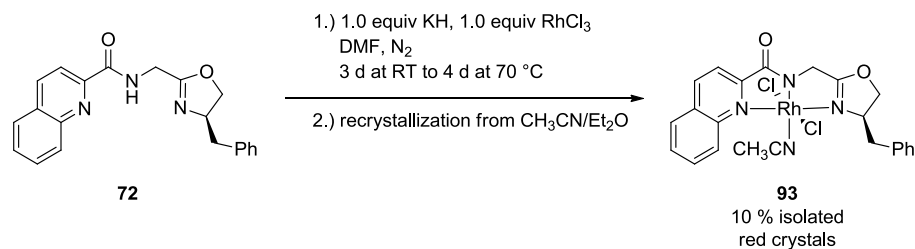
unsuccessful with complex **90**, with a potassium counterion. Counterion exchanges with tetraethyl ammonium bromide to form complex **91** and with tetraphenyl phosphonium chloride to form **92** were attempted. Unfortunately, crystallization was still unsuccessful.

**Scheme 2.40.** Metalation of quinoline-oxazoline ligand **72** with  $\text{CoCl}_2$  to form cobalt(II) complexes **90**, **91**, and **92** (tentatively characterized by mass spectrometry).



Metalation with  $\text{RhCl}_3$  was more promising, as the  $\text{RhCl}_3$  salt was slightly more soluble than the  $\text{IrCl}_3$  salt. Metalation with potassium hydride and  $\text{RhCl}_3$  in dimethylformamide with three days stirring at room temperature and four days at  $70\text{ }^\circ\text{C}$  gave rhodium(III) complex **93** (Scheme 2.41). Finally, crystallization from acetonitrile and diethyl ether afforded 10 % of complex **93**.

**Scheme 2.41.** Metalation of quinoline-oxazoline ligand **72** with  $\text{RhCl}_3$  and crystallization from acetonitrile and diethyl ether to yield rhodium(III) complex **93**.



Potential for facial ligand coordination in complex **93** was of concern, given the flexibility of the ligand backbone (right, Figure 2.6). We were concerned facial coordination might negatively impact reactivity and selectivity.



**Figure 2.6.** Possible coordination modes for rhodium(III) quinoline-oxazoline amide complex **93**.

Upon crystallization from acetonitrile and diethyl ether, x-ray crystallography revealed the coordination geometry of **93** shown in Figure 2.7. Fortunately, the crystal structure showed the desired 1:1 ligand-to-metal meridional coordination geometry, with acetonitrile bound equatorially, and chloride ligands in axial positions. The crystal structure also confirmed the absolute stereochemistry of the ligand.

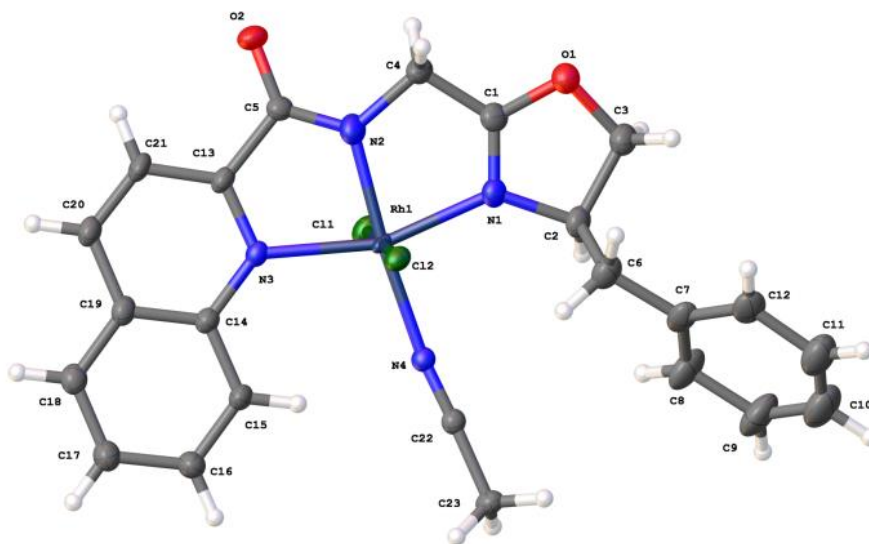


**Figure 2.7.** Crystal structure of rhodium(III) quinoline-oxazoline amide complex **93**.

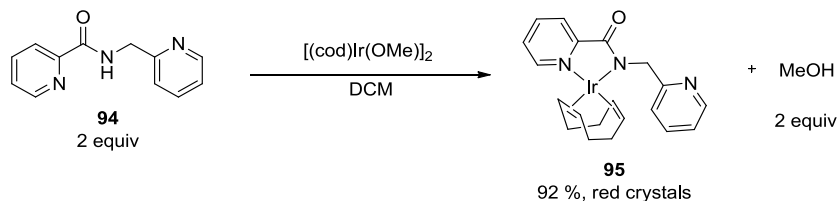
Unfortunately, it was difficult to isolate additional quantities of the rhodium(III) complex **93**. With the prolonged heating that was found necessary to form the complex, this route was not practical synthetically. Despite numerous attempts, we were unable to isolate the iridium(III) complex.

For these reasons, we next targeted the synthesis of an iridium(I) quinoline-oxazoline amide complex. In collaboration with Professor Cora MacBeth and Dr. Omar Villanueva, we designed a route to the iridium(I) complex with plans to subsequently oxidize it to the iridium(III) complex. This method would avoid the solubility problems with iridium(III) salts entirely.

Tejel and coworkers report the use of  $[(\text{cod})\text{Ir}(\text{OMe})]_2$  for metalation of amide ligand **94** (Scheme 2.42).<sup>80</sup> This iridium(I) dimer was able to deprotonate the amide with the methoxy anion and then undergo metalation to form the iridium(I) complex **95** with a

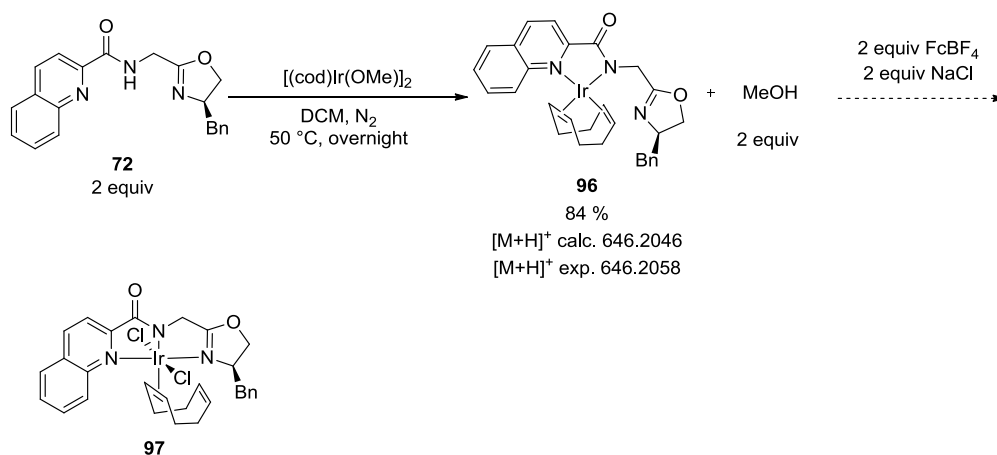
bi-coordinate amidate ligand. The reaction yielded 92 % of **95** with methanol as the only byproduct.

**Scheme 2.42.** Tejel and coworkers' metalation of amide ligand **94** with  $[(\text{cod})\text{Ir}(\text{OMe})_2]$  to form iridium(I) complex **95**.<sup>80</sup>



Dr. Omar Villanueva was able to metalate quinoline-oxazoline amide **72** by exposure to  $[(\text{cod})\text{Ir}(\text{OMe})_2]$  in dichloromethane at 50 °C overnight to yield complex **96** (84 %, Scheme 2.43). Complex **96** could alternatively be synthesized by stirring at room temperature over two days. Crystallization of **96** was unsuccessful, and the geometry shown in Scheme 2.43 is tentative.

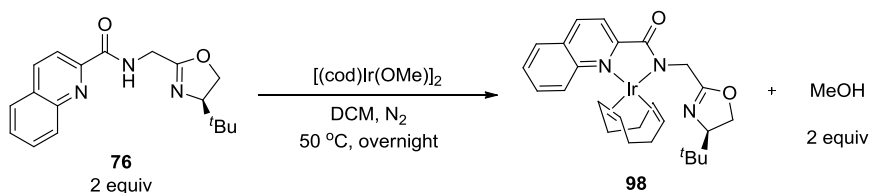
**Scheme 2.43.** Metallation of quinoline-oxazoline amide ligand **72** to form iridium(I) complex **96** and proposed oxidation to iridium(III) complex **97**.



Oxidation of iridium(I) complex **96** was attempted with ferrocenium tetrafluoroborate as oxidant and sodium chloride as a chloride source. Unfortunately, even after multiple attempts, the oxidation was unsuccessful, and iridium(III) complex **97** was not observed.

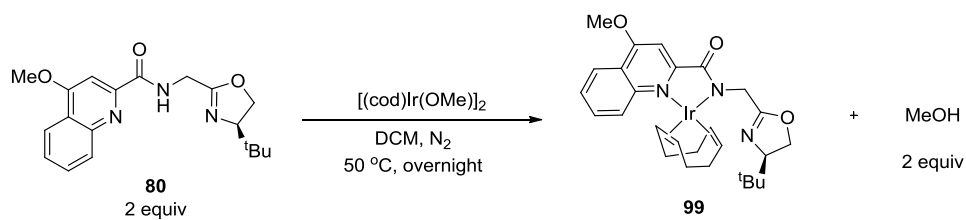
In order to enable better crystallization of the iridium(I) quinoline-oxazoline amide complex, *tert*-butyl-substituted iridium(I) complex **98** was synthesized under the established conditions (Scheme 2.44). The complex was isolated and confirmed by  $^1\text{H}$  NMR. Crystallization from 2-methyl-tetrahydrofuran was accomplished, but crystals suitable for x-ray diffraction could not be obtained.

**Scheme 2.44.** Metallation of quinoline-oxazoline amide ligand **76** to form iridium(I) complex **98**.



For our catalysis studies, we sought to increase the electron density of the iridium(I) complex to aid in stabilization of the metallonitrene for C–H amination. For this reason, methoxy-substituted ligand **80** was metalated with  $[(\text{cod})\text{Ir}(\text{OMe})_2]$  to form iridium(I) complex **99** (Scheme 2.45). This complex was also unable to be crystallized for X-ray crystallography.

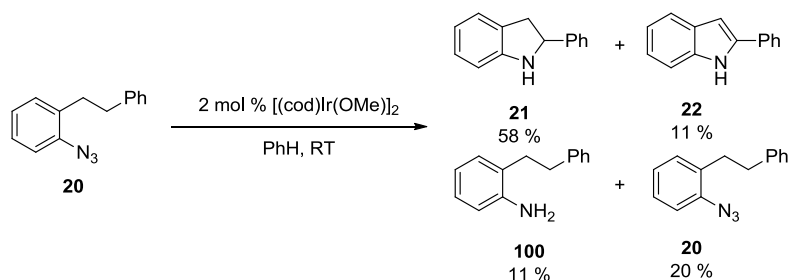
**Scheme 2.45.** Metallation of quinoline-oxazoline amide ligand **80** to form iridium(I) complex **99**.



### 2.3.3 Iridium(I) quinoline-oxazoline amide Catalyzed C–H Amination with Aryl Azides

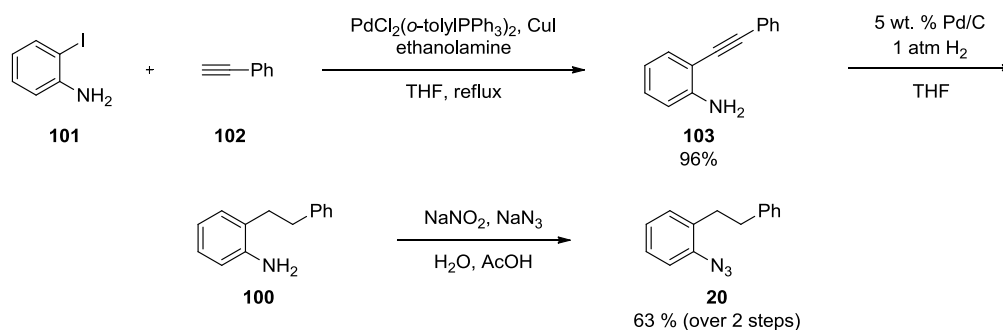
Although the iridium(III) quinoline-oxazoline amide complexes were not able to be isolated, an iridium(I) complex has been previously shown to catalyze benzylic C – H amination with aryl azide **20** (Scheme 2.46).<sup>37</sup> In this work from Driver and coworkers, indole **22** is also observed from *in situ* oxidation of the indoline **21**. Aniline **100** is also formed as a byproduct, and a portion of azide **20** is recovered. It is important to note that when purified by column chromatography, further quantities of indoline are oxidized to indole. Based on this precedent, our iridium(I) quinoline-oxazoline amide complexes were studied for aryl azide C–H amination.

**Scheme 2.46.** Driver and coworkers' iridium(I) catalyzed benzylic C–H amination with aryl azide **20** to form indoline **21**, indole **22** and aniline **100**.<sup>37</sup>



Aryl azide **20** was synthesized according to a method modified from Driver and coworkers (Scheme 2.47).<sup>37</sup> Sonogashira coupling of 2-iodoaniline (**101**) and ethynylbenzene (**102**) gave the desired alkyne **103** in 96 % yield. Subsequent hydrogenation of the alkyne afforded aniline **100**. Aniline **100** was carried forward without purification, and formation of the diazonium salt and displacement using sodium azide gave aryl azide **20** in 63 % yield from alkyne **103**.

**Scheme 2.47.** Synthesis of aryl azide **20**.

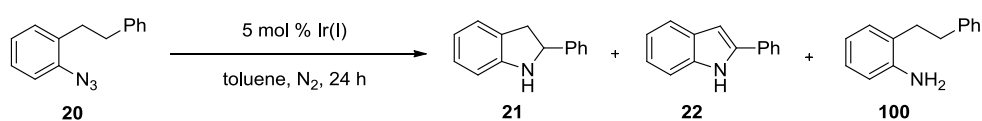


For initial screening of the iridium(I) quinoline-oxazoline amide complexes, we exposed aryl azide **20** to 5 mol % benzyl-substituted complex **96** and *tert*-butyl-

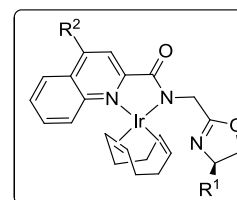


substituted complex **98** at room temperature for 24 hours in toluene in the glove box (Table 2.4, entries 1 and 2). These conditions resulted in no decomposition of azide with either complex. Increasing the temperature to 60 °C with benzyl-substituted iridium(I) complex **96** resulted in slight formation of indole **22** and aniline **100**, but no indoline **21** was observed (entry 3). Heating the reaction to reflux in toluene resulted in significantly increased conversion, but indoline **21** was still not formed (entry 4). The *tert*-butyl-substituted complex **98** gave a greater ratio of both products indole **22** and aniline **100** to starting azide **20**, but still no indoline **21** was produced (entry 5). Methoxy-substituted iridium(I) complex **99** was synthesized to increase the electron density of the iridium center in an effort to reduce the reactivity of the metallonitrene and hinder over-oxidation. However, use of **99** resulted in nearly identical conversion as complex **98** (entry 6).

**Table 2.4.** Iridium(I) quinoline-oxazoline amide catalyst optimization for benzylic C–H amination with aryl azide **20**.



entry	R <sup>1</sup>	R <sup>2</sup>	T (°C)	<sup>1</sup> H NMR ratio (20:21:22:100)
1	Bn	H	RT	100:0:0:0
2	<sup>t</sup> Bu	H	RT	100:0:0:0
3	Bn	H	60	91:0:4:5
4	Bn	H	110	26:0:25:49
5	<sup>t</sup> Bu	H	110	12:0:37:51
6	<sup>t</sup> Bu	OMe	110	15:0:25:60



As far as a mechanistic hypothesis for the source of oxidant to form indole **22**, it is possible that the nitrene is itself performing the oxidation of the indoline to indole,

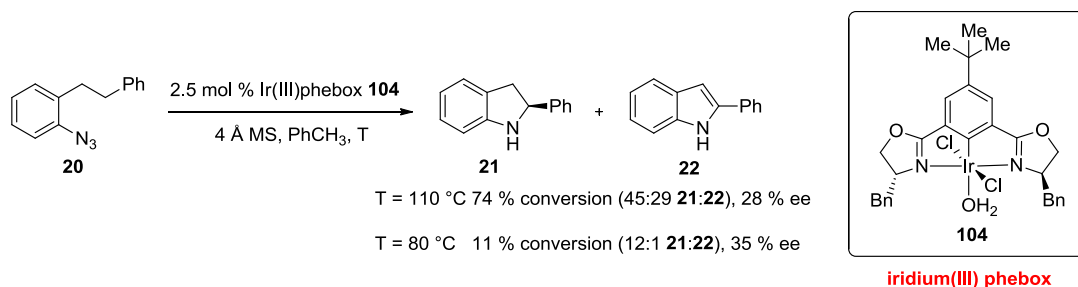
producing aniline **100** as the byproduct. However, aniline **100** and indole **22** were not consistently found in equal ratios in the product mixture. Changing the solvent to trifluorotoluene to eliminate the benzylic C–H bonds of toluene might be helpful in suppressing aniline. Additionally, future studies should include the addition of molecular sieves to remove any adventitious water.

Unfortunately, indoline **21** was never produced, and so we do not have any indication of whether the quinoline-oxazoline amide ligand system is capable of inducing enantioselectivity. For this reason, we were not able to investigate our planned collaboration with the Sigman group for mathematical modeling of the effect of quinoline-oxazoline amide ligand substitution on enantioselectivity.

#### **2.3.4 Iridium(III) Phebox and Phebim Catalyzed Enantioselective C–H Amination with Aryl Azides**

During initial studies in our laboratory by Dr. Clayton Owens of the iridium(III) phenyl bis(oxazoline) (phebox) complexes developed for C–H functionalization (see Chapter 3), azide **20** was exposed to 2.5 mol % of benzyl-substituted iridium(III) phebox **104** in toluene (Scheme 2.48).<sup>81</sup> At 110 °C, 74 % conversion to a mixture of indoline **21** with an ee of 28 % and indole **22** was observed. Lowering the temperature to 80 °C reduced the conversion to 11 % but gave an ee of 35 %.

**Scheme 2.48.** Iridium(III) phebox **104** catalyzed enantioselective amination with aryl azide **20** to form indoline **21** and indole **22**.<sup>81</sup>



Since that time, a number of additional iridium(III) phebox catalysts were synthesized for work in enantioselective carbene chemistry by Dr. Clayton Owens,<sup>81</sup> which had not yet been studied further in metallonitrene chemistry. Additionally, the newly developed iridium(III) phenyl bis(imidazoline) (phebim) catalysts had not been studied for C–H amination (Figure 2.8). The phenyl bis(imidazoline) system provides the added benefit of electronic tuning through the aryl ring in the R<sup>2</sup> position (see Chapter 3).

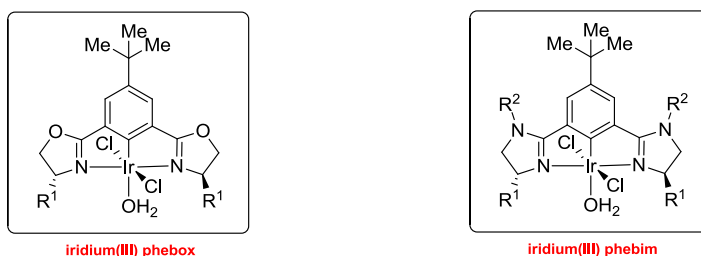
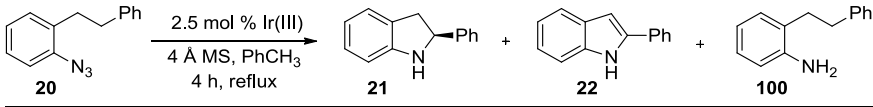


**Figure 2.8.** Comparison of iridium(III) phebox and iridium(III) phebim complexes.

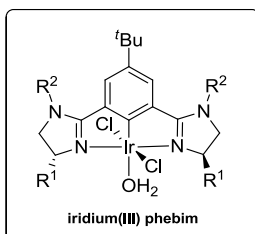
In investigating the iridium(III) phebim catalyst system, we first examined substitution at the R<sup>2</sup> position, while holding R<sup>1</sup> constant with isopropyl substitution

(Table 2.5). When aryl azide **20** is exposed to 2.5 mol % of catalyst with 4 Å powdered molecular sieves for four hours in refluxing toluene, we observed excellent conversion to indoline **21** in all cases, with no formation of indole **22** or aniline **100** (entries 1-3). Enantioselectivities with all three catalysts were similar, with the best ee of 13 % observed for 4-CF<sub>3</sub>-phenyl-substituted iridium(III) phebim (entry 2). For this reason, 4-CF<sub>3</sub>-phenyl substitution was carried forward at the R<sup>2</sup> position for further optimization.

**Table 2.5.** Optimization of iridium(III) phebim R<sup>2</sup> substitution for enantioselective C–H amination with aryl azide **20**.



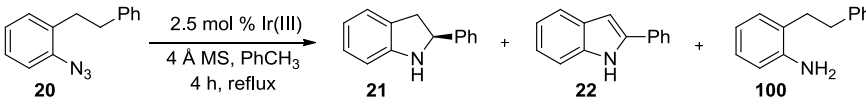
entry	catalyst	R <sup>1</sup>	R <sup>2</sup>	solvent	<sup>1</sup> H NMR ratio ( <b>20</b> : <b>21</b> : <b>22</b> : <b>100</b> )	ee (%)
1	phebim	<sup>i</sup> Pr	Ph	C <sub>6</sub> H <sub>5</sub> CH <sub>3</sub>	8:92:0:0	10
2	phebim	<sup>i</sup> Pr	4-CF <sub>3</sub> Ph	C <sub>6</sub> H <sub>5</sub> CH <sub>3</sub>	8:92:0:0	13
3	phebim	<sup>i</sup> Pr	3,5-(CF <sub>3</sub> ) <sub>2</sub> Ph	C <sub>6</sub> H <sub>5</sub> CH <sub>3</sub>	10:90:0:0	11



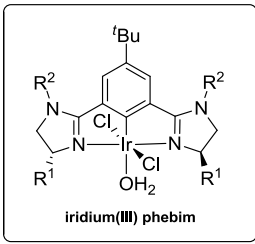
**iridium(III) phebim**

Next, imidazoline substitution at the R<sup>2</sup> position of iridium(III) phebim was studied (Table 2.6). Isopropyl, isobutyl, and *sec*-butyl substitution all gave clean conversion to the indoline **21** (entries 1-3), while benzyl substitution did result in some indole **22** and aniline **100** formation (entry 4). *Sec*-butyl gave the lowest ee of 6 %, and isobutyl gave the highest ee of 27 % (entries 2 and 3). Therefore, isobutyl substitution at the R<sup>1</sup> position was carried forward in iridium(III) phebim optimization.

**Table 2.6.** Optimization of iridium(III) phebim R<sup>1</sup> substitution for enantioselective C–H amination with aryl azide **20**.

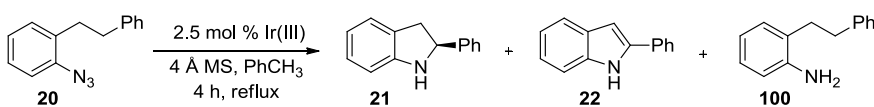


entry	catalyst	R <sup>1</sup>	R <sup>2</sup>	solvent	<sup>1</sup> H NMR ratio ( <b>20</b> : <b>21</b> : <b>22</b> : <b>100</b> )	ee (%)
1	phebim	<sup>i</sup> Pr	<i>p</i> -CF <sub>3</sub> Ph	C <sub>6</sub> H <sub>5</sub> CH <sub>3</sub>	8:92:0:0	13
2	phebim	<sup>t</sup> Bu	<i>p</i> -CF <sub>3</sub> Ph	C <sub>6</sub> H <sub>5</sub> CH <sub>3</sub>	9:91:0:0	27
3	phebim	<sup>s</sup> Bu	<i>p</i> -CF <sub>3</sub> Ph	C <sub>6</sub> H <sub>5</sub> CH <sub>3</sub>	9:91:0:0	6
4	phebim	Bn	<i>p</i> -CF <sub>3</sub> Ph	C <sub>6</sub> H <sub>5</sub> CH <sub>3</sub>	8:78:10:4	18

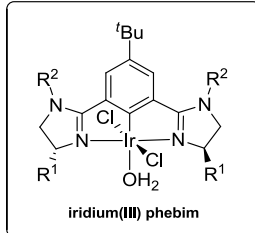


In a study of the effect of the halogen ancillary ligand, bromide ligands were substituted for chloride (Table 2.7). In the ruthenium-pybox system for enantioselective C–H amination, replacing the chloride ligands with bromide resulted in a significant improvement in enantioselectivity.<sup>82</sup> However, in this system, bromide substitution resulted in a minor improvement from 27 % to 32 % ee (entry 2).

**Table 2.7.** Optimization of iridium(III) phebim ancillary ligand for enantioselective C–H amination with aryl azide **20**.



entry	catalyst	R <sup>1</sup>	R <sup>2</sup>	halogen	<sup>1</sup> H NMR ratio ( <b>20</b> : <b>21</b> : <b>22</b> : <b>100</b> )	ee (%)
1	phebim	<sup>t</sup> Bu	<i>p</i> -CF <sub>3</sub> Ph	Cl	9:91:0:0	27
2	phebim	<sup>t</sup> Bu	<i>p</i> -CF <sub>3</sub> Ph	Br	5:83:8:4	32



When the reaction temperature is decreased from 110 °C to 80 °C, conversion is reduced, and the enantioselectivity is increased slightly to 30 % (Table 2.8, entry 2).

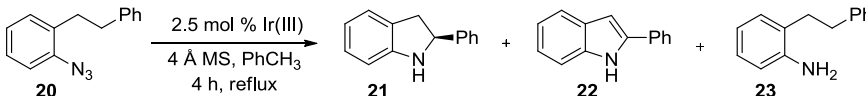
**Table 2.8.** Optimization of iridium(III) phehim reaction temperature for enantioselective C–H amination with aryl azide **20**.

entry	catalyst	R <sup>1</sup>	R <sup>2</sup>	T (°C)	<sup>1</sup> H NMR ratio ( <b>20</b> : <b>21</b> : <b>22</b> : <b>100</b> )	ee (%)
1	phehim	<sup>t</sup> Bu	<i>p</i> -CF <sub>3</sub> Ph	110	9:91:0:0	27
2	phehim	<sup>t</sup> Bu	<i>p</i> -CF <sub>3</sub> Ph	80	53:47:0:0	30

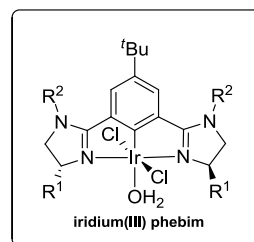
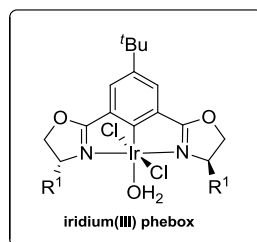
iridium(III) phehim

As mentioned previously, a wider range of iridium(III) phebox catalysts were now available for study as well. For both the isopropyl and benzyl R<sup>1</sup>-substituted iridium(III) phebox and iridium(III) phehim, iridium(III) phebox outperformed iridium(III) phehim by at least 10 % ee (Table 2.9, entries 1-4). The best conversion was observed with isopropyl-substituted iridium(III) phehim (entry 1). The previously observed enantioselectivity with benzyl-substituted phebox was reproduced at 28 % ee (entry 3). Finally, the *tert*-butyl R<sup>1</sup>-substituted iridium(III) phebox gave the highest ee of 55 %, though conversion was somewhat reduced (entry 5).

**Table 2.9.** Optimization of iridium(III) phebox and phebim R<sup>1</sup>-substitution for enantioselective C–H amination with aryl azide **20**.

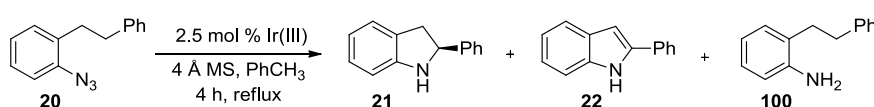


entry	catalyst	R <sup>1</sup>	R <sup>2</sup>	solvent	<sup>1</sup> H NMR ratio ( <b>20</b> : <b>21</b> : <b>22</b> : <b>100</b> )	ee (%)
1	phebim	<sup>i</sup> Pr	<i>p</i> -CF <sub>3</sub> Ph	C <sub>6</sub> H <sub>5</sub> CH <sub>3</sub>	8:92:0:0	13
2	phebox	<sup>i</sup> Pr	-	C <sub>6</sub> H <sub>5</sub> CH <sub>3</sub>	14:86:0:0	26
3	phebim	Bn	<i>p</i> -CF <sub>3</sub> Ph	C <sub>6</sub> H <sub>5</sub> CH <sub>3</sub>	8:78:10:4	18
4	phebox	Bn	-	C <sub>6</sub> H <sub>5</sub> CH <sub>3</sub>	26:56:10:9	28
5	phebox	<sup>t</sup> Bu	-	C <sub>6</sub> H <sub>5</sub> CH <sub>3</sub>	37:63:0:0	55

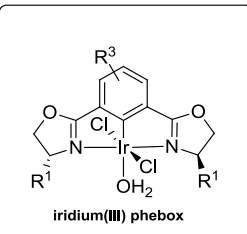


In further tuning the 4-*tert*-butyl-substituted phebox catalyst, we found replacing the 4-*tert*-butyl substitution of the phebox aryl backbone with 3,5-dimethyl substitution increased the conversion significantly but lowered the enantioselectivity slightly (51 %, Table 2.10, entry 2).

**Table 2.10.** Optimization of iridium(III) phebox backbone substitution for enantioselective C–H amination with aryl azide **20**.



entry	catalyst	R <sup>1</sup>	R <sup>3</sup>	solvent	<sup>1</sup> H NMR ratio ( <b>20</b> : <b>21</b> : <b>22</b> : <b>100</b> )	ee (%)
1	phebox	<sup>t</sup> Bu	4- <sup>t</sup> Bu	C <sub>6</sub> H <sub>5</sub> CH <sub>3</sub>	37:63:0:0	55
2	phebox	<sup>t</sup> Bu	3,5-di-Me	C <sub>6</sub> H <sub>5</sub> CH <sub>3</sub>	9:91:0:0	51



iridium(III) phebox

In conducting a solvent screen, benzene was found to give very similar enantioselectivity to toluene, with lower conversion to **21** (Table 2.11, entries 1 and 2). Chlorobenzene gave almost equivalent conversion to **21** as toluene, with a lower enantioselectivity (48 %, entry 3). The enantioselectivity observed in trifluorotoluene appeared extremely promising, with an ee of > 90 % by chiral HPLC (entry 4). However, low conversion resulted in such a small quantity of material for analysis that the minor enantiomer could not be distinguished from the baseline with accuracy, giving a large margin of error ( $\pm 10$  %). In an effort to increase conversion to allow accurate determination of enantioselectivity, the reaction time was extended. Unfortunately, increasing the reaction time from four hours to overnight resulted in over-oxidation to indole **22** and formation of aniline **100**, with a majority of unreacted azide **20** (entry 5).

**Table 2.11.** Solvent optimization for iridium(III) phebox catalyzed enantioselective C–H amination with aryl azide **20**.

entry	catalyst	R <sup>1</sup>	R <sup>2</sup>	solvent	<sup>1</sup> H NMR ratio ( <b>20</b> : <b>21</b> : <b>22</b> : <b>100</b> )	ee (%)
1	phebox	<sup>t</sup> Bu	-	C <sub>6</sub> H <sub>5</sub> CH <sub>3</sub>	37:63:0:0	55
2	phebox	<sup>t</sup> Bu	-	C <sub>6</sub> H <sub>6</sub>	88:12:0:0	54
3	phebox	<sup>t</sup> Bu	-	C <sub>6</sub> H <sub>5</sub> Cl	39:61:0:0	48
4	phebox	<sup>t</sup> Bu	-	C <sub>6</sub> H <sub>5</sub> CF <sub>3</sub>	90:10:0:0	>90
5 <sup>a</sup>	phebox	<sup>t</sup> Bu	-	C <sub>6</sub> H <sub>5</sub> CF <sub>3</sub>	74:1:10:14	n.d.

iridium(III) phebox

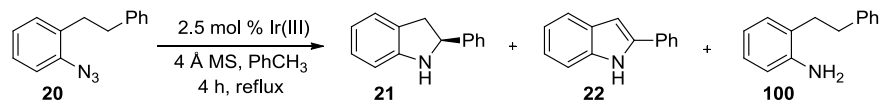
<sup>a</sup>20 h reaction time.

Doubling the catalyst loading of *tert*-butyl substituted iridium(III) phebox from 2.5 mol % to 5 mol % resulted in an identical enantioselectivity of 55 % and nearly equivalent conversion (Table 2.12, entries 1 and 2). In a control reaction, the absence of

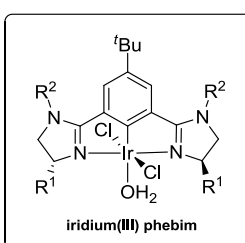


catalyst gave negligible conversion, indicating that no significant thermal decomposition of azide **20** was occurring under reaction conditions (entry 3).

**Table 2.12.** Control reactions for iridium(III) phebox catalyzed enantioselective C–H amination with aryl azide **20**.



entry	catalyst	R <sup>1</sup>	R <sup>2</sup>	mol % catalyst	<sup>1</sup> H NMR ratio ( <b>20</b> : <b>21</b> : <b>22</b> : <b>100</b> )	ee (%)
1	phebox	<sup>t</sup> Bu	-	2.5	37:63:0:0	55
2	phebox	<sup>t</sup> Bu	-	5	30:70:0:0	55
3	none	-	-	-	98:1:0:1	-



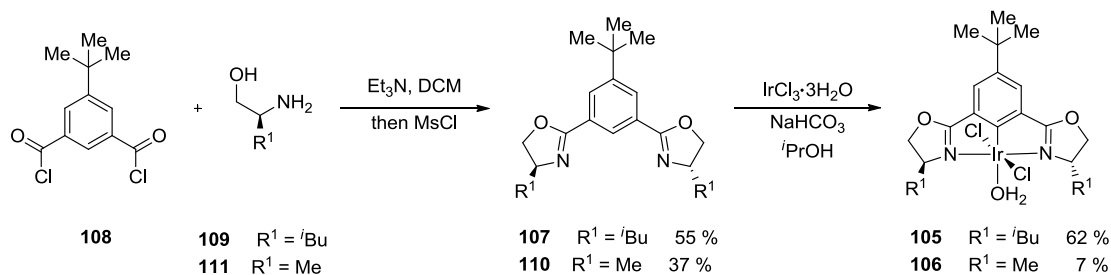
iridium(III) phebox

During discussions with the Sigman group, they indicated that it might be possible to apply two-dimensional mathematical modeling techniques to describe the relationship between the steric bulk at the R<sup>1</sup> position of our iridium(III) phebox and the enantioselectivity. In order to accomplish this, a wider variety of substituents at the R<sup>1</sup> position was needed to obtain a useful spread of data. Based on their suggestion, we synthesized the methyl- and isobutyl-substituted iridium(III) phebox catalysts. Methylene-cyclohexyl-substituted and indanyl-substituted iridium(III) phebox catalysts synthesized for our carbene chemistry studies were also applied.

Synthesis of novel iridium(III) phebox complexes **105** and **106** proceeded according to the literature method (Scheme 2.49).<sup>73</sup> Isobutyl ligand **107** was afforded in one step from diacyl chloride **108** and (*S*)-leucinol (**109**) in 55 % yield. Synthesis of methyl-substituted phebox **110** proceeded in reduced yield of 37 % from **108** and (*S*)-alaninol (**111**). Metalation of isobutyl-substituted ligand **107** afforded iridium(III)

phebox **105** in 62 % yield, but metalation of methyl-substituted **110** gave very poor conversion to **106** (7 %).

**Scheme 2.49.** Synthesis of *i*Bu- and Me-substituted iridium(III) phebox complexes **105** and **106**.



Somewhat surprisingly, both methyl-substituted and isobutyl-substituted iridium(III) phebox complexes gave similar enantioselectivities (37 % and 39 %, respectively; Table 2.13, entries 1 and 3). Methylene-cyclohexyl-substituted iridium(III) phebox (synthesized by Dr. Clayton Owens, see Chapter 3) also gave an enantioselectivity of 36 % (entry 5).

**Table 2.13.** Study of iridium(III) phebox  $R^1$  substitution for enantioselective C–H amination with aryl azide **20**.

entry	$R^1$	$^1\text{H NMR}$ ratio ( <b>20:21:22:100</b> )	ee (%)
1	Me	44:54:2:0	37
2	<i>i</i> Pr	14:86:0:0	26
3	<i>i</i> Bu	10:80:8:3	39
4	Bn	26:56:10:9	28
5	$\text{CH}_2\text{-Cy}$	4:85:7:4	36
6	<i>t</i> Bu	37:63:0:0	55
7	indanyl	9:91:0:0	24

**iridium(III) phebox**

Though we were hopeful that introduction of the often privileged,<sup>53</sup> rigid indanyl substitution of iridium(III) phebox **112** (Figure 2.9, synthesized by Dr. Andrew Schafer) might provide a dramatic increase in enantioselectivity (as was observed with Ru-pybox catalyzed C–H amination with sulfamate esters),<sup>82</sup> the enantioselectivity was actually decreased significantly to 24 % (Table 2.13, entry 7).

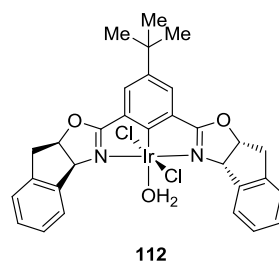
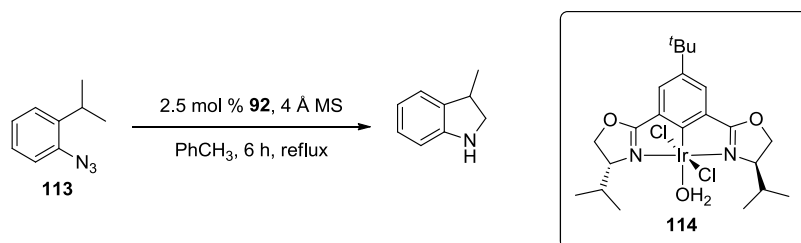


**Figure 2.9.** Iridium(III) indanyl phebox **112** structure, synthesized by Dr. Andrew Schafer.

Unfortunately, due to the narrow distribution of enantioselectivity, mathematical modeling to predict an optimal catalyst structure was unsuccessful. In order to further investigate enantioselective C–H amination with aryl azides, future studies will examine optimization of aryl azide substrates. For example, azide **113** was examined for unactivated primary  $sp^3$  C–H amination, but no product was observed with isopropyl-substituted phebox **114** (Scheme 2.50).

**Scheme 2.50.** Examination of aryl azide **113** for unactivated primary  $sp^3$  C–H insertion with iridium(III) phebox **114**.



Though to this point we have discussed azides as metallonitrene precursors, sulfamate esters are also competent for the formation of nitrenes (see Chapter 1, Section 1.1.2). In a preliminary study by Dr. Clayton Owens of sulfamate ester **115** with iridium(III) phebox **104** for benzylic amination, up to 41 % enantioselectivity was observed (Table 2.14, entry 5).<sup>81</sup>

**Table 2.14.** Preliminary optimization of iridium(III) phebox **104** catalyzed enantioselective benzylic C–H amination with sulfamate ester **115**.<sup>81</sup>

Reaction scheme showing the conversion of sulfamate ester **115** to a benzylic amination product. The reaction conditions are 5 mol % cat.,  $\text{PhI}(\text{O}_2\text{C}^t\text{Bu})_2$  (1.1 equiv.), solvent, additives, 40 °C. The structure of the iridium(III) phebox catalyst **104** is shown in a box. It features an iridium center coordinated to two chlorine atoms, a hydroxyl group, and two chiral ligands derived from a 1,2-diphenylethane-1,2-diol backbone with a tert-butyl group and a hydroxyl group on the central carbon, and a benzyl group on the nitrogen atoms.

entry	solvent	additive(s)	conversion (%) <sup>a</sup>	ee (%) <sup>b</sup>
1	PhH	-	52	32
2	PhH	4 Å MS	61	40
3	PhH	4 Å MS, $\text{AgOTf}^c$	75	37
4	$\text{CH}_2\text{Cl}_2$	4 Å MS, $\text{AgOTf}^c$	63	36
5	$\text{PhCF}_3$	4 Å MS, $\text{AgOTf}^c$	74	41

<sup>a</sup>As determined by  $^1\text{H}$  NMR of the crude reaction mixture. <sup>b</sup>Determined by chiral HPLC. <sup>c</sup>5 mol %. The absolute configuration of the product was determined by comparison to the literature optical rotation value.

From this preliminary result, we sought to optimize enantioselective benzylic C–H amination with sulfamate ester **116** in collaboration with Professor Huw Davies and

Dr. Sandeep Raikar (Table 2.15). Sulfamate ester **116** was designed with methyl ester substitution at the 3-position as a model substrate for a total synthesis in progress in the Davies laboratory. Similar to aryl azide **20**, amination with sulfamate ester **116** proceeded in higher enantioselectivity with iridium(III) phebox than phevim (48 % and 19 %, respectively; entries 1 and 2). Surprisingly, isopropyl-substituted iridium(III) phebox gave the best enantioselectivity of 48 %, with *tert*-butyl-substituted iridium(III) phebox giving an enantioselectivity of 25 % (entry 4). Excluding silver triflate, used for halide abstraction, resulted in a 10 % reduction in enantioselectivity and very low yield (entry 6).

**Table 2.15.** Optimization of iridium(III) phebox and phevim catalyzed enantioselective C–H amination with sulfamate ester **116**.

**116**

$\xrightarrow[\text{4 \AA MS, PhCH}_3, 40\text{ }^\circ\text{C}]{\text{5 mol \% Ir, 5 mol \% AgOTf, 1.5 equiv PhI(O}_2\text{C}^t\text{Bu)}_2}$

entry	catalyst	R <sup>1</sup>	R <sup>2</sup>	yield (%) <sup>a</sup>	ee (%) <sup>b</sup>
1	phevim	<sup>i</sup> Pr	3,5-(CF <sub>3</sub> ) <sub>2</sub> Ph	52	19
2	phebox	<sup>i</sup> Pr	-	64	48
3	phebox	<sup>t</sup> Bu	-	nd	14
4	phebox	<sup>t</sup> Bu	-	50	25
5	phebox	Bn	-	52	39
6 <sup>c</sup>	phebox	<sup>t</sup> Bu	-	nd	4

iridium(III) phebox

iridium(III) phevim

<sup>a</sup>Isolated yield. <sup>b</sup>Determined by chiral HPLC. <sup>c</sup>No AgOTf additive.

Although the catalysts screened did not provide useful levels of enantioselectivity for total synthesis, future studies could focus on further optimization with sulfamate esters. As enantioselectivity seemed to increase with decreasing steric bulk, methyl-

substituted phebox should be screened as well for this reaction. Additionally, the synthetic strategy of the total synthesis could be redesigned to change the substitution of the sulfamate ester for C–H amination.

## 2.4 Cobalt(II) Catalyzed C–H Amination with Aryl Azides

### 2.4.1 Catalysis with a Cobalt(II) Dimer with Redox-Active Ligand Scaffold $\text{NH}(o\text{-PhNHC(O)}^i\text{Pr})_2$

During collaborations with Professor Cora MacBeth and Dr. Omar Villanueva for metalation of our quinoline-oxazoline amide iridium(I) complexes (see Section 2.3.2), we became interested in investigating their cobalt(II) dimers **117-120** with a redox active ligand framework for aryl azide C–H amination. Currently, cobalt(II) complexes that incorporate redox-active ligands for catalytic intramolecular C–H amination are unknown. MacBeth and coworkers previously reported cobalt(II) complexes supported by this tridentate redox-active ligand,  $\text{NH}(o\text{-PhNHC(O)}^i\text{Pr})_2$  scaffold, which are capable of promoting catalytic dioxygen activation for O-atom transfer.<sup>74</sup>

Encouraged by these results and the precedent of Betley and coworkers for cobalt-mediated intraligand amination with a redox-active ligand framework, we sought to explore catalytic C–H amination reactions with aryl azides using the MacBeth group's cobalt(II) catalyst family **117-120** (Figure 2.10). We rationalized that incorporating a robust redox-active ligand scaffold would promote C–H amination at cobalt(II) centers.

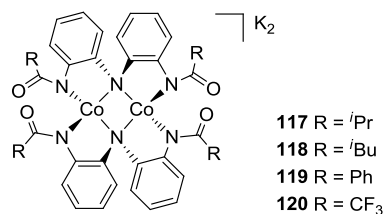
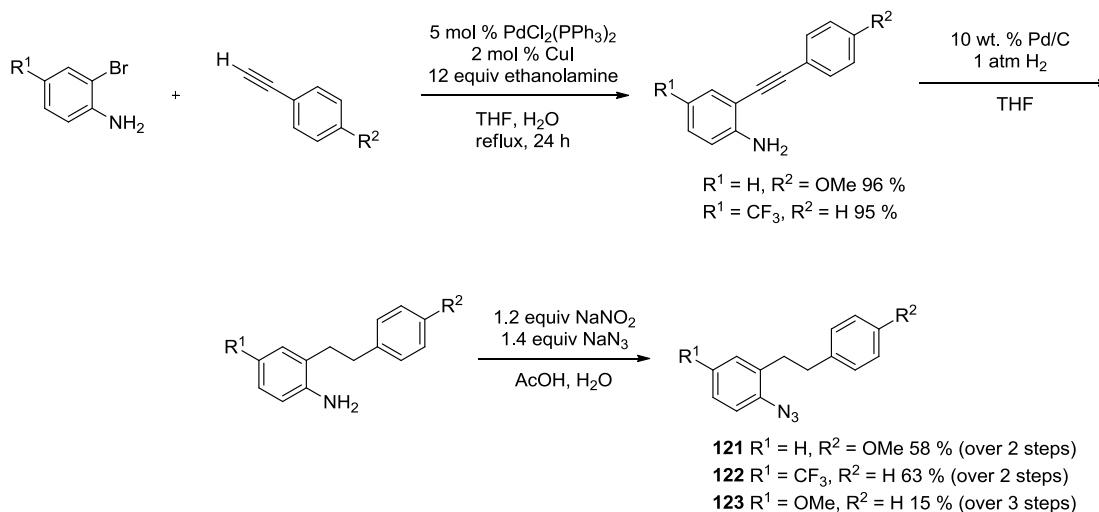


**Figure 2.10.** MacBeth dinuclear cobalt(II) complexes with redox active NH(*o*-PhNHC(O)*i*Pr)<sub>2</sub> ligand scaffold.

## 2.4.2 Aryl Azide Substrate Syntheses

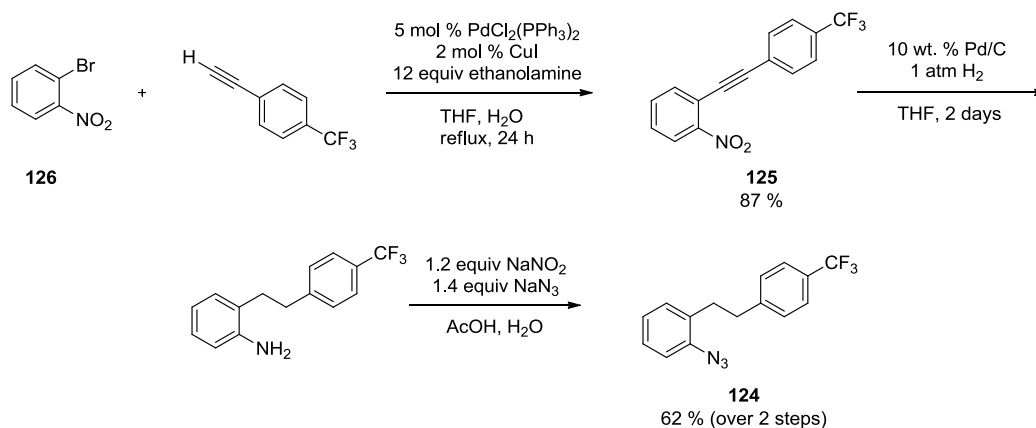
To this end, a variety of substituted aryl azides were synthesized for our investigations. In order to study the effects of aryl substitution of the azide, a variety of azides substituted with electron-donating and electron-donating groups were produced, according to the method described by Driver and coworkers (Scheme 2.51).<sup>37</sup> The sequence proceeded smoothly for azides **121** and **122**. The yield was significantly lower overall for methoxy-substituted azide **123**.

**Scheme 2.51.** Synthesis of methoxy- and trifluoromethyl-substituted aryl azides **121**, **122**, and **123**.



For trifluoromethyl-substituted azide **124**, the Sonogashira coupling afforded significantly higher yield of alkyne **125** from the 2-nitro-bromobenzene **126**, versus 2-bromoaniline (87 % versus 63 %, Scheme 2.52). Hydrogenation of nitrobenzene **125** required an additional 24 hours than hydrogenation of the previous anilines.

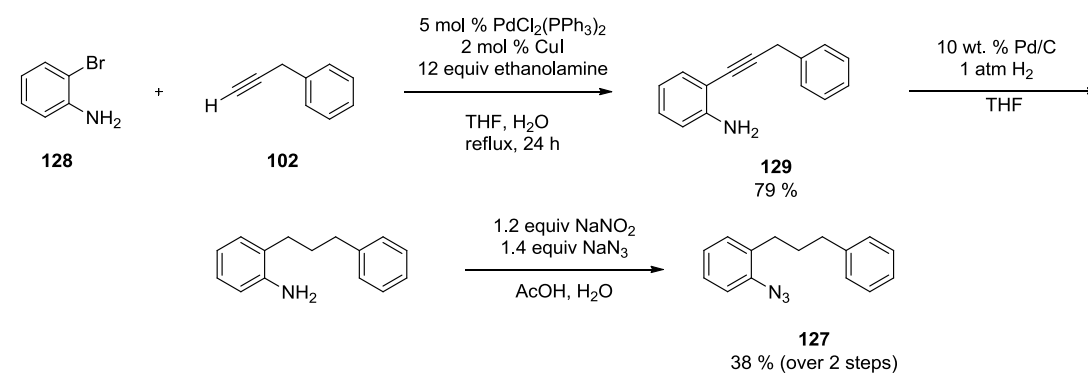
**Scheme 2.52.** Synthesis of trifluoromethyl-substituted aryl azide **124**.





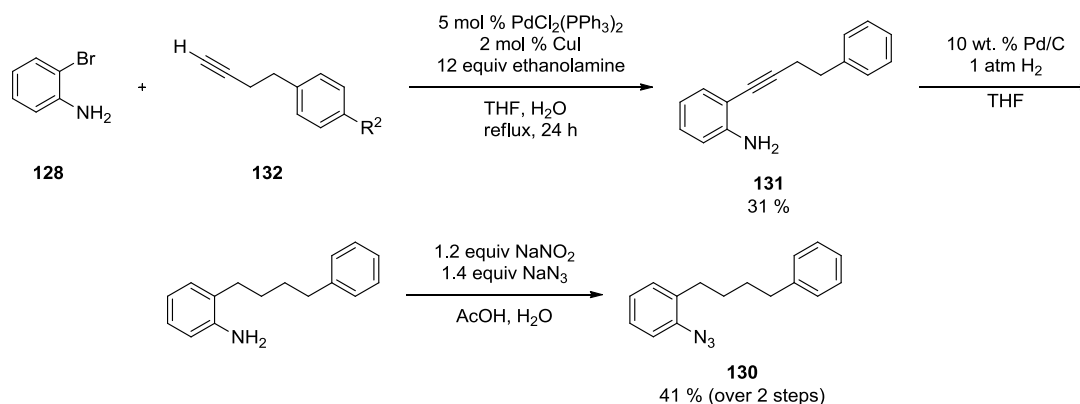
Azide **127** was synthesized to gauge selectivity of the cyclization: whether it would favor formation of the five-membered ring or amination of the benzylic position to afford the six-membered ring (Scheme 2.53). Similar to previous azide syntheses, a Sonogashira reaction of 2-bromoaniline (**128**) and ethynylbenzene (**102**) gave desired alkyne **129** in 79 % yield. Hydrogenation and azide-transfer proceeded in an overall yield of 38 %, making this method roughly twice as efficient for the synthesis of **127**.

**Scheme 2.53.** Optimized synthesis of azide **127** by Sonogashira coupling.



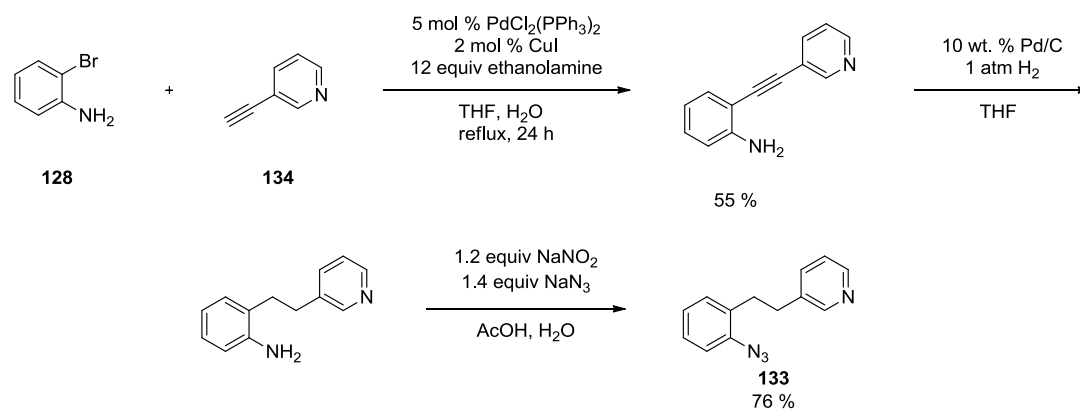
In order to determine the efficacy of reaction conditions for benzylic insertion to form a seven-membered ring, azide **130** was synthesized (Scheme 2.54). Sonogashira reaction to give aniline **131** proceeded in diminished yield from homobenzylic alkyne **132**, possibly due to the instability of **132** and potential for isomerization of the alkyne. Hydrogenation and formation of the azide gave 41 % yield of azide **130**, previously unstudied for C–H amination.

**Scheme 2.54.** Synthesis of azide **130** by Sonogashira reaction.



For applications in pharmaceutical science, we also studied insertion into C–H bonds  $\alpha$  to medicinally relevant heterocycles, such as pyridine and indole. To form the 3-pyridyl azide **133**, 3-ethynyl-pyridine (**134**) undergoes Sonogashira coupling with 2-bromoaniline (**128**) in moderate yield (55 %, Scheme 2.55). Reduction and standard conditions for azide transfer from azide **133** in 76 % yield on gram-scale.

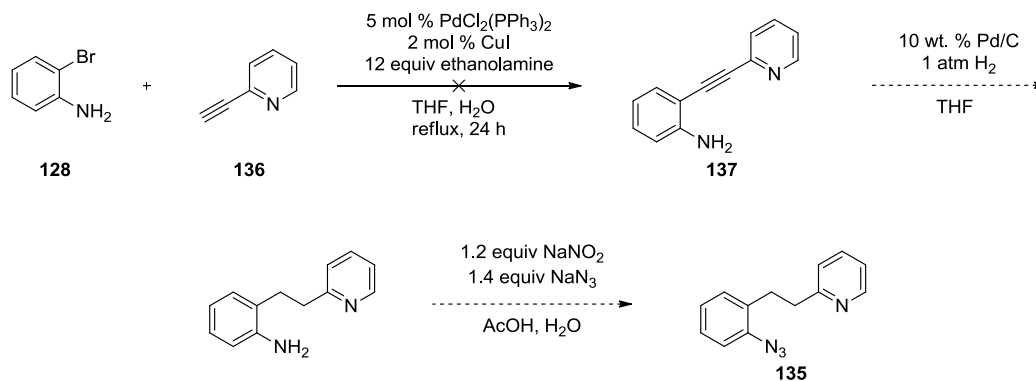
**Scheme 2.55.** Synthesis of pyridinyl azide **133**.



Unfortunately, synthesizing 2-pyridinyl azide **135** did not proceed smoothly (Scheme 2.56). Sonogashira coupling with 2-ethynyl-pyridine (**136**) and 2-bromoaniline

(**128**) under standard conditions gave only trace amounts of aniline **137**, even upon repetition.

**Scheme 2.56.** Failed Sonogashira coupling with 2-ethynyl-pyridine (**136**) and 2-bromoaniline (**128**) in the synthesis of 2-pyridinyl azide **135**.



A similar Sonogashira coupling with 2-ethynyl-pyridine (**136**) was observed by Zhu and coworkers with 2-bromobenzaldehyde (**138**), under slightly altered conditions, though the yield was not reported (Scheme 2.57).<sup>83</sup>

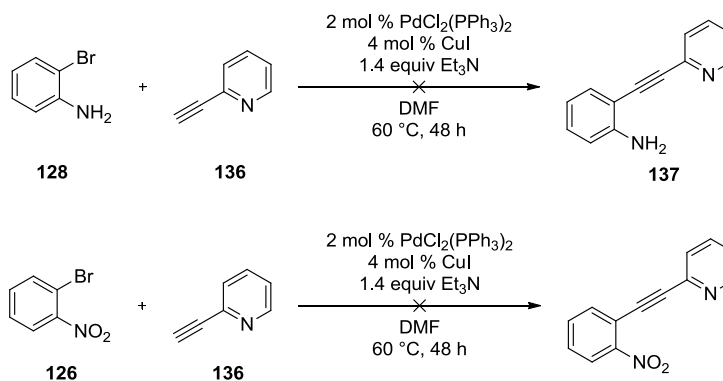
**Scheme 2.57.** Sonogashira coupling with 2-ethynyl-pyridine (**136**) and 2-bromobenzaldehyde (**138**).<sup>83</sup>



The coupling of 2-ethynyl-pyridine (**136**) with 2-bromoaniline (**128**) under these altered conditions still only yielded trace amounts of aniline **137** (Scheme 2.58). In order

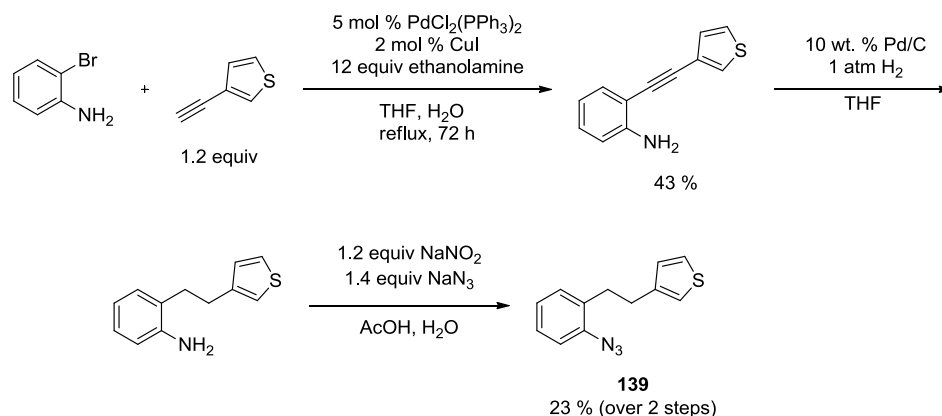
to employ a coupling partner with more similarities to aniline **138**, with an electron-withdrawing aldehyde substituent, the nitrobenzene **126** was utilized under the same conditions. However, this alteration still resulted in observation of only trace amounts of product, and 2-pyridinyl azide **135** was not synthesized.

**Scheme 2.58.** Failed Sonogashira coupling with 2-ethynyl-pyridine (**136**).



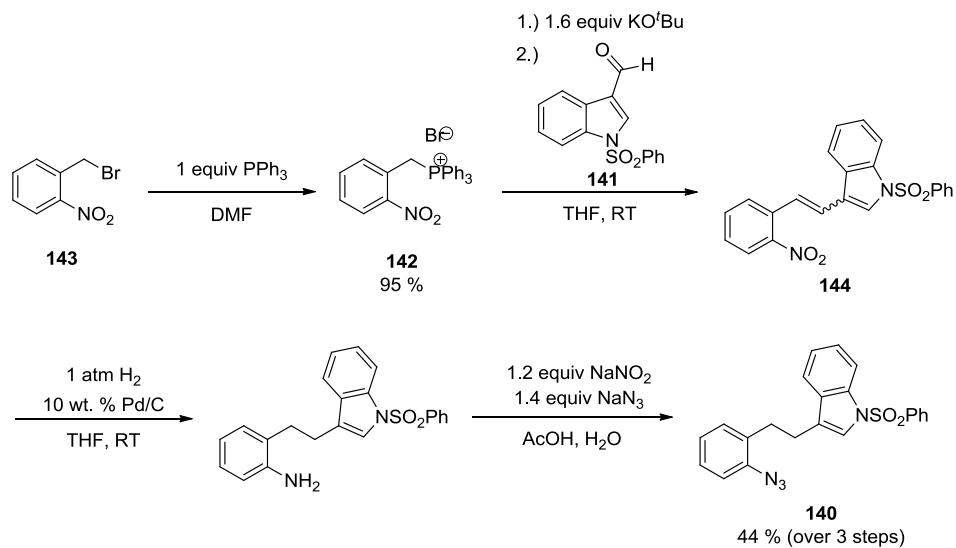
3-Thiophenyl azide **139** was synthesized smoothly, though in poor yield (Scheme 2.59). Because of the poor yield, the azide **139** was not afforded in a synthetically useful quantity, but the synthetic route was successful and could be executed on larger scale for use in the future.

**Scheme 2.59.** Synthesis of 3-thiophenyl azide **139**.

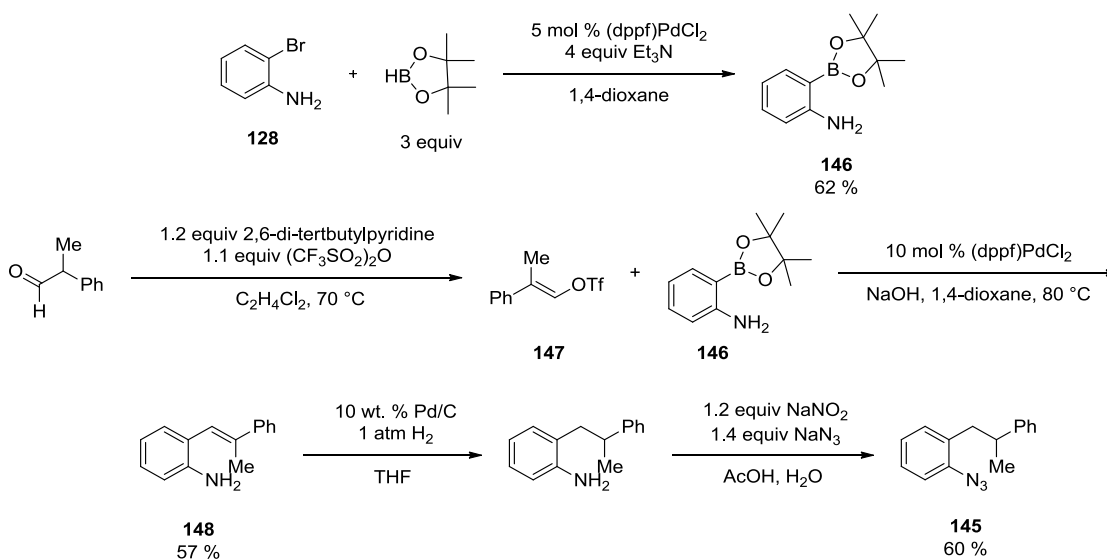


For the synthesis of indolyl azide **140**, a Wittig-olefination strategy was pursued due to the greater availability of indolyl aldehyde **141** in comparison to the 3-ethynyl-indole needed for the Sonagashira coupling strategy employed previously (Scheme 2.60). The phosphonium salt **142** was afforded in excellent yield from benzyl bromide **143**. Synthesis of alkene **144** proceeded efficiently via Wittig-olefination, and the *E/Z* selectivity was not measured, as the alkene **144** was carried on as crude material for hydrogenation.<sup>84</sup> Azide **140** was afforded in 44 % overall yield from phosphonium salt **142** and indolyl aldehyde **141**.

**Scheme 2.60.** Synthesis of indolyl azide **140**.

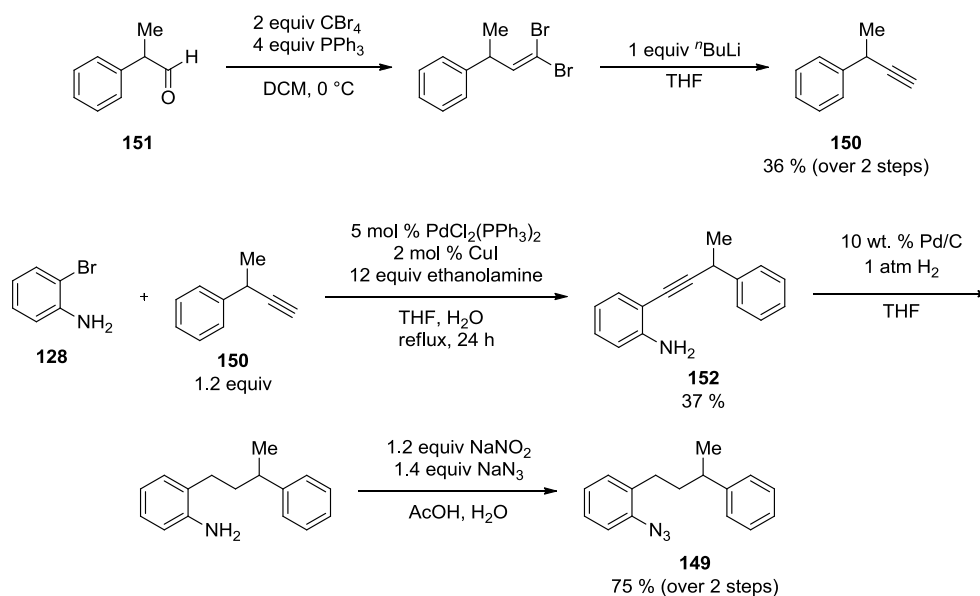


In order to gauge the ability of our system to catalyze C–H amination of a tertiary  $\text{sp}^3$  C–H bond, azide **145** was synthesized (Scheme 2.61).<sup>38</sup> Boronic ester **146** was synthesized from 2-bromoaniline (**128**) in 62 % yield. Coupling of **146** with vinyl triflate **147** gave aniline **148** in 57 % yield and further reduction and azide transfer afforded azide **145** in 60 % yield.

Scheme 2.61. Synthesis of azide **145**.

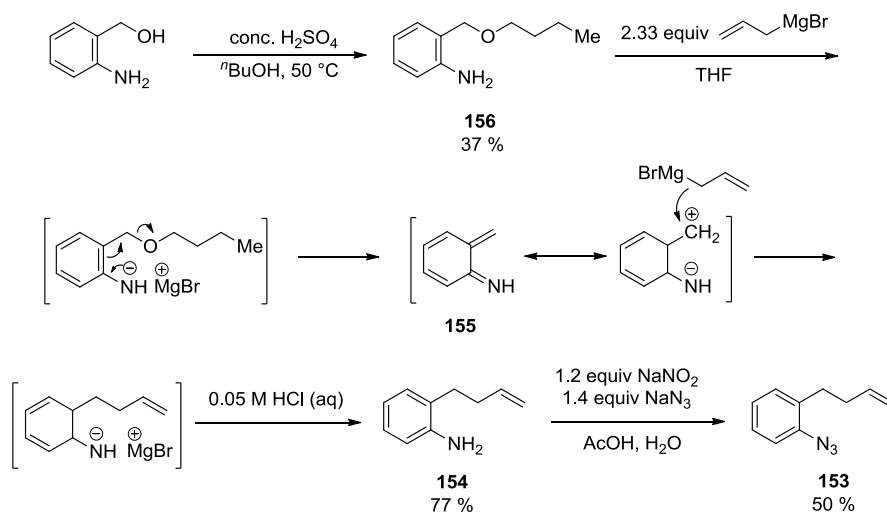
For determining the influence of the length of the tether on intramolecular C–H amination of a tertiary  $\text{sp}^3$  C–H bond, azide **149** was synthesized (Scheme 2.62). In order to access this azide, alkyne **150** was afforded from aldehyde **151** via Corey-Fuchs homologation.<sup>85</sup> Sonogashira reaction yielded the aniline **152**, which was smoothly transformed to 75 % azide **149**.

**Scheme 2.62.** Synthesis of alkyne **150** and use toward azide **149**.

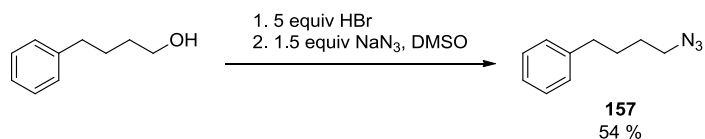


Due to evidence for a H-atom abstraction/radical recombination mechanism for C–H amination with the cobalt(II) dimer system (Section 2.4.3), we anticipated that allylic C–H insertion would be possible without competing aziridination. To this purpose, azide **153** was generated (Scheme 2.63). The aniline **154** was synthesized according to the method of Görl and Alt, involving the generation of aza-ortho-xylylene intermediate **155** from benzyl ether **156** and subsequent attack by allyl magnesium bromide.<sup>86</sup> From aniline **154**, the *ortho*-homoallylic aryl azide **153** was generated in 50% yield. Unfortunately, azide **153** was very unstable, potentially due to intramolecular reaction of the azide and olefin. Storage as a frozen benzene solution was necessary to prevent decomposition.



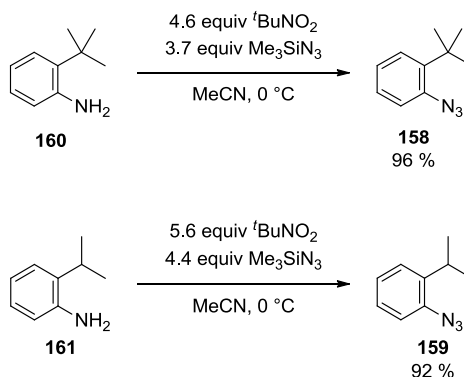
**Scheme 2.63.** Synthesis of *ortho*-homoallylic aryl azide **153**.

Evaluation of the system for benzylic C–H amination with an alkyl azide was also planned. To that end, alkyl azide **157** used by Betley and coworkers was synthesized (Scheme 2.64).<sup>39</sup>

**Scheme 2.64.** Synthesis of alkyl azide **157** for intramolecular benzylic C–H amination.

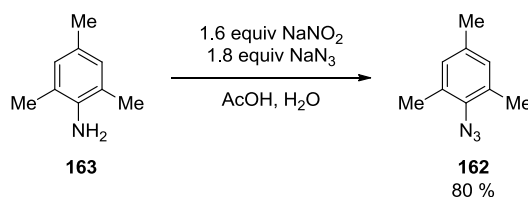
In order to test the catalyst system for C–H amination of unactivated  $\text{sp}^3$  C–H bonds, *ortho*-alkyl azides **158** and **159** were synthesized (Scheme 2.65).<sup>38</sup> *Ortho-tert*-butyl azide (**158**) was generated from *ortho-tert*-butyl aniline (**160**) in 96 % yield. *Ortho*-isopropyl azide (**159**) was also synthesized from the corresponding aniline **161**.

**Scheme 2.65.** Synthesis of *ortho*-alkyl azides **158** and **159**.



Finally, mesityl azide (**162**) was targeted for gauging intermolecular C–H amination with an aryl azide (Scheme 2.66). Synthesis from the corresponding aniline **163** afforded **162** in 80 % yield.<sup>87</sup>

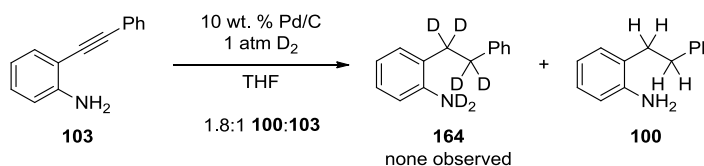
**Scheme 2.66.** Synthesis of mesityl azide (**162**).



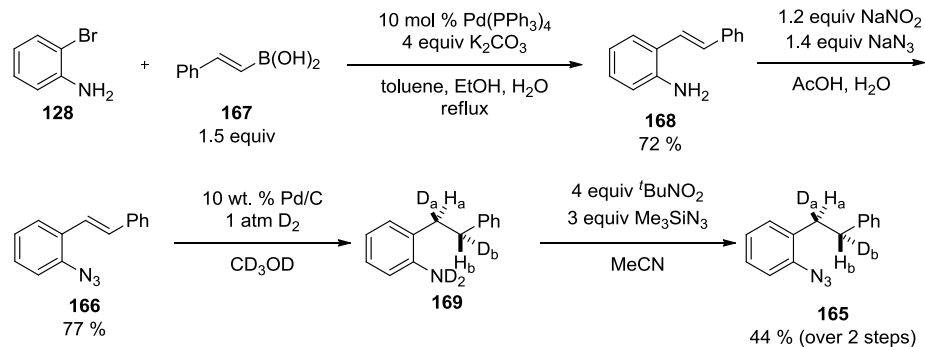
For kinetic isotope effect experiments, synthesis of a deuterated *ortho*-homobenzylic azide was attempted. Initially, alkyne **103** was reduced under an atmosphere of D<sub>2</sub> gas, in the presence of Pd/C (Scheme 2.67). The deuterated azide **164** was intended for use in a competition study in a 1:1 ratio with azide **13** to calculate kinetic isotope effect. Unfortunately, reduction of **103** showed incomplete conversion by crude <sup>1</sup>H NMR to give hydrogenated aniline **100** in a 1.8:1 ratio of **100:103**, with no signs

of deuterated **164**. This degree of hydrogen-incorporation was surprising, but may have resulted from tetrahydrofuran as a hydrogen source.

**Scheme 2.67.** Failed synthesis of deuterated azide **164**.



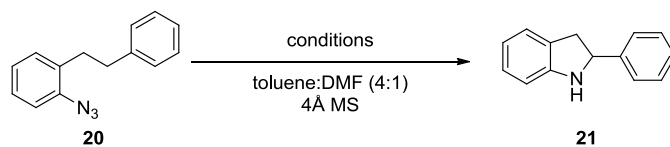
Due to this difficulty, as well as an improved reaction design, substrate **165** for an intramolecular competition experiment was synthesized. Styryl azide **166** was afforded according to the method of Driver and coworkers (Scheme 2.68).<sup>33</sup> Suzuki coupling of 2-bromoaniline (**128**) with (*E*)-styrylboronic acid (**167**) gave 72 % styryl aniline **168**. Formation of the diazonium salt and displacement with sodium azide gave styryl azide **166** in 77 %. Concerns about hydrogen/deuterium exchange with tetrahydrofuran in our previous effort (Scheme 2.67) led to the use of conditions established by Driver and coworkers for reduction in deuterated methanol (Scheme 2.68).<sup>38</sup> The Pd/C catalyst was also rinsed with deuterated methanol prior to use. Under these conditions, deuterium incorporation was successful to yield deuterated aniline **169**, which then afforded deuterated azide **165** in 44 % yield from azide **166**. Aniline **169** was afforded with a ratio of deuterium incorporation of 1:1 H<sub>b</sub>:D<sub>b</sub> and 0.82:1 H<sub>a</sub>:D<sub>a</sub> (see Figure 2.11).

**Scheme 2.68.** Synthesis of deuterated aryl azide **165** via reduction of styryl azide **166**.

### 2.4.3 Cobalt(II) Catalyzed C–H Amination Results

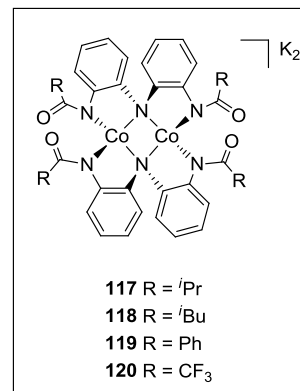
With a selection of azides designed for probing the capabilities of the catalyst system, C–H amination with cobalt(II) catalyst family **117-120** was investigated in collaboration with Dr. Omar Villanueva.<sup>88</sup> Optimization of the reaction with *ortho*-homobenzyl aryl azide **20** established the standard reaction conditions of 1 mol % cobalt(II) dimer **117** in a 4:1 mixture of dimethylformamide and toluene at 110 °C over 48 hours with 4 Å MS to yield indoline **21** (82 %, Table 2.16). Without the incorporation of molecular sieves, it was found that aniline **100** was the dominant product, with minor formation of indoline **21**.

**Table 2.16.** Optimization of intramolecular benzylic C–H amination with *ortho*-homobenzyl aryl azide **20**.<sup>88</sup>

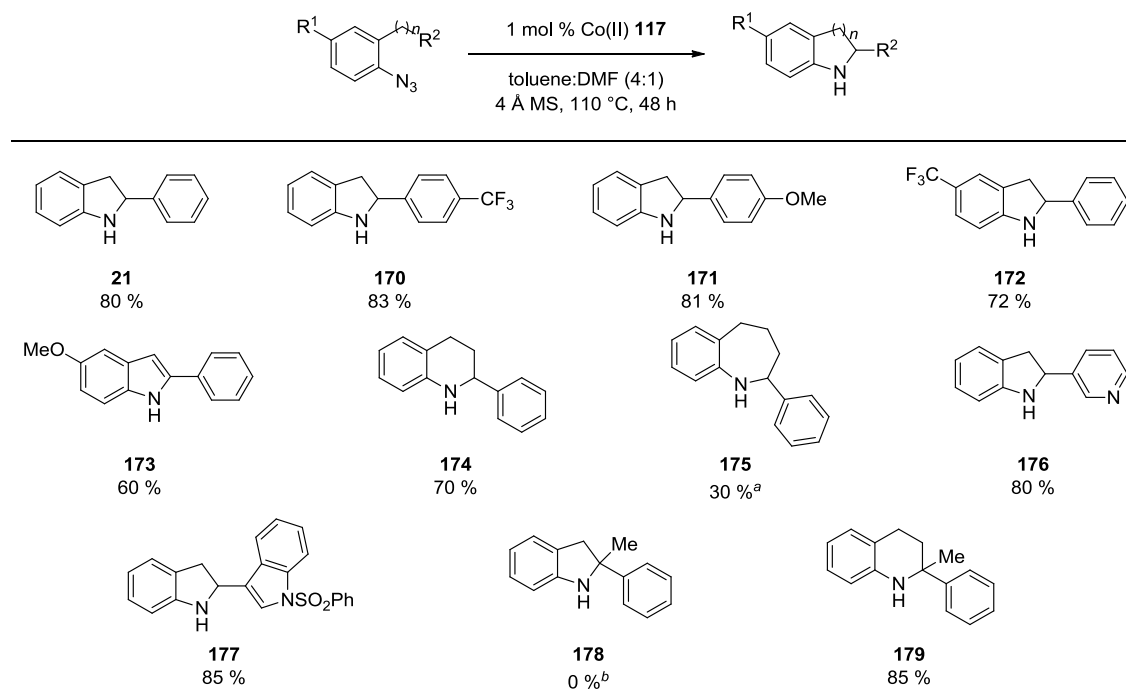


entry	catalyst	loading (mol %)	time (h)	T (°C)	yield (%) <sup>a</sup>
1	<b>117</b>	10	24	25	0
2	<b>117</b>	10	24	110	43
3	<b>118</b>	10	24	110	20
4	<b>119</b>	10	24	110	10
5	<b>120</b>	10	24	110	trace
6	<b>117</b>	1	24	110	11
7	<b>117</b>	1	48	110	82
8	—	—	48	110	0
9	CoBr <sub>2</sub>	1	48	110	0

<sup>a</sup>Yield by <sup>1</sup>H NMR with 1,3,5-trimethoxybenzene as an internal standard.



The reaction yield was not influenced by electronic substitution of the homobenzyl aryl ring (**170** and **171**, 83 % and 81 %, respectively; Table 2.17). Trifluoromethyl substitution of the aryl azide resulted in a slight decrease in efficiency (**172**, 72 %). Most remarkably, methoxy substitution of the aryl azide, which shut down the reaction with the [(cod)Ir(OMe)]<sub>2</sub> catalyst system,<sup>37</sup> resulted in 60 % of indole **173**, oxidized from the corresponding indoline, which was observed by crude <sup>1</sup>H NMR.

**Table 2.17.** Substrate scope of cobalt(II) catalyzed C–H amination with aryl azides.<sup>88</sup>

<sup>a</sup>5 mol % catalyst loading. <sup>b</sup>90 % azide recovered from crude reaction.

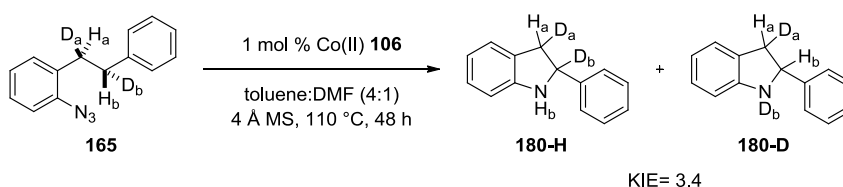
Six- and seven-membered ring formation was possible (**174** and **175**, 70 % and 30 %, respectively; Table 2.17), though formation of **175** in tolerable yield required an increased catalyst loading of 5 mol %. Additionally, the C–H amination conditions were capable of insertion adjacent to medicinally relevant heterocycles to form pyridine-substituted **176** and protected-indole **177** (80 % and 85 %, respectively). Notably, catalyst turnover was not inhibited by coordination of the pyridine moiety of **176**.

Extending the reaction beyond insertion into secondary  $sp^3$  C–H bonds, methyl-substituted aryl azide **145** showed no C–H amination to form indoline **178**, and 90 % starting azide **145** was recovered. In contrast, when the alkyl linker was extended, tertiary C–H insertion was efficient to yield 85 % indoline **179**.

Under standard conditions, cobalt(II) dimer **117** showed no insertion into the unactivated  $sp^3$  C – H bonds of aryl azides **158** or **159**. Likewise, our studies of alkyl azide **157** did not provide any evidence of C–H amination with our system. Studies with aryl azide **153** yielded a complex mixture, but no allylic C–H insertion product was isolated. The above results are detailed in the Ph. D. thesis of Dr. Omar Villanueva.<sup>89</sup>

Using deuterium-labeled aryl azide **165**, an intramolecular competition kinetic isotope effect (KIE) experiment was conducted to calculate a KIE of 3.4 (Scheme 2.69). KIE was measured by comparison of insertion into the C–D<sub>b</sub> bond or the C–H<sub>b</sub> bond of azide **165** under standard amination conditions. A hydrogen/deuterium KIE is defined as  $k_H/k_D$ , which is, in this instance, the percentage of C–H insertion divided by the percentage of C–D insertion of **165**.<sup>37</sup> Because the ratio of H<sub>b</sub> to D<sub>b</sub> was not perfectly 1:1 when azide **165** was synthesized, this initial inequality must be accounted for in the following calculation.

**Scheme 2.69.** Kinetic isotope effect experiment with aryl azide **165**.<sup>88</sup>



By analyzing the  $^1\text{H}$  NMR spectra of azide **165** and aniline precursor **169**, integration reveals a 0.82:1.18 ratio of H<sub>b</sub>:D<sub>b</sub> in starting azide **165** (Figure 2.11). Following complete consumption of azide **165**, comparison of indolines **180-H** and **180-D** yielded a ratio of 0.12:0.88 H<sub>b</sub>:D<sub>b</sub>. Using the relationship: % consumed =

$(H_b \text{ initial} - H_b \text{ final}) / (H_b \text{ initial})$ , it was calculated that 85 % of  $H_b$  was consumed by C- $H_b$  insertion. Applying this relationship to the consumption of  $H_D$ , 25 % of  $D_b$  was consumed by C- $D_b$  insertion. Finally, these percentages were used to calculate  $KIE = 0.85/0.25 = 3.4$ .

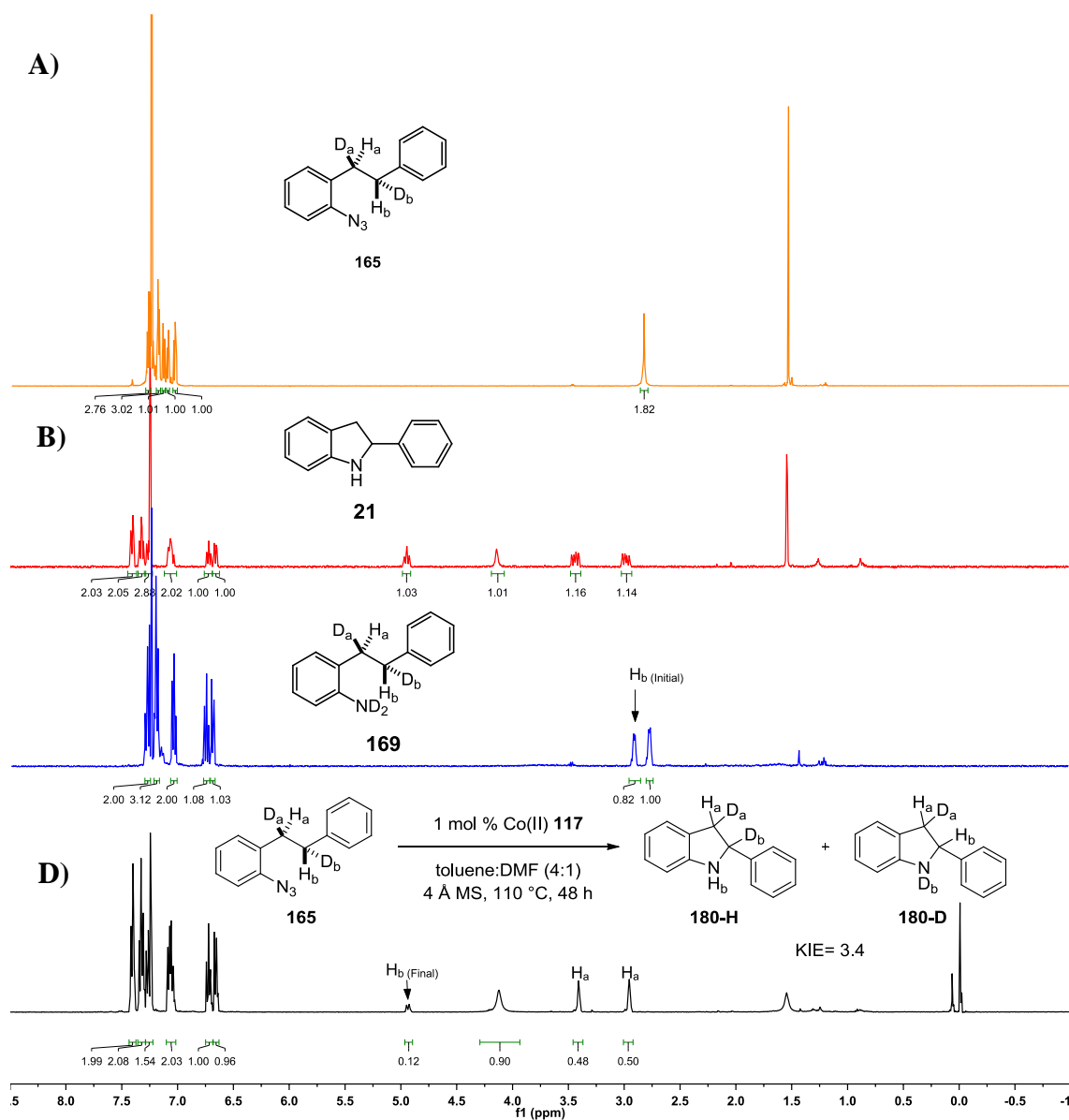


**Figure 2.11.**  $^1\text{H}$  NMR spectra for A) deuterated azide **165**, B) indoline product **21**, C) aniline precursor **169** and azide **165**, and D) reaction mixture of indoline products **180-H** and **180-D**.<sup>88</sup>



KIE was calculated from the  $^1\text{H}$  NMR analysis found in Figure 2.11 as follows:

Before Reaction ( $\text{H}_b$  initial): 0.82  $\text{H}_b$

After Reaction ( $\text{H}_b$  final): 0.12  $\text{H}_b$

$\text{H}_b$  consumed : ( $\text{H}_b$  initial) - ( $\text{H}_b$  final) = (0.82 - 0.12) = 0.70

% of  $\text{H}_b$  consumed = (0.70/0.82) x 100% = 85%

Before Reaction ( $\text{D}_b$  initial): 2.0 - ( $\text{H}_b$  initial) = 2.0 - 0.82 = 1.18  $\text{D}_b$

After Reaction ( $\text{D}_b$  final): 1 - ( $\text{H}_b$  final) = 1.0 - 0.12 = 0.88

$\text{D}_b$  consumed : ( $\text{D}_b$  initial) - ( $\text{D}_b$  final) = (1.18 - 0.88) = 0.30

% of  $\text{D}_b$  consumed = (0.30 / 1.18) x 100% = 25%

$$\mathbf{KIE} = K_{\text{H}} / K_{\text{D}} = 0.85 / 0.25 = \mathbf{3.4}$$

This kinetic isotope effect is in agreement with the mechanistic hypothesis of hydrogen-atom abstraction/radical recombination (Scheme 2.71). In terms of comparison to other C–H aminations, Driver and coworkers observed a KIE of 5.06 with aryl azides and [(cod)Ir(OMe)]<sub>2</sub>.<sup>37</sup> Zhang and coworkers report a KIE of 6.2 for sulfonyl azide allylic insertion,<sup>22</sup> and Betley and coworkers found a KIE of 5.3 for their iron system for alkyl azide amination.<sup>39</sup> While these values are greater than that which we observed, our

observation is higher than the KIE for intramolecular amination with sulfamate esters (1.9).<sup>90</sup>

## 2.5 Conclusions

In conclusion, we report the development of a new quinoline-oxazoline amide ligand framework, as well as the synthesis of corresponding iridium(I) complexes. These iridium(I) complexes were found active for C–H amination with aryl azides, though they produced indole, not allowing for any induction of enantioselectivity. Based on our later results with the cobalt(II) system, the iridium(I) quinoline-oxazoline amide catalyst family should be revisited with the addition of 4Å molecular sieves.

Additionally, oxidation of iridium(I) complex **96** to iridium (III) complex **96** should be re-examined with other oxidants (Scheme 2.43). 2,3,4,5,6,6-Hexachloro-2,4-cyclohexadien-1-one is a promising oxidant for the transformation, which would also serve as a source of chlorine in complex **96**.<sup>91</sup> Alternatively, bromine could also be investigated in the oxidation.

This catalyst framework could also be further studied for other classes of reactions, including strategies involving addition of ligand and metal salts to form active catalyst *in situ*.

Aryl azide C–H amination was explored with our iridium(III) phevim and phebox catalyst families. In contrast to the results observed for enantioselective acceptor-only diazoacetate C–H insertion (Chapter 3), the iridium(III) phebox family was found to perform C–H amination with aryl azides and sulfamate esters with higher

enantioselectivity than iridium(III) phehim. A maximum ee of 55 % was observed for C–H amination with *tert*-butyl substituted iridium(III) phebox (Table 2.13, entry 6). Future studies would further increase the steric bulk of the ligand, perhaps with adamantyl-substitution. Additionally, our results with sulfamate esters as precursors for enantioselective C–H amination showed a different steric influence of catalyst substitution on enantioselectivity, with isopropyl-substituted phebox providing a maximum ee of 48 % (Table 2.15, entry 2). These results indicate the specificity of a particular catalyst and substrate combination for achieving high selectivity. It also provides an indication that another class of nitrene precursor might yet prove successful in attaining high levels of enantioselectivity with the iridium(III) phebox and phehim catalyst families.

Cobalt(II) dimers with redox-active ligands **117-120** were used in the first catalytic C–H amination utilizing aryl azides with cobalt in collaboration with Professor Cora MacBeth and Dr. Omar Villanueva. Further studies could continue to examine the other aryl and alkyl azides described previously that have not yet been successful. Additionally, intermolecular reaction could be further studied with this system. Work in the MacBeth laboratory has since also been directed towards a chiral ligand scaffold for cobalt(II), which if effective in inducing enantioselectivity, would be an important achievement in azide C–H amination. As with the iridium(III) phebox family, the cobalt(II) dimers could also be studied for amination with other classes of nitrene precursors.

Overall, our results, alongside the body of work in C – H amination, emphasize the need for new catalyst systems. Most ligand/metal systems reported in C–H

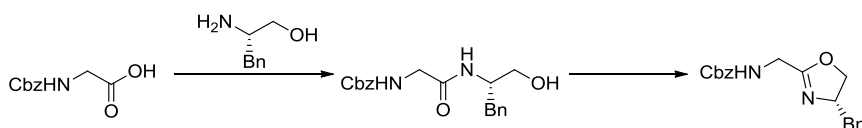
amination, particularly with aryl azides, have been found specific to certain classes of substrates, often with surprising limitations. Development of a generalizable catalyst system with compatibility for an array of nitrene precursors, which could also be tuned for chemoselectivity for a particular class of C–H bonds, remains an important goal in the field.

## 2.6 Experimental Procedures and Compound Characterization

$^1\text{H}$  and  $^{13}\text{C}$  NMR spectra were recorded on a Varian Inova 600 spectrometer (600 MHz  $^1\text{H}$ , 150 MHz  $^{13}\text{C}$ ) and a Varian Inova 400 spectrometer (400 MHz  $^1\text{H}$ , 100 MHz  $^{13}\text{C}$ ) at room temperature in  $\text{CDCl}_3$  (neutralized and dried with anhydrous  $\text{K}_2\text{CO}_3$ ) with internal  $\text{CHCl}_3$  as the reference (7.27 ppm for  $^1\text{H}$  and 77.23 ppm for  $^{13}\text{C}$ ). Chemical shifts ( $\delta$  values) were reported in parts per million (ppm) and coupling constants ( $J$  values) in Hz. Multiplicity is indicated using the following abbreviations: s = singlet, d = doublet, t = triplet, q = quartet, qn = quintet, sext = sextet, m = multiplet, b = broad signal. ). Infrared (IR) spectra were recorded using Thermo Electron Corporation Nicolet 380 FT-IR spectrometer. Solid-state Infrared spectra were recorded as KBr pellets on a Varian Scimitar 800 Series FT-IR spectrophotometer. UV-Visible absorption spectra were recorded on a Cary50 spectrophotometer using 1.0 cm quartz cuvettes. High-resolution mass spectra were obtained using a Thermo Electron Corporation Finigan LTQFTMS (at the Mass Spectrometry Facility, Emory University). X-ray diffraction studies were carried out in the X-ray Crystallography Laboratory at Emory University on a Bruker Smart 1000 CCD diffractometer. We acknowledge the use of

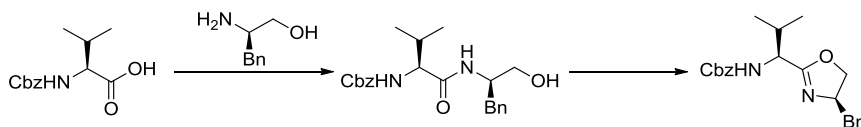
shared instrumentation provided by grants from the NIH and the NSF. Analytical thin layer chromatography (TLC) was performed on precoated glass backed EMD 0.25 mm silica gel 60 plates. Visualization was accomplished with UV light or ethanolic anisaldehyde, followed by heating. Flash column chromatography was carried out using Silicycle® silica gel 60 (40-63  $\mu\text{m}$ ).

All reactions were conducted with anhydrous solvents in oven-dried and nitrogen-charged glassware or conducted in an MBraun Labmaster 130 drybox under a nitrogen atmosphere. Anhydrous solvents were purchased from Sigma-Aldrich and further purified by sparging with Ar gas followed by passage through activated alumina columns. Anhydrous solvents were stored inside an inert atmosphere dry box under freshly activated 4Å molecular sieves. Solvents for workup, extraction and column chromatography were used as received from commercial suppliers. All reagents used were purchased from commercial vendors and used as received unless otherwise noted.



**(S)-Benzyl ((4-benzyl-4,5-dihydrooxazol-2-yl)methyl)carbamate (51).** Prepared according to a procedure modified from the literature:<sup>59</sup> *N*-methylmorpholine (0.540 mL, 4.9 mmol) was slowly added via syringe to a solution of Cbz-Gly-OH (860 mg, 4.11 mmol) in  $\text{CH}_2\text{Cl}_2$  (17 mL) at 0 °C. The solution was stirred for 10 min at 0 °C. Isobutyl chloroformate (0.54 mL, 4.16 mmol) was added dropwise, and the solution was stirred for 45 min at 0 °C. (*S*)-2-amino-3-phenyl propanol (540  $\mu\text{L}$ , 4.9 mmol) was added. Reaction mixture was warmed to room temperature and stirred until thin layer

chromatography indicated consumption of starting material. Reaction was quenched by addition of 1 M HCl and CH<sub>2</sub>Cl<sub>2</sub>. The organic layer was washed with H<sub>2</sub>O and brine, dried over Na<sub>2</sub>SO<sub>4</sub>, and concentrated *in vacuo*. The crude mixture was taken up in CH<sub>2</sub>Cl<sub>2</sub> (30 mL) and triethylamine (15 mL) and cooled to 0 °C. *p*-Toluenesulfonyl chloride (950 mg, 4.98 mmol) was added in three portions. The reaction mixture was warmed to room temperature and stirred until thin layer chromatography indicated consumption of the starting material. The mixture was heated to reflux for 17 h. Reaction mixture was cooled to room temperature and diluted with CH<sub>2</sub>Cl<sub>2</sub> and washed with saturated aqueous NaHCO<sub>3</sub> (3 x), H<sub>2</sub>O, and brine. Organic layer was dried over Na<sub>2</sub>SO<sub>4</sub>, concentrated *in vacuo* and purified by flash chromatography (1:1 Et<sub>2</sub>O/hexanes → 7:3 hexanes: acetone) to afford the Cbz protected oxazoline amine (510 mg, 38 % yield over two steps); **R<sub>f</sub>** 0.29 (7:3 hexanes: acetone); **IR** (thin film, cm<sup>-1</sup>) 2961, 2251, 1710, 1516, 1250, 1052; **<sup>1</sup>H NMR** (CDCl<sub>3</sub>, 400 MHz) δ 7.36-7.16 (m, 10H), 5.37 (br s, 1H), 5.15-5.11 (m, 2H), 4.41-4.35 (m, 1H), 4.25 (t, *J* = 8.8 Hz, 1H), 4.06-3.99 (m, 3H), 3.07 (dd, *J* = 13.9, 5.3 Hz, 1H), 2.65 (dd, *J* = 13.7, 8.2 Hz, 1H); **<sup>13</sup>C NMR** (CDCl<sub>3</sub>, 100 MHz) δ 165.2, 156.6, 137.8, 136.7, 129.4, 128.7, 128.6, 128.2, 126.7, 74.4, 72.6, 67, 41.6, 38.4; **HMRS** (+APCI) calculated for C<sub>19</sub>H<sub>21</sub>N<sub>2</sub>O<sub>3</sub> 325.1547 found 325.1547 [M+H]<sup>+</sup>.



**Benzyl ((S)-1-((R)-4-benzyl-4,5-dihydrooxazol-2-yl)-2-methylpropyl)carbamate (54).**

Prepared according to the literature,<sup>59</sup> using Cbz-Val-OH (515 mg, 2.05 mmol 1 equiv), *N*-methylmorpholine (0.300 mL, 2.73 mmol, 1.2 equiv), isobutyl chloroformate (0.300 mL, 2.28 mmol, 1.1 equiv), (*R*)-2-amino-3-phenyl-propanol (340 mg, 2.25 mmol, 1.1 equiv), and *p*-toluenesulfonyl chloride (500 mg, 2.66 mmol, 1.3 equiv). Flash chromatography afforded 353 mg (47 % yield over two steps) of title compound (cf. 84 % reported). <sup>1</sup>H NMR was identical to that reported;<sup>59</sup> <sup>1</sup>H NMR (CDCl<sub>3</sub>, 400 MHz) δ 7.36-7.16 (m, 10H), 5.34 (d, *J* = 8.8 Hz, 1H), 5.10 (q, *J* = 12.1 Hz, 2H), 4.42-4.33 (m, 2H), 4.22 (t, *J* = 8.8 Hz, 1H), 3.98 (t, *J* = 7.9 Hz, 1H), 3.07 (dd, *J* = 13.9, 5.0 Hz, 1H), 2.61 (dd, *J* = 13.7, 8.5 Hz, 1H), 2.13-2.05 (m, 1H), 0.88 (d, *J* = 6.7 Hz, 6H).



**(S)-1-((R)-4-benzyl-4,5-dihydrooxazol-2-yl)-2-methylpropan-1-amine (53).**

Prepared according to the literature,<sup>59</sup> using oxazoline **54** (137 mg, 0.37 mmol) and 10 % Pd/C (34 mg) at 1 atm H<sub>2</sub> for 4 h. The <sup>1</sup>H NMR was identical to that reported;<sup>59</sup> <sup>1</sup>H NMR (CDCl<sub>3</sub>, 400 MHz) δ 7.28-7.25 (m, 2H), 7.20-7.16 (m, 3H), 4.40-4.33 (m, 1H), 4.17 (t, *J* = 8.8 Hz, 1H), 3.97 (t, *J* = 7.4 Hz, 1H), 3.41 (s, 2H), 3.28 (d, *J* = 5.9 Hz, 1H), 3.08 (dd, *J* = 13.7, 5.1 Hz, 1H), 2.62 (dd, *J* = 13.7, 8.6 Hz, 1H), 1.92 (dq, *J* = 13.5, 6.6 Hz, 1H), 0.91 (dd, *J* = 9.8, 7.0 Hz, 6H);

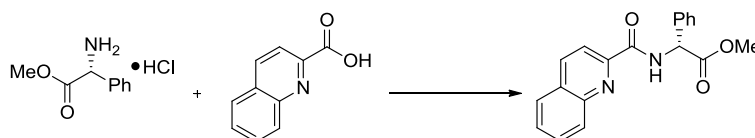
**General procedure A for preparation of methyl ester-amides.** Procedure from the literature<sup>70</sup> was modified as follows: *N*-methylmorpholine (1.5 equiv) was added dropwise via syringe to a solution of quinaldic acid (1 equiv) in CH<sub>2</sub>Cl<sub>2</sub> (0.26 M) at 0 °C. Isobutyl chloroformate (1.15 equiv) was added dropwise via syringe after stirring for 20 min at 0 °C. Additional *N*-methylmorpholine (1.15 equiv) was added dropwise via syringe after stirring for 30 min at 0 °C. Appropriate amino methyl ester hydrochloride (1.15 equiv) was added in three portions. Reaction mixture was warmed to 25 °C and stirred until thin layer chromatography indicated complete consumption of starting material. Reaction was quenched by addition of 1 M HCl and diluted with CH<sub>2</sub>Cl<sub>2</sub>. The organic layer was washed with water and brine. The organic layer was dried over Na<sub>2</sub>SO<sub>4</sub>, filtered, and concentrated *in vacuo*. Purification by mixed solvent recrystallization afforded the desired methyl ester-amide.

**General procedure B for preparation of cyclization precursors.** Procedure from the literature was modified as follows:<sup>71</sup> *n*-Butyllithium (1.1 equiv) was added dropwise to a solution of starting amino alcohol (1.1 equiv) in toluene (0.48 M) and THF (0.72 M) at 0 °C. After stirring for 15 mins, methyl ester-amide (1 equiv) was added in five portions. Reaction mixture was warmed to 25 °C and stirred until thin layer chromatography indicated complete consumption of starting material. Reaction was cooled to 0 °C and water was added dropwise to quench. Organic solvent was removed under reduced pressure and remaining aqueous solution was extracted with CH<sub>2</sub>Cl<sub>2</sub>. The combined organic extracts were dried over Na<sub>2</sub>SO<sub>4</sub>, filtered, and concentrated *in vacuo*. Purification by mixed solvent recrystallization afforded the desired compound.



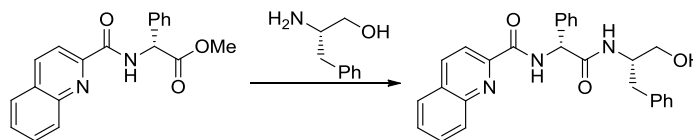
**General procedure C for one-pot preparation of cyclization precursors.** Procedures from the literature were modified as follows:<sup>70,71</sup> *N*-methyldmorpholine (1.5 equiv) was added dropwise via syringe to a solution of quinaldic acid (1 equiv) in CH<sub>2</sub>Cl<sub>2</sub> (0.26 M) at 0 °C. Isobutyl chloroformate (1.15 equiv) was added dropwise via syringe after stirring for 20 min at 0 °C. Additional *N*-methyldmorpholine (1.15) was added dropwise via syringe after stirring for 30 min at 0 °C. Appropriate amino methyl ester hydrochloride (1.15 equiv) was added in three portions. Reaction mixture was warmed to 25 °C and stirred until thin layer chromatography indicated complete consumption of starting material. Reaction was quenched by addition of 1 M HCl and diluted with CH<sub>2</sub>Cl<sub>2</sub>. The organic layer was washed with water and brine. The organic layer was dried over Na<sub>2</sub>SO<sub>4</sub>, filtered, and concentrated *in vacuo*. *n*-Butyllithium (1.1 equiv) was added dropwise to a solution of starting amino alcohol (1.1 equiv) in toluene (0.48 M) and THF (0.72 M) at 0 °C. After stirring for 15 mins, crude residue (1 equiv) was added slowly to this mixture as a solution in THF. Reaction mixture was warmed to 25 °C and stirred until thin layer chromatography indicated complete consumption of starting material. Reaction was cooled to 0 °C and water was added dropwise to quench. Organic solvent was removed under reduced pressure and remaining aqueous solution was extracted with CH<sub>2</sub>Cl<sub>2</sub>. The combined organic extracts were dried over Na<sub>2</sub>SO<sub>4</sub>, filtered, and concentrated *in vacuo*. Purification by mixed solvent recrystallization afforded the desired compound.

**General procedure D for preparation of oxazolines.** Procedure from the literature<sup>70</sup> was modified as follows: triphenylphosphine (1.2 equiv) was added to a solution of oxazoline precursor (1 equiv) in THF (0.15 M). Diisopropyl azodicarboxylate (1.2 equiv) was added dropwise via syringe, allowing color to dissipate between drops. The reaction was stirred at room temperature until thin layer chromatography indicated complete consumption of starting material. The reaction was concentrated *in vacuo* and purified by flash chromatography on silica gel as indicated to afford the desired oxazoline.



**(R)-methyl 2-phenyl-2-(quinoline-2-carboxamido)acetate (58).** Prepared by general procedure A using quinaldic acid (500 mg, 2.89 mmol), *N*-methylmorpholine (0.5 mL and 0.375 mL, 4.54 mmol and 3.41 mmol), isobutyl chloroformate (0.45 mL, 3.47 mmol), and (*R*)-(-)-2-phenylglycine methyl ester hydrochloride (680 mg, 3.37 mmol). Mixed solvent recrystallization (EtOAc/hexanes) afforded the title compound as a white solid (753 mg, 81 %);  $R_f$  0.59 (7:3 hexanes/EtOAc); **IR** (thin film,  $\text{cm}^{-1}$ ) 3385, 2952, 1742, 1675, 1493, 1339, 1171;  **$^1\text{H NMR}$**  ( $\text{CDCl}_3$ , 400 MHz)  $\delta$  9.15 (br d,  $J = 7$  Hz, 1H), 8.27 (q,  $J = 8.6$  Hz, 2H), 8.16 (d,  $J = 8.6$  Hz, 1H), 7.86 (d,  $J = 7.8$  Hz, 1H), 7.77 (td,  $J = 7.8, 1.2$  Hz, 1H), 7.62 (t,  $J = 7$  Hz, 1H), 7.52 (d,  $J = 7.4$  Hz, 2H), 7.42-7.33 (m, 3H), 5.82 (d,  $J = 7.4$  Hz, 1H), 3.79 (s, 3H);  **$^{13}\text{C NMR}$**  ( $\text{CDCl}_3$ , 100 MHz)  $\delta$  171.4, 164.2, 149.3, 146.8, 137.7, 136.8, 130.3, 130.2, 129.6, 129.3, 128.8, 128.3, 127.9,

127.7, 119, 57, 53.1; **HMRS** (+APCI) calculated for C<sub>19</sub>H<sub>17</sub>N<sub>2</sub>O<sub>3</sub> 321.1234, found 321.1231 [M+H]<sup>+</sup>.



***N*-((*R*)-2-(((*S*)-1-hydroxy-3-phenylpropan-2-yl)amino)-2-oxo-1-**

**phenylethyl)quinoline-2-carboxamide (60).** Prepared by general procedure **B** using (*S*)-

(-)-2-amino-3-phenyl-1-propanol (156 mg, 1.03 mmol), *n*-butyllithium (0.45 mL,

1.03 mmol, 2.3 M solution in hexanes), and methyl ester-amide **58** (290 mg, 0.91 mmol).

Mixed solvent recrystallization (Et<sub>2</sub>O/hexanes) afforded the title compound as a white

solid (190 mg, 48 %); **R<sub>f</sub>** (0.30 7:3 hexanes: acetone); **IR** (thin film, cm<sup>-1</sup>) 3303, 3062,

2927, 1651, 1496, 1041; **<sup>1</sup>H NMR** (CDCl<sub>3</sub>, 400 MHz) δ 9.23 (br d, *J* = 7.3 Hz, 1H), 8.25

(t, *J* = 8.1 Hz, 1H), 8.19 (dd, *J* = 8.5, 5.2 Hz, 1H), 8.12 (dt, *J* = 8.5, 4.3 Hz, 1H), 7.83 (dd,

*J* = 10.8, 8.4 Hz, 1H), 7.74 (qd, *J* = 7.2, 1.2 Hz, 1H), 7.59 (qd, *J* = 7.3, 0.9 Hz, 1H), 7.44-

7.38 (m, 2H), 7.35-7.27 (m, 3H), 7.22-7.15 (m, 2H), 7.12 (dd, *J* = 7, 4.6 Hz, 3H), 6.98

(dd, *J* = 6.4, 2.7 Hz, 1H), 6.72 (dd, *J* = 17.7, 7.9 Hz, 1H), 5.72 (dd, *J* = 9, 4.7 Hz, 1H),

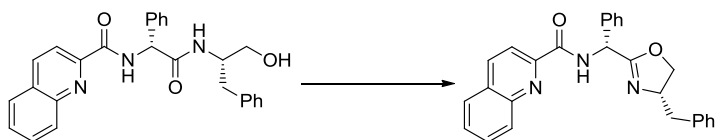
4.19-4.13 (m, 1H), 3.67 (dd, *J* = 6.7, 3.7 Hz, 1H), 3.56 (dt, *J* = 11.4, 4.4 Hz, 1H), 2.86 (d,

*J* = 7.3 Hz, 1H), 2.78 (t, *J* = 7.2 Hz, 1H); **<sup>13</sup>C NMR** (CDCl<sub>3</sub>, 100 MHz) δ 170.4, 164.8,

164.6, 149.1, 146.8, 137.8, 137.5, 130.4, 130.2, 129.6, 129.4, 129.3, 128.8, 128.7, 128.4,

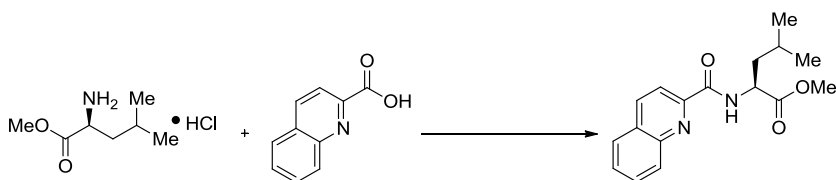
127.9, 127.7, 126.7, 119, 63.7, 58.2, 53.9, 37; **HMRS** (+APCI) calculated for

C<sub>27</sub>H<sub>26</sub>N<sub>3</sub>O<sub>3</sub> 440.1969, found 440.1964 [M+H]<sup>+</sup>.



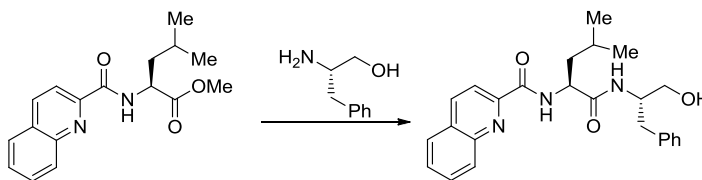
***N*-((*R*)-((*S*)-4-benzyl-4,5-dihydrooxazol-2-yl)(phenyl)methyl)quinoline-2-**

**carboxamide (61).** Prepared by general procedure **D** using **60** (149 mg, 0.34 mmol), triphenylphosphine (109 mg, 0.42 mmol), and diisopropyl azodicarboxylate (0.081 mL, 0.41 mmol) to afford title compound as a 1.3:1 mixture of epimers;  $R_f$  0.41 (7:3 hexanes/acetone); **IR** (thin film,  $\text{cm}^{-1}$ ) 3367, 2981, 2611, 2372, 2199, 2049, 1726, 1497, 1232;  **$^1\text{H NMR}$**  ( $\text{CDCl}_3$ , 400 MHz)  $\delta$  9.3 (d, 1H,  $J = 7.6$  Hz), 8.27 (quin, 2H,  $J = 8.2$  Hz), 8.19 (d,  $J = 9.5$  Hz, 1H), 7.87-7.83 (m, 1H), 7.77 (td,  $J = 7.15$ , 1.4 Hz, 1H), 7.63-7.57 (m, 1H), 7.51 (dd,  $J = 8.6$ , 2.4 Hz, 1H), 7.38-7.34 (m, 4H), 7.32-7.28 (m, 2H), 7.23-7.16 (m, 3H), 5.92 (dd,  $J = 13.8$ , 8.1 Hz, 1H), 4.55-4.46 (m, 1H), 4.24 (td,  $J = 8.8$ , 2.4 Hz, 1H), 4.09 (td,  $J = 7.9$ , 2.4 Hz, 1H), 3.11 (dd,  $J = 13.6$ , 5.5 Hz, 1H), 2.76-2.71 (m, 1H);  **$^{13}\text{C NMR}$**  ( $\text{CDCl}_3$ , 100 MHz)  $\delta$  166.3, 160.9, 149.3, 146.5, 137.6, 130.3, 129.6, 129.2, 129.1, 128.8, 128.7, 128.5, 128.2, 127.9, 127.6, 127.5, 127.1, 126.8, 119.1, 73, 70.3, 52.1, 41.8; **HMRS** (+NSI) calculated for  $\text{C}_{27}\text{H}_{24}\text{N}_3\text{O}_2$  422.1863, found 422.1862  $[\text{M}+\text{H}]^+$ .



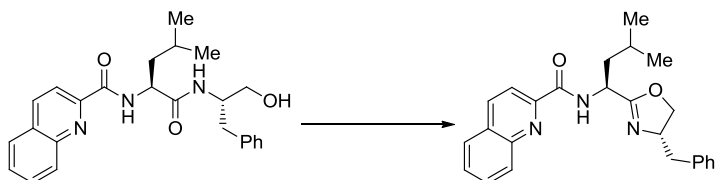
**(*S*)-methyl 4-methyl-2-(quinoline-2-carboxamido)pentanoate (63).** Prepared by general procedure **A** using quinaldic acid (500 mg, 2.89 mmol), *N*-methylmorpholine (0.5 mL and 0.375 mL, 4.54 mmol and 3.41 mmol), isobutyl chloroformate (0.45 mL,

3.47 mmol), and L-leucine methyl ester hydrochloride (600 mg, 3.30 mmol). Mixed solvent recrystallization (Et<sub>2</sub>O/hexanes) afforded the title compound as a white solid (493 mg, 57 %); **R<sub>f</sub>** 0.54 (7:3 hexanes/EtOAc); **IR** (thin film, cm<sup>-1</sup>) 3383, 2955, 1741, 1672, 1522, 1498, 1166; **<sup>1</sup>H NMR** (CDCl<sub>3</sub>, 400 MHz) δ 8.58 (d, *J* = 9 Hz, 1H), 8.28 (dd, *J* = 13.7, 9.0 Hz, 2H), 8.15 (d, *J* = 8.6 Hz, 1H), 7.87 (dd, *J* = 8.2, 1.2 Hz, 1H), 7.77 (ddd, *J* = 8.5, 6.9, 1.4 Hz, 1H), 7.62 (ddd, *J* = 8.2, 7.0, 1.2 Hz, 1H), 4.89 (td, *J* = 8.6, 5.9 Hz, 1H), 3.77 (s, 3H), 1.87-1.74 (m, 3H), 1.00 (dd, *J* = 6.3, 4.7 Hz, 6H); **<sup>13</sup>C NMR** (CDCl<sub>3</sub>, 100 MHz) δ 173.6, 164.51, 149.4, 146.7, 137.7, 130.3, 130.1, 129.6, 128.2, 127.9, 119.1, 52.6, 51.1, 42, 25.2, 23.2, 22.2; **HMRS** (+APCI) calculated for C<sub>17</sub>H<sub>21</sub>N<sub>2</sub>O<sub>3</sub> 301.1547 found 301.1546 [M+H]<sup>+</sup>.



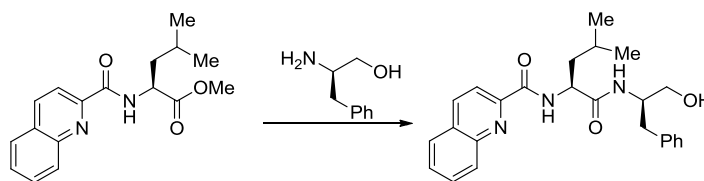
***N*-((*S*)-1-(((*S*)-1-hydroxy-3-phenylpropan-2-yl)amino)-4-methyl-1-oxopentan-2-yl)quinoline-2-carboxamide (66).** Prepared by general procedure **B** using (*S*)-(-)-2-amino-3-phenyl-1-propanol (414 mg, 2.74 mmol), *n*-butyllithium (1.19 mL, 2.73 mmol, 2.3 M solution in hexanes), and methyl ester-amide **63** (718 mg, 2.39 mmol). Mixed solvent recrystallization (Et<sub>2</sub>O/hexanes) afforded the title compound as a white solid (805 mg, 80 %); **R<sub>f</sub>** 0.45 (7:3 hexanes/acetone); **<sup>1</sup>H NMR** (CDCl<sub>3</sub>, 400 MHz) δ 8.41 (br d, *J* = 7.9 Hz, 2H), 8.33 (d, *J* = 8.5 Hz, 1H), 8.24 (d, *J* = 8.5 Hz, 1H), 8.12 (d, *J* = 8.5 Hz, 1H), 7.9 (d, *J* = 7.9 Hz, 1H), 7.79 (ddd, *J* = 8.5, 7.0, 1.2 Hz, 1H), 7.64 (td, *J* = 7.6, 1.1 Hz, 1H), 7.11 (d, *J* = 7 Hz, 2H), 7.03 (t, *J* = 7.6 Hz, 2H), 6.93 (t, *J* = 7.3 Hz, 1H), 6.53 (br d, *J* = 7 Hz, 1H), 4.6 (td, *J* = 8.5, 5.5 Hz, 1H), 4.20-4.13 (m, 1H), 3.72 (dd, *J* = 11.0,

3.4 Hz, 1H), 3.60 (dd,  $J = 11.1, 5.3$  Hz, 1H), 2.87 (dd,  $J = 13.7, 7.0$  Hz, 1H), 2.78 (dd,  $J = 13.7, 7.9$  Hz, 1H), 1.88-1.81 (m, 1H), 1.75-1.66 (m, 2H), 0.94 (dd,  $J = 9.9, 6.3$  Hz, 6H).

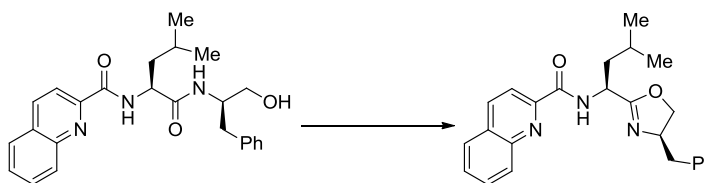


***N*-((*S*)-1-((*S*)-4-benzyl-4,5-dihydrooxazol-2-yl)-3-methylbutyl)quinoline-2-**

**carboxamide (64).** Prepared by general procedure **D** using **66** (805 mg, 1.92 mmol), triphenylphosphine (604 mg, 2.30 mmol), and diisopropyl azodicarboxylate (0.460 mL, 2.33 mmol). Purification by flash chromatography (9:1 hexanes/acetone) afforded **64** as a colorless viscous oil (546 mg, 71 %) with a ratio of 3:1 inseparable epimers;  $R_f$  0.61 (7:3 hexanes/acetone); **IR** (thin film,  $\text{cm}^{-1}$ ) 3381, 2957, 2246, 1663, 1522, 1498, 1165;  **$^1\text{H}$  NMR** ( $\text{CDCl}_3$ , 400 MHz)  $\delta$  1H NMR (500 MHz;  $\text{CDCl}_3$ )  $\delta$  8.57 (br d,  $J = 9.2$  Hz, 1H), 8.32-8.25 (m, 2H), 8.14 (dd,  $J = 16.2, 8.2$  Hz, 1H), 7.85 (dd,  $J = 16.5, 8.2$  Hz, 1H), 7.74 (dd,  $J = 14.0, 7.0$  Hz, 1H), 7.62-7.57 (m, 1H), 7.34-7.27 (m, 1H), 7.25-7.20 (m, 2H), 7.17 (d,  $J = 7.6$  Hz, 2H), 5.02 (dd,  $J = 15.9, 7.0$  Hz, 1H), 4.42 (td,  $J = 8.5, 6.7$  Hz, 1H), 4.23 (t,  $J = 8.8$  Hz, 1H), 4.04 (dd,  $J = 8.2, 7.3$  Hz, 1H), 3.06 (dd,  $J = 13.6, 5.3$  Hz, 1H), 2.67 (dd,  $J = 13.6, 8.4$  Hz, 1H), 1.85-1.72 (m, 3H), 0.98 (dd,  $J = 6.1, 3.7$  Hz, 6H);  **$^{13}\text{C}$  NMR** ( $\text{CDCl}_3$ , 100 MHz)  $\delta$  186.1, 167.8, 164.2, 149.6, 137.7, 130.1, 129.6, 129.2, 128.7, 128.2, 127.9, 127, 126.7, 119.2, 72.4, 67.4, 53.2, 46.3, 42.7, 38.9, 25.1, 22.4; **HMRS** (+APCI) calculated for  $\text{C}_{25}\text{H}_{28}\text{N}_3\text{O}_2$  402.2176, found 402.2172  $[\text{M}+\text{H}]^+$ .

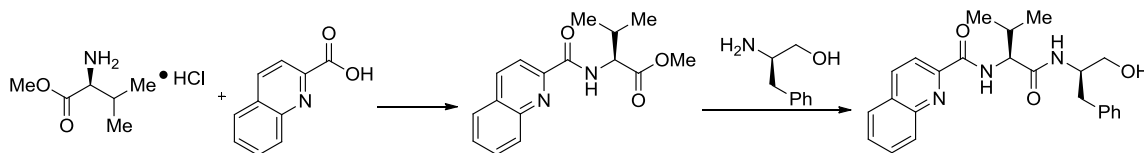


***N*-((*S*)-1-(((*R*)-1-hydroxy-3-phenylpropan-2-yl)amino)-4-methyl-1-oxopent-2-yl)quinoline-2-carboxamide (67).** Prepared by general procedure **B** using (*R*)-(+)-2-amino-3-phenyl-1-propanol (222 mg, 1.47 mmol), *n*-butyllithium (0.64 mL, 1.47 mmol, 2.3 M solution in hexanes), and methyl ester-amide **54** (402 mg, 1.34 mmol). Mixed solvent recrystallization (Et<sub>2</sub>O/hexanes) afforded the title compound as a white solid (512 mg, 91 %); **R<sub>f</sub>** 0.45 (7:3 hexanes/acetone); **IR** (thin film, cm<sup>-1</sup>) 3303, 2955, 1648, 1524, 1468, 1041; **<sup>1</sup>H NMR** (CDCl<sub>3</sub>, 400 MHz) δ 8.5 (br d, *J* = 7.8 Hz, 2H), 8.3 (d, *J* = 8.6 Hz, 1H), 8.22 (d, *J* = 8.6 Hz, 1H), 8.11 (d, *J* = 8.6 Hz, 1H), 7.87 (d, *J* = 8.2 Hz, 1H), 7.77 (dd, *J* = 8.2, 7.0 Hz, 1H), 7.62 (dd, *J* = 8.6, 7.0 Hz, 1H), 7.18 (d, *J* = 4.7 Hz, 3H), 7.12 (dd, *J* = 9.0, 4.7 Hz, 2H), 6.37 (br d, *J* = 5.9 Hz, 1H), 4.49 (q, *J* = 7.4 Hz, 1H), 4.22-4.16 (m, 1H), 3.72 (dd, *J* = 11.2, 3.3 Hz, 1H), 3.57 (dd, *J* = 11.3, 5.1 Hz, 1H), 2.88 (dd, *J* = 15.7, 7.4 Hz, 2H), 1.79 (dt, *J* = 13.9, 7.1 Hz, 1H), 1.67 (dd, *J* = 13.7, 6.3 Hz, 1H), 1.58 (dt, *J* = 13.2, 6.5 Hz, 1H), 0.9 (dd, *J* = 6.5, 2.5 Hz, 6H); **<sup>13</sup>C NMR** (CDCl<sub>3</sub>, 100 MHz) δ 172.5, 165, 149, 146.7, 137.7, 130.4, 130.1, 129.4, 128.7, 128.4, 127.9, 126.7, 118.9, 66.7, 64.2, 53.2, 52.8, 41.4, 37.2, 25, 23, 22.5; **HMRS** (+APCI) calculated for C<sub>25</sub>H<sub>30</sub>N<sub>3</sub>O<sub>3</sub> 420.2282, found 420.2275 [M+H]<sup>+</sup>.



***N*-((*S*)-1-((*R*)-4-benzyl-4,5-dihydrooxazol-2-yl)-3-methylbutyl)quinoline-2-**

**carboxamide (65).** Prepared by general procedure **D** using **67** (200 mg, 0.48 mmol), triphenylphosphine (155 mg, 0.58 mmol), and diisopropyl azodicarboxylate (0.113 mL, 0.58 mmol) to afford title compound as a 1:2 mixture of inseparable epimers; **R<sub>f</sub>** 0.61 (7:3 hexanes/acetone); **IR** (thin film, cm<sup>-1</sup>) 3302, 2980, 1714, 1663, 1499, 1226, 1107; **<sup>1</sup>H NMR** (CDCl<sub>3</sub>, 400 MHz) δ 8.62 (br d, *J* = 8.6 Hz, 1H), 8.31-8.29 (m, 1H), 8.24 (d, *J* = 8.2 Hz, 1H), 8.17-8.13 (m, 1H), 7.86 (d, *J* = 8.2 Hz, 1H), 7.76 (t, *J* = 7.6 Hz, 1H), 7.61 (t, *J* = 7.4 Hz, 1H), 7.30-7.24 (m, 3H), 7.21-7.17 (m, 2H), 4.85 (td, *J* = 8.6, 5.5 Hz, 1H), 4.23 (t, *J* = 9.0 Hz, 1H), 4.04 (t, *J* = 7.8 Hz, 1H), 3.07 (dd, *J* = 14.3, 4.9 Hz, 1H), 2.88-2.83 (m, 1H), 2.68-2.62 (m, 1H), 1.93-1.72 (m, 3H), 0.99 (d, *J* = 6.3 Hz, 6H); **<sup>13</sup>C NMR** (CDCl<sub>3</sub>, 100 MHz) δ 168.1, 164.2, 156.8, 149.5, 146.7, 137.7, 130.3, 130.1, 129.6, 129, 128.7, 128.2, 127.9, 126.7, 119.2, 72.3, 70, 46.1, 42.7, 37.9, 25, 22.2; **HMRS** (+APCI) calculated for C<sub>25</sub>H<sub>28</sub>N<sub>3</sub>O<sub>2</sub> 402.2176, found 402.2171 [M+H]<sup>+</sup>.

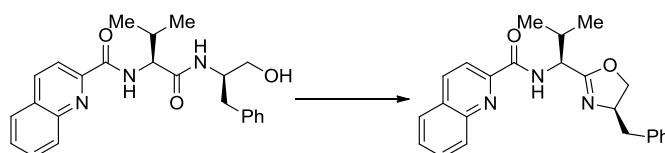


***N*-((*S*)-1-(((*R*)-1-hydroxy-3-phenylpropan-2-yl)amino)-3-methyl-1-oxobutan-2-**

**yl)quinoline-2-carboxamide (68).** Prepared by general procedure **C** using quinaldic acid (2.0g, 11.55 mmol), *N*-methylmorpholine (1.9 mL and 1.5 mL, 17.2 mmol and 13.6 mmol), isobutyl chloroformate (1.7 mL, 13.1 mmol), L-valine methyl ester



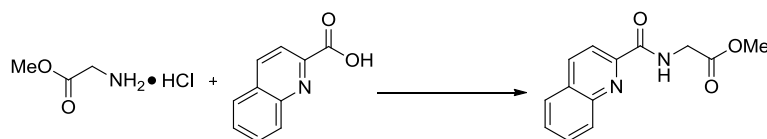
hydrochloride (2.228 g, 13.3 mmol), (*R*)-(+)-2-amino-3-phenyl-1-propanol (1.930 g, 12.76 mmol), and *n*-butyllithium (5.5 mL, 12.7 mmol, 2.3 M solution in hexanes). Mixed solvent recrystallization (Et<sub>2</sub>O/hexanes) afforded the title compound as a white solid (3.526 g, 84 %); **R<sub>f</sub>** (0.43 7:3 hexanes: acetone); **IR** (thin film, cm<sup>-1</sup>) 3364, 2961, 1652, 1498, 1040; **<sup>1</sup>H NMR** (CDCl<sub>3</sub>, 400 MHz) δ 8.69 (br d, *J* = 8.6 Hz, 2H), 8.3 (d, *J* = 10.0 Hz, 1H), 8.23 (d, *J* = 9.5 Hz, 1H), 8.13 (d, *J* = 8.6 Hz, 1H), 7.86 (d, *J* = 7.6 Hz, 1H), 7.76 (td, *J* = 7.6, 1.0 Hz, 1H), 7.62 (td, *J* = 7.6, 1.0 Hz, 1H), 7.31-7.12 (m, 5H), 6.28 (br d, *J* = 7.1 Hz, 1H), 4.27-4.22 (m, 2H), 3.71 (dd, *J* = 11.2, 3.6 Hz, 1H), 3.58 (dd, *J* = 11.2, 5.0 Hz, 1H), 2.92 (dd, *J* = 13.8, 6.7 Hz, 1H), 2.84 (dd, *J* = 13.8, 8.1 Hz, 1H), 2.25 (dq, *J* = 13.6, 6.9 Hz, 1H), 0.89 (d, *J* = 6.7 Hz, 6H); **<sup>13</sup>C NMR** (CDCl<sub>3</sub>, 100 MHz) δ 171.5, 165.1, 149.1, 146.7, 138.9, 137.7, 130.4, 130.2, 129.4, 128.8, 128.3, 128.2, 127.9, 126.6, 119.1, 66.7, 57.7, 54.4, 37.3, 31.8, 19.5; **HMRS** (+APCI) calculated for C<sub>24</sub>H<sub>28</sub>N<sub>3</sub>O<sub>3</sub> 406.2125, found 406.2123 [M+H]<sup>+</sup>.



***N*-((*S*)-1-((*R*)-4-benzyl-4,5-dihydrooxazol-2-yl)-2-methylpropyl)quinoline-2-**

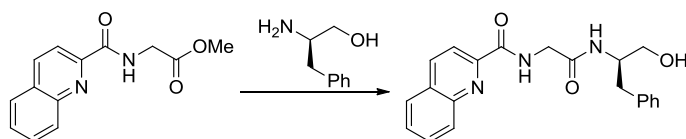
**carboxamide (68).** Procedure from the literature<sup>72</sup> was modified as follows: freshly distilled triethylamine (450 μL, 3.2 mmol, 2.3 equiv) was added via syringe to stirring solution of **69** (500 mg, 1.38 mmol, 1 equiv) and 4-(dimethylamino)pyridine (18 mg, 0.15 mmol, 0.1 equiv) in CH<sub>2</sub>Cl<sub>2</sub> (7 mL) at room temperature. *p*-Toluenesulfonyl chloride (263 mg, 1.39, 1 equiv) in CH<sub>2</sub>Cl<sub>2</sub> (1 mL) was added via cannula to stirring solution in a room temperature water bath and rinsed with 1 mL CH<sub>2</sub>Cl<sub>2</sub>. After 27 h, the

solution was quenched with CH<sub>2</sub>Cl<sub>2</sub> (4 mL) and saturated aqueous NH<sub>4</sub>Cl (6 mL). Water (4 mL) was added, and the aqueous layer was extracted with CH<sub>2</sub>Cl<sub>2</sub> (3 x 5 mL). Combined organic extracts were washed with saturated aqueous NaHCO<sub>3</sub> (5 mL). Aqueous layer was extracted with CH<sub>2</sub>Cl<sub>2</sub> (3 x 5 mL). Combined organic extracts were dried over Na<sub>2</sub>SO<sub>4</sub> and concentrated *in vacuo*. Purification by flash chromatography (8:2 hexanes/acetone) afforded **68** as a colorless viscous oil (261 mg, 55 %); *R<sub>f</sub>* 0.65 (7:3 hexanes/acetone); *IR* (thin film, cm<sup>-1</sup>) 2965, 2249, 1662, 1498, 907; <sup>1</sup>H NMR (CDCl<sub>3</sub>, 400 MHz) δ 8.73 (br d, *J* = 9.5 Hz, 1H), 8.29-8.24 (m, 2H), 8.13 (t, *J* = 9.2 Hz, 1H), 7.81 (d, *J* = 8.2 Hz, 1H), 7.74-7.69 (m, 1H), 7.56 (ddd, *J* = 13.7, 8.2, 1.2 Hz, 1H), 7.27-7.13 (m, 5H), 4.85 (dd, *J* = 8.5, 5.8 Hz, 1H), 4.46-4.38 (m, 1H), 4.21 (td, *J* = 8.8, 2.7 Hz, 1H), 4.02 (td, *J* = 7.9, 2.7 Hz, 1H), 3.13 (dd, *J* = 13.7, 4.9 Hz, 1H), 2.69-2.62 (m, 1H), 2.29 (dq, *J* = 13, 6.7 Hz, 1H), 1.02 (dd, *J* = 6.7, 1.8 Hz, 6H); <sup>13</sup>C NMR (CDCl<sub>3</sub>, 100 MHz) δ 184.3, 166.9, 164.4, 149.6, 146.7, 137.7, 130.2, 129.6, 129.1, 128.8, 128.7, 128.2, 127.9, 126.8, 119.2, 72.3, 67.3, 59.5, 41.9, 32.1, 19.4; *HMRS* (+APCI) calculated for C<sub>24</sub>H<sub>26</sub>N<sub>3</sub>O<sub>2</sub> 388.2019, found 388.3015 [M+H]<sup>+</sup>.



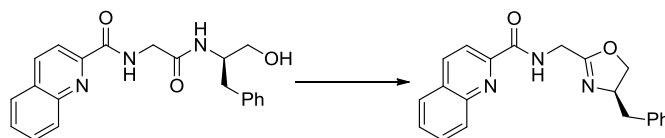
**Methyl 2-(quinoline-2-carboxamido)acetate (73).** Prepared by general method **A** using quinaldic acid (4.00 g, 23.1 mmol), *N*-methylmorpholine (3.8 mL and 3.0 mL, 34.4 mmol and 26.6 mmol), isobutyl chloroformate (3.5 mL, 26.1 mmol), and glycine methyl ester hydrochloride (3.34 g, 13.0 mmol). Mixed solvent recrystallization (EtOAc/hexanes) afforded the title compound as a white solid (4.66 g, 83 %). <sup>1</sup>H NMR (CDCl<sub>3</sub>, 400 MHz)

$\delta$  8.69 (br s, 1H), 8.32-8.26 (m, 2H), 8.12 (d,  $J = 8.5$  Hz, 1H), 7.87 (d,  $J = 8.2$  Hz, 1H), 7.76 (ddd,  $J = 8.4, 6.9, 1.5$  Hz, 1H), 7.61 (ddd,  $J = 8.2, 6.9, 1.1$  Hz, 1H), 4.33 (d,  $J = 5.8$  Hz, 2H), 3.80 (s 3H).



**(R)-N-(2-((1-hydroxy-3-phenylpropan-2-yl)amino)-2-oxoethyl)quinoline-2-**

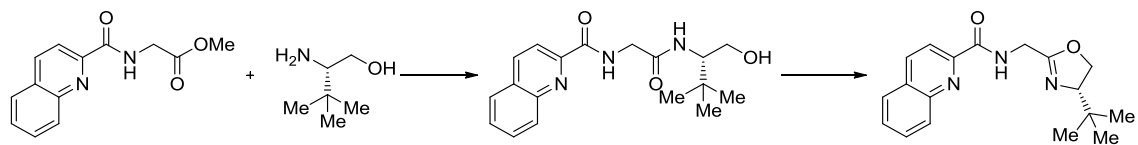
**carboxamide (75).** Prepared by general procedure **B** using **73** (4.33 g, 17.7 mmol), (*R*)-(+)-2-amino-3-phenyl-1-propanol (2.95 g, 19.5 mmol), and *n*-butyllithium (8.5 mL, 19.6 mmol, 2.3 M solution in hexanes). Mixed solvent recrystallization (DCM/hexanes) afforded the title compound as a white solid (6.0 g, 93 %);  $R_f$  0.3 (hexanes/EtOAc); **IR** (thin film,  $\text{cm}^{-1}$ ) 3305, 2928, 1655, 1528, 1042;  **$^1\text{H NMR}$**  ( $\text{CDCl}_3$ , 400 MHz)  $\delta$  8.72 (br m, 2H), 8.34 (d,  $J = 8.2$  Hz, 1H), 8.26 (d,  $J = 8.5$  Hz, 1H), 8.11 (d,  $J = 8.5$  Hz, 1H), 7.90 (d,  $J = 8.2$  Hz, 1H), 7.79 (ddd,  $J = 8.5, 6.9, 1.4$  Hz, 1H), 7.65 (ddd,  $J = 8.2, 6.9, 1.1$  Hz, 1H), 7.14-7.04 (m, 5H), 6.42 (d,  $J = 7.9$  Hz, 1H), 4.15 (dd,  $J = 14, 6.1$  Hz, 2H), 4.19-4.16 (m, 1H), 3.71 (dd,  $J = 11, 3.7$  Hz, 1H), 3.61 (dd,  $J = 11, 5.2$  Hz, 1H), 2.88-2.84 (dd,  $J = 10.4, 7.3$  Hz, 2H);  **$^{13}\text{C NMR}$**  ( $\text{CDCl}_3$ , 100 MHz)  $\delta$  169.5, 165.6, 148.9, 146.7, 137.8, 137.7, 130.5, 130, 129.6, 129.4, 128.8, 128.5, 127.9, 126.8, 118.9, 64.1, 53.4, 43.9, 37.2; **HMRS** (+APCI) calculated for  $\text{C}_{21}\text{H}_{22}\text{N}_3\text{O}_3$  364.1656, found 364.1654  $[\text{M}+\text{H}]^+$ .



**(R)-N-((4-benzyl-4,5-dihydrooxazol-2-yl)methyl)quinoline-2-carboxamide (72).**

Procedures from the literature<sup>59,72</sup> were modified as follows: freshly distilled triethylamine (5.0 mL, 35.8 mmol, 2.2 equiv) was added via syringe to stirring solution of **75** (5.9 g, 16.3 mmol, 1 equiv) and 4-(dimethylamino)pyridine (200 mg, 1.63 mmol, 0.1 equiv) in CH<sub>2</sub>Cl<sub>2</sub> (60 mL) at room temperature. *p*-Toluenesulfonyl chloride (3.11 g, 16.3 mmol, 1 equiv) in CH<sub>2</sub>Cl<sub>2</sub> (13 mL) was added via cannula to stirring solution in a room temperature water bath and rinsed with 3 mL CH<sub>2</sub>Cl<sub>2</sub>. After 27 h, the solution was quenched with CH<sub>2</sub>Cl<sub>2</sub> (40 mL) and saturated aqueous NH<sub>4</sub>Cl (67 mL). Water (40 mL) was added, and the aqueous layer was extracted with CH<sub>2</sub>Cl<sub>2</sub> (3 x 54 mL). Combined organic extracts were washed with saturated aqueous NaHCO<sub>3</sub> (54 mL). Aqueous layer was extracted with CH<sub>2</sub>Cl<sub>2</sub> (3 x 54 mL). Combined organic extracts were dried over Na<sub>2</sub>SO<sub>4</sub> and concentrated *in vacuo*. Purification by flash chromatography (8:2 hexanes/acetone) afforded the title compound as a colorless viscous oil (3.8 g, 67 %); **R<sub>f</sub>** 0.32 (7:3 hexanes/acetone); **IR** (thin film, cm<sup>-1</sup>) 3387, 2924, 1663, 1523, 1497, 1201, 972; **<sup>1</sup>H NMR** (CDCl<sub>3</sub>, 400 MHz) δ 8.71 (br t, 1H), 8.30-8.28 (m, 2H), 8.14 (d, *J* = 8.6 Hz, 1H), 7.86 (d, *J* = 8.6 Hz, 1H), 7.77-7.73 (m, 1H), 7.62-7.58 (m, 1H), 7.28 (q, *J* = 7.3 Hz, 2H), 7.22-7.2 (m, 3H), 4.47-4.42 (m, 1H), 4.33 (dd, *J* = 10.5, 5.2 Hz, 2H), 4.27 (dd, *J* = 18.1, 8.6 Hz, 1H), 4.06 (dd, *J* = 15.7, 8.1 Hz, 1H), 3.14 (dd, *J* = 13.6, 5.5 Hz, 1H), 2.69 (dd, *J* = 13.6, 8.3 Hz, 1H); **<sup>13</sup>C NMR** (CDCl<sub>3</sub>, 100 MHz) δ 164.9, 164.6, 149.4, 146.7, 137.9, 137.7, 130.3, 130.1, 129.6, 129.5, 128.8, 128.2, 127.9, 126.8,

119.1, 72.7, 67.4, 41.8, 37.2; **HMRS** (+APCI) calculated for  $C_{21}H_{20}N_3O_2$  346.1550 found 346.1547  $[M+H]^+$ .



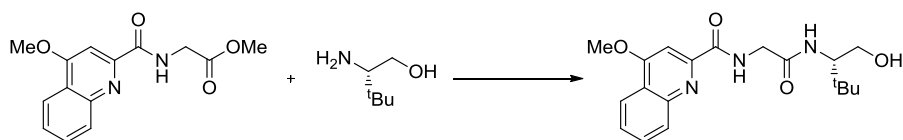
**(S)-N-((4-(tert-butyl)-4,5-dihydrooxazol-2-yl)methyl)quinoline-2-carboxamide (76).**

Procedures from the literature were modified as follows:<sup>71,72</sup> Butyllithium (4.6 mL, 10.6 mmol, 2.3 M solution in hexanes) was added dropwise to a solution of (*S*)-*t*-leucinol (1.23 g, 10.5 mmol) in toluene (0.48 M) and THF (0.72 M) at 0 °C. After stirring for 15 mins, methyl ester-amide **73** (2.33 g, 9.5 mmol), was added in five portions. Reaction mixture was warmed to 25 °C and stirred until thin layer chromatography indicated complete consumption of starting material. Reaction was cooled to 0 °C and water was added dropwise to quench. Organic solvent was removed under reduced pressure and remaining aqueous solution was extracted with  $CH_2Cl_2$ . The combined organic extracts were dried over  $Na_2SO_4$ , filtered, and concentrated *in vacuo*. Freshly distilled triethylamine (3 mL, 21.5 mmol) was added via syringe to stirring solution of the crude reaction mixture and 4-(dimethylamino)pyridine (124 mg, 1.02 mmol) in  $CH_2Cl_2$  (7 mL) at room temperature. *p*-Toluenesulfonyl chloride (1.89 g, 9.9 mmol) in  $CH_2Cl_2$  (1 mL) was added via cannula to stirring solution in a room temperature water bath and rinsed with 1 mL  $CH_2Cl_2$ . After 27 h, the solution was quenched with  $CH_2Cl_2$  and saturated aqueous  $NH_4Cl$ . Water was added, and the aqueous layer was extracted with  $CH_2Cl_2$  (3 x). Combined organic extracts were washed with saturated aqueous  $NaHCO_3$ . Aqueous layer was extracted with  $CH_2Cl_2$  (3 x). Combined organic extracts were dried

over  $\text{Na}_2\text{SO}_4$ . The reaction was concentrated *in vacuo* and purification by flash chromatography (7:3 hexanes/acetone) afforded the title compound as a colorless oil (1.06 g, 34 % over two steps);  $R_f$  0.5 (7:3 hexanes/acetone); **IR** (thin film,  $\text{cm}^{-1}$ ) 3393, 2954, 1667, 1525, 1500, 1200, 1169;  **$^1\text{H NMR}$**  ( $\text{CDCl}_3$ , 400 MHz)  $\delta$  8.72 (br s, 1H), 8.29 (s, 2H), 8.13 (d,  $J = 8.5$  Hz, 1H), 7.87 (d,  $J = 7.9$  Hz, 1H), 7.79-7.71 (m, 1H), 7.63-7.59 (m, 1H), 4.34 (t,  $J = 6.1$  Hz, 2H), 4.27 (t,  $J = 9.8$  Hz, 1H), 4.15 (t,  $J = 8.5$  Hz, 1H), 3.92 (t,  $J = 8.8$  Hz, 1H), 0.92 (s, 9H);  **$^{13}\text{C NMR}$**  ( $\text{CDCl}_3$ , 100 MHz)  $\delta$  164.8, 163.7, 149.5, 146.8, 137.7, 130.3, 129.6, 128.2, 127.9, 119.1, 75.8, 69.7, 37.2, 33.8, 30.1, 26.0; **HMRS** (+NSI) calculated for  $\text{C}_{18}\text{H}_{22}\text{N}_3\text{O}_2$  312.1707, found 312.1706  $[\text{M}+\text{H}]^+$ .



**Methyl 2-(4-methoxyquinoline-2-carboxamido)acetate (77).** Prepared by general method **A** using quinaldic acid (2.00 g, 9.85 mmol), *N*-methylmorpholine (1.6 mL and 1.3 mL, 14.5 mmol and 11.4 mmol), isobutyl chloroformate (1.5 mL, 11.6 mmol), and glycine methyl ester hydrochloride (2.00 g, 11.3 mmol). Mixed solvent recrystallization ( $\text{Et}_2\text{O}$ /hexanes) afforded the title compound as a white solid (2.03 g, 75 %);  $R_f$  (0.34 7:3 hexanes/acetone);  **$^1\text{H NMR}$**  ( $\text{CDCl}_3$ , 400 MHz)  $\delta$  8.72 (br s, 1H), 8.21 (d,  $J = 8.2$  Hz, 1H), 8.04 (d,  $J = 7.9$  Hz, 1H), 7.73 (ddd,  $J = 8.4, 6.9, 1.5$  Hz, 1H), 7.67 (s, 1H), 7.56 (ddd,  $J = 8.2, 7, 1.2$  Hz, 1H), 4.32-4.30 (m, 2H), 4.12 (s, 3H), 3.80 (s, 3H);  **$^{13}\text{C NMR}$**  ( $\text{CDCl}_3$ , 100 MHz)  $\delta$  170.4, 165.26, 163.8, 150.7, 147.8, 130.5, 129.5, 127.2, 122.1, 98.1, 98.0, 56.4, 52.6, 41.6; **HMRS** (+NSI) calculated for  $\text{C}_{14}\text{H}_{15}\text{N}_2\text{O}_4$  275.1026, found 275.1027  $[\text{M}+\text{H}]^+$ .



**(S)-N-(2-((1-hydroxy-3,3-dimethylbutan-2-yl)amino)-2-oxoethyl)-4-**

**methoxyquinoline-2-carboxamide (79).** Prepared by general procedure **B** using

*n*-butyllithium (1.9 mL, 4.4 mmol, 2.3 M solution in hexanes), *S*-*t*-leucinol (500 mg, 4.3 mmol), and **77** (1.06 g, 3.9 mmol). Purification by flash chromatography (7:3

hexanes/acetone) afforded the title compound as a colorless oil (1.05 g, 74 % over two

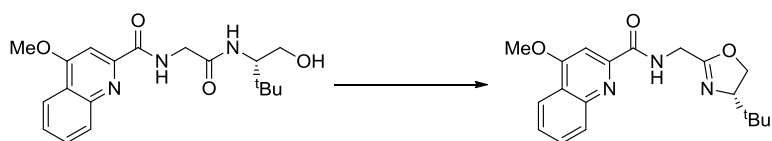
steps);  $R_f$  0.1 (7:3 hexanes/acetone); **IR** (thin film,  $\text{cm}^{-1}$ ) 3324, 2965, 2251, 1656, 1504,

1115;  $^1\text{H NMR}$  ( $\text{CDCl}_3$ , 400 MHz)  $\delta$  8.91 (br t,  $J = 5.6$  Hz, 1H), 8.23 (d,  $J = 8.2$  Hz, 1H), 8.03 (d,  $J = 8.5$  Hz, 1H), 7.75 (ddd,  $J = 8.5, 7, 1.5$  Hz, 1 H), 7.66 (s, 1H), 7.58 (td,

$J = 7.6, 1.2$  Hz, 1H), 6.50 (d,  $J = 9.1$  Hz, 1H), 4.24 (d,  $J = 6.2$  Hz, 2H), 4.14 (s, 3H), 3.87 (dd,  $J = 8.6, 5.4$  Hz, 2H), 3.56 (dd,  $J = 11.9, 8.6$  Hz, 1H), 2.50 (br s, 1H), 0.94 (s, 9H);

$^{13}\text{C NMR}$  ( $\text{CDCl}_3$ , 100 MHz)  $\delta$  170.3, 165.7, 163.5, 150.4, 147.5, 130.3, 129.4, 127.0, 122.0, 97.8, 97.7, 62.13, 60.1, 56.2, 56.1, 43.8, 39.9; **HMRS** (+NSI) calculated for

$\text{C}_{19}\text{H}_{26}\text{N}_3\text{O}_4$  360.1918, found 360.1923  $[\text{M}+\text{H}]^+$ .



**(S)-N-((4-(tert-butyl)-4,5-dihydrooxazol-2-yl)methyl)-4-methoxyquinoline-2-**

**carboxamide (80).** Procedure from the literature was modified as follows:<sup>72</sup> freshly

distilled triethylamine (0.77 mL, 5.5 mmol) was added via syringe to stirring solution of

**79** (903 mg, 2.5 mmol) and 4-(dimethylamino)pyridine (30 mg, 0.25 mmol) in  $\text{CH}_2\text{Cl}_2$

(7 mL) at room temperature. *p*-Toluenesulfonyl chloride (477 mg, 2.5 mmol) in  $\text{CH}_2\text{Cl}_2$

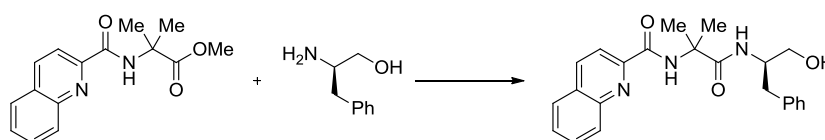
(1 mL) was added via cannula to stirring solution in a room temperature water bath and rinsed with 1 mL CH<sub>2</sub>Cl<sub>2</sub>. After 27 h, the solution was quenched with CH<sub>2</sub>Cl<sub>2</sub> and saturated aqueous NH<sub>4</sub>Cl. Water was added, and the aqueous layer was extracted with CH<sub>2</sub>Cl<sub>2</sub> (3 x). Combined organic extracts were washed with saturated aqueous NaHCO<sub>3</sub>. Aqueous layer was extracted with CH<sub>2</sub>Cl<sub>2</sub> (3 x). Combined organic extracts were dried over Na<sub>2</sub>SO<sub>4</sub>. The reaction was concentrated *in vacuo* and purified by flash chromatography on silica gel (7:3 hexanes/acetone) to afford the title compound as a white solid (453 mg, 53 %); **R<sub>f</sub>** 0.4 (7:3 hexanes/acetone); **IR** (thin film, cm<sup>-1</sup>) 3385, 2954, 2247, 1666, 1503, 1420, 1187, 1113; **<sup>1</sup>H NMR** (CDCl<sub>3</sub>, 400 MHz) δ 8.75 (br t, *J* = 4.8 Hz, 1H), 8.21 (d, *J* = 8.6 Hz, 1H), 8.04 (d, *J* = 8.6 Hz, 1H), 7.72 (td, *J* = 6.9, 1.4 Hz, 1H), 7.68 (s, 1H), 7.55 (td, *J* = 7.6, 1.0 Hz, 1H), 4.38-4.29 (m, 2H), 4.26 (dd, *J* = 10.0, 9.1 Hz, 1H), 4.14 (t, *J* = 8.3 Hz, 1H), 4.11 (s, 3H), 3.91 (t, *J* = 9.1 Hz, 1H), 0.91 (s, 9H); **<sup>13</sup>C NMR** (CDCl<sub>3</sub>, 100 MHz) δ 165.0, 163.7, 150.9, 147.7, 130.4, 129.6, 127.1, 122.3, 122.3, 122.1, 98.1, 75.8, 69.6, 56.4, 37.2, 33.8, 26.0; **HMRS** (+NSI) calculated for C<sub>19</sub>H<sub>24</sub>N<sub>3</sub>O<sub>3</sub> 342.1812, found 342.1813 [M+H]<sup>+</sup>.



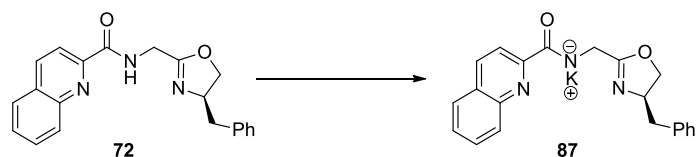
**Methyl 2-methyl-2-(quinoline-2-carboxamido)propanoate (82).** Prepared by general method **A** using quinaldic acid (1.95 g, 11.2 mmol), *N*-methylmorpholine (1.9 mL and 1.5 mL, 17.2 mmol and 13.6 mmol), isobutyl chloroformate (1.75 mL, 13.5 mmol), and methyl 2-amino-2-methylpropanoate hydrochloride (2.00 g, 13.0 mmol). Mixed solvent recrystallization (Et<sub>2</sub>O/hexanes) afforded the title compound as a white solid (2.16 g,



71 %); **R<sub>f</sub>** (0.41 7:3 hexanes: acetone); **IR** (thin film,  $\text{cm}^{-1}$ ) 3387, 2989, 2950, 2253, 1738, 1673, 1522, 1499, 1427; **<sup>1</sup>H NMR** ( $\text{CDCl}_3$ , 400 MHz)  $\delta$  8.72 (s, 1H), 8.27 (q, 2H,  $J = 8.3$  Hz), 8.13 (d, 1H,  $J = 8.6$  Hz), 7.87 (d, 1H,  $J = 8.2$  Hz), 7.76 (t, 1H,  $J = 7.6$  Hz), 3.78 (s, 3H), 1.73 (s, 6H); **<sup>13</sup>C NMR** ( $\text{CDCl}_3$ , 100 MHz)  $\delta$  175.1, 163.9, 149.8, 146.6, 137.7, 130.3, 129.9, 129.5, 128.1, 127.9, 118.8, 56.6, 52.9, 25.2; **HMRS** (+NSI) calculated for  $\text{C}_{15}\text{H}_{17}\text{N}_2\text{O}_3$  273.1234, found 273.1236  $[\text{M}+\text{H}]^+$ .

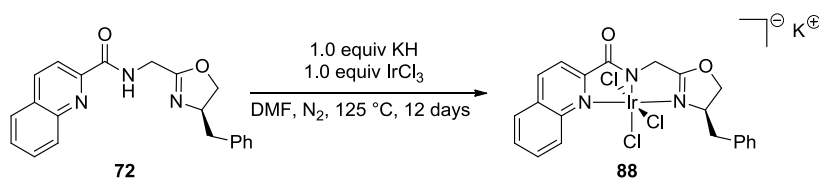


**(R)-N-(1-((1-Hydroxy-3-phenylpropan-2-yl)amino)-2-methyl-1-oxopropan-2-yl)quinoline-2-carboxamide (83)**. Prepared by general procedure **B** using *(R)*-(+)-2-amino-3-phenyl-1-propanol (1.11 g, 7.4 mmol), *n*-butyllithium (3.2 mL, 7.36 mmol, 2.3 M solution in hexanes), and methyl ester-amide **82** (2.00 g, 7.3 mmol). Purification by flash chromatography (1:1 hexanes/EtOAc) afforded the title compound as a white solid (1.55 g, 54 %); **R<sub>f</sub>** 0.25 (1:1 hexanes/EtOAc); **IR** (thin film,  $\text{cm}^{-1}$ ) 3359, 2940, 2248, 1661, 1519, 1221, 1041; **<sup>1</sup>H NMR** ( $\text{CDCl}_3$ , 400 MHz)  $\delta$  8.56 (s, 1H), 8.33 (d,  $J = 8.6$  Hz, 1H), 8.24 (d,  $J = 8.6$  Hz, 1H), 8.12 (d,  $J = 8.2$  Hz, 1H), 7.9 (d,  $J = 7.8$  Hz, 1H), 7.79 (t,  $J = 7.6$  Hz, 1H), 7.64 (t,  $J = 7.8$  Hz, 1H), 7.18-7.09 (m, 5H), 6.48 (d,  $J = 7.8$  Hz, 1H), 4.17 (br s, 1H), 3.81 (dd,  $J = 11.3, 3.1$  Hz, 1H), 3.54 (dd,  $J = 11.7, 5.5$  Hz, 1H), 2.84 (dd,  $J = 7.4, 2.7$  Hz, 2H), 1.64 (s, 3H), 1.60 (s, 3H); **<sup>13</sup>C NMR** ( $\text{CDCl}_3$ , 100 MHz)  $\delta$  174.5, 164.9, 149.3, 146.5, 138.0, 130.6, 129.8, 129.6, 129.4, 128.6, 128.5, 128.0, 126.6, 118.8, 63.6, 57.5, 53.4, 36.9, 25.8, 25.3; **HMRS** (+NSI) calculated for  $\text{C}_{23}\text{H}_{26}\text{N}_3\text{O}_3$  392.1969, found 392.1971  $[\text{M}+\text{H}]^+$ .



**Potassium (R)-((4-benzyl-4,5-dihydrooxazol-2-yl)methyl)(quinoline-2-**

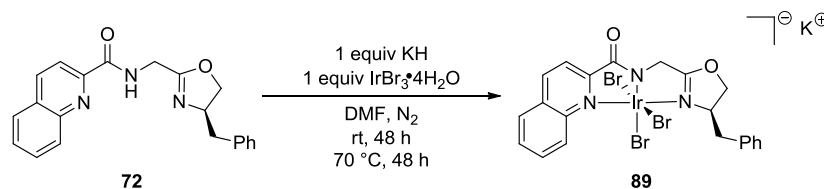
**carbonyl)amide (87).** In an inert atmosphere dry box using degassed reagents and solvents, potassium hydride (75 mg, 1.87 mmol) was added to a solution of (R)-N-((4-benzyl-4,5-dihydrooxazol-2-yl)methyl)quinoline-2-carboxamide (639 mg, 1.85 mmol) in 20 mL DMF. The solution turned orange and bubbling was observed upon addition. After stirring overnight, the reaction was concentrated to yield the title ligand-potassium salt;  $^1\text{H NMR}$  ( $\text{CDCl}_3$ , 400 MHz)  $\delta$  8.29-8.27 (m, 2H), 8.12 (d,  $J = 8.5$  Hz, 1H), 7.86 (dd,  $J = 8.2, 1.2$  Hz, 1H), 7.77-7.72 (m, 1H), 7.60 (t,  $J = 7.5$  Hz, 1H), 7.28-7.26 (m, 2H), 7.20-7.18 (m, 3H), 4.44-4.41 (m, 1H), 4.32-4.30 (m, 2H), 4.25 (t,  $J = 8.8$  Hz, 1H), 4.04 (t,  $J = 7.2$  Hz, 1H), 3.10-3.09 (m, 1H), 2.69-2.64 (m, 1H).



**[(R)-N-((4-benzyl-4,5-dihydrooxazol-2-yl)methyl)quinoline-2-carboxamide]IrCl<sub>3</sub>(K)**

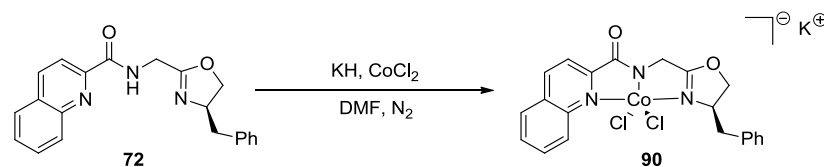
**(88).** In an inert atmosphere dry box using degassed reagents and solvents, potassium hydride (17 mg, 0.42 mmol) was added to a solution of (R)-N-((4-benzyl-4,5-dihydrooxazol-2-yl)methyl)quinoline-2-carboxamide (148 mg, 0.42 mmol) in 1 mL DMF. The solution turned light orange and bubbled upon addition. After stirring for forty minutes, anhydrous  $\text{IrCl}_3$  (130 mg, 0.42 mmol) was added. The reaction was transferred to a pressure tube, removed from the dry box, and heated to 125 °C for 12

days, with monitoring by HRMS every 2 days until ligand was consumed. The crude mixture was concentrated, taken up in CH<sub>3</sub>CN, filtered, and concentrated. Complex **88** was not isolated and is tentatively characterized by HRMS; **HMRS** (-NSI) calculated for C<sub>21</sub>H<sub>18</sub>Cl<sub>3</sub>IrN<sub>3</sub>O<sub>2</sub> 642.0094, found 642.0095 [M-K].



**[(*R*)-*N*-((4-benzyl-4,5-dihydrooxazol-2-yl)methyl)quinoline-2-carboxamide]IrCl<sub>3</sub>(K)**

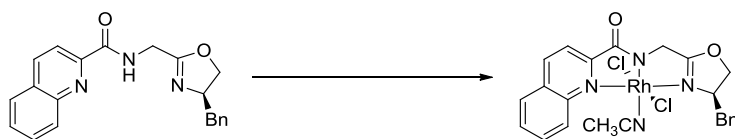
**(89).** In an inert atmosphere dry box using degassed reagents and solvents, potassium hydride (25 mg, 0.63 mmol) was added to a solution of (*R*)-*N*-((4-benzyl-4,5-dihydrooxazol-2-yl)methyl)quinoline-2-carboxamide (218 mg, 0.63 mmol) in 1 mL DMF. The solution turned light orange and bubbled upon addition. After stirring for 5 h, anhydrous IrBr<sub>3</sub>•4H<sub>2</sub>O (318 mg, 0.63 mmol) was added. The reaction was stirred for 48 h at RT, then transferred to a pressure tube, removed from the dry box, and heated to 70 °C for 48 h. The crude mixture was concentrated, taken up in CH<sub>3</sub>CN, filtered, and concentrated. Complex **89** was not isolated and is tentatively characterized by HRMS; **HMRS** (-NSI) calculated for C<sub>21</sub>H<sub>18</sub>Br<sub>3</sub>IrN<sub>3</sub>O<sub>2</sub> 773.8584, found 773.8549 [M-K].



**[(*R*)-*N*-((4-benzyl-4,5-dihydrooxazol-2-yl)methyl)quinoline-2-carboxamide]CoCl<sub>2</sub>(K)**

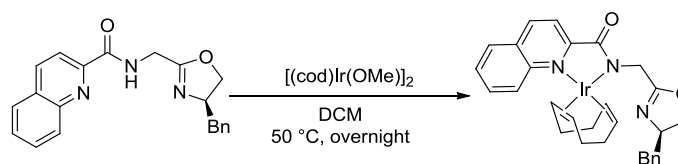
**(90).** In an inert atmosphere dry box using degassed reagents and solvents, potassium

hydride (23 mg, 0.58 mmol) was added to a solution of (*R*)-*N*-((4-benzyl-4,5-dihydrooxazol-2-yl)methyl)quinoline-2-carboxamide (214 mg, 0.62 mmol) in 1 mL DMF. The solution turned light orange and bubbled upon addition. After stirring for 30 minutes, anhydrous CoCl<sub>2</sub> (81 mg, 0.62 mmol) was added. The reaction was stirred for 3 h at RT. The crude mixture was concentrated, taken up in CH<sub>3</sub>CN, filtered, and concentrated. Complex **90** was not isolated and is tentatively characterized by HRMS; **HMRS** (-NSI) calculated for C<sub>21</sub>H<sub>18</sub>Cl<sub>2</sub>CoN<sub>3</sub>O<sub>2</sub> 473.0114, found 473.0114 [M-K]<sup>-</sup>.



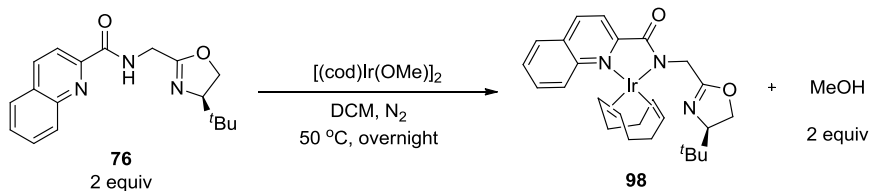
**[(*R*)-*N*-((4-benzyl-4,5-dihydrooxazol-2-yl)methyl)quinoline-2-carboxamide]RhCl<sub>2</sub>(CH<sub>3</sub>CN) (**93**).** In an inert atmosphere dry box using degassed reagents and solvents, potassium hydride (17 mg, 0.42 mmol) was added to a solution of (*R*)-*N*-((4-benzyl-4,5-dihydrooxazol-2-yl)methyl)quinoline-2-carboxamide (145 mg, 0.42 mmol) in 1 mL DMF. The solution turned light orange and bubbled upon addition. After stirring for forty minutes, anhydrous RhCl<sub>3</sub> was added. The reaction was transferred to a pressure tube, removed from the dry box, and heated to 70 ° C for 6 days. The reaction was heated further to 90 ° C for 12 days until mass spectrometry indicated ligand was consumed. The crude mixture was concentrated, taken up in CH<sub>3</sub>CN, and filtered. Recrystallization out of CH<sub>3</sub>CN/Et<sub>2</sub>O yielded 23 mg (10 % yield, 0.042 mmol) of the title compound as a red crystalline solid; **IR** (thin film, cm<sup>-1</sup>) 3524, 2924, 2034, 1978, 1632, 1419, 1238; **<sup>1</sup>H NMR** (CDCl<sub>3</sub>, 400 MHz) δ 8.87 (d, *J* = 8.87 Hz, 1H), 8.42 (d, *J* = 8.2 Hz, 1H), 8.24 (d, *J* = 8.2 Hz, 1H), 7.94 (d, *J* = 8.2 Hz, 1H), 7.83 (t, *J* = 7.8 Hz,

1H), 7.69 (t,  $J = 7.8$  Hz, 1H), 7.36-7.17 (m, 5H), 4.79 (s, 2H), 4.74-4.68 (m, 2H), 4.53 (dd,  $J = 7.4, 4.7$  Hz, 1H), 3.7 (d,  $J = 14.1$  Hz, 1H), 2.95 (dd,  $J = 14.9, 10.6$  Hz, 1H); **HMRS** (-ESI) calculated for  $C_{21}H_{18}N_3O_2Cl_3Rh$  551.9526, found 551.9525  $[M+Cl]^-$ .



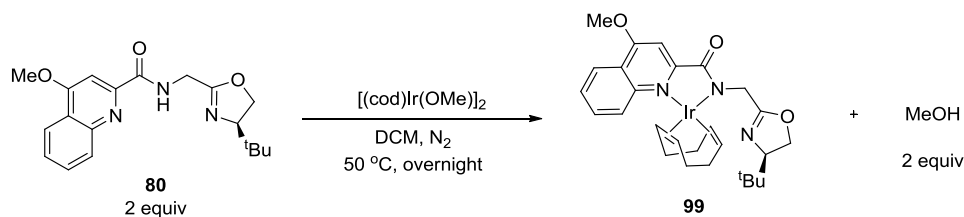
**[(*R*)-*N*-((4-benzyl-4,5-dihydrooxazol-2-yl)methyl)quinoline-2-carboxamide]Ir(cod)**

**(96)**. Inside a nitrogen-filled atmosphere dry box, a 20 mL scintillation vial was charged with a magnetic stir bar and ligand **72** (215 mg, 0.63 mmol) in DCM (0.19 M).  $[(cod)Ir(OMe)_2]_2$  (208 mg, 0.31 mmol) was stirred in DCM (10 mL) and added to solution of ligand in DCM. Immediate color change to deep red was observed. The reaction mixture was transferred to a sealed pressure tube and heated in an oil bath outside the glove box at 50 °C overnight. The reaction vessel was returned to the glovebox and DCM was removed under vacuum to yield **96** (339 mg, 84 % yield) as a light red powder;  **$^1H$  NMR** ( $CDCl_3$ , 400 MHz)  $\delta$  8.47 (dd,  $J = 11.6, 8.8$  Hz, 1H), 8.25 (d,  $J = 8.8$  Hz, 1H), 7.93 (d,  $J = 7.6$  Hz, 1H), 7.81-7.52 (m, 2H), 7.64 (q,  $J = 6.4$  Hz, 1H), 7.31-7.18 (m, 5H), 4.32-4.15 (m, 7H), 3.97 (t,  $J = 8.0$  Hz, 2H), 3.07 (br d,  $J = 14.0$  Hz, 1H), 2.65 (dd,  $J = 22.0, 8.8$  Hz, 1H), 2.24 (br s, 4H), 1.69-1.63 (m, 4H); **HMRS** (+ESI) calculated for  $C_{29}H_{31}IrN_3O_2$  646.2046, found 646.2059  $[M+H]^+$ .



**[(*R*)-*N*-((4-(*tert*-butyl)-4,5-dihydrooxazol-2-yl)methyl)quinoline-2-**

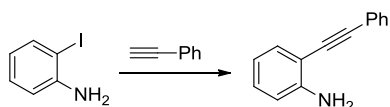
**carboxamide]Ir(cod) (**98**).** Inside a nitrogen-filled atmosphere dry box, a 20 mL scintillation vial was charged with a magnetic stir bar and ligand **76** (250 mg, 0.74 mmol) in DCM (0.19 M). [(cod)Ir(OMe)<sub>2</sub>] (251 mg, 0.37 mmol) was stirred in DCM (10 mL) and added to solution of ligand in DCM. Immediate color change to deep red was observed. The reaction mixture was transferred to a sealed pressure tube and heated in an oil bath outside the glove box at 50 °C overnight. The reaction vessel was returned to the glovebox and DCM was removed under vacuum to yield **98** as a light red powder; <sup>1</sup>H NMR (CDCl<sub>3</sub>, 400 MHz) δ 8.47 (d, *J* = 8.4 Hz, 1H), 8.26 (dd, *J* = 13.6, 8.0 Hz, 1H), 7.90 (d, *J* = 6.8 Hz, 1H), 7.93-7.75 (m, 2H), 7.63 (br s, 1H), 4.38-4.27 (m, 4H), 4.17-4.00 (m, 4H), 3.84 (dt, *J* = 22.8, 7.6 Hz, 1H), 3.24 (br s, 4H), 1.64 (br d, *J* = 9.2 Hz, 4H), 0.90 (s, 9H); **HMRS** (+ESI) calculated for C<sub>26</sub>H<sub>33</sub>IrN<sub>3</sub>O<sub>2</sub> 612.2202, found 612.2296 [M+H]<sup>+</sup>.



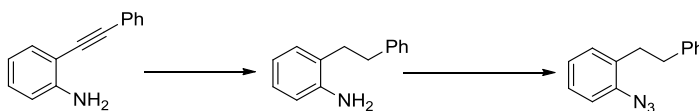
**[(*R*)-*N*-((4-(*tert*-butyl)-4,5-dihydrooxazol-2-yl)methyl)-4-methoxyquinoline-2-**

**carboxamide]Ir(cod) (**99**).** Inside a nitrogen-filled atmosphere dry box, a 20 mL scintillation vial was charged with a magnetic stir bar and ligand **80** (111 mg, 0.33 mmol) in DCM (0.19 M). [(cod)Ir(OMe)<sub>2</sub>] (108 mg, 0.16 mmol) was stirred in DCM (10 mL)

and added to solution of ligand in DCM. Immediate color change to deep red was observed. The reaction mixture was transferred to a sealed pressure tube and heated in an oil bath outside the glove box at 50 ° C overnight. The reaction vessel was returned to the glovebox and DCM was removed under vacuum to yield **99** as a light red powder;  $^1\text{H NMR}$  ( $\text{CDCl}_3$ , 400 MHz)  $\delta$  8.25 (d,  $J = 8.0$  Hz, 1H), 7.72-7.66 (m, 3H), 7.57 (d,  $J = 6.0$  Hz, 1H), 4.19-4.12 (m, 8H), 4.04 (dd,  $J = 16.0, 8.0$  Hz, 2H), 3.83 (t,  $J = 8.0$  Hz, 2H), 2.24 (br s, 4H), 1.64 (br s, 4H), 0.86 (s, 9H).



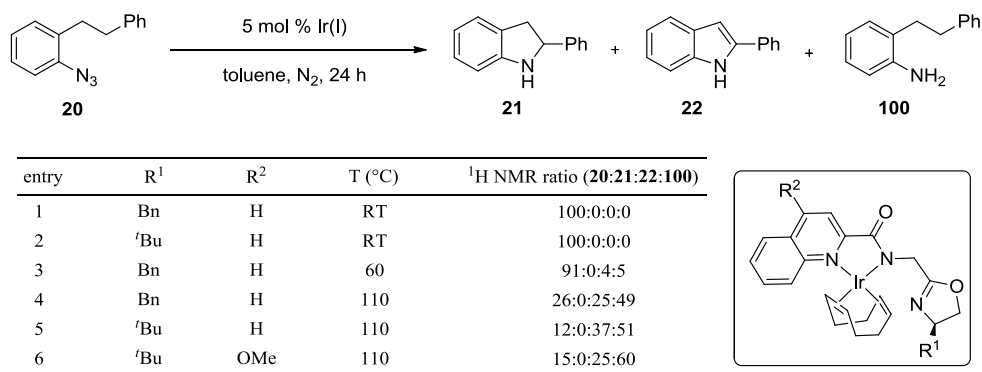
**2-(phenylethynyl)aniline (103)**. Prepared according to the literature,<sup>37</sup> using 1-iodo-2-iodobenzene (2.02 g, 9.2 mmol), ethynylbenzene (1.2 mL, 10.9 mmol),  $\text{PdCl}_2(\text{PPh}_3)_2$  (340 mg, 0.48 mmol),  $\text{CuI}$  (42 mg, 0.22 mmol), and ethanolamine (6.6 mL, 109 mmol). Flash chromatography afforded 1.7 g (96 % yield) of title compound.  $^1\text{H NMR}$  was identical to that reported;<sup>37</sup>  $^1\text{H NMR}$  ( $\text{CDCl}_3$ , 400 MHz)  $\delta$  7.51 (dd,  $J = 7.9, 1.7$  Hz, 2H), 7.36-7.31 (m, 4H), 7.13 (t,  $J = 7.6$  Hz, 1H), 6.71 (t,  $J = 8.6$  Hz, 2H), 4.26 (br s, 2H).



**1-azido-2-phenethylbenzene (20)**. Prepared according to the literature,<sup>37</sup> using **103** (4.37 g, 23 mmol),  $\text{Pd/C}$  (1.54 g),  $\text{H}_2$  gas, sodium nitrite (1.87 g, 27 mmol), and sodium azide (2.07 g, 32 mmol). Flash chromatography afforded 3.16 g (63 % yield over 2 steps) of title compound.  $^1\text{H NMR}$  was identical to that reported;<sup>37</sup>  $^1\text{H NMR}$  ( $\text{CDCl}_3$ , 400 MHz)

$\delta$  7.32-7.27 (m, 3H), 7.24-7.16 (m, 3H), 7.14-7.10 (m, 2H), 7.07-7.02 (m, 1H), 2.87 (m, 4H).

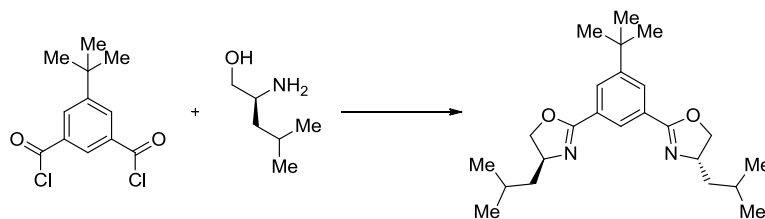
**Table 2.4.** Iridium(I) quinoline-oxazoline amide catalyst optimization for benzylic C–H amination with aryl azide **20**.



**General procedure for iridium(I) complex screening for C–H amination with 1-azido-2-phenethylbenzene.** The following procedure was modified from the literature.<sup>37</sup>

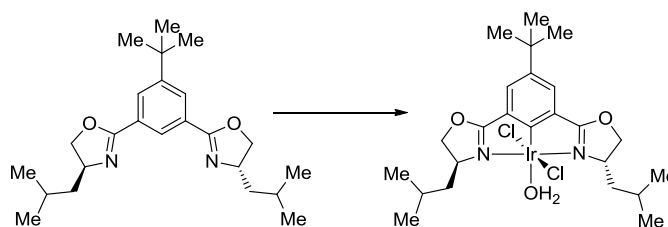
In an inert atmosphere dry box using degassed reagents and solvents, to a mixture of 1-azido-2-phenethylbenzene (30 mg, 0.13 mmol) and iridium(I) complex (5 mol %) in a sealed tube was added 1 mL of solvent. The reaction mixture was removed from the glove box and was stirred at the specified temperature for 20 h. The mixture was filtered through Celite. The filtrate was concentrated *in vacuo*. The ratio of products and starting material was determined by comparing C–H peaks of each compound (reported in the literature) by crude <sup>1</sup>H NMR in CDCl<sub>3</sub>.





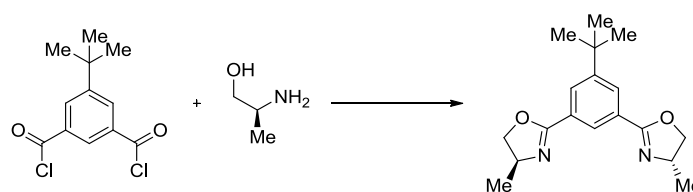
**(4*S*,4'*S*)-2,2'-(5-(*tert*-butyl)-1,3-phenylene)bis(4-isobutyl-4,5-dihydrooxazole) (107).**

Prepared according to the literature,<sup>73</sup> using 5-*t*-butylisophthaloyl dichloride (500 mg, 1.9 mmol) in CH<sub>2</sub>Cl<sub>2</sub> (8 mL), (*S*)-(+)-Leucinol (0.5 mL, 4.2 mmol), Et<sub>3</sub>N (4.0 mL, 28.6 mmol) in CH<sub>2</sub>Cl<sub>2</sub> (15 mL), and methanesulfonyl chloride (0.33 mL, 4.3 mmol). Purification by flash chromatography (7:3 pentane/EtOAc) afforded the title compound as a white solid (400 mg, 55 %); R<sub>f</sub> 0.7 (7:3 hexanes/EtOAc); **IR** (thin film, cm<sup>-1</sup>) 2956, 1649, 1592, 1467, 1366, 1244, 980; **<sup>1</sup>H NMR** (CDCl<sub>3</sub>, 400 MHz) δ 8.27 (t, *J* = 1.5 Hz, 1H), 8.05 (d, *J* = 1.5 Hz, 2H), 4.47 (dd, *J* = 1.2, 9.4 Hz, 2H), 4.30 (quint, *J* = 7.8, 1.8 Hz, 2H), 3.96 (t, *J* = 7.8 Hz, 2H), 1.84-1.65 (m, 4H), 1.39-1.33 (m, 11H), 0.94 (dd, *J* = 6.4, 4.4 Hz, 12H); **<sup>13</sup>C NMR** (CDCl<sub>3</sub>, 100 MHz) δ 163.2, 151.8, 128.2, 125.7, 73.3, 65.5, 45.8, 35.1, 31.4, 25.7, 23.2, 22.8; **HMRS** (+NSI) calculated for C<sub>24</sub>H<sub>37</sub>N<sub>2</sub>O<sub>2</sub> 385.2850, found 385.2849 [M+H]<sup>+</sup>.



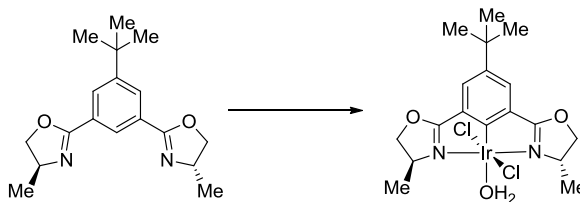
**[(*S*, *S*)-*t*-ButylPhebox-*i*-Butyl]IrCl<sub>2</sub>(H<sub>2</sub>O) (105).** Prepared according to the literature,<sup>73</sup> using **107** (187 mg, 0.62 mmol), IrCl<sub>3</sub>·3H<sub>2</sub>O (243 mg, 0.69 mmol), sodium bicarbonate (61 mg, 0.73 mmol), and isopropanol (24 mL) at reflux for 5 hours. Purification by preparatory thin layer chromatography (7:3 hexanes/EtOAc) afforded the title compound

as an orange solid (213 mg, 62 %);  $R_f$  0.4 (7:3 hexanes/EtOAc); **IR** (thin film,  $\text{cm}^{-1}$ ) 2690, 2231, 1621, 1452, 1379, 1284;  **$^1\text{H}$  NMR** ( $\text{CDCl}_3$ , 400 MHz)  $\delta$  7.51 (s, 2H), 5.07 (t,  $J = 9.1$  Hz, 2H), 4.5 (t,  $J = 7.1$  Hz, 2H), 4.07-4.03 (m, 1H), 3.75-3.71 (m, 1H), 1.46 (s, 2H), 1.34 (s, 9H), 1.24-1.21 (m, 6H);  **$^{13}\text{C}$  NMR** ( $\text{CDCl}_3$ , 100 MHz)  $\delta$  163.2, 151.8, 128.2, 128.1, 125.7, 73.3, 65.5, 45.8, 35.1, 31.4, 25.7, 23.2; **HMRS** (+APCI) calculated for  $\text{C}_{24}\text{H}_{35}\text{N}_2\text{O}_2\text{Cl}_2\text{Ir}$  646.1699, found 646.1711  $[\text{M}-\text{H}_2\text{O}]^+$ .



**(4*S*,4'*S*)-2,2'-(5-(*tert*-butyl)-1,3-phenylene)bis(4-methyl-4,5-dihydrooxazole) (110).**

Prepared according to the literature,<sup>73</sup> using 5-*t*-butylisophthaloyl dichloride (504 mg, 1.9 mmol) in  $\text{CH}_2\text{Cl}_2$  (8 mL), (*S*)-(+)-2-amino-1-propanol (0.31 mL, 4.0 mmol),  $\text{Et}_3\text{N}$  (4.0 mL, 28.6 mmol) in  $\text{CH}_2\text{Cl}_2$  (15 mL), and methanesulfonyl chloride (0.33 mL, 4.3 mmol). Purification by flash chromatography (7:3  $\rightarrow$  6:4 pentane/EtOAc) afforded the title compound as a white solid (213 mg, 37 %);  $R_f$  0.4 (7:3 hexanes/EtOAc); **IR** (thin film,  $\text{cm}^{-1}$ ) 3721, 2634, 2897, 2420, 2330, 2154, 2005, 1648, 1591, 1236;  **$^1\text{H}$  NMR** ( $\text{CDCl}_3$ , 400 MHz)  $\delta$  8.28 (t,  $J = 1.4$  Hz, 1H), 8.08 (d,  $J = 1.4$  Hz, 2H), 4.5 (dd,  $J = 9.5$ , 8.1 Hz, 2H), 4.40-4.34 (m, 2H), 3.94 (t,  $J = 7.9$  Hz, 2H), 1.36-1.34 (m, 15H);  **$^{13}\text{C}$  NMR** ( $\text{CDCl}_3$ , 100 MHz)  $\delta$  163.4, 151.9, 128.2, 128.1, 125.7, 74.3, 62.4, 35.2, 31.5, 21.7; **HMRS** (+NSI) calculated for  $\text{C}_{18}\text{H}_{25}\text{N}_2\text{O}_2$  301.1911, found 301.1911  $[\text{M}+\text{H}]^+$ .



[(*S,S*)-*t*-ButylPhebox-Me]IrCl<sub>2</sub>(H<sub>2</sub>O) (**106**). Prepared according to the literature,<sup>73</sup> using **110** (187 mg, 0.52 mmol), IrCl<sub>3</sub>·3H<sub>2</sub>O (219 mg, 0.62 mmol), sodium bicarbonate (57 mg, 0.68 mmol), and isopropanol (22 mL) at reflux for 5 hours. Purification by preparatory thin layer chromatography (7:3 hexanes/EtOAc) afforded the title compound as an orange solid (25.1 mg, 7 %); R<sub>f</sub> 0.3 (7:3 hexanes/EtOAc); **IR** (thin film, cm<sup>-1</sup>) 2967, 2228, 2055, 1579, 1448, 1289, 1108; **<sup>1</sup>H NMR** (CDCl<sub>3</sub>, 400 MHz) δ 7.50 (s, 2H), 5.03 (t, *J* = 9.1 Hz, 2H), 4.84 (t, *J* = 8.1 Hz, 2H), 4.28 (q, *J* = 8.1 Hz, 2H), 2.10 (tt, *J* = 10.0, 2.4 Hz, 2H), 1.59 (t, *J* = 8.1 Hz, 2H), 1.34 (s, 9H), 0.99 (dd, *J* = 6.4, 4 Hz, 6H); **HMRS** (+APCI) calculated for C<sub>18</sub>H<sub>23</sub>N<sub>2</sub>O<sub>2</sub>ClIr 527.1072, found 527.1083 [M-H<sub>2</sub>O-Cl]<sup>+</sup>.

**Table S2.1.** Optimization of iridium(III) phebox and phebim catalyzed enantioselective C–H amination with aryl azide **20**.

entry	catalyst	R <sup>1</sup>	R <sup>2</sup>	solvent	<sup>1</sup> H NMR ratio ( <b>20</b> : <b>21</b> : <b>22</b> : <b>100</b> )	ee (%)
1	phebim	<sup>i</sup> Pr	Ph	C <sub>6</sub> H <sub>5</sub> CH <sub>3</sub>	8:92:0:0	10
2	phebim	<sup>i</sup> Pr	4-CF <sub>3</sub> Ph	C <sub>6</sub> H <sub>5</sub> CH <sub>3</sub>	8:92:0:0	13
3	phebim	<sup>i</sup> Pr	3,5-(CF <sub>3</sub> ) <sub>2</sub> Ph	C <sub>6</sub> H <sub>5</sub> CH <sub>3</sub>	10:90:0:0	11
4	phebox	<sup>i</sup> Pr	-	C <sub>6</sub> H <sub>5</sub> CH <sub>3</sub>	14:86:0:0	26
5	phebim	<sup>t</sup> Bu	<i>p</i> -CF <sub>3</sub> Ph	C <sub>6</sub> H <sub>5</sub> CH <sub>3</sub>	9:91:0:0	27
6	phebox	<sup>t</sup> Bu	-	C <sub>6</sub> H <sub>5</sub> CH <sub>3</sub>	10:80:8:3	39
7	phebim	Bn	<i>p</i> -CF <sub>3</sub> Ph	C <sub>6</sub> H <sub>5</sub> CH <sub>3</sub>	8:78:10:4	18
8	phebox	Bn	-	C <sub>6</sub> H <sub>5</sub> CH <sub>3</sub>	26:56:10:9	28
9	phebox	CH <sub>2</sub> -Cy	-	C <sub>6</sub> H <sub>5</sub> CH <sub>3</sub>	4:85:7:4	36
10	phebox	<sup>t</sup> Bu	-	C <sub>6</sub> H <sub>5</sub> CH <sub>3</sub>	37:63:0:0	55
11	phebox	Me	-	C <sub>6</sub> H <sub>5</sub> CH <sub>3</sub>	44:54:2:0	37
12	phebox	CH <sub>2</sub> -Cy	-	C <sub>6</sub> H <sub>5</sub> CH <sub>3</sub>	4:85:7:4	36
13	phebox	indanyl	-	C <sub>6</sub> H <sub>5</sub> CH <sub>3</sub>	9:91:0:0	24
14 <sup>a</sup>	phebox	<sup>t</sup> Bu	-	C <sub>6</sub> H <sub>5</sub> CH <sub>3</sub>	9:91:0:0	51
15 <sup>b</sup>	phebim	<sup>t</sup> Bu	<i>p</i> -CF <sub>3</sub> Ph	C <sub>6</sub> H <sub>5</sub> CH <sub>3</sub>	5:83:8:4	32
16 <sup>c</sup>	phebim	<sup>t</sup> Bu	<i>p</i> -CF <sub>3</sub> Ph	C <sub>6</sub> H <sub>5</sub> CH <sub>3</sub>	53:47:0:0	30
17	phebox	<sup>t</sup> Bu	-	C <sub>6</sub> H <sub>6</sub>	88:12:0:0	54
18	phebox	<sup>t</sup> Bu	-	C <sub>6</sub> H <sub>5</sub> Cl	39:61:0:0	48
19	phebox	<sup>t</sup> Bu	-	C <sub>6</sub> H <sub>5</sub> CF <sub>3</sub>	90:10:0:0	>90
20 <sup>d</sup>	phebox	<sup>t</sup> Bu	-	C <sub>6</sub> H <sub>5</sub> CF <sub>3</sub>	74:1:10:14	n.d.
21 <sup>e</sup>	phebox	<sup>t</sup> Bu	-	C <sub>6</sub> H <sub>5</sub> CH <sub>3</sub>	30:70:0:0	55
22 <sup>f</sup>	-	-	-	C <sub>6</sub> H <sub>5</sub> CH <sub>3</sub>	98:1:0:1	-

<sup>a</sup>3,5-di-Me phebox (instead of <sup>t</sup>Bu) catalyst backbone. <sup>b</sup>Bromide ancillary ligands in place of chloride. <sup>c</sup>T = 80 °C.

<sup>d</sup>20 h. <sup>e</sup>5 mol % catalyst loading. <sup>f</sup>No catalyst.

**General procedure for iridium(III) phebox and phebim complex screening for decomposition of 1-azido-2-phenethylbenzene.** To activated powdered 4 Å M.S. (80 mg) and iridium complex (2.5 mol %)<sup>81</sup> was added 1-azido-2-phenethylbenzene (35 mg, 0.16 mmol) in toluene (3.2 mL). The mixture was heated to reflux for four hours, after which the reaction was cooled and filtered through a pad of Celite. The mixture was concentrated and the crude residue was dissolved in hexanes and analyzed by HPLC (AS-H, 2 → 5 % IPA/HEX, 1 mL/min, λ 254 nm, t<sub>r</sub>(maj) = 6.56 min, t<sub>r</sub>(min) = 10.75 min) to determine enantiomeric excess. The crude mixture was analyzed by

$^1\text{H}$  NMR and the ratio of products and starting material was determined by comparing C–H peaks of each compound, reported in the literature.<sup>37</sup>

HPLC trace for Table S2.1, entry 10 (AS-H, 2  $\rightarrow$  5 % IPA/HEX, 1 mL/min)  $\lambda$  254 nm,  $t_r(\text{maj}) = 6.56$  min,  $t_r(\text{min}) = 10.75$  min

Time [Min]	Height [mAU]	Area [mAU.Min]	Area [%]
6.56	708.7	9791	77.4
10.75	78.8	2856	22.6

Racemic Indoline:

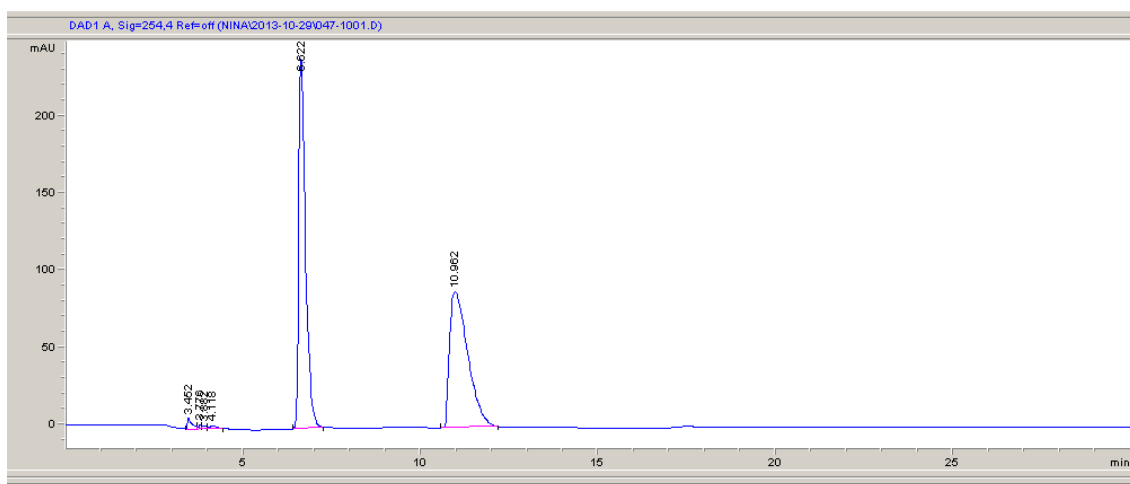
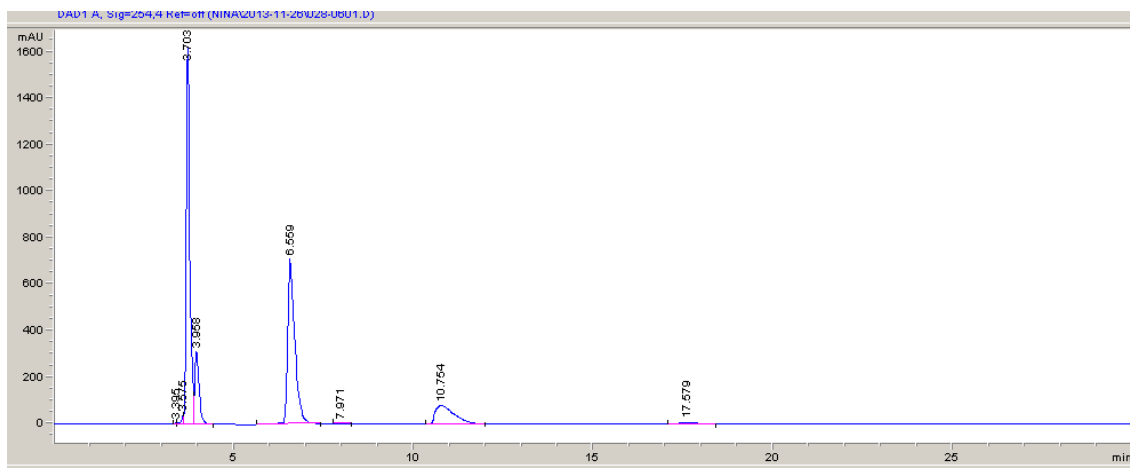
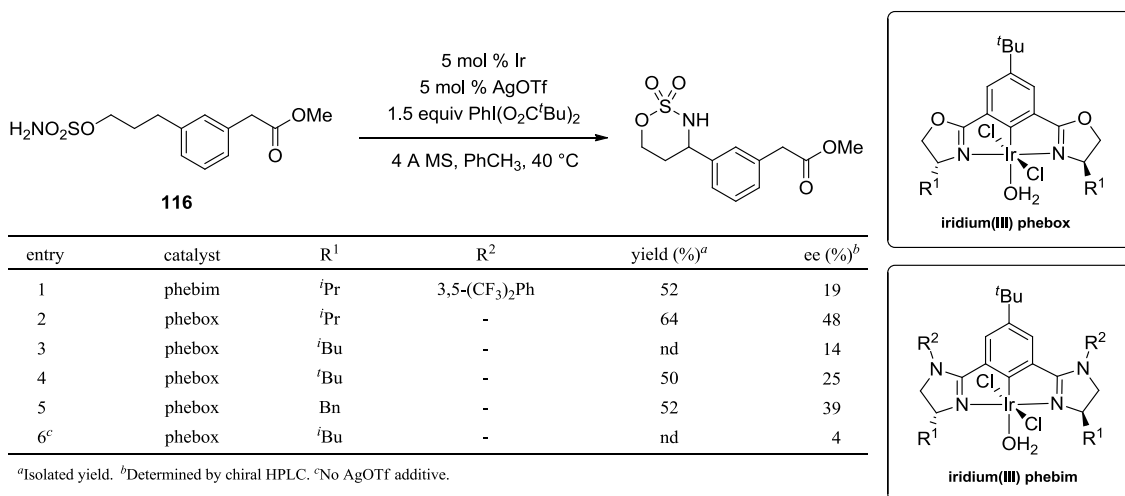


Table S2.1, entry 10:



**Table 2.15.** Optimization of iridium(III) phebox and phebim catalyzed enantioselective C–H amination with sulfamate ester **116**.

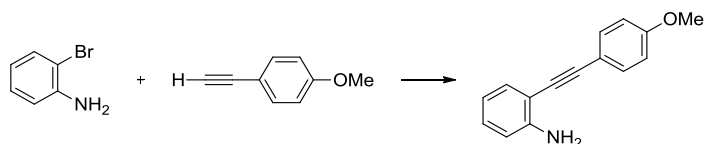


**General procedure for iridium(III) phebox and phebim complex screening for C–H amination to give methyl 2-(3-(2,2-dioxido-1,2,3-oxathiazinan-4-yl)phenyl)acetate.**

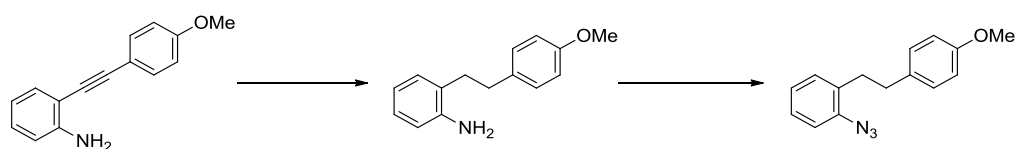
A round bottom flask was charged with a magnetic stir bar, sulfamate **115** (11 mg, 0.038 mmol, 1 equiv), PhI(O<sub>2</sub>C<sup>t</sup>Bu)<sub>2</sub> (23 mg, 0.057 mmol, 1.5 equiv), iridium(III) phebox or phebim (5 mol %),<sup>81</sup> AgOTf (0.5 mg, 0.0019 mmol, 5 mol %), and 4 Å molecular sieves (17 mg). PhCF<sub>3</sub> (0.75 mmol) was added and the solution was heated to 40 °C for 18 h. The reaction mixture was then filtered through a plug of silica gel, and concentrated *in vacuo* and purified by flash chromatography (7:3 hexanes/EtOAc) to afford the title compound in the indicated yield; <sup>1</sup>H NMR (CDCl<sub>3</sub>, 400 MHz) δ 7.35 (t, *J* = 7.6 Hz, 1H), 7.27 (t, *J* = 2.9 Hz, 2H), 7.11-7.05 (m, 1H), 4.84 (td, *J* = 12.4 Hz, 2H), 4.64 (ddd, *J* = 11.7, 5.0, 1.4 Hz, 1H), 4.33 (br d, *J* = 9.1 Hz, 1H), 3.68-3.66 (m, 1H), 3.62 (s, 3H), 3.59-3.57 (m, 1H), 2.26-2.19 (m, 1H), 2.04-2.00 (m, 1H).

**General Procedure E.** Procedure from the literature<sup>37</sup> was modified as follows: alkyne (1.2 equiv.) was added to a solution of 2-bromoaniline (1.0 equiv), PdCl<sub>2</sub>(PPh<sub>3</sub>)<sub>3</sub> (5 mol %), and CuI (2 mol %) in THF at room temperature. N<sub>2</sub> was bubbled through the stirring mixture for 30 mins, after which a solution of ethanolamine in H<sub>2</sub>O (3.0 M, 12 equiv) was added slowly. The mixture was heated to reflux until thin layer chromatography indicated complete consumption of starting material. The reaction was cooled to room temperature and extracted with DCM. The combined organic extracts were washed with brine, dried over Na<sub>2</sub>SO<sub>4</sub>, and concentrated *in vacuo*. Purification by flash chromatography on silica gel as indicated afforded the desired product.

**General Procedure F.** Procedure from the literature<sup>37</sup> was modified as follows: aniline (1.0 equiv.) and Pd/C (10 wt. %, 0.1 equiv.) in THF (0.12 M) were stirred at room temperature under a balloon of H<sub>2</sub>. After thin layer chromatography indicated complete consumption of the starting material, the mixture was filtered through Celite and washed with Et<sub>2</sub>O to afford crude product. NaNO<sub>2</sub> (1.2 equiv.) was added to a stirring solution of crude aniline (1.0 equiv.) in a 1:1 mixture of AcOH and H<sub>2</sub>O (0.8 M) at 0 °C. The mixture was stirred for two hours, and NaN<sub>3</sub> (1.4 equiv.) was added. The reaction was warmed to room temperature. After 30 minutes, H<sub>2</sub>O and Et<sub>2</sub>O were added. Na<sub>2</sub>CO<sub>3</sub> was added slowly to neutralize the solution until pH 7 was reached. The phases were separated, and the aqueous phase was extracted with Et<sub>2</sub>O. The combined organic extracts were washed with brine, dried over Na<sub>2</sub>SO<sub>4</sub>, and concentrated *in vacuo*. Purification by flash chromatography on silica gel as indicated afforded the azide.

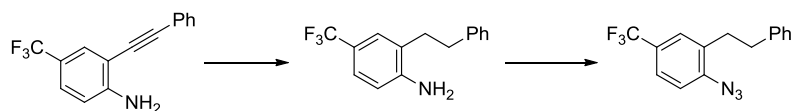


**2-((4-methoxyphenyl)ethynyl)aniline.** Prepared according general procedure **E**, using 2-bromobenzene-1-amine (1.75 mL, 15.5 mmol), 4-ethynylanisole (1.55 mL, 12.0 mmol), PdCl<sub>2</sub>(PPh<sub>3</sub>)<sub>2</sub> (353 mg, 0.50 mmol), CuI (38 mg, 0.20 mmol), and ethanolamine (7.2 mL, 121 mmol). Flash chromatography afforded 2.56 g (96 % yield) of the title compound. <sup>1</sup>H NMR was identical to that reported;<sup>37</sup> <sup>1</sup>H NMR (CDCl<sub>3</sub>, 400 MHz) δ 7.45 (dt, *J* = 9.1, 1.9 Hz, 2H), 7.33 (dd, *J* = 7.6, 1.4 Hz, 1H), 7.12-7.07 (m, 1H), 6.87 (dt, *J* = 9.1, 2.9 Hz, 2H), 6.71 (dd, *J* = 7.9, 3.1 Hz, 2H), 4.24 (br s, 2H), 3.82 (s, 3H).

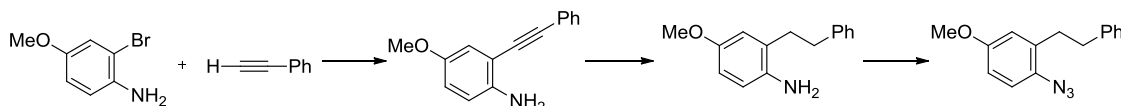


**1-azido-2-(4-methoxyphenethyl)benzene (121).** Prepared according to general procedure **F**, using 2-((4-methoxyphenyl)ethynyl)aniline (856 mg, 3.8 mmol), Pd/C (271 mg), balloon H<sub>2</sub>, sodium nitrite (326 mg, 4.7 mmol), and sodium azide (360 mg, 5.5 mmol). Flash chromatography afforded 560 mg (58 % yield over 2 steps) of title compound **110**. <sup>1</sup>H NMR was identical to that reported;<sup>37</sup> <sup>1</sup>H NMR (CDCl<sub>3</sub>, 400 MHz) δ 7.24-7.21 (m, 1H), 7.12 (d, *J* = 8.1 Hz, 1H), 7.09-7.07 (m, 3H), 7.02 (td, *J* = 7.2, 1.0 Hz, 1H), 6.81 (dt, *J* = 8.6, 1.9 Hz, 2H), 3.77 (s, 3H), 2.83-2.80 (m, 2H), 2.79-2.76 (m, 2H).

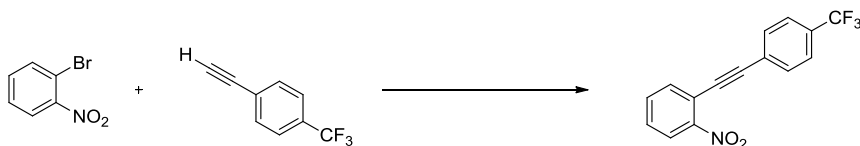




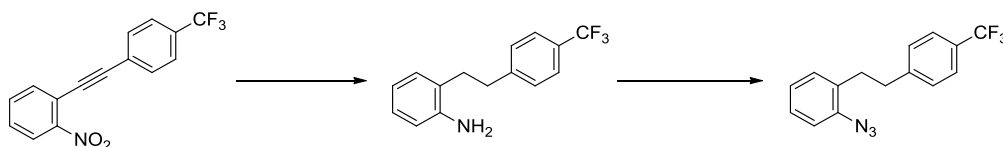
**1-azido-2-phenethyl-4-(trifluoromethyl)benzene (122).** Prepared according to general procedure **F**, using 2-(phenylethynyl)-4-(trifluoromethyl)aniline (1.39 g, 5.3 mmol), Pd/C (361 mg), 1 atm H<sub>2</sub>, sodium nitrite (427 mg, 6.19 mmol), and sodium azide (519 mg, 7.98 mmol). Flash chromatography afforded 981 mg (63 % yield over 2 steps) of title compound **111**. <sup>1</sup>H NMR was identical to that reported;<sup>37</sup> <sup>1</sup>H NMR (CDCl<sub>3</sub>, 400 MHz) δ 7.48 (dd, *J* = 8.3, 1.7 Hz, 1H), 7.32 (s, 1H), 7.27 (td, *J* = 7.2, 1.4 Hz, 2H), 7.2 (dd, *J* = 8.6 Hz, 2H), 7.16 (dd, *J* = 7.1, 1.0 Hz, 2H), 2.90-2.88 (m, 2H), 2.86-2.83 (m, 2H).



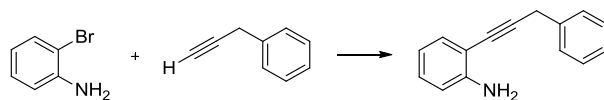
**1-azido-4-methoxy-2-phenethylbenzene (123).** Prepared according general procedures **E** and **F**, without intermediate purification, using 2-bromo-4-methoxyaniline (2.06 g, 10.2 mmol), phenylacetylene (1.32 mL, 12.0 mmol), PdCl<sub>2</sub>(PPh<sub>3</sub>)<sub>2</sub> (355 mg, 0.51 mmol), CuI (41 mg, 0.22 mmol), ethanolamine (7.2 mL, 119 mmol), Pd/C (806 mg), 1 atm H<sub>2</sub>, sodium nitrite (875 mg, 12.7 mmol), and sodium azide (960 mg, 14.8 mmol) to give 369 mg (15 % yield over 3 steps) of title compound **123**; <sup>1</sup>H NMR was identical to that reported;<sup>37</sup> <sup>1</sup>H NMR (CDCl<sub>3</sub>, 400 MHz) δ 7.26 (q, *J* = 7.6 Hz, 3H), 7.19-7.17 (m, 3H), 6.77 (dd, *J* = 8.8, 3.1 Hz, 1H), 6.63 (d, *J* = 2.9 Hz, 1H), 3.72 (s, 3H), 2.82 (s, 4H).



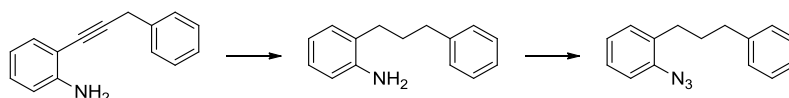
**1-nitro-2-((4-(trifluoromethyl)phenyl)ethynyl)benzene (125).** Prepared according to general procedure **E**, using 1-bromo-2-nitrobenzene (2.2 g, 11.0 mmol, 1 equiv), 1-ethynyl-4-(trifluoromethyl)benzene (2.3 g, 13.2 mmol, 1.2 equiv), PdCl<sub>2</sub>(PPh<sub>3</sub>)<sub>2</sub> (387 mg, 0.55 mmol, 5 mol %), CuI (58 mg, 0.30 mmol, 2 mol %), and ethanolamine (8.0 mL, 13.2 mmol, 1.2 equiv) to give **114** (2.5 g, 87 % yield); <sup>1</sup>H NMR (CDCl<sub>3</sub>, 400 MHz) δ 8.11 (d, *J* = 8.6 Hz, 1H), 7.74-7.68 (m, 2H), 7.62-7.61 (m, 2H), 7.51 (t, *J* = 8.2 Hz, 1H).



**1-azido-2-(4-(trifluoromethyl)phenethyl)benzene (124).** Prepared according to general procedure **F**, using **125** (2.5 g, 8.6 mmol, 1 equiv), Pd/C (858 mg, 10 wt. %), 1 atm H<sub>2</sub>, sodium nitrite (710 mg, 10.3 mmol, 1.2 equiv), and sodium azide (769 mg, 12.0 mmol, 1.4 equiv). Flash chromatography afforded 1.56 g (62 % yield over 2 steps) of title compound. <sup>1</sup>H NMR was identical to that reported;<sup>37</sup> <sup>1</sup>H NMR (CDCl<sub>3</sub>, 400 MHz) δ 7.51 (d, *J* = 8.1 Hz, 2H), 7.27-7.24 (m, 3H), 7.13 (d, *J* = 7.6 Hz, 1H), 7.07-7.01 (m, 2H), 2.91-2.89 (m, 2H), 2.87-2.84 (m, 2H).

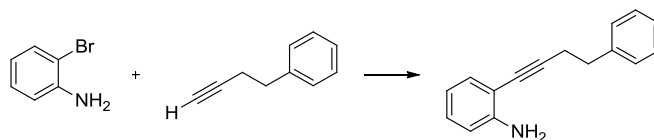


**2-(3-phenylprop-1-yn-1-yl)aniline (129).** Prepared by general procedure **E** using  $\text{PdCl}_2(\text{PPh}_3)_3$  (211 mg, 0.3 mmol), CuI (22 mg, 0.12 mmol), 2-bromoaniline (1.04 g, 6.0 mmol), 3-phenyl-1-propyne (0.9 mL, 7.2 mmol), and ethanolamine (4.4 mL, 72 mmol). Purification by flash chromatography (95:5 hexanes/EtOAc) afforded the title compound as an orange oil (988 mg, 79 %);  $R_f$  0.28 (9:1 hexanes/EtOAc); **IR** (thin film,  $\text{cm}^{-1}$ ) 3474, 3378, 3028, 1612, 1492, 1307, 906, 729;  **$^1\text{H NMR}$**  ( $\text{CDCl}_3$ , 400 MHz)  $\delta$  7.43 (d,  $J = 8.2$  Hz, 2H), 7.37-7.24 (m, 4H), 7.11 (t,  $J = 7.6$  Hz, 1H) 6.71-6.67 (m, 2H), 4.14 (br s, 2H), 3.90 (s, 2H);  **$^{13}\text{C NMR}$**  ( $\text{CDCl}_3$ , 100 MHz)  $\delta$  147.8, 136.8, 132.2, 129.1, 128.6, 127.9, 126.7, 117.8, 114.2, 108.4, 92.9, 79.2, 26.0; **HRMS** (+ESI) calculated for  $\text{C}_{15}\text{H}_{14}\text{N}$  208.1121, found 208.1117  $[\text{M}+\text{H}]^+$ .

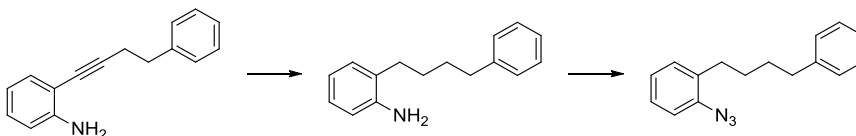


**1-azido-2-(3-phenylpropyl)benzene (127).** Prepared by general procedure **F** using 2-(3-phenylprop-1-yn-1-yl)aniline (947 mg, 4.6 mmol), Pd/C (450 mg, 10 wt. %),  $\text{NaNO}_2$  (380 mg, 5.5 mmol), and  $\text{NaN}_3$  (420 mg, 6.6 mmol). Purification by flash chromatography (hexanes  $\rightarrow$  97:3 hexanes/EtOAc) afforded the title compound as a light yellow oil (410 mg, 38 % over two steps);  $R_f$  0.85 (95:5 hexanes/EtOAc); **IR** (thin film,  $\text{cm}^{-1}$ ) 3025, 2990, 2858, 2116, 1581, 1488, 1450, 1282, 745;  **$^1\text{H NMR}$**  ( $\text{CDCl}_3$ , 400 MHz)  $\delta$  7.29-7.22 (m, 3H), 7.21-7.10 (m, 5H), 7.04 (t,  $J = 7.4$  Hz, 1H), 2.66-2.58 (m, 4H), 1.89 (quin,  $J = 7.8$  Hz, 2H);  **$^{13}\text{C NMR}$**  ( $\text{CDCl}_3$ , 100 MHz)  $\delta$  142.2, 138.0, 133.8, 130.4, 128.5,

128.3, 127.3, 125.8, 124.7, 118.1, 35.7, 31.9, 31.0; **HRMS** (+ESI) calculated for  $C_{15}H_{18}N$  212.1434, found 212.1431  $[M-2N+3H]^+$ .

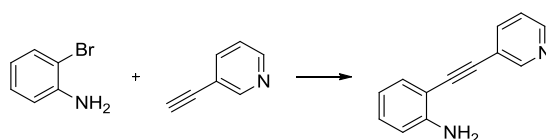


**2-(4-phenylbut-1-yn-1-yl)aniline (131).** Prepared by general procedure **E** using  $PdCl_2(PPh_3)_3$  (416 mg, 0.59 mmol), CuI (45 mg, 0.24 mmol), 2-bromoaniline (2.04 g, 11.9 mmol), 4-phenyl-1-butyne (2.0 mL, 14.2 mmol), and ethanolamine (8.6 mL, 142 mmol). Purification by flash chromatography (95:5 hexanes/EtOAc) afforded the title compound as an orange oil (820 mg, 31 %);  $R_f$  0.28 (9:1 hexanes/EtOAc); **IR** (thin film,  $cm^{-1}$ ) 3471, 3375, 3026, 2925, 1612, 1491, 1454, 1307, 905, 744;  $^1H$  **NMR** ( $CDCl_3$ , 400 MHz)  $\delta$  7.32-7.27 (m, 4H), 7.24-7.19 (m, 2H), 7.05 (td,  $J = 7.7, 1.3$  Hz, 1H) 6.63 (t,  $J = 7.5$  Hz, 2H), 3.95 (br s, 2H), 2.93 (t,  $J = 7.5$  Hz, 2H), 2.78 (t,  $J = 7.5$  Hz, 2H);  $^{13}C$  **NMR** ( $CDCl_3$ , 100 MHz)  $\delta$  147.8, 140.6, 131.9, 128.9, 128.6, 128.4, 126.3, 117.7, 114.1, 108.5, 94.6, 77.9, 35.1, 21.7; **HRMS** (+ESI) calculated for  $C_{16}H_{16}N$  222.1277, found 222.1273  $[M+H]^+$ .

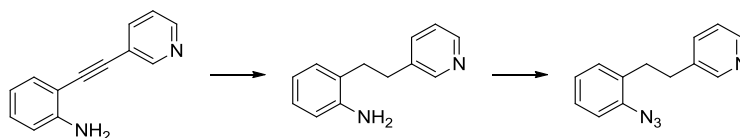


**1-azido-2-(4-phenylbutyl)benzene (130).** Prepared by general procedure **F** using 2-(4-phenylbut-1-yn-1-yl)aniline (820 mg, 3.7 mmol), Pd/C (370 mg, 10 wt. %),  $NaNO_2$  (306 mg, 4.4 mmol), and  $NaN_3$  (331 mg, 5.2 mmol). Purification by flash chromatography (hexanes  $\rightarrow$  97:3 hexanes/EtOAc) afforded the title compound as a light

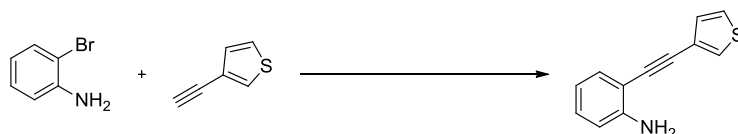
yellow oil (383 mg, 41 % over two steps); **R<sub>f</sub>** 0.87 (95:5 hexanes/EtOAc); **IR** (thin film,  $\text{cm}^{-1}$ ) 3024, 2929, 2857, 2113, 1581, 1488, 1451, 1283, 747; **<sup>1</sup>H NMR** ( $\text{CDCl}_3$ , 400 MHz)  $\delta$  7.29-7.10 (m, 8H), 7.03 (td,  $J = 7.0, 1.2$  Hz, 1H), 2.65-2.56 (m, 4H), 1.69-1.55 (m, 4H); **<sup>13</sup>C NMR** ( $\text{CDCl}_3$ , 100 MHz)  $\delta$  142.5, 137.9, 134.0, 130.4, 128.4, 128.2, 127.2, 125.6, 124.6, 118.0, 35.8, 31.2, 31.0, 29.9; **HRMS** (+ESI) calculated for  $\text{C}_{16}\text{H}_{20}\text{N}$  226.1590, found 226.1586  $[\text{M}-2\text{N}+3\text{H}]^+$ .



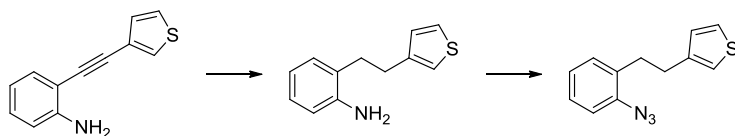
**2-(pyridin-3-ylethynyl)aniline.** Prepared by general procedure **E** using  $\text{PdCl}_2(\text{PPh}_3)_3$  (550 mg, 0.78 mmol), CuI (73 mg, 0.38 mmol), 2-bromoaniline (1.9 mL, 16.8 mmol), 3-ethynylpyridine (2.1 g, 20.4 mmol), and ethanolamine (12.3 mL, 204 mmol). Purification by flash chromatography (9:1  $\rightarrow$  8:2 hexanes/EtOAc) afforded the title compound as an orange oil (1.78 g, 55 %); **R<sub>f</sub>** 0.20 (7:3 hexanes/EtOAc); **IR** (thin film,  $\text{cm}^{-1}$ ) 3456, 3324, 3192, 3030, 2211, 1615, 1493, 1407, 1314, 748; **<sup>1</sup>H NMR** ( $\text{CDCl}_3$ , 400 MHz)  $\delta$  8.75 (dd,  $J = 2.3, 0.8$  Hz, 1H), 8.53 (dd,  $J = 4.9, 1.8$  Hz, 1H), 7.78 (dt,  $J = 7.8, 2.0$  Hz, 1H), 7.37 (dd,  $J = 8.0, 1.4$  Hz, 1H), 7.27 (ddd,  $J = 8.4, 4.3, 1.0$  Hz, 1H), 7.16 (ddd,  $J = 8.1, 7.1, 1.6$  Hz, 1H), 6.74-6.70 (m, 2H), 4.31 (br s, 2H); **<sup>13</sup>C NMR** ( $\text{CDCl}_3$ , 100 MHz)  $\delta$  152.03, 148.5, 147.9, 138.2, 132.2, 130.3, 123.0, 120.5, 118.0, 114.4, 107.1, 91.2, 89.3; **HRMS** (+ESI) calculated for  $\text{C}_{13}\text{H}_{11}\text{N}_2$  195.0917, found 195.0914  $[\text{M}+\text{H}]^+$ .



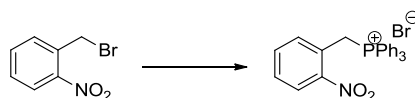
**3-(2-azidophenethyl)pyridine (133).** Prepared by general procedure **F** using 2-(pyridin-3-ylethynyl)aniline (1.5 g, 7.73 mmol), Pd/C (880 mg, 10 wt. %), NaNO<sub>2</sub> (640 mg, 9.28 mmol), and NaN<sub>3</sub> (700 mg, 10.94 mmol). Purification by flash chromatography (8:2 hexanes/EtOAc) afforded the title compound as a light yellow oil (1.32 g, 76 % over two steps); **R<sub>f</sub>** 0.35 (7:3 hexanes/EtOAc); **IR** (thin film, cm<sup>-1</sup>) 3027, 2928, 2118, 1709, 1579, 1489, 1284, 906, 712; **<sup>1</sup>H NMR** (CDCl<sub>3</sub>, 400 MHz) δ 8.42 (tt, *J* = 5.1, 1.2 Hz, 2H), 7.47 (d, *J* = 7.9 Hz, 1H), 7.27-7.23 (m, 1H), 7.20 (dd, *J* = 7.8, 4.7 Hz, 1H), 7.13 (d, *J* = 7.9 Hz, 1H), 7.06-7.0 (m, 2H), 2.85 (s, 4H); **<sup>13</sup>C NMR** (CDCl<sub>3</sub>, 100 MHz) δ 149.7, 147.3, 137.9, 136.8, 136.1, 132.1, 130.5, 127.7, 124.7, 123.2, 118.1, 33.5, 32.9; **HRMS** (+ESI) calculated for C<sub>13</sub>H<sub>13</sub>N<sub>4</sub> 225.1135, found 225.1134 [M+H]<sup>+</sup>.



**2-(thiophen-3-ylethynyl)aniline.** Prepared by general procedure **E** using 2-bromoaniline (800 μL, 6.9 mmol, 1 equiv), 3-ethynylthiophene (820 μL, 8.3 mmol, 1 equiv), PdCl<sub>2</sub>(PPh<sub>3</sub>)<sub>2</sub> (250 mg, 0.35 mmol, 5 mol %), CuI (26 mg, 0.18 mmol, 2 mol %), and ethanolamine (5 mL, 82.8 mmol, 12 equiv). Purification by flash chromatography (95:5 hexanes/EtOAc) afforded the title compound as a orange oil (590 mg, 43 %); **R<sub>f</sub>** 0.41 (9:1 hexanes/EtOAc); **<sup>1</sup>H NMR** (CDCl<sub>3</sub>, 400 MHz) δ 7.50 (dd, *J* = 2.9, 1.4 Hz, 1H), 7.34 (d, *J* = 8.2 Hz, 1H), 7.31-7.28 (m, 1H), 7.18 (dt, *J* = 5.1, 1.2 Hz, 1H), 7.12 (t, *J* = 7.8 Hz, 1H), 6.70 (t, *J* = 7.4 Hz, 2H), 4.24 (br s, 2H).

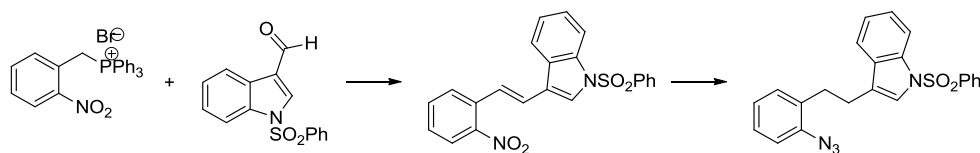


**3-(2-azidophenethyl)thiophene (139).** Prepared by general procedure **F** using 2-(thiophen-3-ylethynyl)aniline (580 mg, 2.9 mmol, 1 equiv), Pd/C (200 mg, 10 wt. %), 1 atm H<sub>2</sub>, NaNO<sub>2</sub> (240 mg, 3.5 mmol, 1.2 equiv), and NaN<sub>3</sub> (264 mg, 4.1 mmol, 1.4 equiv). Purification by preparative thin layer chromatography (99:1 hexanes/EtOAc) afforded the title compound as a light yellow oil (155 mg, 23 % over two steps); **R<sub>f</sub>** 0.7 (hexanes); **<sup>1</sup>H NMR** (CDCl<sub>3</sub>, 400 MHz) δ 7.25 (dd, *J* = 4.5, 1.4 Hz, 1H), 7.18-7.11 (m, 3H), 7.05 (td, *J* = 7.4, 1.2 Hz, 1H), 6.96-6.93 (m, 2H), 2.89 (s, 4H).



**Phosphonium salt (142).** Procedure from the literature<sup>91</sup> was modified as follows: to a solution of 2-nitrobenzyl bromide (10.1 g, 46.9 mmol, 1 equiv.) in DMF (33 mL) was added triphenylphosphine (12.3, g, 46.9 mmol, 1 equiv.). The reaction mixture was stirred 26 h at room temperature, at which point it was diluted with toluene (1 M) and filtered. The filter was washed with DCM to dissolve the solid filtrate. The product solution was concentrated *in vacuo* and recrystallized out of DCM/Et<sub>2</sub>O to yield pure phosphonium salt as a white solid (21.2 g, 94 %); **IR** (thin film, cm<sup>-1</sup>) 3420, 3058, 2856, 2160, 1525, 1437, 1340, 1110, 722; **<sup>1</sup>H NMR** (CDCl<sub>3</sub>, 400 MHz) δ 8.12 (dt, *J* = 7.5, 3.1 Hz, 1H), 7.91 (d, *J* = 8.3 Hz, 1H), 7.77 (td, *J* = 7.5, 0.9 Hz, 3H) 7.68 (dd, *J* = 12.7, 8.3 Hz, 6H), 7.63-7.59 (m, 7H), 7.46 (tt, *J* = 7.5, 2.2 Hz, 1H) 6.13 (d, *J* = 14.9 Hz, 1H);

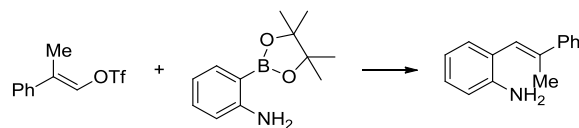
$^{13}\text{C}$  NMR (CDCl<sub>3</sub>, 100 MHz)  $\delta$  135.2, 134.3, 134.2, 130.3, 130.2, 125.7, 117.6, 117.0, 28.7; HRMS (+ESI) calculated for C<sub>25</sub>H<sub>21</sub>NO<sub>2</sub>P 398.1310, found 398.1282 [M-Br]<sup>+</sup>.



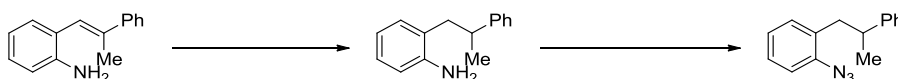
**3-(2-azidophenethyl)-1-(phenylsulfonyl)-1H-indole (140).** Procedure from the literature<sup>92</sup> was modified as follows: a solution of phosphonium salt (2.04 g, 4.3 mmol, 1.2 equiv) in THF (0.2 M) was cooled to 0 °C, and KO<sup>t</sup>Bu (630 mg, 5.6 mmol, 1.6 equiv) was added. The solution was stirred for 30 min at 0 °C, and 1-(phenylsulfonyl)-3-indolecarboxaldehyde (980 mg, 3.5 mmol, 1.0 equiv.) was added. The mixture was warmed to room temperature overnight and quenched with H<sub>2</sub>O and EtOAc after 22 h. The phases were separated, and the aqueous phase was extracted with EtOAc. The combined organic extracts were washed with brine, dried over MgSO<sub>4</sub>, and concentrated *in vacuo*. The crude mixture was dissolved in EtOAc and passed through a plug of silica. The crude filtrate was concentrated *in vacuo* and carried on through general procedure **F** using Pd/C (300 mg, 10 wt. %), NaNO<sub>2</sub> (100 mg, 1.43 mmol), and NaN<sub>3</sub> (113 mg, 1.67 mmol). Purification by flash chromatography (8:2 → 7:3 hexanes/EtOAc) afforded the title compound as an orange solid (320 mg, 44 % over three steps); **R<sub>f</sub>** 0.7 (7:3 hexanes/EtOAc); **IR** (thin film, cm<sup>-1</sup>) 3065, 2928, 2119, 1446, 1365, 1280, 1173, 905, 725; **<sup>1</sup>H NMR** (CDCl<sub>3</sub>, 400 MHz)  $\delta$  7.97 (dd, *J* = 8.2, 0.8 Hz, 1H), 7.81 (d, *J* = 8.6 Hz, 2H); 7.52 (t, *J* = 7.4 Hz, 2H), 7.41 (t, *J* = 7.4 Hz, 2H), 7.32-7.21 (m, 4H), 7.13 (d, *J* = 8.2 Hz, 1H), 7.05-6.97 (m, 2H), 2.91 (s, 4H); **<sup>13</sup>C NMR** (CDCl<sub>3</sub>, 100 MHz)  $\delta$  138.3, 138.0, 135.3, 133.6, 132.7, 131.0, 130.5, 129.2, 127.6, 126.7, 124.7, 123.1, 122.8, 122.7,



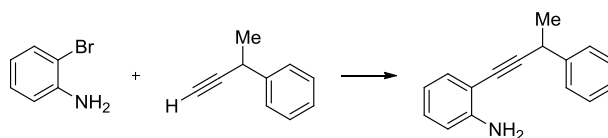
119.5, 118.1, 113.7, 31.0, 25.6; **HRMS** (+ESI) calculated for  $C_{22}H_{21}O_2N_2S$  377.1318, found 377.1319  $[M-2N+3H]^+$ .



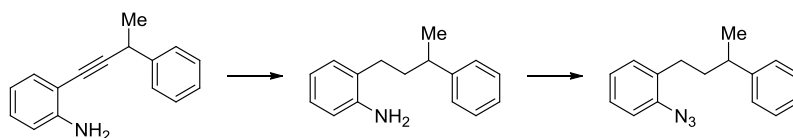
**(E)-2-(2-phenylprop-1-en-1-yl)aniline (148)**. Prepared according to the literature:<sup>37</sup> using boronic ester **146** (2.05 g, 9.4 mmol, 1 equiv), vinyl triflate **147** (2.2 g, 8.2 mmol, 1.6 equiv), and (dppf)PdCl<sub>2</sub>•DCM (817 mg, 0.51 mmol, 10 mol %). Purification by flash column chromatography (9:1 hexanes/EtOAc) afforded the title compound **148** (1.112 g, 57 % yield); **R<sub>f</sub>** 0.62 (9:1 hexanes/EtOAc); <sup>1</sup>H NMR was identical to that reported;<sup>37</sup> <sup>1</sup>H NMR (CDCl<sub>3</sub>, 400 MHz) δ 7.22-7.15 (m, 5H), 6.97 (td, *J* = 7.8, 1.2 Hz, 1H), 6.74 (d, *J* = 7.8 Hz, 1H), 6.62 (d, *J* = 7.8 Hz, 1H), 6.52 (t, *J* = 7.4 Hz, 1H), 6.41 (s, 1H), 3.67 (br s, 2H), 2.28 (d, *J* = 1.6 Hz, 3H).



**1-azido-2-(2-phenylpropyl)benzene (145)**. Prepared according to general procedure **F** using aniline **148** (1.112 g, 5.3 mmol, 1 equiv), Pd/C (360 mg, 10 wt. %), NaNO<sub>2</sub> (450 mg, 6.5 mmol, 1.2 equiv), and NaN<sub>3</sub> (482 mg, 7.4 mmol, 1.4 equiv). Purification by flash column chromatography (hexanes → 97:3 hexanes/EtOAc → 95:5 hexanes/EtOAc) afforded the title compound **137** (753 mg, 60 % yield); **R<sub>f</sub>** 0.9 (9:1 hexanes/EtOAc); <sup>1</sup>H NMR was identical to that reported;<sup>37</sup> <sup>1</sup>H NMR (CDCl<sub>3</sub>, 400 MHz) δ 7.29-7.17 (m, 6H), 7.10 (d, *J* = 7.8 Hz, 1H), 6.98-6.96 (m, 2H), 3.03 (sxt, *J* = 7.0 Hz, 1H), 2.84 (dd, *J* = 13.3, 6.6 Hz, 1H), 2.75 (dd, *J* = 13.3, 8.6 Hz, 1H), 1.22 (d, *J* = 7.0, 3H).

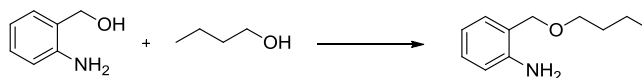


**2-(3-phenylbut-1-yn-1-yl)aniline (152).** Prepared by general procedure **E** using PdCl<sub>2</sub>(PPh<sub>3</sub>)<sub>3</sub> (211 mg, 0.3 mmol), CuI (23 mg, 0.12 mmol), 2-bromoaniline (1.04 g, 6.0 mmol), (1-methyl-2-propyn-1-yl)-benzene<sup>85</sup> (940 mg, 7.2 mmol), and ethanolamine (4.4 mL, 72 mmol). Purification by flash chromatography (95:5 hexanes/EtOAc) afforded the title compound as an orange oil (498 mg, 36 %); **R<sub>f</sub>** 0.31 (95:5 hexanes/EtOAc); **IR** (thin film, cm<sup>-1</sup>) 3472, 3378, 3027, 2974, 1611, 1491, 1453, 1305, 747; **<sup>1</sup>H NMR** (CDCl<sub>3</sub>, 400 MHz) δ 7.44 (d, *J* = 7.0 Hz, 2H), 7.33 (tt, *J* = 7.7, 1.76, 2H), 7.27-7.22 (m, 2H), 7.07 (td, *J* = 7.8, 1.5 Hz, 1H), 6.67-6.64 (m, 2H), 4.13 (br s, 2H), 4.03 (q, *J* = 7.0 Hz, 1H), 1.59 (d, *J* = 7.0 Hz, 3H); **<sup>13</sup>C NMR** (CDCl<sub>3</sub>, 100 MHz) δ 147.7, 143.4, 132.1, 129.1, 128.6, 126.9, 126.7, 117.8, 114.2, 108.5, 98.1, 78.9, 32.8, 24.8; **HRMS** (+ESI) calculated for C<sub>16</sub>H<sub>16</sub>N 222.1277, found 222.1279 [M+H]<sup>+</sup>.

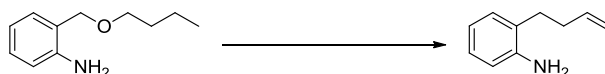


**1-azido-2-(3-phenylpropyl)benzene (149).** Prepared by general procedure **B** using 2-(3-phenylbut-1-yn-1-yl)aniline (438 mg, 2.0 mmol), Pd/C (200 mg, 10 wt. %), NaNO<sub>2</sub> (166 mg, 2.4 mmol), and NaN<sub>3</sub> (180 mg, 2.8 mmol). Purification by flash chromatography (hexanes → 97:3 hexanes/EtOAc) afforded the title compound as a light yellow oil (371 mg, 75 % over two steps); **R<sub>f</sub>** 0.9 (95:5 hexanes/EtOAc); **IR** (thin film, cm<sup>-1</sup>) 2958, 2116, 1489, 1450, 1283, 905, 727; **<sup>1</sup>H NMR** (CDCl<sub>3</sub>, 400 MHz) δ 7.32-7.28 (m, 2H), 7.22-7.18 (m, 4H), 7.08 (td, *J* = 8.0, 1.6 Hz, 2H), 7.01 (td, *J* = 7.4, 1.2 Hz, 1H),

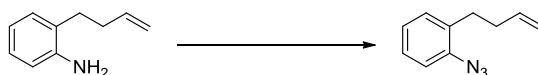
2.71 (sxt,  $J = 7.1$  Hz, 1H), 2.53-2.37 (m, 2H), 1.87-1.78 (m, 2H), 1.27 (d,  $J = 7.0$  Hz, 3H);  $^{13}\text{C}$  NMR ( $\text{CDCl}_3$ , 100 MHz)  $\delta$  147.2, 137.9, 134.0, 130.3, 128.4, 127.2, 127.1, 126.0, 124.6, 118.0, 39.8, 38.6, 29.5, 22.6; HRMS (+ESI) calculated for  $\text{C}_{15}\text{H}_{18}\text{N}$  212.1434, found 212.1431  $[\text{M}-2\text{N}+3\text{H}]^+$ .



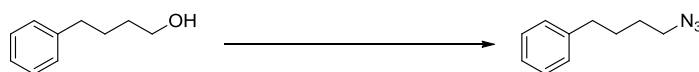
**2-(butoxymethyl)aniline (156).** Prepared according to the literature<sup>86</sup> using 2-aminobenzyl alcohol (5.0 g, 40.6 mmol, 1 equiv), *n*-butanol (275 mL), and sulfuric acid (4 g, 40.8 mmol, 1 equiv). Purification by flash chromatography (7:3 hexanes/EtOAc) afforded the title compound **156** (2.66 g, 37 % yield).  $^1\text{H}$  NMR was identical to that reported;<sup>86</sup>  $^1\text{H}$  NMR ( $\text{CDCl}_3$ , 400 MHz)  $\delta$  7.11 (t,  $J = 7.6$  Hz, 1H), 7.04 (d,  $J = 7.4$  Hz, 1H), 6.68 (dd,  $J = 12.4, 7.4$  Hz, 2H), 4.50 (s, 2H), 4.17 (br s, 2H), 3.42 (td,  $J = 6.6, 0.8$  Hz, 2H), 1.60-1.53 (m, 2H), 1.36 (sxt,  $J = 7.4$  Hz, 2H), 0.89 (td,  $J = 7.4, 0.8$  Hz, 2H).



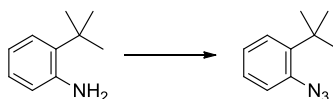
**2-(but-3-en-1-yl)aniline (154).** Prepared according to the literature<sup>86</sup> using **156** (2.66 g, 14.8 mmol, 1 equiv) and allyl magnesium bromide (35 mL, 34.5 mmol, 2.33 equiv). Purification by flash chromatography (9:1 hexanes/EtOAc) afforded **154** (1.68 g, 77 %).  $^1\text{H}$  NMR was identical to that reported;<sup>86</sup>  $^1\text{H}$  NMR ( $\text{CDCl}_3$ , 400 MHz)  $\delta$  7.07-7.04 (m, 2H), 6.75 (t,  $J = 7.2$  Hz, 1H), 6.69 (d,  $J = 7.4$  Hz, 1H), 5.92 (ddt,  $J = 16.9, 10.3, 6.6$  Hz, 1H), 5.10 (dd  $J = 17.2, 1.6$  Hz, 1H), 5.03 (d,  $J = 10.2$  Hz, 1H), 3.62 (br s, 2H), 2.62-2.58 (m, 2H), 2.39 (q,  $J = 7.04$  Hz, 2H).



**1-azido-2-(but-3-en-1-yl)benzene (153).** Prepared according to general procedure **F** using aniline **154** (1.68 g, 11.4 mmol, 1 equiv), NaNO<sub>2</sub> (946 mg, 13.7 mmol, 1.2 equiv), NaN<sub>3</sub> (1.04 g, 16.0 mmol, 1.4 equiv). Purification by flash chromatography (hexanes → 95:5 hexanes/EtOAc) afforded **153** (996 mg, 50 % yield) as an oil; **R<sub>f</sub>** 0.87 (9:1 hexanes/EtOAc); **<sup>1</sup>H NMR** (CDCl<sub>3</sub>, 400 MHz) δ 7.27 (t, *J* = 7.4 Hz, 1H), 7.20-7.15 (m, 2H), 7.09 (t, *J* = 7.4 Hz, 1H), 5.94-5.83 (m, 1H), 5.10-5.00 (m, 2H), 2.70 (t, *J* = 7.8 Hz, 2H), 2.36 (q, *J* = 7.2 Hz, 2H); **<sup>13</sup>C NMR** (CDCl<sub>3</sub>, 100 MHz) δ 138.0, 133.3, 130.5, 127.4, 124.7, 118.1, 115.0, 34.3, 30.8; **HRMS** (+NSI) calculated for C<sub>10</sub>H<sub>12</sub>N<sub>3</sub> 174.1026, found 174.1024 [M+H]<sup>+</sup>.

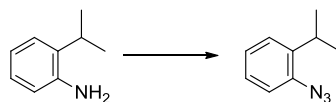


**(4-azidobutyl)benzene (157).** Prepared according to the literature,<sup>39</sup> using 4-phenyl-1-butanol (3.0 mL, 20.0 mmol, 1 equiv), HBr (10 mL, 48 % aq.), NaN<sub>3</sub> (1.98 g, 30.0 mmol, 1.5 equiv). Purification by flash chromatography (9:1 hexanes/EtOAc) afforded **157** (1.89 g, 50 % yield). **<sup>1</sup>H NMR** was identical to that reported;<sup>39</sup> **<sup>1</sup>H NMR** (CDCl<sub>3</sub>, 400 MHz) δ 7.27 (t, *J* = 7.6 Hz, 2H), 7.19-7.15 (m, 3H), 3.27 (t, *J* = 6.7 Hz, 2H), 2.63 (t, *J* = 7.3 Hz, 2H), 1.74-1.59 (m, 4H).

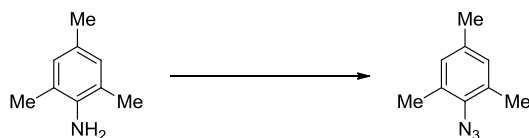


**1-azido-2-(tert-butyl)benzene (158).** Prepared according to the literature,<sup>38</sup> using 2-*tert*-butylaniline (0.93 mL, 5.1 mmol), *tert*-butyl nitrite (2.8 mL, 23.5 mmol), and

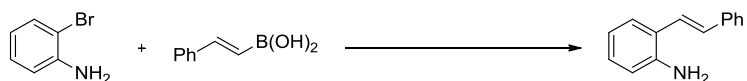
azidotrimethylsilane (2.5 mL, 18.8 mmol). Flash chromatography afforded 856 mg (96 % yield) of title compound.  $^1\text{H NMR}$  was identical to that reported;<sup>38</sup>  $^1\text{H NMR}$  ( $\text{CDCl}_3$ , 400 MHz)  $\delta$  7.33 (d,  $J = 7.9$  Hz, 1H), 7.24 (t,  $J = 7.2$  Hz, 1H), 7.15 (d,  $J = 7.6$  Hz, 1H), 7.06 (t,  $J = 7.6$  Hz, 1H), 1.39 (s, 9H).



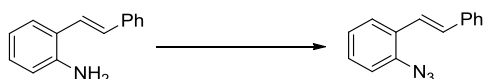
**1-azido-2-(tert-butyl)benzene (159).** Prepared according to the literature,<sup>38</sup> using 2-isopropylaniline (1.41 mL, 7.2 mmol), *tert*-butyl nitrite (4.8 mL, 40.4 mmol), and azidotrimethylsilane (4.2 mL, 31.6 mmol). Flash chromatography afforded 1.07 g (92 % yield) of title compound.  $^1\text{H NMR}$  was identical to that reported;<sup>38</sup>  $^1\text{H NMR}$  ( $\text{CDCl}_3$ , 400 MHz)  $\delta$  7.23-7.20 (m, 2H), 7.10 (qd,  $J = 7.6, 1.0$  Hz, 2H), 3.19 (spt,  $J = 6.9$  Hz, 1H), 1.19 (d,  $J = 7.1$  Hz, 6H).



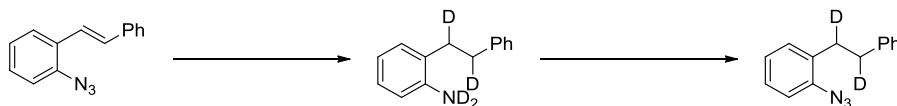
**2-azido-1,3,5-trimethylbenzene (162).** Prepared according to the literature,<sup>87</sup> using 2,4,6-trimethylaniline (1.04 mL, 7.4 mmol, 1 equiv),  $\text{NaNO}_2$  (790 mg, 11.5 mmol, 1.6 equiv), and  $\text{NaN}_3$  (880 mg, 13.5 mmol, 1.8 equiv). Flash chromatography (9:1 hexanes/EtOAc) afforded **162** (959 mg, 80 % yield).  $^1\text{H NMR}$  was identical to that reported;<sup>87</sup>  $^1\text{H NMR}$  ( $\text{CDCl}_3$ , 400 MHz)  $\delta$  6.82 (s, 2H), 2.30 (s, 6H), 2.23 (s, 3H).



**(E)-2-styrylaniline (168).** Prepared according to the literature,<sup>33</sup> using 2-bromoaniline (1.5 mL, 13.5 mmol, 1 equiv), *trans*-2-phenyl-vinyl boronic acid (3.0 g, 20.3 mmol, 1.5 equiv), Pd(PPh<sub>3</sub>)<sub>4</sub> (1.56 g, 1.35 mmol, 10 mol %), and K<sub>2</sub>CO<sub>3</sub> (7.5 g, 54.0 mmol, 4 equiv). Flash chromatography (9:1 hexanes/EtOAc) afforded **168** (1.9 g, 72 %) as a yellow solid. <sup>1</sup>H NMR was identical to that reported;<sup>33</sup> <sup>1</sup>H NMR (CDCl<sub>3</sub>, 400 MHz) δ 7.50 (d, *J* = 7.8 Hz, 2H), 7.40-7.33 (m, 3H), 7.27-7.23 (m, 1H), 7.15 (d, *J* = 16.0 Hz, 1H), 7.09 (t, *J* = 7.6 Hz, 1H), 6.98 (d, *J* = 16.4 Hz, 1H), 6.8 (t, *J* = 7.8 Hz, 1H), 6.7 (d, *J* = 7.8 Hz, 1H), 3.79 (br s, 2H).

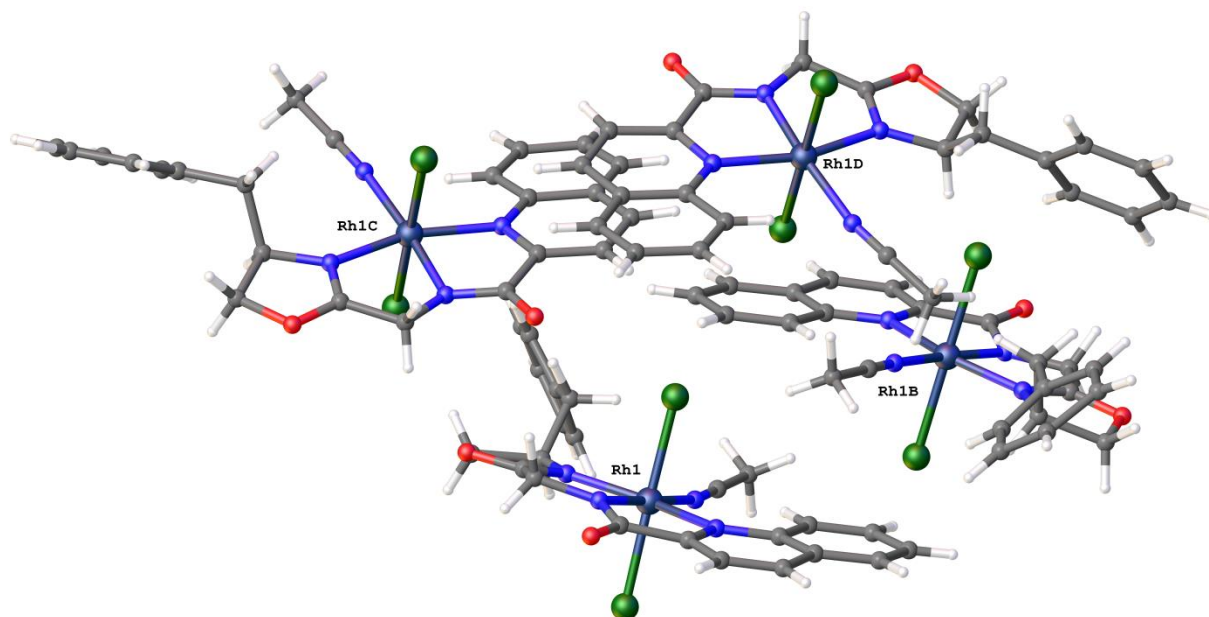
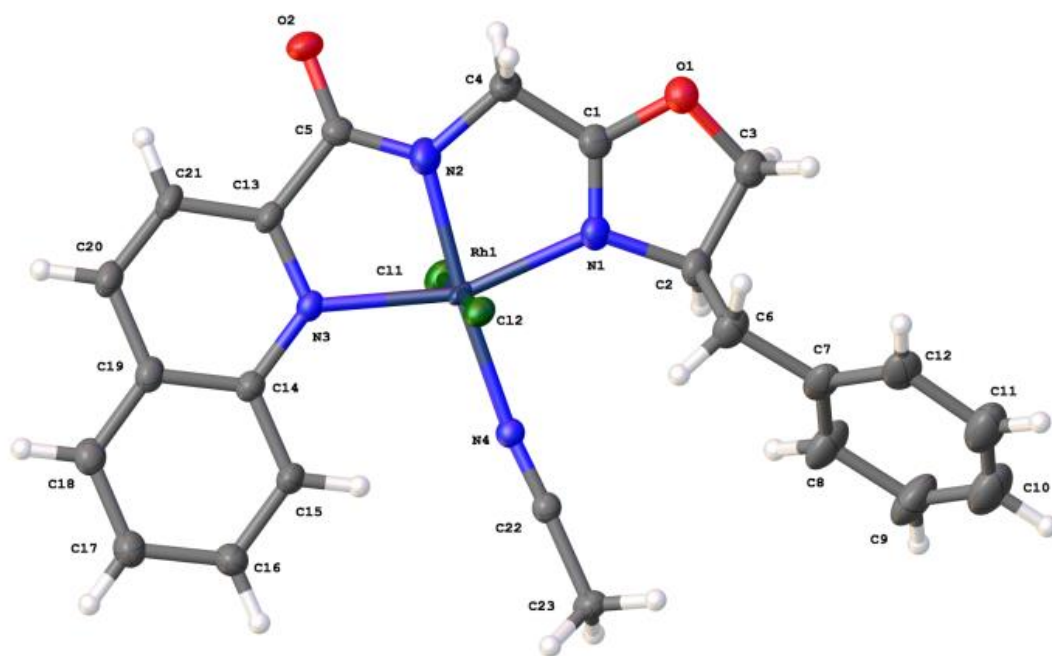


**(E)-1-azido-2-styrylbenzene (166).** Prepared according to the literature,<sup>33</sup> using **168** (1.9 g, 9.1 mmol, 1 equiv), NaNO<sub>2</sub> (873 mg, 12.7 mmol, 1.4 equiv), and NaN<sub>3</sub> (878 mg, 13.5 mmol, 1.5 equiv). Flash chromatography (95:5 hexanes/EtOAc) afforded **166** (1.6 g, 77 %). <sup>1</sup>H NMR was identical to that reported;<sup>33</sup> <sup>1</sup>H NMR (CDCl<sub>3</sub>, 400 MHz) δ 7.63 (d, *J* = 7.4 Hz, 1H), 7.52 (d, *J* = 7.4 Hz, 2H), 7.37-7.33 (m, 3H), 7.29-7.25 (m, 2H), 7.17-7.11 (m, 2H), 7.07 (d, *J* = 16.4 Hz, 1H).



**Azide 165.** Prepared according to the literature,<sup>38</sup> using **166** (811 mg, 3.6 mmol, 1 equiv), Pd/C rinsed with CD<sub>3</sub>OD (362 mg, 10 wt. %), CD<sub>3</sub>OD (10 mL), <sup>t</sup>BuNO<sub>2</sub> (1.7 mL,

14.3 mmol, 4 equiv), and  $\text{Me}_3\text{SiN}_3$  (1.3 mL, 9.8 mmol, 3 equiv). Flash chromatography (hexanes) afforded **160** (360 mg, 44 %) as a yellow oil.  $^1\text{H}$  NMR was identical to that reported;  $^1\text{H}$  NMR ( $\text{CDCl}_3$ , 400 MHz)  $\delta$  7.29-7.26 (m, 3H), 7.20-7.17 (m, 3H), 7.14 (d,  $J$  = 8.2 Hz, 1H), 7.10 (dd,  $J$  = 7.6, 1.8 Hz, 1H), 7.04 (td,  $J$  = 7.6, 1.2 Hz, 1H), 2.83 (s, 2H).

X-Ray Crystallographic Data for **93**.



**Table S2.2.** Crystal data and structure refinement for **93**.

Empirical formula	C <sub>23</sub> H <sub>21</sub> Cl <sub>2</sub> N <sub>4</sub> O <sub>2</sub> Rh
Formula weight	559.25
Temperature	110(2) K
Wavelength	0.71073 Å
Crystal system	Monoclinic
Space group	C 1 2 1
Unit cell dimensions	a = 25.6672(9) Å b = 11.3911(4) Å c = 34.3405(12) Å
Volume	9982.4(6) Å <sup>3</sup>
Z	16
Density (calculated)	1.488 Mg/m <sup>3</sup>
Absorption coefficient	0.924 mm <sup>-1</sup>
F(000)	4512
Crystal size	0.444 x 0.265 x 0.14 mm <sup>3</sup>
Theta range for data collection	1.193 to 27.103°.
Index ranges	-32<=h<=27, -14<=k<=13, -44<=l<=39
Reflections collected	46636
Independent reflections	19066 [R(int) = 0.0595]
Completeness to theta = 25.242°	99.4 %
Absorption correction	Semi-empirical from equivalents
Max. and min. transmission	0.7460 and 0.6012

Refinement method	Full-matrix least-squares on $F^2$
Data / restraints / parameters	19066 / 946 / 1121
Goodness-of-fit on $F^2$	1.110
Final R indices [ $I > 2\sigma(I)$ ]	R1 = 0.0833, wR2 = 0.2029
R indices (all data)	R1 = 0.0928, wR2 = 0.2086
Absolute structure parameter	0.069(14)
Extinction coefficient	n/a
Largest diff. peak and hole	2.676 and -1.913 e.Å <sup>-3</sup>

## References

- (1) Du Bois, J. *Org. Process Res. Dev.* **2011**, *15*, 758.
- (2) Turner, N. J. *Curr. Opin. Chem. Biol.* **2011**, *15*, 234.
- (3) Heberling, M. M.; Wu, B.; Bartsch, S.; Janssen, D. B. *Curr. Opin. Chem. Biol.* **2013**, *17*, 250.
- (4) McIntosh, J. A.; Coelho, P. S.; Farwell, C. C.; Wang, Z. J.; Lewis, J. C.; Brown, T. R.; Arnold, F. H. *Angew. Chem., Int. Ed.* **2013**, *52*, 9309.
- (5) Hyster, T. K.; Farwell, C. C.; Buller, A. R.; McIntosh, J. A.; Arnold, F. H. *J. Am. Chem. Soc.* **2014**, *136*, 15505.
- (6) Jeffrey, J. L.; Sarpong, R. *Chem. Sci.* **2013**, *4*, 4092.
- (7) Collet, F.; Dodd, R. H.; Dauban, P. *Chem. Commun.* **2009**, 5061.
- (8) Anslyn, E. V.; Dougherty, D. A.. *Moddern Physical Organic Chemistry*; University Science Books: Sausalito, CA, 2006; pp 69-70.
- (9) Dequirez, G.; Pons, V.; Dauban, P. *Angew. Chem., Int. Ed.* **2012**, *51*, 7384.
- (10) Scriven, E. F. V.; Turnbull, K. *Chem. Rev.* **1988**, *88*, 297.
- (11) Lu, H.; Zhang, X. P. *Chem. Soc. Rev.* **2011**, *40*, 1899.
- (12) Katsuki, T. *Chem. Lett.* **2005**, *34*, 1304.
- (13) Driver, T. G. *Nat. Chem.* **2013**, *5*, 736.
- (14) Driver, T. G. *Org. Biomol. Chem.* **2010**, *8*, 3831.
- (15) Kwart, H.; Khan, A. A. *J. Am. Chem. Soc.* **1967**, *89*, 1951.
- (16) Fantauzzi, S.; Caselli, A.; Gallo, E. *Dalton Trans.* **2009**, 5434.

- (17) Cenini, S.; Gallo, E.; Penoni, A.; Ragaini, F.; Tollari, S. *Chem. Commun.* **2000**, 2265.
- (18) Ragaini, F.; Penoni, A.; Gallo, E.; Tollari, S.; Gotti, C. L.; Lapadula, M.; Mangioni, E.; Cenini, S. *Chem.—Eur. J.* **2003**, *9*, 249.
- (19) Ruppel, J. V.; Kamble, R. M.; Zhang, X. P. *Org. Lett.* **2007**, *9*, 4889.
- (20) Lu, H.; Tao, J.; Jones, J. E.; Wojtas, L.; Zhang, X. P. *Org. Lett.* **2010**, *12*, 1248.
- (21) Lu, H.; Jiang, H.; Wojtas, L.; Zhang, X. P. *Angew. Chem., Int. Ed.* **2010**, *49*, 10192.
- (22) Lu, H.; Jiang, H.; Hu, Y.; Wojtas, L.; Zhang, X. P. *Chem. Sci.* **2011**, *2*, 2361.
- (23) Lu, H.; Hu, Y.; Jiang, H.; Wojtas, L.; Zhang, X. P. *Org. Lett.* **2012**, *14*, 5158.
- (24) Lu, H.; Subbarayan, V.; Tao, J.; Zhang, X. P. *Organometallics* **2010**, *29*, 389.
- (25) Kim, J. Y.; Park, S. H.; Ryu, J.; Cho, S. H.; Kim, S. H.; Chang, S. *J. Am. Chem. Soc.* **2012**, *134*, 9110.
- (26) Ryu, J.; Shin, K.; Park, S. H.; Kim, J. Y.; Chang, S. *Angew. Chem., Int. Ed.* **2012**, *51*, 9904.
- (27) Kim, J.; Chang, S. *Angew. Chem., Int. Ed.* **2014**, *53*, 2203.
- (28) Kang, T.; Kim, Y.; Lee, D.; Wang, Z.; Chang, S. *J. Am. Chem. Soc.* **2014**, *136*, 4141.
- (29) Ryu, J.; Kwak, J.; Shin, K.; Lee, D.; Chang, S. *J. Am. Chem. Soc.* **2013**, *135*, 12861.
- (30) Lee, D.; Kim, Y.; Chang, S. *J. Org. Chem.* **2013**, *78*, 11102.
- (31) Stokes, B. J.; Dong, H.; Leslie, B. E.; Pumphrey, A. L.; Driver, T. G. *J. Am. Chem. Soc.* **2007**, *129*, 7500.

- (32) Shen, M.; Driver, T. G. *Org. Lett.* **2008**, *10*, 3367.
- (33) Shen, M.; Leslie, B. E.; Driver, T. G. *Angew. Chem., Int. Ed.* **2008**, *47*, 5056.
- (34) Stokes, B. J.; Jovanović, B.; Dong, H.; Richert, K. J.; Riell, R. D.; Driver, T. G. *J. Org. Chem.* **2009**, *74*, 3225.
- (35) Stokes, B. J.; Richert, K. J.; Driver, T. G. *J. Org. Chem.* **2009**, *74*, 6442.
- (36) Dong, H.; Shen, M.; Redford, J. E.; Stokes, B. J.; Pumphrey, A. L.; Driver, T. G. *Org. Lett.* **2007**, *9*, 5191.
- (37) Sun, K.; Sachwani, R.; Richert, K. J.; Driver, T. G. *Org. Lett.* **2009**, *11*, 3598.
- (38) Nguyen, Q.; Sun, K.; Driver, T. G. *J. Am. Chem. Soc.* **2012**, *134*, 7262.
- (39) Hennessy, E. T.; Betley, T. A. *Science* **2013**, *340*, 591.
- (40) Shin, K.; Baek, Y.; Chang, S. *Angew. Chem., Int. Ed.* **2013**, *52*, 8031.
- (41) Liu, Y.; Wei, J.; Che, C. M. *Chem. Commun.* **2010**, *46*, 6926.
- (42) King, E. R.; Sazama, G. T.; Betley, T. A. *J. Am. Chem. Soc.* **2012**, *134*, 17858.
- (43) Badiei, Y. M.; Dinescu, A.; Dai, X.; Palomino, R. M.; Heinemann, F. W.; Cundari, T. R.; Warren, T. H. *Angew. Chem., Int. Ed.* **2008**, *47*, 9961.
- (44) Aguila, M. J. B.; Badiei, Y. M.; Warren, T. H. *J. Am. Chem. Soc.* **2013**, *135*, 9399.
- (45) Luca, O. R.; Crabtree, R. H. *Chem. Soc. Rev.* **2013**, *42*, 1440.
- (46) Vlcek, A. *Coord. Chem. Rev.* **2010**, *254*, 1357.
- (47) Chirik, P. J.; Wieghardt, K. *Science* **2010**, *327*, 794.
- (48) Ichinose, M.; Suematsu, H.; Yasutomi, Y.; Nishioka, Y.; Uchida, T.; Katsuki, T. *Angew. Chem., Int. Ed.* **2011**, *50*, 9884.
- (49) Nishioka, Y.; Uchida, T.; Katsuki, T. *Angew. Chem., Int. Ed.* **2013**, *125*, 1783.

- (50) McIntosh, J. A.; Coelho, P. S.; Farwell, C. C.; Wang, Z. J.; Lewis, J. C.; Brown, T. R.; Arnold, F. H. *Angew. Chem., Int. Ed.* **2013**, *52*, 9309.
- (51) Knowles, W. S. *Acc. Chem. Res.* **1983**, *16*, 106.
- (52) Harper, K. C.; Bess, E. N.; Sigman, M. S. *Nat. Chem.* **2012**, *4*, 366.
- (53) Yoon, T. P.; Jacobsen, E. N. *Science* **2003**, *299*, 1691.
- (54) Ghosh, A. K.; Mathivanan, P.; Cappiello, J. *Tetrahedron: Asymmetry* **1998**, *9*, 1.
- (55) McManus, H. A.; Guiry, P. J. *Chem. Rev.* **2004**, *104*, 4151.
- (56) Braunstein, P.; Naud, F. *Angew. Chem., Int. Ed.* **2001**, *40*, 680.
- (57) Harper, K. C.; Sigman, M. S. *Science* **2011**, *333*, 1875.
- (58) Harper, K. C.; Vilardi, S. C.; Sigman, M. S. *J. Am. Chem. Soc.* **2013**, *135*, 2482.
- (59) Miller, J. J.; Sigman, M. S. *Angew. Chem., Int. Ed.* **2008**, *47*, 771.
- (60) Harper, K. C.; Sigman, M. S. *Proc. Natl. Acad. Sci. U.S.A.* **2011**, *108*, 2179.
- (61) Sigman, M. S.; Miller, J. J. *J. Org. Chem.* **2009**, *74*, 7633.
- (62) Milo, A.; Neel, A. J.; Toste, F. D.; Sigman, M. S. *Science* **2015**, *347*, 737.
- (63) Bess, E. N.; DeLuca, R. J.; Tindall, D. J.; Oderinde, M. S.; Roizen, J. L.; Du Bois, J.; Sigman, M. S. *J. Am. Chem. Soc.* **2014**, *136*, 5783.
- (64) Harper, K. C.; Sigman, M. S. *J. Org. Chem.* **2013**, *78*, 2813.
- (65) Michel, B. W.; Steffens, L. D.; Sigman, M. S. *J. Am. Chem. Soc.* **2011**, *133*, 8317.
- (66) Stokes, B. J.; Opra, S. M.; Sigman, M. S. *J. Am. Chem. Soc.* **2012**, *134*, 11408.
- (67) McDonald, R. I.; White, P. B.; Weinstein, A. B.; Tam, C. P.; Stahl, S. S. *Org. Lett.* **2011**, *13*, 2830.
- (68) Kikushima, K.; Holder, J. C.; Gatti, M.; Stoltz, B. M. *J. Am. Chem. Soc.* **2011**, *133*, 6902.

- (69) Rajaram, S.; Sigman, M. S. *Org. Lett.* **2002**, *4*, 3399.
- (70) Miller, J. J.; Sigman, M. S. *J. Am. Chem. Soc.* **2007**, *129*, 2752.
- (71) Miller, J. J.; Rajaram, S.; Pfaffenroth, C.; Sigman, M. S. *Tetrahedron* **2009**, *65*, 3110.
- (72) Evans, D. A.; Peterson, G. S.; Johnson, J. S.; Barnes, D. M.; Campos, K. R.; Woerpel, K. A. *J. Org. Chem.* **1998**, *63*, 4541.
- (73) Owens, C. P.; Varela-Alvarez, A.; Boyarskikh, V.; Musaev, D. G.; Davies, H. M. L.; Blakey, S. B. *Chem. Sci.* **2013**, *4*, 2590.
- (74) Sharma, S. K.; May, P. S.; Jones, M. B.; Lense, S.; Hardcastle, K. I.; MacBeth, C. *E. Chem. Commun.* **2011**, *47*, 1827.
- (75) Shirin, Z.; Hammes, B. S.; Young, V. G.; Borovik, A. S. *J. Am. Chem. Soc.* **2000**, *122*, 1836.
- (76) MacBeth, C. E.; Hammes, B. S.; Young, V. G.; Borovik, A. S. *Inorg. Chem.* **2001**, *40*, 4733.
- (77) MacBeth, C. E.; Gupta, R.; Mitchell-Koch, K. R.; Young, V. G.; Lushington, G. H.; Thompson, W. H.; Hendrich, M. P.; Borovik, A. S. *J. Am. Chem. Soc.* **2004**, *126*, 2556.
- (78) Shirin, Z.; S. Borovik, A.; G. Young Jr, V. *Chem. Commun.* **1997**, 1967.
- (79) Mukherjee, J.; Lucas, R. L.; Zart, M. K.; Powell, D. R.; Day, V. W.; Borovik, A. *S. Inorg. Chem.* **2008**, *47*, 5780.
- (80) Tejel, C.; del Río, M. P.; Ciriano, M. A.; Reijerse, E. J.; Hartl, F.; Zális, S.; Hetterscheid, D. G. H.; Tschlis i Spithas, N.; de Bruin, B. *Chem. –Eur. J.* **2009**, *15*, 11878.

- (81) Owens, C. P. Design, Synthesis, and Utilization of Iridium(III) Bis(oxazolinyl)phenyl and Iridium(III) Bis(imidazolinyl)phenyl Complexes for Catalytic Enantioselective Atom Transfer C–H Functionalization.. Ph. D. Dissertation, Emory University, Atlanta, GA, 2014.
- (82) Milczek, E.; Boudet, N.; Blakey, S. *Angew. Chem., Int. Ed.* **2008**, *47*, 6825.
- (83) Zhu, S.; Guo, Z.; Huang, Z.; Jiang, H. *Chem. – Eur. J.* **2014**, *20*, 2425.
- (84) Wu, K.-J.; Dai, L.-X.; You, S.-L. *Org. Lett.* **2012**, *14*, 3772.
- (85) Henrion, G.; Chavas, T. E. J.; Le Goff, X.; Gagosz, F. *Angew. Chem., Int. Ed.* **2013**, *52*, 6277.
- (86) Görl, C.; Alt, H. G. *J. Mol. Cat. A: Chem.* **2007**, *273*, 118.
- (87) Brown, D. G.; Sangantrakun, N.; Schulze, B.; Schubert, U. S.; Berlinguette, C. *P. J. Am. Chem. Soc.* **2012**, *134*, 12354.
- (88) Villanueva, O. Mace Weld, N.; Blakey, S. B.; MacBeth, C. E. *Chem. Sci.* Accepted **2015**.
- (89) Villanueva, O. Design and Development of Novel Bis(amidophenyl)amine Redox-active Ligands to Promote Novel Reactivity at First-row Transition Metal Centers. Ph. D. Dissertation, Emory University, Atlanta, GA, 2015.
- (90) Fiori, K. W.; Espino, C. G.; Brodsky, B. H.; Du Bois, J. *Tetrahedron* **2009**, *65*, 3042.
- (91) De Kimpe, N. 2,3,4,5,6,6-Hexachloro-2,4-cyclohexadien-1-one. *e-EROS Encyclopedia of Reagents for Organic Synthesis* **2001**.
- (92) Rousseaux, S.; García-Fortanet, J.; Del Aguila Sanchez, M. A.; Buchwald, S. L. *J. Am. Chem. Soc.* **2011**, *133*, 9282.



**Chapter 3. Enantioselective Acceptor-Only Metallocarbene  
C–H Functionalization**

### 3.1 Introduction to Enantioselective C–H Functionalization Utilizing Metalcarbenes

Similar to the utility of metallonitrenes for C–H amination and group transfer reactions, metalcarbenes (**1**) have found broad applicability in C–H functionalization and other transformations (Figure 3.1).<sup>1-6</sup> Diazoacetate compounds (**2**) are appealing metalcarbene precursors, with three main classes: donor/acceptor, acceptor-only, and acceptor/acceptor diazoacetates. Donor/acceptor metalcarbenes have been extensively used in enantioselective C–H functionalization, including the synthesis of complex natural products.<sup>7,8</sup> In contrast, acceptor-only metalcarbenes have received significantly less study in enantioselective transformations, though a few notable examples have been discovered. Acceptor/acceptor metalcarbenes have been used in an even more limited number of C–H insertion reactions than acceptor-only metalcarbenes, with no enantioselective variants known.<sup>9-11</sup>

Mechanistically, C–H functionalization with diazoacetates proceeds in a similar manner to C–H amination with azides (Chapter 2). Coordination of metal catalyst **3**, often a dirhodium tetracarboxylate complex, to diazoacetate **2** results in extrusion of nitrogen to form metalcarbene **1** (Figure 3.1). Metalcarbene **1** then inserts into a C–H bond, often activated in some way, such as the ethereal bond of tetrahydrofuran (**4**), to form product **5**.

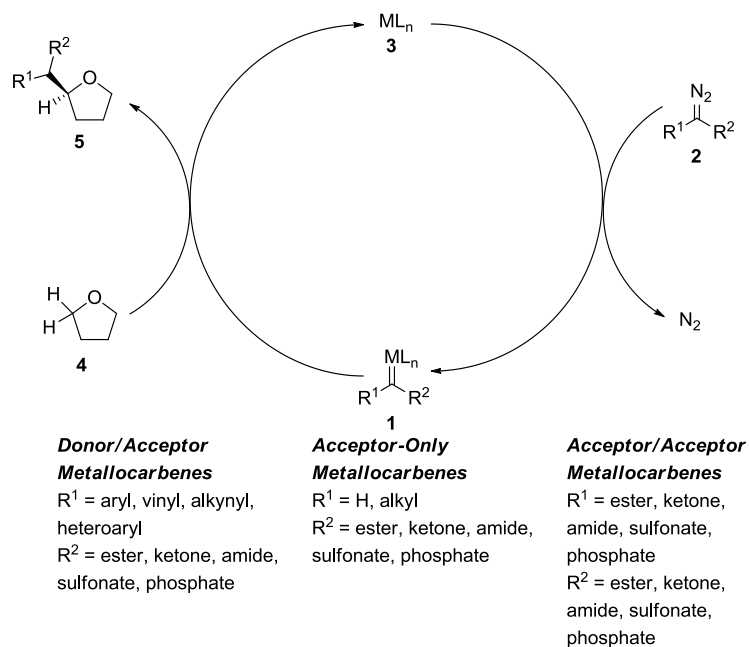


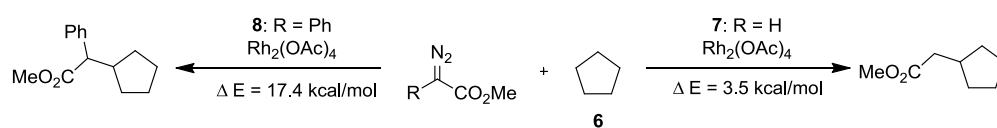
**Figure 3.1.** Metalcarbene C–H functionalization mechanism.<sup>8</sup>

### 3.1.1 Intermolecular Enantioselective C–H Insertion with Acceptor-Only Diazoacetate Metalcarbene Precursors

Donor/acceptor metalcarbenes have found wide application in enantioselective catalysis due in part to their relatively lower electrophilicity, induced by the electron donating group, which enables a sufficient energy barrier to C–H insertion to allow for induction of enantioselectivity. In contrast, acceptor-only metalcarbenes are extremely reactive. For example, the barrier for  $\text{Rh}_2(\text{OAc})_4$  catalyzed insertion into unactivated cyclopentane (**6**) with methyl diazoacetate (**7**) was calculated to be 3.5 kcal/mol (Scheme 3.1).<sup>12</sup> This energy barrier is significantly lower than the calculated energy barrier of 17.4 kcal/mol for methyl phenyldiazoacetate (**8**) into cyclopentane (**6**). The

difference in energy barriers between insertion with these two classes explains the selectivity challenge in utilizing acceptor-only carbenes. Catalysts for C–H functionalization with acceptor-only diazoacetates must provide additional stabilization of the carbene to tame the inherent reactivity of this diazoacetate class.

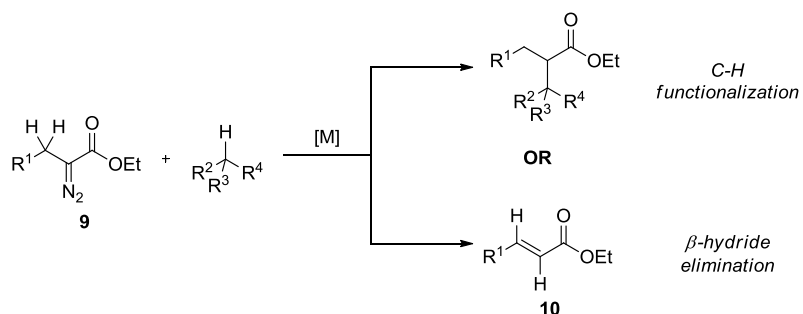
**Scheme 3.1.** Calculated energy barriers for  $\text{Rh}_2(\text{OAc})_4$  catalyzed C–H insertion of methyl diazoacetate (**7**) and methyl phenyldiazoacetate (**8**) into cyclopentane (**6**).<sup>12</sup>



### 3.1.1.1 Intermolecular Enantioselective C–H Insertion with Alkyl Diazoacetates

Though dirhodium tetracarboxylate complexes have excellent applicability in promoting highly selective C–H insertion reactions with donor/acceptor diazoacetates, alkyl-substituted acceptor-only diazoacetates (**9**) present a particular challenge (Scheme 3.2). With this diazoacetate class,  $\beta$ -hydride elimination to give alkenes (**10**) is the dominant reaction in competition with intermolecular C–H functionalization.<sup>13,14</sup> Though alkyl diazoacetates have been well-established for intramolecular C–H insertion, intermolecular insertion remains an outstanding challenge.<sup>15-18</sup>

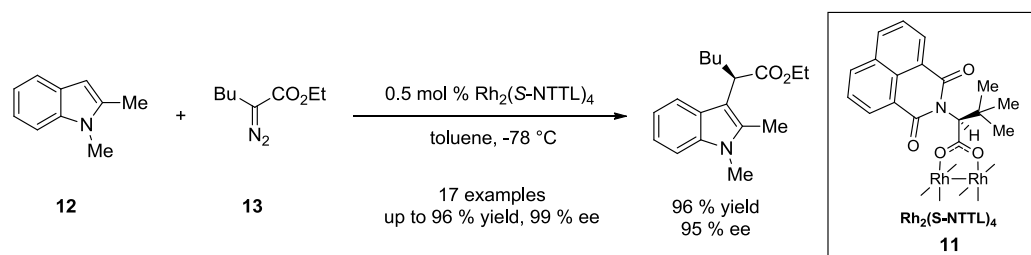
**Scheme 3.2.** Competitive  $\beta$ -hydride elimination of alkyl diazoacetates (**9**) to give alkenes (**10**).



In addressing this challenge, Fox and coworkers have found the use of sterically demanding dirhodium tetracarboxylates led to dramatic improvements in both intermolecular cyclopropanation<sup>19</sup> and cyclopropanation<sup>20</sup> with alkyl diazoacetates. Key to the development of enantioselective methods for cyclopropanation,<sup>21</sup> as well as C–H insertion with alkyl diazoacetates,<sup>22</sup> was the recognition of the utility of the chiral, sterically demanding dirhodium carboxylates  $\text{Rh}_2(\text{S-PTTL})_4$  and  $\text{Rh}_2(\text{S-NTTL})_4$ .  $\text{Rh}_2(\text{S-PTTL})_4$  was developed by Hashimoto and coworkers,<sup>23</sup> and used by them for intramolecular benzylic C–H insertion with alkyl diazoacetates in high enantioselectivity, among a myriad of other transformations.<sup>24</sup> These results led to studies of the structurally similar  $\text{Rh}_2(\text{S-NTTL})_4$  (**11**) developed by Müller and coworkers<sup>25</sup> in intermolecular C–H functionalization with alkyl diazoacetates

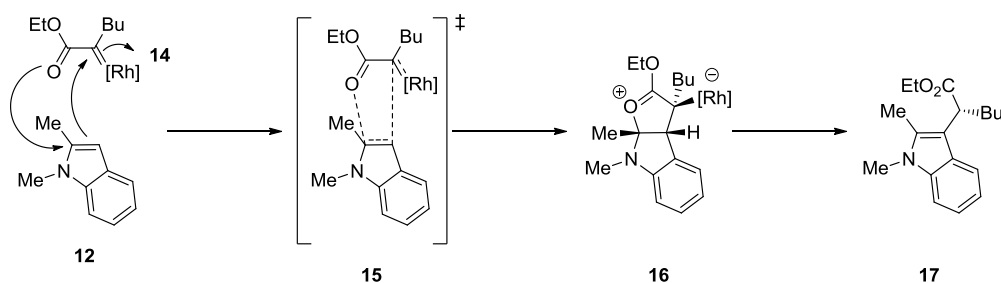
Fox and coworkers found  $\text{Rh}_2(\text{S-NTTL})_4$  (**11**) catalyzed the C–H functionalization of indoles, such as **12**, with  $\alpha$ -alkyl- $\alpha$ -diazoester **13** in excellent enantioselectivity (Scheme 3.3).<sup>22</sup>

**Scheme 3.3.**  $\text{Rh}_2(\text{S-NTTL})_4$  (**11**) catalyzed enantioselective C–H insertion of  $\alpha$ -alkyl- $\alpha$ -diazoester **13** with indole **12**.<sup>22</sup>



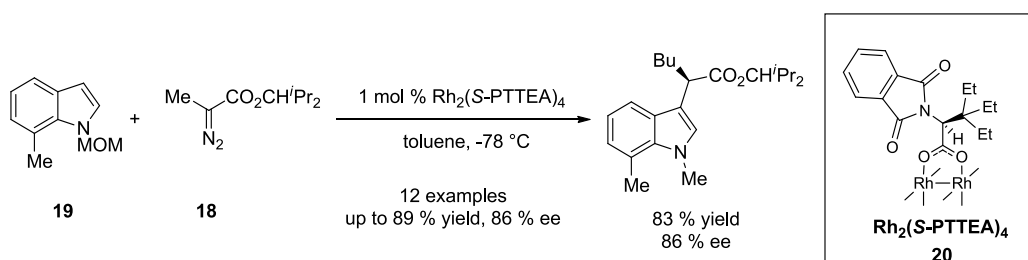
Control experiments provided evidence against a cyclopropanation/fragmentation mechanism, suggesting instead an ylide formation/proton-transfer pathway, which is also supported by DFT calculations (Scheme 3.4).<sup>22</sup> In this mechanism, end-on approach of the indole **12** to metalcarbene **14** gives transition state **15**. Formation of a C–C bond and C–O bond provides rhodium-ylide intermediate **16**. Aromatization of the indole and protonolysis of the C–Rh bond affords indole **17**. While the lack of  $\beta$ -hydride elimination of metalcarbene **14** is notable, the involvement of the indole  $\pi$ -bond in this proposed mechanism differentiates it from a typical C–H insertion. Thus far, this method has not been generalizable to other classes of C–H bonds

**Scheme 3.4.** Proposed mechanism of  $\text{Rh}_2(\text{S-NTTL})_4$  (**11**) catalyzed enantioselective C–H insertion of alkyl metalcarbene **14** with indole **12**.<sup>22</sup>



Hashimoto and coworkers observed a similar enantioselective C–H insertion of  $\alpha$ -diazopropionate **18** with 2,3-unsubstituted indole **19** using  $\text{Rh}_2(\text{R-PTTEA})_4$  (**20**), presumably through a similar mechanism (Scheme 3.5).<sup>26</sup> Incorporation of the MOM protecting group of indole **19** was necessary for high levels of induction of enantioselectivity.

**Scheme 3.5.**  $\text{Rh}_2(\text{S-PTTEA})_4$  (**20**) catalyzed enantioselective C–H insertion of  $\alpha$ -diazopropionate **18** with 2,3-unsubstituted indole **19**.<sup>26</sup>



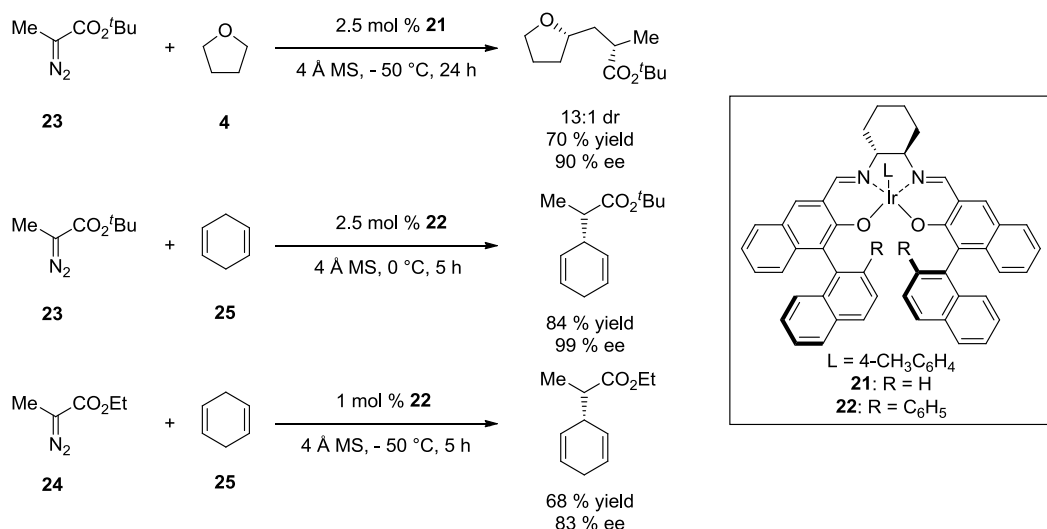
Though the use of low reaction temperatures and bulky dirhodium tetracarboxylate catalysts have been observed as aiding in suppression of  $\beta$ -hydride

migration of alkyl diazoacetates, a detailed explanation for the role of the catalyst in preventing this migration has not been proposed. In enantioselective  $\text{Rh}_2(\text{OPiv})_4$  catalyzed cyclopropanation with alkyl diazoacetates, Fox and coworkers propose, with computational support, that these bulky dirhodium tetracarboxylates align the carbonyl relative to the carbene in such a manner as to increase the rate of intermolecular cyclopropanation versus  $\beta$ -hydride elimination. A more detailed explanation of the suppression of  $\beta$ -hydride elimination has not been proposed.

In a shift from these dirhodium tetracarboxylate-catalyzed transformations, an earlier report from Katsuki and coworkers used iridium-salen catalysts **21** and **22** in the first examples of intermolecular enantioselective insertion of  $\alpha$ -alkyl- $\alpha$ -diazoacetates **23** and **24** into tetrahydrofuran (**4**) and 1,4-cyclohexadiene (**25**, Scheme 3.6).<sup>27</sup> This catalyst family has not been pursued further in C–H insertion with alkyl diazoacetates, but provides an intriguing use of iridium for acceptor-only diazoacetate C–H insertion. In the subsequent development of Si–H insertion using alkyl diazoacetates, Katsuki and coworkers also attributed the prevention of  $\beta$ -hydride elimination to the bulky salen ligand structure regulating the conformation of the metallocarbene intermediate, though a more thorough mechanistic hypothesis is not provided.<sup>28</sup>



**Scheme 3.6.** Iridium-salen **21** and **22** catalyzed enantioselective C–H insertion of alkyl diazoacetates **23** and **24** into tetrahydrofuran (**4**) and 1,4-cyclohexadiene (**25**).<sup>27</sup>

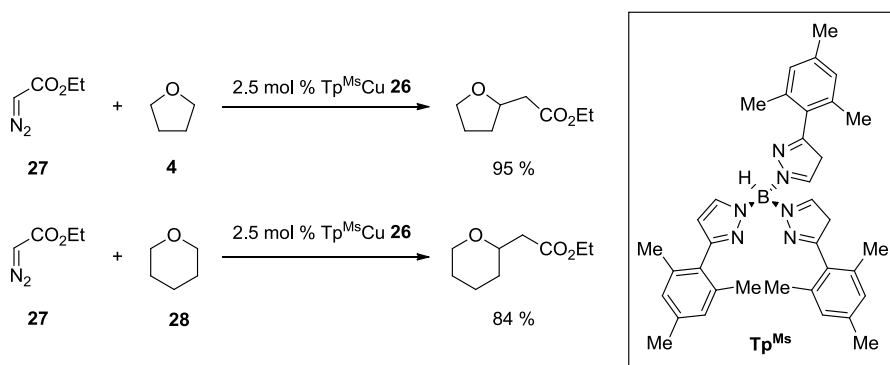


### 3.1.1.2 Racemic C–H Insertion and Enantioselective Cyclopropanation with Ethyl

#### Diazoacetate

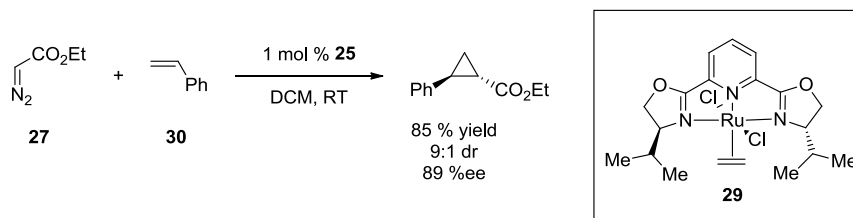
Ethyl diazoacetate has been widely studied for C–H insertion and cyclopropanation, with the first example of ethereal C–H functionalization with ethyl diazoacetate disclosed over 25 years ago.<sup>29</sup> A number of racemic C–H functionalization methods have been developed, with the current state-of-the-art method utilizing bulky copper(I) homoscorpionate catalyst **26** for ethyl diazoacetate (**27**) insertion into tetrahydrofuran (**4**) and tetrahydropyran (**28**, Scheme 3.7).<sup>30</sup> A modified silver(I) scorpionate catalyst was also effective for ethyl diazoacetate C–H insertion into tetrahydrofuran, though competing dimerization was a problem.<sup>31</sup>

**Scheme 3.7.**  $\text{Tp}^{\text{Ms}}\text{Cu}$  **26** Catalyzed racemic C–H functionalization with ethyl diazoacetate (**27**) into tetrahydrofuran (**4**) and tetrahydropyran (**28**).<sup>30</sup>



Until now, no enantioselective C–H insertions have been reported with ethyl diazoacetate (**27**), though a number of enantioselective cyclopropanations have been developed.<sup>32,33</sup> A notable example was disclosed by Nishiyama and coworkers using ruthenium bis(oxazolonyl)pyridine (pybox) **29** and acceptor-only diazoacetates such as ethyl diazoacetate (**27**) for cyclopropanation of styrene (**30**, Scheme 3.8).<sup>34</sup> The success of ruthenium pybox **29** in inducing enantioselectivity with ethyl diazoacetate (**27**) indicated that bis(oxazolonyl) ligands might be useful in enantioselective C–H functionalization as well.

**Scheme 3.8.** Ruthenium pybox **29** catalyzed enantioselective cyclopropanation of styrene (**30**) with ethyl diazoacetate (**27**).<sup>34</sup>



### 3.1.2 Iridium(III) Phebox and Phebim Catalysts for C–H Functionalization

In taming the reactivity of acceptor-only carbenes, we hypothesized that the use of iridium catalysts in place of more standard dirhodium tetracarboxylates would enable enantioselective reactions, in a similar manner to the iridium-salen catalyzed C–H functionalization with alkyl diazoacetates (Scheme 3.5).<sup>27</sup> Though no diiridium(II) tetracarboxylate complexes have been reported, iridium(III) complexes have been shown to mediate enantioselective group transfer reactions with acceptor-only carbenes as well as acceptor/acceptor carbenes.<sup>35</sup> Due to the recent emergence of these highly selective iridium-catalyzed metallocarbene transformations, we sought to utilize iridium(III) complexes for enantioselective C–H insertion with acceptor-only diazoacetates.

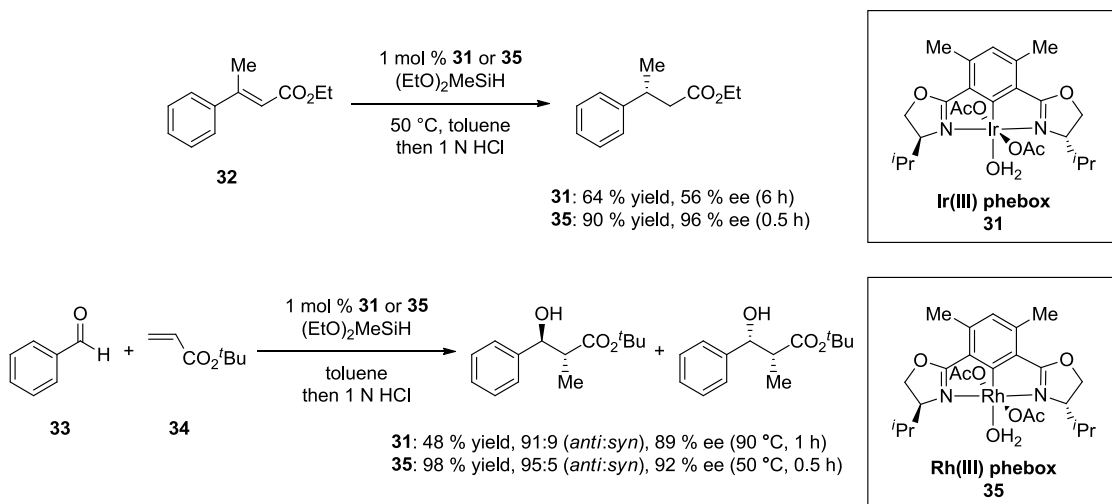
#### 3.1.2.1 Development and Previous Uses of the Phebox and Phebim Ligand Scaffolds

With the precedent of ruthenium-pybox **29** catalyzed enantioselective cyclopropanation with ethyl diazoacetate, the bis(oxazolinyl)phenyl (phebox) ligand

system showed great promise for our studies. The phebox ligand class is a type of chiral  $C_2$ -symmetric N,C,N-tridentate ligand, first synthesized independently by Denmark and coworkers and Stark and Richards.<sup>36,37</sup> Since then, this ligand structure has found use in a number of highly enantioselective reactions with a variety of transition metals.<sup>38-44</sup>

Iridium(III) phebox **31** was used for conjugate reduction of ester **32** and asymmetric reductive aldol reaction with benzaldehyde (**33**) and *t*-butyl acrylate (**34**, Scheme 3.9).<sup>45</sup> However, rhodium(III) phebox **35** proved both more active and more enantioselective in both reactions.

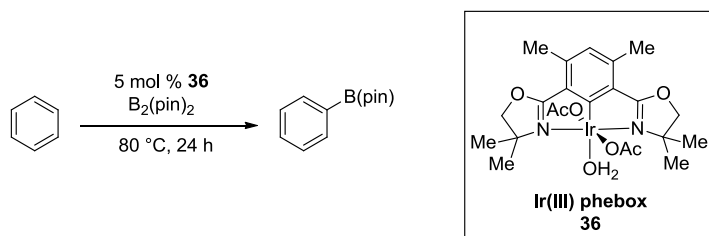
**Scheme 3.9.** Iridium(III) phebox **31** and rhodium(III) phebox **35** catalyzed conjugate reduction and asymmetric reductive aldol reaction.<sup>45</sup>



In terms of C–H functionalization with iridium(III) phebox complexes, iridium(III) phebox **36** was capable of stoichiometric insertion into aryl C–H bonds.<sup>46</sup>

Iridium(III) phebox **36** was also able to perform catalytic C–H borylation of arenes with bis(pinacolato)diboron or pinacolborane (Scheme 3.10).

**Scheme 3.10.** Iridium(III) phebox **36** catalyzed borylation of arenes.<sup>46</sup>



In our studies of iridium(III) phebox catalyzed C–H functionalization (Section 3.1.2.2), the bis(imidazoliny)phenyl ligand (phebim) framework **37** presented an attractive complement to the phebox framework **38** (Figure 3.2).<sup>47</sup> The phebim structure provided the added benefit of electronic tuning through introduction of an aryl ring at the R<sup>2</sup> position.

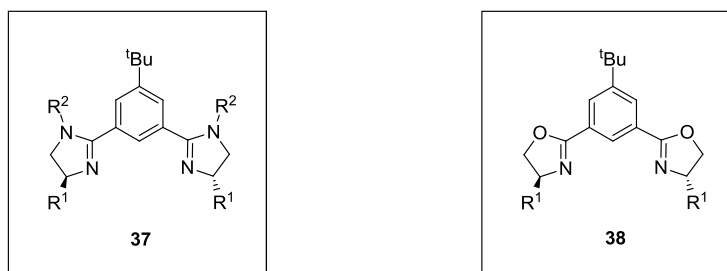
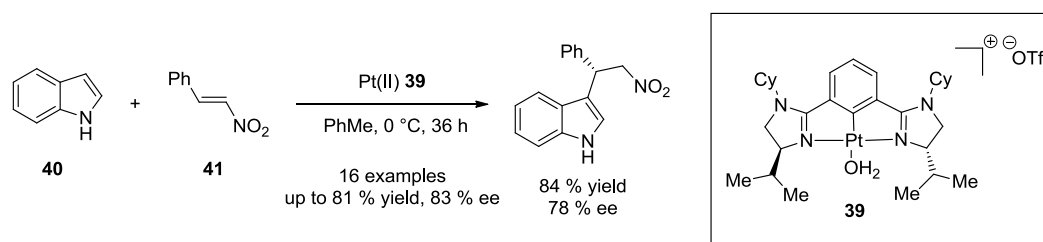


**Figure 3.2.** Phebim **37** and phebox **38** ligand frameworks.

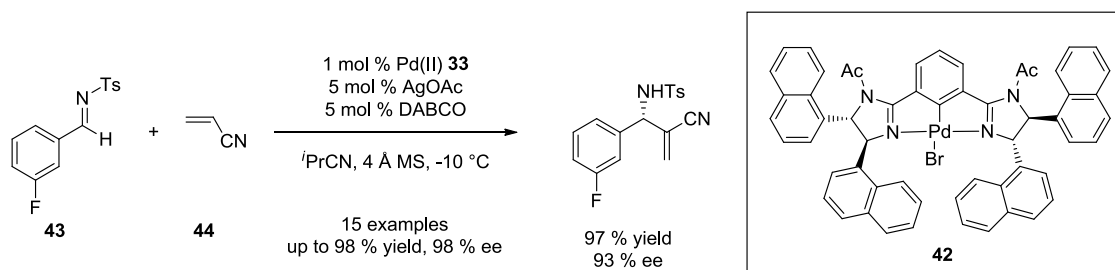
The phebim ligand was first reported in 2006 with the corresponding platinum complexes.<sup>48</sup> Since that time, phebim ligands have been used for a number of applications. Cationic platinum(II) phebim **39** was found capable of asymmetric Friedel-Crafts alkylation of indole **40** using nitroalkene **41** (Scheme 3.11).<sup>49</sup> For this study, several phebim analogues were synthesized, with the optimal catalyst **39** providing good yields and moderate enantioselectivity.

**Scheme 3.11.** Platinum(II) phebim **39** catalyzed asymmetric Friedel-Crafts alkylation of indole **40** with nitroalkene **41**.<sup>49</sup>



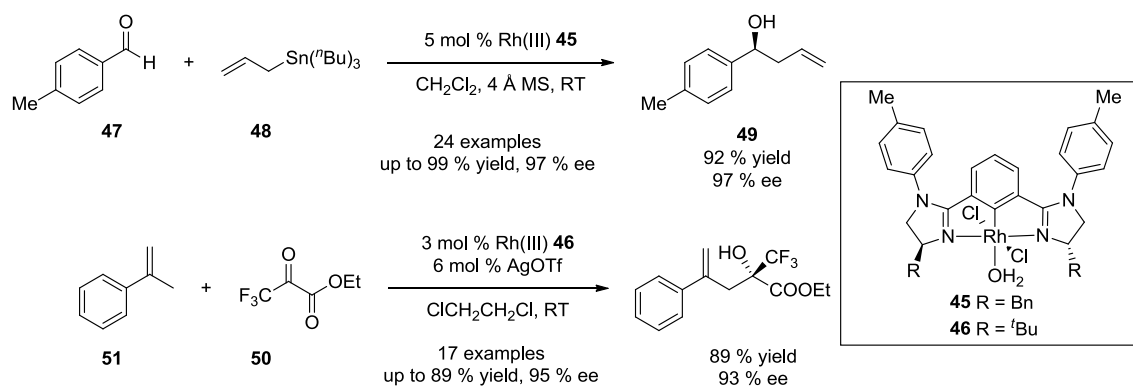
The extremely bulky palladium(II) phebim complex **42** catalyzed the aza-Morita-Baylis-Hillman reaction of imine **43** with nitrile **44** in excellent yield and enantioselectivity (Scheme 3.12).<sup>50</sup> This methodology also took advantage of the capacity of the phebim ligand structure for tuning at the 5-position of the imidazolines of **42**.

**Scheme 3.12.** Palladium(II) phebim **42** catalyzed enantioselective aza-Morita-Baylis-Hillman reaction of imine **43** with nitrile **44**.<sup>50</sup>



Gong, Song, and coworkers reported the use of rhodium(III) phebim complexes **45** and **46** for enantioselective allylation of aldehyde **47** with allyltributyltin (**48**) to afford chiral allyl alcohol **49** and for the asymmetric carbonyl-ene reaction of ethyl trifluoropyruvate (**50**) with 2-arylpropene **51** (Scheme 3.13).<sup>51</sup> For the carbonyl-ene reaction, the inclusion of two equivalents of AgOTf with respect to the rhodium(III) phebim **46** was necessary for removal of the chloride ancillary ligands, as well as for enhancing the Lewis acidity of the catalyst. Phebim complexes have also been synthesized with first row transition metals, such as the four-coordinate nickel(II) phebim complexes.<sup>52,53</sup> Use of an iridium(III) phebim catalyst system for metalcarbene generation and enantioselective C–H insertion would be a significant departure mechanistically from its previous roles as chiral Lewis acids and in reductive manifolds.

**Scheme 3.13.** Rhodium(III) phehim **45** and **46** catalyzed allylation of aldehyde **47** and carbonyl-ene reaction.<sup>51</sup>

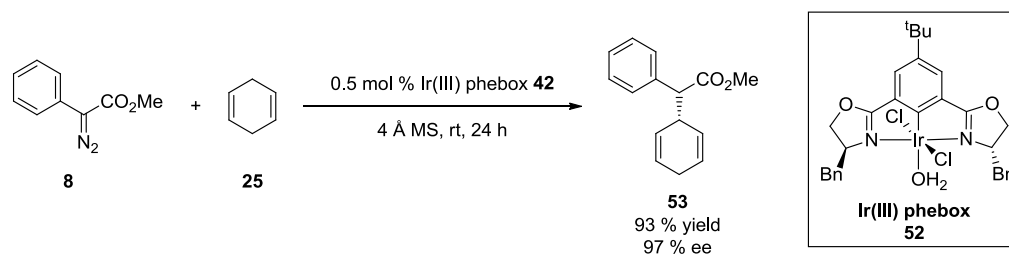


### 3.1.2.2 Enantioselective Iridium(III) Phebox Catalyzed Donor/Acceptor Metallocarbene C–H Functionalization

With the aim of developing iridium(III) phebox catalysis for acceptor-only metallocarbene C–H functionalization, Blakey and coworkers first established proof-of-principle for the capability of iridium(III) phebox **52** for diazo decomposition and carbene stabilization for enantioselective C–H insertion (Scheme 3.14).<sup>54</sup> Screening of a variety of phebox substitution patterns and conditions afforded a maximum yield of 93 % and ee of 97 % for the insertion of methyl phenyldiazoacetate (**8**) into 1,4-cyclohexadiene (**25**) to form chiral cyclohexadiene derivative **53**.

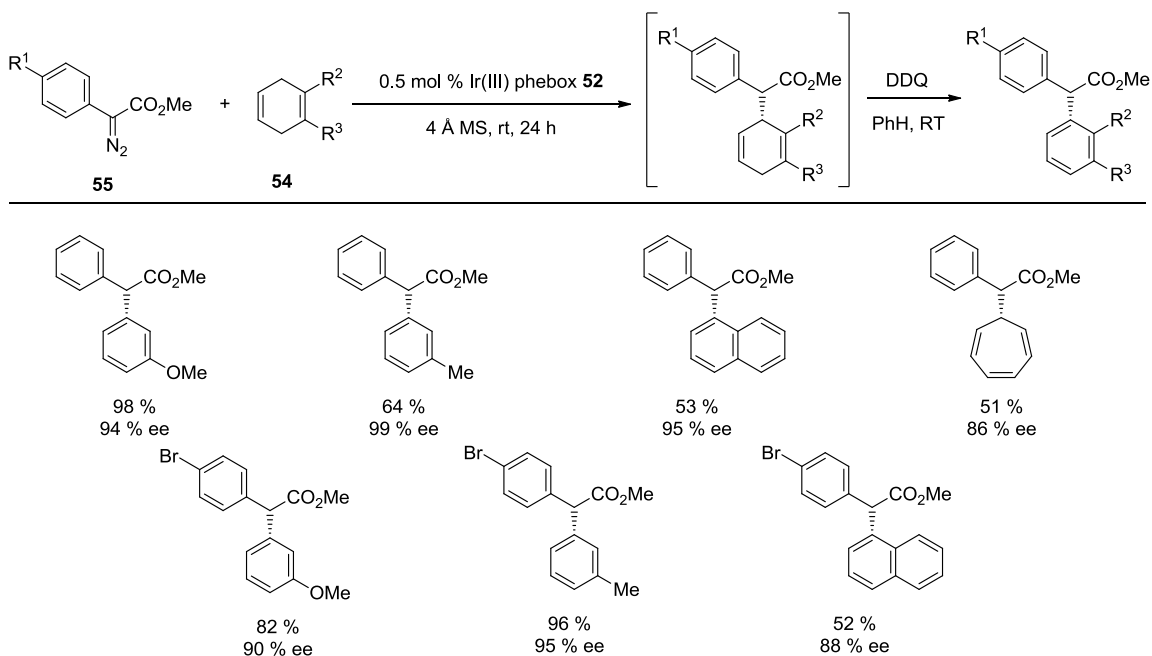


**Scheme 3.14.** Iridium(III) phebox **52** catalyzed enantioselective C–H functionalization of 1,4-cyclohexadiene (**25**) with methyl phenyldiazoacetate (**8**).<sup>54</sup>



The insertion was found compatible with several substituted cyclohexadiene substrates (**54**) and donor/acceptor diazoacetates (**55**, Table 3.1). Notably, a very low catalyst loading (0.5 mol %) was required, and gradual addition of the diazoacetate was not necessary. This use of the phebox ligand scaffold represents a departure from previous uses as chiral Lewis acids and in reductive manifolds.

**Table 3.1.** Iridium(III) phebox **52** catalyzed enantioselective C–H functionalization of cyclohexadiene derivatives (**54**) with methyl phenyldiazoacetates (**55**).<sup>54</sup>

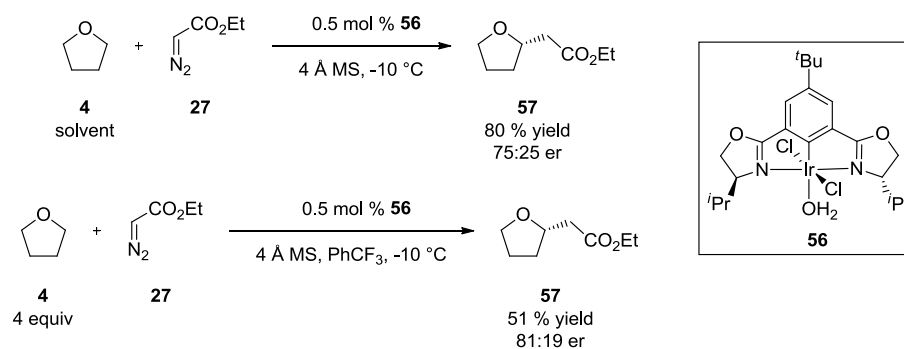


### 3.1.2.3 Enantioselective Iridium(III) Phebox Catalyzed Ethyl Diazoacetate C–H Functionalization

With the iridium(III) phebox catalyzed insertion with donor/acceptor diazoacetates established, the insertion of ethyl diazoacetate (**27**) into tetrahydrofuran (**4**) was studied, in work conducted by Dr. Clayton Owens.<sup>47,55</sup> Initially, it was discovered that iridium (III) phebox **56** catalyzed the enantioselective insertion of ethyl diazoacetate (**27**) into tetrahydrofuran (**4**) to afford 80 % insertion product **57** in 75:25 er (Scheme 3.15). Notably, when four equivalents of tetrahydrofuran (**4**) were used in

trifluorotoluene, in place of tetrahydrofuran as solvent, the enantioselectivity increased to 81:19 er.

**Scheme 3.15.** Iridium(III) phebox **56** catalyzed enantioselective insertion of ethyl diazoacetate (**27**) into tetrahydrofuran (**4**) to give insertion product **57**.<sup>47</sup>



Using the CPCM-M06L/{LANL08(f)Ir + [6-31G(d,p)]} level of theory, Dr. Jamal Musaev, Dr. Shentan Chen, and Dr. Adrian Varela-Alvarez calculated the structure and free energy of pro-*S* transition state (**TS1**) and pro-*R* transition state (**TS2**) for ethyl diazoacetate insertion into phthalan (Figure 3.3).<sup>55</sup> The  $\Delta\Delta G^\ddagger$  value between **TS1** and **TS2** was calculated to be very small (0.5 kcal/mol), and the favored transition state **TS1** has a short O1-H2 distance of 2.308 Å because of a ligand-substrate electrostatic interaction.

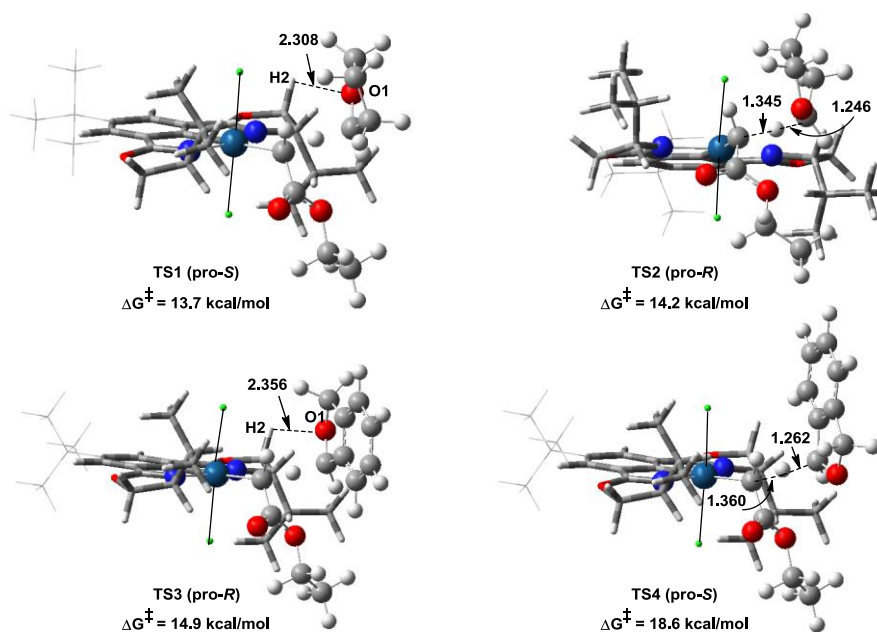
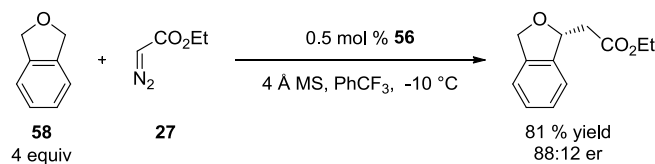


**Figure 3.3.** Calculated pro-*R* and pro-*S* transition states of ethyl diazoacetate (27) insertion into tetrahydrofuran (top) and phthalan (bottom) with Ir(III)-phebox 56.<sup>55</sup>

In terms of reaction optimization, by replacing tetrahydrofuran (4) with phthalan (49), the  $\Delta\Delta G^\ddagger$  between TS3 and TS4 was calculated to increase to 3.7 kcal/mol. This prediction was correct qualitatively, as the use of phthalan (58) increased enantioselectivity to 88:12 er (Scheme 3.16).<sup>55</sup>

**Scheme 3.16.** Iridium(III) phebox 56 catalyzed enantioselective insertion of ethyl diazoacetate (27) into phthalan (58).<sup>47</sup>

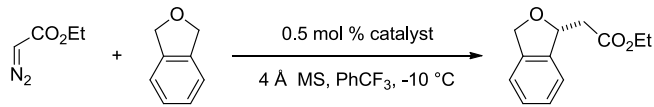


Because of the insight into the electrostatic interaction between O1 of phthalan (**58**) and H2 of iridium(III) phebox **56** in the favored transition state **TS3**, it was theorized that enantioselectivity could be improved by increasing the charge density of H2 through electronic modulation of the iridium(III) ligand structure. (Figure 3.3)

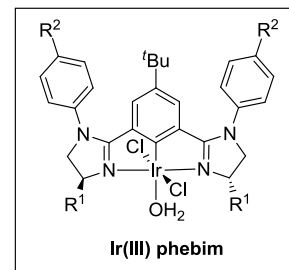
### **3.2 Enantioselective Iridium(III) Phebim Catalyzed Acceptor-Only Diazoacetate C–H Functionalization**

The capacity of the phechim ligand structure for electronic tuning made it the next logical step from the phebox ligand structure for optimizing enantioselectivity of the ethyl diazoacetate C–H insertion. In work conducted by Dr. Clayton Owens, by varying substitution on the aryl ring at the R<sup>2</sup>-position, trifluoromethyl-substituted isopropyl phechim gave an improvement in enantioselectivity to 90:10 er (Table 3.2, entry 4).<sup>47</sup> Changing the steric bulk of the chiral pocket by adjusting R<sup>1</sup> substitution gave a maximum enantioselectivity of 95:5 with both isobutyl- and methylene-cyclohexyl-substituted iridium(III) phechim catalysts (entries 6 and 9).

**Table 3.2.** Catalyst optimization of enantioselective ethyl diazoacetate (**27**) insertion into phthalan (**58**)<sup>a, 47</sup>



entry	R <sup>1</sup>	R <sup>2</sup>	yield (%) <sup>b</sup>	er <sup>c</sup>
1	<sup>i</sup> Pr	H	85	88:12
2	<sup>i</sup> Pr	OMe	26	89:11
3	<sup>i</sup> Pr	NO <sub>2</sub>	70	90:10
4	<sup>i</sup> Pr	CF <sub>3</sub>	73	90:10
5 <sup>d</sup>	<sup>i</sup> Pr	CF <sub>3</sub>	83	88:12
6	<sup>i</sup> Bu	CF <sub>3</sub>	95	95:5
7	<sup>s</sup> Bu	CF <sub>3</sub>	81	92:8
8	<sup>c</sup> Hex	CF <sub>3</sub>	83	90:10
9	CH <sub>2</sub> <sup>c</sup> Hex	CF <sub>3</sub>	80	95:5



<sup>a</sup>General conditions: 0.29 M solution of ethyl diazoacetate in PhCF<sub>3</sub> was added over 5 h to a mixture of catalyst, phthalan (4 equiv), and 4 Å MS in PhCF<sub>3</sub> at -10 °C. <sup>b</sup>Isolated yields. <sup>c</sup>Determined by chiral HPLC. <sup>d</sup>Chloride ancillary ligands replaced with bromide ligands.

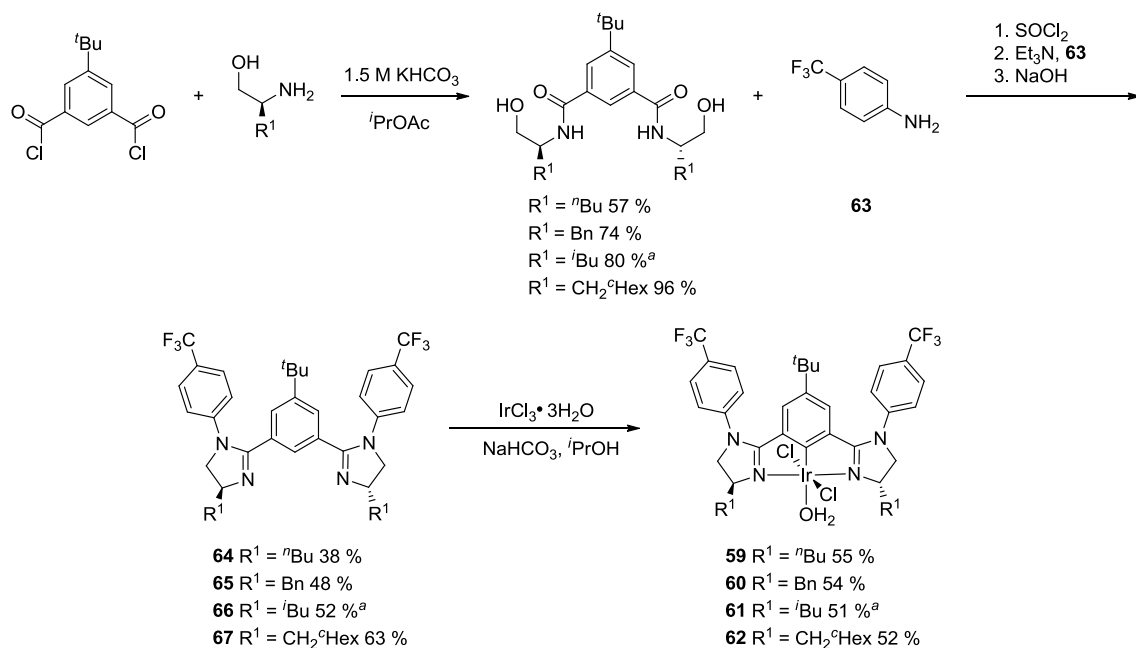
As discussed in Chapter 2, using linear regression mathematical modeling techniques of catalyst optimization data can predict the optimal catalyst structure for a reaction (Section 2.2.2). In collaboration with the Sigman group, we sought to model the effect of iridium(III) phebim R<sup>1</sup> substitution in inducing enantioselectivity. For this purpose, we synthesized an array of catalysts.

### 3.2.1 Iridium(III) Phebim Catalyst Synthesis

In order to widen the spread of steric parameters of iridium(III) phebim R<sup>1</sup> substitution, we synthesized iridium(III) phebim **59** with *n*-butyl substitution and **60** with benzyl substitution (Scheme 3.17). Additionally, upon repetition, the efficiency of the synthesis of our most effective iridium(III) phebim catalysts **61** and **62** was increased on

larger scale. Using a method adapted from the literature,<sup>56,57</sup> the amidation reaction showed efficiency of up to 96 %. Addition of the 4-trifluoromethyl aniline **63** to form the phebim proceeded in low to moderate yield of phebim ligands **64-67**.<sup>58</sup> Metalation proceeded smoothly with  $\text{IrCl}_3 \cdot 3\text{H}_2\text{O}$  and sodium bicarbonate in refluxing isopropanol<sup>45,54</sup> to yield the new iridium(III) phebim complexes **59** and **60** and an improved overall yield of complexes **61** and **62**.

**Scheme 3.17.** Synthesis of iridium(III) phebim complexes **59-62**.

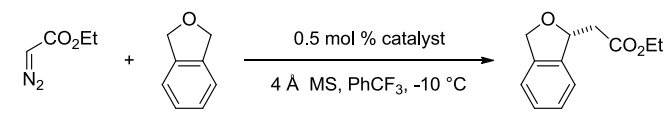


<sup>a</sup>Opposite catalyst enantiomer was synthesized.

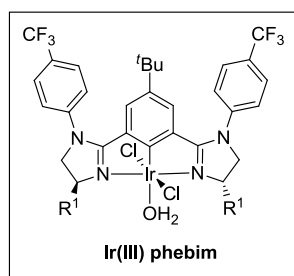
### 3.2.2 Iridium(III) Phebim Catalyst Optimization with Ethyl Diazoacetate

With these new additions to the catalyst library, we were able to complete our R<sup>1</sup> optimization table (Table 3.3). *n*-Butyl- and benzyl-substituted catalysts **59** and **60** gave the lowest enantioselectivities observed (13:87 and 86:14, entries 6 and 7, respectively). A wide spread of data is actually advantageous for the linear regression mathematical modeling that was undertaken in collaboration with the Sigman group.

**Table 3.3.** Additional catalyst optimization of enantioselective ethyl diazoacetate (**27**) insertion into phthalan (**58**)<sup>a</sup>.



entry	R <sup>1</sup>	yield (%) <sup>b</sup>	er <sup>c</sup>
1 <sup>d</sup>	<sup>i</sup> Pr	73	90:10
2 <sup>d</sup>	<sup>i</sup> Bu	95	95:5
3 <sup>d</sup>	<sup>s</sup> Bu	81	92:8
4 <sup>d</sup>	<sup>c</sup> Hex	83	90:10
5 <sup>d</sup>	CH <sub>2</sub> <sup>c</sup> Hex	80	95:5
6	<sup>n</sup> Bu	54	13:87 <sup>e</sup>
7	Bn	36	86:14



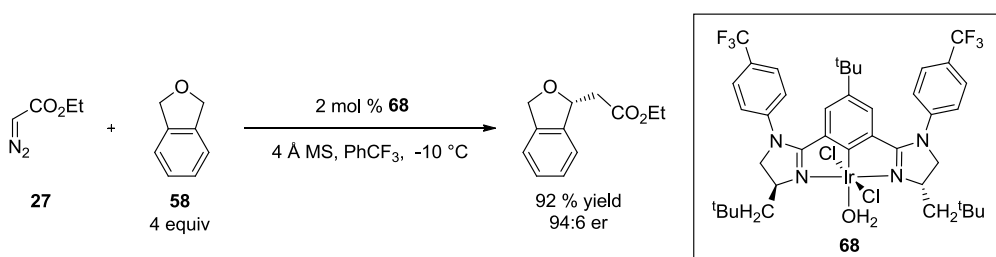
<sup>a</sup>General conditions: 0.29 M solution of ethyl diazoacetate in PhCF<sub>3</sub> was added over 5 h to a mixture of catalyst, phthalan (4 equiv), and 4 Å MS in PhCF<sub>3</sub> at -10 °C. <sup>b</sup>Isolated yields. <sup>c</sup>Determined by chiral HPLC. <sup>d</sup>Results by Dr. Clay Owens. <sup>e</sup>Catalyst **59** is a member of the opposite enantio-series.

By analyzing a variety of steric parameters (Sterimol, Charton/Taft, and Austel values), Zachary Niemeyer and Professor Matthew Sigman calculated the mathematical relationship of iridium(III) phebam R<sup>1</sup>-substitution to enantioselectivity.<sup>59</sup> The relationship required balancing of the branching (Austel value) and spherical size



(Charton/Taft value) of  $R^1$  to attain optimal selectivity. From this model, it was predicted that methylene-*tert*-butyl-substituted iridium(III) phebim **68** would give an er of 94:6 (Scheme 3.18). Dr. Andrew Schafer synthesized catalyst **68** and found the observed enantioselectivity was in agreement with this prediction.

**Scheme 3.18.**  $\text{CH}_2$ -*t*Bu-substituted iridium(III) phebim **68** catalyzed C–H insertion with ethyl diazoacetate accomplished by Dr. Andrew Schafer (**27**).

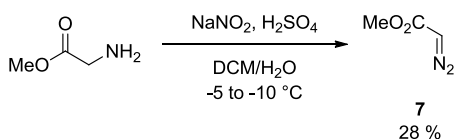


### 3.2.3 Acceptor-Only Diazoacetate Scope

Employing the two iridium(III) phebim catalysts providing the highest enantioselectivity in our model reaction, isobutyl-substituted **61** and methylene-cyclohexyl-substituted **62**, the effect of diazoacetate substitution was explored in an effort to further increase enantioselectivity. As ester substituent size has been previously found to have a large impact on donor/acceptor carbene C–H insertion,<sup>2</sup> we moved from ethyl diazoacetate (**27**) to methyl diazoacetate (**7**). In synthesizing **7**, careful control of reaction temperature was necessary for formation of diazoacetate **7** (Scheme 3.19). Additionally, volatility required care in purification of diazoacetate **7**. Additional

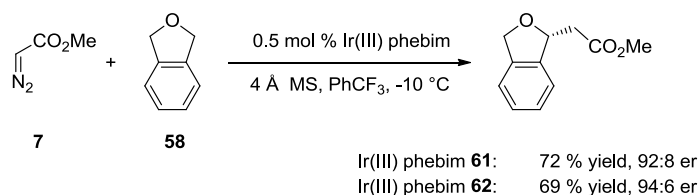
acceptor-only diazoacetate compounds were synthesized by Cameron Herting, following literature precedent.

**Scheme 3.19.** Synthesis of methyl diazoacetate (**7**).



In our system, we observed only a minor difference in selectivity, with the enantioselectivity dropping slightly from that observed with ethyl diazoacetate (**27**) to 94:6 with catalyst **62** (Scheme 3.20).

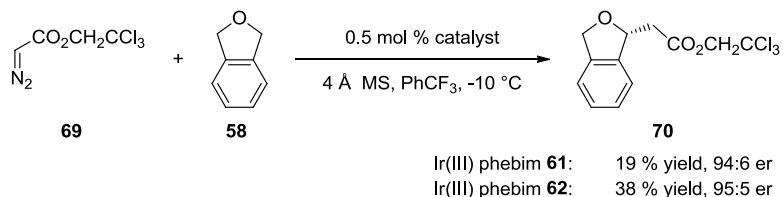
**Scheme 3.20.** Iridium(III) phebim **61** and **62** catalyzed C–H insertion with phthalan (**58**) and methyl diazoacetate (**7**).



2,2,2-Trichloroethyl diazoacetate (**69**) has been recently shown to provide significant improvement for some catalyst classes in dirhodium(II) tetracarboxylate-catalyzed donor/acceptor C–H insertion.<sup>60</sup> Under standard conditions of 0.5 mol % catalyst loading, the reaction yield was poor with both iridium(III) phebim **61** and **62**

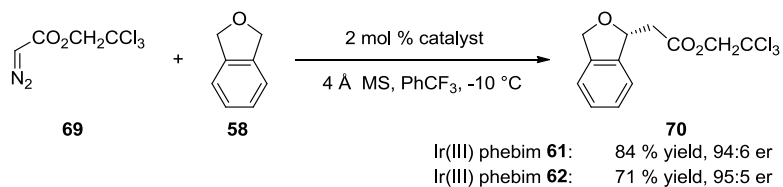
(Scheme 3.21). Significant amounts of unreacted diazoacetate **69** were observed by  $^1\text{H}$  NMR, even after stirring overnight.

**Scheme 3.21.** Iridium(III) phebim **61** and **62** catalyzed C–H insertion with phthalan (**58**) and 2,2,2-trichloroethyl diazoacetate (**69**) at 0.5 mol % catalyst loading.



When the catalyst loading was increased to 2 mol %, diazoacetate **69** was completely consumed to afford 84 % insertion product **70** with isobutyl-substituted **61** and 71 % with methylene-cyclohexyl-substituted **62** (Scheme 3.22). Enantioselectivity remained at similar levels to previous diazoacetates.

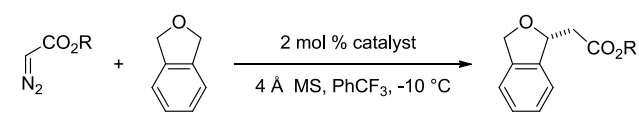
**Scheme 3.22.** Iridium(III) phebim **61** and **62** catalyzed C–H insertion with phthalan (**58**) and 2,2,2-trichloroethyl diazoacetate (**69**) at 2 mol % catalyst loading.



This increased catalyst loading of 2 mol % was applied to the remainder of diazoacetates studied. Introduction of a 2-(trimethylsilyl)ethyl ester in donor/acceptor

diazoacetate insertion with Rh catalysts can result in an intramolecular reaction to form allyl silanes.<sup>61</sup> However, 2-trimethylsilyl diazoacetate was observed to give C–H insertion in good er of 94:6 with iridium(III) phebim **62** (Table 3.4, entry 6). A range of substituted phenyl diazoacetates were tolerated, with enantioselectivity up to 93:7 for the unsubstituted phenyl diazoacetate (entries 7–12). Although none of the additional diazoacetates studied gave improved selectivity, all substitution patterns investigated were well-tolerated, suggesting broad substrate variation at this position is possible. Additionally, we observed that isobutyl-substituted catalyst **61** generally gave slightly higher yield, while methylene-cyclohexyl-substituted catalyst **62** gave slightly higher enantioselectivity in the C–H insertion reaction. For this reason, catalyst **62** was used for further studies of substrate scope.

**Table 3.4.** Diazoacetate scope for C–H insertion into phthalan with iridium(III) phebim complexes **61** and **62**.



entry	R	catalyst	yield (%) <sup>b</sup>	er <sup>c</sup>
1 <sup>d</sup>	Me	<b>61</b>	72	92:8
2 <sup>d</sup>	Me	<b>62</b>	69	94:6
3	CH <sub>2</sub> CCl <sub>3</sub>	<b>61</b>	84	94:6
4	CH <sub>2</sub> CCl <sub>3</sub>	<b>62</b>	71	95:5
5	CH <sub>2</sub> CH <sub>2</sub> Si(CH <sub>3</sub> ) <sub>3</sub>	<b>61</b>	62	93:7
6	CH <sub>2</sub> CH <sub>2</sub> Si(CH <sub>3</sub> ) <sub>3</sub>	<b>62</b>	67	94:6
7	Ph	<b>61</b>	65	91:9
8	Ph	<b>62</b>	68	93:7
9	4-OMe-Ph	<b>61</b>	57	91:9
10	4-OMe-Ph	<b>62</b>	70	92:8
11	4-CF <sub>3</sub> -Ph	<b>61</b>	78	90:10
12	4-CF <sub>3</sub> -Ph	<b>62</b>	69	92:8

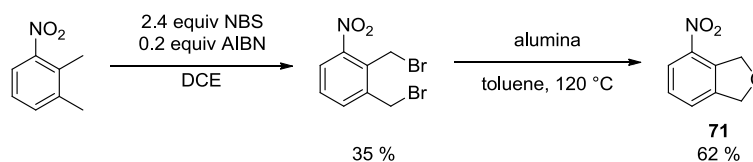
<sup>a</sup>General conditions: 0.29 M solution of diazoacetate in PhCF<sub>3</sub> was added over 5 h to a mixture of catalyst, phthalan (4 equiv), and 4 Å MS in PhCF<sub>3</sub> at -10 °C. <sup>b</sup>Isolated yields. <sup>c</sup>Determined by chiral HPLC. <sup>d</sup>0.5 mol % catalyst loading.

During these studies, we discovered a few practical considerations to account for when conducting these reactions. While these catalysts are shelf-stable over a period of months, when using catalysts synthesized over a year prior, we found it useful to monitor the purity by  $^1\text{H}$  NMR, as well as conducting a known test reaction, such as phthalan insertion with ethyl diazoacetate. It was also found that commercially available phthalan does not contain an inhibitor and is thus susceptible to oxidation. Phthalan should be freshly distilled prior to use to avoid O–H insertion of the oxidized phthalan.

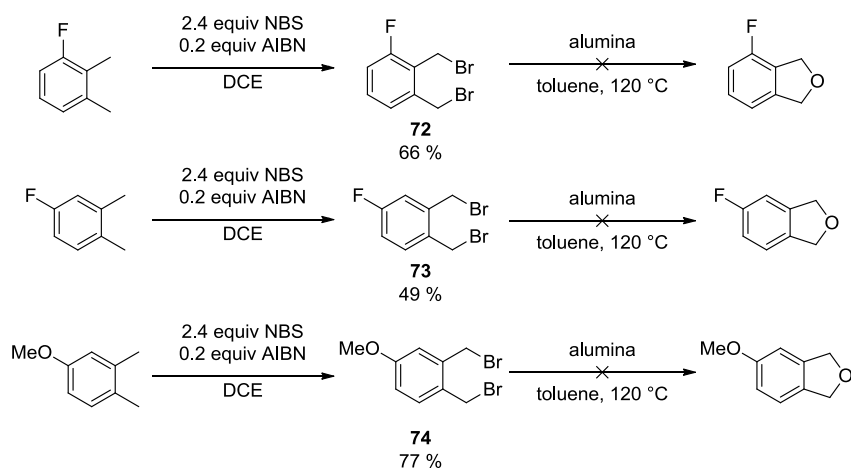
### 3.2.4 Phthalan-Derived Substrate Synthesis

In order to study the substrate scope of the iridium(III) phebim catalyzed acceptor-only diazoacetate C–H functionalization, a divergent route to synthesize phthalan derivatives was needed to study electronic and steric tuning of the reaction. Based on a literature method for radical bromination, followed by cyclization on the surface of alumina, 3-nitro-substituted phthalan **71** was synthesized (Scheme 3.23).<sup>62</sup> The radical bromination procedure called for carbon tetrachloride, but it was found successful in dichloroethane, albeit in reduced yield.

**Scheme 3.23.** Synthesis of 3-nitro-substituted phthalan **71**.

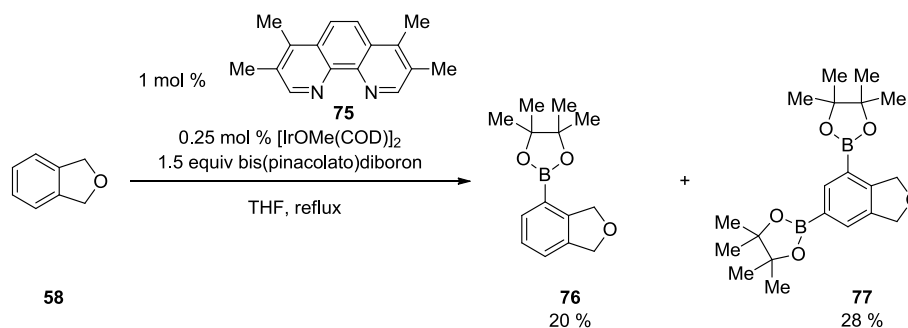


Unfortunately, though the bromination was generalizable to other 1,2-dimethyl-substituted benzene derivatives, the cyclization was not successful with 3-fluoro-substituted **72**, 4-fluoro-substituted **73**, or 4-methoxy-substituted **74** (Scheme 3.24).

**Scheme 3.24.** Unsuccessful syntheses of phthalan derivatives.

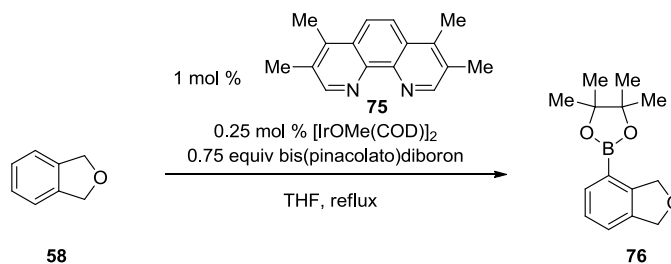
In another approach, arene C–H borylation was utilized for the functionalization of phthalan.<sup>63</sup> When phthalan is exposed to 0.25 mol % [(OMe)Ir(cod)]<sub>2</sub> with 1 mol % 3,4,7,8-tetramethyl-1,10-phenanthroline ligand (**75**) and 1.5 equiv of bis(pinacolato)diboron, 3-borylated product **76** is observed, alongside diborylated **77** (Scheme 3.25).

**Scheme 3.25.** Arene C–H borylation of phthalan (**58**) to afford phthalan derivatives **76** and **77**.



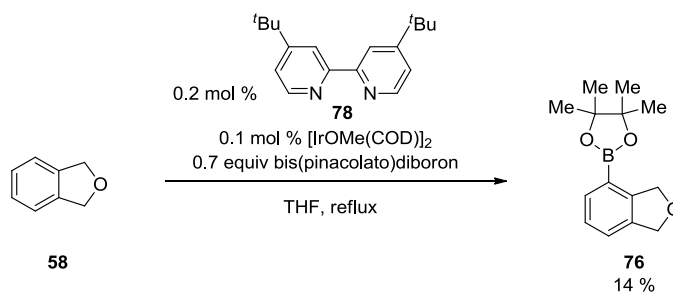
In an effort to prevent diborylation, the excess of bis(pinacolato)diboron was reduced, and an improved yield of 32 % **76** was observed, though not without competing diborylation (Scheme 3.26).

**Scheme 3.26.** Improved arene C–H borylation of phthalan (**58**) to afford phthalan derivative **76**.



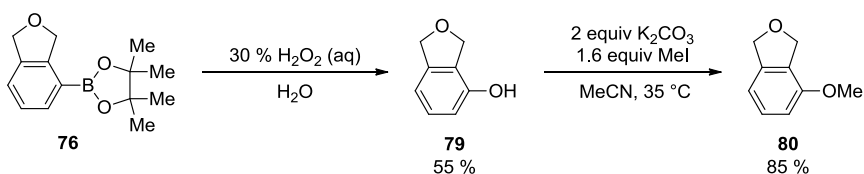
Though an extensive optimization was not conducted, the conditions were altered to vary the ligand to 4,4'-di-*tert*-butyl-2,2'-dipyridyl (**78**), resulting in a reduction in yield (Scheme 3.27).<sup>50</sup>

**Scheme 3.27.** Arene C–H borylation of phthalan (**58**) with 4,4'-di-*tert*-butyl-2,2'-dipyridyl ligand (**78**) to afford phthalan derivative **76**.



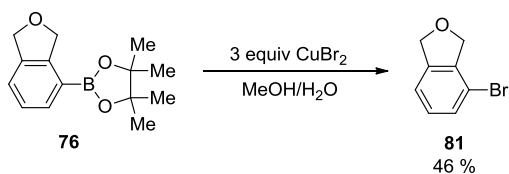
From the pinacol boronate **76**, oxidation with hydrogen peroxide gave alcohol **79** (Scheme 3.28). Methylation with methyl iodide afforded 3-methoxy-phthalan (**80**).

**Scheme 3.28.** Synthesis of 3-methoxy phthalan (**80**).



Bromination of pinacol boronate **76** with copper(II) bromide afforded 3-bromo-phthalan (**81**) in moderate yield (Scheme 3.29).<sup>64</sup>

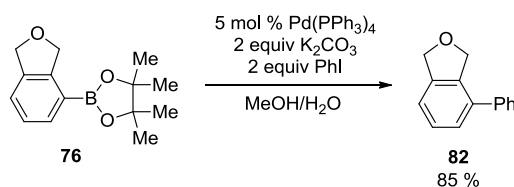
**Scheme 3.29.** Bromination of pinacol boronate **76** to yield 3-bromo-phthalan (**81**).



Suzuki–Miyaura cross-coupling was carried out smoothly with pinacol boronate **76** and phenyl iodide to afford 3-phenyl-phthalan (**82**) in good yield (Scheme 3.30).<sup>65</sup>

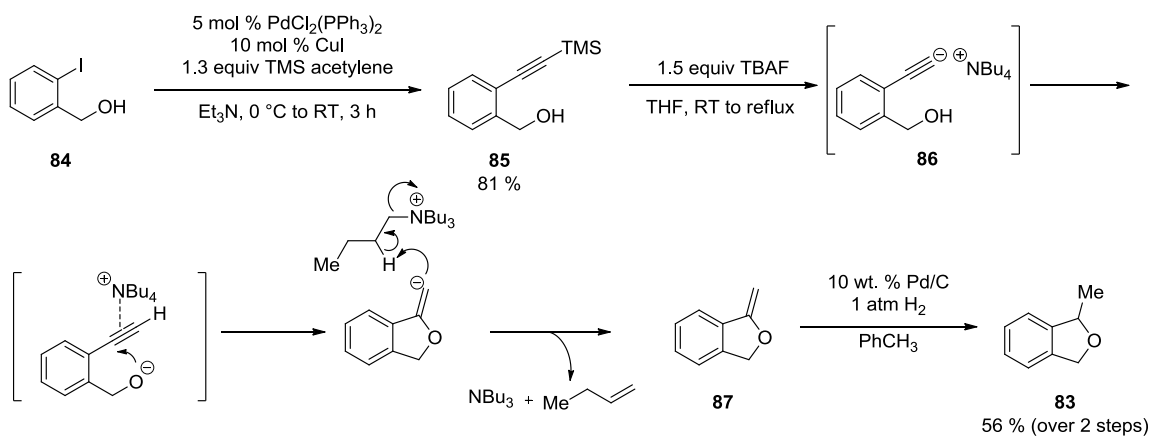


**Scheme 3.30.** Suzuki-Miyaura cross-coupling of pinacol boronate **76** and phenyl iodide to yield 3-phenyl-phthalan (**82**).



Finally, racemic 2-methyl-phthalan (**83**) was synthesized to assess the possibility of kinetic resolution (Scheme 3.31). Sonogashira coupling of trimethylsilyl acetylene and aryl iodide **84** afforded 81 % of the 2-ethynylbenzyl alcohol derivative **85**. Initial exposure of **85** to TBAF at room temperature causes the detrimethylsilyl reaction to yield alcohol **86**. Warming to reflux initiates the TBAF-promoted cyclization to give **87**, which was then reduced to 2-methyl-phthalan (**83**).<sup>66</sup>

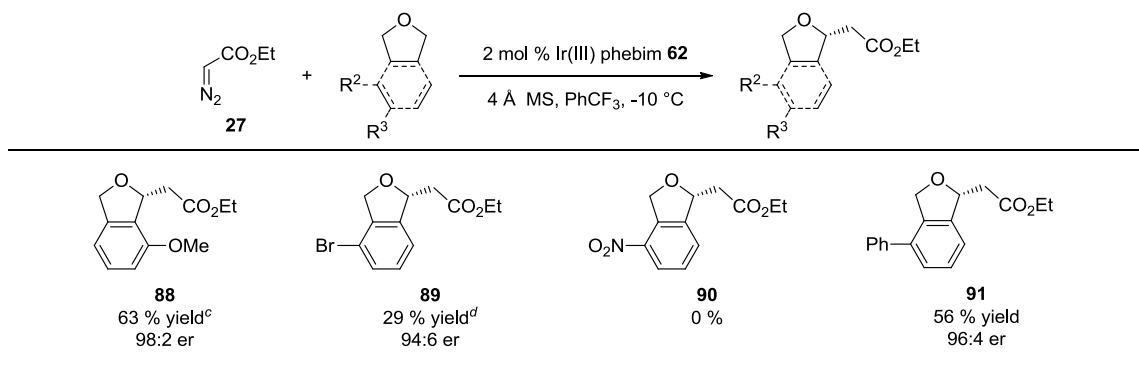
**Scheme 3.31.** Synthesis of 2-methyl-phthalan (**83**) by TBAF-promoted cyclization of alcohol **85**.



### 3.2.5 Ethyl Diazoacetate C–H Insertion Substrate Scope

Substrate substitution was found to have a significant impact on both the efficiency and selectivity of the iridium(III) phebim catalyzed acceptor-only diazoacetate C–H functionalization. 3-Methoxy-phthalan (**80**) favored insertion at the electronically favored 2-position to give major product **88** in 63 % yield and the highest enantiomeric ratio observed of 98:2 (Table 3.5). The minor 2,6-regioisomer was produced in 19 % yield and an er of 94:6. The 3-bromo-phthalan (**81**) showed a bias for the sterically favored 2,6-substituted product **89** in 29 % yield and 94:6 er. An additional 10 % of the electronically favored 2,3-regioisomer was formed as well. 3-Nitro-substituted **71** was not a viable substrate, forming no insertion product **90**, even with warming to room temperature overnight. 3-Phenyl substituted **82** showed steric blocking of the 2-position, yielding only 2,6-substituted product **91** in 56 % yield and 96:4 er.

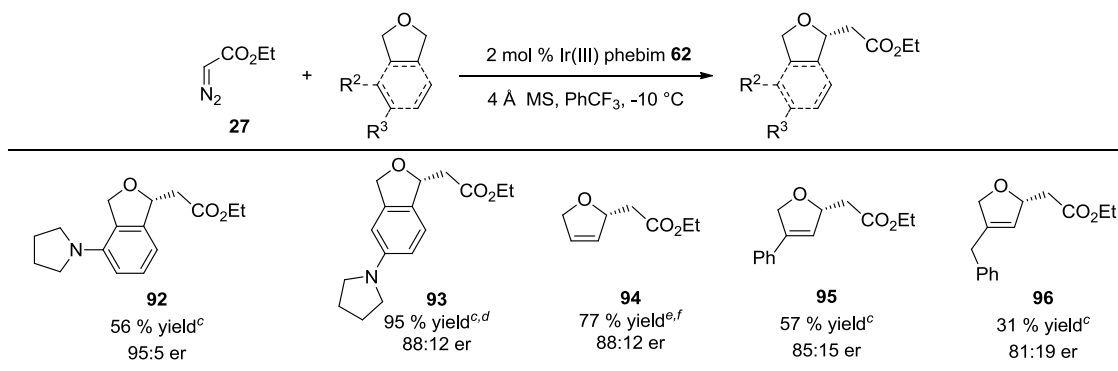
**Table 3.5.** Phthalan derivative substrate scope of iridium(III) phebim **62** catalyzed enantioselective C–H functionalization with ethyl diazoacetate (**27**).<sup>a,b</sup>



<sup>a</sup>General conditions: 0.29 M solution of ethyl diazoacetate in PhCF<sub>3</sub> was added over 5 h to a mixture of catalyst, substrate (4 equiv), and 4 Å MS in PhCF<sub>3</sub> at -10 °C. <sup>b</sup>Isolated yields are given. <sup>c</sup>The 2,6-regioisomer is also observed in an additional 19 % yield and 94:6 er. <sup>d</sup>The 2,3-regioisomer is also observed in an additional 10 % yield.

In work conducted by Dr. Andrew Schafer, 3-pyrrolidinyl-phthalan gave the sterically less hindered insertion product **92** in 56 % yield and 95:5 er (Table 3.6). 4-pyrrolidinyl-phthalan removed the steric bias and showed a majority of insertion at the electronically favored position to give the 2,5-isomer **93** and 2,4-isomer in a 4:1 ratio. Extending beyond phthalan derivatives, Dr. Clayton Owens established smooth insertion into 2,5-dihydrofuran to give 77 % yield of **94** in 88:12 er.<sup>47</sup> Dr. Andrew Schafer found reaction with 3-phenyl-2,5-dihydrofuran gave sterically favored dihydrofuran **95** (57 % yield, 85:15 er). Similarly, 3-benzyl-2,5-dihydrofuran gave dihydrofuran **96** in 31 % yield and 81:19 er. No competing cyclopropanation was observed for 2,5-dihydrofuran or its derivatives.

**Table 3.6.** Further phthalan 2,5-dihydrofuran derivative substrate scope of iridium(III) phebim **62** catalyzed enantioselective C–H functionalization with ethyl diazoacetate (**27**) by Dr. Clay Owens and Dr. Andrew Schafer.<sup>a,b</sup>

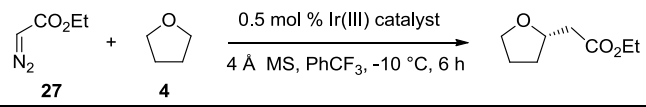


<sup>a</sup>General conditions: 0.29 M solution of ethyl diazoacetate in PhCF<sub>3</sub> was added over 5 h to a mixture of catalyst, substrate (4 equiv), and 4 Å MS in PhCF<sub>3</sub> at -10 °C. <sup>b</sup>Isolated yields are given. <sup>c</sup>Result by Dr. Andrew Schafer. <sup>d</sup>Product was isolated as a 4:1 inseparable mixture of the 2,5 (major) and 2,4 (minor) regioisomers. <sup>e</sup>Result by Dr. Clay Owens. <sup>f</sup>0.5 mol % catalyst loading.

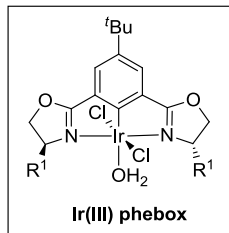
Returning to the initial problem of ethyl diazoacetate (**27**) insertion into tetrahydrofuran (**4**), a new library of iridium(III) phebox and phebim catalysts were available. Initially, Dr. Clayton Owens found isopropyl-substituted phebim gave an optimal er of 80:20 (Table 3.7, entry 1).<sup>47</sup> Using both the phebox and phebim analogues for the optimal isobutyl- and methylene-cyclohexyl-substituted iridium(III) catalysts, phebox performed about significantly better than phebim (entries 2-5). However, both isobutyl-phebox and methylene-cyclohexyl iridium(III) phebox gave slightly lower enantioselectivity than isopropyl-phebox (entries 1, 3, and 5). The bulky indanyl-substituted iridium(III) phebox (Section 2.3.4) gave a slightly higher enantioselectivity than the isopropyl-substituted, but still did not reach the levels of enantioselectivity obtained with phthalan as substrate (entry 6). The contrast in the catalyst optimization of

tetrahydrofuran with the optimization of phthalan highlights the specificity of a particular catalyst structure to a class of substrates.

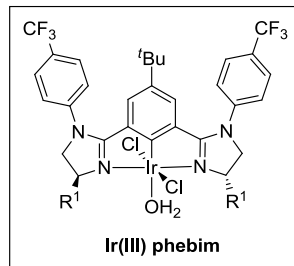
**Table 3.7.** Optimization of iridium(III) phebox- and phebox-catalyzed acceptor-only C–H functionalization of tetrahydrofuran (**4**) with ethyl diazoacetate (**27**).



entry	ligand	R <sup>1</sup>	yield (%) <sup>b</sup>	er
1 <sup>c</sup>	phebox	<sup>i</sup> Pr	51	80:20
2 <sup>c</sup>	phebim	<sup>t</sup> Bu	53	68:32
3	phebox	<sup>t</sup> Bu	30	79:21 <sup>d</sup>
4	phebim	CH <sub>2</sub> <sup>c</sup> Hex	14	68:32 <sup>d</sup>
5	phebox	CH <sub>2</sub> <sup>c</sup> Hex	22	77:23 <sup>d</sup>
6	phebox	indanyl	32	83:17 <sup>d</sup>



**Ir(III) phebox**



**Ir(III) phebox**

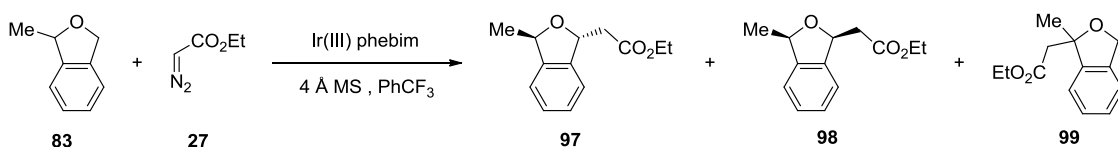
<sup>a</sup>General conditions: 0.29 M solution of ethyl diazoacetate in PhCF<sub>3</sub> was added over 5 h to a mixture of catalyst, substrate (4 equiv), and 4 Å MS in PhCF<sub>3</sub> at -10 °C <sup>b</sup>Isolated yield. <sup>c</sup>Result by Dr. Clay Owens. <sup>d</sup>Enantiomeric excess based on p-nitro-benzoate derivative.

### 3.2.6 Kinetic Resolution

In expanding the substrate scope of our acceptor-only carbene insertion, we sought to apply it in a kinetic resolution. Initial studies were conducted using 2-methyl-tetrahydrofuran, but the difficulty of isolation due to product volatility, as well as our growing success with phthalan derivatives, caused us to pursue 2-methyl-phthalan (**83**) as substrate. Standard insertion conditions followed by warming to room temperature overnight gave an optimal yield of 60 % of products **97**, **98**, and **99** in a ratio of 85:5:10

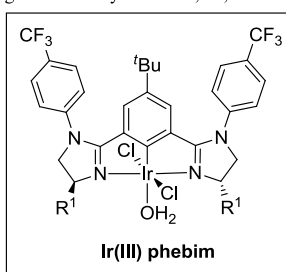
and an er of 88:12 of **97** (Table 3.8, entry 1). Increasing the catalyst loading to 2 mol % or doubling the equivalents of **83** resulted in a dramatic decrease in yield (entries 2 and 3). Using the isobutyl-substituted catalyst **61**, the yield was also considerably lower (entry 4). Conducting the reaction entirely at room temperature resulted primarily in carbene dimerization to form diethyl fumarate and diethyl maleate, with only trace product observed.

**Table 3.8.** Optimization of iridium(III) phebim-catalyzed kinetic resolution of 2-methylphthalan (**83**) with ethyl diazoacetate (**27**).



entry	R <sup>1</sup>	equiv <b>83</b>	catalyst loading (mol %)	T (°C)	GC ratio ( <b>97</b> : <b>98</b> : <b>99</b> )	yield (%) <sup>c</sup>	er <b>97</b>
1	CH <sub>2</sub> Cy	4	0.5	-10 to RT <sup>b</sup>	85:5:10	60	88:12
2	CH <sub>2</sub> Cy	4	2	-10	16:1:2	22 <sup>d</sup>	87:13
3	CH <sub>2</sub> Cy	8	0.5	-10	19:1:3	trace	-
4	<sup>t</sup> Bu	4	2	-10	17:1:2	18 <sup>d</sup>	87:13

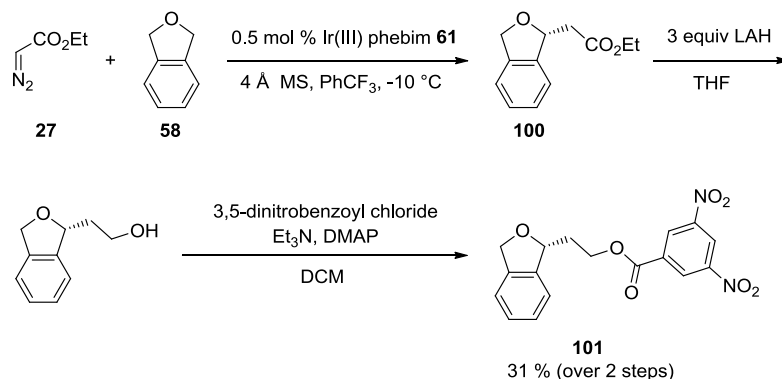
<sup>a</sup>General conditions: 0.29 M solution of ethyl diazoacetate in PhCF<sub>3</sub> was added over 5 h to a mixture of catalyst, substrate (4 equiv), and 4 Å MS in PhCF<sub>3</sub> at -10 °C <sup>b</sup>Allowed to warm to RT overnight. <sup>c</sup>Isolated yield of **97**, **98**, and **99**. <sup>d</sup>Significant dimer in reaction mixture.



### 3.2.7 Determination of Absolute Stereochemistry of C–H Insertion Products

Through most of our studies, the products of C–H insertion were colorless oils, rather than crystalline solids. For this reason, we initially sought to derivatize the phthalan insertion product **100** by reduction and acylation to form the 3,5-dinitrobenzoate **101** (Scheme 3.32). Unfortunately, **101** was an amorphous solid, and crystallization attempts were unsuccessful.

**Scheme 3.32.** Derivatization of insertion product **100** to form the 3,5-dinitrobenzoate **101**.



In the course of our studies of diazoacetate scope, the product of 4-trifluoromethyl-phenyl diazoacetate insertion was found to be crystalline (Table 3.4, entries 11 and 12). Though crystallization was possible, the trifluoromethyl group caused too much disorder for accurate determination of absolute stereochemistry. Fortunately, insertion with 4-methoxy-phenyl diazoacetate resulted in crystalline product **102**, and a

crystal structure was obtained with confidence in the absolute stereochemistry shown (Table 3.4, entries 9 and 10; Figure 3.4).

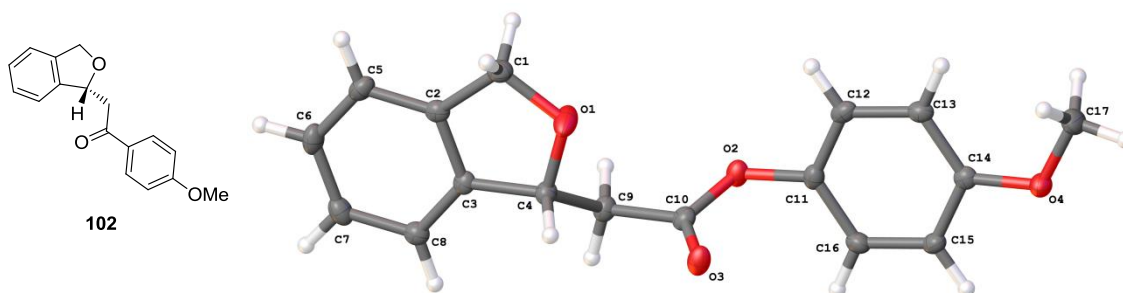


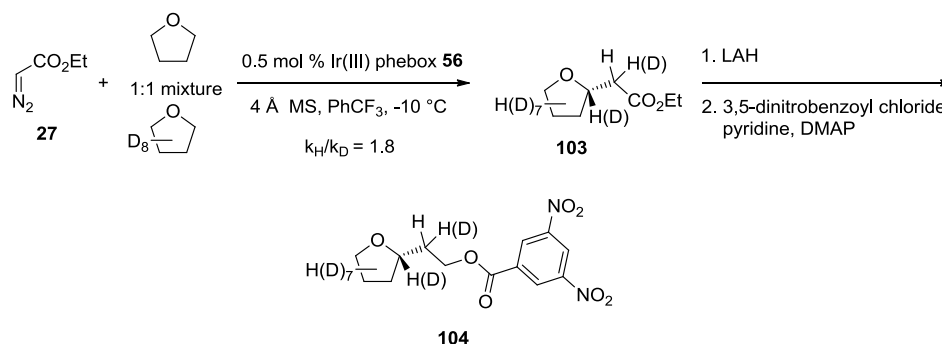
**Figure 3.4.** Crystal structure of 4-methoxy-phenyl diazoacetate insertion product **102**.<sup>55</sup>

### 3.2.8 Kinetic Isotope Effect of Ethyl Diazoacetate C–H Insertion into Tetrahydrofuran

Though extensive mechanistic studies were not undertaken to this point, a kinetic isotope effect was calculated for the insertion of ethyl diazoacetate (**27**) into tetrahydrofuran (**4**, Scheme 3.33). For calculation of the kinetic isotope effect (KIE) by  $^1\text{H}$  NMR, a 1:1 mixture of tetrahydrofuran and its fully deuterated analogue was exposed to ethyl diazoacetate and iridium(III) phebox **56** under standard conditions for C–H insertion.



**Scheme 3.33.** Kinetic isotope effect for ethyl diazoacetate (**27**) insertion into tetrahydrofuran (**4**).



For kinetic isotope effect calculations, the insertion product **103** was derivatized to the 3,5-dinitrobenzoate **104** to avoid concerns with the volatility of **103**. Based on the crude  $^1H$  NMR spectrum of the 3,5-dinitrobenzoate derivative **104**, 64 % of the product resulted from C–H insertion, while 36 % resulted from C–D insertion (Figure 3.5). Using the kinetic isotope effect formula of  $k_H/k_D = KIE$ , a kinetic isotope effect of 1.8 was calculated (0.64/0.36). This is in agreement with the kinetic isotope effect of 1.7 calculated previously by Dr. Clayton Owens using mass spectrometry analysis.<sup>47</sup> Both values are consistent with a concerted C–H insertion mechanism. The kinetic isotope effect for our system is very similar to those reported for the dirhodium tetracarboxylate-catalyzed donor/acceptor C–H insertion into cyclohexane (2.0) and tetrahydrofuran (3.0).<sup>67</sup>

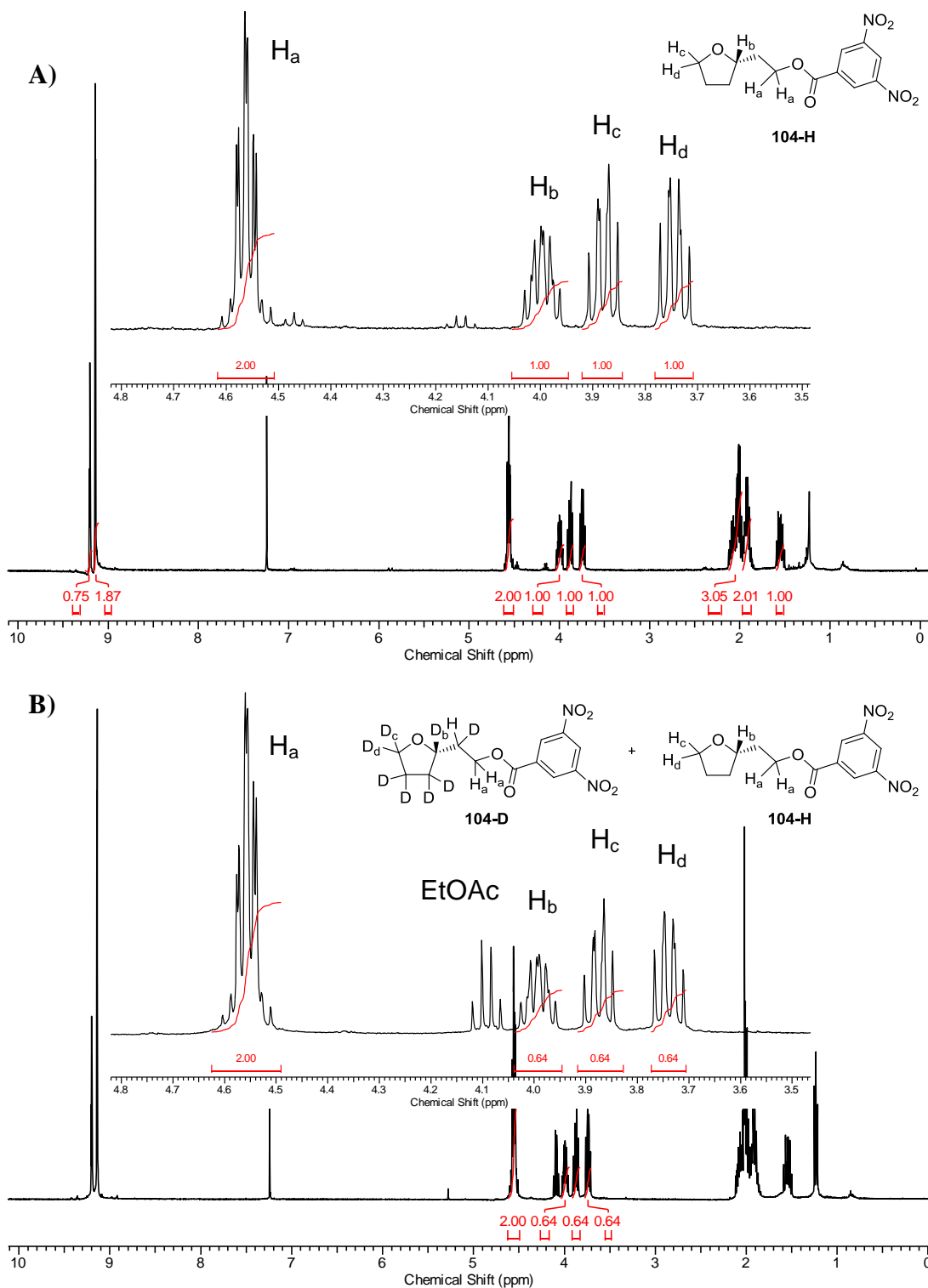


**Figure 3.5.**  $^1\text{H}$  NMR spectra for determination of kinetic isotope effect: **A)**  $^1\text{H}$  NMR spectrum of **104-H**; **B)**  $^1\text{H}$  NMR spectrum of kinetic isotope effect experiment.

**Calculations used for the determination of KIE value from  $^1\text{H}$  NMR analysis:**

$$H_a = 2.0$$

$$H_b = 0.64$$

$$D_b = 1 - 0.64 = 0.36$$

$$H_c = 0.64$$

$$D_c = 1 - 0.64 = 0.36$$

$$H_d = 0.64$$

$$D_d = 1 - 0.64 = 0.36$$

$$\% \text{ H incorporated} = 0.64 / 1.0 = 64 \%$$

$$\% \text{ D incorporated} = 0.36 / 1.0 = 36 \%$$

$$\mathbf{KIE} = k_H / k_D = 0.64 / 0.36 = \mathbf{1.8}$$

### 3.3 Conclusions

In conclusion, our study of the iridium(III) phebox and phevim catalyzed enantioselective C–H insertion of acceptor-only diazoacetates into phthalan derivatives represents the first enantioselective C–H insertion of this type. Catalyst optimization was guided by computational analysis and mathematical modeling, resulting in the optimal methylene-cyclohexyl substituted iridium(III) phevim catalyst **62**. Diazoacetate

substitution was found to have little effect on reaction yield and enantioselectivity. In contrast, substrate substitution was found to have a profound effect on selectivity.

To this point, when optimized conditions were applied in the enantioselective functionalization of tetrahydrofuran, the high enantioselectivity levels achieved with phthalan were not reached. In fact, ligand class and ligand substitution seemed to have a very different relationship to enantioselectivity with tetrahydrofuran. Tetrahydrofuran insertion still presents a difficulty and highlights the specificity of the iridium(III) phebim and phebox catalyst systems for a particular class of substrate. Mathematical modeling of insertion into tetrahydrofuran could be useful for increasing enantioselectivity. Further mechanistic studies could also help to elucidate the relationship between substrate and catalyst.

Development of new ligand and catalyst systems is also needed, not only for insertion into tetrahydrofuran, but also for enantioselective insertion with alkyl diazoacetates. Previous studies in our group established that our iridium(III) phebox catalyst family was not capable of insertion with alkyl diazoacetates, and competing  $\beta$ -hydride elimination was observed.<sup>47</sup> The relationship between catalyst structure and suppression of  $\beta$ -hydride elimination needs to be better understood.

The iridium(III) phebim catalyzed acceptor-only C–H insertion showcases the power of rational catalyst design in enantioselective group transfer reactions.

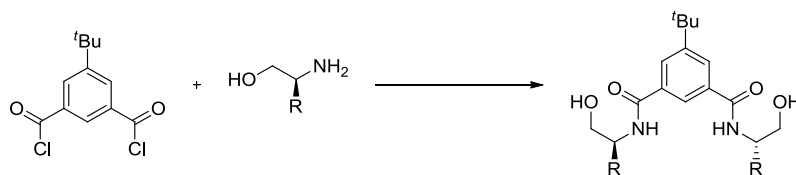
### 3.4 Experimental Procedures and Compound Characterization

#### General Considerations

$^1\text{H}$  and  $^{13}\text{C}$  NMR spectra were recorded on a Varian Inova 600 spectrometer (600 MHz  $^1\text{H}$ , 150 MHz  $^{13}\text{C}$ ) and a Varian Inova 400 spectrometer (400 MHz  $^1\text{H}$ , 100 MHz  $^{13}\text{C}$ ) at room temperature in  $\text{CDCl}_3$  (neutralized and dried with anhydrous  $\text{K}_2\text{CO}_3$ ) with internal  $\text{CHCl}_3$  as the reference (7.27 ppm for  $^1\text{H}$  and 77.23 ppm for  $^{13}\text{C}$ ) or  $(\text{CD}_3)_2\text{SO}$  with internal  $(\text{CH}_3)_2\text{SO}$  as the reference (2.50 ppm for  $^1\text{H}$  and 39.51 ppm for  $^{13}\text{C}$ ). Chemical shifts ( $\delta$  values) were reported in parts per million (ppm) and coupling constants ( $J$  values) in Hz. Multiplicity is indicated using the following abbreviations: s = singlet, d = doublet, t = triplet, q = quartet, qn = quintet, sext = sextet, m = multiplet, br = broad signal. ). Infrared (IR) spectra were recorded using Thermo Electron Corporation Nicolet 380 FT-IR spectrometer. High-resolution mass spectra were obtained using a Thermo Electron Corporation Finigan LTQFTMS (at the Mass Spectrometry Facility, Emory University). X-ray diffraction studies were carried out in the X-ray Crystallography Laboratory at Emory University on a Bruker Smart 1000 CCD diffractometer. Gas chromatography (GC) was carried out on an Agilent 6850 Network GC System equipped with a CHIRASIL-DEX CB column. High performance liquid chromatography (HPLC) was carried out on an Agilent 1100 Series equipped with Chirasil Chiralpak OJ-H and OD-H columns and a variable wavelength detector. We acknowledge the use of shared instrumentation provided by grants from the NIH and the

NSF. Analytical thin layer chromatography (TLC) was performed on precoated glass backed EMD 0.25 mm silica gel 60 plates. Visualization was accomplished with UV light or ethanolic anisaldehyde, followed by heating. Flash column chromatography was carried out using Silicycle® silica gel 60 (40-63  $\mu\text{m}$ ).

All reactions were conducted with anhydrous solvents in oven-dried and nitrogen-charged glassware. Anhydrous solvents were purified by passage through activated alumina using a *Glass Contours* solvent purification system unless otherwise noted.  $\text{PhCF}_3$  was dried over activated 4 Å molecular sieves and deoxygenated by bubbling through  $\text{N}_2$ . Solvents for workup, extraction and column chromatography were used as received from commercial suppliers. All reagents used were purchased from commercial vendors and used as received unless otherwise noted. Phthalan was obtained from Alfa Aesar or Sigma Aldrich and distilled before use. Ethyl diazoacetate (EDA) was obtained from Sigma Aldrich containing 14 % (w/w %) dichloromethane and used without further purification. 4 Å powdered molecular sieves were activated by heating to 100 ° C under reduced pressure (0.2 torr) for 12 hours. Pyridine and  $\text{Et}_3\text{N}$  were purified by distillation from calcium hydride.  $\text{IrCl}_3 \cdot 3\text{H}_2\text{O}$  and  $\text{IrBr}_3 \cdot 4\text{H}_2\text{O}$  were purchased from Strem. Amino alcohols were purchased from Sigma Aldrich or Combi-Blocks.



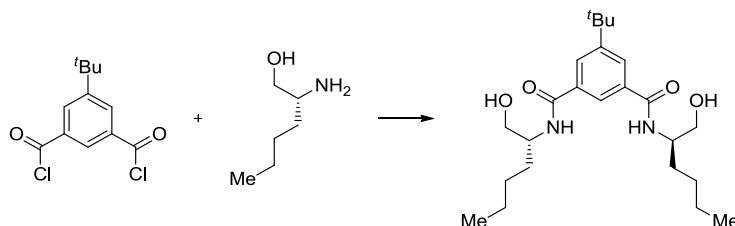
### General Procedure A

A procedure was adapted from the literature as follows:<sup>56</sup> A 0.5 M solution of 5-*tert*-butylisophthaloyl chloride (1.0 equiv.) in CH<sub>2</sub>Cl<sub>2</sub> was added dropwise to a 0 °C mixture of amino alcohol (2.0 equiv.) and Et<sub>3</sub>N (2.0 equiv.) in CH<sub>2</sub>Cl<sub>2</sub> (0.29 M). The reaction mixture was warmed to ambient temperature and stirred approximately 20 h. Water was added (5 mL/1 mmol acyl chloride), and the mixture was stirred for 10 minutes. The phases were separated and the organic phase was dried over Na<sub>2</sub>SO<sub>4</sub> and concentrated *in vacuo*. The resulting solid was purified as indicated to give the title amide.

### General Procedure B

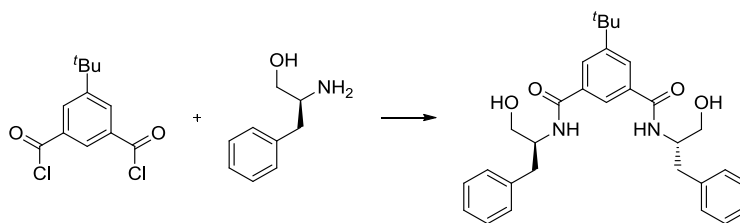
A procedure was adapted from the literature as follows:<sup>57</sup> A round bottom flask was charged with amino alcohol or amino alcohol·TFA salt (2.0 equiv) in isopropyl acetate (0.13 M in acyl chloride). The mixture was heated to 65 °C with vigorous stirring, and aqueous 1.5 M KHCO<sub>3</sub> (10 equiv.) was added. 5-*tert*-Butyl isophthaloyl dichloride (1.0 equiv) was added as a solid in three equal portions over the course of 30 minutes, and the mixture was aged at 65 °C for 12 h. The mixture was cooled to room temperature and poured into a separatory funnel. The phases were separated, and the aqueous phase was extracted with isopropyl acetate (3 x). The organics were combined, dried over

sodium sulfate, filtered, and concentrated *in vacuo*. The resulting solid was purified as indicated to give the title amide.



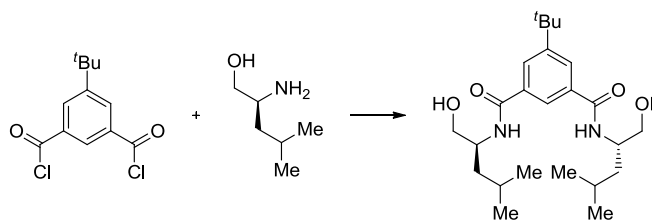
**5-(*tert*-butyl)-*N*1,*N*3-bis((*R*)-1-hydroxyhexan-2-yl)isophthalamide.** Prepared by general procedure **B** using 5-*tert*-butylisophthaloyl dichloride (504 mg, 2.0 mmol), (*R*)-2-amino-1-hexanol (509 mg, 4.3 mmol),  $\text{KHCO}_3$  (13 mL, 19.4 mmol). Mixed solvent recrystallization (EtOAc/hexanes) afforded the title compound as a white amorphous solid (463 mg, 57 %); **IR** (thin film,  $\text{cm}^{-1}$ ) 3294, 2957, 2871, 1633, 1537, 1460, 1260, 1063;  **$^1\text{H NMR}$**  (400 MHz,  $\text{CDCl}_3$ )  $\delta$  7.86-7.69 (m, 3H), 7.43 (d,  $J = 7.9$  Hz, 2H), 4.78 (br s, 2H), 4.11 (br s, 2H), 3.78-3.76 (m, 2H), 3.70-3.62 (m, 2H), 1.56-1.49 (m, 4H) 1.30-1.23 (m, 10H), 1.14 (s, 9H) 0.84 (t,  $J = 6.9$  Hz, 6H);  **$^{13}\text{C NMR}$**  (100 MHz,  $\text{CDCl}_3$ )  $\delta$  206.3, 168.8, 134.7, 127.5, 67.7, 64.9, 52.7, 35.0, 31.3, 28.6, 22.8, 14.2; **HMRS** (+APCI) calculated for  $\text{C}_{24}\text{H}_{40}\text{N}_2\text{O}_4\text{Na}$  443.2880, found 443.2880  $[\text{M}+\text{Na}]^+$ .  $[\alpha]_{\text{D}}^{20} +68.4^\circ$  ( $c$  1.0,  $\text{CHCl}_3$ ).





**5-(*tert*-butyl)-*N*1,*N*3-bis((*S*)-1-hydroxy-3-phenylpropan-2-yl)isophthalamide.**

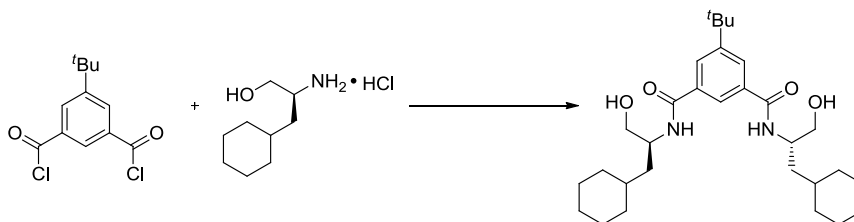
Prepared by general procedure **B** using 5-*tert*-butylisophthaloyl dichloride (500 mg, 1.9 mmol) in isopropyl acetate (1.5 mL, 0.13 M in acyl chloride), (*S*)-2-amino-3-phenyl-1-propanol (590 mg, 3.9 mmol), 1.5 M KHCO<sub>3</sub> (13 mL, 19.4 mmol). Mixed solvent recrystallization (EtOAc/hexanes) afforded the title compound as a white solid (703 mg, 74 %); **mp** 76-79 ° C; **IR** (thin film, cm<sup>-1</sup>) 3283, 2964, 1636, 1542, 1041; **<sup>1</sup>H NMR** (400 MHz, CDCl<sub>3</sub>) δ 7.73 (s, 1H), 7.61 (s, 2H), 7.28-7.19 (m, 10H), 7.08 (d, *J* = 12.8 Hz, 2H), 4.31 (br s, 2H), 3.76 (dd, *J* = 11.1, 2.9 Hz, 2H), 3.64 (dd, *J* = 11.6, 6.1 Hz, 2H), 2.96-2.86 (m, 4H), 1.15 (s, 9H); **<sup>13</sup>C NMR** (100 MHz, CDCl<sub>3</sub>) δ 172.5, 168.2, 151.9, 137.7, 134.4, 129.3, 128.6, 127.2, 126.6, 122.1, 63.6, 53.7, 37.1, 34.8, 30.9; **HMRS** (+NSI) calculated for C<sub>30</sub>H<sub>36</sub>N<sub>2</sub>O<sub>4</sub> 489.2748, found 489.2743 [M+H]<sup>+</sup>; [α]<sup>20</sup><sub>D</sub> -84.6 ° (c 1.0, CHCl<sub>3</sub>).



**5-(*tert*-butyl)-*N*1,*N*3-bis((*S*)-1-hydroxy-4-methylpentan-2-yl)isophthalamide.**

Prepared by general procedure **A** using 5-*tert*-butylisophthaloyl chloride (1.04 g,

4.0 mmol) in  $\text{CH}_2\text{Cl}_2$  (8 mL), (*S*)-leucinol (943 mg, 1.03 mL, 8.0 mmol), and  $\text{Et}_3\text{N}$  (1.16 mL, 8.0 mmol) in  $\text{CH}_2\text{Cl}_2$  (14 mL). Recrystallization from boiling  $\text{CH}_2\text{Cl}_2$  afforded the title amide as a white solid (1.36 g, 80 %); **mp** 161-164 ° C; **IR** (thin film,  $\text{cm}^{-1}$ ) 3291, 2957, 2870, 1637, 1543;  **$^1\text{H}$  NMR** (400 MHz,  $\text{CDCl}_3$ )  $\delta$  7.85 (bs, 1H), 7.77 (bs, 2H), 6.93 (bs, 2H), 4.28 (bs, 2H), 3.82 (dd,  $J = 11.3, 3.2$  Hz, 2H), 3.66 (dd,  $J = 11.0, 6.5$  Hz, 2H), 3.08-3.05 (m, 2H), 1.67 (dq,  $J = 13.6, 6.7$  Hz, 2H), 1.59-1.52 (m, 2H), 1.43-1.37 (m, 2H), 1.23 (s, 9H), 0.94 (d,  $J = 6.5$  Hz, 12H);  **$^{13}\text{C}$  NMR** (100 MHz,  $\text{CDCl}_3$ )  $\delta$  168.6, 154.9, 134.6, 127.1, 121.6, 65.5, 50.6, 40.2, 30.9, 25.0, 22.9, 22.4; **HRMS** [+APCI] calculated for  $\text{C}_{24}\text{H}_{41}\text{N}_2\text{O}_4$  421.3061, found 421.3060  $[\text{M}+\text{H}]^+$ ;  **$[\alpha]_D^{20}$**  -43.7 ° ( $c$  1.0,  $\text{CHCl}_3$ ).



**5-(*tert*-butyl)-*N*1,*N*3-bis((*S*)-1-cyclohexyl-3-hydroxypropan-2-yl)isophthalamide.**

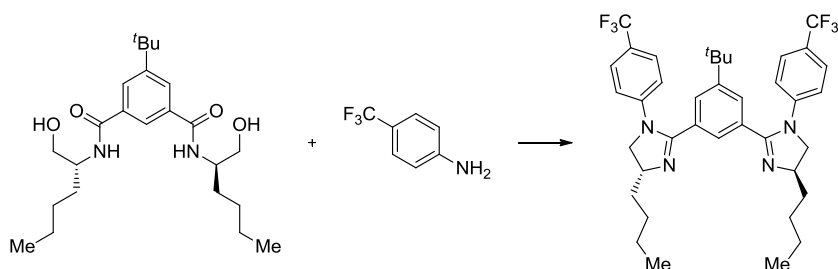
Prepared by general procedure **B** using (*S*)-2-amino-3-cyclohexylpropanol hydrochloride (1.08 g, 5.2 mmol, 2.0 equiv) in isopropyl acetate (20 mL, 0.13 M in acyl chloride), 1.5 M  $\text{KHCO}_3$  (17 mL, 26 mmol, 10 equiv), and 5-*tert*-butyl isophthaloyl dichloride (671 mg, 2.6 mmol, 1.0 equiv). Diethyl ether (40 mL) was added to the crude solid with stirring, and the solid was collected by vacuum filtration to give the title amide as a white solid (1.25 g, 96 %); **mp** 88-90 ° C; **IR** (thin film,  $\text{cm}^{-1}$ ) 3253, 2918, 2848, 1628, 1547, 1029, 902;  **$^1\text{H}$  NMR** (600 MHz,  $\text{CDCl}_3$ )  $\delta$  7.91 (d,  $J = 15.7$  Hz, 2H), 7.25 (s, 1H), 6.29

(d,  $J = 7.6$  Hz, 2H), 4.33-4.28 (m, 2H), 3.8 (dd,  $J = 11.0, 2.9$  Hz, 2H), 3.66 (dd,  $J = 11.0, 5.7$  Hz, 2H), 1.75-1.62 (m, 6H), 1.54-1.46 (m, 8H), 1.35 (s, 9H), 1.23-1.13 (m, 8H), 1.01-0.88 (m, 4H);  $^{13}\text{C}$  NMR (150 MHz,  $(\text{CD}_3)_2\text{SO}$ )  $\delta$  166.4, 151.1, 135.2, 126.9, 124.2, 64.3, 49.3, 35.2, 34.4, 34.0, 32.6, 31.5, 26.6, 26.2; HRMS [+APCI] calculated for  $\text{C}_{30}\text{H}_{49}\text{N}_2\text{O}_4$  501.3687, found 501.3685  $[\text{M}+\text{H}]^+$ ;  $[\alpha]_D^{20} -15.5^\circ$  ( $c$  0.5,  $\text{CHCl}_3$ ).

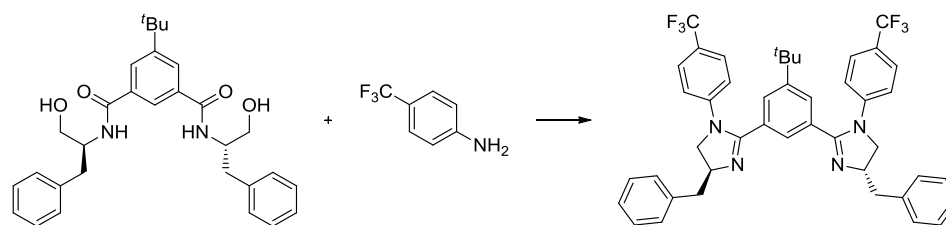


### General Procedure C

A procedure was adapted from the literature as follows:<sup>58</sup> A 10 mL flask was charged with amide (1.0 equiv) fitted with a reflux condenser, and evacuated and backfilled with dry nitrogen.  $\text{SOCl}_2$  (16 equiv) was added via syringe, and the mixture was refluxed for approximately 7 h. Excess  $\text{SOCl}_2$  was removed directly under high vacuum. The residue was dissolved in dry  $\text{CH}_2\text{Cl}_2$  (0.18 M) and cooled to  $0^\circ\text{C}$ .  $\text{Et}_3\text{N}$  (6.0 equiv) and the primary aniline (2.2 equiv) were added sequentially, and the mixture was stirred overnight at ambient temperature. 10 % aqueous  $\text{NaOH}$  (15 equiv) was added and stirred for 30 minutes. The phases were separated, and the aqueous phase was extracted with  $\text{CH}_2\text{Cl}_2$  (3 x). The combined organics were dried over  $\text{Na}_2\text{SO}_4$ , filtered, and concentrated *in vacuo*. The residue was purified by flash column chromatography on silica gel as indicated to give the title compound.



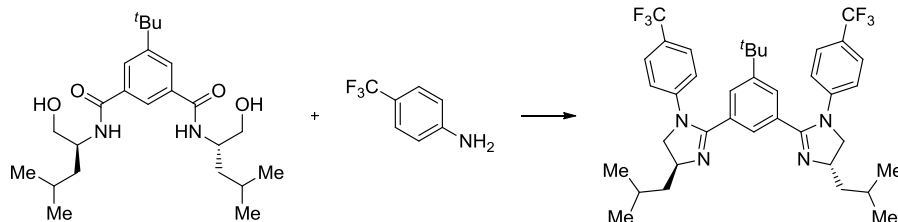
**(4R,4'R)-2,2'-(5-(*tert*-butyl)-1,3-phenylene)bis(4-butyl-1-(4-(trifluoromethyl)phenyl)-4,5-dihydro-1H-imidazole) (64).** Prepared according to general procedure **C** using 5-(*tert*-butyl)-*N*1,*N*3-bis((*R*)-1-hydroxyhexan-2-yl)isophthalamide (193 mg, 0.43 mmol), SOCl<sub>2</sub> (0.7 mL), Et<sub>3</sub>N (0.4 mL, 2.9 mmol), CH<sub>2</sub>Cl<sub>2</sub> (2.3 mL), 4-trifluoromethylaniline (0.12 mL, 0.96 mmol), and 10 % aq. NaOH (2.5 mL). Flash chromatography (EtOAc → 9:1 EtOAc:methanol) afforded the title ligand as an oil (110 mg, 38 %); **R<sub>f</sub>** 0.32 (9:1 EtOAc:methanol); **IR** (thin film, cm<sup>-1</sup>) 2962, 2933, 2873, 1612, 1522, 1323, 1123, 1070; **<sup>1</sup>H NMR** (400 MHz, CDCl<sub>3</sub>) δ 7.79 (s, 1H), 7.33 (d, *J* = 8.5 Hz, 4H), 7.24 (s, 2H), 6.72 (d, *J* = 8.2 Hz, 4H), 4.24-4.14 (m, 4H), 3.66 (t, *J* = 7.3 Hz, 2H), 1.83-1.77 (m, 2H), 1.59-1.52 (m, 2H), 1.43-1.33 (m, 8H), 0.94 (t, *J* = 4.9 Hz, 9H), 0.91 (t, *J* = 6.9 Hz, 6H); **<sup>13</sup>C NMR** (150 MHz, CDCl<sub>3</sub>) δ 159.6, 156.2, 151.0, 145.1, 130.9, 127.8, 126.4, 125.6, 121.0, 64.5, 58.0, 36.0, 34.5, 30.6, 30.5, 27.9, 22.7, 13.9; **HMRS** (+NSI) calculated for C<sub>38</sub>H<sub>45</sub>N<sub>4</sub>F<sub>6</sub> 671.3554, found 671.3550 [M+H]<sup>+</sup>; [**α**]<sub>D</sub><sup>20</sup> +8.1 ° (*c* 1.0, CHCl<sub>3</sub>).



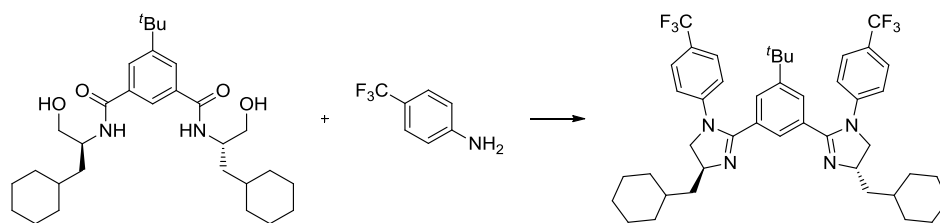
**(4*S*,4'*S*)-2,2'-(5-(*tert*-butyl)-1,3-phenylene)bis(4-benzyl-1-(4-**

**(trifluoromethyl)phenyl)-4,5-dihydro-1H-imidazole) (65).** Prepared according to

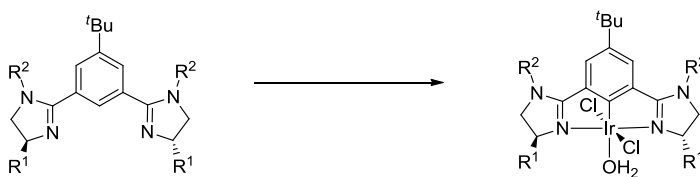
general procedure C, using 5-(*tert*-butyl)-*N*1,*N*3-bis((*S*)-1-hydroxy-3-phenylpropan-2-yl)isophthalamide (420 mg, 0.86 mmol), SOCl<sub>2</sub> (1.1 mL), Et<sub>3</sub>N (0.73 mL, 5.2 mmol), CH<sub>2</sub>Cl<sub>2</sub> (4.7 mL), 4-trifluoromethylaniline (0.25 mL, 2.0 mmol), and 10 % aq. NaOH (5 mL). Flash chromatography (EtOAc → 9:1 EtOAc:MeOH) afforded the title compound as a yellow amorphous solid (303 mg, 48 %); **R<sub>f</sub>** 0.24 (9:1 EtOAc:methanol); **IR** (thin film, cm<sup>-1</sup>) 2969, 2195, 1611, 1521, 1376, 1321, 1163; **<sup>1</sup>H NMR** (400 MHz, CDCl<sub>3</sub>) δ 7.72 (t, *J* = 1.5 Hz, 1H), 7.29 (dd, *J* = 4.9, 3.4 Hz, 6H), 7.21-7.15 (m, 10H), 6.54 (d, *J* = 8.5 Hz, 4H), 4.58-4.51 (m, 2H), 4.11 (t, *J* = 9.6 Hz, 2H), 3.70 (dd, *J* = 9.5, 6.1 Hz, 2H), 3.16 (dd, *J* = 13.7, 4.6 Hz, 2H), 2.81 (dd, *J* = 13.6, 8.1 Hz, 2H), 0.98 (s, 9H); **<sup>13</sup>C NMR** (100 MHz, CDCl<sub>3</sub>) δ 160.6, 151.5, 145.3, 137.9, 131.1, 129.7, 128.6, 128.1, 128.06, 126.7, 126.5, 125.8, 124.8, 124.5, 123.0, 121.3, 65.5, 57.3, 42.0, 34.8, 30.8; **HMRS** (+NSI) calculated for C<sub>44</sub>H<sub>41</sub>N<sub>4</sub>F<sub>6</sub> 739.3229, found 739.3227 [M+H]<sup>+</sup>; [α]<sub>D</sub><sup>20</sup> +164.4 ° (c 1.0, CHCl<sub>3</sub>).



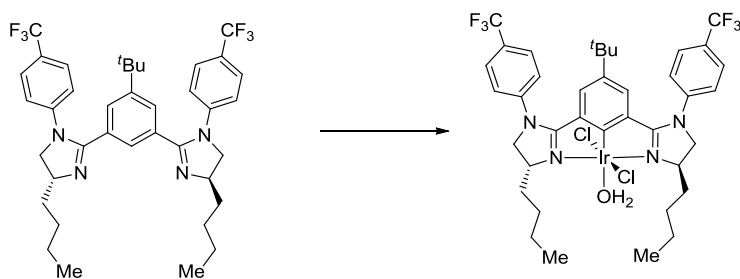
**(4*S*,4'*S*)-2,2'-(5-(*tert*-butyl)-1,3-phenylene)bis(4-isobutyl-1-(4-(trifluoromethyl)phenyl)-4,5-dihydro-1H-imidazole) (66).** Prepared by general procedure **C** using 5-(*tert*-butyl)-*N*1,*N*3-bis((*S*)-1-hydroxy-4-methylpentan-2-yl)isophthalamide (950 mg, 2.3 mmol), SOCl<sub>2</sub> (2.8 mL), Et<sub>3</sub>N (2.0 mL, 14.3 mmol), CH<sub>2</sub>Cl<sub>2</sub> (13 mL), 4-trifluoromethylaniline (180 mg, 1.12 mmol), and 10 % aq. NaOH (14 mL). Flash chromatography (4:5 EtOAc:hexanes) afforded the title ligand as a colorless oil (793 mg, 52 %); **R<sub>f</sub>** 0.66 (1:1 hexanes:EtOAc); **IR** (thin film) 2959, 2158, 2009, 1613, 1324, 1122, 750; **<sup>1</sup>H NMR** (400 MHz, CDCl<sub>3</sub>) δ 7.76 (s, 1H), 7.33 (d, *J* = 8.6 Hz, 4H), 7.24 (s, 2H), 6.71 (d, *J* = 8.6 Hz, 4H), 4.31-4.23 (m, 2H), 4.17 (t, *J* = 9.2 Hz, 2H), 3.63 (t, *J* = 8.2 Hz, 2H), 1.83 (dt, *J* = 13.3, 6.7 Hz, 2H), 1.74 (dt, *J* = 13.3, 6.7 Hz, 2H), 1.43-1.41 (m, 2H), 0.98-0.94 (m, 21H); **<sup>13</sup>C NMR** (100 MHz, CDCl<sub>3</sub>) δ 159.8, 151.2, 145.4, 131.1, 128.1, 126.7, 125.9, 121.1, 63.1, 58.8, 46.1, 34.7, 30.8, 25.5, 23.2, 22.8; **HRMS** [+NSI] calculated for C<sub>38</sub>H<sub>45</sub>N<sub>4</sub>F<sub>6</sub> 671.3543, found 671.3523 [M+H]<sup>+</sup>; [α]<sup>20</sup><sub>D</sub> -31.1 ° (*c* 1.0, CHCl<sub>3</sub>).



**(4*S*,4'*S*)-2,2'-(5-(*tert*-butyl)-1,3-phenylene)bis(4-(cyclohexylmethyl)-1-(4-(trifluoromethyl)phenyl)-4,5-dihydro-1*H*-imidazole) (67).** Prepared by general procedure **C** using 5-(*tert*-butyl)-*N*1,*N*3-bis((*S*)-1-cyclohexyl-3-hydroxypropan-2-yl)isophthalamide (130 mg, 0.26 mmol), SOCl<sub>2</sub> (0.31 mL), Et<sub>3</sub>N (0.4 mL, 2.9 mmol), CH<sub>2</sub>Cl<sub>2</sub> (1.4 mL), 4-trifluoromethylaniline (51 μL, 0.56 mmol), and 10 % aq. NaOH (1.5 mL). Flash chromatography (1:1 hexanes:EtOAc → 3:7 hexanes:EtOAc → EtOAc) afforded the title ligand as a white amorphous solid (123 mg, 63 %); **R<sub>f</sub>** 0.57 (3:7 hexanes/EtOAc); **IR** (thin film) 3843, 3019, 2344, 2147, 1710, 1214, 744; **<sup>1</sup>H NMR** (600 MHz, CDCl<sub>3</sub>) δ 7.80 (s, 1H), 7.32 (d, *J* = 8.6 Hz, 4H), 7.23 (t, *J* = 1.4 Hz, 2H), 6.71 (d, *J* = 8.6 Hz, 4H), 4.31 (dt, *J* = 15.9, 7.8 Hz, 2H), 4.17 (t, *J* = 9.3 Hz, 2H), 3.62 (t, *J* = 8.3 Hz, 2H), 1.82-1.73 (m, 6H), 1.72-1.63 (m, 8H), 1.50 (ddd, *J* = 10.6, 7.0, 3.8 Hz, 2H), 1.38 (dt, *J* = 13.6, 7.0 Hz, 2H), 1.28-1.23 (m, 4H), 1.19-1.15 (m, 2H) 1.00-0.96 (m, 4H), 0.93 (s, 9H); **<sup>13</sup>C NMR** (150 MHz, CDCl<sub>3</sub>) δ 159.7, 145.5, 131.3, 128.0, 126.7, 125.8, 121.1, 62.5, 58.9, 44.8, 34.9, 33.9, 33.5, 30.8, 26.8, 26.5; **HRMS** [+APCI] calculated for C<sub>44</sub>H<sub>53</sub>F<sub>6</sub>N<sub>4</sub> 751.4169, found 751.4172 [M+H]<sup>+</sup>; [α]<sub>D</sub><sup>20</sup> - 26.3 ° (*c* 1.0, CHCl<sub>3</sub>).



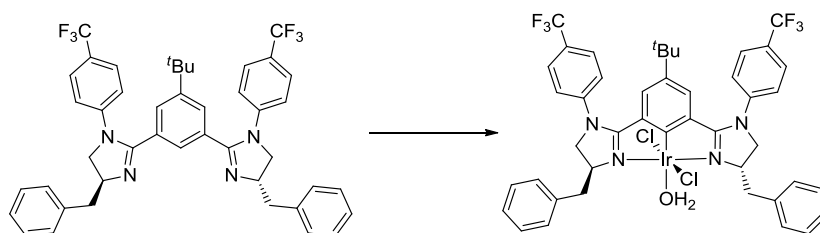
**General procedure D.** A procedure was adapted from the literature as follows:<sup>54</sup> a dry round bottom flask was charged with ligand (1.0 equiv.),  $\text{IrCl}_3 \cdot 3\text{H}_2\text{O}$  or  $\text{IrBr}_3 \cdot 4\text{H}_2\text{O}$  (1.1 equiv), and  $\text{NaHCO}_3$  (1.1 equiv). The flask was fitted with a reflux condenser and evacuated and backfilled with nitrogen. *i*PrOH (0.03 M) was added, and the mixture was refluxed until the ligand was consumed as judged by thin-layer chromatography. The reaction mixture was cooled to room temperature and concentrated *in vacuo*. The crude solid was purified by flash column chromatography on silica gel or by preparative thin layer chromatography as indicated to give the iridium(III) phebim complex.



**[(*R,R*)-*t*-ButylPhebim-4- $\text{CF}_3\text{Ph}$ -*n*-Bu]IrCl<sub>2</sub>(H<sub>2</sub>O) (**59**).** Prepared by general procedure **D** using **64** (110 mg, 0.16 mmol),  $\text{IrCl}_3 \cdot 3\text{H}_2\text{O}$  (65 mg, 0.18 mmol), and  $\text{NaHCO}_3$  (17 mg, 0.20 mmol). The reaction was refluxed in *i*PrOH (5 mL) for 5 h. Preparative thin layer chromatography (7:3 hexanes:EtOAc) afforded iridium(III) phebim **59** as an orange solid (83 mg, 55 %);  $R_f$  0.45 (7:3 hexanes:EtOAc);  $mp$  230 ° C; **IR** (thin film,  $\text{cm}^{-1}$ ) 3334, 2959, 2049, 1614, 1526, 1453, 1323, 1127, 1069; **<sup>1</sup>H NMR** (400 MHz,  $\text{CDCl}_3$ )  $\delta$  7.60 (d,

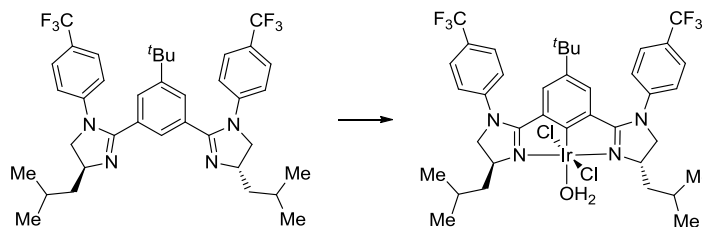


$J = 9.2$  Hz, 4H), 7.41 (d,  $J = 7.9$  Hz, 4H), 6.68 (s, 2H), 4.54 (t,  $J = 9.8$  Hz, 2H), 4.35 (br s, 2H), 4.07 (dd,  $J = 9.1, 6.7$  Hz, 2H), 2.15 (br s, 2H), 1.82-1.74 (m, 2H), 1.47-1.24 (m, 9H) 0.91-0.82 (m, 14H);  $^{13}\text{C}$  NMR (100 MHz,  $\text{CDCl}_3$ )  $\delta$  171.7, 145.9, 143.2, 131.9, 126.5, 126.4, 126.1, 126.0, 64.7, 59.0, 34.2, 30.9, 26.9, 22.5, 13.9; **HMRS** (+APCI) calculated for  $\text{C}_{38}\text{H}_{43}\text{Cl}_2\text{F}_6\text{N}_4\text{Ir}$  932.2393, found 932.2388  $[\text{M}-\text{H}_2\text{O}]^+$ ;  $[\alpha]_{\text{D}}^{20} -18.9^\circ$  ( $c$  0.1,  $\text{CHCl}_3$ ).

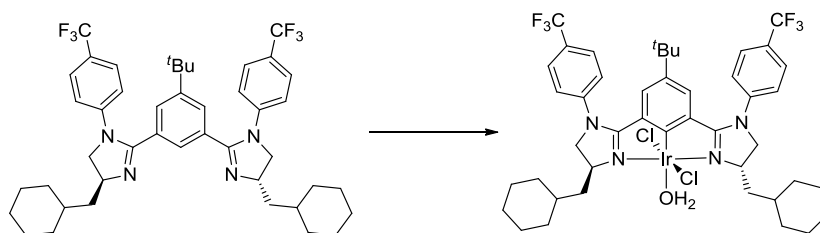


**[(*S,S*)-*t*-ButylPhebim-*p*-CF<sub>3</sub>Ph-Bn]IrCl<sub>2</sub>(H<sub>2</sub>O) (60)**. Prepared by general procedure D using ligand **65** (140 mg, 0.19 mmol), IrCl<sub>3</sub>·3H<sub>2</sub>O (78 mg, 0.22 mmol), and NaHCO<sub>3</sub> (18 mg, 0.22 mmol). The reaction was refluxed in *i*PrOH (6 mL) for 6 h. Preparative thin layer chromatography (7:3 hexanes:EtOAc) afforded iridium(III) phehim **60** as an orange solid (104 mg, 54 %);  $R_f$  0.41 (7:3 hexanes:EtOAc); **mp** 180 ° C; **IR** (thin film,  $\text{cm}^{-1}$ ) 3338, 2962, 2231, 2046, 1525, 1452, 1321, 1125, 1068;  $^1\text{H}$  NMR (400 MHz,  $\text{CDCl}_3$ )  $\delta$  7.69 (d,  $J = 8.6$  Hz, 4H), 7.39 (d,  $J = 8.2$  Hz, 4H), 7.35-7.32 (m, 4H), 7.29-7.23 (m, 6H), 6.71 (s, 2H), 4.63 (tdd,  $J = 7.1, 3.9$  Hz, 2H), 4.28 (t,  $J = 10.1$  Hz, 2H), 4.04 (dd,  $J = 9.9, 7.2$  Hz, 2H), 3.68 (dd,  $J = 14.0, 3.9$  Hz, 2H), 2.96 (dd,  $J = 14.0, 10.5$  Hz, 2H), 0.84 (s, 9H);  $^{13}\text{C}$  NMR (100 MHz,  $\text{CDCl}_3$ )  $\delta$  174.2, 172.2, 146.2, 136.5, 131.9, 129.3, 128.9, 126.9, 126.5, 126.4, 126.3, 126.2, 65.8, 58.7, 40.9, 34.6, 30.9; **HMRS** (+APCI)

calculated for  $C_{44}H_{38}ClF_6N_4Ir$  964.2313, found 964.2306  $[M-H_2O-Cl-H]^+$ ;  $[\alpha]_D^{20} + 20.5^\circ$  ( $c$  0.1,  $CHCl_3$ ).



**[(*S,S*)-*t*-ButylPhebim-4-CF<sub>3</sub>-Ph-*i*-Bu]IrCl<sub>2</sub>(H<sub>2</sub>O) (61)**. Prepared by general procedure **D** using ligand **66** (749 mg, 1.12 mmol), IrCl<sub>3</sub>·3H<sub>2</sub>O (445 mg, 1.23 mmol), and NaHCO<sub>3</sub> (103 mg, 1.23 mmol). The reaction was refluxed in *i*PrOH (37 mL) for 4.5 h. Flash chromatography (7:3 hexanes:EtOAc) afforded iridium(III) phebim **61** as a dark red solid (545 mg, 51 %);  $R_f$  0.56 (7:3 hexanes:EtOAc);  $mp$  218 ° C; **IR** (thin film,  $cm^{-1}$ ) 3734, 3045, 2357, 2024, 1699, 1558, 1226, 782, 694; **<sup>1</sup>H NMR** (400 MHz, CDCl<sub>3</sub>)  $\delta$  7.68 (d,  $J = 8.6$  Hz, 4H), 7.39 (d,  $J = 8.2$  Hz, 4H), 6.65 (s, 2H), 4.53 (t,  $J = 10.6$  Hz, 2H), 4.41-4.34 (m, 2H), 4.07 (dd,  $J = 9.2, 6.8$  Hz, 2H), 2.77 (s, 2H), 2.20-2.13 (m, 2H), 1.74-1.65 (m, 4H), 1.02 (t,  $J = 6.5$  Hz, 12H), 0.86 (s, 9H); **<sup>13</sup>C NMR** (150 MHz, CDCl<sub>3</sub>)  $\delta$  169.7, 144.4, 142.9, 132.2, 128.6, 126.4, 125.44, 125.31, 62.3, 60.0, 43.7, 34.4, 31.3, 25.7, 24.1, 21.8, 18.6; **HRMS** [+APCI] calculated for  $C_{38}H_{43}N_4Cl_2F_6Ir$  932.2393, found 932.2400  $[M-H_2O]^+$ ;  $[\alpha]_D^{20} + 15.9^\circ$  ( $c$  0.1,  $CHCl_3$ ).

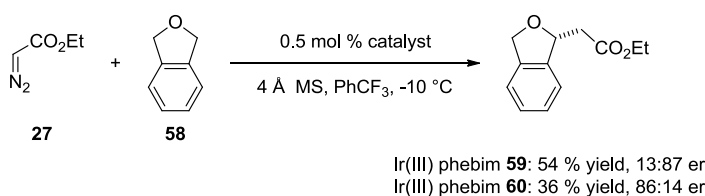


[(*S,S*)-*t*-ButylPhebim-4-CF<sub>3</sub>Ph-CH<sub>2</sub><sup>c</sup>Hex]IrCl<sub>2</sub>(H<sub>2</sub>O) (**62**). Prepared by general procedure **D** using ligand **67** (595 mg, 0.79 mmol), IrCl<sub>3</sub>·3H<sub>2</sub>O (314 mg, 0.89 mmol), and NaHCO<sub>3</sub> (75 mg, 0.89 mmol). The reaction was refluxed in *i*PrOH (26 mL) for 4.5 h. Flash chromatography (7:3 hexanes:EtOAc) afforded iridium(III) phebim **62** as a light orange solid (428 mg, 52 %); **R<sub>f</sub>** 0.63 (7:3 hexanes:EtOAc); **mp** 236 ° C; **IR** (thin film, cm<sup>-1</sup>) 3019, 2347, 2039, 1710, 1214, 745, 667; **<sup>1</sup>H NMR** (600 MHz, CDCl<sub>3</sub>) δ 7.68 (d, *J* = 8.4 Hz, 4H), 7.40 (d, *J* = 8.4 Hz, 4H), 6.70 (s, 2H), 4.56 (t, *J* = 9.7 Hz, 2H), 4.42-4.37 (m, 2H), 4.06 (dd, *J* = 9.0, 7.0 Hz, 2H), 2.20 (ddd, *J* = 13.6, 10.3, 2.7 Hz, 2H), 1.95 (br s, 2H), 1.87 (d, *J* = 12.8 Hz, 2H), 1.77-1.67 (m, 8H), 1.40-1.34 (m, 2H), 1.25-1.13 (m, 8H), 1.12-1.00 (m, 4H), 0.88 (s, 9H); **<sup>13</sup>C NMR** (150 MHz, CDCl<sub>3</sub>) δ 187.1, 169.6, 144.5, 143.1, 132.2, 126.5, 125.5, 125.4, 124.9, 123.1, 61.9, 60.2, 42.6, 35.4, 34.7, 34.6, 32.7, 31.4, 26.6, 26.5; **HRMS** [+APCI] calculated for C<sub>44</sub>H<sub>51</sub>N<sub>4</sub>Cl<sub>2</sub>F<sub>6</sub>Ir 1012.3019, found 1012.3025 [M-H<sub>2</sub>O]<sup>+</sup>; [**α**]<sub>D</sub><sup>20</sup> +24.2 ° (*c* 0.1, CHCl<sub>3</sub>).

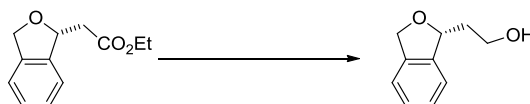
### General procedure E

A round bottom flask was charged with iridium phebim catalyst (0.5 mol % or 2 mol %, as indicated), 4Å molecular sieves and a stir bar, then evacuated and backfilled with N<sub>2</sub>. Substrate (4 equiv) and anhydrous PhCF<sub>3</sub> (1.7 M in substrate) were added via

syringe, and the reaction mixture was cooled to  $-10^{\circ}\text{C}$  in an ice/salt bath. A solution of ethyl diazoacetate (1 equiv, 13 % wt.  $\text{CH}_2\text{Cl}_2$ ) in anhydrous  $\text{PhCF}_3$  (0.29 M in diazoacetate) was added over 5 h via syringe pump. The temperature of the reaction mixture was maintained between  $-10^{\circ}\text{C}$  and  $-5^{\circ}\text{C}$ . After addition, once ethyl diazoacetate was completely consumed as judged by TLC, the mixture was concentrated *in vacuo*. The residue was purified as indicated to give the insertion product.

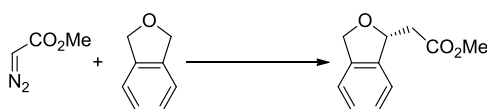


**Catalyst Optimization.** Prepared by general procedure **E** using ethyl diazoacetate (100 mg, 0.75 mmol) in  $\text{PhCF}_3$  (3 mL), phthalan (380  $\mu\text{L}$ , 3.52 mmol) in  $\text{PhCF}_3$  (2 mL), iridium(III) phebim catalyst **59** or **60** (0.5 mol %), and 4 Å MS (176 mg). Flash chromatography (8:2 pentane: $\text{Et}_2\text{O}$ ) afforded the title compound as a colorless oil in the yield and enantioselectivity indicated. Compound was confirmed by  $^1\text{H}$  NMR identical to the literature.<sup>47</sup>



**(R)-2-(1,3-Dihydroisobenzofuran-1-yl)ethanol.** A solution of **100** (0.44 mmol, 1.0 equiv) in THF (2 mL, 0.2 M) was cooled to  $0^{\circ}\text{C}$ . LAH (1.3 mL, 1 M in  $\text{Et}_2\text{O}$ , 3 equiv) was added dropwise. The reaction was warmed to room temperature. Once thin

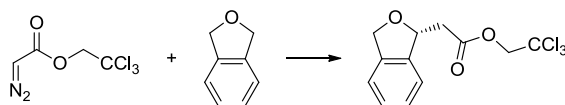
layer chromatography indicated complete consumption of starting material (1 h), the reaction mixture was poured into a vigorously stirring solution of Et<sub>2</sub>O and a saturated aqueous Rochelle's salt solution. Et<sub>2</sub>O was added and the resulting biphasic mixture was stirred vigorously for 3 h. The organic layer was separated, washed with brine, dried over MgSO<sub>4</sub> and concentrated *in vacuo*. Preparative thin layer chromatography (7:3 hexanes:EtOAc) afforded the title compound as a light yellow oil (62 mg, 86 %); **R<sub>f</sub>** 0.26 (7:3 hexanes:EtOAc); **IR** (thin film, cm<sup>-1</sup>) 3398, 2855, 1461, 1046, 725; **<sup>1</sup>H NMR** (600 MHz, CDCl<sub>3</sub>) δ 7.28-7.21 (m, 3H), 7.15-7.12 (m, 1H), 5.41 (dd, *J* = 8.8, 1.8 Hz, 1H), 5.13 (dd, *J* = 12.3, 2.3 Hz, 1H), 5.05 (dd, *J* = 12.3, 1.2 Hz, 1H), 3.88-3.82 (m, 2H), 2.76 (br s, 1H), 2.17-2.12 (m, 1H), 1.94-1.89 (m, 1H); **<sup>13</sup>C NMR** (150 MHz, CDCl<sub>3</sub>) δ 141.4, 138.9, 127.6, 127.4, 121.0, 120.9, 83.7, 72.5, 60.8, 37.8; **HRMS** [+NSI] calculated for C<sub>10</sub>H<sub>13</sub>O<sub>2</sub> 165.0910, found 165.0909 [M+H]<sup>+</sup>; **HPLC** (Daicel OJ-H, 5 % IPA:HEX, 1 mL/min), λ 210 nm, t<sub>R</sub>(maj) = 14.2 min, t<sub>R</sub>(min) = 15.9 min.



**(R)-Methyl 2-(1,3-dihydroisobenzofuran-1-yl)acetate.** Prepared by general procedure **E** using methyl diazoacetate<sup>68</sup> (57 mg, 0.57 mmol) in PhCF<sub>3</sub> (2 mL), phthalan (255 μL, 2.3 mmol) in PhCF<sub>3</sub> (1.3 mL), **61** (2.7 mg, 0.5 mol %), and 4Å MS (118 mg). Flash chromatography (8:2 pentane:Et<sub>2</sub>O) afforded the title compound as a colorless oil (79 mg, 72 % yield, 92:8 er). The title compound was subjected to the LAH reduction procedure above to give (*R*)-2-(1,3-dihydroisobenzofuran-1-yl)ethanol for HPLC analysis. **R<sub>f</sub>** 0.6

(7:3 pentane:Et<sub>2</sub>O); **IR** (thin film, cm<sup>-1</sup>) 2951, 2859, 1733, 1436, 1365, 1161, 1036, 750; **<sup>1</sup>H NMR** (400 MHz, CDCl<sub>3</sub>) δ 7.28-7.16 (m, 4H), 5.67-5.64 (m, 1H), 5.16-5.05 (m, 2H), 3.73 (d, *J* = 0.8 Hz, 3H), 2.83-2.69 (m, 2H); **<sup>13</sup>C NMR** (150 MHz, CDCl<sub>3</sub>) δ 171.3, 140.6, 139.1, 127.9, 127.4, 121.1, 80.3, 72.7, 51.8, 41.4; **HRMS** [+NSI] calculated for C<sub>11</sub>H<sub>13</sub>O<sub>3</sub> 193.0859, found 193.0858 [M+H]<sup>+</sup>; [α]<sub>D</sub><sup>20</sup> +45.8 ° (*c* 1.0, CHCl<sub>3</sub>).

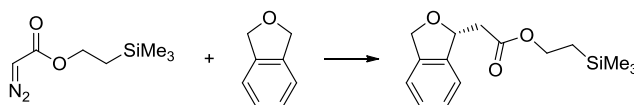
**(R)-Methyl 2-(1,3-dihydroisobenzofuran-1-yl)acetate.** Prepared by general procedure **E** using methyl diazoacetate<sup>68</sup> (56 mg, 0.55 mmol) in PhCF<sub>3</sub> (2 mL), phthalan (255 μL, 2.3 mmol) in PhCF<sub>3</sub> (1.3 mL), **62** (3 mg, 0.5 mol %), and 4 Å MS (118 mg). Flash chromatography (8:2 pentane:Et<sub>2</sub>O) afforded the title compound as a colorless oil (73 mg, 69 % yield, 94:6 er). Compound was confirmed by <sup>1</sup>H NMR identical to above. The title compound was subjected to the LAH reduction procedure above to give (*R*)-2-(1,3-dihydroisobenzofuran-1-yl)ethanol for HPLC analysis.



**(R)-2,2,2-Trichloroethyl 2-(1,3-dihydroisobenzofuran-1-yl)acetate (70).** Prepared by general procedure **E** using trichloroethyl diazoacetate (76 mg, 0.35 mmol) in PhCF<sub>3</sub> (1.2 mL), phthalan (155 μL, 1.57 mmol) in PhCF<sub>3</sub> (0.8 mL), **61** (7 mg, 2 mol %), and 4 Å MS (80 mg). Flash chromatography (95:5 pentane:Et<sub>2</sub>O) afforded the title compound as a colorless oil (90 mg, 84 % yield, 94:6 er). The title compound was subjected to the LAH reduction procedure above to give (*R*)-2-(1,3-dihydroisobenzofuran-1-yl)ethanol for HPLC analysis. **R<sub>f</sub>** 0.28 (95:5 pentane:Et<sub>2</sub>O); **IR** (thin film, cm<sup>-1</sup>) 3019, 2361, 1754,

1148, 1039, 749;  $^1\text{H NMR}$  (400 MHz,  $\text{CDCl}_3$ )  $\delta$  7.30-7.20 (m, 4H), 5.7 (td,  $J = 5.1$ , 2.3 Hz, 1H), 5.17 (dd,  $J = 12.1$ , 2.0 Hz, 1H), 5.08 (dd,  $J = 12.1$ , 1.6 Hz, 1H), 4.83 (dd,  $J = 12.1$ , 2.4 Hz, 1H), 4.75 (dd,  $J = 11.7$ , 2.4 Hz, 1H), 2.97 (dd,  $J = 16.0$ , 4.7 Hz, 1H), 2.88 (dd,  $J = 16.0$ , 8.2 Hz, 1H);  $^{13}\text{C NMR}$  (150 MHz,  $\text{CDCl}_3$ )  $\delta$  169.2, 140.1, 139.1, 128.0, 127.5, 121.2, 121.1, 94.7, 79.7, 74.1, 72.8, 41.2; **HRMS** [+NSI] calculated for  $\text{C}_{12}\text{H}_{12}\text{O}_3\text{Cl}_3$  308.9847, found 308.9848  $[\text{M}+\text{H}]^+$ ;  $[\alpha]_{\text{D}}^{20} +35.2^\circ$  ( $c$  1.0,  $\text{CHCl}_3$ ).

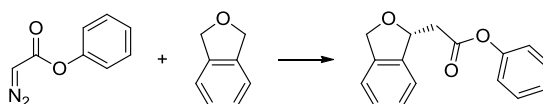
**(R)-2,2,2-Trichloroethyl 2-(1,3-dihydroisobenzofuran-1-yl)acetate (61)**. Prepared by general procedure **E** using trichloroethyl diazoacetate (76 mg, 0.35 mmol) in  $\text{PhCF}_3$  (1.2 mL), phthalan (155  $\mu\text{L}$ , 1.57 mmol) in  $\text{PhCF}_3$  (0.8 mL), **62** (7 mg, 2 mol %), and 4 Å MS (80 mg). Flash chromatography (95:5 pentane: $\text{Et}_2\text{O}$ ) afforded the title compound as a colorless oil (77 mg, 71 % yield, 95:5 er). Compound was confirmed by  $^1\text{H NMR}$  identical to above. The title compound was subjected to the LAH reduction procedure above to give (*R*)-2-(1,3-dihydroisobenzofuran-1-yl)ethanol for HPLC analysis.



**(R)-2-(Trimethylsilyl)ethyl 2-(1,3-dihydroisobenzofuran-1-yl)acetate**. Prepared by general procedure **E** using trimethylsilyl ethyl diazoacetate (66 mg, 0.35 mmol) in  $\text{PhCF}_3$  (1.2 mL), phthalan (155  $\mu\text{L}$ , 1.57 mmol) in  $\text{PhCF}_3$  (0.8 mL), **61** (7 mg, 2 mol %), and 4 Å MS (80 mg). Flash chromatography (95:5 pentane: $\text{Et}_2\text{O}$ ) afforded the title compound as a colorless oil (60 mg, 62 % yield, 93:7 er). The title compound was subjected to the LAH reduction procedure above to give (*R*)-2-(1,3-dihydroisobenzofuran-1-yl)ethanol for

HPLC analysis.  $R_f$  0.24 (95:5 pentane:Et<sub>2</sub>O); **IR** (thin film, cm<sup>-1</sup>) 2953, 2897, 1729, 1248, 1158, 1038, 833, 749; **<sup>1</sup>H NMR** (600 MHz, CDCl<sub>3</sub>)  $\delta$  7.28-7.17 (m, 4H), 5.67-5.64 (m, 1H), 5.16-5.04 (m, 2H), 4.22 (td,  $J = 8.6, 2.3$  Hz, 2H), 2.77 (dd,  $J = 15.7, 4.7$  Hz, 1H), 2.71 (dd,  $J = 15.7, 7.8$  Hz, 1H), 1.01-0.97 (m, 2H) 0.03 (s, 9H); **<sup>13</sup>C NMR** (150 MHz, CDCl<sub>3</sub>)  $\delta$  170.9, 140.7, 139.2, 127.8, 127.4, 121.1, 121.0, 80.3, 72.7, 62.9, 41.8, 17.3, -1.5; **HRMS** [+NSI] calculated for C<sub>15</sub>H<sub>23</sub>O<sub>3</sub>Si 279.1411, found 279.1414 [M+H]<sup>+</sup>;  $[\alpha]_D^{20} +39.3^\circ$  ( $c$  1.0, CHCl<sub>3</sub>).

**(R)-2-(trimethylsilyl)ethyl 2-(1,3-dihydroisobenzofuran-1-yl)acetate.** Prepared by general procedure **E** using trimethylsilyl ethyl diazoacetate (66 mg, 0.35 mmol) in PhCF<sub>3</sub> (1.2 mL), phthalan (154  $\mu$ L, 1.57 mmol) in PhCF<sub>3</sub> (0.8 mL), **62** (7 mg, 2 mol %), and 4 Å MS (80 mg). Flash chromatography (95:5 pentane/Et<sub>2</sub>O) afforded the title compound as a colorless oil (66 mg, 67 % yield, 94:6 er). Compound was confirmed by <sup>1</sup>H NMR identical to above. The title compound was subjected to the LAH reduction procedure above to give (*R*)-2-(1,3-dihydroisobenzofuran-1-yl)ethanol for HPLC analysis.

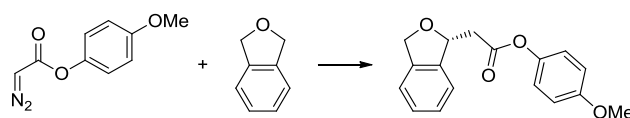


**(R)-Phenyl 2-(1,3-dihydroisobenzofuran-1-yl)acetate.** Prepared by general procedure **E** using phenyl diazoacetate<sup>69</sup> (57 mg, 0.35 mmol) in PhCF<sub>3</sub> (1.2 mL), phthalan (154  $\mu$ L, 1.57 mmol) in PhCF<sub>3</sub> (0.8 mL), **61** (7 mg, 2 mol %), and 4 Å MS (80 mg). Flash chromatography (8:2 pentane:Et<sub>2</sub>O) afforded the title compound as a white solid (58 mg, 65 % yield, 91:9 er). The title compound was subjected to the LAH reduction procedure



above to give (*R*)-2-(1,3-dihydroisobenzofuran-1-yl)ethanol for HPLC analysis. **R<sub>f</sub>** 0.35 (8:2 hexanes:EtOAc); **mp** 46-48 ° C; **IR** (thin film, cm<sup>-1</sup>) 3019, 2362, 1753, 1592, 1492, 1214, 1140, 919, 750; **<sup>1</sup>H NMR** (600 MHz, CDCl<sub>3</sub>) δ 7.39-7.19 (m, 7H), 7.07-7.04 (m, 2H), 5.78-5.75 (m, 1H), 5.22-5.09 (m, 2H), 3.06 (dd, *J* = 15.7, 4.7 Hz, 1H), 2.98 (dd, *J* = 15.7, 7.4 Hz, 1H); **<sup>13</sup>C NMR** (150 MHz, CDCl<sub>3</sub>) δ 172.5, 169.3, 158.3, 150.5, 140.4, 139.2, 129.4, 128.0, 127.5, 128.9, 121.5, 121.2, 121.1, 80.3, 72.9, 41.7; **HRMS** [+NSI] calculated for C<sub>16</sub>H<sub>15</sub>O<sub>3</sub> 255.1016, found 255.1014 [M+H]<sup>+</sup>; **[α]<sub>D</sub><sup>20</sup>** + 34.0 ° (*c* 1.0, CHCl<sub>3</sub>).

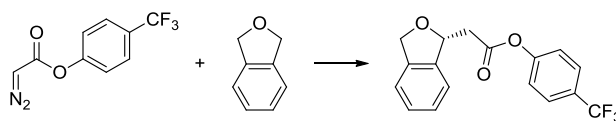
**(*R*)-Phenyl 2-(1,3-dihydroisobenzofuran-1-yl)acetate.** Prepared by general procedure **E** using phenyl diazoacetate<sup>69</sup> (57 mg, 0.35 mmol) in PhCF<sub>3</sub> (1.2 mL), phthalan (154 μL, 1.57 mmol) in PhCF<sub>3</sub> (0.8 mL), **62** (7 mg, 2 mol %), and 4 Å MS (80 mg). Flash chromatography (8:2 pentane:Et<sub>2</sub>O) afforded the title compound as a white solid (61 mg, 68 % yield, 93:7 er). Compound was confirmed by <sup>1</sup>H NMR identical to above. The title compound was subjected to the LAH reduction procedure above to give (*R*)-2-(1,3-dihydroisobenzofuran-1-yl)ethanol for HPLC analysis.



**(*R*)-4-Methoxyphenyl 2-(1,3-dihydroisobenzofuran-1-yl)acetate (102).** Prepared by general procedure **E** using 4-methoxy-phenyl diazoacetate<sup>70</sup> (68 mg, 0.35 mmol) in PhCF<sub>3</sub> (1.2 mL), phthalan (154 μL, 1.57 mmol) in PhCF<sub>3</sub> (0.8 mL), **61** (7 mg, 2 mol %), and 4 Å MS (80 mg). Flash chromatography (8:2 pentane:Et<sub>2</sub>O) afforded the title

compound as a white solid (57 mg, 57 % yield, 91:9 er). The title compound was subjected to the LAH reduction procedure above to give (*R*)-2-(1,3-dihydroisobenzofuran-1-yl)ethanol for HPLC analysis. **R<sub>f</sub>** 0.45 (7:3 hexanes:EtOAc); **mp** 44-47 ° C; **IR** (thin film, cm<sup>-1</sup>) 3019, 2361, 1751, 1506, 1214, 920, 748; **<sup>1</sup>H NMR** (600 MHz, CDCl<sub>3</sub>) δ 7.31-7.26 (m, 4H), 6.98-6.95 (m, 2H), 6.87-6.84 (m, 2H), 5.76-5.74 (m, 1H), 5.19 (dd, *J* = 11.9, 2.6 Hz, 1H), 5.1 (d, *J* = 11.9 Hz, 1H), 3.78 (s, 3H), 3.02 (dd, *J* = 15.4, 4.8 Hz, 1H), 2.95 (dd, *J* = 15.4, 7.5 Hz, 1H); **<sup>13</sup>C NMR** (150 MHz, CDCl<sub>3</sub>) δ 172.5, 169.6, 157.2, 144.0, 140.4, 139.2, 128.0, 127.5, 122.3, 121.2, 121.1, 114.4, 80.3, 72.8, 55.6, 41.6; **HRMS** [+NSI] calculated for C<sub>17</sub>H<sub>17</sub>O<sub>4</sub> 285.1121, found 285.1118 [M+H]<sup>+</sup>; [**α**]<sub>D</sub><sup>20</sup> +36.1 ° (*c* 1.0, CHCl<sub>3</sub>).

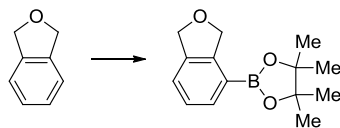
**(*R*)-4-Methoxyphenyl 2-(1,3-dihydroisobenzofuran-1-yl)acetate (102)**. Prepared by general procedure **E** using 4-methoxy-phenyl diazoacetate<sup>70</sup> (68 mg, 0.35 mmol) in PhCF<sub>3</sub> (1.2 mL), phthalan (154 μL, 1.57 mmol) in PhCF<sub>3</sub> (0.8 mL), **62** (7 mg, 2 mol %), and 4 Å MS (80 mg). Flash chromatography (8:2 pentane:Et<sub>2</sub>O) afforded the title compound as a white solid (70 mg, 70 % yield, 92:8 er). Compound was confirmed by <sup>1</sup>H NMR identical to above. The title compound was subjected to the LAH reduction procedure above to give (*R*)-2-(1,3-dihydroisobenzofuran-1-yl)ethanol for HPLC analysis.



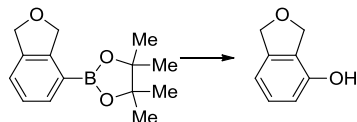
**(R)-4-(Trifluoromethyl)phenyl 2-(1,3-dihydroisobenzofuran-1-yl)acetate.** Prepared by general procedure **E** using 4-trifluoromethyl-phenyl diazoacetate (81 mg, 0.35 mmol) in PhCF<sub>3</sub> (1.2 mL), phthalan (154 μL, 1.57 mmol) in PhCF<sub>3</sub> (0.8 mL), **61** (7 mg, 2 mol %), and 4 Å MS (80 mg). Flash chromatography (9:1 pentane:Et<sub>2</sub>O) afforded the title compound as a white solid (88 mg, 78 % yield, 90:10 er). The title compound was subjected to the LAH reduction procedure above to give (*R*)-2-(1,3-dihydroisobenzofuran-1-yl)ethanol for HPLC analysis. **R<sub>f</sub>** 0.5 (8:2 hexanes:EtOAc); **mp** 70-72 ° C; **IR** (thin film, cm<sup>-1</sup>) 3019, 2925, 2363, 1710, 1362, 1214, 922, 754; **<sup>1</sup>H NMR** (600 MHz, CDCl<sub>3</sub>) δ 7.62 (d, *J* = 8.2 Hz, 2H), 7.33-7.28 (m, 2H), 7.27-7.25 (m, 2H), 7.17 (d, *J* = 8.2 Hz, 2H), 5.77-5.74 (m, 1H), 5.19 (dd, *J* = 12.3, 2.9 Hz, 1H), 5.11 (d, *J* = 12.3 Hz, 1H), 3.08 (dd, *J* = 15.2, 4.1 Hz, 1H), 2.98 (dd, *J* = 15.2, 8.2 Hz, 1H); **<sup>13</sup>C NMR** (150 MHz, CDCl<sub>3</sub>) δ 168.8, 156.4, 153.0, 140.0, 139.2, 128.1, 127.6, 126.8, 122.1, 121.2, 121.1, 115.4, 80.2, 72.9, 41.6, 29.7; **HRMS** [+NSI] calculated for C<sub>17</sub>H<sub>14</sub>O<sub>3</sub>F<sub>3</sub> 323.0890, found 323.0890 [M+H]<sup>+</sup>; [α]<sub>D</sub><sup>20</sup> + 7.7 ° (*c* 1.0, CHCl<sub>3</sub>).

**(R)-4-(Trifluoromethyl)phenyl 2-(1,3-dihydroisobenzofuran-1-yl)acetate.** Prepared by general procedure **E** using 4-trifluoromethyl-phenyl diazoacetate (81 mg, 0.35 mmol) in PhCF<sub>3</sub> (1.2 mL), phthalan (154 μL, 1.57 mmol) in PhCF<sub>3</sub> (0.8 mL), **62** (7 mg, 2 mol %), and 4 Å MS (80 mg). Flash chromatography (9:1 pentane:Et<sub>2</sub>O) afforded the title compound as a white solid (78 mg, 69 % yield, 92:8 er). Compound was confirmed by <sup>1</sup>H NMR identical to above. The title compound was subjected to the LAH reduction

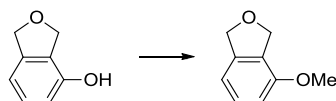
procedure above to give (*R*)-2-(1,3-dihydroisobenzofuran-1-yl)ethanol for HPLC analysis.



**2-(1,3-Dihydroisobenzofuran-4-yl)-4,4,5,5-tetramethyl-1,3,2-dioxaborolane (76).** An oven-dried flask equipped with a reflux condenser was charged with phthalan (2.4 mL, 21.9 mmol, 1 equiv), [Ir(OMe)(cod)]<sub>2</sub> (39 mg, 0.06 mmol, 0.25 mol %), 3,4,7,8-tetramethyl-1,10-phenanthroline (62 mg, 0.26 mmol, 1 mol %), and bis(pinacolato)diboron (4.2 g, 16.7 mmol, 0.75 equiv) in tetrahydrofuran (108 mL). The mixture was heated to reflux for 22 h with vigorous stirring. The reaction mixture was cooled to room temperature and filtered through silica gel. The filtrate was concentrated *in vacuo* and flash chromatography (95:5 hexanes:EtOAc) afforded the title compound as a white solid (1.7 g, 32 %); **R<sub>f</sub>** 0.55 (9:1 hexanes/EtOAc); **mp** 74-76 ° C; **IR** (thin film, cm<sup>-1</sup>) 2978, 2857, 1603, 1350, 1129, 1047, 967; **<sup>1</sup>H NMR** (400 MHz, CDCl<sub>3</sub>) δ 7.68 (d, *J* = 7.0 Hz, 1H), 7.31 (d, *J* = 7.4 Hz, 1H), 7.27-7.23 (m, 1H), 5.23 (t, *J* = 2.0 Hz, 2H), 5.11-5.09 (m, 2H), 1.31 (s, 12H); **<sup>13</sup>C NMR** (100 MHz, CDCl<sub>3</sub>) δ 146.1, 138.2, 133.9, 126.5, 123.6, 83.8, 74.8, 73.2, 24.9; **HRMS** [+NSI] calculated for C<sub>14</sub>H<sub>19</sub>O<sub>3</sub>BNa 269.1319, found 269.1319 [M+Na]<sup>+</sup>.

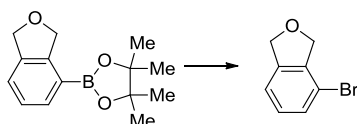


**1,3-Dihydroisobenzofuran-4-ol (79).** H<sub>2</sub>O<sub>2</sub> (5 ml, 30 wt. % in H<sub>2</sub>O) was added to a solution of **76** (1.7 g, 6.9 mmol, 1 equiv) in H<sub>2</sub>O (5 mL) at room temperature. The reaction was stirred until thin layer chromatography indicated complete consumption of starting material (1 h). The mixture was transferred to a separatory funnel and the aqueous layer was extracted with CH<sub>2</sub>Cl<sub>2</sub> (3 x). The combined organic extracts were washed with brine, dried over MgSO<sub>4</sub> and concentrated *in vacuo*. Flash chromatography (7:3 hexanes:EtOAc) afforded the title compound as a white solid (518 mg, 55 %); <sup>1</sup>H NMR (400 MHz, CDCl<sub>3</sub>) δ 7.14-7.11 (m, 2H), 6.8 (d, *J* = 7.6 Hz, 1H), 6.63 (d, *J* = 8.2 Hz, 1H), 5.11 (d, *J* = 2.9 Hz, 4H). All spectral data matched those previously reported.<sup>71</sup>

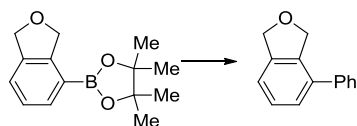


**4-Methoxy-1,3-dihydroisobenzofuran (80).** An oven-dried round bottom flask was charged with **79** (518 mg, 3.8 mmol, 1 equiv) and K<sub>2</sub>CO<sub>3</sub> (1.06 g, 7.7 mmol, 2 equiv) in MeCN (15 mL). MeI (390 μL, 6.3 mmol, 1.6 equiv) was added via syringe. The reaction mixture was heated to 35 ° C. Once thin layer chromatography indicated complete consumption of starting material (24 h), the reaction was quenched by the addition of NH<sub>4</sub>Cl (aq). The biphasic mixture was transferred to a separatory funnel and the aqueous layer was extracted with CH<sub>2</sub>Cl<sub>2</sub> (3 x). The combined organic extracts were washed with

brine, dried over  $\text{MgSO}_4$  and concentrated *in vacuo*. Flash chromatography (8:2 pentane:Et<sub>2</sub>O) afforded the title compound as a white solid (484 mg, 85 %); <sup>1</sup>H NMR (400 MHz, CDCl<sub>3</sub>)  $\delta$  7.24-7.21 (m, 1H), 6.81 (d,  $J = 7.5$  Hz, 1H), 6.72 (d,  $J = 8.3$  Hz, 1H), 5.09 (s, 4H), 3.82-3.81 (m, 3H). All spectral data matched those previously reported.<sup>72</sup>

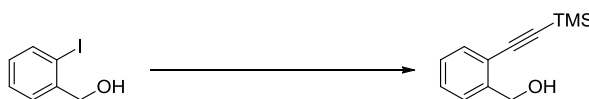


**4-Bromo-1,3-dihydroisobenzofuran (81).** Prepared according to literature procedure<sup>64</sup> using **76** (740 mg, 3.0 mmol),  $\text{CuBr}_2$  (2 g, 9.0 mmol), MeOH (38 mL), and H<sub>2</sub>O (38 mL). After heating for 6 h, flash chromatography (95:5 hexanes:EtOAc) afforded the title compound as a white amorphous solid (275 mg, 46 % yield);  $R_f$  0.65 (9:1 hexanes:EtOAc); IR (thin film,  $\text{cm}^{-1}$ ) 2852, 1720, 1574, 1447, 1128, 1045, 881; <sup>1</sup>H NMR (400 MHz, CDCl<sub>3</sub>)  $\delta$  7.37-7.34 (m, 1H), 7.15-7.08 (m, 2H), 5.15 (d,  $J = 7.8$  Hz, 2H), 5.06 (d,  $J = 7.8$  Hz, 2H) 4.18 (t,  $J = 7.2$  Hz, 2H); <sup>13</sup>C NMR (100 MHz, CDCl<sub>3</sub>)  $\delta$  141.0, 139.8, 130.2, 129.2, 119.7, 115.9, 74.7, 74.6; HRMS [+APCI] calculated for C<sub>8</sub>H<sub>8</sub>OBr 198.9753, found 198.9752 [M+H]<sup>+</sup>.

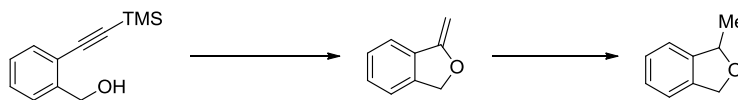


**4-Phenyl-1,3-dihydroisobenzofuran (82).** Prepared according to literature procedure<sup>65</sup> using **76** (50 mg, 0.20 mmol, 1 equiv), Pd(PPh<sub>3</sub>)<sub>4</sub> (12 mg, 5 mol %), K<sub>2</sub>CO<sub>3</sub> (56 mg,

0.41 mmol, 2 equiv), and PhI (50  $\mu$ L, 0.45 mmol, 2 equiv) in DMF (0.6 mL). After heating for 19 h, flash chromatography (9:1 hexanes:EtOAc) afforded the title compound as a white solid (34 mg, 85 % yield);  $^1\text{H NMR}$  (400 MHz,  $\text{CDCl}_3$ )  $\delta$  7.45-7.30 (m, 7H), 7.22 (d,  $J = 7.4$  Hz, 1H), 5.19 (d,  $J = 2.0$  Hz, 2H), 5.17 (d,  $J = 2.0$  Hz, 2H). All spectral data matched those previously reported.<sup>72</sup>

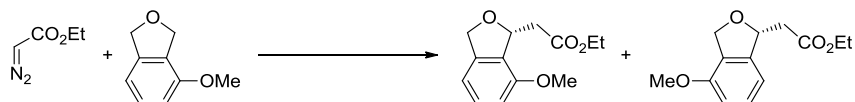


**(2-((Trimethylsilyl)ethynyl)phenyl)methanol (85)**. Prepared according to literature procedure<sup>66</sup> using trimethylsilyl acetylene (8.0 mL, 56.2 mmol, 1.2 equiv),  $\text{PdCl}_2(\text{PPh}_3)_2$  (1.5 g, 2.1 mmol, 5 mol %), CuI (820 mg, 4.3 mmol, 10 mol %), and 2-iodobenzyl alcohol (10.0 g, 42.7 mmol, 1 equiv). After stirring for 3 h, flash chromatography (9:1  $\rightarrow$  7:3 hexanes/EtOAc) followed by short path distillation afforded the title compound as a colorless oil (7.35 g, 84 %);  $^1\text{H NMR}$  (400 MHz,  $\text{CDCl}_3$ )  $\delta$  7.45 (d,  $J = 7.4$  Hz, 1H), 7.40 (d,  $J = 7.4$  Hz, 1H), 7.22 (m, 1H), 7.31 (t,  $J = 7.4$  Hz, 1H), 4.80 (d,  $J = 6.3$  Hz, 2H), 2.28 (t,  $J = 6.7$  Hz, 1H), 0.25 (s, 9H). All spectral data matched those previously reported.<sup>66</sup>

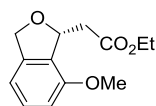


**1-Methyl-1,3-dihydroisobenzofuran (83)**. Prepared according to literature procedure<sup>66</sup> using (2-((trimethylsilyl)ethynyl)phenyl)methanol (7.35 g, 35.9 mmol, 1 equiv), TBAF (54.0 mL, 1 M in THF, 1.5 equiv), Pd/C (1.0 g, 10 wt. %), and  $\text{H}_2$  (1 atm). Short path

distillation afforded the title compound as a colorless oil (2.51 g, 52 %);  $^1\text{H NMR}$  (400 MHz,  $\text{CDCl}_3$ )  $\delta$  7.26-7.24 (m, 2H), 7.21-7.19 (m, 1H), 7.15-7.14 (m, 1H), 5.3 (q,  $J = 5.7$  Hz, 1H), 5.1 (d,  $J = 12.3$  Hz, 1H), 5.0 (d,  $J = 12.3$  Hz, 1H), 1.48 (dd,  $J = 6.4$ , 1.5 Hz, 3H). All spectral data matched those previously reported.<sup>66</sup>



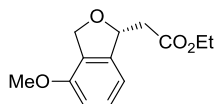
Prepared by general procedure **E** using ethyl diazoacetate (44 mg, 0.33 mmol) in  $\text{PhCF}_3$  (1.1 mL), **80** (200 mg, 1.3 mmol) in  $\text{PhCF}_3(0.75)$ , **62** (7 mg, 2 mol %), and 4 Å MS (66 mg). Flash chromatography (9:1  $\rightarrow$  8:2 pentane: $\text{Et}_2\text{O}$ ) afforded the title compounds as a mixture of separable regioisomers (49 mg, 63 % yield, 98:2 er **88**; 15 mg, 19 % yield, 94:6 er **S1**);



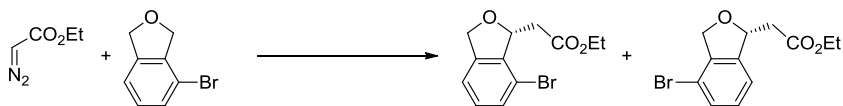
**(R)-Ethyl 2-(7-methoxy-1,3-dihydroisobenzofuran-1-yl)acetate (88)**. The title compound was isolated as 49 mg of a white amorphous solid (63 % yield, 98:2 er);  $R_f$  0.28 (9:1 pentane:  $\text{Et}_2\text{O}$ ); **IR** (thin film,  $\text{cm}^{-1}$ ) 3019, 2032, 1730, 1614, 1485, 1270, 922, 749, 667;  $^1\text{H NMR}$  (600 MHz,  $\text{CDCl}_3$ )  $\delta$  7.26-7.24 (m, 1H), 6.79 (d,  $J = 7.5$  Hz, 1H), 6.73 (d,  $J = 8.3$  Hz, 1H), 5.72 (d,  $J = 9.2$  Hz, 1H), 5.15 (dd,  $J = 12.3$ , 2.6 Hz, 1H), 5.04 (d,  $J = 12.3$  Hz, 1H), 4.16 (q,  $J = 7.0$  Hz, 2H), 3.81 (s, 3H), 3.1 (dd,  $J = 15.6$ , 2.9 Hz, 1H), 2.57 (dd,  $J = 15.6$ , 9.0 Hz, 1H), 1.23 (t,  $J = 7.2$  Hz, 3H);  $^{13}\text{C NMR}$  (100 MHz,  $\text{CDCl}_3$ )  $\delta$  172.5, 171.3, 154.3, 141.2, 129.7, 113.2, 108.9, 79.9, 73.2, 60.5, 55.1, 39.9, 14.2; **HRMS**



[+NSI] calculated for  $C_{13}H_{17}O_4$  237.1121, found 237.1119  $[M+H]^+$ ;  $[\alpha]^{20}_D + 69.5^\circ$  ( $c$  1.0,  $CHCl_3$ ); **HPLC** (Daicel OJ-H, 0.5 % IPA:HEX, 1 mL/min),  $\lambda$  230 nm,  $t_R(\text{min}) = 25.8$  min,  $t_R(\text{maj}) = 33.2$  min.

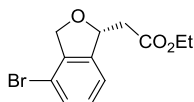


**(R)-Ethyl 2-(4-methoxy-1,3-dihydroisobenzofuran-1-yl)acetate (S1).** The title compound was isolated as 15 mg of a white amorphous solid (19 % yield, 94:6 er);  $R_f$  0.30 (9:1 pentane:Et<sub>2</sub>O); **IR** (thin film,  $cm^{-1}$ ) 3019, 2342, 1731, 1599, 1487, 1267, 1038, 924, 889, 751; **<sup>1</sup>H NMR** (600 MHz,  $CDCl_3$ )  $\delta$  7.25-7.24 (m, 1H), 6.75 (t,  $J = 7.5$  Hz, 2H), 5.66-5.64 (m, 1H), 5.12 (dd,  $J = 12.7, 2.6$  Hz, 1H), 5.04 (d,  $J = 12.3$  Hz, 1H), 4.18, (q,  $J = 7.0$  Hz, 2H), 3.81 (s, 3H), 2.76 (dd,  $J = 15.8, 4.4$  Hz, 1H), 2.7 (dd,  $J = 15.8, 8.3$  Hz, 1H), 1.25 (t,  $J = 7.2$  Hz, 3H); **<sup>13</sup>C NMR** (100 MHz,  $CDCl_3$ )  $\delta$  172.5, 129.3, 113.2, 110.0, 109.3, 80.9, 71.3, 60.7, 55.2, 41.7, 14.2; **HRMS** [+NSI] calculated for  $C_{13}H_{17}O_4$  237.1121, found 237.1119  $[M+H]^+$ ;  $[\alpha]^{20}_D + 31.0^\circ$  ( $c$  1.0,  $CHCl_3$ ); **HPLC** (Daicel OJ-H, 0.5 % IPA:HEX, 1 mL/min),  $\lambda$  210 nm,  $t_R(\text{min}) = 24.3$  min,  $t_R(\text{maj}) = 31.8$  min.

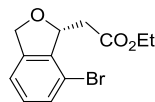


Prepared by general procedure **E** using ethyl diazoacetate (45 mg, 0.34 mmol) in  $PhCF_3$  (1.2 mL), **72** (272 mg, 1.37 mmol) in  $PhCF_3$  (0.8 mL), **62** (8 mg, 2 mol %), and 4 Å MS (68 mg). Flash chromatography (100:0  $\rightarrow$  95:5 pentane:Et<sub>2</sub>O) afforded the title

compounds as a mixture of separable regioisomers (28 mg, 29 % yield, 94:6 er **89**; 9.5 mg, 10 % yield **S2**);

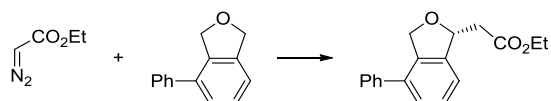


**(R)-Ethyl 2-(4-bromo-1,3-dihydroisobenzofuran-1-yl)acetate (89).** The title compound was isolated as 28 mg of a white amorphous solid (29 % yield, 94:6 er);  $R_f$  0.28 (9:1 hexanes:EtOAc); **IR** (thin film,  $\text{cm}^{-1}$ ) 3019, 2359, 1733, 1361, 1214, 1042, 923, 750, 668;  **$^1\text{H NMR}$**  (400 MHz,  $\text{CDCl}_3$ )  $\delta$  7.39 (d,  $J = 6.6$  Hz, 1H), 7.17-7.10 (m, 2H), 5.73 (t,  $J = 7.4$  Hz, 1H), 5.10 (dd,  $J = 12.9, 2.7$  Hz, 1H), 5.02 (dd,  $J = 12.9, 1.6$  Hz, 1H), 2.76-2.74 (m, 2H), 1.25 (t,  $J = 7.2$  Hz, 3H);  **$^{13}\text{C NMR}$**  (150 MHz,  $\text{CDCl}_3$ )  $\delta$  170.5, 142.6, 139.9, 130.8, 129.5, 120.0, 115.9, 81.5, 73.8, 60.8, 41.5, 29.7, 14.1; **HRMS** [+NSI] calculated for  $\text{C}_{12}\text{H}_{14}\text{O}_3\text{Br}$  285.0121, found 285.0120  $[\text{M}+\text{H}]^+$ ;  $[\alpha]_D^{20} + 12.8^\circ$  ( $c$  1.0,  $\text{CHCl}_3$ ); **HPLC** (Daicel OJ-H, 1 % IPA:HEX, 1 mL/min),  $\lambda$  210 nm,  $t_R(\text{min}) = 10.8$  min,  $t_R(\text{maj}) = 17.0$  min.

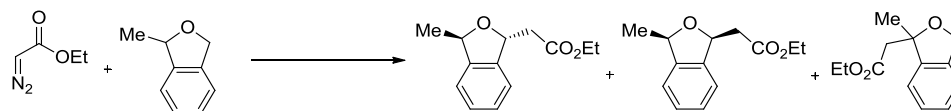


**(R)-Ethyl 2-(7-bromo-1,3-dihydroisobenzofuran-1-yl)acetate (S2).** The title compound was isolated as 9.5 mg of a white amorphous solid (10 % yield);  $R_f$  0.26 (9:1 hexanes:EtOAc); **IR** (thin film,  $\text{cm}^{-1}$ ) 3019, 2357, 2196, 1733, 1214, 920, 889, 753, 665;  **$^1\text{H NMR}$**  (400 MHz,  $\text{CDCl}_3$ )  $\delta$  7.40-7.38 (m, 1H), 7.16-7.15 (m, 2H), 5.67 (dt,  $J = 8.9, 2.4$  Hz, 1H), 5.22 (dd,  $J = 12.5, 2.7$  Hz, 1H), 5.08 (dd,  $J = 12.5, 0.8$  Hz, 1H), 4.16 (q,  $J = 7.0$  Hz, 2H), 3.18 (dd,  $J = 15.6, 2.7$  Hz, 1H), 2.66 (dd,  $J = 15.6, 9.0$  Hz, 1H), 1.24

(t,  $J = 7.0$  Hz, 3H);  $^{13}\text{C}$  NMR (150 MHz,  $\text{CDCl}_3$ )  $\delta$  170.7, 141.6, 140.0, 131.0, 129.8, 120.0, 116.3, 81.7, 73.0, 60.7, 39.3, 14.1; HRMS [+NSI] calculated for  $\text{C}_{12}\text{H}_{14}\text{O}_3\text{Br}$  285.0121, found 285.0118  $[\text{M}+\text{H}]^+$ ;  $[\alpha]_D^{20} + 56.6^\circ$  ( $c$  0.5,  $\text{CHCl}_3$ ).

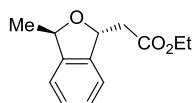


**(R)-Ethyl 2-(4-phenyl-1,3-dihydroisobenzofuran-1-yl)acetate (91).** Prepared by general procedure **E** using **83** (102 mg, 0.51 mmol), ethyl diazoacetate (17 mg, 0.13 mmol), **62** (2.6 mg, 2 mol %), and 4 Å MS (27 mg). Flash chromatography (100 % pentane  $\rightarrow$  95:5 pentane: $\text{Et}_2\text{O}$ ) afforded the title compound as a colorless oil (20 mg, 56 % yield, 96:4 er);  $R_f$  0.28 (9:1 pentane: $\text{Et}_2\text{O}$ ); IR (thin film,  $\text{cm}^{-1}$ ) 3020, 2007, 1732, 1214, 920, 756;  $^1\text{H}$  NMR (400 MHz,  $\text{CDCl}_3$ )  $\delta$  7.44-7.32 (m, 7H), 7.17 (d,  $J = 7.0$  Hz, 1H), 5.71 (t,  $J = 5.3$  Hz, 1H), 5.21 (dd,  $J = 12.5, 2.3$  Hz, 1H), 5.15 (dd,  $J = 12.9, 2.0$  Hz, 1H), 4.20 (q,  $J = 7.3$  Hz, 2H), 2.86-2.74 (m, 2H), 1.26 (t,  $J = 7.2$  Hz, 3H);  $^{13}\text{C}$  NMR (150 MHz,  $\text{CDCl}_3$ )  $\delta$  170.8, 141.5, 139.8, 137.1, 136.1, 128.7, 128.2, 128.0, 127.8, 127.5, 120.0, 80.4, 72.5, 60.7, 41.6, 24.9, 14.2; HRMS [+NSI] calculated for  $\text{C}_{18}\text{H}_{19}\text{O}_3$  283.1329, found 283.1326  $[\text{M}+\text{H}]^+$ ;  $[\alpha]_D^{20} + 6.9^\circ$  ( $c$  1.0,  $\text{CHCl}_3$ ); HPLC (Daicel OJ-H, 1 % IPA:HEX, 1 mL/min),  $\lambda$  254 nm,  $t_R(\text{min}) = 21.9$  min,  $t_R(\text{maj}) = 24.9$  min.



**Ethyl 2-((1R,3R)-3-methyl-1,3-dihydroisobenzofuran-1-yl)acetate (97, 98, 99).**

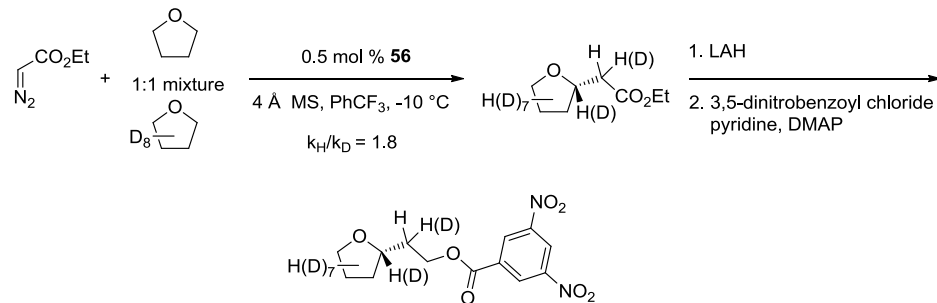
Prepared by general procedure **E** using ethyl diazoacetate (117 mg, 0.88 mmol) in PhCF<sub>3</sub> (3 mL), **83** (472 mg, 3.5 mmol) in PhCF<sub>3</sub> (2 mL), **62** (4.5 mg, 0.5 mol %), and 4 Å MS (176 mg). Ethyl diazoacetate solution was added to the substrate solution at -10 °C and warmed to room temperature overnight. Flash chromatography (97:3 → 95:5 → 9:1 pentane:Et<sub>2</sub>O) afforded the title compounds as a 85:5:10 mixture of **97:98:99** by GC and crude <sup>1</sup>H NMR. (116 mg, 60 % yield). **GC** (CHIRASIL DEX, 120 → 140 °C, 1 °C/min) t<sub>r</sub>(**99**) = 18.596 min, t<sub>r</sub>(**97**) = 21.839 min, t<sub>r</sub>(**98**) = 23.556 min. Major product **97** was characterized as follows (88:12 er).



**ethyl 2-((1R,3R)-3-methyl-1,3-dihydroisobenzofuran-1-yl)acetate (97). R<sub>f</sub> 0.41**

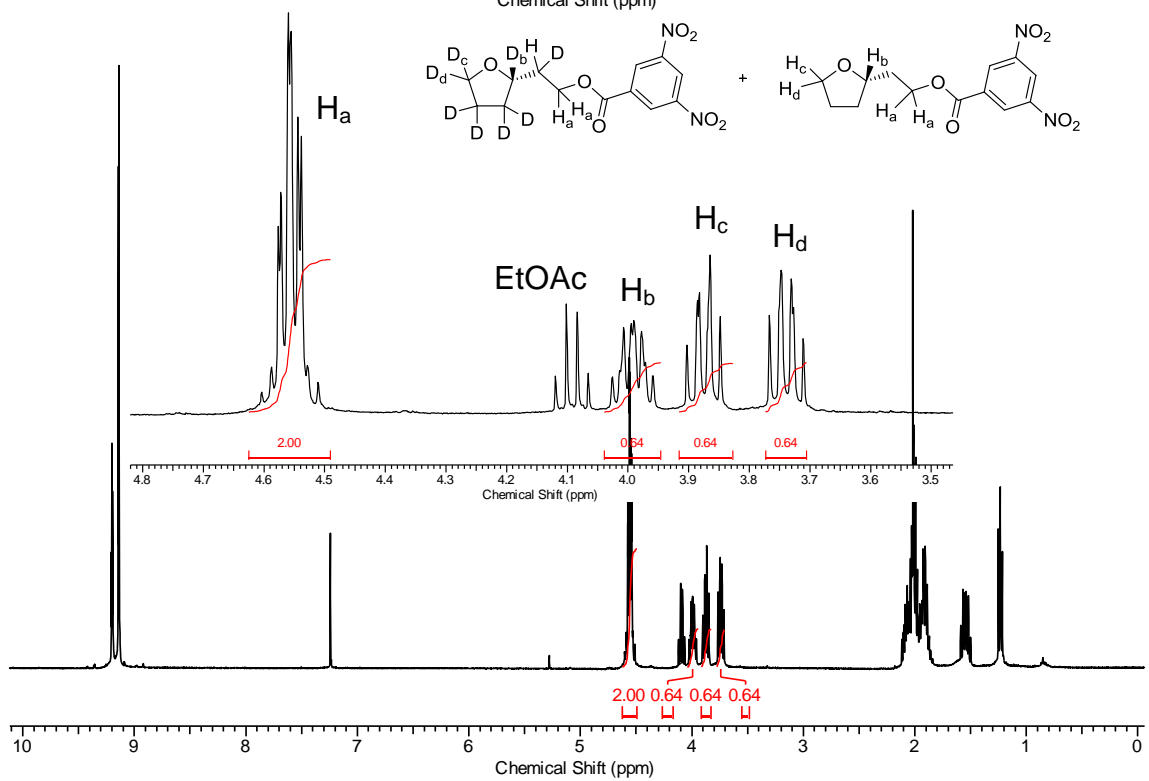
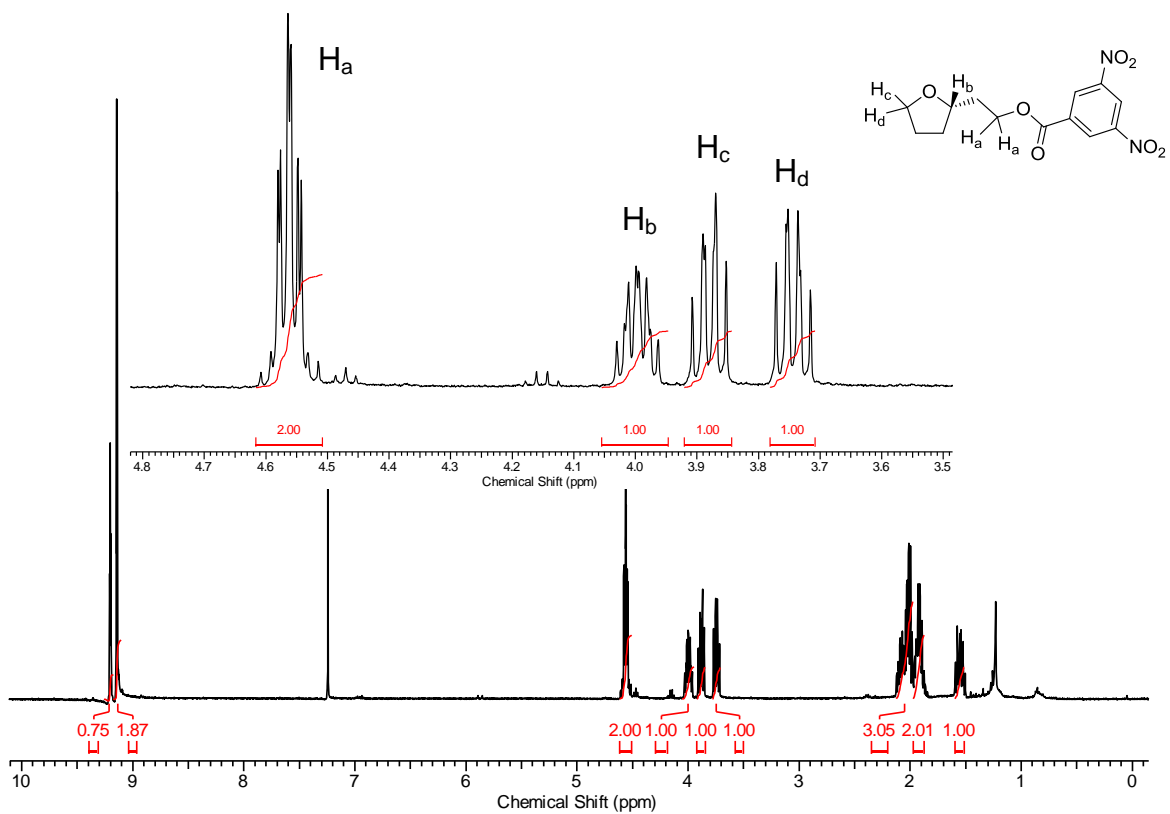
(9:1 pentane:Et<sub>2</sub>O); **IR** (thin film, cm<sup>-1</sup>) 3019, 2162, 2010, 1731, 1214, 1033, 920, 752, 668; **<sup>1</sup>H NMR** (400 MHz, CDCl<sub>3</sub>) δ 7.33-7.25 (m, 2H), 7.20-7.14 (m, 2H), 5.70 (td, *J* = 6.4, 2.9 Hz, 1H), 5.39 (qd, *J* = 6.3, 2.6 Hz, 1H), 4.19 (q, *J* = 7.2 Hz, 2H), 2.72 (d, *J* = 6.4 Hz, 2H), 1.48 (d, *J* = 6.4 Hz, 3H), 1.26 (t, *J* = 7.0 Hz, 3H); **<sup>13</sup>C NMR** (150 MHz, CDCl<sub>3</sub>) δ 170.9, 143.4, 140.7, 127.9, 127.5, 121.2, 121.0, 79.1, 79.0, 60.6, 41.8, 22.0, 14.2; **HRMS** [+NSI] calculated for C<sub>13</sub>H<sub>17</sub>O<sub>3</sub> 221.1172, found 221.1170 [M+H]<sup>+</sup>; [α]<sub>D</sub><sup>20</sup> + 10.2 ° (*c* 1.0, CHCl<sub>3</sub>); **HPLC** (Daicel OJ-H, 1 % IPA:HEX, 1 mL/min), λ 254 nm, t<sub>R</sub>(min) = 8.4 min, t<sub>R</sub>(maj) = 9.7 min.

### Kinetic Isotope Effect



**(S)-2-(tetrahydrofuran-2-yl)ethyl 3,5-dinitrobenzoate (104)**. Prepared by general procedure **E** using ethyl diazoacetate (336 mg, 2.5 mmol) in PhCF<sub>3</sub> (8.6 mL), THF (408 μL, 5.0 mmol) and d<sup>8</sup>-THF (409 μL, 5.0 mmol) in PhCF<sub>3</sub> (5.7 mL), [(*S,S*)-<sup>t</sup>BuPhebox-<sup>i</sup>Pr]IrCl<sub>2</sub>(H<sub>2</sub>O) **56**<sup>54</sup> (8 mg, 0.5 mol %), and 4 Å MS (502 mg). The crude residue was taken forward without further purification. A dry round bottom flask was charged with the crude residue and dissolved in Et<sub>2</sub>O (5 mL). The reaction mixture was cooled to 0 °C. LiAlH<sub>4</sub> (7.6 mL, 1 M in Et<sub>2</sub>O, 3.0 equiv) was added dropwise, and the reaction was stirred overnight. Once thin layer chromatography indicated complete consumption of starting material, the reaction mixture was poured into a vigorously stirring solution of Et<sub>2</sub>O (30 mL) and a saturated aqueous Rochelle's salt solution (15 mL). Et<sub>2</sub>O (60 mL) was added and the resulting biphasic mixture was stirred vigorously for approximately 3 h. The organic layer was separated, washed with brine, dried over MgSO<sub>4</sub> and concentrated in vacuo. The crude product was dissolved in CH<sub>2</sub>Cl<sub>2</sub> (8 mL). Pyridine (610 μL, 7.6 mmol, 3.0 equiv) and DMAP (31 mg, 0.26 mmol, 10 mol %) were added to the solution under N<sub>2</sub> and stirred for 10 min. 3,5-dinitrobenzoyl chloride (1.15 g, 5.0 mmol, 2.0 equiv) was added in one portion, and the mixture was

stirred for 1.5 h.  $\text{NH}_4\text{Cl}$  (aq) was added to the reaction mixture and extracted with  $\text{CH}_2\text{Cl}_2$  (3 x). The combined organic layers were washed with  $\text{NaHCO}_3$  (aq). The aqueous layer was extracted with  $\text{CH}_2\text{Cl}_2$  (3 x). The combined organic layers were dried with  $\text{MgSO}_4$ , filtered, and concentrated *in vacuo*. Flash chromatography (8:2 hexanes:EtOAc) afforded the title compound as a light yellow oil (192 mg, 25 % yield over 3 steps).



**Calculations used for the determination of KIE value from  $^1\text{H}$  NMR analysis:**

$$H_a = 2.0$$

$$H_b = 0.64$$

$$D_b = 1 - 0.64 = 0.36$$

$$H_c = 0.64$$

$$D_c = 1 - 0.64 = 0.36$$

$$H_d = 0.64$$

$$D_d = 1 - 0.64 = 0.36$$

$$\% \text{ H incorporated} = 0.64 / 1.0 = 64 \%$$

$$\% \text{ D incorporated} = 0.36 / 1.0 = 36 \%$$

$$\mathbf{KIE} = K_H / K_D = 0.64 / 0.36 = \mathbf{1.8}$$



## X-Ray Crystallographic Information

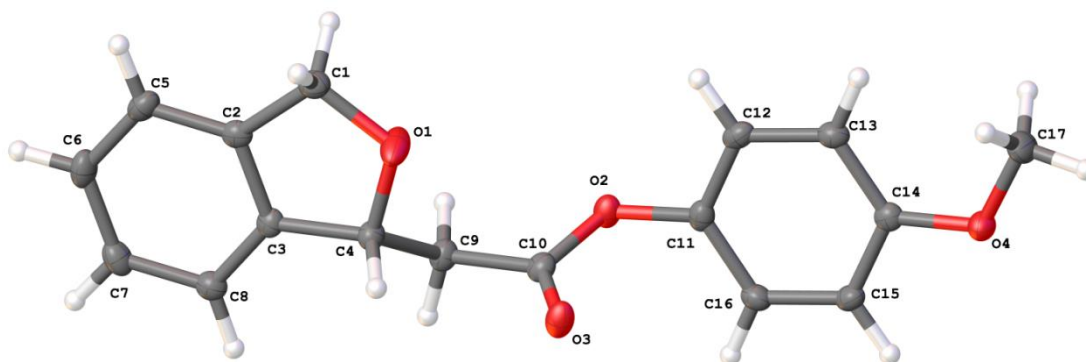
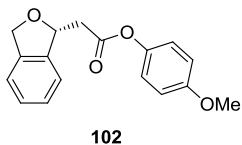


**Table S3.1.** Structural refinement data for (*R*)-4-methoxyphenyl 2-(1,3-dihydroisobenzofuran-1-yl)acetate (**102**).

<b>102</b>	
<b>Formula</b>	C <sub>17</sub> H <sub>16</sub> O <sub>4</sub>
<b>Form. Wt. (g/mol)</b>	284.30
<b>T (K)</b>	100.02
<b>Crystal system</b>	Orthorhombic
<b>Space group</b>	P2 <sub>1</sub> 2 <sub>1</sub> 2 <sub>1</sub>
<b><i>a</i> (Å)</b>	7.47301(10)

<b><i>b</i></b> (Å)	12.08020(15)
<b><i>c</i></b> (Å)	15.6344(2)
<b><math>\alpha</math></b> (°)	90
<b><math>\beta</math></b> (°)	90
<b><math>\gamma</math></b> (°)	90
<b>V</b> (Å <sup>3</sup> )	1411.40(3)
<b>Z</b>	4
<b><math>\rho_{\text{calc}}</math></b> (g/cm <sup>3</sup> )	1.338
<b><math>\mu</math></b> /mm <sup>-1</sup>	0.781
<b>F(000)</b>	600.0
<b>Crystal size</b> (mm <sup>3</sup> )	0.23 × 0.185 × 0.176
<b>Radiation</b>	CuK $\alpha$ ( $\lambda$ = 1.54178)
<b>2<math>\theta</math> range</b>	9.252 to 146.698
<b>Index ranges</b>	-9 ≤ <i>h</i> ≤ 8, -15 ≤ <i>k</i> ≤ 14, -19 ≤ <i>l</i> ≤ 19
<b>Reflns. Collected</b>	24525
<b>Unique reflns.</b>	2805 [ $R_{\text{int}}$ = 0.0236, $R_{\text{sigma}}$ = 0.0108]

<b>Data/rest./par.</b>	2805/36/242
<b>GOF</b>	1.101
<b>Final R indexes [<math>I &gt; 2\sigma(I)</math>]</b>	$R_1 = 0.0270$ , $wR_2 = 0.0668$
<b>All data</b>	$R_1 = 0.0273$ , $wR_2 = 0.0670$
<b>Largest diff. peak/hole / <math>e \text{ \AA}^{-3}</math></b>	0.17/-0.26
<b>Flack parameter</b>	0.06(4)

---

## References

- (1) Doyle, M. P.; Forbes, D. C. *Chem. Rev.* **1998**, *98*, 911.
- (2) Davies, H. M. L.; Beckwith, R. E. J. *Chem. Rev.* **2003**, *103*, 2861.
- (3) Davies, H. M. L.; Manning, J. R. *Nature* **2008**, *451*, 417.
- (4) Thu, H.-Y.; Tong, G. S.-M.; Huang, J.-S.; Chan, S. L.-F.; Deng, Q.-H.; Che, C.-M. *Angew. Chem., Int. Ed.* **2008**, *47*, 9747.
- (5) Lu, H. J.; Zhang, X. P. *Chem. Soc. Rev.* **2011**, *40*, 1899.
- (6) Davies, H. M. L.; Lian, Y. *Acc. Chem. Res.* **2012**, *45*, 923.
- (7) Davies, H. M. L.; Denton, J. R. *Chem. Soc. Rev.* **2009**, *38*, 3061.
- (8) Davies, H. M. L.; Morton, D. *Chem. Soc. Rev.* **2011**, *40*, 1857.
- (9) Mbuvi, H. M.; Woo, L. K. *Organometallics* **2008**, *27*, 637.
- (10) Davies, H. M. L.; Mark Hodges, L.; Matasi, J. J.; Hansen, T.; Stafford, D. G. *Tetrahedron Lett.* **1998**, *39*, 4417.
- (11) Müller, P.; Tohill, S. *Tetrahedron* **2000**, *56*, 1725.
- (12) Hansen, J.; Autschbach, J.; Davies, H. M. L. *J. Org. Chem.* **2009**, *74*, 6555.
- (13) Ikota, N.; Takamura, N.; Young, S. D.; Ganem, B. *Tetrahedron Lett.* **1981**, *22*, 4163.
- (14) Taber, D. F.; Herr, R. J.; Pack, S. K.; Geremia, J. M. *J. Org. Chem.* **1996**, *61*, 2908.
- (15) Taber, D. F.; Hennessy, M. J.; Louey, J. P. *J. Org. Chem.* **1992**, *57*, 436.
- (16) Taber, D. F.; You, K. K. *J. Am. Chem. Soc.* **1995**, *117*, 5757.

- (17) Taber, D. F.; You, K. K.; Rheingold, A. L. *J. Am. Chem. Soc.* **1996**, *118*, 547.
- (18) Takeda, K.; Oohara, T.; Anada, M.; Nambu, H.; Hashimoto, S. *Angew. Chem., Int. Ed.* **2010**, *49*, 6979.
- (19) Panne, P.; Fox, J. M. *J. Am. Chem. Soc.* **2007**, *129*, 22.
- (20) Panne, P.; DeAngelis, A.; Fox, J. M. *Org. Lett.* **2008**, *10*, 2987.
- (21) DeAngelis, A.; Dmitrenko, O.; Yap, G. P. A.; Fox, J. M. *J. Am. Chem. Soc.* **2009**, *131*, 7230.
- (22) DeAngelis, A.; Shurtleff, V. W.; Dmitrenko, O.; Fox, J. M. *J. Am. Chem. Soc.* **2011**, *133*, 1650.
- (23) Watanabe, N.; Ogawa, T.; Ohtake, Y.; Ikegami, S.; Hashimoto, S.-I. *Synlett* **1996**, *1996*, 85.
- (24) Minami, K.; Saito, H.; Tsutsui, H.; Nambu, H.; Anada, M.; Hashimoto, S. *Adv. Synth. Catal.* **2005**, *347*, 1483.
- (25) Muller, P.; Allenbach, Y.; Robert, E. *Tetrahedron-Asymmetry* **2003**, *14*, 779.
- (26) Goto, T.; Natori, Y.; Takeda, K.; Nambu, H.; Hashimoto, S. *Tetrahedron: Asymmetry* **2011**, *22*, 907.
- (27) Suematsu, H.; Katsuki, T. *J. Am. Chem. Soc.* **2009**, *131*, 14218.
- (28) Yasutomi, Y.; Suematsu, H.; Katsuki, T. *J. Am. Chem. Soc.* **2010**, *132*, 4510.
- (29) Adams, J.; Poupart, M.-A.; Grenier, L.; Schaller, C.; Ouimet, N.; Frenette, R. *Tetrahedron Lett.* **1989**, *30*, 1749.
- (30) Díaz-Requejo, M. M.; Belderraín, T. R.; Nicasio, M. C.; Trofimenko, S.; Pérez, P. *J. Am. Chem. Soc.* **2002**, *124*, 896.

- (31) Dias, H. V. R.; Browning, R. G.; Richey, S. A.; Lovely, C. J. *Organometallics* **2004**, *23*, 1200.
- (32) Caballero, A.; Prieto, A.; Díaz-Requejo, M. M.; Pérez, P. J. *Eur. J. Inorg. Chem.* **2009**, *2009*, 1137.
- (33) Doyle, M. P. *Recueil des Travaux Chimiques des Pays-Bas* **1991**, *110*, 305
- (34) Nishiyama, H.; Itoh, Y.; Matsumoto, H.; Park, S.-B.; Itoh, K. *J. Am. Chem. Soc.* **1994**, *116*, 2223.
- (35) Schafer, A. G.; Blakey, S. B. *Chem.Soc Rev.* **2015**, DOI: 10.1039/C5CS00354G.
- (36) Denmark, S. E.; Stavenger, R. A.; Faucher, A.-M.; Edwards, J. P. *J. Org. Chem.* **1997**, *62*, 3375.
- (37) Stark, M. A.; Richards, C. J. *Tetrahedron Lett.* **1997**, *38*, 5881.
- (38) Motoyama, Y.; Koga, Y.; Kobayashi, K.; Aoki, K.; Nishiyama, H. *Chem. –Eur. J.* **2002**, *8*, 2968.
- (39) Motoyama, Y.; Koga, Y.; Nishiyama, H. *Tetrahedron* **2001**, *57*, 853.
- (40) Nishiyama, H.; Ito, J.-I. *Chem. Commun.* **2010**, *46*, 203.
- (41) Nishiyama, H. *Chem. Soc. Rev.* **2007**, *36*, 1133.
- (42) Motoyama, Y.; Okano, M.; Narusawa, H.; Makihara, N.; Aoki, K.; Nishiyama, H. *Organometallics* **2001**, *20*, 1580.
- (43) Tsuchiya, Y.; Uchimura, H.; Kobayashi, K.; Nishiyama, H. *Synlett* **2004**, 2099.
- (44) Nishiyama, H.; Shiomi, T.; Tsuchiya, Y.; Matsuda, I. *J. Am. Chem. Soc.* **2005**, *127*, 6972.
- (45) Ito, J. I.; Shiomi, T.; Nishiyama, H. *Adv. Synth. Catal.* **2006**, *348*, 1235.

- (46) Ito, J.-i.; Kaneda, T.; Nishiyama, H. *Organometallics* **2012**, *31*, 4442.
- (47) Owens, C. P. Design, Synthesis, and Utilization of Iridium(III) Bis(oxazoliny)phenyl and Iridium(III) Bis(imidazoliny)phenyl Complexes for Catalytic Enantioselective Atom Transfer C–H Functionalization.. Ph. D. Dissertation, Emory University, Atlanta, GA, 2014.
- (48) Hao, X.-Q.; Gong, J.-F.; Du, C.-X.; Wu, L.-Y.; Wu, Y.-J.; Song, M.-P. *Tetrahedron Lett.* **2006**, *47*, 5033.
- (49) Hao, X.-Q.; Xu, Y.-X.; Yang, M.-J.; Wang, L.; Niu, J.-L.; Gong, J.-F.; Song, M.-P. *Organometallics* **2012**, *31*, 835.
- (50) Hyodo, K.; Nakamura, S.; Shibata, N. *Angew. Chem., Int. Ed.* **2012**, *51*, 10337.
- (51) Wang, T.; Hao, X.-Q.; Huang, J.-J.; Niu, J.-L.; Gong, J.-F.; Song, M.-P. *J. Org. Chem.* **2013**, *78*, 8712.
- (52) Shao, D.-D.; Niu, J.-L.; Hao, X.-Q.; Gong, J.-F.; Song, M.-P. *Dalton Trans.* **2011**, *40*, 9012.
- (53) Yang, M.-J.; Liu, Y.-J.; Gong, J.-F.; Song, M.-P. *Organometallics* **2011**, *30*, 3793.
- (54) Owens, C. P.; Varela-Alvarez, A.; Boyarskikh, V.; Musaev, D. G.; Davies, H. M. L.; Blakey, S. B. *Chem. Sci.* **2013**, *4*, 2590.
- (55) Mace Weldy, N. Schafer, A. G.; Owens, C. P.; Herting, C. J.; Varela-Alvarez, A.; Chen, S.; Niemeyer, Z.; Musaev, D. G.; Sigman, M. S.; Davies, H. M. L.; Blakey, S. B. **2015**, Submitted.

- (56) Wu, L.-Y.; Hao, X.-Q.; Xu, Y.-X.; Jia, M.-Q.; Wang, Y.-N.; Gong, J.-F.; Song, M.-P. *Organometallics* **2009**, *28*, 3369.
- (57) Davies, I. W.; Gerena, L.; Lu, N.; Larsen, R. D.; Reider, P. J. *J. Org. Chem.* **1996**, *61*, 9629.
- (58) Ma, K.; You, J. *Chem.–Eur. J.* **2007**, *13*, 1863.
- (59) Karcher, W. D., J. Practical Applications of Quantitative Structure-Activity Relationships (QSAR) in Environmental Chemistry and Toxicology; Springer Netherlands, 1990.
- (60) Guptill, D. M.; Davies, H. M. L. *J. Am. Chem. Soc.* **2014**, *136*, 17718.
- (61) Guptill, D. M.; Cohen, C. M.; Davies, H. M. L. *Org. Lett.* **2013**, *15*, 6120.
- (62) Favor, D. A.; Johnson, D. S.; Powers, J. J.; Li, T.; Madabattula, R. *Tetrahedron Lett.* **2007**, *48*, 3039.
- (63) Mkhaliid, I. A. I.; Barnard, J. H.; Marder, T. B.; Murphy, J. M.; Hartwig, J. F. *Chem. Rev.* **2010**, *110*, 890.
- (64) Murphy, J. M.; Liao, X.; Hartwig, J. F. *J. Am. Chem. Soc.* **2007**, *129*, 15434.
- (65) Mo, F.; Jiang, Y.; Qiu, D.; Zhang, Y.; Wang, J. *Angew. Chem., Int. Ed.* **2010**, *49*, 1846.
- (66) Hiroya, K.; Jouka, R.; Kameda, M.; Yasuhara, A.; Sakamoto, T. *Tetrahedron* **2001**, *57*, 9697.
- (67) Davies, H. M. L.; Hansen, T.; Churchill, M. R. *J. Am. Chem. Soc.* **2000**, *122*, 3063.



- (68) Kornilova, T.; Ukolov, A.; Kostikov, R.; Zenkevich, I. *Russ. J. Gen. Chem.* **2012**, *82*, 1675.
- (69) Toma, T.; Shimokawa, J.; Fukuyama, T. *Org. Lett.* **2007**, *9*, 3195.
- (70) Candish, L.; Lupton, D. W. *J. Am. Chem. Soc.* **2013**, *135*, 58.
- (71) Martín-Matute, B.; Cárdenas, D. J.; Echavarren, A. M. *Angew. Chem., Int. Ed.* **2001**, *40*, 4754.
- (72) García, D.; Foubelo, F.; Yus, M. *Tetrahedron* **2008**, *64*, 4275.